Hosna Khajeh

# Improving the Flexibility of Future Power Systems

Provision of Flexibility Services to the System Operators by Different Energy Resources

ACTA WASAENSIA 547

Vaasan yliopisto
UNIVERSITY OF VAASA

ISBN 978-952-395-171-6 (print)
978-952-395-172-3 (online)

ISSN 0355-2667 (Acta Wasaensia 547, print)
2323-9123 (Acta Wasaensia 547, online)

URN https://urn.fi/URN:ISBN:978-952-395-172-3

PunaMusta Oy, Joensuu, 2024.

ACADEMIC DISSERTATION

*To be presented, with the permission of the Board of the School of Technology and Innovations of the University of Vaasa, for public examination on the 3rd of December, 2024, at noon.*

Article based dissertation, School of Technology and Innovations, Electrical Engineering

Author Hosna Khajeh https://orcid.org/0000-0001-5020-0279

Supervisor(s) Professor Hannu Laaksonen
University of Vaasa. School of Technology and Innovations, Electrical Engineering.

Postdoctoral Researcher Elahe Doroudchi
University of Vaasa. School of Technology and Innovations, Electrical Engineering.

Custos Professor Hannu Laaksonen
University of Vaasa. School of Technology and Innovations, Electrical Engineering.

Reviewers Professor Matti Lehtonen
Aalto University. Department of Electrical Engineering and Automation, Power Systems and High Voltage Engineering.

Professor Samuli Honkapuro
LUT University. School of Energy Systems, Electrical Engineering.

Opponent Professor Pertti Järventausta
Tampere University, Faculty of Information Technology and Communication Sciences, Electrical Engineering.

## Tiivistelmä

Tulevaisuuden sähköjärjestelmien tulee olla entistä joustavampia laajamittaisen uusiutuvien energialähteiden ja sähköajoneuvojen integroimisen mahdollistamiseksi. Sen vuoksi kanta- ja jakeluverkko-operaattorit tarvitsevat yhä enemmän teknisiä joustopalveluita, jotka tehostavat sähköjärjestelmän toimintaa ja parantavat verkon olemassa olevan kapasiteetin hyödyntämistä sallittujen jännite- ja virtarajojen puitteissa.

Vaikka joustopalvelut ja niihin liittyvät tekniset lisäarvopalvelumarkkinat kantaverkkoyhtiöille ovat olleet olemassa jo pitkään erityisesti taajuuden ja sähköjärjestelmän tehotasapainon hallintaan liittyen, niin jakeluverkkoyhtiöille suunnatut tekniset joustopalvelut ovat saaneet vähemmän huomiota tähän päivään mennessä. Väitöskirja keskittyy jakeluverkko-operaattoreiden joustopalveluiden suunnitteluun ja esittää uusia periaatteita joustavien energiaresurssien tehokkaaseen hyödyntämiseen jakeluverkoissa.

Joustavat energiaresurssit voivat olla joko energian tuottajia tai kuluttajia, jotka pystyvät ohjaamaan sähkön kulutustaan tai -tuotantoaan kanta- ja jakeluverkko-operaattoreiden tarpeiden mukaan. Väitöskirja analysoi erilaisia joustavia energiaresursseja, mukaan lukien sähköakkuvarastot, kotitalouksien ohjattavat sähkölaitteet, sähköajoneuvot ja paikalliset energiayhteisöt sekä tuulivoimaan integroidut vetyjärjestelmät. Näitä joustoresursseja hyödynnetään tuottamaan joustopalveluita sekä kanta- että jakeluverkkoyhtiöille.

Väitöskirja esittelee sekä optimointipohjaisen että sumeaan logiikkaan perustuvat menetelmät joustavien energiaresurssien pätö- ja loistehon hallintaan joustopalveluiden tuottamiseksi kanta- ja jakeluverkko-operaattoreiden kasvaviin joustotarpeisiin. Erilaiset epävarmuustekijät voivat kuitenkin hankaloittaa joustoresurssien hyödyntämistä ja joustotarpeiden täyttämistä. Tämän vuoksi väitöskirjassa esitetään suunnitelma, joka mahdollistaa optimaalisten valintojen tekemisen erilaiset epävarmuustekijät, ajalliset vaihtelut ja niihin liittyvät skenaariot huomioiden. Kaikki väitöskirjassa esitetyt menetelmät on testattu erilaisissa tapaustutkimuksissa käytännön sovellettavuuden sekä joustopalveluiden taloudellisen kannattavuuden varmistamiseksi.

Avainsanat: Joustopalvelu, joustavat energiaresurssit, energiankäytön optimointi, kanta- ja jakeluverkko-operaattorit, energian hallintajärjestelmät.

## Abstract

Future power systems must become more flexible to enable the increased integration of intermittent, weather-dependent renewable energy sources (RES) and electric vehicles. To address this, power system operators increasingly need various flexibility services. These services enable more efficient system operation, better utilisation of existing assets, and increased hosting capacity by managing voltage, current, or thermal limit-related congestions.

While flexibility services for transmission system operators (TSOs) have been well-developed, less attention has been given to those for distribution system operators (DSOs). Hence, this dissertation addresses the key features needed for designing flexibility services at the DSO level and offers guidance for efficient utilisation of Flexible Energy Resources (FERs) in distribution networks.

FERs can be defined as customers, consumers and/or producers, who can control their electricity use or production based on system operators' needs. This dissertation analyses various FERs, including battery energy storage system (BESS), controllable devices in smart homes like electric water heater, heating and ventilation air conditioner, and electric vehicle, a local energy community with shared controllable devices, as well as a wind-integrated hydrogen system with an electrolyser, compressor, and hydrogen storage. These FERs are scheduled to provide flexibility services for DSO and TSO.

This dissertation introduces two general methods for managing FERs: mathematically modelled optimisation-based systems and fuzzy logic control for coordinated active and reactive power management. These methods enable FERs to provide flexibility services for the system operators. By using the proposed approaches, system operators can better address the challenges of integrating renewable energy, while FERs can achieve financial benefits. However, uncertainties can complicate achievement of these goals. Therefore, the dissertation proposes a roadmap to make informed and optimal decisions under various uncertainties. It also implements methods to generate scenarios based on the nature of the related scheduling problem.

All the methodologies proposed in this dissertation have been applied to various case studies using real-world data from Finnish power systems to ensure practical relevance. Additionally, different comparison models have been developed to show how financially profitable the flexibility services provision could be for FERs.

Keywords: Flexibility Service, Flexible Energy Resource, Energy Optimisation, System Operators, Energy Management System.

# ACKNOWLEDGEMENT

This dissertation was carried out at the School of Innovation and Technology at the University of Vaasa during 2019 to 2024. I am very thankful for the financial support that made this work possible: the Fleximar Project (2019-2021), a grant from the Ella and Georg Ehrnrooth Foundation (2022), and funding from the Finnish Foundation for Technology Promotion (2023-2024). I am also grateful for the doctoral researcher position provided by the School of Innovation and Technology from 2021 to 2024.

I would like to express my deepest gratitude to my supervisor, Prof. Hannu Laaksonen. He has made my research journey both successful and enjoyable. He has consistently supported my ideas and provided me with the freedom to explore and be creative. His knowledge and guidance have been invaluable to my work, and his support has meant the world to me. I couldn't have asked for a better or more encouraging supervisor, and I feel incredibly fortunate to have had him by my side.

I also want to thank my other collaborators: Hooman Firoozi, Chethan Parthasarathy, Sahar Seyyedeh-Barhagh, Prof. Marcelo Godoy Simões, and Dr. Elahe Doroudchi. I am especially grateful to Hooman for his significant contributions to the papers included in this dissertation—his innovative ideas and technical skills have greatly enriched my work.

I would like to express my deep gratitude to Dr. Mohammad Reza Hesamzadeh for graciously hosting me at KTH University. I am also thankful for the opportunity to collaborate with Dr. Sambuddha Chakrabarti, whose guidance has been invaluable in teaching me the fundamentals of programming with Python and Julia, as well as the importance of professional collaboration through version control systems.

I am deeply thankful to my parents, who taught me the importance of both science and kindness. My research journey started over ten years ago when my master's supervisor told me that while studying for a course is like walking, research is more like climbing a mountain—it's not meant to be easy. Now, ten years later, I can confirm that my path has indeed been challenging, with many ups and downs, but I have enjoyed every part of the ride.

Moving to Finland was a major turning point in my life. While I miss the support of my family and friends back home, having a good friend here has made all the difference. I am truly thankful for my best friend in Finland, Ensieh

Ghorbanzadeh, who has been a great source of support and friendship. To Farzaneh and Navid, thank you for being such wonderful friends to us!

Lastly, I cannot put into words how much emotional support I have received from my husband throughout this journey. He has always encouraged me to do my best and has been there for me in every situation. He has helped me believe in myself and my abilities, and I am so grateful for his constant love and encouragement.

# Contents

## Figures

## Tables

## Abbreviations

| | |
|---|---|
| AC | Alternating Current |
| aFRR | Automatic Frequency Restoration Reserve |
| ANM | Active Network Management |
| BESS | Battery Energy Storage Systems |
| BSP | Balance Service Provider |
| CDF | Cumulative Distribution Function |
| CM | Comparison Model |
| DBU | Degree of BESS Utilisation |
| DC | Direct Current |
| DER | Distributed Energy Resource |
| DSO | Distribution System Operator |
| ECMC | Energy Community Management Centre |
| EMS | Energy Management System |
| EV | Electric Vehicle |
| EWH | Electric Water Heater |
| FACTS | flexible AC Transmission System |
| FC | Fuel Cells |
| FCR | Frequency Containment Reserve |
| FCR-D | Frequency Containment Reserve for Disturbances |
| FCR-N | Frequency Containment Reserve for Normal operations |
| FER | Flexible Energy Resource |
| FFR | Fast Frequency Reserve |
| FLC | Fuzzy Logic Control |
| FRR | Frequency Restoration Reserve |
| HEMS | Home Energy Management System |
| HV | High Voltage |
| HVAC | Heating Ventilation and Air Conditioning |
| HVDC | High Voltage Direct Current |
| ICT | Information and Communication Technology |
| LV | Low Voltage |
| mFRR | Manual Frequency Restoration Reserve |
| MV | Medium Voltage |
| OLTC | On-Load Tap Changing |
| PDF | Probability Density Function |
| Pf | Active Power-Frequency |
| PST | phase-shifting transformer |
| QU | Reactive Power-Voltage |
| RES | Renewable Energy Resource |
| SOC | State of Charge |
| TES | Thermal Energy Storages |
| TSO | Transmission System Operator |
| WAMPAC | Wide-Area Monitoring Protection and Control |

# Formulas

## List of Publications

Publication I: **Hosna Khajeh** & Hannu Laaksonen, (2022, September). Potential ancillary service markets for future power systems. In 2022 18th International Conference on the European Energy Market (EEM) (pp. 1-6). IEEE. https://doi.org/10.1109/EEM54602.2022.9921133. © 2022, IEEE. Reprinted with permission.

Publication II: **Hosna Khajeh**, Sahar Seyyedeh-Barhagh, Hannu Laaksonen. (2024, Jun), Quantifying the Impact of Day-ahead Renewable Forecasts on DER Hosting Capacity Estimation in CIRED 2024 Vienna Workshop.

Publication III: **Hosna Khajeh** & Hannu Laaksonen, (2022). Applications of probabilistic forecasting in smart grids: A review. Applied Sciences, 12(4), 1823. https://doi.org/10.3390/app12041823. © 2022 by the authors. Published by MDPI. CC BY.

Publication IV: **Hosna Khajeh**, Hooman Firoozi, & Hannu Laaksonen, (2022). Flexibility potential of a smart home to provide TSO-DSO-level services. Electric Power Systems Research, 205, 107767.
https://doi.org/10.1016/j.epsr.2021.107767. © 2021 The Author(s). Published by Elsevier. CC BY.

Publication V: **Hosna Khajeh**, Hannu Laaksonen, & Marcelo G. Simões, (2023). A fuzzy logic control of a smart home with energy storage providing active and reactive power flexibility services. Electric Power Systems Research, 216, 109067. https://doi.org/10.1016/j.epsr.2022.109067. © 2022 The Author(s). Published by Elsevier. CC BY.

Publication VI: Hooman Firoozi, **Hosna Khajeh**, & Hannu Laaksonen, (2020). Optimized operation of local energy community providing frequency restoration reserve. IEEE Access, 8, 180558-180575.
https://doi.org/10.1109/ACCESS.2020.3027710. Published by IEEE. CC BY.

Publication VII: Hooman Firoozi, **Hosna Khajeh**, & Hannu Laaksonen, (2022). Flexibility of Microgrids with Energy Management Systems. In Artificial Intelligence-Based Energy Management Systems for Smart Microgrids (pp. 1-29). CRC Press. https://doi.org/10.1201/b22884-1. © 2022 Taylor & Francis Group.

Publication VIII: **Hosna Khajeh**, Chethan Parthasarathy, Elahe Doroudchi, & Hannu Laaksonen, (2023). Optimized siting and sizing of distribution-network-connected battery energy storage system providing flexibility services for system operators. Energy, 285, 129490. https://doi.org/10.1016/j.energy.2023.129490. 

Publication IX: **Hosna Khajeh**, Sahar Seyyedeh-Barhagh, Hannu Laaksonen, (2024), Optimized Operation of Hybrid Wind-Hydrogen System to Provide Flexibility for Transmission System Needs, Submitted to IEEE Transactions on Sustainable Energy.

## Author’s contributions

Publication I: Hosna Khajeh: Conceptualisation, Investigation, Visualisation, Writing - Original Draft; Hannu Laaksonen: Writing - Review & Editing, Supervision.

Publication II: Hosna Khajeh: Conceptualisation, Investigation, Methodology, Software, Visualisation, Writing - Original Draft; Sahar Seyyedeh-Barhagh: Conceptualisation, Writing - Original Draft; Hannu Laaksonen: Writing - Review & Editing, Supervision, Project Administration.

Publication III: Hosna Khajeh: Conceptualization, Investigation, Visualization, Writing - Original Draft; Hannu Laaksonen: Writing - Review & Editing, Supervision.

Publication IV: Hosna Khajeh: Conceptualisation, Methodology, Investigation, Simulation, Writing - Original Draft; Hooman Firoozi: Conceptualisation, Methodology, Investigation, Simulation; Hannu Laaksonen: Writing - Reviewing & Editing, Supervision, Project Administration, Fund Acquisition.

Publication V: Hosna Khajeh: Conceptualisation, Methodology, Investigation, Simulation, Visualisation, Writing - Original Draft; Hannu Laaksonen: Supervision, Validation, Writing - Review & Editing; Marcelo G. Simões: Validation, Writing – Review & Editing.

Publication VI: Hosna Khajeh: Conceptualisation, Methodology, Investigation, Simulation, Writing - Original Draft; Hooman Firoozi: Conceptualisation, Methodology, Investigation, Visualisation, Writing - Original Draft; Hannu Laaksonen: Writing- Reviewing & Editing, Supervision, Project Administration, Fund Acquisition.

Publication VII: Hosna Khajeh: Conceptualisation, Methodology, Investigation, Writing - Original Draft; Hooman Firoozi: Methodology, Investigation, Writing -

Original Draft, Visualisation; Hannu Laaksonen: Writing- Reviewing & Editing, Supervision, Project Administration, Fund Acquisition.

Publication VIII: Hosna Khajeh: Conceptualisation, Methodology, Investigation, Simulation, Visualization, Writing – Original Draft; Chethan Parthasarathy: Conceptualization, Writing – Original Draft; Elahe Doroudchi: Writing – Review & Editing, Hannu Laaksonen: Conceptualization, Supervision, Validation, Writing – Review & Editing, Project Administration.

Publication IX: Hosna Khajeh: Conceptualisation, Methodology, Investigation, Simulation, Visualization, Writing – Original Draft; Sahar Seyyedeh-Barhagh: Conceptualisation, Visualisation, Writing – Original Draft; Hannu Laaksonen: Conceptualization, Supervision, Writing – Review & Editing, Project Administration.

## Other relevant publications

The following are the list of author’s relevant publications that are not included in the thesis:

**H. Khajeh**, H. Firoozi, M. R. Hesamzadeh, H. Laaksonen, and M. Shafie-Khah, ‘A local capacity market providing local and system-wide flexibility services’, IEEE Access, vol. 9, pp. 52336–52351, 2021.

**H. Khajeh**, H. Firoozi, H. Laaksonen, and M. Shafie-khah, ‘A new local market structure for meeting customer-level flexibility needs’, presented at the 2020 International Conference on Smart Energy Systems and Technologies (SEST), IEEE, 2020, pp. 1–6.

H. Firoozi, **H. Khajeh**, H. Laaksonen, and M. Shaterabadi, ‘Active Building as an Electricity Network Service Provider’, in Active Building Energy Systems: Operation and Control, Springer, 2022, pp. 273–293.

H. Firoozi, M. A. R. Nezhad, **H. Khajeh**, and H. Laaksonen, ‘Active management of distribution networks’, Active Electrical Distribution Network: A Smart Approach, pp. 155–176, 2021.

H. Laaksonen, C. Parthasarathy, **H. Khajeh**, and M. Shafie-khah, ‘Adaptation of DER Control Schemes and Functions During MV Network Back-up Connection’, presented at the 2021 International Conference on Smart Energy Systems and Technologies (SEST), IEEE, 2021, pp. 1–6.

**H. Khajeh**, M. Shafie-khah, and H. Laaksonen, ‘Blockchain-based demand response using prosumer scheduling’, in Blockchain-based Smart Grids, Elsevier, 2020, pp. 131–144.

**H. Khajeh**, H. Firoozi, H. Laaksonen, and M. Shafie-Khah, ‘Business Models for Different Future Electricity Market Players’, in Deregulated Electricity Structures and Smart Grids, CRC Press, 2022, pp. 63–81.

**H. Khajeh**, H. Firoozi, H. Laaksonen, and M. Shafie-khah, ‘Comparison of optimised operation of energy community’s flexibility considering different regulations and trading structures’, presented at the CIRED 2021-The 26th International Conference and Exhibition on Electricity Distribution, IET, 2021, pp. 3102–3106.

H. Laaksonen, C. Parthasarathy, H. Hafezi, M. Shafie-khah, and **H. Khajeh**, ‘Control and management of distribution networks with flexible energy resources’, Int. Rev. Electr. Eng, vol. 15, no. 3, pp. 213–223, 2020.

H. Firoozi, **H. Khajeh**, and H. Laaksonen, ‘Demand Response Techniques and Smart Home Energy Management Systems’, Active Electrical Distribution Network: A Smart Approach, pp. 517–537, 2021.

C. Parthasarathy, **H. Khajeh**, H. Firoozi, H. Laaksonen, and H. Hafezi, ‘Distributed generation, storage and active network management’, in Deregulated Electricity Structures and Smart Grids, CRC Press, 2022, pp. 83–111.

**H. Khajeh**, C. Parthasarathy, and H. Laaksonen, ‘Effects of battery aging on BESS participation in frequency service markets–Finnish case study’, presented at the 2022 18th International Conference on the European Energy Market (EEM), IEEE, 2022, pp. 1–6.

M. A. Rajabinezhad, H. Firoozi, **H. Khajeh**, and H. Laaksonen, ‘Electrical energy storage devices for active buildings’, in Active Building Energy Systems: Operation and Control, Springer, 2022, pp. 51–69.

M. Shaterabadi, **H. Khajeh**, H. Firoozi, and H. Laaksonen, ‘Energy Management Systems of Grid-Connected Active Buildings’, in Active Building Energy Systems: Operation and Control, Springer, 2022, pp. 251–271.

H. Firoozi, **H. Khajeh**, and H. Laaksonen, ‘Flexibility Forecast at Local Energy Community Level’, presented at the 2021 IEEE PES Innovative Smart Grid Technologies Europe (ISGT Europe), IEEE, 2021, pp. 1–5.

H. Laaksonen, C. Parthasarathy, **H. Khajeh**, M. Shafie-Khah, and N. Hatziargyriou, ‘Flexibility services provision by frequency-dependent control of on-load tap-changer and distributed energy resources’, IEEE Access, vol. 9, pp. 45587–45599, 2021.

**H. Khajeh** and H. Laaksonen, ‘Flexibility Utilisation Enabling Business Models and Tariff Structures’, presented at the 2023 19th International Conference on the European Energy Market (EEM), IEEE, 2023, pp. 1–6.

H. Laaksonen, C. Parthasarathy, H. Hafezi, M. Shafie-khah, and **H. Khajeh**, ‘Flexible control and management methods for future distribution networks’, presented at the CIRED 2020 Berlin Workshop (CIRED 2020), IET, 2020, pp. 66–69.

M. G. Simoes, F. A. Farret, **H. Khajeh**, M. Shahparasti, and H. Laaksonen, 'Future renewable energy communities based flexible power systems', Applied Sciences, vol. 12, no. 1, p. 121, 2021.

E. Doroudchi, **H. Khajeh**, and H. Laaksonen, 'Increasing self-sufficiency of energy community by common thermal energy storage', IEEE Access, vol. 10, pp. 85106–85113, 2022.

A. S. Gazafroudi, **H. Khajeh**, M. Shafie-khah, H. Laaksonen, and J. M. Corchado, 'Local market models', in Local electricity markets, Elsevier, 2021, pp. 79–90.

**H. Khajeh**, H. Firoozi, H. Laaksonen, and M. Shafie-khah, 'Microgrids as energy and flexibility providers for TSO-level networks', presented at the CIRED 2020 Berlin Workshop (CIRED 2020), IET, 2020, pp. 787–790.

H. Laaksonen, **H. Khajeh**, and N. Hatziargyriou, 'Novel DER and OLTC Management Scheme for Coordinated TSO-DSO Flexibility Services Provision', presented at the 2023 IEEE PES Innovative Smart Grid Technologies Europe (ISGT EUROPE), IEEE, 2023, pp. 1–5.

H. Firoozi, **H. Khajeh**, and H. Laaksonen, 'Optimised operation of local energy community with flexible energy resources providing local and system-wide flexibility services for DSO and TSO needs', presented at the CIRED 2021-The 26th International Conference and Exhibition on Electricity Distribution, IET, 2021, pp. 2028–2032.

**H. Khajeh**, A. S. Gazafroudi, H. Laaksonen, M. Shafie-Khah, P. Siano, and J. P. Catalão, 'Peer-to-peer electricity market based on local supervision', IEEE access, vol. 9, pp. 156647–156662, 2021.

**H. Khajeh**, H. Firoozi, H. Laaksonen, and M. Shafie-khah, 'Peer-to-peer flexibility trading of end-users at distribution networks', presented at the CIRED 2020 Berlin Workshop (CIRED 2020), IET, 2020, pp. 797–799.

**H. Khajeh**, R. Zheng, H. Firoozi, H. Laaksonen, and M. Shafie-Khah, 'Role of Smart Homes and Smart Communities in Flexibility Provision', in Flexibility in Electric Power Distribution Networks, CRC Press, 2021, pp. 21–40.

H. Laaksonen, C. Parthasarathy, H. Hafezi, M. Shafie-khah, **H. Khajeh**, and N. Hatziargyriou, 'Solutions to increase PV hosting capacity and provision of services from flexible energy resources', Applied Sciences, vol. 10, no. 15, p. 5146, 2020.

S. Talari, **H. Khajeh**, M. Shafie-khah, B. Hayes, H. Laaksonen, and J. P. Catalão, 'The role of various market participants in blockchain business model', in Blockchain-based Smart Grids, Academic Press, 2020, pp. 75–102.

**H. Khajeh**, H. Laaksonen, A. S. Gazafroudi, and M. Shafie-Khah, 'Towards flexibility trading at TSO-DSO-customer levels: A review', Energies, vol. 13, no. 1, p. 165, 2019.

H. Laaksonen, **H. Khajeh**, C. Parthasarathy, M. Shafie-khah, and N. Hatziargyriou, 'Towards flexible distribution systems: Future adaptive management schemes', Applied Sciences, vol. 11, no. 8, p. 3709, 2021.

S. Chakrabarti, **H. Khajeh**, T. R. Nudell, M. R. Hesamzadeh, and R. Baldick, 'Transmission Investment Coordination using MILP Lagrange Dual Decomposition and Auxiliary Problem Principle', IEEE Transactions on Energy Markets, Policy and Regulation, 2023.

# 1 INTRODUCTION

Europe aims to achieve a 55% reduction in greenhouse gas emissions by 2030 according to the European Climate Law (Regulation 2021). To achieve this goal, the European Commission has undertaken several measures and strategies. These strategies include the EU energy system integration strategy (European Commission 2020c), the strategy for increasing offshore renewable energy (European Commission 2020e), the strategy associated with sustainable and smart mobility (European Commission 2020d), the renovation wave (European Commission 2020b), and the EU strategy related to hydrogen (European Commission 2020a) (Chyong et al. 2024).

In addition to the designed strategies, following the crisis triggered by Russia's invasion of Ukraine, the European Commission published its RePowerEU plan in May 2022 (Baldursson, Banet, and Chyong 2023), which outlines a set of measures and goals to ban fossil fuel-based energy imports from Russia before 2030. The RePowerEU plan encourages independence from energy imports and aligns with the EU's net-zero targets (Chyong et al. 2024). However, being net zero with high share of renewables in generation mix causes difficulties in ensuring a stable energy supply, especially in the short term. Thus, Europe is seeking Flexible Energy Resources (FERs) to achieve a fully decarbonized renewable-based European energy system by 2050 (Chyong et al. 2024).

FERs aim to increase power system flexibility by providing flexibility services. The International Energy Agency defines power system flexibility as "the ability of a power system to reliably and cost-effectively manage the variability and uncertainty of supply and demand across all relevant timescales" (IEA 2018). Therefore, flexibility services are defined as services in the form of active and reactive power, aiming to improve power system flexibility.

FERs can be connected to different voltage levels, including low voltage (LV) and medium voltage (MV) networks, which are mainly operated by DSOs, as well as high voltage (HV) networks under the operation of TSOs. In distribution networks, FERs can increase the hosting capacity of the networks and facilitate the efficient integration of Renewable Energy Sources (RES) by providing active and reactive power to control voltage, current, and thermal limit-related congestions. Additionally, FERs can offer frequency control services, transmission network congestion management, and voltage control services to TSOs (Sijakovic et al. 2022).

FERs include various types of storages such as mechanical, thermal, and electrical. However, FERs are not limited to storages. Any producer and consumer with the power control capability to flexibly produce and consume electricity can be considered as FER. Consequently, recent research has focused on identifying FERs by flexibly scheduling various types of controllable energy production and consumption resources.

## 1.1 Background and motivation

FER operations should align with the flexibility requirements of the power system. Figure 1 shows a mind map from FERs maximum utilisation viewpoint outlining the background and necessary steps when trying to maximise the utilisation of FERs for system operators' flexibility needs. Maximum utilisation of FERs means that if TSOs and DSOs, who operate energy system at different voltage levels, call for flexibility from FERs, all flexible production and consumption sources align their activities and operations with system operators' requests. This harmonization can be achieved manually, by transferring signals from system operators to FERs, or automatically, by measuring and reacting to deviations in frequency and/or local voltage from the standard or target values/ranges.

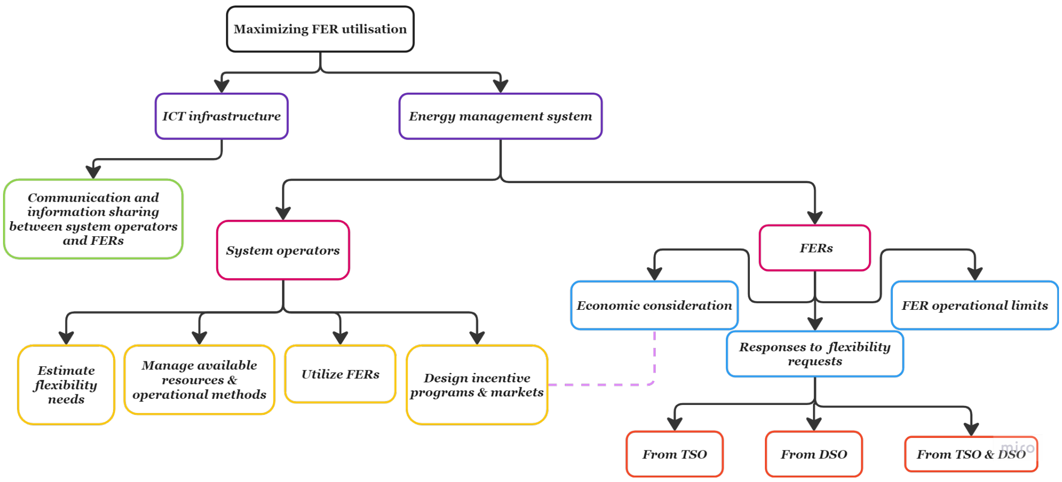


**Figure 1.** Necessary steps towards maximising the utilisation of FERs by system operators.

As a first step (Figure 1) to integrating FERs at all levels of power systems, a suitable Information and Communication Technology (ICT) infrastructure should be constructed. This infrastructure facilitates the communication and information sharing between system operators and FERs. Research such as (Jindal et al. 2020) has analysed the requirements for a flexible ICT architecture that supports communication between FERs and system operators. The reference also developed a dashboard to streamline communication and allow grid control by the DSO. Another example is (Guerrero Alonso et al. 2020) which proposed integrating the OpenADR protocol with a blockchain-based decentralized permissioned marketplace. It was proved that the proposed approach enhances communication, regulatory compliance, and provides a flexible solution for FERs, ensuring robust monitoring, management, and adaptability to different national regulations.

The second step (Figure 1) towards maximum utilisation of FERs involves developing Energy Management Systems (EMS) for both system operators and FERs. For system operators, the EMS needs to estimate network flexibility requirements, manage existing resources and network operational methods, utilise FERs to ensure secure network operation and design incentive programs and markets to motivate FERs. For example, (Laaksonen, Khajeh, and Hatziargyriou 2023) presented an adaptive management scheme for Distributed Energy Resources (DER) and On-Load Tap Changing (OLTC) transformer, considering frequency deviation intensity and DER location to enhance effective operation of the grid. Another example is the study proposed by (Rodrigues, Soares, and Morais 2023), which developed a reactive power management model for DSOs to address voltage issues using DERs, OLTC transformers, and capacitor banks.

Incentives for FERs can be created through market designs that require active participation, dynamic tariffs or prices for network usage, or agreements that offer financial benefits to FERs. TSOs and DSOs need to consider the different perspectives and motivations of FERs, and design incentive programs and markets tailored to various FER's clusters (Sridhar et al. 2023b). For example, (Sridhar et al. 2023a) suggested that residential households (as FERs) can be categorised as Adopters, Followers, or Neutrals, each requiring different incentive programs. Authors in (Khalili et al. 2019) analysed the impact of different incentive programs so that the consumers contribute more effectively to the improved reliability of a microgrid. In addition to aligning incentive programs, appropriate settings, rules, and universal/European regulations should be developed to ensure fairness and to maximize the incentives for all FERs (Cired Working Group 2023).

Given that the incentive programs are well-designed and effective, the EMS of FERs schedules responses to system operators' requests for flexibility. Initially, the EMS should ensure that FERs adhere to their operational constraints. Economic considerations, such as cost minimisation and profit maximisation, are regarded as key objectives of FER scheduling. Research has explored various FER management and scheduling strategies so that they participate in various markets and programs designed by TSOs and DSOs. For instance, studies have assessed battery as an FER and its participation in primary, secondary, and tertiary control reserve markets like (Astero and Evens 2020), (Fleer et al. 2017), (Merten et al. 2020), and (Nitsch et al. 2021). Some research examined flexible Electric Vehicle (EV) charging aligned with frequency deviations and considers EV as an FER, such as (Osório et al. 2021), (Cui, Hu, and Luo 2020), (Liu et al. 2021) and (Figgener et al. 2022). Smart buildings and houses can also provide flexibility through aggregation methods, either via an aggregator or an energy community (Manna and Sanjab 2023). Large-scale electrolyser have been proposed as an FER providing flexibility services and aligning its hydrogen production with grid requirements (Saretta, Raheli, and Kazempour 2023) (Lüth et al. 2024).

FERs can also assist DSOs with network operations, such as voltage control and congestion management. Research has proposed concepts like BESS as a service for DSOs (Alaperä et al. 2019; Berg, Rana, and Farahmand 2023, n.d.) and market-based methodologies for EV users and households to manage congestion and maintain power quality in the local distribution networks (Menghwar et al. 2024).

While significant research has been done on FERs providing flexibility services for either TSOs or DSOs, fewer studies have focused on the provision of coordinated flexibility services from FER's perspective. FERs in distribution networks can provide services for both TSOs and DSOs cooperatively. For example, if DSO voltage control requires an FER to increase active power ($P$) consumption while frequency deviation requires decreased active power consumption, FERs need clear instructions for such conflicting scenarios. Similarly, FERs in transmission networks must balance providing congestion management and frequency control services without compromising network security. This coordination has primarily been analysed using centralized, market-based approaches. For example, (Vagropoulos, Biskas, and Bakirtzis 2022) and (Vicente-Pastor et al. 2019) have designed flexibility market clearing approaches for trading flexibility between FERs and system operators. However, less research has focused on FERs' flexibility provision, their scheduling and the operational reactions to different scenarios, especially when system operators' flexibility needs conflict.

## 1.2 The objective of the thesis

This PhD thesis analyses how flexibility can be extracted from different FERs to be used as a flexibility service offered to DSOs and/or TSOs. The analyses are mostly from the perspective of FER EMSs. The FERs analysed include:

- A Battery Energy Storage System (BESS)

- A smart home with controllable devices such as Heating Ventilation and Air Conditioning (HVAC), EV, a battery, and an Electric Water Heater (EWH)
- A local energy community with a shared BESS and EVs with flexible charging capabilities
- A wind-integrated hydrogen system with an electrolyser, a compressor, and hydrogen storage

This dissertation is focused on and tries to answer the following research questions (see Figure 2):

Q1. Decision-making Under Uncertainties: What is the roadmap towards optimal decision-making from FER's and system operator's perspectives in a smart grid environment?

Q2. Distribution Network Enhancement: How can a DSO analyse its flexibility needs and strengthen the network using FERs?

Q3. Flexibility Estimation: How is the flexibility of FERs quantified?

Q4. FER Scheduling: How should FERs be scheduled to meet the flexibility requirements of system operators?

Q5. TSO-DSO Flexibility Coordination: How can FERs provide coordinated TSO-DSO flexibility?

Q6. Profitability Analysis: Is flexibility provision financially beneficial for FER owners?

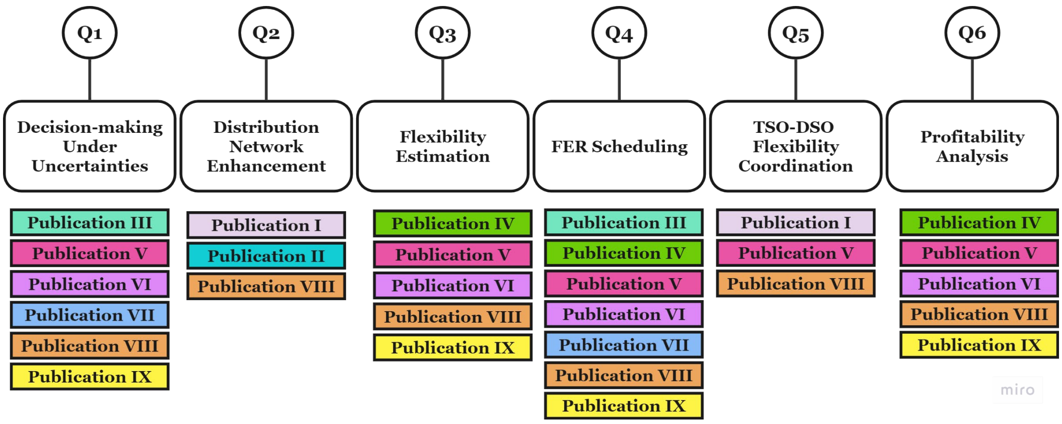


**Figure 2.** Research questions (Q) answered in this dissertation and the publications associated with each question.

The dissertation employs various methods to address the mentioned questions. Each question is answered by at least one publication developed during this research work, as illustrated by Figure 2. The following numbering points detail how the questions are answered:

1. For the first question, state-of-the-art research is reviewed and integrated to understand the path to optimised operations and planning for both system operators and FERs. The reviewed uncertainty-handling models are then utilised in some research articles shown by Figure 2.

2. To answer the second question, an optimisation-based approach is developed to estimate the total and nodal hosting capacities of the network. Steps are discussed for a DSO to revise its estimation and react to ensure network security. Additionally, research is dedicated to siting and sizing a BESS in a distribution network to maintain secure operations under worst-case scenarios.

3. The third question is addressed using an optimisation-based approach to differentiate between normal and flexible operations of FERs and find the potential flexible capacity of different FERs that can be offered to capacity markets.

4. The fourth question is answered by developing optimisation problems and Fuzzy Logic-based Control (FLC)-integrated EMS aimed at minimising net costs or maximising profits, ensuring that flexibility provision is profitable for FERs while adhering to market rules and requirements associated with each flexibility service.

5. For the fifth question, scenarios are discussed in which DSO and TSO request different flexibility signals, and how FERs would respond if operators' requirements conflict.

6. The sixth question is answered by developing comparison cases to evaluate the financial benefits of flexibility provision for FERs. Different cases are developed as comparative examples to determine if flexibility provision is profitable for FERs

To implement the suggested methodology, this thesis utilises Matlab, GAMS, Python, and Julia. Matlab is used for developing the FLC system, while optimisation problems are addressed with GAMS, CVXPY (Python), and JuMP (Julia).

## 1.3 Main contributions

The main contributions of the thesis can be summarized as follows:

1) Analysis of Flexible Operation of FERs:

- Including a BESS, smart home with HVAC, BESS, EWH, EV, an energy community with a shared BESS and EVs, and a wind-integrated hydrogen system.
- Reviewing potential FERs in microgrids and the EMS designed to manage them.
- Incorporating constraints involving the primary functionality of each device, such as thermal comfort for HVAC and EWH, and charging schedules proposed by EV owners.

2) Bidding Strategy:

- Development of bidding strategies for smart homes, energy communities, and wind-integrated hydrogen systems to participate in capacity markets.
- Estimating the flexible capacity of different resources for use in day-ahead capacity markets.
- Modelling market characteristics and technical requirements needed for the flexibility services.
- Developing guidelines for coordinated flexibility services provision.

3) Siting and Sizing of BESS in Distribution Networks for FCR-N Provision:

- Siting BESSs in distribution networks to strengthen the local distribution network in worst-case scenarios.
- Sizing the BESS to maximise profit by participating in the FCR-N market considering most probable scenarios.

4) Solutions for DSOs:

    - Developing an optimisation approach to estimate DSO's nodal and total hosting capacities.

- Proposing a strategy for DSOs to manage networks based on the hosting capacity estimations and nodal RES forecasts.

5) Uncertainty Handling:

- Considering worst-case flexibility activation and wind power scenarios to build a robust bidding strategy for the wind-integrated hydrogen system.
- Defining control parameters for a BESS to reserve part of its capacity for handling uncertainties from forecast errors.
- Taking into account worst-case situations when estimating the flexible capacity of an EWH.
- Proposing a roadmap towards optimised decision making under uncertainties.

6) Techno-Economic Analysis:

- Developing comparison models with different objectives.
- Comparing the various operations and economic outcomes of FERs.

More details about content and individual contribution of each publication I-IX (page XVI) included in this dissertation can be found from Section 1.4.

## 1.4 Summary and contribution of publications

Figure 3 categorises the publications I-IX (page XVI) into five different groups (types of FER, EMS, simulation tools, flexibility services used in the publications and the type of research publication) to emphasise the differences between their contributions. Also, this section summarises the publications with emphasis on their unique contributions. Author's individual contributions of each publication I-IX (page XVI) can be found on page XVII.

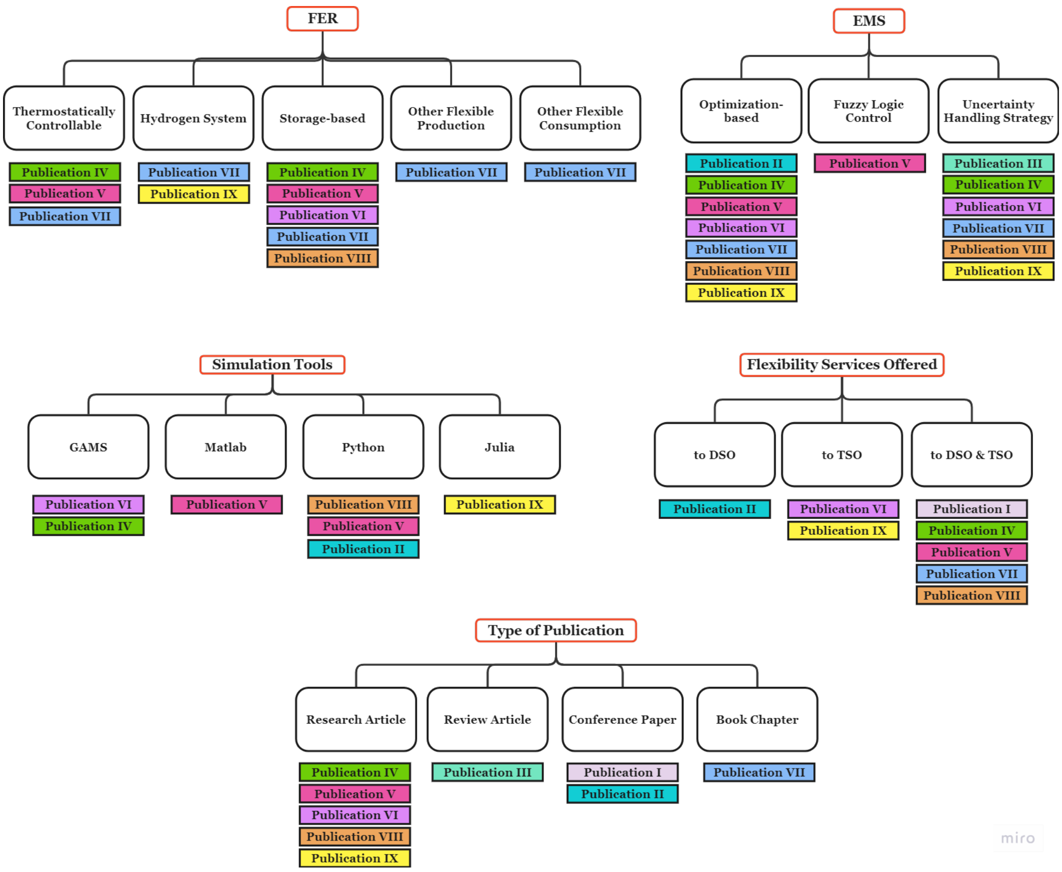


**Figure 3.** Categorisation of the publications of this dissertation in terms of different factors, including the types of FER, EMS, simulation tools, and flexibility services used in the publications, as well as the type of research publication.

**Publication I *(Potential ancillary service markets for future power systems)*:**

This publication first introduces the existing TSO-level ancillary service markets, with a focus on the Nordic and Finnish markets, highlighting their characteristics, prices, and capacity trading. It then explores the potential markets at the DSO level and the projects aimed at designing DSO-level markets. Finally, the paper discusses potential future ancillary and flexibility service markets, which are proposed to enable the participation of small-scale FERs in providing flexibility services at both the TSO and DSO levels.

**Publication II *(Quantifying the Impact of Day-ahead Renewable Forecasts on DER Hosting Capacity Estimation)*:**

This paper aims to examine the impacts of RES forecasts on nodal and total hosting capacities of distribution networks. The main contributions of Publication II are as follows:

- Proposing a new optimisation-based method using a piecewise linearized power flow model to estimate the hosting capacity of distribution networks.
- Suggesting that the DSO revises estimated short-term (day-ahead) hosting capacity based on day-ahead RES forecasts. This approach allows the DSO to ensure network operational security and reliability effectively.
- Using a real-world Finnish urban distribution network model to estimate hosting capacities with the proposed method and conducting thorough sensitivity analyses to show how individual node RES forecasts can affect nodal and total hosting capacities.

**Publication III *(Applications of probabilistic forecasting in smart grids: A review)*:**

This paper presents a roadmap for optimised decision-making under uncertainties. It begins by introducing probabilistic forecasting models and reviewing how the distributions of uncertain parameters are predicted based on previous research. Next, it describes the common methods for generating scenarios from these predicted distributions. Publication III then discusses how the generated scenarios can aid smart grid management systems in making informed decisions under various uncertain conditions. Finally, it explores two advanced applications of probabilistic forecasting that could be expanded in future work. In the conclusion and discussion section, the paper proposes several future applications based on the evolving flexibility needs of power systems.

**Publication IV *(Flexibility potential of a smart home to provide TSO-DSO-level services)*:**

This paper explores how smart home can provide flexibility services for system operators, introducing a comprehensive model that includes thermostatically controllable appliances (HVAC and EWH) and storage-based devices (EV and BESS). It uniquely examines the simultaneous operation of these four appliances to provide flexibility, a topic not previously addressed in the literature. Additionally, the paper estimates the flexible capacity of households by comparing normal and flexible operations of these appliances, a critical metric for system operators, household aggregators, and the households themselves to develop effective bidding strategies and allocate monetary values.

**Publication V *(A fuzzy logic control of a smart home with energy storage providing active and reactive power flexibility services)*:**

Publication V develops an EMS for a smart home equipped with an inverter-interfaced BESS. The system controls the home's appliances to provide coordinated flexibility services for both the local DSO and the TSO. The proposed EMS uses an FLC method with the following features:

- The smart home supplies FCR-N while also offering flexibility services to the local DSO. When the needs of the TSO and DSO conflict, the system prioritizes the local DSO to maintain the quality of electricity supply. Frequency control services are provided using active power ($P$) flexibility, while DSO-level flexibility uses both active ($P$) and reactive power ($Q$) flexibility.

- A minimal-rule FLC is designed to manage household appliances, such as the HVAC, EV charging schedule, and the active/reactive power from the BESS. The system ensures that the operational constraints of the appliances are respected even when responding to flexibility signals.

- The fuzzy logic rules are designed to prioritize essential appliances for flexibility services and minimise the use of the BESS due to its operating costs unless high flexibility is required by the DSO.

**Publication VI *(Optimised operation of local energy community providing frequency restoration reserve)*:**

This article presents a two-stage model for a PV-equipped local energy community with EVs and a shared BESS to provide manual Frequency Restoration Reserve (mFRR) services. The first stage involves day-ahead scheduling, where the community estimates its flexible capacities and submits offers for mFRR services. The second stage involves real-time scheduling based on the assigned and activated reserve power. The main contributions are:

- Publication VI is the first to assess the participation of a community in providing mFRR (tertiary reserve) services, considering the specific trading structures required by TSO-level reserves.

- It considers a local energy community as a potential reserve provider by leveraging various distribution-network-located FERs and motivating members to manage their consumption. Members can share resources, such as a PV system and a BESS, to increase profits and share the capital costs. The community also includes EVs that contribute to flexibility, considering the charging satisfaction of EV owners.

- The article defines control parameters related to the BESS State of Charge (SOC) to handle uncertainties in the day-ahead stage. It calculates different control parameters for a case study and discusses their impact on the community's real-time operation and profitability.

**Publication VII *(Flexibility of Microgrids with Energy Management Systems)*:**

This book chapter (publication VII) begins with an overview of FERs in microgrids and their characteristics. It then delves into modelling approaches for microgrid EMS, covering different management methods and objectives. These approaches utilise optimisation algorithms tailored to microgrid and grid constraints. microgrid constraints relate to the physical limitations of local resources, while the objective functions involve addressing congestion, reducing emissions, and minimising energy losses.

Furthermore, the study explores the application of microgrid EMS featuring FERs such as energy storage, EVs, and thermostatically controllable loads. These components interact with the grid, providing flexibility services. The publication concludes with a summary and discussion of the potential roles microgrids can play in enhancing grid stability and efficiency through their flexible operations.

**Publication VIII *(Optimised siting and sizing of distribution-network-connected battery energy storage system providing flexibility services for system operators)*:**

This paper stands out by sizing and siting a distribution-network-connected BESS to provide DSO and TSO flexibility services simultaneously. The BESS ensures voltage stability and respects power flow constraints while enhancing profitability through FCR-N services. This study is the first, to author's knowledge, to specifically size a BESS for FCR-N provision.

Key contributions include:

- Introducing a two-stage stochastic optimisation model where the first stage allocates the BESS to secure local network operation and determine minimum size, while the second stage optimises profitability through FCR-N.

- Proposing scenario extraction methods where worst-case scenarios ensure network security in the first stage, while high-probability historical scenarios used for the second stage.

- Simulating four comparison models to optimise BESS size, comparing outcomes of FCR-N provision versus day-ahead market operations using 2021-2022 real-world data, and analysing effects of cycle aging and capacity fade on profitability.

**Publication IX *(Optimised Operation of Hybrid Wind-Hydrogen System to Provide Flexibility for Transmission System Needs)*:**

Publication IX introduces an optimisation framework aimed at coordinating the operations of a hydrogen storage, electrolyser, and a wind farm to offer flexibility services to the TSO. It focuses on supporting frequency control through participation in FCR markets and addressing congestion management issues near the system's transmission lines. The study explores how the system can simultaneously engage in FCR-N, upward FCR-D, and downward FCR-D markets while providing essential congestion management services to enhance grid reliability and efficiency.

Furthermore, the paper analyses the operational dynamics of the wind-integrated hydrogen system by examining the *Pf* droop relationships that govern active power response to frequency deviations, leveraging historical frequency activation data to assess real-time operational impacts. It also introduces a robust methodology to mitigate uncertainties associated with wind power forecasting and real-time activation scenarios. Comparative analysis includes evaluating the proposed operational strategy against alternatives such as optimising based on spot market prices and adopting self-sufficiency-focused strategies.

## 1.5 Outline of the thesis

This dissertation is comprised of a summary section and the attached original publications. The summary is categorised into seven chapters, as described in the following:

Chapter 1 provides the background behind the research and the motivation to further explore the subject. It identifies the objective and the main scientific contribution of this dissertation. It also specifies the outline of the thesis and summarizes the main publications.

Chapter 2 provides a comprehensive definition of flexibility in power systems and describes the flexibility needs and services designed for each system operator, TSO, and DSO. It describes the increasing need for TSO-DSO coordinated flexibility provision. Additionally, it outlines the flexibility scheduling and forecasting from both the system operators' and FERs' perspectives by introducing the path towards optimal decision-making under uncertainties. Chapter 2 includes the main contributions of Publications I, II and III of this dissertation.

Chapter 3 outlines methods to schedule flexible and controllable appliances and devices in a smart home to provide flexibility services to DSO and TSO. Both optimisation-based and FLC are utilised to flexibly schedule smart home’s flexible appliances. Chapter 3 describes the main contributions of Publications IV and V.

Chapter 4 goes a step further and analyses the flexible scheduling of FERs within an energy community and a microgrid. This chapter models a local energy community providing mFRR. It also assesses the flexibility potential of a microgrid, identifies its FERs, and describes the EMS used for flexibility scheduling. Chapter 4 presents the main contributions of Publications VI and VII.

Chapter 5 focuses on scheduling a BESS as an FER. The chapter discusses the optimal allocation of the BESS and its FCR-N provision for boosting economic profitability. Chapter 5 includes the main contributions of Publication VIII.

Chapter 6 summarises a research work in which a wind-integrated hydrogen system provides FCR-N and FCR-D while ensuring that the nearby transmission network is safely operated. Chapter 6 presents the main contributions of Publication IX.

Chapter 7 concludes the summary and discusses future directions for continuing the research work.

# 2 ROLE OF FLEXIBILITY IN THE FUTURE POWER SYSTEM

Modern power systems face the challenge of integrating a significant share of intermittent RESs. RESs offer sustainability, environmental friendliness, and lower marginal costs, aligning with the political pressure to reduce carbon emissions and the subsidisation of renewable energy. However, RES power generation is highly weather-dependent, intermittent, and difficult to predict accurately. The inherent variability and unpredictability of RES power generation causes a significant challenge to the secure operation of power systems, necessitating system operators to utilise flexibility services from FER's controllable active and reactive power across different timescales. Flexibility services enable system operators to dynamically adjust their network operating points so that e.g. frequency, voltage and current/thermal limits are not violated due to real-time fluctuations in RES power output, uncertainty of EV charging behavior or other unpredictable factors resulting from electrification trends (Khajeh et al. 2019). By utilising various active and reactive power control services from FER at different voltage levels, system operators can effectively manage the complexities of transitioning to future renewable-based power systems, enabling more efficient and reliable system operation.

## 2.1 Increasing need for flexibility in the future power systems

Both system operators, including TSO and DSO, need flexibility services to address challenges posed by the future renewable-based power systems. TSOs utilise active power control related flexibility services in real-time to manage power system frequency and maintain a balance between system generation and consumption, ensuring the system operates within its normal state. Regarding European power system, normal state of the system has a frequency between 49.9 to 50.1 Hz. TSOs may also employ active and reactive power control flexibility services to manage congestion on both inter-regional and intra-regional transmission lines, as well as for voltage control within their networks. It is evident that the needs for balance between generation and consumption as well as those to solve congestion management and voltage control are increasing due to the high injection of intermittent weather-dependent RES. This leads TSOs requiring more flexibility services.

In addition to the TSOs' issues, DSO's traditional management methods for network operation cannot solve the challenges caused by the high integration of renewable-based DERs. The problem deteriorates as the traditional power system transitions to a more decentralized and bi-directional operation, with numerous DERs being integrated into distribution networks. In this sense, DSOs need to utilise active and reactive power control flexibility services for the operational management and control of future renewable-based distribution networks. This includes complementary supports for managing active and reactive power flow to control node voltages, manage congestion on feeders, and ensure a steady supply of power (Venizelou et al. 2023).

The provision of active and reactive power control flexibility services across multiple timescales is a key solution to addressing the challenges faced by system operators. Flexibility services can be provided by various FERs, which exist at different levels of power systems, including the TSO and DSO levels.

- At the TSO level, FERs are typically large-scale resources connected to HV feeders.
- At the DSO level, FERs are generally smaller in scale, connected to MV or LV feeders, and located closer to end users.

### 2.1.1 Different sources of flexibility

FERs at TSO levels can be divided into three main categories: production-based, consumption-based, and technology-based resources. Consumption-based resources involve transmission-network-located consumers with sufficient capacity that can adjust consumption to meet TSO flexibility needs. Production-based resources include traditional generators, wind farms and solar parks, storage facilities, virtual power plants, and other large-scale energy sources capable of adjusting production levels while being connected to transmission networks.

Furthermore, TSOs can utilise technology and devices to enhance transmission network flexibility. Solutions like Flexible AC Transmission System (FACTS) and High Voltage Direct Current (HVDC) technologies improve controllability and flexibility of the network (ISGAN 2013). Integrating Wide Area Monitoring Protection and Control (WAMPAC) with FACTS and HVDC enhances transmission network flexibility and TSO's control over power flows (Nikoobakht et al. 2019). Traditional technologies like OLTC transformers and Phase-Shifting Transformers (PST) also contribute to regulating voltage magnitude (Khajeh et al. 2019).

At the DSO level, DERs are crucial FERs. DERs encompass various resources of different sizes, including individual and aggregated EVs, storage systems, wind turbines, solar panels, and buildings (residential, commercial, and industrial) equipped with controllable devices and appliances. Combining these resources with active network management (ANM) schemes enables DSOs to maximise network flexibility (Laaksonen et al. 2021). Figure 4 summarizes the types of flexible energy resources at both TSO and DSO levels in a power system.

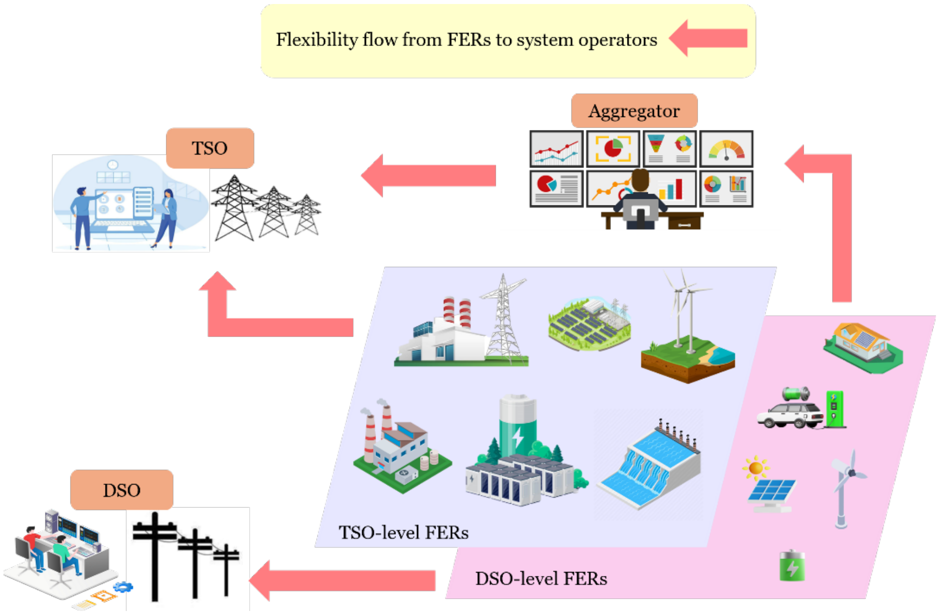


**Figure 4.** Different types of FER at both TSO and DSO levels in a power system.

### 2.1.2 Need for TSO-DSO coordination

Power systems are moving towards decentralization, with more DERs being integrated into distribution networks while large, fuel-based generation units located in transmission networks are being phased out. Consequently, the operation of transmission networks is becoming increasingly dependent on distribution networks, and the controllability of TSOs is decreasing as dispatchable fuel-based power plants are replaced by less controllable renewable-based DERs in distribution networks.

On the other hand, DSOs are not completely self-sufficient, as many generation units are still located in transmission networks, and TSOs handle crucial tasks related to security of supply and system balancing. Therefore, effective utilisation of FERs at the system level and avoiding the risk of a system-wide blackout require enhanced cooperation between TSOs and DSOs.

To achieve this, coordination between DSOs and TSOs must ensure maximum utilisation of flexibility within distribution networks to meet both local and system-wide needs (Laaksonen, Khajeh, and Hatziargyriou 2023). This means that FERs in distribution networks should not only provide local services like congestion management and voltage control for DSOs but also contribute to system-wide services, such as frequency control services. Moreover, the flexibility provision of FERs for one system operator should not adversely affect the secure operation of the system when the flexibility needs of DSOs and TSOs diverge.

### 2.1.3 Markets and tariff structures for enhanced flexibility utilisation

In order to exploit the maximum potential of FERs at all levels of power system, incentive mechanisms should be thoroughly defined. The incentive mechanisms motivate FERs to cooperate with system operators by responding to the signals and orders sent by system operators.

Flexibility markets aim to create this incentive by providing a competitive and fair platform for all types of FERs to sell their flexibility to system operators. These flexibility markets have been widely designed for the TSO, although only large flexibility owners and aggregators can participate in these markets. Local-level flexibility markets are rarely seen in the real world (LCP Delta & SmartEn 2023).

The local flexibility markets can be organized by DSOs to help with congestion management in the local network, voltage control, and some other services such as network investment deferral as well as pre-fault, post-fault and restoration services (FUSION Project Report 2023).

In addition to flexibility markets, dynamic tariffs in distribution networks can provide an incentive and thus exploit the available flexibility of the network. However, thorough studies need to be done to understand how tariffs can reflect network constraints, which depend on factors like location (local vs global) and time (seasons, weekdays, time of day). This is also important to ensure tariffs do not become overly complicated for small-scale FERs (Khajeh and Laaksonen 2023).

Some countries already use the concept of nodal pricing, where different prices are charged at different locations on the grid. However, this nodal pricing approach may not exploit the maximum flexibility of the network and cannot work in a fair way as local flexibility issues often depend heavily on the specific locations of grid constraints. Both "implicit flexibility" (where customers respond to price signals) and "explicit flexibility" (where third parties control customers' assets) need to be used to help address flexibility challenges in distribution networks (Nouicer, Meeus, and Delarue 2020). Also, dynamic tariffs would be more effective if they can be combined with local flexibility markets.

### 2.1.4 Regulatory developments for DSO and TSO flexibility utilisation

The European Union has funded projects in various European countries to incentivize flexible production, consumption, and the use of storage to provide system operators with flexibility (Production 2023). In this context, flexibility platforms should be designed to incentivise sellers and facilitate efficient access for market participants to sell their flexibility and meet their flexibility requirements. The market platform showcased many local projects led by TSOs, DSOs, and third parties who need flexibility. The goal of these projects has been to implement flexibility markets beyond the traditional TSO-level markets to manage flexibility at all levels of the system.

Although TSO-level flexibility markets are widely used in most countries, only three countries—Great Britain, the Netherlands, and France—have developed commercial markets to provide DSOs with flexibility (LCP Delta & SmartEn 2023). Additionally, Norway and Sweden have advanced trial offerings (LCP Delta & SmartEn 2023). Figure 5 ranks the progress of different European countries in implementing local flexibility markets (LCP Delta & SmartEn 2023). This ranking considers whether they have commercial DSO flexibility markets, the number of flexibility-based pilot projects, and the volume of flexibility being sold and purchased in the market (Cired Working Group 2023).

The European electricity market landscape is diverse, with each country taking a different approach to encourage flexibility and consumer participation (Cired Working Group 2023). Common challenges include regulatory barriers for aggregators, economic obstacles, and delays in smart meter rollouts (Cired Working Group 2023). In the Nordic countries, financial incentives and smart meters empower consumers. Finland and Norway have implemented 15-minute measurement intervals to enhance their tariff structures. Spain recently included demand-side and storage installations in the balancing market, but regulatory openness for aggregators remains limited. Italy is opening its market to distributed resources through pilot projects, while the UK has established local flexibility markets despite facing issues like price volatility and market complexity. Belgium allows consumer participation but imposes significant barriers for aggregators. Greece focuses on system stability through interruptible loads, and Cyprus faces a lack of support for flexibility services. Germany permits participation in wholesale and balancing markets but deals with administrative burdens and regulatory opposition to flexible network charges (Cired Working Group 2023).

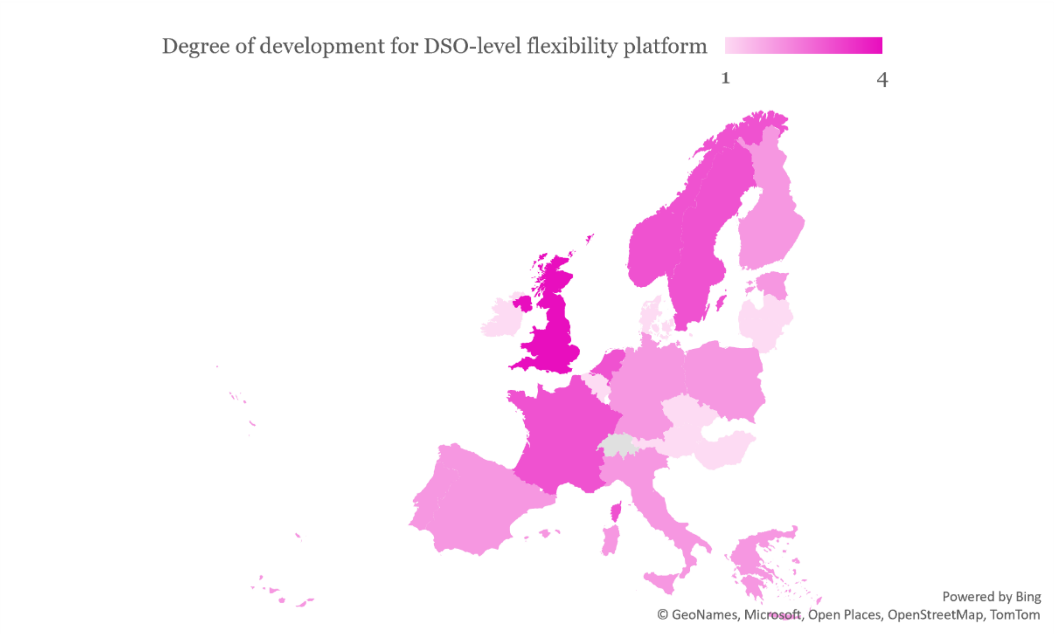


**Figure 5.** European degree of advancement regarding developing platform for DSO-level flexibility trading.

While some countries have made progress in developing flexibility platform, many are still behind as there is no EU-level regulation for integrating flexibility in electricity markets. The current regulatory frameworks fail to develop flexibility markets across all European countries as they pose challenges, such as (Cired Working Group 2023):

- Markets not being open to aggregators in many countries
- High competition in ancillary services
- Economic obstacles like price volatility and low profits for large generators
- Technical issues, such as delayed implementation of advanced metering infrastructure and complex market rules

Standardized regulations could accelerate renewable integration and improve the use of flexibilities at all voltage levels including medium and low voltage levels. A recommendation is to establish European-level business rules, metrics, and key performance indicators for flexibility trading.

## 2.2 TSO-level Flexibility: Requirements and Services

The major share of physical electricity trading is conducted in a day-ahead wholesale market, also known as the spot market. However, it is practically impossible to precisely balance the system a day before physical delivery due to uncertainties associated with renewable generation and demand behavior. These uncertainties often lead to imbalances in the system. To address this issue, market participants are responsible for adhering to the bids they have submitted to the spot market. Any deviation from these bids can result in imbalance costs for the participants. In order to compensate for imbalances, market participants can utilise intra-day markets, which operate continuously until shortly before delivery.

In real-time and near real-time, TSOs take on the responsibility of managing imbalances and maintaining the standard frequency of the system. In Europe, the standard frequency is 50 Hz. An imbalance between consumption and production leads to frequency deviations. As long as frequency deviations are lower than 0.1 Hz in either direction, the system remains within a normal situation. However, sustained deviations higher than 0.1 Hz can push the system into alert and emergency situations. It is important to note that the system situations are determined not only by the magnitude of the frequency deviations but also by the duration for which the deviations persist, as illustrated in Figure 6 (Modig et al. 2022).

TSOs define various types of active power control related flexibility services to fulfill their flexibility requirements in each state. These flexibility services are also called frequency control reserves, aiming to manage system imbalances and control frequency deviations in the power system. In terms of Nordic power system terminology, there are three main categories of reserves: Frequency Containment Reserve (FCR), Frequency Restoration Reserve (FRR), and Fast Frequency Reserve (FFR). FCRs and FFR are activated based on local frequency deviations, whereas FRRs take into account the Nordic synchronous system. Figure 7 overviews the details of each reserve service and its market specifications for Finnish TSO, Fingrid.

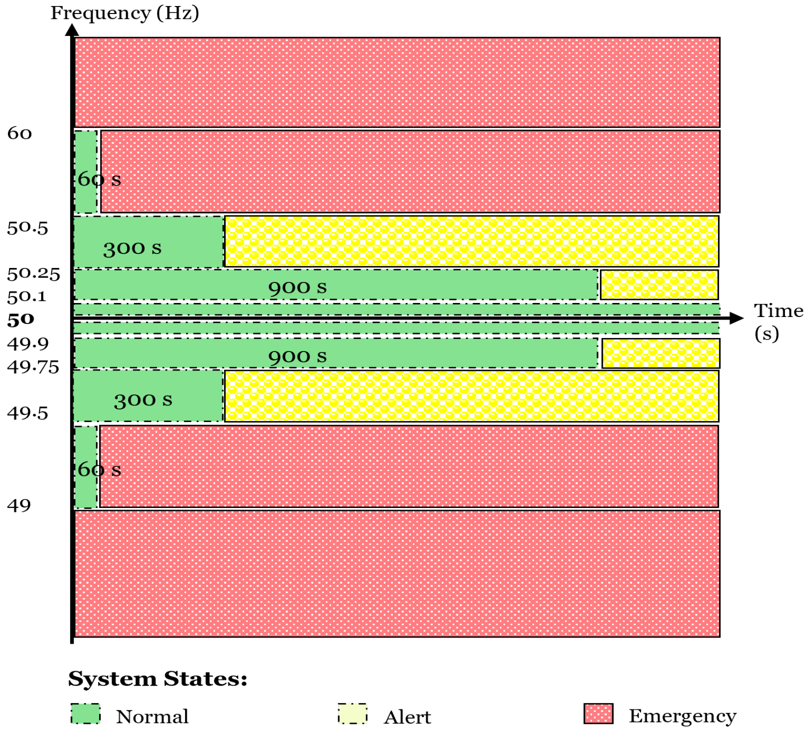


**Figure 6.** Different states of the power system according to its frequency.

| | FFR | FCR-D | FCR-N | aFRR | mFRR |
|---|---|---|---|---|---|
| **Capacity Market Gate Closure (EET, EEST)** | 18 | 18.30 | 18.30 | 8.30 | 9.30 |
| **Minimum Bid Size (MW)** | 1 | 1 | 0.1 | 1 | 1 or 5 |
| **Capacity / Energy Fee** | Just Capacity | Just Capacity | Both | Both | Both |
| **Procurement Channel *** | HM<br>EST | YM<br>HM<br>NC<br>EST | YM<br>HM<br>NC<br>EST | HM<br>EST | BEM<br>BCM<br>Fingrid Reserves |
| Activation Time (s) | 0.7 -1 - 1.3 | 7.5 | 60-180 | 300 | 750 |

* Reserve procurement can be from:
**HM:** Hourly Market, **YM:** Yearly Market, **EST:** Trading with Estonia, **NC:** Trading with other Nordic counties, **BCM:** Balancing Capacity Market, **BEM:** Balancing Energy Market
**Fingrid Reserves:** Fingrid's reserve units and leasing power plants

**Figure 7.** Finnish frequency control service specifications in 2024: capacity market gate closure, minimum bid size in capacity markets, fees for capacity and energy remuneration, procurment channels in Finland and their required activation speed.

### 2.2.1 Frequency Containment Reserves (FCR)

FCR is subcategorized into two types: FCR for Normal operation (FCR-N) and FCR for Disturbances (FCR-D). FCR-N and FCR-D are automatically activated based on locally measured frequency deviations. The purpose of FCRs is to maintain the frequency within the normal operating range during both normal operation and disturbances (ENTSO-E 2023).

FCR-N is continuously activated to ensure that the system operates within the normal frequency range of 49.9 Hz to 50.1 Hz. On the other hand, FCR-D is activated when the frequency deviates from the normal range. A reserve provider offering these services needs to monitor frequency deviations constantly and adjust its production/consumption according to the droop curve defined for FCR-N and FCR-D (ENTSO-E 2023). The droop curves for production units are illustrated in Figure 8.

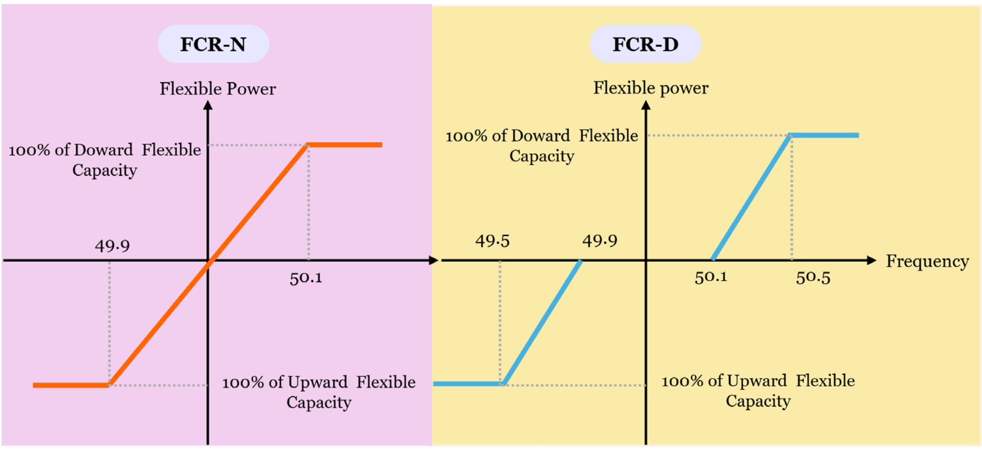


**Figure 8.** Droops indicating the change of flexible capacities of FCR providers according to the measured frequency deviations.

FCR-N is a symmetrical product, meaning that the reserve provider must be capable of both increasing power production or decreasing consumption during up regulation (when the frequency drops below 50 Hz) and decreasing power production or increasing consumption during down regulation (when the frequency exceeds 50 Hz). FCR-D, on the other hand, is divided into separate up-regulation and down-regulation products, each with its own capacity markets. TSOs organize yearly and hourly capacity markets to procure the necessary FCR-N and FCR-D services in advance (Fingrid 2024f).

In Finland, the Finnish TSO, Fingrid, procures the required FCR from national yearly and hourly markets, as well as through foreign trades via Estonian HVDC links and trades with other Nordic countries. Fingrid's domestic procurement occurs in yearly and hourly capacity markets. Yearly markets are held once a year at a fixed price, while hourly markets are settled once a day (one day before actual physical delivery) using the marginal pricing principle (Fingrid 2024f). FCR-N, upward FCR-D, and downward FCR-D each have their own yearly and hourly capacity markets. Both yearly and hourly markets maintain the same technical requirements (Fingrid 2024f). Reserve providers must be located within the TSO's operating zone to participate in capacity markets.

If a reserve provider offers FCR-N, it earns revenue according to the price of the yearly or hourly FCR-N capacity market. In addition to capacity remunerations, an FCR-N provider receives revenue based on the up-regulation price when the FCR-N activates in the upward direction, meaning the provider decreases consumption or increases production. However, the FCR-N provider incurs a payment if the FCR-N activation is in the downward direction, in accordance with the hourly down-regulation prices. In contrast, FCR-D services do not entail energy remuneration cost or revenue. The FCR-D provider only receives payment (capacity remunerations) according to the FCR-D capacity market prices and its accepted bids (Fingrid 2024f).

### 2.2.2 Fast Frequency Reserve (FFR)

Previously, synchronous generators were an important source that helped the power system resist sudden changes in system frequency. All synchronously connected rotating machines contribute to this resistance, also known as inertia, through their kinetic energy (Ørum et al. n.d.). However, the phasing out of conventional generating units and their substitution with renewable energy such as wind and solar power decreases the system's ability to resist these abrupt changes. In the modern power system, FFR service is designed to handle these situations, referred to as low-inertia situations.

Figure 9 illustrates the variation of frequency over time when a big disturbance happens to two systems with different inertial responses: 100 MWs and 200 MWs. In the figure, the nadir frequency is the lowest frequency reached after the disturbance. The slopes of the orange and gray lines represent the rate of change of frequencies (RoCoF) of Systems I and II, respectively. The RoCoF represents the dynamic behavior of frequency, i.e. *df/dt*, during the time in which FFRs are activated. A lower inertial response results in a steeper RoCoF line, meaning that the system is more prone to frequency fluctuations and instability if a disturbance occurs.

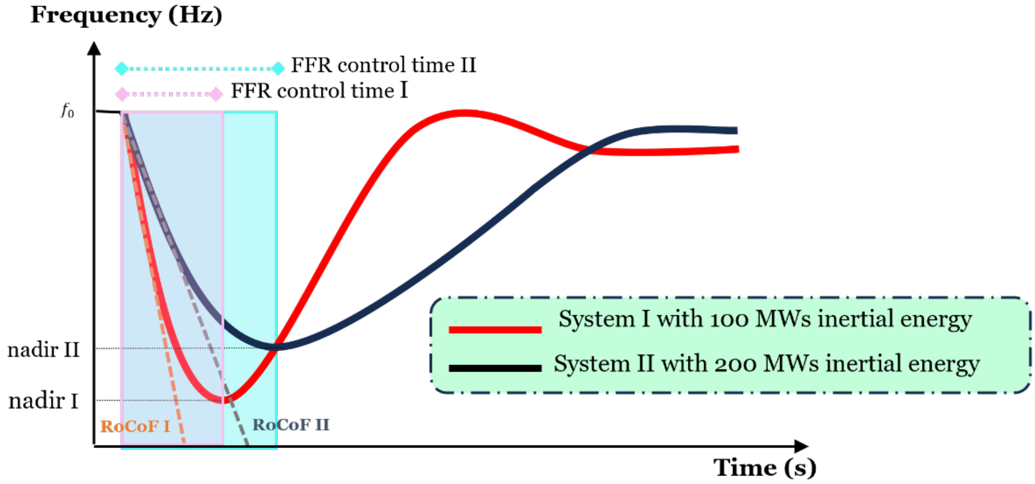


**Figure 9.** The comparison between frequency reaction curve for two systems with different inertial energy.

The Nordic power system must be operated in a way that the loss of a single generating unit or an HVDC link does not result in the frequency falling below 49.0 Hz (ENTSO-E 2019). The magnitude of the frequency drop depends on factors such as the degree of disturbance, system inertia, and FFR activation speed. Accordingly, Nordic TSOs procure FFR based on their forecasts of prevailing system inertia and the potential size of incidents that could occur.

FFR is the newest reserve service introduced in May 2020. Nordic TSOs procure FFR through their national market. Potential FFR providers must meet technical requirements and pass prequalification tests to participate in the FFR market. Similar to FCRs, FFR activation is based on locally measured frequency deviations, and Fingrid does not send control signals (ENTSO-E 2019).

The flexible capacity accepted in the FFR capacity market must be fully activated within the required activation time when the frequency drops below a certain threshold. The TSO offers three options to FFR providers, and the reserve provider should respond to the frequency deviation according to the selected option (ENTSO-E 2019).

FFR procurement only occurs when the system inertia is predicted to be lower than its limit. In the Nordics, the need for FFR procurement is highest in the spring, summer, and autumn months when renewable energy contribution is highest and conventional generation has a lower share compared to winter. Fingrid publishes the required FFR requirements one week in advance, providing insight to participants intending to take part in the FFR market.

Fingrid organizes the FFR capacity market at the national level. In the hourly FFR capacity market, bids for tomorrow's hours are submitted, and hourly prices are determined according to marginal pricing principles. Interestingly, the FFR provider can submit a combined bid that includes FFR and upward FCR-D and FCR-N (Fingrid 2024e).

The FFR provider earns a capacity remuneration from the TSO if its bid is accepted, and it activates its flexibility according to the selected option. Like FCR-D, it does not receive any energy remuneration for its activations (Fingrid 2024e).

### 2.2.3 Frequency Restoration Reserves (FRR)

FRRs consist of two reserve services: manual FRR (mFRR) and automatic FRR (aFRR) (Fingrid 2024c). The main goal of aFRR is to restore the frequency to the standard value. It is activated automatically based on signals sent by the TSO every 10 seconds, aiming to compensate for frequency deviations within the Nordic synchronous area (Fingrid 2019).

The Finnish TSO, Fingrid, procures aFRR capacity from its national hourly market and through inter-TSO trades with neighboring countries (Fingrid 2024a). Automatic FRR is only procured for hours expected to have higher variations. Providers of aFRR can submit their hourly flexible capacities to upward and/or downward aFRR capacity markets. These markets are settled according to the marginal price principle (Fingrid 2024d). Unlike FCR-D and FFR, aFRR providers are subjected to energy remunerations in addition to their earnings from aFRR capacity markets (Fingrid 2024d). At the time of writing this dissertation, aFRR is set to have a separate centralized market for energy remuneration, called the aFRR energy market (eSett 2024).

Similar to aFRR, mFRR aims to restore the frequency to the standard level and is the only manual reserve service used in the Nordics. Manual FRR requires manual activation, ordered from the TSO's Main Grid Control Center (Fingrid 2024b). The TSO orders mFRR activation to reduce existing imbalances or address forecasted imbalances expected in the near future. Manual FRR has both capacity and energy markets, known as balancing capacity and balancing energy markets, respectively. The balancing capacity market is organized on a day-ahead basis, with a separate price for each hour settled according to the marginal principle. However, the market gate closure for the balancing energy market is 45 minutes before physical delivery (Fingrid 2023).

An mFRR provider whose capacity has been accepted in the balancing capacity market is required to participate in the balancing energy (regulation) market as well and is remunerated accordingly. Nordic TSOs collaboratively operate balancing energy markets, and the hourly settled prices are also referred to as up-regulation and down-regulation prices (Fingrid 2024b).

## 2.3 DSO-level flexibility: requirements and potential services

The rise of renewable-based DER, such as rooftop photovoltaic panels, is resulting in bidirectional power flow within distribution grids. This, combined with the unpredictable charging patterns of EVs, can lead to voltage issues and congestion in distribution networks (Firoozi et al. 2021). Consequently, DSOs must enhance the DER hosting capacity of their networks to accommodate the increasing integration of renewable energy.

DER hosting capacity denotes the maximum quantity of DERs that can be integrated into a distribution network without surpassing operational limits, necessitating control adjustments or infrastructure upgrades (Alturki et al. 2018). In this regard, in order to increase hosting capacity, DSOs must reconsider their network management strategies (Firoozi et al. 2021).

One solution is to implement a more dynamic approach in network operation such as ANM. This involves leveraging FERs within the grid, such as DERs and adaptable EV charging (Parthasarathy et al. 2022). In this sense, DSOs can organize local markets at the distribution level to procure the necessary flexible capacities, incentivizing different energy resources to support the grid while earning a profit (Khajeh et al. 2021). For instance, flexible DER which are connected to the distribution network can participate in the local markets. By participating, DERs provide voltage control services through their converters' local voltage control functions, such as reactive power-voltage *(QU)* droop and active power-voltage *(PU)* droop functionalities.

Local markets provide ANM with the necessary flexibility. However, it is important to emphasize that cooperation between DSO and TSO should be integrated into the ANM scheme to optimise management efficiency. Figure 10 illustrates the interaction among FERs, a local market, the DSO, and the TSO. This figure exemplifies the management of FERs located in distribution networks within a local market platform. In this setup, the DSO manages and settles the local markets. Nevertheless, some studies such as (Khajeh et al. 2021) suggest that the

DSO can assign the task of operating the local market to another entity known as the local market operator.

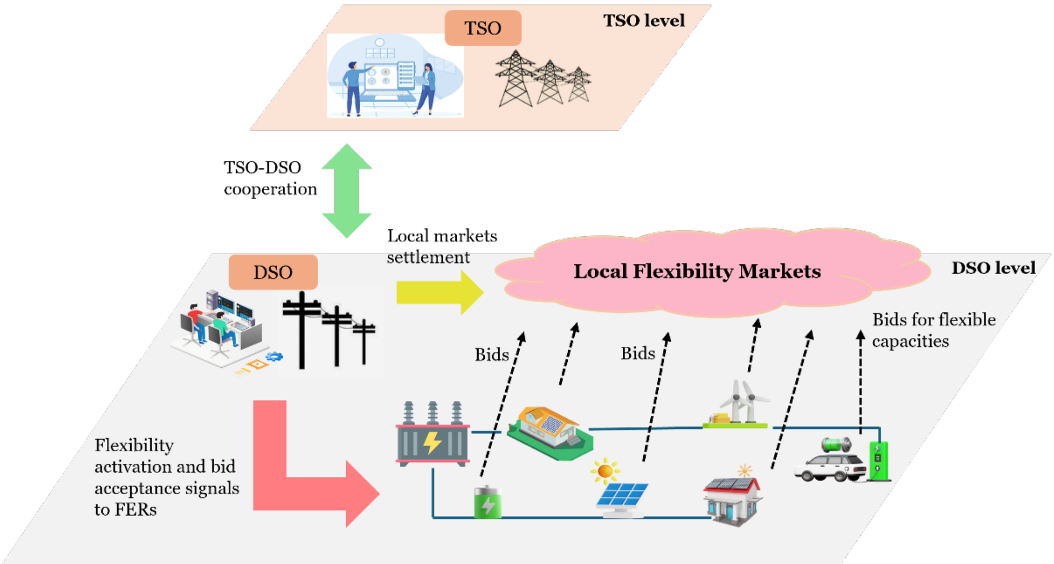


**Figure 10.** An example of a local flexible capacity market organized by the DSO, the interaction among FERs, local markets, the DSO, and the TSO.

By 2050, it is expected that about half of all households in the European Union will have renewable energy sources like solar panels. This could generate enough energy to meet almost 45% of Europe's total energy demand (European Environment Agency 2024). Additionally, households are becoming more conscious of their energy usage patterns, especially with fluctuating prices due to increased use of renewables. As more homes adopt Home Energy Management Systems (HEMS), they will be better able to adjust to price changes automatically.

In the future, distribution networks can take advantage of this price sensitivity by implementing dynamic tariffs, set by DSOs (Khajeh and Laaksonen 2023). Currently, certain customers, like those in Finland, can consume electricity based on fluctuating spot market prices but still pay a fixed tariff to the DSO for network usage. However, this DSO tariff could adapt to meet flexibility needs, varying based on time and customer location within the network (Khajeh and Laaksonen 2023). Customers who respond to DSO’s flexibility requirements positively should pay lower distribution network tariffs as a reward for their contribution (Khajeh and Laaksonen 2023).

### 2.3.1 Potential flexibility services for DSOs (Publication I)

To efficiently utilise existing resources through market mechanisms, DSOs must provide tangible definitions of their required flexibility services. Publication I recommends that these DSO-level services should tap into both reactive power ($Q$) and active power ($P$) flexibility within the distribution network. This means not only active power providers but also reactive power resources like inverter-based DERs can join the DSO-organized markets.

Publication I also suggests another concept: coordinated flexibility services. This means that both TSO and DSO are involved in procuring flexibility from distribution networks and its procurement should enhance the cooperation between the TSO and the DSO. In this regard, clear rules should be established for different operational scenarios of TSO and DSO, ensuring that flexible resources respond appropriately.

Sometimes, the flexibility requirements of TSO and DSO may conflict. For instance, while the DSO might need upward flexibility at certain nodes, the TSO balancing requirements might demand downward flexibility. In such cases, leveraging reactive power flexibility by the DSO can prevent adverse effects on grid frequency. Therefore, DSO-defined services should incorporate both active and reactive power to facilitate collaboration between DSOs and TSOs.

Future DSOs need to define various services to meet their flexibility needs across different distribution network states: normal, alert, and emergency situations. These services should have their own capacity markets, organized in advance (e.g., day-ahead), ensuring the DSO meets its flexibility requirements and optimises resource scheduling.

Pricing of DSO-level flexibility services is crucial, as it can incentivize or prevent local market participation. Separate pricing for reactive and active power flexibility services, as well as for upward and downward capacities, can be implemented. Pricing based on marginal principle encourages flexible resources to submit their marginal costs as offered prices. The time horizon and granularity of local capacity markets should align with distribution network flexibility requirements.

For real-time flexibility activation, Publication I suggests that the DSO communicates with flexible resources via flexibility signals, indicating whether they should react upwards or downwards. However, in some cases, activation can be automatic based on the locally measured voltages, especially for services addressing voltage fluctuations. Figure 11 summarizes the key features of the potent DSO-level flexibility services proposed by Publication I.

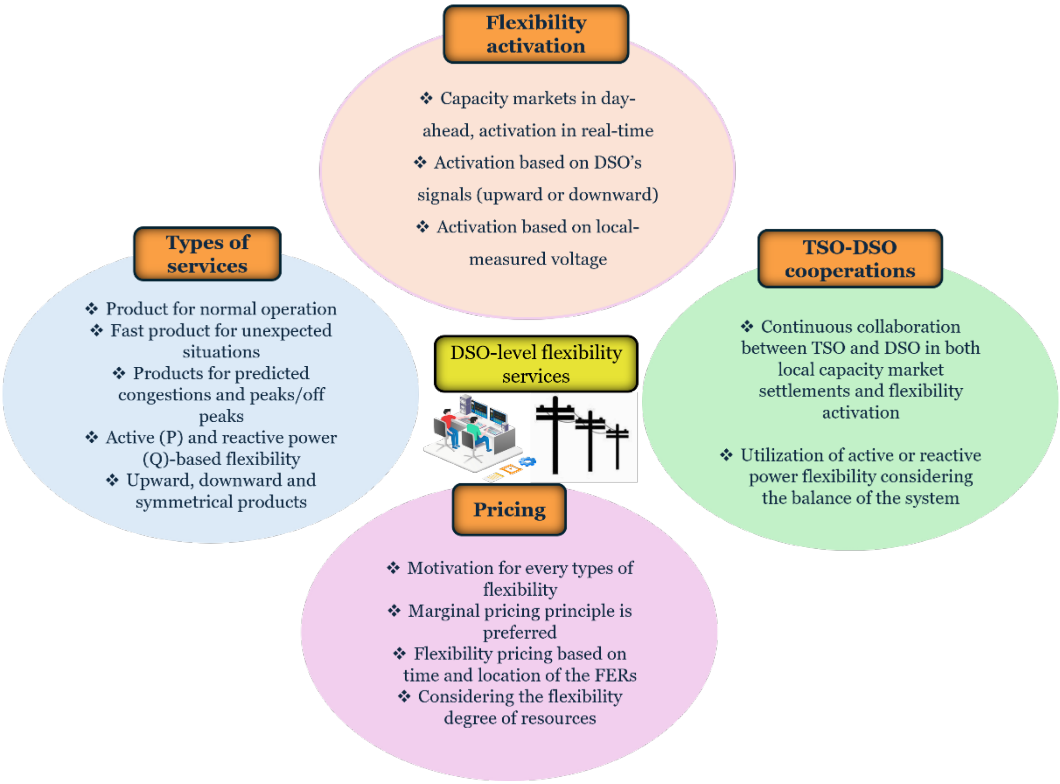


**Figure 11.** Key features of the potential flexibility services for future DSOs proposed by Publication I.

### 2.3.2 Hosting capacity estimation and effects of RES forecasting (Publication II)

Before organizing local markets and acquiring the necessary flexibility, a DSO needs to estimate its hosting capacity. This estimation provides insight into how much DER its network can accommodate. Publication II outlines steps for DSOs to estimate hosting capacity and revise the estimation based on RES forecasts.

In Publication II, hosting capacity is estimated through an optimisation problem aimed at maximising the sum of injection into each node of the network. The objective function is constrained by the power flow limitations of the distribution network. Publication II employs piecewise linearized power flow equations as described by (Khajeh et al. 2021). Constraints include active and reactive power balance requirements, voltage and current limits within feeders, as well as linear equations relating voltage and current squares to active and reactive power, along with inequalities associated with piecewise linearization of active and reactive power. Figure 12 summarizes the optimisation problem for hosting capacity estimation.

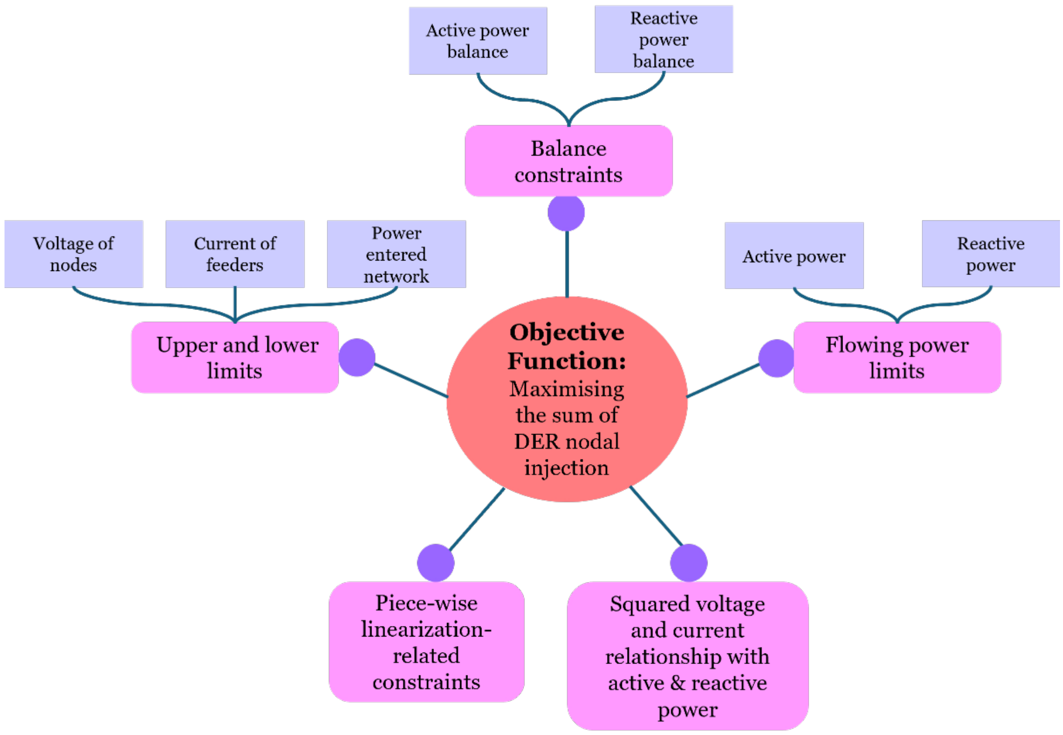


**Figure 12.** An illustration of the optimisation problem estimating the hosting capacity of the distribution network.

Following the optimisation, nodal hosting capacities and the total hosting capacity are determined as output and decision variables of the optimisation. Nodal hosting capacities represent the maximum injection possible at each node, while the total hosting capacity sums up all nodal hosting capacities.

After solving the optimisation problem and determining maximum nodal injection values (nodal hosting capacities), the DSO compares them with forecasted RES for each node. Three cases may arise:

- Case I) Forecasted RES generation is equal to or lower than nodal hosting capacities for all nodes.
- Case II) Forecasted RES generation for some nodes exceeds their estimated nodal hosting capacities.
- Case III) Forecasted RES generation for all nodes exceeds their estimated nodal hosting capacities.

Publication II suggests actions for the DSO to ensure network security, as depicted in Figure 13:

✓ In Case I, no action is needed.

✓ In Case II, the DSO adjusts nodal hosting capacities to match the higher RES forecasts and re-runs the optimisation to determine unviolated nodal hosting capacities. If feasible, this provides revised estimates for nodal and total hosting capacities. If not feasible, FERs may be employed via local markets or other incentive programs to maintain network security.

✓ In Case III, local network security is compromised. To mitigate this, the DSO can employ measures like leveraging FERs via local markets or dynamic tariffs for distribution networks.

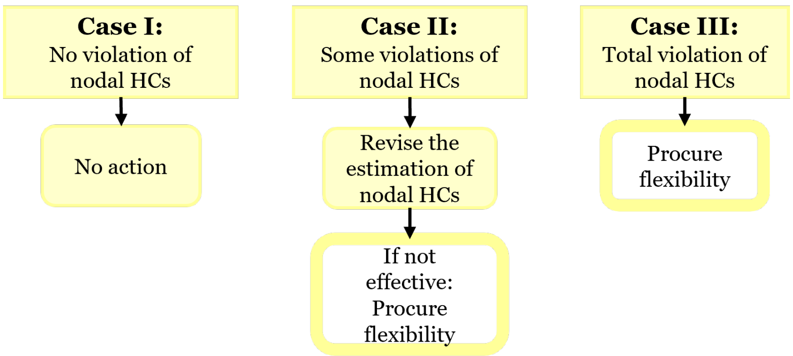


**Figure 13.** Actions suggested by Publication II for DSO's action after estimating the nodal hosting capacities (HC) and receiving the forecasted RES values for each node.

Publication II applies the proposed hosting capacity estimator to a Finnish urban LV network model, yielding the following results:

- Nodes closer to the beginning of the LV feeder and nearer to the MV/LV transformer have greater hosting capacities, as expected.

- Nodes closer to the transformer, with higher hosting capacities, are more sensitive to forecasting errors. Even 40% errors in their RES forecasts, can significantly impact the hosting capacity of the entire network, emphasizing the importance of accurate RES forecasts, especially for nodes near the transformer.

- Based on Publication II's outcomes, DSOs are advised to conduct sensitivity analyses to understand the impact of different RES forecast levels on estimated hosting capacities. This can guide investments in improving RES forecast accuracy, especially for critical nodes.

## 2.4 Flexibility forecasting and scheduling

Flexibility must be forecasted before system operators can utilise it. This involves predicting both the available and required flexibility at different timescales. The required flexibility forecast, which is from the perspective of system operators, should be conducted separately by TSOs and DSOs. They need to figure out how much flexible power is required at each node to ensure effective network operation.

Each type of flexibility service should be forecasted independently. For this purpose, TSOs forecast amounts of flexible power required for each type of service on the next day. For instance, TSOs must estimate the volume of fast-responding flexibility needed for each time slot of the following day to manage inertia decreases. Similarly, DSOs should define services with various speeds and characteristics tailored to their specific flexibility needs, such as real-time voltage control and congestion management at nodes. They should then forecast the flexibility requirements for each service to manage both expected and unexpected network situations.

Flexibility availability refers to the flexibility provided by FERs that can be used by DSOs and TSOs. This flexibility can come in the form of both active ($P$) and reactive ($Q$) power and can be sourced from various levels of the power system. For example, (Firoozi, Khajeh, and Laaksonen 2021) attempted to forecast flexibility from residential end users in a local energy community, predicting how these users would respond to requests from system operators. If the system operator requests downward flexibility, the increased consumption is forecasted. If it orders upward flexibility, the algorithm predicts how much consumption will decrease after receiving the flexibility signal.

FERs need to be scheduled according to the flexibility signals sent by system operators. If an upward flexibility request is made, FERs should reduce their power consumption or/and increase production. Conversely, for downward flexibility, they should increase their power withdrawal from the grid. This rescheduling occurs in real-time or close to real-time. However, the actual provision of active or reactive power related flexibility is dependent on specific market requirements and can be also provided based on FERs corresponding functions that utilise local frequency, voltage, active and reactive power measurements.

Furthermore, FERs should estimate their available flexibility in advance and communicate this to system operators. This allows system operators to plan based on the available flexibility to ensure the secure operation of their networks. Both flexibility estimation and real-time rescheduling of FERs should be framed as optimisation problems or other control methods, taking into account the significant impact of uncertainties in flexibility scheduling and estimation.

### 2.4.1 Uncertainty-aware scheduling of flexibility (Publication III)

In order for both system operators (TSO and DSO) and FER owners to make informed decisions on managing their networks and scheduling their resources, Publication III proposes a roadmap framework towards uncertainty-aware decision making. The roadmap begins with using probabilistic forecasting models to predict uncertain variables such as renewable energy, energy consumption, and energy prices. It continues with generating different scenarios based on the predicted distribution of these uncertain variables. The scenarios are then utilised by stochastic, robust, and chance-constrained optimisations to make decisions according to the strategies selected by the decision makers. The proposed roadmap is illustrated in Figure 14.

A probabilistic forecast aims to create a predictive distribution of values, whereas non-probabilistic forecasts provide single points as the forecasted values. The distribution of predicted values facilitates the process of generating different scenarios and the probability associated with each scenario.

Publication III first reviews parametric and non-parametric probabilistic forecasting models. Parametric probabilistic models make assumptions about the Probability Density Function (PDF) of the forecast, whereas non-parametric models do not consider known PDFs. The publication then reviews literature on developing forecasting models for solar and wind generation, loads, and energy prices. The uncertainty modeling and scenario generation are discussed using the output of the probabilistic forecasts.

Publication III highlights that future power systems will become smart, decentralized, weather-driven, and uncertain with the high integration of renewables, EVs, and other uncertain productions and consumptions. This results in numerous agents and stakeholders facing uncertainties within their operational and planning decision-making problems. Some examples are as follows:

- A power plant owner with renewable energy resources, aiming to participate in spot and reserve markets while considering the uncertainties of its renewable energy.

- Strategic agents dealing with uncertain market prices and competitors' strategies when constructing their optimal bidding strategies.

- Retailers purchasing electricity in advance while considering their customers' uncertain demand.

- Balancing responsible parties utilising their flexibility, such as scheduling their batteries, to maintain the balance between their intermittent production and uncertain consumption.

- System operators, TSOs, and DSOs making decisions on their required flexibility to effectively operate their networks, maintain the security of supply, and ensure the reliability of the networks within defined limits. In this context, uncertainties in renewables and customer behavior impact their secure operations.

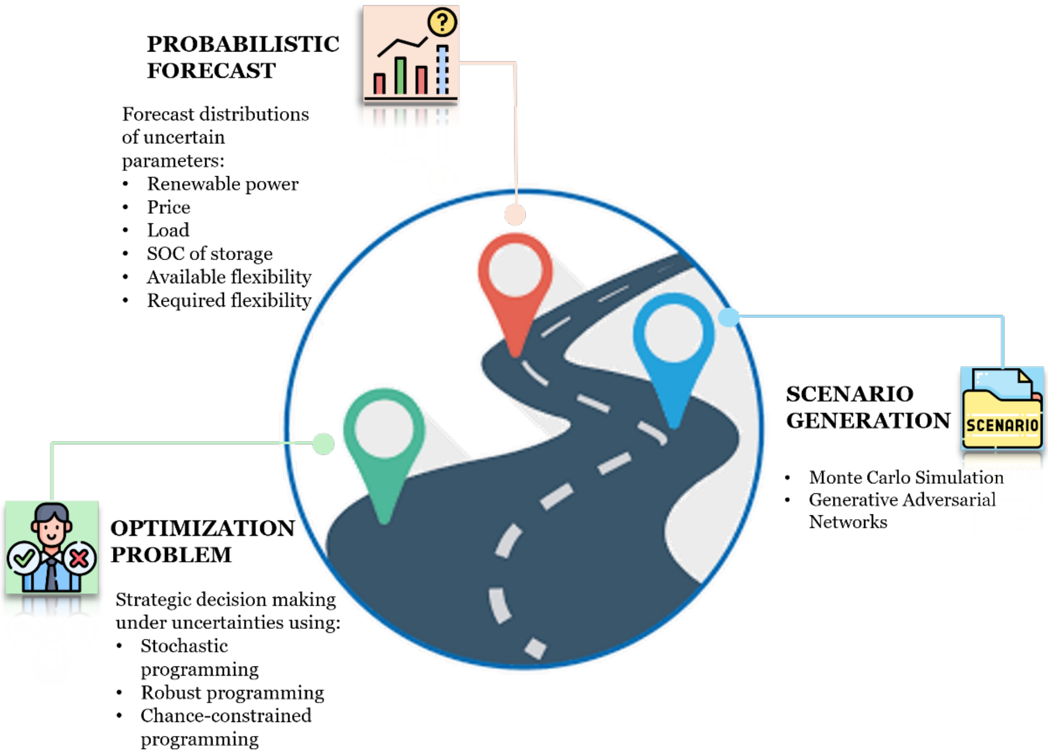


**Figure 14.** A roadmap proposed by Publication III which outlines the path towards decision-making under uncertainties.

Hence, the lack of accurate information affects optimal decision making. In this regard, stochastic, robust, and chance-constrained models can be useful by considering uncertainties in the optimisation and decision-making process. A stochastic optimisation problem considers the probabilities of input occurrences and creates a single solution based on different scenarios and their associated probabilities. The robust optimisation approach focuses on finding an optimal solution considering worst-case scenarios. Chance-constrained optimisation programming allows for optimisation constraints to be fulfilled up to a certain level. Publication III devotes three subsections to review the literature and categorize the applications of these three optimisations in a smart grid environment.

The proposed decision-making roadmap can increase the flexibility of the power system and make it less prone to uncertainties. As power systems become more weather-dependent, handling uncertainty in determining the available flexibility by FERs and the required flexibility by TSOs and DSOs can lead to more reliable decisions.

Publication III also discusses the need for probabilistically forecasting flexibility-related variables in the smart grid environment. This includes forecasting both the required and available flexibility in the network. For instance, in the future, probabilistic forecasts could predict the flexible capacities of EVs available for the next day, which can be used for providing FCRs. Another example is forecasting the flexibility of heating and cooling systems in buildings based on the weather conditions expected for the next day.

# 3 SMART HOMES AS FLEXIBLITY PROVIDERS

Today, an increasing number of homes are equipped with RESs like rooftop solar panels coupled with batteries, which can be further optimised through EMSs. Additionally, governmental regulations are facilitating the transition to electric transportation, thereby promoting the use of EVs.

In addition to storage-based FERs, smart homes often feature appliances whose operations can be scheduled to maximise household economic benefits. For instance, dishwashers and washing machines can be activated when the grid has overproduction. The operation of HVACs can also be adjusted to meet the flexibility needs of the grid operators without compromising occupants' comfort.

Furthermore, EWHs can be controlled based on grid requirements, enabling them to contribute as FERs without sacrificing their primary function of meeting hot water demand. Similarly, the charging schedule of EVs can be adapted to provide flexibility to system operators.

With at least one of these appliances likely present in most households, nearly all homes have the potential to serve as flexibility providers. However, two key factors are essential for realizing this potential: firstly, the implementation of a HEMS and the ICT infrastructure to automate flexible operations and connect homes with system operators; and secondly, the motivation of households to adopt such systems and respond to the flexibility needs of the grid.

## 3.1 Estimating the flexibility potential of a smart home (Publication IV)

As most flexible capacities are procured on day-ahead capacity markets, the flexible capacities of smart homes need to be estimated and offered to the markets, either directly or through aggregators. Therefore, it is crucial to estimate the available flexible capacity of each household in advance based on its controllable devices. This prior estimation allows the HEMS to conduct cost-benefit analyses and select the best markets to sell their flexible capacities. Additionally, accurate flexibility estimation ensures that system operators can assign fair monetary compensation based on the flexible capacities offered and the real-time activation of the smart home devices.

However, distinguishing between actual and flexible demand-side behaviour can be challenging. Publication IV proposes methods to estimate the flexible capacities of smart homes by analysing the capabilities of their controllable appliances to respond to flexibility signals. It suggests that the flexible capacity of each controllable device should be estimated by comparing its normal operation with its flexible operation. The HEMS estimates both flexible and non-flexible operations of each device and subtracts these values to obtain the appliance's flexible capacity. Flexibility orders (signals) from system operators also influence the estimation of flexible capacity. For instance, if system operators require upward flexibility, the maximum reduced consumption of an appliance is estimated as its flexible capacity. This flexible capacity is then communicated to system operators, either directly to the DSO or through an aggregator to the TSO.

The publication examines two thermostatically controllable devices, including HVAC and EHW, as well as two storage-based devices, an EV and a battery. Figure 15 illustrates the interaction between system operators, HEMS, and controllable appliances of the smart home.

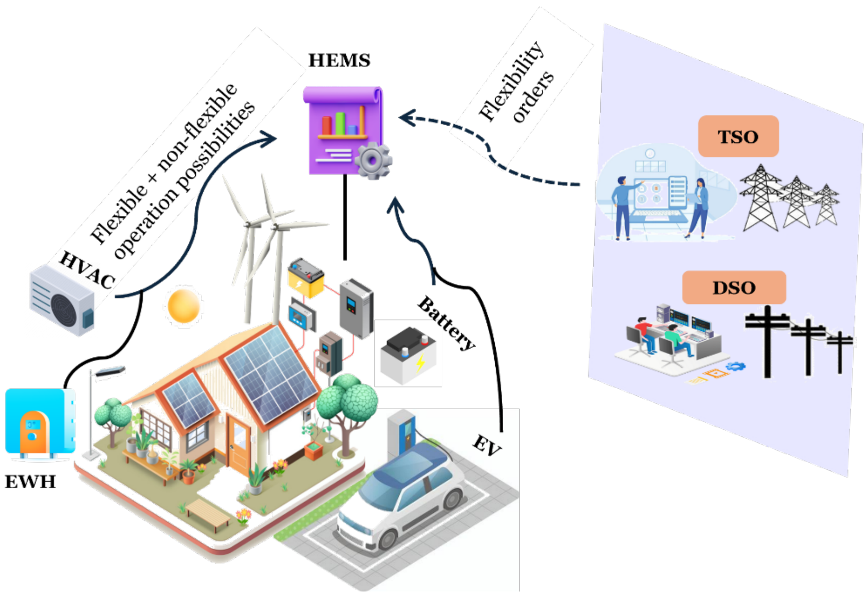


**Figure 15.** Controllable appliances of the smart home considered in Publication IV, the estimation of flexibility of each controllable device by HEMS and the role of flexibility orders from system operators.

Each controllable appliance operates in both normal and flexible modes. In HVAC systems, normal operation aims to minimise the difference between indoor and desired temperatures, while flexible operation minimises energy consumption when there's a need for upward flexibility or maximises the electricity usage when the grid needs downward flexibility. Indoor temperature limits are crucial constraints for both modes. Additionally, operational constraints of the HVAC should apply to the problem.

HEMS aims to minimise the difference between desired and actual water temperatures in EWH during normal operation. In flexible mode, power operation in EWH is determined by flexibility signals, but meeting hot water demand and device constraints remain priorities.

For EVs, fast charging is considered normal operation since the owner normally desires maximum charging speed upon plugging in without any interruption in the charging process (Andrenacci and Valentini 2023). Flexible operation allows for variable charging speeds based on received signals, with owner-set availability for charging and EV battery operational limits being optimisation constraints.

Battery operation is fully flexible according to Publication IV, charging during downward-flexibility-required periods and discharging during the time when the grid required upward flexibility. Recovery periods, not aligned with system needs, occur during non-flexibility periods or when the battery is idle. The optimisation process depicted in the Figure 16 resolves scheduling optimisation problems for both flexible and normal operations of controllable appliances.

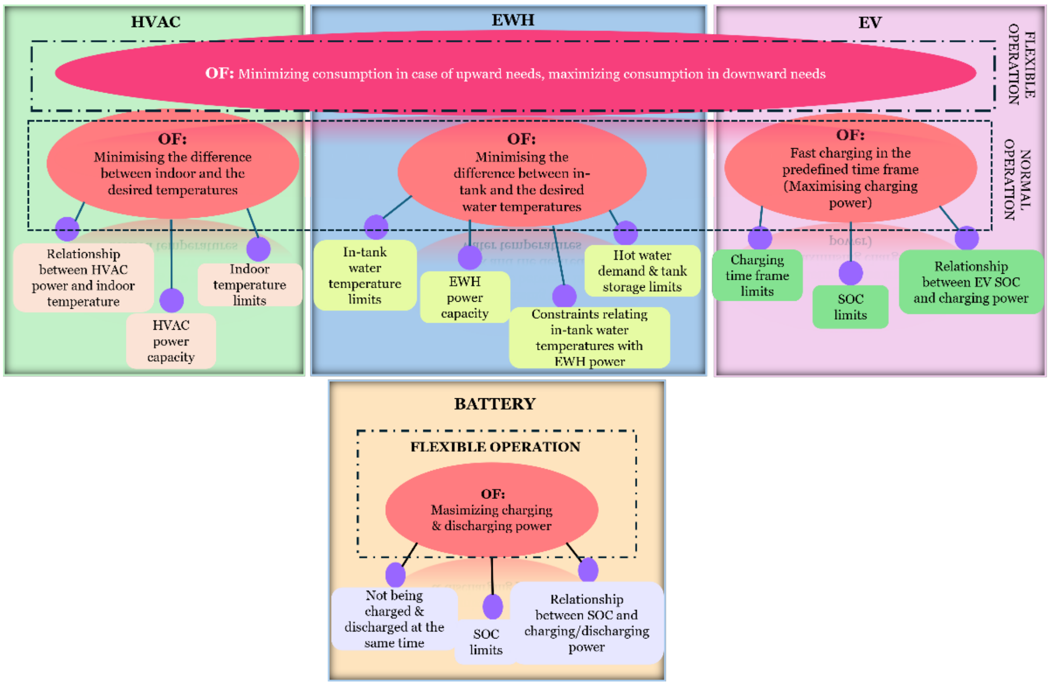


**Figure 16.** Illustration of Objective Functions (OFs) and optimisation problems solved for flexible and normal operations of HVAC, EWH, EV, and battery.

The difference between normal and flexible operation at each hour determines the available flexibility of the smart home. Publication IV suggests adopting a robust method to estimate the flexible capacity of the EWH. This involves generating various scenarios from the forecasted hot water consumption and selecting the worst-case scenario (minimum flexibility) as the available flexible capacity of the EWH. This ensures that the smart home maintains the required capacity despite uncertainties in hot water demand.

In the simulation section, a smart home with several controllable devices is considered. Flexibility signals are derived from mFRR signals activated on 1.9.2020 in Finland using an API connected to the Fingrid open data platform. The optimisation problems are solved using GAMS and the CPLEX solver, and the house ambient temperatures are taken from the Finnish Meteorological Institute for the same date. Figure 17 illustrates the factors considered in the simulation.

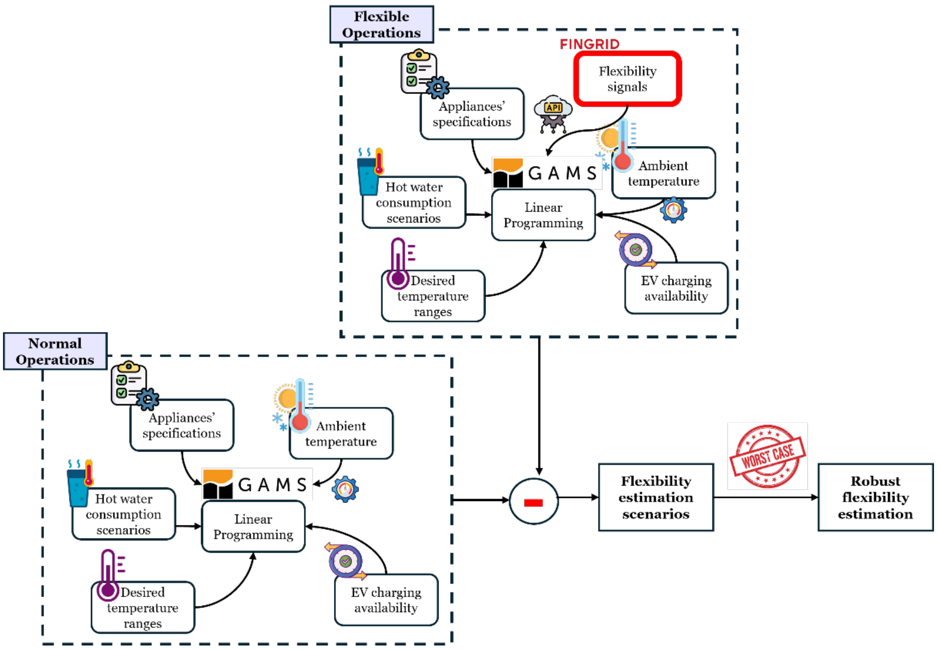


**Figure 17.** The inputs considered in the simulation of a smart home for estimating the flexible and non-flexible operations of controllable devices.

The simulation results of Publication IV show that all controllable devices respond to the flexibility signals, although their flexibility intensity varies according to their operational limits. The battery demonstrates the highest flexibility compared to the EV and thermostatically controllable loads. The primary function of the battery is to provide flexibility, whereas the EV, EWH, and HVAC systems have other main functions. Thermal comfort and meeting the household's hot water demand are more critical for thermostatically controllable devices, making them less responsive to flexibility signals. The charging availability of the EV is a crucial factor affecting its degree of flexibility.

## 3.2 Applications of fuzzy logic-based control method (Publication V)

Publication V proposes a fuzzy logic-based control method for the HEMS of a smart home to schedule controllable appliances and devices. The controllable devices include an inverter-interfaced BESS, HVAC, and EV. The smart home provides coordinated flexibility services for both the DSO and the TSO. It offers active power ($P$) support as a frequency control service for the TSO, while supporting the DSO with both active power ($P$) and reactive power ($Q$). The publication assumes the BESS inverter has an oversizing option and can control both consumed and produced active ($P$) and reactive power ($Q$) within their permissible ranges.

### 3.2.1 Membership functions

As a first step of designing an FLC, membership functions for inputs and outputs should be defined. The membership functions considered in Publication V are illustrated in Figure 18.

The inputs of the control system include EV availability set by the EV owner, real-time data of EV SOC and BESS SOC, online measurements of indoor temperatures, measured frequency deviation for TSO-level flexibility provision, and flexibility signals from the DSO. The EV can be either available or unavailable for charging. The SOC levels of the EV's battery and BESS can be low (L), medium (M), or high (H). Similarly, the indoor temperature can be low (L), medium (M), or high (H). Publication V defines frequency changes as upward (U), downward (D), or none (N). The flexibility signals from the DSO are UB, US, N, DS, and DB. UB indicates a large upward flexibility requirement, US indicates a small upward flexibility need, N means no flexibility is required, DS indicates a small downward flexibility need, and DB indicates a large downward flexibility need.

The outputs of the fuzzy control system include the operating power of the HVAC, the charging power of the EV, and the active and reactive power output of the inverter connected to the BESS. The inverter's active power output can be negative big (NB), negative small (NS), zero (ZE), positive small (PS), or positive big (PB). The reactive power output can be negative (N), zero (ZE), or positive (P). The

HVAC power ranges from zero to its maximum nominal power (in kW) and can be zero (ZE) or a positive value (P). Similarly, the EV charging power can be zero (ZE) or a positive value (P), varying from 0 to its nominal power in kW.

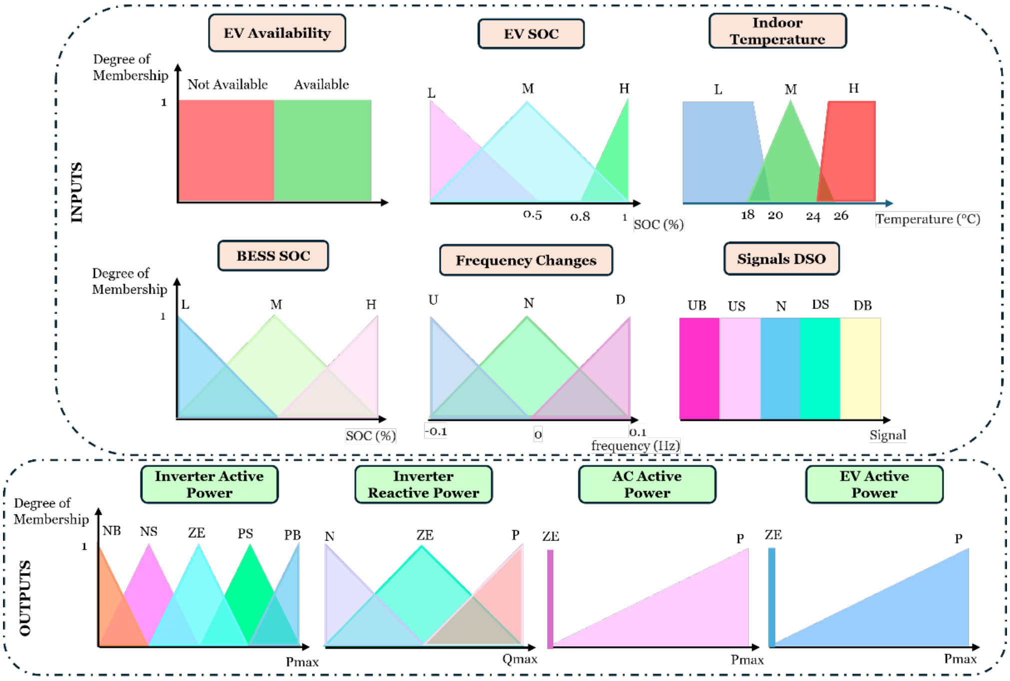


**Figure 18.** Membership functions defined for input and output variables of the fuzzy logic controller designed by Publication V.

### 3.2.2 Fuzzy rules and defuzzification method

Following the definition of the membership functions, fuzzy rules should be designed for the control system. These rules define the relationship between input and output values, determining how to make decisions based on different combinations of inputs.

Publication V defines 42 rules related to the active and reactive outputs of the inverter-interfaced BESS. The rules are defined around the following meta rules:

- If the SOC level is low (L), the active power tends to become positive (PB, PS), i.e. charging state to reach the medium (M) level of the SOC, as a medium SOC provides more flexibility for both the DSO and the TSO.

- Correspondingly, if the SOC level is high (H), the active power tends towards negative values (NB, NS) in discharging mode to inch towards the medium (M) level.

- The BESS's active power does not respond to the DSO's small flexibility needs (US and DS), allowing must-run appliances, i.e. EV and HVAC, to fulfil these non-emergency requirements as the operation of must-run appliances incurs less cost.

- The BESS responds weakly (PS and NS) to positive and negative frequency changes, respectively, and reacts strongly (PB and NB) if the DSO needs higher flexibility (UB, DB).

- The active power output is zero when the DSO's and TSO's flexibility needs do not align, in which case the inverter utilises and adjusts reactive power instead of active power.

- If the DSO's and TSO's needs align, the BESS responds strongly (PB and NB).

- The BESS does not change its operation if neither the DSO nor the TSO requires flexibility.

For the HVAC, 9 rules are defined with the following meta rules:

- The HVAC fully responds to the flexibility signals from the DSO: it outputs zero for an upward flexibility requirement and a positive value for a downward flexibility requirement.

- The HVAC prioritizes the DSO's needs, responding to the DSO's signals even if they contradict the TSO's flexibility needs.

- The HVAC also reacts to frequency changes (TSO flexibility requirements) if they align with the DSO's requirements.

- The HVAC does not change its operation if neither the DSO nor the TSO requires flexibility.

Regarding the EV, Publication V defines 13 rules considering the meta rules below:

- The EV fully responds to frequency changes if they align with the DSO's flexibility needs.

- The EV completely reacts to the DSO's flexibility signals.

- The EV prioritizes the DSO's needs if the DSO's and TSO's requirements contradict each other.

- The EV does not change its operation if neither the DSO nor the TSO requires flexibility.

Publication V uses the Largest of Maximum (LoM) method to determine the outputs' crisp values. LoM maximises the output fuzzy set and is chosen to achieve the maximum flexibility provision by the smart home.

### 3.2.3 Comparison with other cases and simulation results

Publication V implements the proposed fuzzy logic controller with enhanced performance and introduces three comparison models. Figure 19 provide details on the proposed and Comparison Models (CM). The CMs are as follows:

CM 1) An FLC model that works based on spot market prices and tries to minimise energy costs in real time. When the price is low, the BESS is charged, and other appliances operate as much as possible. When the price is high, the smart home consumes less and produces more, meaning the BESS is discharged, and other appliances are scheduled to consume as little energy as possible. Additionally, other operational rules related to indoor temperature and EV availability and the SOCs are taken into account.

CM 2) The second model, named self-sufficient, ignores prices and flexibility signals, aiming to use its BESS as much as possible to meet household consumption. It tries not to compromise the indoor temperature and consider constraints associated with EV availabilities and the SOCs.

CM 3) This model also works based on spot market prices. However, an optimisation problem is designed to minimise energy usage costs, considering the operational limits of the devices as well as factors related to indoor temperature and EV availability.

The controllable appliances are scheduled from January 1, 2021, to March 31, 2021, across four cases. Each controllable device is modelled linearly to assess the control strategy. For the HVAC, ambient and previous temperatures affect the current temperature, with ambient temperatures sourced from real-world data in Vaasa for the defined time period. The EV SOC is modelled based on its charging power and availability, while the BESS model relates SOC to its charging and discharging power.

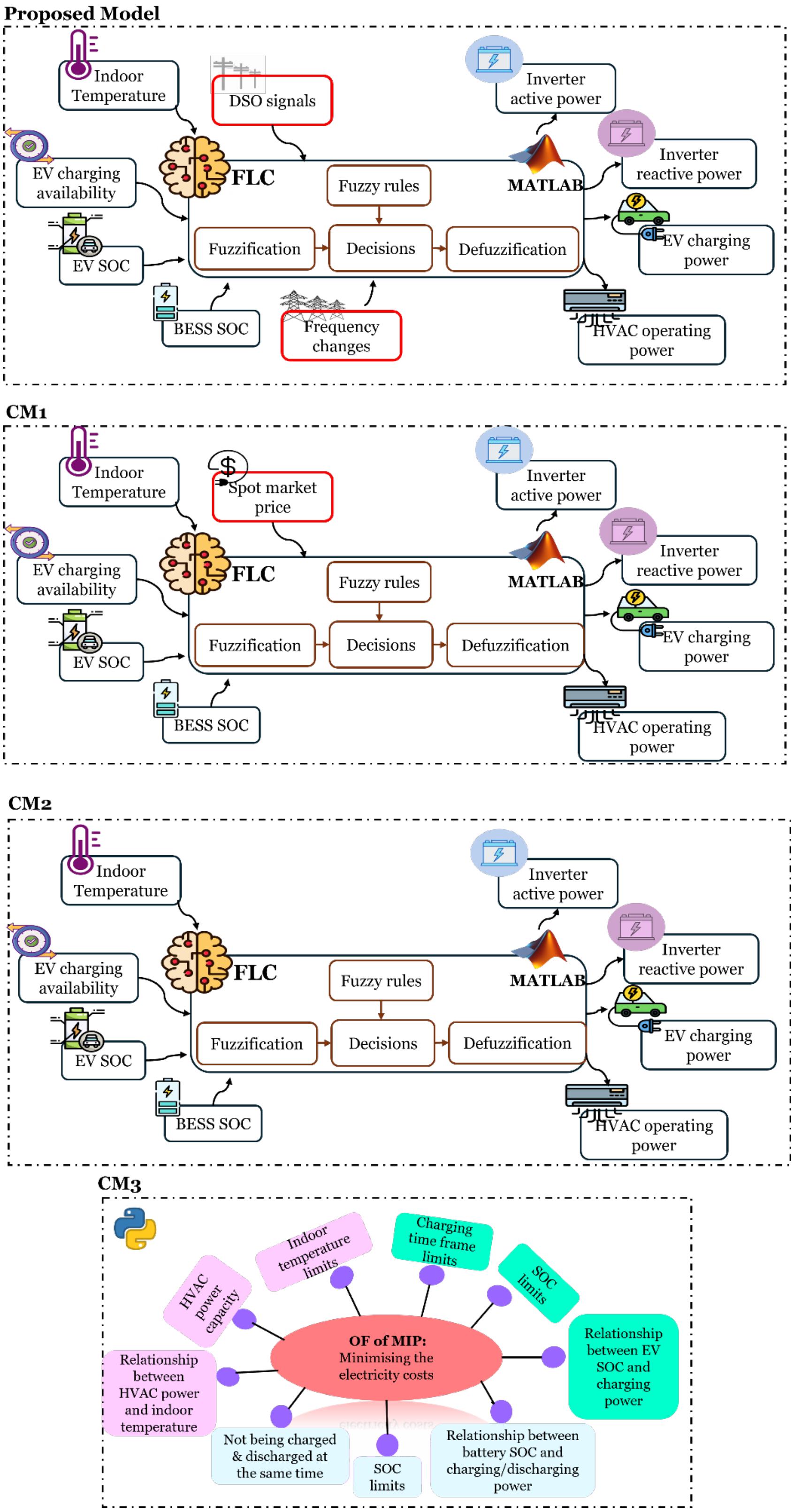


**Figure 19.** Implementation of the proposed FLC model and the introduced comparison models (CMs).

Household devices are scheduled every three minutes. Real-time frequency data is extracted from Fingrid open data (Fingrid 2021) via API for January to April 2021. The FLC developed in MATLAB using Fuzzy Logic Toolbox and the optimisation problems were implemented using CVXPY in Python.

Publication V conducts a three-month economic analysis for the smart home, scheduling devices based on the four models. Results show that the proposed model's total cost over three months was about one-fifth of the other three models. Additionally, the proposed model received a significant capacity payment (around €216), offsetting household costs and generating profits. Figure 20 compares the net cost (cost minus revenue) of the proposed model with those of CMs. In total, the proposed model generates profits with negative net cost. The self-sufficient model incurred the highest cost, while the spot-price-based models were intermediate in cost efficiency. The results also indicate that the FLC-integrated price-based model performed as well as that using mathematical optimisation to minimise energy costs.

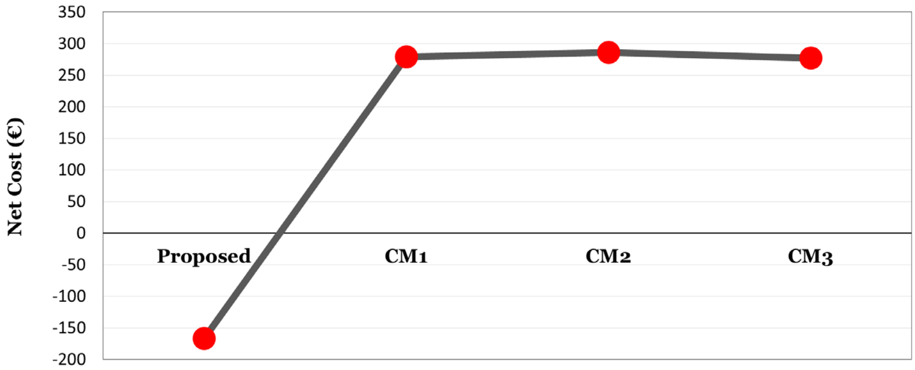


**Figure 20.** Comparison of the three-month monetary cost of a case study considering the proposed FLC-based models and three introduced CMs.

# 4 FLEXIBILITY FROM MICROGRIDS AND ENERGY COMMUNITIES

Energy communities and microgrids offer a platform to aggregate small-scale FERs, such as flexible households and buildings, to provide flexibility services to system operators. An example of these services can be frequency control in the microgrid’s grid-connected mode. Microgrid’s FERs can also generate profits by offering services in islanded mode and enhancing the microgrid's resilience and flexibility when islanded.

In addition to the microgrid operation with islanded operation capability, small-scale FERs can form an energy community to maximise profits by supporting the grid. Typically, energy communities are not equal to microgrids by definition, ownership and operation structure (Hatziargyriou 2023). Mainly energy communities are operating only in grid-connected mode without island operation capability of the certain part network with existing FERs. Energy communities can include various members, such as residential, commercial, and industrial buildings with flexible devices, or the owners of other FERs such as EV charging station owners.

An energy community might have shared assets like bulk energy storage systems (thermal, mechanical, or electrical), wind turbines, and PV panels. These shared assets enable all members to benefit financially from participating in flexibility markets while supporting the integration of more renewable energy into the grid. The capital costs of these shared assets are shared among community members, making it more affordable compared to each member purchasing individual FERs to participate in energy markets and make profits (Doroudchi, Khajeh, and Laaksonen 2022).

## 4.1 An energy community providing mFRR (Publication VI)

Publication VI analyses the operation of a local energy community providing mFRR services for the TSO. The local energy community consists of members and assets that are geographically close, allowing locally produced energy to be consumed within the community. The community owns shared assets, including a PV park and a BESS. Additionally, several EVs within the community can be charged flexibly.

A non-profit manager oversees the scheduling of these flexible devices through an Energy Community Management Centre (ECMC). The primary goal is to maximise the community's total profit by providing mFRR through optimised management of its FERs, including EVs and the BESS.

Publication VI suggests that the ECMC estimates the community's upward and downward flexible capacity and sends this information to a Balancing Service Provider (BSP). The BSP aggregates the FERs from multiple communities and other small-scale resources and develops bidding strategies for participation in the mFRR capacity and energy markets, known as balancing capacity and energy markets.

The TSO then clears these balancing markets and assigns mFRR capacity to each BSP. In real-time, when the TSO calls for mFRR energy activation, the ECMC updates the schedules of the community's flexible devices (EVs and the BESS) to ensure the reserve is activated as promised. Figure 21 illustrated the relationship between the local energy community with the upstream BSP and the TSO. The colourful blocks highlight the focus of the Publication VI.

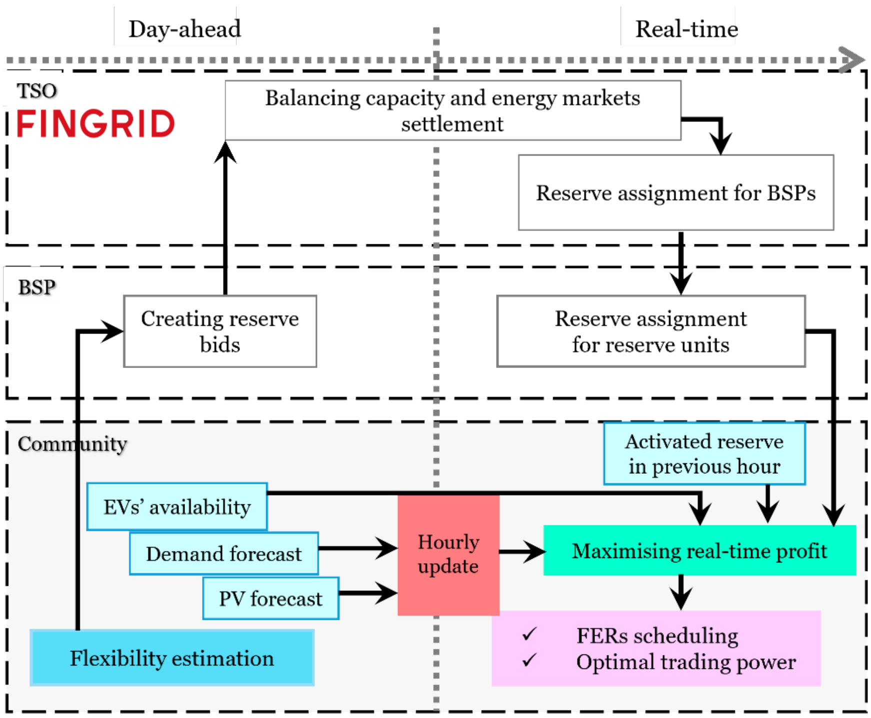


**Figure 21.** The interaction between the energy community and the BSP aggregating the flexible capacity and the TSO who organizes and clears the balancing markets.

For each time slot, the community provides its upward flexible capacity based on its surplus production and downward flexible capacity based on the status and the availability of its BESS and EVs to increase their consumption. If the community has overproduction, it submits the surplus as upward flexible capacity. Conversely, the maximum capacity to increase consumption determines the downward flexible capacity.

In the day-ahead capacity market, the community may offer both upward and downward flexible capacities if it has a positive surplus and the capability to increase consumption. However, only one direction will be activated in real-time.

The ECMC runs a stochastic optimisation problem in the day-ahead market to maximise revenue from offering flexible capacities to the balancing capacity market. The optimisation problem, as shown in Figure 22, aims to maximise potential revenue from both upward and downward capacities.

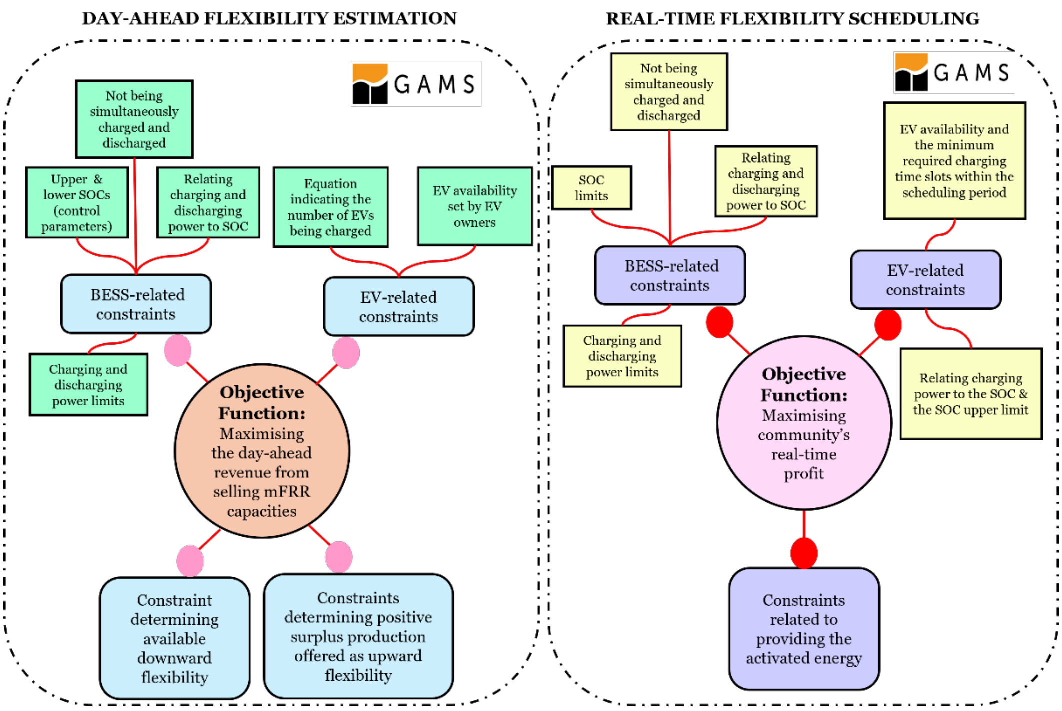


**Figure 22.** Day-ahead and real-time optimisation problems proposed by publication VI in order to estimate the flexible capacities of the community in day-ahead and reschedule the community in real-time to activate the flexibility required by the TSO.

To handle uncertainties in mFRR real-time activation and the forecasting errors, Publication VI proposes two control parameters that determine the minimum and maximum bounds of BESS SOC. These parameters reserve a portion of the BESS capacity, preventing battery's capacity from being fully offered as flexibility in the day-ahead market. This reserved capacity helps real-time schedules have more flexibility. This can mitigate the risk of penalties for failing to provide the assigned mFRR. The SOC control parameters are visually shown in Figure 23.

In real-time, ECMC runs an optimisation problem with the objective of maximising the community's profit. The primary priority of the local energy community's real-time scheduling is to provide the activated flexibility, considering the activation and the direction of the mFRR ordered by the TSO.

The real-time scheduling optimisation problem also takes into account the availability of EVs for charging and sets a constraint that determines the minimum number of 15-minute time slots in which the EVs should be charged, so as not to compromise the EV's predefined charging schedule. The defined optimisation problem developed for the real-time scheduling is illustrated on the right-hand side of Figure 22.

Publication VI considers a hypothetical community consists of 50 households a 100kW PV system, a 50kW/200kWh (Vanadium Redox Flow) BESS and 10 EVs, as a case study. Optimisation problems were solved using GAMS and CPLEX solver. The data of mFRR prices and activation extracted from the Fingrid open data on July 7, 2019.

Regarding day-ahead scheduling, Publication VI analyses 15 cases that have different bounds of minimum and maximum SOC as control parameters. According to the results, all of the considered cases lead to three pairs of total upward and downward flexibility offers, as Figure 23 illustrates. In light of this conclusion, Publication VI narrows down all 15 cases into three groups, namely G1, G2 and G3.

The results demonstrate that day-ahead control parameters significantly impact the community's profitability. According to the simulation results in Publication VI, the group that reserves more BESS capacity, i.e. G3 is more profitable compared to those with high BESS utilisation, G1 and G2. Furthermore, groups with lower BESS capacity deployment (G2, G3) are more profitable than that where the LEC does not provide mFRR (Figure 24).

The simulations indicate that participating in mFRR provision can be profitable for the community. Hence, providing mFRR ancillary services not only assists the TSO but also increases profits for the community. However, careful estimation of the community's day-ahead available flexibility is crucial for real-time profitability and its optimal operation.

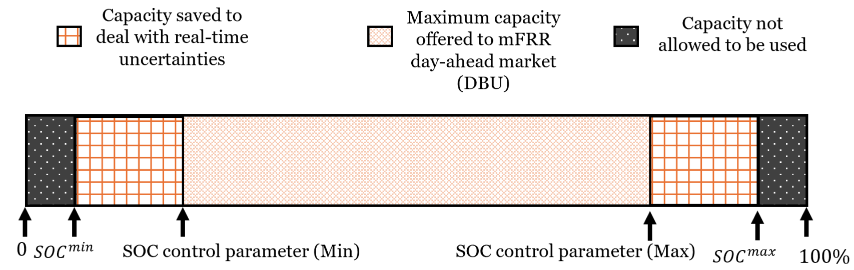


| Case No. | Control Parameters | | Total Daily Upward Flexibility Offer (kW) | Total Daily Downward Flexibility Offer (kW) | DBU (%) |
|---|---|---|---|---|---|
| | *min* | *max* | | | |
| 1 | 0.2 | 0.8 | 583.9 | 780.5 | 100 |
| 2 | 0.3 | 0.8 | 583.9 | 780.5 | 83 |
| 3 | 0.4 | 0.8 | 133.9 | 130.5 | 67 |
| 4 | 0.5 | 0.8 | 83.9 | 80.5 | 50 |
| 5 | 0.2 | 0.7 | 583.9 | 780.5 | 83 |
| 6 | 0.3 | 0.7 | 83.9 | 80.5 | 67 |
| 7 | 0.4 | 0.7 | 83.9 | 80.5 | 50 |
| 8 | 0.5 | 0.7 | 83.9 | 80.5 | 33 |
| 9 | 0.2 | 0.6 | 133.9 | 130.5 | 67 |
| 10 | 0.3 | 0.6 | 83.9 | 80.5 | 50 |
| 11 | 0.4 | 0.6 | 83.9 | 80.5 | 33 |
| 12 | 0.5 | 0.6 | 83.9 | 80.5 | 17 |
| 13 | 0.2 | 0.5 | 133.9 | 130.5 | 50 |
| 14 | 0.3 | 0.5 | 83.9 | 80.5 | 33 |
| 15 | 0.4 | 0.5 | 83.9 | 80.5 | 17 |

G1 G2 G3

**Figure 23.** Illustration of control parameters and the results of the day-ahead optimisation problem solved for the case study in Publication VI.

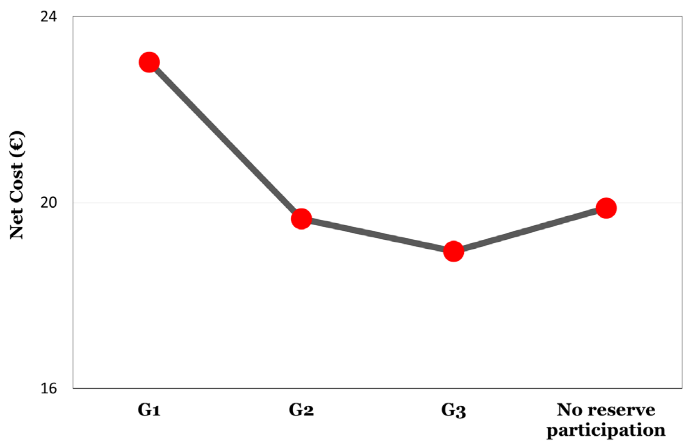


**Figure 24.** The daily net cost (cost minus revenue) obtained for the case study considering different control parameters and the case in which the community does not provide mFRR.

## 4.2 Microgrid’s flexibility potential (Publication VII)

Publication VII discusses how microgrids equipped with EMS can enhance flexibility of the grid and assist system operators in managing their networks. Microgrids are viewed as valuable sources of flexibility for addressing network operation challenges, as they contain several controllable FERs that can be operated in alignment with network requirements. Microgrids can also be disconnected from the grid in urgent situations, such as during a blackout. In this regard, FERs can provide services to support the microgrid’s stand-alone operation.

### 4.2.1 Flexible energy resources in microgrids

Publication VII introduces FERs in microgrids and their adaptable characteristics. Figure 25 showcases a hypothetical microgrid with potential FERs.

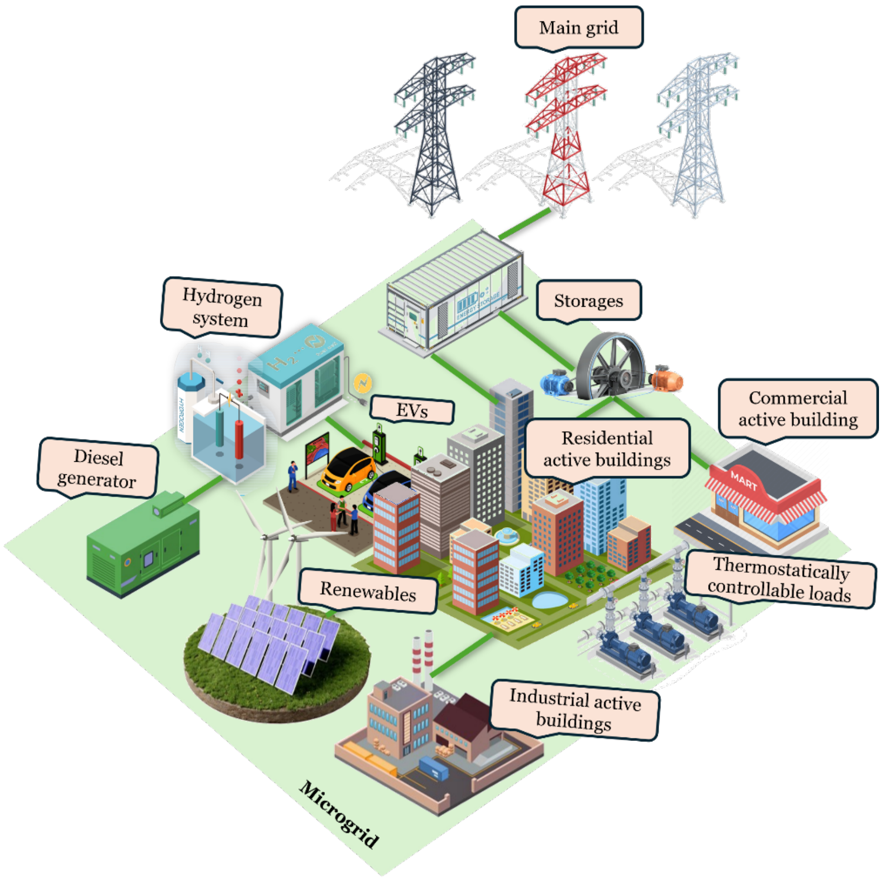


**Figure 25**. Illustration of a grid-connected microgrid with different flexible energy resources.

The publication VII categorises FERs based on their flexibility into two main types:

- ✓ Low-to-medium FERs such as solar and wind generation units: These units have mostly uncontrollable or less controllable output that can be curtailed if downward flexibility is needed in the network.
- ✓ Medium-to-high FERs: such as energy storages, EVs, and thermostatically controllable loads: These resources have continuously controllable outputs, though their operational constraints might limit the flexibility they can provide.

The publication details various storage-based high-flexible energy resources available in microgrids, including:

- EVs: EVs offer adjustability, shiftability, and fast response capabilities, making them valuable high-flexible resources for system operators and microgrid operations. EVs with vehicle-to-grid capability are more flexible compared to those without it as they enable bi-directional flow of power.
- BESS: BESSs provide rapid-response solutions for stability, resiliency, and flexibility in the microgrid. They come in various sizes and materials, such as Lithium ion and Vanadium Redox Flow batteries. Their mathematical modelling is similar to that of EVs, but EVs have additional constraints related to their charging availability and vehicle-to-grid capability.
- Thermal Energy Storage (TES): TESs store thermal energy from sources like combined heat and power units, waste heat, or industrial units. This stored heat can be used during high-price periods to avoid using expensive electricity for heating. TESs can be seasonal, storing cold in winters for use in summers. The publication includes a table detailing typical TES types and their characteristics, including capacity, power, efficiency, cost, and storage time.
- Flywheels: These mechanical energy storage devices store kinetic energy by speeding up a rotational part. The stored energy can be released back to the grid as needed. Flywheels are modelled based on their mass, radius, and rotational speed.

The publication also reviews production-side FERs in microgrids, including:

- Fuel Cell (FC): FCs convert chemical energy from hydrogen-oxygen reactions into electrical energy. They operate in alignment with renewables, producing power when renewables are not available. For example, electrolysers produce hydrogen when there is surplus renewable production, and FCs use this hydrogen when renewable production is insufficient.

- Diesel generators: They provide backup power or upward flexibility when needed. Their sizing and ramping rates are limited and should be considered in their mathematical modelling.

- Renewable production: As previously mentioned, their production can be curtailed in cases where the grid requires decreased production.

Microgrid's FERs in the demand side include residential appliances, industrial controllable devices, and commercial building systems, located in the microgrid:

- Thermostatically controllable devices: Devices known as heating and cooling systems like EWH, HVAC systems, heat pumps, and refrigerators can adjust their power consumption via thermostat control.

- Shiftable loads: Devices like dishwashers and washing machines cannot control power consumption but can be scheduled to operate during low-price hours or when they receive flexibility orders from system operators.

- Curtailable loads: Lighting devices and other similar loads can adjust power consumption without significantly affecting user comfort.

In demand-side resources, customer comfort is the highest priority. Figure 26 summarizes the FERs that can be available in a microgrid.

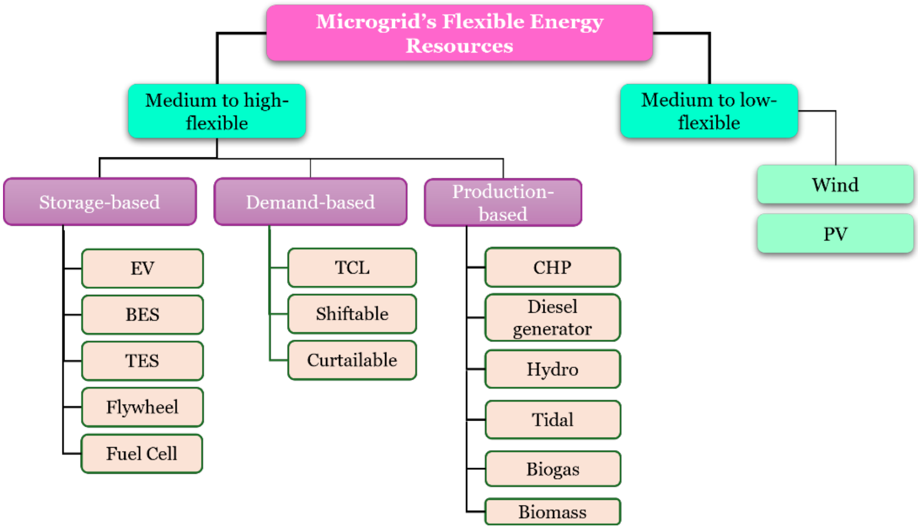


**Figure 26.** Categorization of microgrid's potential FERs that can provide flexibility according to their degree of flexibility.

### 4.2.2 Energy management systems in microgrids

The active utilisation of high-flexible FERs can enhance microgrid's flexibility through EMS. In this regard, Publication VI presents various EMS designed for microgrids with objectives ranging from cost reduction (fuel costs, devices operational and maintenance costs, and the costs of purchasing electricity from the upstream grid) and revenue maximisation (revenues from selling electricity to the grid and customers as well as providing flexibility services to TSOs and DSOs) to emission reduction and self-sufficiency.

The publication outlines three different approaches for microgrid's EMS:

- Centralized management: Controls all FER operations based on global optimal points.
- Decentralized management: Meets individual preferences of each FER owner, giving them more freedom of operation.
- Distributed management: Uses a game-theoretic approach where FER owners make independent decisions and trade signals to achieve a global optimum.

Publication VII emphasizes the importance of considering uncertainties of renewable energy generation and demand in microgrid's planning and operation. It explores various optimisation techniques, including stochastic programming, robust optimisation, and Benders' decomposition, to address these uncertainties.

The publication explains the Model Predictive Control approach for making real-time operational decisions of FERs by solving an approximate model over future horizon. Model Predictive Control is used to handle intermittency, binary variables, and sudden changes. It also reviews the applications of Model Predictive Control in microgrid’s EMS.

Additionally, the publication discusses game theory as a potential approach for microgrid’s operation, enabling distributed decision-making and handling multiple agents of FERs. Game theory approaches are explored for multi-objective optimisation and coordinated control in microgrids, involving multiple decision-makers with potentially conflicting interests.

# 5 BATTERY ENERGY STORAGE SYSTEMS AS FLEXIBLE ENERGY RESOURCES

Publication VIII assumes that a private company aims to design a specific type of Lithium-ion BESS. This BESS consists of battery cells connected in series and parallel, along with the necessary equipment to integrate it with the grid, including a converter, transformer, and control system. The primary purpose of the BESS is to ensure the secure operation of the local distribution network by providing the DSO with the required flexibility.

Additionally, the BESS is designed to enhance profitability by participating in the Finnish FCR-N market. The main architecture of the publication is showcased by Figure 27.

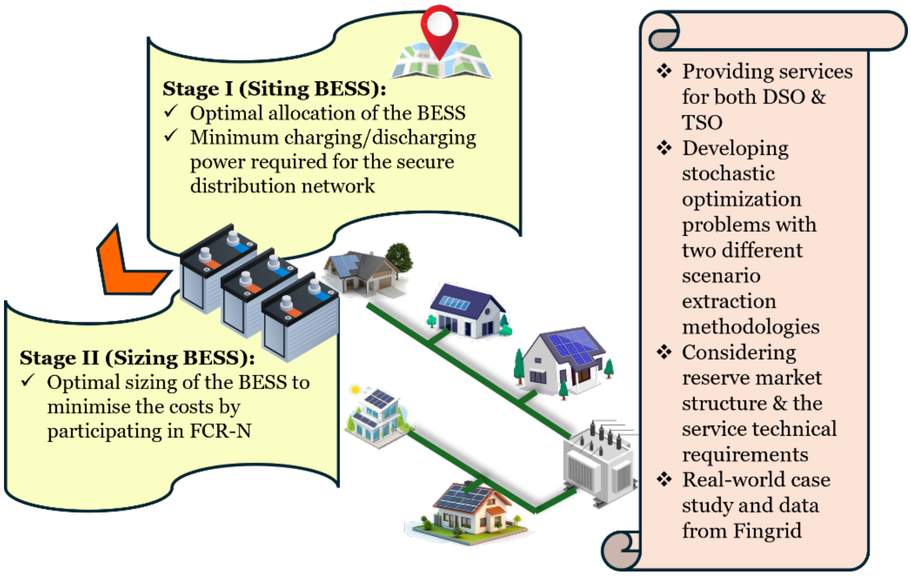


**Figure 27.** The main architecture and contribution presented by Publication VIII.

BESS planning model focuses on two main objectives:

- Network security: Determine the place and minimum size of the BESS to prevent voltage violations and avoid exceeding the thermal limits of feeders.
- Profit maximisation: Size the BESS to increase overall profits by providing the FCR-N service for the TSO.

To achieve these objectives, the planning model runs in two stages:

- Stage I (required allocation and sizing): In this stage, the BESS is optimally placed within the local network and the minimum charging and discharging power capacities are set to ensure the security of the local network even in worst-case scenarios.

- Stage II (cost minimisation): This stage focuses on minimising the net costs (costs minus revenues) of the BESS while ensuring the secure operation of the network for the DSO.

## 5.1 Battery allocation for DSO-level flexibility provision (Publication VIII)

The first stage involves deploying a mathematical model of the distribution network to understand the relationship between injected/withdrawn flexible power at each node, node voltages, and power flow within the feeders. For this, Publication VIII uses a piecewise-linearized power flow model, also employed in Publication I.

Upward flexibility is achieved by discharging the BESS to inject power into the local network, while downward flexibility is achieved by charging the BESS to withdraw power from the grid. The objective of this stage is to minimise the amount of flexibility injected into and withdrawn from the grid under worst-case scenarios to minimise the flexible capacity invested for having a secure distribution network.

The optimisation problem utilised for the first stage has the same structure and formulations to model the distribution network as that of Publication I, which is displayed in Figure 12. However, some adjustments are made to determine the location of the BESS. In this regard, the publication assumes that each candidate node has an associated binary variable, indicating whether the BESS can be located at that node. Candidate nodes are selected among the network's weak nodes that experience highest voltage fluctuations.

Publication VIII considers that designers have predefined the maximum number of BESS units that can be placed in the distribution network. As mentioned, the additional constraints are included in the power flow problem to determine the optimal locations for these BESS units:

$$P_{cn,s,t}^{up} \leq M\, u_{cn}^{BESS} \qquad \textbf{(1)}$$

$$P_{cn,s,t}^{down} \leq M\, u_{cn}^{BESS} \qquad \textbf{(2)}$$

$$\sum_{cn} u_{cn}^{BESS} \leq N^{BESS} \qquad \textbf{(3)}$$

Where, $P_{cn,s,t}^{up}$ and $P_{cn,s,t}^{down}$ are upward and downward flexibility provided by candidate node $cn$ at time $t$ for scenario $s$. Parameter $M$ is a large number. The binary variable $u_{cn}^{BESS}$ equals one only if the node has a BESS. For nodes without a BESS, $u_{cn}^{BESS}$ is set to zero, and consequently $P_{cn,s,t}^{up}$ and $P_{cn,s,t}^{down}$ are set to zero. Constraint (3) limits the number of nodes with BESS, based on the designer's predefined maximum number of BESS units.

Optimisation problem is solved and the outputs are the optimal values for upward and downward flexibility at the optimal BESS locations (OBP), $P_{n=OBP,s,t}^{up,optimal}$ and $P_{n=OBP,s,t}^{down,optimal}$. As a result, the minimum BESS charging and discharging power, $P^{BESS,min}$, is set to the maximum charging and discharging power across all worst-case scenarios:

$$P^{BESS,min} = \max\left(\max\left(P_{n=OBP,s,t}^{up,optimal}\right), max\left(P_{n=OBP,s,t}^{down,optimal}\right)\right) \qquad \textbf{(4)}$$

This means that the maximum flexible power needed by the network is set as a minimum capacity power of the BESS.

Publication VIII proposes the following scenario generation algorithm to identify the worst-case scenarios for the local network, as detailed in Figure 28:

**Inputs:** Historical data on daily net load at each node and each hour.

**Outputs:** Scenarios for daily net loads at each node and each hour.

The algorithm works as follows:

**Time-Series clustering:** Utilises time-series clustering to categorize nodes into clusters and determine the probability for each cluster combination.

**Selection of extreme days**: Selects probable days with the highest total hourly loads and the highest production.

**Normalisation:** Normalises the probabilities so that their sum equals 1.

Publication VIII utilises two case studies—the IEEE 33-bus radial distribution system and a Finnish rural network—to implement the first stage of BESS allocation and minimum sizing. The CVXPY package in Python was used to model both the first- and second-stage optimisation problems.

In the IEEE case study, the maximum number of BESS units was systematically increased by modifying the right side of constraint (3). The study then compared the aggregated capacities of all BESS units required to ensure secure operation of the distribution network, with the results shown in

**Table 1**. Notably, increasing the number of BESS units up to 7 resulted in a reduction in the required aggregated BESS capacity. However, adding an eighth battery led to a higher aggregated BESS capacity.

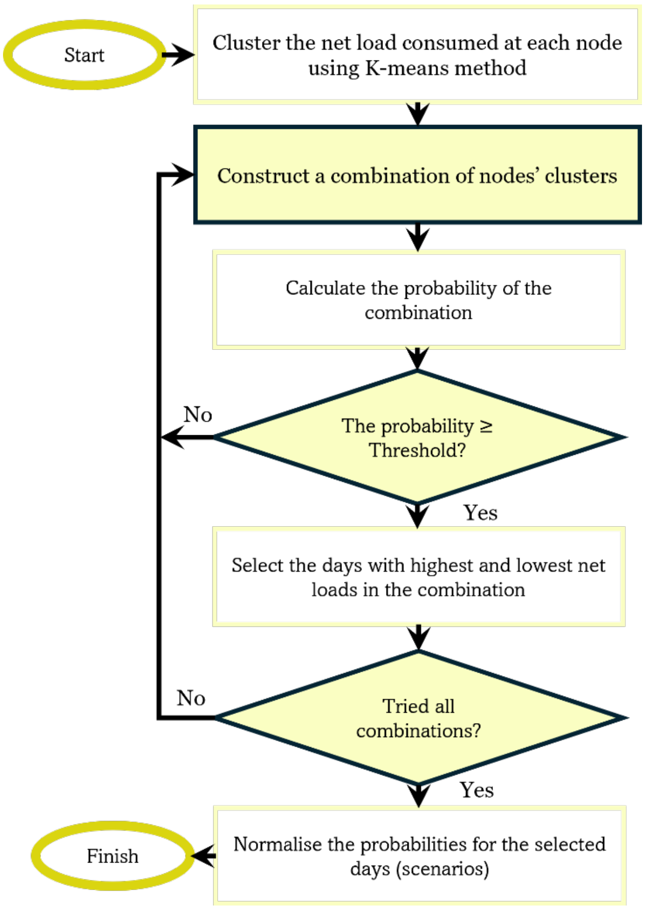


**Figure 28.** Details on scenario extraction algorithm utilised for the first-stage stochastic optimisation problem proposed by Publication VIII.

**Table 1.** The aggregated capacities and the location of the BESS(s) required for the secure operation of IEEE 33 bus system if the number of BESS units varies.

| Number of BESS units | Optimum location (nodes) | Aggregated power capacities of all BESS units [kW] | Aggregated energy capacities of all BESS units [kWh] |
|---|---|---|---|
| 1 | 12 | 2.799 | 10.106 |
| 2 | 16, 33 | 1.829 | 6.604 |
| 3 | 15, 18, 33 | 2.147 | 7.753 |
| 4 | 14, 16, 18, 33 | 2.387 | 8.619 |
| 5 | 14, 16, 17, 18, 33 | 2.470 | 8.918 |
| 6 | 13, 14, 16, 17, 18, 33 | 2.602 | 9.396 |
| 7 | 13, 14, 15, 16, 17, 18, 33 | 2.694 | 9.727 |
| 8 | 13, 14, 15, 16, 17, 18, 32, 33 | 2.826 | 10.203 |

For the Finnish rural network, increasing the number of BESS units did not affect the results, as the local network required only one battery located at its weak node. The results also demonstrated significantly improved voltage levels for both local networks using the BESS units. The minimum power capacity of the BESS, determined in the first stage, is then used as a constraint in the second stage.

## 5.2 Battery sizing for FCR-N provision (Publication VIII)

The second stage focuses on designing the BESS to achieve optimal energy and power capacities, maximising revenue from the FCR-N markets. This stage aims to minimise the daily net costs of operating the BESS by considering the most likely scenarios. The objective function accounts for several factors:

- **Daily based maintenance and operational costs:** These are calculated per kilowatt (kW) of BESS charging and discharging.
- **Cycling cost:** This arises from the wear and tear on the BESS due to charging and discharging cycles.
- **Cost of FCR-N provision**: This includes earnings (negative cost) from reserving symmetrical FCR capacity, by participating in FCR-N capacity markets and revenue (negative cost) from activating FCR-N energy in the

upward direction, plus the costs of activating FCR-N energy in the downward direction.

- **Cost of spot markets:** This is the cost of charging the BESS at spot market prices minus the revenue from discharging the BESS at those prices.

The constraints of the second-stage problem can be summarized as follow:

Active power balance equation as a constraint models the downward-activated FCR-N and the charging power traded at day-ahead prices as consumption with negative signs. Correspondingly, the upward-activated FCR-N and discharging power traded at day-ahead prices are modelled as production with positive signs. These production and consumption activities occur at the BESS-located node, which was determined from the first-stage problem. In addition to the BESS, the net load consumption at each node has a negative sign, while the power entering the local network from the outer grid is considered production with a positive sign. The reactive power balance equation includes only the consumption term from demand, as the publication assumes that the BESS unit does not inject or withdraw reactive power.

Publication VIII distinguishes between activated FCR-N energy and FCR-N capacity. According to the droop control defined for the FCR-N (see Figure 8), the relationship between activated FCR-N energy and capacity is as follows:

$$Upward\ activated\ FCR-N\ energy = \begin{cases} \frac{(50-frequency)}{0.1} \times FCR-N\ capacity & if\ 49.9 \leq frequency \leq 50 \\ FCR-N\ capacity & if\ frequency \leq 49.9 \end{cases} \quad \textbf{(5)}$$

$$downward\ activated\ FCR-N\ energy = \begin{cases} \frac{(frequency-50)}{0.1} \times FCR-N\ capacity & if\ 50 \leq frequency \leq 50.1 \\ FCR-N\ capacity & if\ frequency \geq 50.1 \end{cases} \quad \textbf{(6)}$$

The other set of constraints determine the power capacity allocated to FCR-N and charging/discharging power based on spot prices. Due to the symmetrical nature of FCR-N, providers must reserve both upward and downward capacity for each time slot.

For downward flexibility, the combined FCR-N power capacity and day-ahead charging power must not exceed the BESS's rated power capacity, as indicated by Constraint (7).

Constraint (8) stipulates that the sum of the FCR-N power capacity and the day-ahead discharging power cannot exceed the BESS's rated active power.

$$FCR - N\ capacity + charging\ with\ spot\ prices\ \leq BESS\ power\ capacity \quad \textbf{(7)}$$

$$FCR - N\ capacity + discharging\ with\ spot\ prices \leq BESS\ power\ capacity \quad \textbf{(8)}$$

When providing reserve services, adhering to current market regulations and characteristics is crucial. For instance, at the time of publication, one key constraint from Fingrid mandated that a BESS must be fully activated for at least 30 minutes in each direction (Astero and Evens 2020). Therefore, Publication VIII includes a constraint ensuring that the BESS's available state of energy at the beginning of each timeslot is sufficient to handle a 30-minute activation of FCR-N power capacity in either direction.

Additionally, the publication defines constraints addressing the operational limitations of the battery. These constraints link the effects of upward and downward energy activation of FCR-N, as well as charging and discharging based on spot prices, on variations in the BESS SOC.

Furthermore, linearized distribution network constraints are considered in the second stage to ensure that providing FCR-N does not compromise the security of distribution networks. Figure 29 summarizes the most important components utilised for developing the second-stage optimisation problem.

The scenarios used for the second-stage optimisation problem are extracted from a different algorithm than the first stage. The algorithm involves generating and reducing scenarios based on historical data including hourly net loads for each node and hourly positive and negative frequency deviations. The algorithm first determines the optimal number of clusters for daily net loads and frequency deviations using the Elbow Method. It then categorizes daily net loads and frequency deviations into these clusters using the K-means clustering algorithm. Probabilities are calculated for each combination of node and frequency deviation clusters. The scenario generation and reduction process involve selecting days with probabilities above a certain threshold and normalising the probabilities of the final selected scenarios so that their sum equals one. Figure 30 provides details on the scenario extraction methodology used for the second stage of BESS-sizing stochastic optimisation problem.

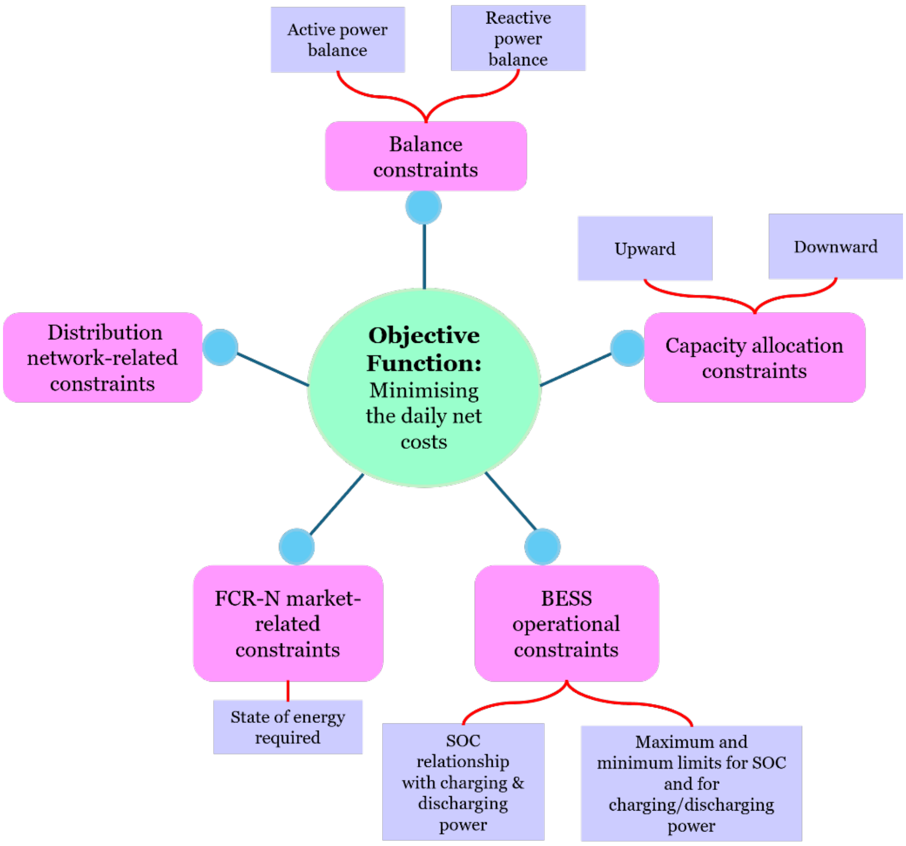


**Figure 29**. Illustration of the optimisation problem developed to model the second stage of the BESS sizing problem.

The second-stage method was applied to the Finnish rural network to assess the impact of increasing prices from 2021 to 2022 and analyse the profitability of participating in FCR-N markets for the BESS. The analysis considered four strategic cases:

- **Case I:** Utilises 2021 price and frequency data, with BESS operation optimised based on the proposed model.
- **Case II:** Utilises 2021 price and frequency data, with BESS operation optimised solely based on spot prices.
- **Case III:** Utilises 2022 price and frequency data, with BESS operation optimised based on the proposed model.
- **Case IV:** Utilises 2022 price and frequency data, with BESS operation optimised solely based on spot prices.

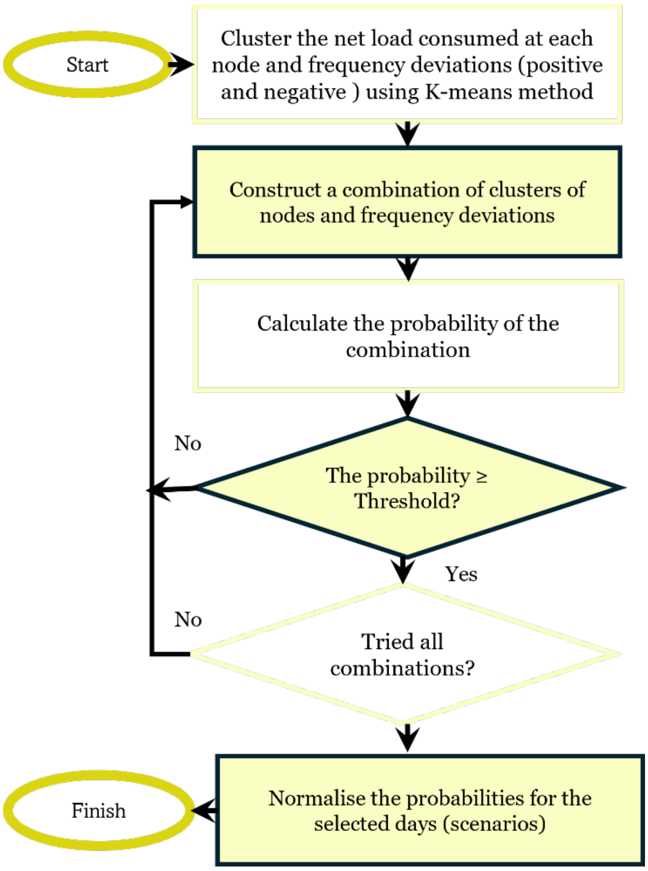


**Figure 30.** Algorithm utilised for second-stage scenario extraction in Publication VIII.

According to the results from Publication VIII, the optimal BESS size is 800 kWh when providing FCR-N services (Cases I & III). This value equals to the maximum energy capacity limited by the transformer's capacity in Finnish rural network case study.

For cases where the BESS does not participate in FCR-N, the optimal energy capacity was 107.399 kWh in 2021 (Case II) and 800 kWh in 2022 (Case IV). This difference is due to the significant increase in market prices in 2022.

Figure 31 compares the daily profits for each case. In 2021 (Case I), the BESS generated €55.8 of profit from FCR-N. In 2022 (Case III), the profit increased to €280.3, which is 3.6 times higher than the profit from operating based solely on spot prices. In 2021, operating based on spot prices resulted in negative profits, indicating that the operational costs exceeded the revenue.

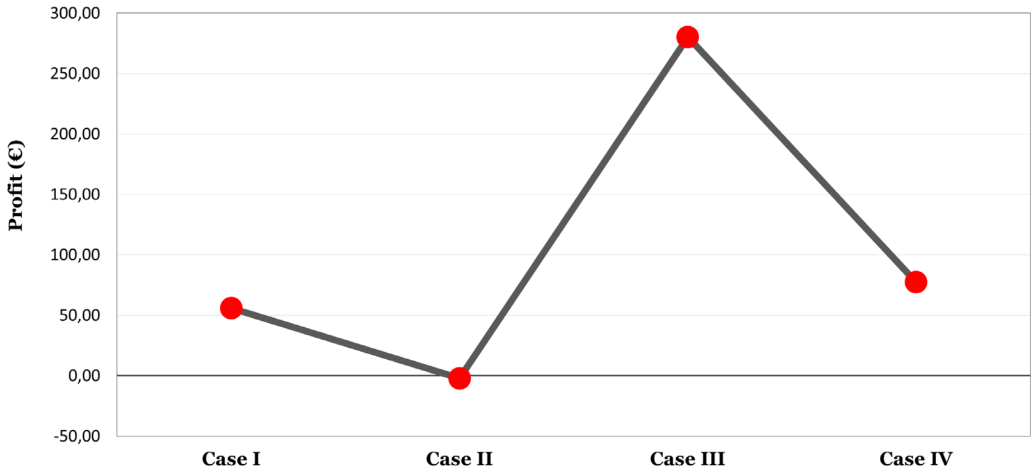


**Figure 31.** Daily profit comparisons estimated by Publication VIII for 800 kWh BESS considering different market participation strategies and for different years.

Publication VIII also examines the impact of cycling aging on the profitability of Li-ion BESS from FCR-N participation. The results indicate that after 800 and 1600 cycles, the daily profit decreases by approximately 3% and 15%, respectively, due to BESS capacity fade.

# 6 WIND-INTEGRATED HYDROGEN SYSTEM PROVIDING FLEXIBILITY FOR TRANSMISSION SYSTEM OPERATOR

Europe is advancing towards developing hydrogen infrastructure and significantly increasing hydrogen production to meet the EU Green Deal's goal of boosting renewable energy resources, with a particular focus on green hydrogen (Iliceto et al. 2023). This effort involves expanding hydrogen valleys across Europe (Iliceto et al. 2023).

While green hydrogen could accelerate the EU's green transition, the large-scale integration of electrolysers presents challenges to local TSOs and broader interconnected energy systems. These challenges include increased congestion, disruption of balance, and larger frequency deviations (Iliceto et al. 2023). To address these issues, coordinated and collaborative scheduling between hydrogen production units and electrical system operators is essential to facilitate the widespread integration of hydrogen.

A key strategy is aligning electrolyser operations with the network's flexibility requirements. This cooperation benefits both parties: electrolysers as an FER can generate additional revenue by supporting the system operator, leading to cheaper hydrogen production through cheaper electricity. Meanwhile, the system operator enhances network flexibility, enabling it to accommodate more renewables and green hydrogen electrolysers. In this context, Publication IX analyses the operation of a hydrogen system participating in FCR-N and FCR-D markets while ensuring that the nearby transmission network operational limits are respected.

## 6.1 Electrolysers providing FCRs (Publication IX)

In Publication IX, a wind-integrated hydrogen system comprising a wind farm, an electrolyser, a compressor, and hydrogen storage is scheduled to provide FCR services for TSOs. These services include FCR-N, upward FCR-D, and downward FCR-D. When the locally measured frequency drops below 50 Hz, the hydrogen system injects wind power into the network. Conversely, when the frequency exceeds 50 Hz, the system consumes more electricity to produce hydrogen, thereby withdrawing more power from the network. Additionally, the publication assumes that a fixed-term contract between the TSO and the hydrogen system ensures the operation of the hydrogen system prevents congestion in the local transmission grid. Figure 32 summarises the optimisation problem developed for scheduling of the wind-integrated hydrogen system.

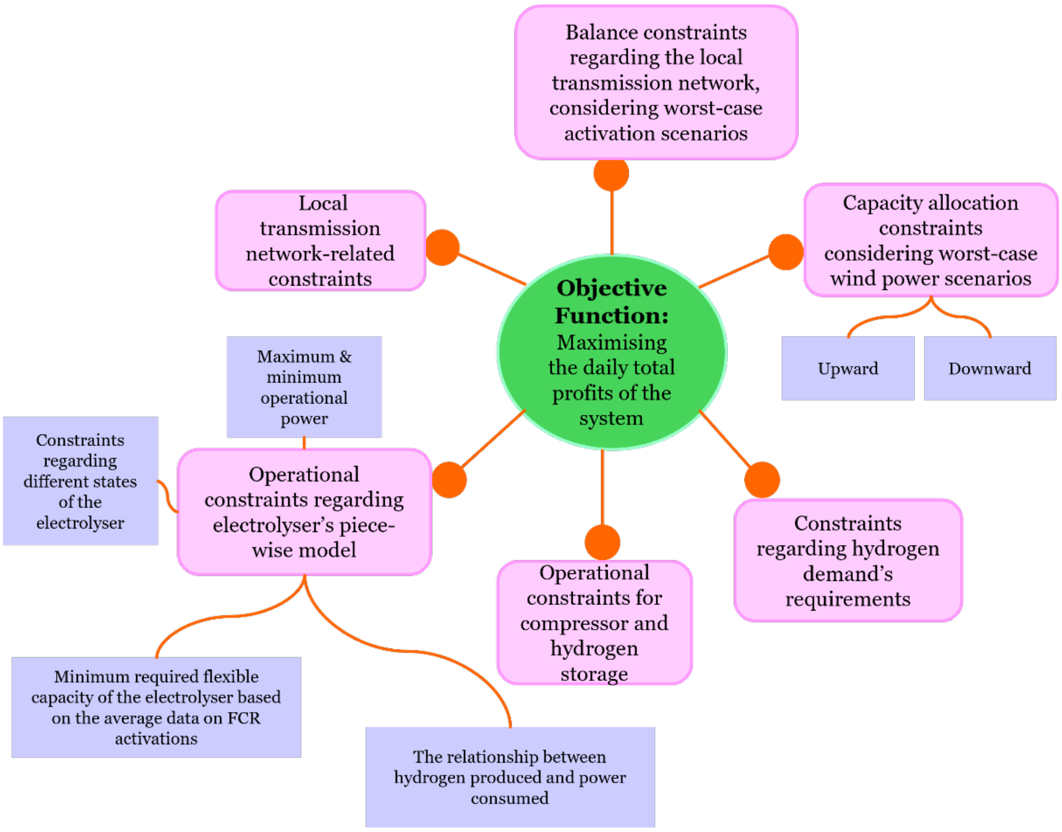


**Figure 32.** The optimisation problem developed by Publication IX that optimises the operation of wind-integrated electrolyser participating in FCR markets.

The objective of our scheduling problem is to maximise daily profit by selling hydrogen and providing FCRs to the TSO. Therefore, the profit from the wind-integrated hydrogen system can be expressed as follows:

$$\begin{aligned}&Daily\ profit = Revenue\ from\ selling\ hydrogen + \\&Revenue\ from\ reserving\ capacity\ for\ FCRs + \\&Activation\ revenue\ from\ upward\ FCR-N - \\&Activation\ cost\ from\ downward\ FCR-D - \\&Electrolyzer's\ startup\ cost\end{aligned} \tag{9}$$

FCR-D services do not include any activation payments, so activation costs and payments apply only to FCR-N services.

The first constraint (Figure 32) is the balance constraint for the local transmission network. In this formulation, upward FCRs inject power into the network, while downward FCRs withdraw power. Additionally, the power flow between two nodes is modelled as the product of the voltage difference between the nodes and the line's susceptance. To model the worst-case activation scenario, two specific scenarios are defined based on historical data. The first scenario assumes that the worst-case FCR-N is activated in only downward direction, with no upward activation. The second scenario assumes the worst-case hourly upward activation, with no downward activation. In both cases, the maximum values for activation are derived from worst-case scenarios of historical data.

Another set of constraints defines the upward and downward flexible capacity that can be offered to the FCR day-ahead capacity markets based on wind power forecasts for the next day. Since Publication IX adopts a robust strategy, it considers worst-case forecasting scenarios to estimate the wind-integrated hydrogen system's flexible capacity for each time slot tomorrow. For each time slot of the next day, these constraints are as follows:

$$FCR - N\ capacity + Upward\ FCR - D\ capacity \leq Minimum\ forecasted\ wind\ power \tag{10}$$

$$FCR - N\ capacity + Downward\ FCR - D\ capacity \leq Maximum\ power\ capacity\ of\ electrolyzer - Maximum\ forecated\ wind\ power \tag{11}$$

Constraint (10) ensures that even if the forecasted wind power drops to its minimum forecasted value, the electrolyser can still inject power, providing upward flexibility to the grid.

Constraint (11) ensures that if the maximum forecasted wind power is realized, the wind-integrated hydrogen system can still consume power, offering downward flexibility.

In Publication IX, the electrolyser is assumed to operate during downward FCR activation. Besides responding to downward activation, the electrolyser must also absorb the non-activated portion of upward FCRs produced by wind turbines. Additionally, since we consider the minimum forecast scenario as upward flexibility, the electrolyser must absorb surplus power generated due to forecasting errors. Thus, the following constraint approximately accounts for the minimum real-time power consumption of the electrolyser, influenced by both FCR service activations and various wind power injection scenarios:

$$\begin{aligned} &Electrolyzer's\ working\ power \\ &\leq The\ average\ estimation\ of\ downward\ activation \\ &+ The\ average\ estimation\ of\ the\ non\ activated\ part\ of\ upward\ capacity \\ &+ The\ average\ error\ of\ wind\ power\ forecast \end{aligned} \tag{12}$$

In (12), the average error is computed by taking the scenario-probability-weighted average of the differences between wind power scenarios and the scenario with the minimum wind power value, which was utilised in constraint (10). It is worth mentioning that the publication estimates the average hourly downward and upward activation based on the historical data to be utilised in (12).

Another set of constraints govern the voltages of nodes and limit the power flowing through the lines within the local transmission network.

Additionally, the hydrogen system, comprising the operation of the electrolyser, compressor, and storage, is modelled. The publication employs a three-state model of the Alkaline electrolyser for this purpose. The model was firstly introduced by (Baumhof et al. 2023).This model includes the following constraints:

- A constraint of binary variables ensures the electrolyser operates in one state only: on, off, or standby.
- Another constraint ensures that power consumption in the on state of the electrolyser remains within specified limits and the maximum power capacity.
- A constraint dictates the fixed power consumption when the electrolyser is in standby mode.
- Startup binary variables are defined to estimate startup costs, with a constraint modelling cold startup, though it is explicitly stated that the electrolyser cannot transition from off to standby mode.

Furthermore, additional constraints model the electrolyser's hydrogen production relative to its electricity consumption. To address the non-linear efficiency of the electrolyser, a piecewise linearization of the function is implemented using binary variables.

Constraints are also established to model the route through which hydrogen demand is fulfilled, either directly from the electrolyser to demand or via the compressor and storage before reaching demand. Capacities of the compressor and storage, as well as the SOC of the storage, are incorporated as constraints in the problem. Figure 33 provides an illustration of the proposed wind-integrated hydrogen system as well as the flow of hydrogen, electricity traded with the main grid and the flexibility provided for the local transmission network.

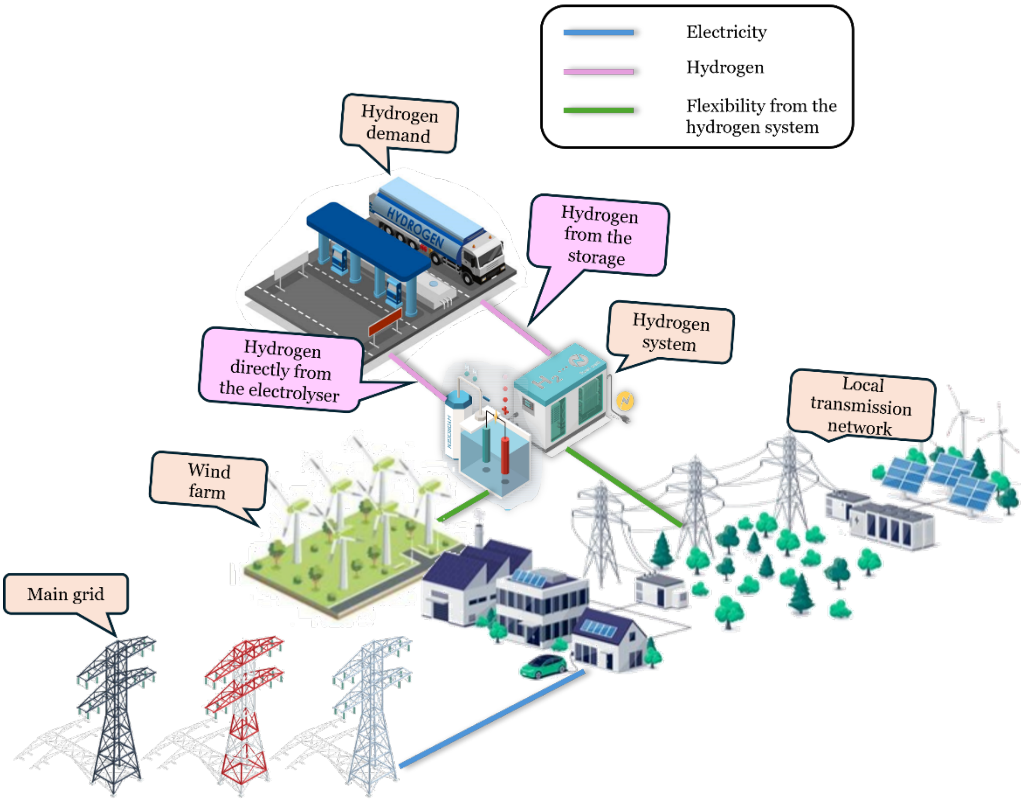


**Figure 33.** Architecture of the wind-integrated hydrogen system providing flexibility for TSO.

To generate various wind power forecast scenarios, the publication utilises an approach involving quantile regression. The methodology includes (Burba 2023):

- Employing quantile regression to model wind power as a function of forecasted wind speed, enabling the prediction of quantiles representing different scenarios.
- Estimating the Cumulative Distribution Function (CDF) by fitting a distribution function to the predicted quantiles using quantile matching.
- Calculating the difference between CDF values at consecutive quantiles to estimate the associated probabilities.
- Normalising the probabilities to ensure their sum equals 1.

## 6.2 Operations comparison (Publication IX)

Publication IX presents a case study showcasing a simplified model of the European HV transmission network. It focuses on the operation of a wind-integrated hydrogen system located at the third node of the local transmission network and other nodes with various types of generation units and demand. Details about hydrogen equipment come from NREL and reference (Baumhof et al. 2023), specifying capacities: 52.25 MWh for the electrolyser, 22 kg for hydrogen storage, and 42 MWh for the wind park. Daily hydrogen demand is assumed to be 1222.44 kg. Real-world price data from Finland in April 2023 is analysed, specifically for FCR markets. Historical frequency data from Finland is examined for activation ratios of FCRs over one year. Activation ratios are computed using equations considering activation droop characteristics. Wind scenarios and their probabilities are determined using quantile regression and the presented scenario generation model. The data related to FCRs, and frequencies were obtained from Fingrid open data platform (Fingrid 2021) and those for wind speed were given from Finnish Meteorological Institute (FMI 2023).

For comparison purposes, Publication IX investigates three distinct operational approaches. While all strategies involve the wind-integrated hydrogen system in managing network congestion, their operational methods differ as outlined below:

- ✓ Proposed operational strategy: The model suggested in the publication, wherein the wind-integrated hydrogen system contributes to both FCR-N and FCR-D provision.
- ✓ Spot strategy: Introduced by (Baumhof et al. 2023), which optimises wind-integrated hydrogen system's operation according to spot market prices.
- ✓ Self-sufficient strategy: Designed to promote local grid self-sufficiency, which aims to minimise power coming into the local transmission network. Costs are also calculated based on spot market prices.

Figure 34 provides a comparison of the daily profits achieved through these three strategies. The findings indicate that engaging in FCR markets can boost wind-integrated hydrogen system's profit by over 2.6 times compared to operating solely based on spot market prices. Moreover, the notable influence of startup costs is apparent in the Self-sufficient strategy, where profits are eight times lower than those in the proposed operational strategy.

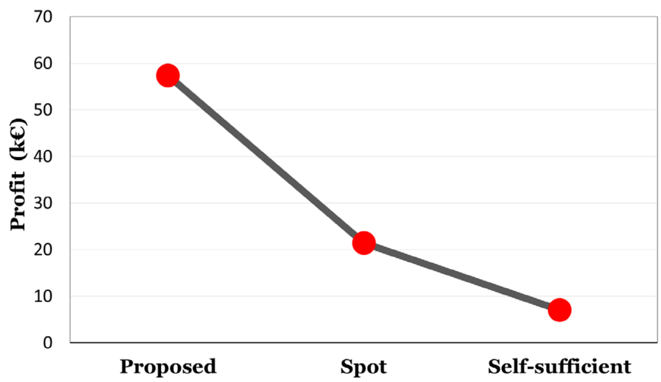


**Figure 34.** Daily profits compared for different cases introduced by Publication IX.

Moreover, the findings indicate that the proposed strategy, which involves participating in FCR markets, results in notably higher hydrogen production compared to other strategies. This is because it utilises the least expensive electricity (FCR activations) for hydrogen production. Conversely, the Self-sufficient operation strategy leads to the least hydrogen production. These results underscore the significant revenue generation potential for the hydrogen system through assisting the TSO.

# 7 CONCLUSION

As power systems increasingly rely on weather-dependent intermittent renewables and phase out conventional generators, their flexibility becomes crucial. Enhancing the flexibility of power systems can be achieved by deploying available FERs across various levels, including distribution and transmission networks. In this sense, this dissertation proposes solutions to better align the operation of FERs with system operators. By doing so, system operators can respond more effectively to both expected and unexpected challenges, thereby improving the overall flexibility and resiliency of power systems.

## 7.1 Research outcomes

The refined answers (A) to the research questions (Q) raised in Chapter 1 (Section 1.2) can be regarded as a part of dissertation's research outcomes:

**Q1 *(Decision-making Under Uncertainties)*:** What is the roadmap towards optimal decision-making from FER's and system operator's perspectives in a smart grid environment?

**A1:** The process of making informed and optimal decisions under various uncertain conditions includes the following steps:

- Specify and Probabilistically Forecast Uncertain Variables: Decision-makers should identify and forecast the uncertain variables in their decision-making process. For FERs, real-time flexibility activation and prices of flexibility services can be considered their uncertain variables whereas system operators can develop probabilistic forecasting models for various parameters such as demand and production within the network, the hosting capacity of their network and their flexibility requirements.

- Generate Scenarios: Based on the probabilistic forecasts, generate scenarios to be used as inputs for the decision-making optimisation problems.

- Develop Optimisation Problems: Depending on the strategy to handle uncertainties, develop a stochastic, robust, or chance-constrained optimisation problem.

For decision-making that demands high resiliency, such as network management or submitting day-ahead bids to capacity markets, a robust strategy is usually preferred. This is because failing to stick to the commitment can result in substantial costs. In contrast, chance-constrained models give the agent more control over specific risks by focusing on meeting constraints with a certain level of confidence. Stochastic models, on the other hand, consider all possible scenarios and their probabilities, providing a comprehensive assessment of potential outcomes.

**Q2 *(Distribution Network Enhancement)*:** How can a DSO analyse its flexibility needs and strengthen the network using FERs?

**A2:** A DSO can analyse the flexibility of its network by estimating its nodal hosting capacity, which indicates the maximum capacity for nodal injection. Consequently, the DSO can take the following steps:

- ➢ Estimate Nodal Hosting Capacity: Use an optimisation-based approach to estimate nodal hosting capacity one day before.
- ➢ Revise Estimates: Adjust the estimate based on the nodal RES forecasts for each node by rerunning the optimisation problem that estimates hosting capacities.
- ➢ Utilise FERs: If the revised hosting capacity estimation does not end up in new values and the optimisation problem does not converge, use available FERs in the network.

To support the final step, a DSO can:

- Define different services and their associated incentive markets for DSO's various flexibility needs, including both expected and unexpected incidents in the network.
- Ensure future DSO-level services provide both active and reactive flexibility.
- Have a continuous collaboration with the TSO regarding flexibility services' design and procurement.

Additionally, the DSO can ask a third company to perform the siting and sizing of BESS(s) to secure the DSO-level network against worst-case scenarios and strengthen the distribution network as much as possible.

**Q3 *(Flexibility Estimation)*:** How is the flexibility of an FER quantified?

**A3:** The flexible capacity of each FER is quantified by estimating the difference between the device's flexible and normal operations. The process involves:

- Downward Flexibility: Quantified by maximising the consumption or minimising the produced power of the device when the system operator needs more withdrawal from the grid.

- Upward Flexibility: Quantified by minimising the consumption or maximising the produced power of the device when the system operator needs more injection to the grid.

Flexible capacity should be estimated considering the operational and technical constraints of the FERs, along with the market needs and strategy adopted by the owners.

**Q4 *(FER Scheduling)*:** How should FERs be scheduled to meet the flexibility requirements of system operators?

**A4:** FER scheduling should prioritize their primary functionalities before addressing system operator flexibility requirements, in line with the services they provide.

For instance, thermostatically controlled appliances should prioritize the thermal comfort of building occupants before adjusting electricity consumption, for example, in response to frequency deviations. For EVs, the priority should be their availability for charging and the final battery status set by the owners before scheduling. BESS has more flexibility but must consider operational constraints like energy and power capacity limits during scheduling.

Developing an optimisation problem can ensure adherence to both device operational limitations and specific flexibility service requirements, while maximising the economic income. Depending on the FER owner's strategy, stochastic, robust, or chance-constrained optimisation problems can be designed.

In addition to solving optimisation problems, FLC methods can effectively manage scheduling by setting rules that account for the operational constraints of FERs, technical requirements, market rules, and the synchronization of different FERs. The FLC method is preferred when the scheduling problem involves complex and non-linear constraints.

**Q5 *(TSO-DSO Flexibility Coordination)*:** How can FERs provide coordinated TSO-DSO flexibility?

**A5:** Clear instructions are essential for FERs when providing flexibility services for both system operators. It is crucial that flexibility provided to one system operator does not compromise the secure operation of another, ensuring the stability of the entire network. Therefore, services for distribution-network-located FERs should be revised to improve TSO-DSO coordination.

For example, if the DSO requires upward flexibility (increased injection) and the TSO needs downward flexibility (decreased injection), FERs with reactive power control can be better options for providing the necessary flexibility to the DSO without disrupting the overall system balance. Additionally, FERs should prioritize flexibility provision according to the urgency of the system's operational requirements.

It is also important to recognize that the DSO's local network has fewer FERs compared to the TSO, which can draw from both DSO-level and TSO-level networks. In scenarios such as a weak distribution network, local FERs should prioritize the DSO’s flexibility needs to maintain local network security.

**Q6 *(Profitability Analysis)*:** Is flexibility provision financially beneficial for FER owners?

**A6:** It has been shown that in Finland, providing flexibility services to the TSO can be considerably more profitable than participating in spot markets or prioritizing self-sufficiency. However, uncertainties must be carefully managed when optimising the FER’s schedule and submitting flexible capacities to day-ahead capacity markets, as failing to meet promised capacities can incur high penalty costs and significant losses. Therefore, the optimisation problem for day-ahead flexible capacity estimation and real-time scheduling must consider all device operational constraints, market requirements, and potential real-time uncertainties such as those related to flexibility activations.

At the time of conducting this research, there are no real-world published prices for DSO-level flexibility services. Future analyses on the profitability of these services can be conducted once DSO-level local markets are realised and real-world data becomes available.

## 7.2 Contributions

In Chapter 1 (Section 1.3), the main contributions were described, and the individual contributions of each publication (I-IX) were outlined in Section 1.4. In this section (7.2), all the dissertation's contributions (I-IX) are listed as follows:

I. **Considering Various FERs:** This dissertation analyses the flexible operation of a range of FERs, including:

- Distribution-network-located resources such as a single BESS, an individual household with EV, EWH, HVAC system, and a small battery, a local energy community with a shared BESS and EVs

- Transmission network-connected resources, such as a wind-integrated hydrogen system

II. **Optimal Scheduling Methodology for FERs:** The dissertation presents an optimal methodology to align the operation of FERs with system operator requirements. Through developed optimisation problems, FERs can respond to flexibility orders based on the chosen service without compromising their primary functionalities. Scheduling is considered in various environments, including smart home and energy community.

III. **Incorporating Service's Technical Requirements & Market Characteristics:** The research emphasises the need for individualized research and modelling for each frequency control reserve service, taking into account the technical requirements and market characteristics of each service in each geographical area. The dissertation incorporates up-to-date technical and market requirements, focusing on Finnish frequency control reserve markets.

IV. **Uncertainty Management Roadmap:** The dissertation outlines a roadmap and strategies for FERs and system operators to manage uncertainties. It offers guidance for making informed decisions in smart grid environments and suggests strategies for robustly submitting flexible capacities of FERs to day-ahead capacity markets. A novel concept, "control parameters of BESS," is introduced to manage real-time uncertainties, along with various scenario generation methodologies tailored for the scheduling and planning problems.

V. **New Optimisation Approach for DSOs:** The dissertation proposes a new optimisation approach for DSOs, estimating maximum injection possibilities at each node and recommending actions based on comparisons between nodal RES forecasts and estimated nodal hosting capacities.

VI. **BESS Sizing and Siting:** The dissertation includes a study on the sizing and siting of a BESS in a distribution network to strengthen the network against worst-case scenarios while maximising BESS profit through participation in a frequency control reserve market, considering the cycle aging characteristics of lithium-ion batteries.

VII. **FERs in Microgrids:** The dissertation reviews potential FERs in microgrids and discusses the development of EMSs for scheduling FERs in microgrids.

VIII. **Coordinated Flexibility Provision:** The dissertation introduces FER's coordinated flexibility provision. It suggests that a transmission-network-located resource provide simultaneous congestion management and frequency control services, while distribution-network-located FERs provide flexibility at both TSO and DSO levels. It also offers guidelines for FERs, particularly when DSO and TSO flexibility needs diverge.

IX. **Profitability Comparison Models:** The dissertation develops comparison models to prove the profitability of frequency control service provision using real-world data and a case study in Finland.

## 7.3 Thesis limitation and future research

Based on the factors that were less focused on in this dissertation, future research can be furthered as follows:

**a) Optimisation of FERs for Providing More Types of Flexibility Services**

This research considered TSO-level services, including FCR-N, FCR-D, mFRR, congestion management, and voltage control in distribution and transmission networks. Future research could explore FER participation in services such as FFR and aFRR, as well as multi-service optimisations. This would involve considering frequency control services, congestion management, and voltage control services simultaneously. In the multi-service optimisation case, the day-ahead flexible capacity of FERs should factor in the forecasted prices of all services in an economic-based objective function. Future works can also include bidding strategies for sending combined bids to upward FCRs and FFR capacity markets. Additionally, FERs participating in multi-service markets must meet prequalification tests and adhere to market rules of all included services. Finally, as local DSO-level markets develop, further analyses should assess the profitability of participating in these markets.

**b) DSO-Level Services Definition & Pricing**

Although this research introduced some key factors for future DSO-level local markets, extensive research is required to define DSO-level services and markets based on the specific needs of each distribution network. Future research should also analyse optimal pricing for DSO-level services. For example, if DSO-level services are priced higher than frequency control services, it may reduce contributions to frequency control and increase imbalance in the system. Therefore, pricing for DSO-level services should be done in relation to TSO-level services, requiring close collaboration between TSOs and DSOs.

**c) Optimisation of Multi-Energy Systems for Flexibility Provision**

This dissertation demonstrated that aligning the hydrogen system's operation with TSO’s flexibility needs yields significant economic benefits for the hydrogen system owner. HVAC and EWH were also optimised to provide flexibility services and profits without compromising customer thermal comfort. This strategy could be extended to optimise and synchronize large-scale hydrogen, gas, heating, and cooling systems with the electrical grid's flexibility needs. This would allow electrical system operators to benefit from various FERs at different levels, while flexibility providers could enjoy monetary benefits and cheaper electricity.

**d) Aggregation Methods for Participating in Flexibility Service Markets**

Analysing aggregation methods was beyond the scope of this dissertation, but extensive work is needed to aggregate different types of FERs for participation in reserve markets. Aggregation methods should account for market limitations regarding the minimum bid for each reserve market and the operational constraints of each FER. Aggregators need to develop methods to maximise FER profits from market participation. Optimising multi-service markets can enhance aggregation profits and mitigate the limitations regarding minimum bids for some services.

# References

Alaperä, Ilari, Tomi Hakala, Elenia Oy, and Samuli Honkapuro. 2019. 'BATTERY SYSTEM AS A SERVICE FOR A DISTRIBUTION SYSTEM OPERATOR'.

Alturki, Mansoor, Amin Khodaei, Aleksi Paaso, and Shay Bahramirad. 2018. 'Optimization-Based Distribution Grid Hosting Capacity Calculations'. *Applied Energy* 219: 350–60. doi:10.1016/j.apenergy.2017.10.127.

Andrenacci, Natascia, and Maria Pia Valentini. 2023. 'A Literature Review on the Charging Behaviour of Private Electric Vehicles'. *Applied Sciences* 13(23): 12877. doi:10.3390/app132312877.

Astero, Poria, and Corentin Evens. 2020. 'Optimum Operation of Battery Storage System in Frequency Containment Reserves Markets'. *IEEE Transactions on Smart Grid* 11(6): 4906–15. doi:10.1109/TSG.2020.2997924.

Baldursson, Friðrik Már, Catherine Banet, and Chi Kong Chyong. 2023. 'Building Resilience in Europe's Energy System'. *Převzaté z: https://cerre.eu/publications/building-resi-lience-in-europes-energy-system/Citované* 5: 2023.

Baumhof, Manuel Tobias, Enrica Raheli, Andrea Gloppen Johnsen, and Jalal Kazempour. 2023. 'Optimization of Hybrid Power Plants: When Is a Detailed Electrolyzer Model Necessary?' In *2023 IEEE Belgrade PowerTech*, Belgrade, Serbia: IEEE, 1–10. doi:10.1109/PowerTech55446.2023.10202860.

Berg, Kjersti, Rubi Rana, and Hossein Farahmand. 2023. 'Quantifying the Benefits of Shared Battery in a DSO-Energy Community Cooperation'. *Applied Energy* 343: 121105. doi:10.1016/j.apenergy.2023.121105.

Berg, Kjersti, Rubi Rana, and Hossein Farahmand. 'Cooperation between an Active DSO and an Energy Community Battery to Improve the Voltage Profile of a Low-Voltage Distribution Grid'. https://www.authorea.com/doi/full/10.36227/techrxiv.21879231.v1?commit=be89f6f54069b611f4de4ba6d61b5d669a027e3f (July 22, 2024).

Burba, Davide. 2023. 'Probabilistic ML with Quantile Matching: An Example with Python'. *Medium*. https://towardsdatascience.com/probabilistic-ml-with-quantile-matching-an-example-with-python-c367eee85f18 (August 12, 2024).

Chyong, Chi Kong, Michael Pollitt, David Reiner, and Carmen Li. 2024. 'Modelling Flexibility Requirements in Deep Decarbonisation Scenarios: The Role of Conventional Flexibility and Sector Coupling Options in the European 2050 Energy System'. *Energy Strategy Reviews* 52: 101322. doi:10.1016/j.esr.2024.101322.

Cired Working Group. 2023. *Network Planning & System Design with Flexibility*.

Cui, Yan, Zechun Hu, and Haocheng Luo. 2020. 'Optimal Day-Ahead Charging and Frequency Reserve Scheduling of Electric Vehicles Considering the Regulation Signal Uncertainty'. *IEEE Transactions on Industry Applications* 56(5): 5824–35. doi:10.1109/TIA.2020.2976839.

Doroudchi, Elahe, Hosna Khajeh, and Hannu Laaksonen. 2022. 'Increasing Self-Sufficiency of Energy Community by Common Thermal Energy Storage'. *IEEE Access* 10: 85106–13. doi:10.1109/ACCESS.2022.3195242.

ENTSO-E. 2019. *Fast Frequency Reserve – Solution to the Nordic Inertia Challenge*. https://www.fingrid.fi/globalassets/dokumentit/en/electricity-market/reserves/fast-frequency-reserve-solution-to-the-nordic-inertia-challenge.pdf (May 12, 2024).

ENTSO-E. 2023. *Technical Requirements for Frequency Containment Reserve Provision in the Nordic Synchronous Area*. https://www.fingrid.fi/globalassets/dokumentit/fi/sahkomarkkinat/reservit/technical-requirements-for-frequency-containment-reserve-provision-in-the-nordic-synchronous-area.pdf (May 13, 2024).

eSett. 2024. 'Picasso'. https://www.esett.com/picasso/ (May 29, 2024).

European Commission. 2020a. 'A Hydrogen Strategy for a Climate-Neutral Europe'. *Communication from the Commission to the European Parliament, the Council, the European Economic and Social Com-Mittee and the Committee of the Regions*.

European Commission. 2020b. 'A Renovation Wave for Europe—Greening Our Buildings, Creating Jobs, Improving Lives'. *Official Journal of the European Union*: 26.

European Commission. 2020c. 'Powering a Climate-Neutral Economy: An EU Strategy for Energy System Integration'.

European Commission. 2020d. 'Sustainable and Smart Mobility Strategy—Putting European Transport on Track for the Future'.

European Commission, EU. 2020e. *An EU Strategy to Harness the Potential of Offshore Renewable Energy for a Climate Neutral Future*. https://eur-lex.europa.eu/legal-content/EN/TXT/HTML/?uri=CELEX%3A52020DC0741.

European Environment Agency. 2024. *Share of Energy Consumption from Renewable Sources in Europe*. https://www.eea.europa.eu/en/analysis/indicators/share-of-energy-consumption-from?activeAccordion=546a7c35-9188-4d23-94ee-005d97c26f2b (May 29, 2024).

Figgener, Jan, Benedikt Tepe, Fabian Rücker, Ilka Schoeneberger, Christopher Hecht, Andreas Jossen, and Dirk Uwe Sauer. 2022. 'The Influence of Frequency Containment Reserve Flexibilization on the Economics of

Electric Vehicle Fleet Operation'. *Journal of Energy Storage* 53: 105138. doi:10.1016/j.est.2022.105138.

Fingrid. 2019. *The Technical Requirements and the Prequalification Process of Automatic Frequency Restoration Reserve (aFRR)*. https://www.fingrid.fi/globalassets/dokumentit/en/electricity-market/reserves/automaattisen-taajuudenhallintareservin-afrr-teknisten-vaatimusten-todentaminen-ja-hyvaksyttamispr_en.pdf (May 29, 2024).

Fingrid. 2021. 'Open Data on the Electricity Market and the Power System'. https://data.fingrid.fi/en.

Fingrid. 2023. *Terms and Conditions for Providers of Manual Frequency Restoration Reserves (mFRR)*. https://www.fingrid.fi/globalassets/dokumentit/fi/sahkomarkkinat/saatosahko/liite-1-mfrr-ehdot-4-2022-hyvaksytyt-ehdot-en.pdf (May 29, 2024).

Fingrid. 2024a. 'Automatic Frequency Restoration Reserve (aFRR)'. https://www.fingrid.fi/en/electricity-market/reserves_and_balancing/automatic-frequency-restoration-reserve/ (May 29, 2024).

Fingrid. 2024b. 'Balancing Energy and Balancing Capacity Markets (mFRR)'. https://www.fingrid.fi/en/electricity-market/reserves_and_balancing/balancing-energy-and-balancing-capacity-markets/ (May 29, 2024).

Fingrid. 2024c. 'Reserves and Balancing Power'. https://www.fingrid.fi/en/electricity-market/reserves_and_balancing/#reserve-obligations-and-procurement-sources (May 29, 2024).

Fingrid. 2024d. *Terms and Conditions for Providers of Automatic Frequency Restoration Reserves (aFRR)*. https://www.fingrid.fi/globalassets/dokumentit/en/electricity-market/reserves/afrr-ehdot-toukokuu2023-muutospyynnon-mukainen_en.pdf (May 29, 2024).

Fingrid. 2024e. *Terms and Conditions for Providers of Fast Frequency Reserves (FFR)*. https://www.fingrid.fi/globalassets/dokumentit/en/electricity-market/reserves/terms-and-conditions-for-providers-of-fast-frequency-reserves-ffr.pdf (May 13, 2024).

Fingrid. 2024f. *Terms and Conditions for Providers of Frequency Containment Reserves (FCR)*. https://www.fingrid.fi/globalassets/dokumentit/en/electricity-market/reserves/terms-and-conditions-for-providers-of-frequency-containment-reserves-fcr-id-391152.pdf (May 13, 2024).

Firoozi, Hooman, Hosna Khajeh, and Hannu Laaksonen. 2021. ‘Flexibility Forecast at Local Energy Community Level’. In *2021 IEEE PES Innovative Smart Grid Technologies Europe (ISGT Europe)*, Espoo, Finland: IEEE, 1–5. doi:10.1109/ISGTEurope52324.2021.9640214.

Firoozi, Hooman, Mohammad Rajabinezhad, Hosna Khajeh, and Hannu Laaksonen. 2021. ‘Active Management of Distribution Networks’. In *Active Electrical Distribution Network: A Smart Approach*,.

Fleer, Johannes, Sebastian Zurmühlen, Jonas Meyer, Julia Badeda, Peter Stenzel, Jürgen-Friedrich Hake, and Dirk Uwe Sauer. 2017. ‘Price Development and Bidding Strategies for Battery Energy Storage Systems on the Primary Control Reserve Market’. *Energy Procedia* 135: 143–57. doi:10.1016/j.egypro.2017.09.497.

FMI. 2023. ‘Download Observations’. https://en.ilmatieteenlaitos.fi/download-observations (August 12, 2024).

FUSION Project Report. 2023. *Role and Value of FUSION Concept in Supporting Cost Effective Electricity System Decarbonisation*. https://www.spenergynetworks.co.uk/userfiles/file/FUSION_CBA_report_Feb_2023.pdf (July 23, 2023).

Guerrero Alonso, Juan Ignacio, Enrique Personal, Sebastián García, Antonio Parejo, Mansueto Rossi, Antonio García, Federico Delfino, Ricardo Pérez, and Carlos León. 2020. ‘Flexibility Services Based on OpenADR Protocol for DSO Level’. *Sensors* 20(21): 6266. doi:10.3390/s20216266.

Hatziargyriou, Nikos. 2023. ‘Differences and Synergies between Local Energy Communities and Microgrids’. *Oxford Open Energy* 2: oiac013. doi:10.1093/ooenergy/oiac013.

IEA. 2018. *Status of Power System Transformation 2018*. https://iea.blob.core.windows.net/assets/ede9f1f7-282e-4a9b-bc97-a8f07948b63c/Status_of_Power_System_Transformation_2018.pdf (August 9, 2024).

Iliceto, Antonio, Natalie Samovich, Nuno Sousa e Silva, and Albana Ilo. 2023. ‘Hydrogen’s Impact on Grids: Impact of Hydrogen Integration on Power Grids and Energy Systems’.

ISGAN. 2013. *Smarter & Stronger Power Transmission: Review of Feasible Technologies for Enhanced Capacity and Flexibility*. https://www.iea-isgan.org/smarter-stronger-power-transmission-review-of-feasible-technologies-for-enhanced-capacity-and-flexibility/ (May 29, 2024).

Jindal, Anish, Jakob Kronawitter, Ramona Kühn, Martin Bor, Hermann de Meer, Antonios Gouglidis, David Hutchison, et al. 2020. ‘A Flexible ICT Architecture to Support Ancillary Services in Future Electricity Distribution Networks: An Accounting Use Case for DSOs’. *Energy Informatics* 3(1): 6. doi:10.1186/s42162-020-00111-x.

Khajeh, Hosna, Hooman Firoozi, Mohammad Reza Hesamzadeh, Hannu Laaksonen, and Miadreza Shafie-Khah. 2021. 'A Local Capacity Market Providing Local and System-Wide Flexibility Services'. *IEEE Access* 9: 52336–51. doi:10.1109/ACCESS.2021.3069949.

Khajeh, Hosna, and Hannu Laaksonen. 2023. 'Flexibility Utilisation Enabling Business Models and Tariff Structures'. In *2023 19th International Conference on the European Energy Market (EEM)*, Lappeenranta, Finland: IEEE, 1–6. doi:10.1109/EEM58374.2023.10161810.

Khajeh, Hosna, Hannu Laaksonen, Amin Shokri Gazafroudi, and Miadreza Shafie-khah. 2019. 'Towards Flexibility Trading at TSO-DSO-Customer Levels: A Review'. *Energies* 13(1): 165. doi:10.3390/en13010165.

Khalili, Tohid, Amirreza Jafari, Mehdi Abapour, and Behnam Mohammadi-Ivatloo. 2019. 'Optimal Battery Technology Selection and Incentive-Based Demand Response Program Utilisation for Reliability Improvement of an Insular Microgrid'. *Energy* 169: 92–104. doi:10.1016/j.energy.2018.12.024.

Laaksonen, Hannu, Hosna Khajeh, and Nikos Hatziargyriou. 2023. 'Novel DER and OLTC Management Scheme for Coordinated TSO-DSO Flexibility Services Provision'. In *2023 IEEE PES Innovative Smart Grid Technologies Europe (ISGT EUROPE)*, Grenoble, France: IEEE, 1–5. doi:10.1109/ISGTEUROPE56780.2023.10407143.

Laaksonen, Hannu, Hosna Khajeh, Chethan Parthasarathy, Miadreza Shafie-khah, and Nikos Hatziargyriou. 2021. 'Towards Flexible Distribution Systems: Future Adaptive Management Schemes'. *Applied Sciences* 11(8): 3709.

LCP Delta & SmartEn. 2023. *2022 Market Monitor for Demand Side Flexibility*.

Liu, Wenjie, Shibo Chen, Yunhe Hou, and Zaiyue Yang. 2021. 'Optimal Reserve Management of Electric Vehicle Aggregator: Discrete Bilevel Optimization Model and Exact Algorithm'. *IEEE Transactions on Smart Grid* 12(5): 4003–15. doi:10.1109/TSG.2021.3075710.

Lüth, Alexandra, Yannick Werner, Ruud Egging-Bratseth, and Jalal Kazempour. 2024. 'Electrolysis as a Flexibility Resource on Energy Islands: The Case of the North Sea'. *Energy Policy* 185: 113921. doi:10.1016/j.enpol.2023.113921.

Manna, Carlo, and Anibal Sanjab. 2023. 'A Decentralized Stochastic Bidding Strategy for Aggregators of Prosumers in Electricity Reserve Markets'. *Journal of Cleaner Production* 389: 135962. doi:10.1016/j.jclepro.2023.135962.

Menghwar, Mohan, Jie Yan, Yongning Chi, M. Asim Amin, and Yongqian Liu. 2024. 'A Market-Based Real-Time Algorithm for Congestion Alleviation Incorporating EV Demand Response in Active Distribution Networks'. *Applied Energy* 356: 122426. doi:10.1016/j.apenergy.2023.122426.

Merten, Michael, Christopher Olk, Ilka Schoeneberger, and Dirk Uwe Sauer. 2020. 'Bidding Strategy for Battery Storage Systems in the Secondary Control Reserve Market'. *Applied Energy* 268: 114951. doi:10.1016/j.apenergy.2020.114951.

Modig, Niklas, Robert Eriksson, Pia Ruokolainen, Jon Nerbø Ødegård, Simon Weizenegger, and Thomas Dalgas Fechtenburg. 2022. *Overview of Frequency Control in the Nordic Power System*. https://www.epressi.com/media/userfiles/107305/1648196866/overview-of-frequency-control-in-the-nordic-power-system-1.pdf (May 13, 2024).

Nikoobakht, Ahmad, Jamshid Aghaei, Roohallah Khatami, Esmaeel Mahboubi-Moghaddam, and Masood Parvania. 2019. 'Stochastic Flexible Transmission Operation for Coordinated Integration of Plug-in Electric Vehicles and Renewable Energy Sources'. *Applied energy* 238: 225–38.

Nitsch, Felix, Marc Deissenroth-Uhrig, Christoph Schimeczek, and Valentin Bertsch. 2021. 'Economic Evaluation of Battery Storage Systems Bidding on Day-Ahead and Automatic Frequency Restoration Reserves Markets'. *Applied Energy* 298: 117267. doi:10.1016/j.apenergy.2021.117267.

Nouicer, Athir, Leonardo Meeus, and Erik Delarue. 2020. 'The Economics of Explicit Demand-Side Flexibility in Distribution Grids: The Case of Mandatory Curtailment for a Fixed Level of Compensation'. doi:10.2139/ssrn.3665989.

Ørum, Erik, Mikko Kuivaniemi, Minna Laasonen, Ivar Bruseth Alf, and Alexander Jansson. *Future System Inertia*.

Osório, Gerardo J., Mohamed Lotfi, Matthew Gough, Mohammad Javadi, Helena M. D. Espassandim, Miadreza Shafie-khah, and João P. S. Catalão. 2021. 'Modeling an Electric Vehicle Parking Lot with Solar Rooftop Participating in the Reserve Market and in Ancillary Services Provision'. *Journal of Cleaner Production* 318: 128503. doi:10.1016/j.jclepro.2021.128503.

Parthasarathy, Chethan, Hosna Khajeh, Hooman Firoozi, Hannu Laaksonen, and Hossein Hafezi. 2022. 'Distributed Generation, Storage and Active Network Management'. In *Deregulated Electricity Structures and Smart Grids*, CRC Press, 83–111.

Production, Flexible Energy. 2023. 'Demand and Storage-Based Virtual Power Plants for Electricity Markets and Resilient DSO Operation'.

Regulation, EU. 2021. '1119 of the European Parliament and of the Council of 30 June 2021 Establishing the Framework for Achieving Climate Neutrality and Amending Regulations (EC) No 401/2009 and (EU) 2018/1999 ("European Climate Law"). Off'. *J. Eur. Union* 50: 243.

Rodrigues, Marta, Tiago Soares, and Hugo Morais. 2023. 'Reactive Power Management Considering Transmission System Operator and

Distribution System Operator Coordination'. *Sustainable Energy, Grids and Networks* 36: 101204. doi:10.1016/j.segan.2023.101204.

Saretta, Marco, Enrica Raheli, and Jalal Kazempour. 2023. 'Electrolyzer Scheduling for Nordic FCR Services'. In *2023 IEEE International Conference on Communications, Control, and Computing Technologies for Smart Grids (SmartGridComm)*, , 1–6. doi:10.1109/SmartGridComm57358.2023.10333890.

Sijakovic, Nenad, Aleksandar Terzic, Georgios Fotis, Ioannis Mentis, Magda Zafeiropoulou, Theodoros I. Maris, Emmanouil Zoulias, et al. 2022. 'Active System Management Approach for Flexibility Services to the Greek Transmission and Distribution System'. *Energies* 15(17): 6134. doi:10.3390/en15176134.

Sridhar, Araavind, Samuli Honkapuro, Fredy Ruiz, Jan Stoklasa, Salla Annala, Annika Wolff, and Antti Rautiainen. 2023a. 'Residential Consumer Preferences to Demand Response: Analysis of Different Motivators to Enroll in Direct Load Control Demand Response'. *Energy Policy* 173: 113420. doi:10.1016/j.enpol.2023.113420.

Sridhar, Araavind, Samuli Honkapuro, Fredy Ruiz, Jan Stoklasa, Salla Annala, Annika Wolff, and Antti Rautiainen. 2023b. 'Toward Residential Flexibility—Consumer Willingness to Enroll Household Loads in Demand Response'. *Applied Energy* 342: 121204. doi:10.1016/j.apenergy.2023.121204.

Vagropoulos, Stylianos I., Pandelis N. Biskas, and Anastasios G. Bakirtzis. 2022. 'Market-Based TSO-DSO Coordination for Enhanced Flexibility Services Provision'. *Electric Power Systems Research* 208: 107883. doi:10.1016/j.epsr.2022.107883.

Venizelou, Venizelos, Apostolos C. Tsolakis, Demetres Evagorou, Christos Patsonakis, Ioannis Koskinas, Phivos Therapontos, Lampros Zyglakis, et al. 2023. 'DSO-Aggregator Demand Response Cooperation Framework towards Reliable, Fair and Secure Flexibility Dispatch'. *Energies* 16(6): 2815. doi:10.3390/en16062815.

Vicente-Pastor, Alejandro, Jesus Nieto-Martin, Derek W. Bunn, and Arnaud Laur. 2019. 'Evaluation of Flexibility Markets for Retailer–DSO–TSO Coordination'. *IEEE Transactions on Power Systems* 34(3): 2003–12. doi:10.1109/TPWRS.2018.2880123.

# Potential Ancillary Service Markets for Future Power Systems

Hosna Khajeh, Hannu Laaksonen
School of Technology and Innovations, Flexible Energy Resources
University of Vaasa
65200 Vaasa, Finland

*Abstract*—**Future renewable-based power systems require more flexible energy resources that provide ancillary services. Ancillary services help transmission system operators (TSO) and distribution system operators (DSO) operate their networks. It is thereby necessary to know the existing ancillary services' technical requirements and market structures in order to design future ancillary or flexibility service markets. In this regard, this paper firstly introduces the existing TSO-level ancillary service markets in Nordic countries. Their technical requirements, capacity prices, and market outcomes are assessed based on the Finnish capacity markets. Then, the DSO-level markets are discussed by introducing the projects that develop markets for DSO needs. Finally, new ancillary service markets are proposed that are designed for the future renewable-based more decentralized system. In the proposed market, local flexible energy resources can provide active and reactive power related flexibility services for both TSO and DSO.**

*Index Terms*—**TSO, DSO, ancillary service markets, frequency regulation, voltage control, congestion management.**

## I. INTRODUCTION

Power systems are going through a major transformation in recent years. The strong growth in the intermittent weather-dependent renewable generation has increased the need for flexibility at different voltage levels of the power system. Both system operators TSO and DSO need to adopt more flexibility to be able to operate their networks in a reliable and efficient manner. At the TSO level, more flexible energy resources (i.e. flexibilities) for frequency control services provision in real-time and near-real-time horizons are needed. In addition, the DSO needs to utilize increasing amount of flexibilities to control local voltages, avoid congestion within feeders, and deal with the issues that arise due to distributed generation (DG) [1].

In this regard, as a first step, clear view about the existing ancillary service markets is required. Then, the new ancillary service markets should be designed to complement the existing ones and also fulfill the increasing future flexibility needs. In the future, also increasing cooperation is needed between DSOs and TSOs in order to maximize the potential collaborative benefits of different flexibilities located at different voltage levels in the system.

Regarding to the first step and existing ancillary service markets, there exists some previous literature. For example, in [2] the existing frequency-related markets in Nordics are briefly described, although some markets are being upgraded at the moment. In addition, the literature focused only on TSO-related ancillary services. However, in future power systems it is expected that also DSOs will need to procure ancillary services. Also, in [3] an evaluation was conducted about the existing ancillary service markets based on their products, architecture, services, and the levels of buyers' and sellers' agreement.

On the other hand, related to the future ancillary service markets, also previous research has been conducted. In [4] a local capacity market was developed for providing DSO needs as well as providing FCR services for the TSO. In [5], the authors presented an interesting framework for trading reactive power as an ancillary service. However, the future ancillary service markets should be able to trade active and reactive power related flexibility services as well as DSO-level flexibility services besides TSO-level ones.

In this paper, first the existing TSO-level ancillary service markets are introduced with a focus on Nordic and Finnish markets. Focus is on the discussion about the characteristics, prices and capacity trading of these services. Then, the paper discusses the DSO-level potential markets and the projects that aim to design markets for DSOs. Finally, the potential future ancillary/flexibility service markets are discussed. These future flexibility markets are proposed to enable participation of small-scale flexible energy resources for the TSO- and DSO-level flexibility services provision.

## II. EXISTING TSO-LEVEL ANCILLARY SERVICE MARKETS

The major share of electricity is traded in the day-ahead spot market. The day-ahead market is settled one day before delivery. Thus, it fails to fulfil the balance requirements of the power system because of forecast errors. There are entities named balance responsible parties (BRP) who are responsible for maintaining the balance within their regions in each trading period. BRPs are allowed to bilaterally trade in the intraday market to compensate for their imbalances. However, taking care of the real-time and near-real-time imbalances is the main responsibility of TSOs. TSOs control real-time imbalances by regulating the system frequency. A frequency deviation indicates the system imbalance. In Europe, the standard frequency is 50 Hz. A small deviation in the range of 0.1 Hz is allowed during normal operation. However, sustained larger deviations result in alert and emergency situations. Fig. 1 illustrates the frequency deviations in which alert and emergency limits are exceeded [6].

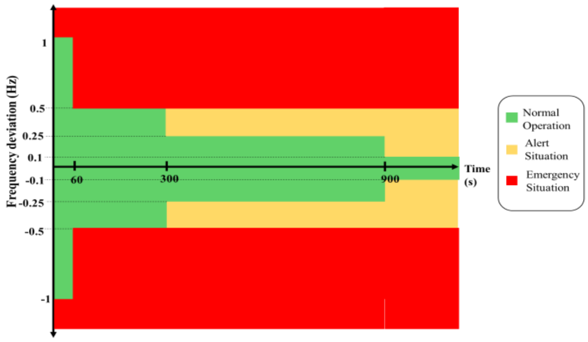


Figure 1. System status based on frequency deviation levels

TSO has different ancillary service markets to reserve the required frequency control capacities. In case of power imbalance (i.e. frequency deviation), full or part of the reserved capacity is activated to compensate/correct the deviation or imbalance. When the frequency is higher than 50 Hz, the TSO needs to increase consumption or decrease the amount of electricity generation. In this case, the TSO activates downward regulation services. Otherwise, if the frequency falls below 50 Hz, the TSO activates upward regulation services to increase the generation or decrease the electricity consumption.

Each level of frequency deviation requires its own frequency regulation service. Table I summarizes the technical requirements of the frequency regulation services, with a focus on the Finnish markets [7]. Fig. 2 is an example obtained from [6] showing which services are activated when a significant disturbance happens in the power system. Frequency deviations during normal operation are compensated by frequency containment reserves for normal operation (FCR-N). FCR-N services react to the frequency deviations in a range of ±0.1 Hz [8], [9]. In disturbance situations, frequency containment reserves for disturbances (FCR-D) are activated. FCR-D responds to the frequency deviations between 0.1-0.5 and -0.5-(-0.1) Hz [9]. Since the deviation in Fig. 2 is larger, it activates FCR-D and FCR-N is not activated. There also exist other services which aim to restore the frequency to the standard range after a disturbance or event. These services are called frequency restoration reserves (FRR). Automatic FRR (aFRR) is activated according to an activation request that is constantly sent by the TSO each 10 seconds. In this way, the volume of frequency deviation in the Nordic synchronous area is measured and the appropriate signal is made accordingly [10]. In case of Finnish aFRR service, when the reserve resource receives the aFRR signal, it should fully activate its reserved capacity in 5 minutes. Manual FRR (mFRR) is the other restoration reserve service. This service compensates for the forecasted imbalances that are expected to happen in a near future. The reserved resource has 15 minutes time to be fully activated when it receives the signal [11].

TABLE I. TECHNICAL REQUIREMENTS AND FEATURES OF RESERVE SERVICES IN FINLAND

| Service | Activation Frequency (Hz) | main feature | Activation time for 100% activation (s) | Minimum bid size (MW) |
|---|---|---|---|---|
| FCR-N | 49.9-50<br>50-50.1 | Symmetrical capacity | 180 | 0.1 |
| FCR-D | 49.5-49.9<br>50.1-50.5 | Upward-downward capacity | 30 | 1 |
| FFR | 49.7, 49.6, 49.5 | Very fast upward capacity | 1.3, 1, 0.7 | 1 |
| aFRR | Not based on frequency | Activated by TSO signals | 350 | 5 |
| mFRR | Not based on frequency | Manual activation requested by TSO | 900 | 5 |

Rather recently, also a service has been introduced and designed for low inertia situations. The modern power system aims to phase out conventional fuel-based generators and replace them with renewable-based units. This will decrease the power system inertia and imposes a risk of high power imbalance. The newly introduced service, named fast frequency reserve (FFR), is responsible for responding extremely fast in a short period of time in situations where the levels of kinetic energy (i.e. inertia) are low. The resource providing FFR is activated in even less than a second when the frequency falls into 49.5 Hz (see Table I) [12].

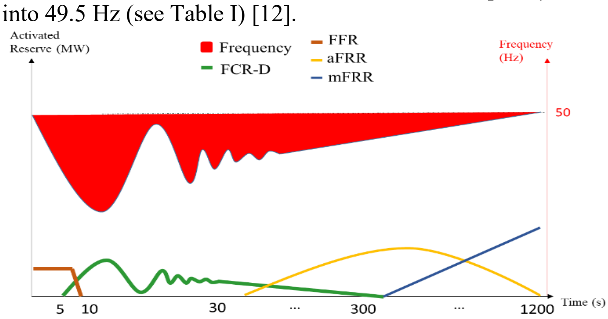


Figure 2. Services activated after a significant disturbance / under-frequency event

Fig. 3 compares the hourly capacity prices of FCR-N, upward FCR-D, FFR, and upward aFRR, in 2021, Finland. As the figure states, FCR-D had some price spikes during the year. Unlike FCR-D, upward aFRR prices did not experience high variations. FFR was more procured during summertime and autumn in low-inertia situations. FCR-N experienced many price volatilities, especially in the summer and autumn. Finnish TSO, Fingrid, has also published the updated annual income if 100 MW resource is reserved for FCR and FFR capacity markets illustrated in Fig. 4. The study considered volume weighted average prices in 2021 and the yearly prices in 2022. As it indicates, participating in the yearly FCR-D down market was the most profitable option while the yearly FCR-D up market leads to less outcome. Since FFR is not being procured as frequent as other services such as FCR-N, it leads to less outcome.

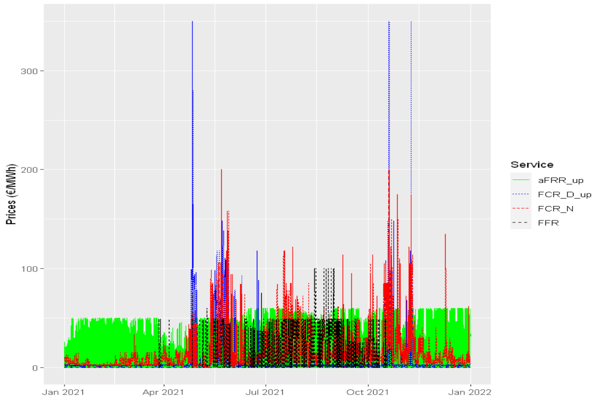


Figure 3. Prices of hourly capacity markets related to upward services in Finland

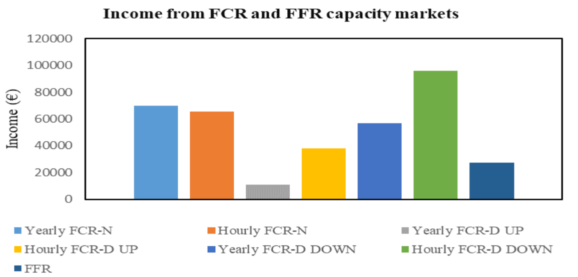


Figure 4. Outcome comparison if 100 MW resource is reserved for providing FCR and FFR services

The following subsection describes with more details the different capacity markets organized for these services.

## A. FCR-N Markets

At the moment, there is not a common FCR-N market in Nordic countries. However, the TSOs may trade FCR-N capacities with each other. Finnish TSO Fingrid organizes yearly and monthly capacity markets. The yearly capacity markets are held every autumn. The highest accepted bid determines the price which will be fixed for each calendar year [13]. On the other hand, the hourly capacity markets for procuring FCR-N are organized before the wholesale day-ahead energy market. Fingrid determines the FCR-N prices for each hour of the next day using the marginal (uniform) pricing principle [13]. Fig. 5 compares the prices of hourly FCR-N capacity markets with that of the yearly capacity market in 2021, Finland. As the figure states, the yearly price guarantees a constant price but the hourly market can have volatile prices which can also increase in the summer and the autumn.

The Swedish TSO, Svenska Kraftnät, and the Danish TSO, Energinet, however, have a common hourly market with two auctions to procure FCR-N capacity: one before and one after the closure of the wholesale day-ahead market [6]. If the capacity of a reserve resource is accepted in the market, it receives payment according to its own offered price. Thus, the settlement is based on the pay-as-bid principle. Statnett, as a Norwegian TSO, also has two national hourly FCR-N sub-markets, before and after the wholesale day-ahead market. It also uses the pay-as-bid principle [6].

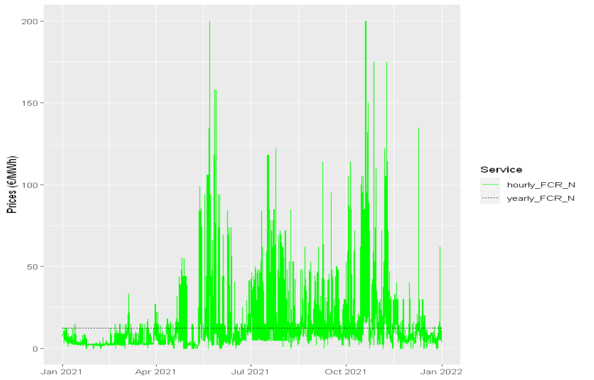


Figure 5. Yearly FCR-N price vs. hourly FCR-N prices in 2021, Finland

## B. FCR-D Markets

Fingrid has two separate hourly and yearly markets to procure upward and downward FCR-D. Also, Energinet and Svenska Kraftnät use the same method as FCR-N and procure FCR-D from their common market. Statnett's FCR-D market follows the same rule as its FCR-N market [6].

## C. FFR Markets

Fingrid purchases the FFR capacity from Estonia and/or the hourly market that is held one day before the actual day, after the wholesale day-ahead market [14]. A reserve provider has the option to submit a combined bid that includes both FCR-D and FFR services. In this way, if the bid is not accepted in the FFR market, it is deployed in the FCR-D market [15]. The FFR market has uniform pricing (marginal) principle.

Svenska Kraftnät organizes two markets for FFR procurement, one with a four-day time horizon (Tuesday-Friday) and the other one with a three-day time horizon (Saturday-Monday). The bids are organized based on a merit-order list and the resources are paid according to the marginal pricing principle [6].

Energinet purchases FFR by organizing hourly markets, similar to Fingrid while Statnett procures the FFR service by organizing a market from May to September. Statnett first reserves the required FFR capacity in the seasonal market. It then requests the short-term capacities from the resources, if needed. The reserve providers are remunerated based on the marginal pricing principle [6].

## D. aFRR Markets

Similar to FCR and FFR markets, there exists no common market for Nordic TSOs procuring aFRR. However, they will define a common market in a near future and at the moment the

TSOs have the opportunity to purchase and sell aFRR bilaterally with each other via inter-TSO trades [16], [17].

At the moment, Fingrid organizes aFRR hourly markets on the day before, based on the marginal pricing principle. From 10th May 2022, Svenska Kraftnät will organize the daily-procured market for aFRR with the same pricing as Fingrid. At the moment Energinet does not have a national market for procuring aFRR [6]. Statnett, on the other hand, has a national hourly market for aFRR. Although it deploys the marginal pricing principle, more expensive bids may be accepted in some situations and be paid based on the pay-as-bid principle [6].

### *E. mFRR Markets*

Although mFRR activation has a common Nordic market, each TSO organizes national markets to procure mFRR capacity. Currently, Fingrid sometimes procures mFRR from mFRR weekly capacity markets. In most of the times, it has its own reserves for providing mFRR[11]. Svenska Kraftnät does not have a national market for mFRR capacity whereas Energinet has an mFRR hourly capacity market for upward regulations within its first zone (DK1). These markets are organized on a day-ahead and marginal pricing basis. Statnett has two seasonal and weekly markets to procure mFRR capacity. One is held every Friday and the other market is organized for wintertime. The mFRR capacity is procured in these two markets based on the current situation of the power system and the related constraints [6].

## III. DSO-level Markets

The increasing integration of inverter-based and intermittent renewable energy sources like solar photovoltaic (PV) in distribution networks and the growing number of electric vehicles (EVs) can lead to voltage limit violations and may create congestions in distribution network lines. Therefore, in order to avoid excessive investments in capacity upgrades by passive network components (lines, transformers etc.) DSOs could increasingly deploy coordinated and adaptive active network management (ANM) schemes based on distributed energy resources (DER) active and reactive power related flexibility services utilization and hosting capacity improvement [18]-[20]. In addition, DSOs may need a market to reserve flexible capacities to use them when needed. For example, flexible DER connected to the distribution network can support voltage control by their local voltage control functions like reactive power-voltage ($QU$) -droop and active power voltage ($PU$) -droop. [18]-[21].

To the best of the authors' knowledge, there is not a real-world DSO-level market that aims to help DSOs operate their networks. However, there are certain pilot projects and research studies that propose DSO-level markets for controlling local voltages and congestion [21], [22]. For example, two pilots have been developed to implement flexibility markets in distribution networks in NODES-project [23], [24]. They aim to analyze if the flexibility markets are able to solve voltage challenges on an island and mainland. The first area is far away from the main power system. The main challenge in this case were under-voltage problems at peak hours. Thus, the flexibility market was implemented to buy flexibility during these periods. The purchased flexibility decreases the loads in order to maintain voltage level between target limits [24]. The second flexibility market is implemented on an island in Norway. A local flexibility market aims to resolve future voltage limit violation issues due to the electrification of the ferry and other future activities related to the growing businesses on the island [22].

Enera is another project with a pilot located in the windy Northwest of Germany [21], [25]. The project aims to unlock flexibility in order to avoid wind power curtailment (i.e. increase wind power hosting capacity). In this project, DSOs purchase flexibility in the intraday timeframe to manage congestion within their networks. GOPACS is another interesting project based in Netherland. It is integrated into a national intraday platform called Energy Trading Platform Amsterdam (ETPA) and it tries to be connected to other market platforms as well. If flexibility offers have a locational tag, they can be sold to GOPACS. Accordingly, GOPACS finds the best and cheapest resources for alleviating congestion within the network [22], [26].

## IV. Potential Flexibility Markets for the Future Power Systems

Renewable-based power systems, with some share of synchronous generation and natural inertia, require ancillary/flexibility service markets that have the following features:

1- The new flexibility (ancillary service) markets should unlock the flexibility of small-scale resources as well as large-scale ones. They are established locally for local participants.
2- They need to provide the local DSO and the TSO with their flexibility requirements in coordinated manner (optimally also collaborative benefit of the flexibility could be simultaneously maximized for the DSO and TSO). In this regard, they should make some rules for local resources so that they would know how to react in different situations.
3- DSOs can utilize the reactive power ($Q$) related flexibility in distribution networks as well as active power ($P$) related flexibility services. Reactive power flexible resources such as inverter-based DER can thereby participate in these markets.

In the first stage, flexible capacities could participate in capacity markets. Capacity markets could be organized locally for each frequency control service. Correspondingly, a local DSO needs to define different services with different activation times for normal, alert, and emergency situations. Future low-/variable inertia power system frequency control may also require restructuring of the frequency markets and respective frequency deviation levels [18], [19]. Each flexibility service needs its own capacity market. Similar to the TSO services, a DSO might also define a fast symmetrical reserve service to overcome the real-time voltage variations resulting from renewable DER during normal operation and another fast service designed for unexpected situations that cause higher voltage deviations and/or congestion. A slower service is also required to avoid predicted congestion and to manage voltage at peak or off-peak hours of the day. The capacity markets guarantee the flexible capacities that are required for the near future (e.g. tomorrow in case of a day-ahead market). Fig. 6 summarizes the proposed markets.

The TSO and the local DSO can submit their flexibility offers as buyers. The DSO deploys both active and reactive-power flexibility. Flexible energy resources owners submit bids separately for their flexible active and reactive power. The DSO has an option to run optimal power flow and select the cheapest service according to the needs. There might be some time in which the needs of the TSO and the DSO contradict each other. For example, a DSO may ask for upward flexibility while the frequency deviation needs downward flexibility. In these situations, the DSO is better to use reactive power flexibility in order not to adversely affect the frequency. Hence, the DSO should reserve enough reactive-power capacity besides active power to operate its network cooperatively and effectively. Coordinated operation of different marketplaces at DSO and TSO level with certain main principles for services prioritization will be important in order to achieve maximum societal and collaborative value of flexibilities. It is also worth mentioning that, for example, voltage control related ANM schemes at DSO level could also be a combination of dynamic distribution tariffs and local flexibility markets.

Flexible resources have different flexibility levels [27]. For example, batteries are highly flexible because their operating time and power are controllable and they can respond to the flexibility signals very fast. However, thermal controllable loads are less flexible since their main objective is to maintain the thermal comfort of their owners at a good level. Thus, similar to the existing capacity markets, each future capacity market should have its technical requirement. The reserved resource must therefore pass the prequalification tests before entering the market.

Pricing is an important factor in organizing a market. It can motivate or discourage participants to continue trading in the market. The pricing principle of the future markets can be uniform pricing similar to most existing capacity markets. Reactive and active power capacity markets can have different prices. Upward and downward capacities can be settled separately. The flexibility providers submit their offers based on their marginal costs. For instance, the reactive power resources may consider the cost of losses, switching costs and lost opportunity costs when they submit their bids [28]. The time horizon and granularity of the capacity markets can be determined based on the flexibility needs of the system and the requirements of the service.

In real-time the resources would react based on the flexibility signals, they receive. TSO-level services mostly require a frequency measurement and the reaction should be according to the frequency deviation. The DSO also may transfer flexibility signals to the resources indicating which types of service it needs and whether it needs upward/downward or active/reactive power flexibility. The activation prices can be the same for all capacity markets or DSOs may determine their own activation prices. However, they should be competitive enough so to incentivize the flexible resources to participate in DSO capacity markets. As mentioned before, the DSO activates reactive power flexibility, rather than active power, if its flexibility needs contradict that of the TSO.

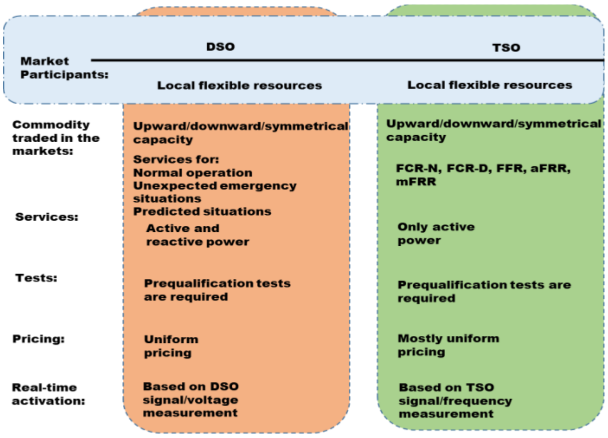


Figure 6. Some characteristics of the future capacity markets that can be organized by TSO and DSO

## V. CONCLUSION

Flexibility/ancillary services play an important role in the future renewable-based power systems. This paper first introduced the existing technical ancillary service markets in Nordic countries. They are mainly designed for TSOs frequency control purposes. Each frequency deviation level requires its own flexibility/ancillary service market. For example, FCR-N reacts to the deviation in normal operation and FFR service is deployed to handle low-inertia situations and FRR services try to restore the frequency. The paper then discussed the technical requirements, market structures and the outcomes that a reserve service provider can achieve after providing these services.

The modern power systems have a number of DER units connected to distribution networks which can adversely affect the operation of the networks. Thus, DSOs also need to establish their local flexibility/ancillary service markets in the future. The paper discussed the related projects in this regard. Finally, we introduced the potential flexibility/ancillary service markets basic structure for the future increasingly decentralized power systems. Unlike the existing ancillary service markets that have a minimum capacity limit for the participants, the proposed markets are established locally for all-sized local resources. They provide both DSO and TSO with reactive and active power-based flexibility services. Each DSO and TSO market could organize separate capacity markets for their various operation needs in a coordinated/collaborative way and some of the related details were discussed in the paper. The work can be continued in the future by developing the proposed flexibility/ancillary service markets in terms of pricing method and market settlement. In addition, more future works are required to develop DSO-level services for normal, alert and emergency situations.

## ACKNOWLEDGEMENT

The work of Hosna Khajeh was supported by the Ella and Georg Ehrnrooth Foundation in Finland.

REFERENCES


[1] A. G. Givisiez, K. Petrou, and L. F. Ochoa, "A Review on TSO-DSO Coordination Models and Solution Techniques," *Electric Power Systems Research*, vol. 189, p. 106659, Dec. 2020, doi: 10.1016/j.epsr.2020.106659.

[2] A. Khodadadi, L. Herre, P. Shinde, R. Eriksson, L. Soder, and M. Amelin, "Nordic Balancing Markets: Overview of Market Rules," in *2020 17th International Conference on the European Energy Market (EEM)*, Stockholm, Sweden, Sep. 2020, pp. 1–6. doi: 10.1109/EEM49802.2020.9221992.

[3] G. Rancilio, A. Rossi, D. Falabretti, A. Galliani, and M. Merlo, "Ancillary services markets in europe: Evolution and regulatory trade-offs," *Renewable and Sustainable Energy Reviews*, vol. 154, p. 111850, Feb. 2022, doi: 10.1016/j.rser.2021.111850.

[4] H. Khajeh, H. Firoozi, M. R. Hesamzadeh, H. Laaksonen, and M. Shafie-Khah, "A Local Capacity Market Providing Local and System-Wide Flexibility Services," *IEEE Access*, vol. 9, pp. 52336–52351, 2021, doi: 10.1109/ACCESS.2021.3069949.

[5] D. Jay and K. S. Swarup, "A comprehensive survey on reactive power ancillary service markets," *Renewable and Sustainable Energy Reviews*, vol. 144, p. 110967, Jul. 2021, doi: 10.1016/j.rser.2021.110967.

[6] N. Modig, R. Eriksson, P. Ruokolainen, J. Odegard, S. Weizenegger, and T. Fechtenburg, "Overview of Frequency Control in the Nordic Power System," Nordic Analysis Group, Mar. 2022. Accessed: Apr. 02, 2022. [Online]. Available: https://www.fingrid.fi/en/pages/news/news/2022/overview-of-frequency-control-in-the-nordic-power-system-published/

[7] H. Khajeh, H. Firoozi, and H. Laaksonen, "Flexibility Potential of a Smart Home to Provide TSO-DSO-level Services," *Electric Power Systems Research*, vol. 205, p. 107767, Apr. 2022, doi: 10.1016/j.epsr.2021.107767.

[8] P. Hasanpor Divshali and C. Evens, "Optimum Operation of Battery Storage System in Frequency Containment Reserves Markets," *IEEE Transactions on Smart Grid*, vol. 11, no. 6, pp. 4906–4915, Nov. 2020, doi: 10.1109/TSG.2020.2997924.

[9] Fingrid, "The technical requirements and the prequalification process of Frequency Containment Reserves (FCR)," no. January, p. 17, 2019.

[10] Fingrid, "The technical requirements and the prequalification process of Automatic Frequency Restoration Reserve (aFRR)," Jan. 2019. Accessed: Mar. 20, 2022. [Online]. Available: https://www.fingrid.fi/globalassets/dokumentit/en/electricity-market/reserves/automaattisen-taajuudenhallintareservin-afrr-teknisten-vaatimusten-todentaminen-ja-hyvaksyttamispr_en.pdf

[11] Fingrid, "Reserves and Balancing Power." https://www.fingrid.fi/en/electricity-market/reserves_and_balancing/#reserve-obligations-and-procurement-sources (accessed Mar. 20, 2022).

[12] Fingrid, "The technical requirements and the prequalification process of Fast Frequency Reserve (FFR)." Accessed: Mar. 20, 2022. [Online]. Available: https://www.fingrid.fi/globalassets/dokumentit/en/electricity-market/reserves/the-technical-requirements-and-the-prequalification-process-of-fast-frequency-reserve-ffr.pdf

[13] Fingrid, "Terms and conditions for providers of Frequency Containment Reserves (FCR)." Accessed: Apr. 01, 2022. [Online]. Available: https://www.fingrid.fi/globalassets/dokumentit/en/electricity-market/reserves/fcr-liite1---ehdot-ja-edellytykset_en.pdf

[14] Fingrid, "Fast Frequency Reserve." https://www.fingrid.fi/en/electricity-market/reserves_and_balancing/fast-frequency-reserve/#technical-requirements (accessed Apr. 01, 2022).

[15] Fingrid, "Terms and conditions for providers of Fast Frequency Reserves (FFR)." Accessed: Apr. 01, 2022. [Online]. Available: https://www.fingrid.fi/globalassets/dokumentit/en/electricity-market/reserves/terms-and-conditions-for-providers-of-ffr.pdf

[16] Fingrid, "Automatic frequency restoration reserve." https://www.fingrid.fi/en/electricity-market/reserves_and_balancing/automatic-frequency-restoration-reserve/ (accessed Apr. 01, 2022).

[17] Fingrid, "Terms and conditions for providers of automatic Frequency Restoration Reserves (aFRR)." Accessed: Apr. 01, 2022. [Online]. Available: https://www.fingrid.fi/globalassets/dokumentit/en/electricity-market/reserves/reservitoimittajien-afrr-ehdot-ja-edellytykset_en.pdf

[18] H. Laaksonen, C. Parthasarathy, H. Khajeh, M. Shafie-Khah, and N. Hatziargyriou, "Flexibility Services Provision by Frequency-Dependent Control of On-Load Tap-Changer and Distributed Energy Resources," *IEEE Access*, vol. 9, pp. 45587–45599, 2021, doi: 10.1109/ACCESS.2021.3067297.

[19] H. Laaksonen, H. Khajeh, C. Parthasarathy, M. Shafie-khah, N. Hatziargyriou, "Towards Flexible Distribution Systems: Future Adaptive Management Schemes," *Applied Sciences*, vol. 11, Issue 8, 3709, MDPI, 2021, https://doi.org/10.3390/app11083709.

[20] H. Laaksonen, C. Parthasarathy, H. Hafezi, M. Shafie-khah, H. Khajeh, N. Hatziargyriou, "Solutions to Increase PV Hosting Capacity and Provision of Services from Flexible Energy Resources," *Applied Sciences*, Vol. 10, Issue 15, 2020, https://doi.org/10.3390/app10155146.

[21] ENTSOE, "Voltage Market (for Distributed Energy Resources)." https://www.entsoe.eu/Technopedia/techsheets/voltage-market-for-distributed-energy-resources (accessed Apr. 01, 2022).

[22] T. Schittekatte and L. Meeus, "Flexibility markets: Q&A with project pioneers," *Utilities Policy*, vol. 63, p. 101017, Apr. 2020, doi: 10.1016/j.jup.2020.101017.

[23] "NODES (Marketplace for trading decentralised flexibility)." https://nodesmarket.com/ (accessed Apr. 01, 2022).

[24] H. Sæle *et al.*, "EXPERIENCE FROM NORWEGIAN INTELLIGENT ELECTRICITY DISTRIBUTION PILOT PROJECTS," in *CIRED 2021 - The 26th International Conference and Exhibition on Electricity Distribution*, Online Conference, 2021, pp. 3339–3343. doi: 10.1049/icp.2021.1924.

[25] "Enera Project." https://www.usef.energy/implementations/enera/ (accessed Apr. 01, 2022).

[26] "GOPACS (The platform to solve congestion in the electricity grid)." https://en.gopacs.eu/ (accessed Apr. 01, 2022).

[27] H. Khajeh, H. Firoozi, H. Laaksonen, and M. Shafie-khah, "A New Local Market Structure for Meeting Customer-Level Flexibility Needs," in *2020 International Conference on Smart Energy Systems and Technologies (SEST)*, Istanbul, Turkey, Sep. 2020, pp. 1–6. doi: 10.1109/SEST48500.2020.9203499.

[28] T. Wolgast, S. Ferenz, and A. Niebe, "Reactive Power Markets: A Review," *IEEE Access*, vol. 10, pp. 28397–28410, 2022, doi: 10.1109/ACCESS.2022.3141235.

CIRED 2024 Vienna Workshop 19 – 20 June 2024

Paper 0070

# Quantifying the Impact of Day-ahead Renewable Forecasts on DER Hosting Capacity Estimation

***Hosna Khajeh*, Sahar Seyyedeh-Barhagh, Hannu Laaksonen***

*Flexible Energy Resources, School of Technology and Innovations, University of Vaasa, Vaasa, Finland*

**hosna.khajeh@uwasa.fi*

**Keywords**: DSO, OPTIMIZATION-BASED HOSTING CAPACITY ESTIMATION, DISTRIBUTION NETWORKS, DER FORECASTS

## Abstract

This research paper presents a novel optimization approach to estimate short-term hosting capacity of distributed energy resources (DER) within a local distribution network. It emphasizes how DER day-ahead forecasts at various nodes can significantly impact both total and nodal hosting capacities. By analysing these forecasts, the distribution system operator (DSO) can proactively adjust the hosting capacity estimation to ensure network short-term operational security under different scenarios. Our study case with Finnish urban network model confirms that nodes at the beginning of the feeder have higher nodal hosting capacity. Crucially, even 40 % variations in DER forecasts for these high-capacity nodes can substantially affect the entire network's hosting capacity. This highlights the paramount importance of accurate DER forecasts, particularly for these critical points within the DSO network.

## 1. Introduction

Estimating the day-ahead hosting capacity (HC) of DER is vital for operational planning of distribution networks and making informed decisions about future actions. DER HC refers to the maximum amount of DERs that can be integrated into a distribution network without surpassing network operation limits, such as voltage or current limits, before needing control adjustments or system upgrades [1], [2]. Accurate DER hosting capacity estimation ensures that DSOs can integrate DERs into the network safely and reliably. However, day-ahead DER HC estimation is greatly affected by day-ahead DER forecasts.

Various research efforts have focused on estimating the HC of distribution networks, as detailed in [3], [4]. Notably, deterministic approaches, such as that analysed by [5], have delved into flexibility from storage, PV power curtailment scenarios, substation overloading possibilities, and different load penetration levels in HC estimation. Reference [6] explored HC by varying DER penetration levels and assessing impacts on voltage fluctuations across various loading conditions. Similarly, [7] aimed for faster convergence in estimating HC, considering composite load models and complex power. Reference [8] investigated relationships between maximum PV generation, feeder impedance, load, and network HC.

In general, HC estimation is affected by factors like load and DER scenarios, alongside network features and limitations such as voltage levels, the current carrying capacity of cables as well as overload limits of transformers, unbalances, harmonics, and flickers [9]. However, previous literature largely overlooked the effects of DER forecasts on HC estimation. This paper, therefore, tries to address this gap by examining the impacts of DER forecasts on nodal and total HCs of networks. The paper's main contributions can be summarised as follows:

- Proposing a new optimization-based method using a piecewise linearized power flow model to estimate HC of distribution networks.
- Suggesting that the DSO revises estimated short-term (day-ahead) HC based on day-ahead DER forecasts. This enables the DSO to ensure network operational security and reliability effectively.
- Utilizing a real-world Finnish urban distribution network model to estimate HCs based on the proposed approach, alongside conducting thorough sensitivity analyses to demonstrate how individual node's DER forecast can affect nodal and total HCs.

The rest of the paper is organised as follows. Section 2 introduces the new optimization-based HC estimation, while Section 3 discusses revised HC estimation and DER forecast effects. Section 4 presents the case study, and Section 5 implements the proposed methodology on the case study and conducts sensitivity analysis. Finally, Section 6 discusses results and concludes the paper.

## 2. Optimization-based Hosting Capacity Estimation

The objective of HC estimation is to determine the maximum amount of power that DERs at all nodes can inject into the network under scenario $s$:

$$\max_{HC_{n,s}} \sum_n HC_{n,s} \qquad (1)$$

Where, $HC_{n,s}$ represents the hosting capacity of node $n$ (i.e. nodal hosting capacity) estimated for scenario $s$. The objective function (1) is limited by distribution network power flow constraints. This paper uses the piecewise linearized power flow equations as described by [10], [11]. These constraints are formulated as follows:

$$P^{2net}_{n=PoC,s} + HC_{n,s} - P^{D}_{n,s} - \sum_{n'}(P^{+}_{n,n',s} - P^{-}_{n,n',s} + R_{n,n'}SI_{n,n',s}) + \sum_{n'}(P^{+}_{n',n,s} - P^{-}_{n',n,s}) = 0 \quad (2)$$

$$Q^{2net}_{n=PoC,s} + Q^{DER}_{n,s}{}_{n,s} - Q^{D}_{n,s} - \sum_{n'}(Q^{+}_{n,n',s} - Q^{-}_{n,n',s} + X_{n,n'}SI_{n,n',s}) + \sum_{n'}(Q^{+}_{n',n,s} - Q^{-}_{n',n,s}) = 0 \quad (3)$$

$$SV_{n,s} - SV_{n',s} - Z^{2}_{n,n'}SI_{n,n',s} - 2R_{n,n'}\left(P^{+}_{n,n',s} - P^{-}_{n,n',s}\right) - 2X_{n,n',s}\left(Q^{+}_{n,n',s} - Q^{-}_{n,n',s}\right) = 0 \quad (4)$$

$$\underline{V}^2 \leq SV_{n,s} \leq \overline{V}^2 \quad (5)$$

$$\underline{I}_{n,n'}{}^2 \leq SI_{n,n',s} \leq \overline{I}_{n,n'}{}^2 \quad (6)$$

$$\underline{P} \leq P^{2net}_{n,s} \leq \overline{P} \quad (7)$$

$$\underline{Q} \leq Q^{2net}_{n,s} \leq \overline{Q} \quad (8)$$

$$P^{+}_{n,n',s} + P^{-}_{n,n',s} \leq V^{rated}\overline{I}_{n,n'} \quad (9)$$

$$Q^{+}_{n,n',s} + Q^{-}_{n,n',s} \leq V^{rated}\overline{I}_{n,n'} \quad (10)$$

$$V^{rated^2}SI_{n,n',s} = \sum_i(2i-1)\,\Delta S_{n,n'}\,\Delta P_{n,n',s,i} + \sum_i(2i-1)\,\Delta S_{n,n'}\,\Delta Q_{n,n',s,i} \quad (11)$$

$$P^{+}_{n,n',s} + P^{-}_{n,n',s} \leq \sum_i \Delta P_{n,n',s,i} \quad (12)$$

$$Q^{+}_{n,n',s} + Q^{-}_{n,n',s} \leq \sum_i \Delta Q_{n,n',s,i} \quad (13)$$

$$0 \leq \Delta P_{n,n',s,i} \leq \Delta S_{n,n'} \quad (14)$$

$$0 \leq \Delta Q_{n,n',s,i} \leq \Delta S_{n,n'} \quad (15)$$

$$\Delta S_{n,n'} = \frac{V^{rated}\,\overline{I}_{n,n'}}{N^{i}} \quad (16)$$

$$P^{+}_{n,n',s}, P^{-}_{n,n',s}, , Q^{+}_{n',n,s}, Q^{-}_{n',n,s}, HC_{n,s}, \Delta P_{n,n',s}, \Delta Q_{n,n',s} \geq 0 \quad (17)$$

Where, constraint (2) is an active power balance equation, keeping balance between the active power entering/leaving the local distribution network, i.e. $P^{2net}_{n=PoC,s}$, the maximum power that can be injected into the network, $HC_{n,s}$, the power consumed by the local demand, $P^{D}_{n,s}$, and the active power flowing through lines, indicating by $\sum_{n'}(P^{+}_{n,n',s} - P^{-}_{n,n',s} + R_{n,n',s}SI_{n,n',s}) + \sum_{n'}(P^{+}_{n',n,s} - P^{-}_{n',n,s})$. In this term, $P^{+}_{n,n',s}$ denotes the active power that flows in a downstream direction from $n$ to $n'$. Correspondingly, $P^{-}_{n,n',s}$ indicates the flowing active power from $n$ to $n'$ in an upstream direction.

Constraint (3) applies the same balance as (2), between the reactive power injections and consumptions. It includes the reactive power entering/leaving the local distribution network at point of coupling (PoC), i.e. $Q^{2net}_{n=PoC,s}$, the reactive power injected by the DER, $Q^{DER}_{n,s}$, the reactive power consumed by the local demand, $Q^{D}_{n,s}$, as well as the reactive power flowing through the lines. Similarly, $Q^{+}_{n,n',s}$ represents the reactive power flowing in a downstream direction from $n$ to $n'$ and $Q^{-}_{n,n',s}$ is the reactive power transmitting from $n$ to $n'$ in an upstream direction. Moreover, $R_{n,n'}, X_{n,n'}$ and $Z_{n,n'}$ refer to the resistance, reactance, and impedance of the line between $n$ and $n'$.

It should be highlighted that (3) and (4) are applied at each node $n$ for each scenario $s$.

Equation (4) describes the relationship between the lines' flowing power and the voltages of nodes. In this constraint, $SV_{n,s}$ serves as an alternative variable equal to the squared voltage at node $n$ under scenario $s$. Also, $SI_{n,n',s}$ is an alternative variable substituting the squared current flowing between $n$ and $n'$ under scenario $s$.

Constraints (5) and (6) restrict the squared voltages and squared currents to stay within their minimum values ($\underline{V}^2, \underline{I}_{n,n'}{}^2$) and their maximum values ($\overline{V}^2, \overline{I}_{n,n'}{}^2$). Similarly, constraints (7) and (8) limit the values of active and reactive power allowed to enter and exit the local distribution network, taking into account the capacity of the transformer. $\underline{P}$ and $\underline{Q}$ represent the minimum active and reactive power, while $\overline{P}$ and $\overline{Q}$ indicate the maximum active and reactive power ranges, respectively.

Constraints (9) and (10) ensure that there is no congestion within the lines, where $V^{rated}$ denotes the rated voltage.

Constraints (11)-(16) pertain to the piecewise linearization technique applied to the power flow equations. In these constraints, $i$ is the index showing the partition used in piecewise linearization and $N^{i}$ indicates the total number of partitions. The parameter $\Delta S_{n,n'}$ refers to the maximum apparent power that can flow between $n$ and $n'$ in the piecewise-linearized power flow. The variables $\Delta P_{n,n',s,i}$ and $\Delta Q_{n,n',s,i}$ represent the discretised active and reactive power for partition $i$ flowing between $n$ and $n'$ under scenario $s$.

After solving optimization problem (1)-(17) and identifying the maximum/optimum amount of nodal DER injection ($HC^{opt}_{n,s}$) for each scenario, the nodal HC of the network is determined by finding the minimum value of the nodal DER injection across all scenarios. This implies that the nodal HC is obtained as follows:

$$Nodal\ HC = HC_n{}^{opt} = \min_s HC_{n,s}^{opt} \qquad (18)$$

The total HC of the network is obtained by summing up the nodal HCs of the distribution network:

$$HC = \sum_n HC_n{}^{opt} \qquad (19)$$

## 3. The Impact of DER Forecasts on HC Estimation

Assume that a DSO executes equations (1)-(18) to determine the maximum values for the nodal HC of its distribution network on a day-ahead basis. Thus, the DSO should utilize forecasted values of nodal consumption for the parameter $P_n^D$. Additionally, it receives forecasts of nodal DER generation. Then, the following situations may arise:

Case I) The forecasted DER generations are all equal or below the nodal HCs of the network.

Case II) At some nodes, the forecasted DER generations exceed their estimated nodal HCs.

Case III) The DER generation forecasts for nodes indicate that all nodes are expected to generate power exceeding their nodal HCs.

The DSO does not need to take action in Case I. However, in Case II, the DSO can implement the following measures to ensure network security:

1) Set the value of the nodal HC with higher DER forecast to be equal to their forecasts:
   $HC_{n,s} = Forecast_n\ if\ Forecast_n \geq HC_n{}^{opt}$ (19)
   Where, $Forecast_n$ is the DER generation forecast for node $n$.
2) Execute (1)-(18) with the fixed parameters of HC for those nodes whose DER forecasts are higher. Subsequently, if the optimization problem is solved, it gives you a new set of values for nodal HCs. Thus, the DSO revises its nodal and total HCs according to the new results.
3) If the optimization problem is not feasible, indicating that the network is not secure. The DSO may employ flexible energy resources, as proposed by [10], [12], to ensure network security.

In Case III, the DSO can take the same measures and utilize flexible energy resources to make sure that its network will remain secure for the following day.

## 4. Case Study

This paper examines a Finnish urban LV network (Fig. 1) as a case study. The line parameters and line current capacities are detailed in [13]. The nominal voltage is set at 1 pu, with minimum and maximum voltage limits defined as 0.95 and 1.05 pu, respectively. Also, the power factor of loads and DERs were set to 0.8.

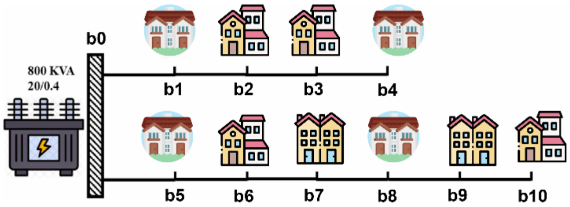


Fig. 1. The studied Finnish urban LV network

At each node of the Fig. 1 LV network, there are two or three detached houses. We extracted representative consumption data for one day from real data collected in 2019 in Finland. This data serves as representative scenarios for the optimization problem (1) to (17). The nodal consumption data is shown in Fig. 2.

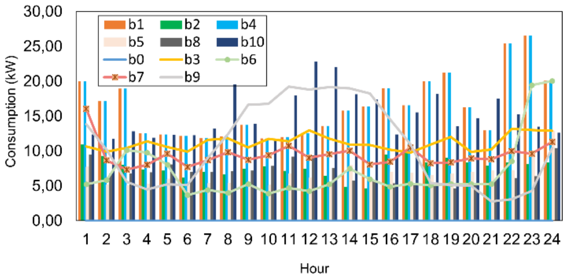


Fig. 2. Nodal consumption of the studied LV network (Fig. 1)

## 5. Simulation Results

### 5.1. *HC Estimation*

First, the optimization problem defined by equations (1)-(17) was modelled and solved. Then, equations (18) and (19) were used to calculate HC for each node (nodal HC) and the total HC for the entire network.

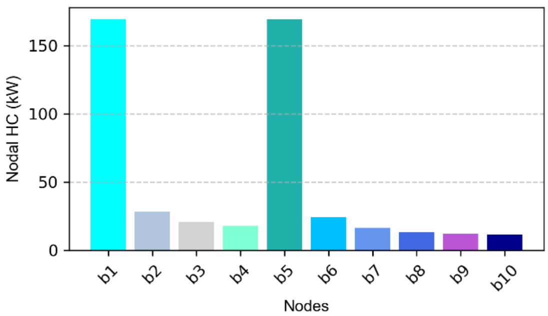


Fig. 3. Nodal HC estimated for the studied urban LV network in Fig. 1

To solve this optimization problem, we used a software package called CVXPY in Python [14]. The calculations were performed on a laptop equipped with 16 GB of RAM and a 13th Gen Intel Core i5-1335U processor.

Fig. 3 displays bar charts representing the HC at each node of the Fig. 1 LV network. The Fig. 3 illustrates that nodes closer to the beginning of the LV feeder exhibit higher HC. Nodes further away from the MV/LV transformer (Fig. 1) have less capacity to accommodate DERs. Therefore, nodes b5 and b7 have the highest HC, while nodes b9 and b10 are the least capable for integrating DERs. For example, the HC of b1 is 14 times higher than that of b10.

### *5.2. Impact of DER Forecasts on HCs*

The HC value of each node was separately increased to observe how the DER forecast of each node affected both the nodal and total HCs. Generally, when the HC of one node increased, which can indicate the DER forecast of that node, the HC of other nodes either stayed the same or decreased. Fig. 4 illustrates how increasing the HC of node b1 affects the hosting capacities of other nodes in the studied LV network (Fig. 1).

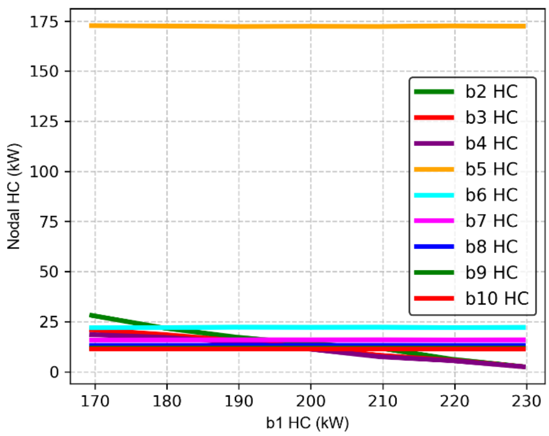


Fig. 4. Variation of nodal hosting capacities (HCs) in relation to the hosting capacity of node b1 in the studied LV network (Fig. 1).

On the other hand, a single HC increase up to a certain level did not affect the total HC of the network. This implies that if the DSO receives a higher DER forecast for a specific node, up to a certain threshold, it does not impact its original total HC estimation of the network.

Fig. 4 illustrates the impact of increasing the HC of each node (in %) on the total HC of the network. As depicted in the Fig. 4, nodes closer to the beginning of the LV feeder (b1 and b5 in Fig. 1) can have a greater effect on changing the total HC. This suggests that the total HC can be more sensitive to DER forecasts of these nodes.

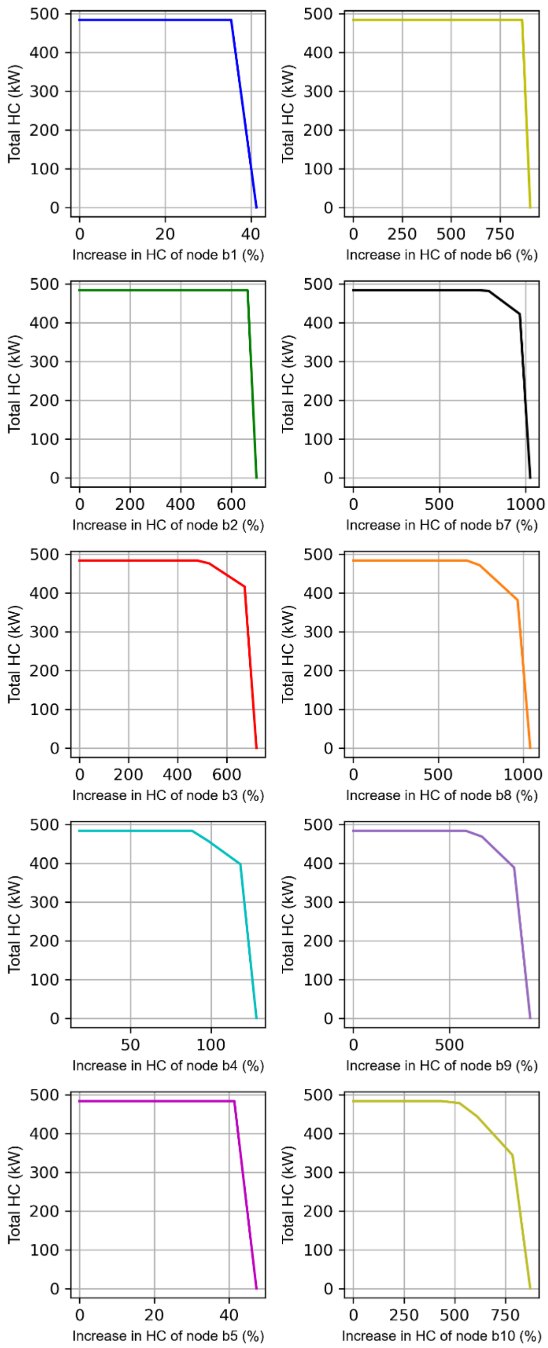


Fig. 5. Variation in total HC concerning changes in the HC of individual nodes in %

In Fig. 5, zero values for both total and nodal HCs indicate that the optimization problem (1)-(17) is infeasible. This infeasibility suggests that the distribution network cannot accommodate the planned amount of DER injection at the node. For example, if the forecasted DER at node b1 is 40

% higher than its primary estimated hosting capacity, the HC estimator optimization will not have a solution. This means that injecting such a high level of DER at b1 would violate one or more security limits of the network.

## 6. Discussion and conclusion

This paper proposed a new optimization-based approach to estimate the total and nodal DER hosting capacities in DSO network. The research emphasized that if the forecasted DER at a particular node exceeds the initial hosting capacity estimate, the DSO needs to revise its estimation of both the total network hosting capacity and the hosting capacity of nodes. This paper also studied different actions the DSO might take depending on the DER forecast scenario.

The proposed hosting capacity estimator was studied with a Finnish urban LV network model. As expected, the results showed that nodes closer to the beginning of the LV feeder and close to the MV/LV transformer have higher hosting capacities. More importantly, the findings revealed that for these nodes with higher hosting capacities, even 40 % variations in the forecasted DER can significantly impact the total network hosting capacity. This underlines the critical role of accurate DER forecasts, especially for these nodes with higher hosting capacity.

Based on the studies, it is recommended that DSOs first conduct a sensitivity analysis to assess how the network's hosting capacity reacts to different DER forecast levels. This analysis could help DSOs to identify which nodes have the greatest influence on the total network hosting capacity depending on the accuracy of the DER forecasts.

## 7. Acknowledgement

This work has been done as a part of “Smart Grid 2.0” project funded by Business Finland with grant No. 1386/31/2022. The work of Hosna Khajeh has been partly supported by “Finnish Foundation for Technology Promotion”.

## 8. References

[1] M. Alturki, A. Khodaei, A. Paaso, and S. Bahramirad, ‘Optimization-based distribution grid hosting capacity calculations’, *Appl. Energy*, vol. 219, pp. 350–360, Jun. 2018, doi: 10.1016/j.apenergy.2017.10.127.

[2] NREL, ‘Advanced Hosting Capacity Analysis’. Accessed: Mar. 08, 2024. [Online]. Available: https://www.nrel.gov/solar/market-research-analysis/advanced-hosting-capacity-analysis.html

[3] N. Qamar, A. Arshad, K. Mahmoud, and M. Lehtonen, ‘Hosting capacity in distribution grids: A review of definitions, performance indices, determination methodologies, and enhancement techniques’, *Energy Sci. Eng.*, vol. 11, no. 4, pp. 1536–1559, Apr. 2023, doi: 10.1002/ese3.1389.

[4] M. Zain Ul Abideen, O. Ellabban, and L. Al-Fagih, ‘A Review of the Tools and Methods for Distribution Networks’ Hosting Capacity Calculation’, *Energies*, vol. 13, no. 11, p. 2758, Jun. 2020, doi: 10.3390/en13112758.

[5] R. Luthander, D. Lingfors, and J. Widén, ‘Large-scale integration of photovoltaic power in a distribution grid using power curtailment and energy storage’, *Sol. Energy*, vol. 155, pp. 1319–1325, Oct. 2017, doi: 10.1016/j.solener.2017.07.083.

[6] D. O. Ampofo, I. K. Otchere, and E. A. Frimpong, ‘An investigative study on penetration limits of distributed generation on distribution networks’, in *2017 IEEE PES PowerAfrica*, Accra, Ghana: IEEE, Jun. 2017, pp. 573–576. doi: 10.1109/PowerAfrica.2017.7991289.

[7] S. S. Parihar and N. Malik, ‘Interval Arithmetic Power Flow Analysis of Radial Distribution System with Probabilistic Load Model and Distributed Generation’, *Process Integr. Optim. Sustain.*, vol. 6, no. 1, pp. 3–15, Mar. 2022, doi: 10.1007/s41660-021-00200-8.

[8] S. Heslop, I. MacGill, J. Fletcher, and S. Lewis, ‘Method for Determining a PV Generation Limit on Low Voltage Feeders for Evenly Distributed PV and Load’, *Energy Procedia*, vol. 57, pp. 207–216, 2014, doi: 10.1016/j.egypro.2014.10.025.

[9] S. Fatima, V. Püvi, and M. Lehtonen, ‘Review on the PV Hosting Capacity in Distribution Networks’, *Energies*, vol. 13, no. 18, p. 4756, Sep. 2020, doi: 10.3390/en13184756.

[10] H. Khajeh, H. Firoozi, M. R. Hesamzadeh, H. Laaksonen, and M. Shafie-Khah, ‘A Local Capacity Market Providing Local and System-Wide Flexibility Services’, *IEEE Access*, vol. 9, pp. 52336–52351, 2021, doi: 10.1109/ACCESS.2021.3069949.

[11] H. Khajeh, C. Parthasarathy, E. Doroudchi, and H. Laaksonen, ‘Optimized siting and sizing of distribution-network-connected battery energy storage system providing flexibility services for system operators’, *Energy*, vol. 285, p. 129490, Dec. 2023, doi: 10.1016/j.energy.2023.129490.

[12] H. Khajeh and H. Laaksonen, ‘Flexibility Utilization Enabling Business Models and Tariff Structures’, in *2023 19th International Conference on the European Energy Market (EEM)*, Lappeenranta, Finland: IEEE, Jun. 2023, pp. 1–6. doi: 10.1109/EEM58374.2023.10161810.

[13] H. Laaksonen, P. Saari, and R. Komulainen, ‘Control of voltage and frequency in inverter and synchronous generator based urban LV microgrid’, presented at the Proceedings The Sixth IASTED International Conference on European Power and Energy Systems, 2006, pp. 26–28.

[14] S. Diamond and S. Boyd, ‘CVXPY: A Python-embedded modeling language for convex optimization’, *J. Mach. Learn. Res.*, vol. 17, no. 83, pp. 1–5, 2016.

applied sciences

MDPI

*Review*

# Applications of Probabilistic Forecasting in Smart Grids: A Review

**Hosna Khajeh and Hannu Laaksonen ***

School of Technology and Innovations, Flexible Energy Resources, University of Vaasa, 65200 Vaasa, Finland; hosna.khajeh@uwasa.fi
* Correspondence: hannu.laaksonen@uwasa.fi

**Abstract:** This paper reviews the recent studies and works dealing with probabilistic forecasting models and their applications in smart grids. According to these studies, this paper tries to introduce a roadmap towards decision-making under uncertainty in a smart grid environment. In this way, it firstly discusses the common methods employed to predict the distribution of variables. Then, it reviews how the recent literature used these forecasting methods and for which uncertain parameters they wanted to obtain distributions. Unlike the existing reviews, this paper assesses several uncertain parameters for which probabilistic forecasting models have been developed. In the next stage, this paper provides an overview related to scenario generation of uncertain parameters using their distributions and how these scenarios are adopted for optimal decision-making. In this regard, this paper discusses three types of optimization problems aiming to capture uncertainties and reviews the related papers. Finally, we propose some future applications of probabilistic forecasting based on the flexibility challenges of power systems in the near future.

**Keywords:** probabilistic forecasting; smart grids; decision making under uncertainty; renewable generation; stochastic programming



**Citation:** Khajeh, H.; Laaksonen, H. Applications of Probabilistic Forecasting in Smart Grids: A Review. *Appl. Sci.* **2022**, *12*, 1823. https://doi.org/10.3390/app12041823

Academic Editors: Hartmann Balint and Joao Miguel C. Sousa

Received: 20 December 2021
Accepted: 8 February 2022
Published: 10 February 2022



## 1. Introduction

### *1.1. Motivation and Contribution*

Smart grids' operation and planning deal with different types of forecasts. The recent advances in information and communication technology (ICT) facilitate the real-time control of devices and resources based on the real-time system states. However, to establish an effective control, the mass of data received from smart meters should be processed and analyzed. These data are utilized to predict future system states. The results of this prediction are then employed to find the optimal control strategy. For example, in many studies, electricity consumption and renewable generation are forecasted and the results are used to determine the optimal commitment of the other conventional generation units and resources.

In this regard, well-trained data-driven forecasting models often give forecasters overconfident and point-forecasted values [1]. This means that the data-driven algorithms giving us point forecasts cannot model the uncertainties and errors of the forecasts. In addition, the decision-making process may be subjected to an information gap. This information gap creates a disparity between the information that a decision maker has and the information that could be known. Thus, the information gap produces possibilities, and this range of possibilities increases as the information gap grows. In this way, decision makers may decide to base their decisions upon the best-informed available model and disregard the uncertainties, which results in insufficient decision-making [2]. To resolve this issue, probabilistic forecasting is suggested.

A probabilistic forecast produces a predictive distribution of values rather than a single value. In general, there are two techniques to generate probabilistic forecasts, named parametric and non-parametric methods. Parametric methods associate a probability distribution with an uncertain variable and then try to estimate the parameters of this probability distribution function (PDF). On the other hand, non-parametric methods use quantiles and ensemble forecasts to derive different forecasted values.

Different types of variables require different probabilistic forecasting models. The goodness of a probabilistic forecasting model should be evaluated according to two properties: "calibration and sharpness" [3]. A calibrated model is able to maintain statistical consistency between forecasts' distribution and the corresponding observations. On the other hand, the sharpness property is more concerned about the concentration of the obtained distribution function [3]. Accordingly, one can conclude that a good probabilistic forecasting model needs to be optimally sharp, subject to being calibrated.

In a smart grid environment, stakeholders and operators employ probabilistic forecasting methods for their uncertain parameter values. Renewable generations, customers' consumption behavior, and electric vehicles' charging/discharging behavior are some examples of uncertain parameters. Thus, a comprehensive review of the applications of probabilistic forecasting can guide forecasters to focus on important uncertain parameters in smart grids. For this purpose, a limited number of reviews have been conducted. For example, ref. [4,5] focused on the recent probabilistic forecasting models aiming to predict wind power. The main focus of [4] was on short-term wind power probabilistic forecasting and compared the forecasting models developed by the previous literature. In contrast, ref. [5] discussed the probabilistic forecasting models up until 2014, considering three different representations of wind power. Similarly, ref. [6–8] reviewed the methods and applications of probabilistic forecasting for PV generation. In this regard, ref. [6] mainly concentrated on integrating PV probabilistic forecasting models into power system decisions, while ref. [7,8] mostly reviewed and compared the probabilistic forecasting techniques. Additionally, the methods applied to predict the distribution of electricity demand were reviewed in [9]. On the other hand, the main contribution of [10] was to review the papers seeking to probabilistically forecast energy prices. This paper is useful for strategic stakeholders that need to make decisions with uncertain prices and participate in the market accordingly. Finally, ref. [11] provided a short review of the parametric and non-parametric probabilistic forecasting models for electricity loads, wind and solar productions. Table 1 compares the existing similar review papers with ours. The first column indicates the reference and the next four columns specify the uncertain parameters for which the probabilistic forecasting models were reviewed. The last column is devoted to the main contribution of the paper that will be discussed later.

**Table 1.** Comparison of this paper with the literature reviewing probabilistic forecasting models and applications in smart grids and power systems.

| Ref. | Load Probabilistic Forecast | Solar Probabilistic Forecast | Wind Probabilistic Forecast | Price Probabilistic Forecast | Pathway towards Decision Making under Uncertainties |
|---|---|---|---|---|---|
| [4] | | | ✓ | | |
| [5] | | | ✓ | | |
| [6] | | ✓ | | | |
| [7] | | ✓ | | | |
| [8] | ✓ | ✓ | | | |
| [9] | ✓ | | | | |
| [10] | | | | ✓ | |
| [11] | ✓ | ✓ | ✓ | | |
| This paper | ✓ | ✓ | ✓ | ✓ | ✓ |

To the best of the authors' knowledge, there is no comprehensive review paper proposing a comprehensive framework for smart grid decision-makers and stakeholders based on the probabilistic forecasting of all uncertain inputs (wind, PV, price, load, etc.). In addition, the applications of probabilistic forecasts and the decision-making pathway were not fully assessed in the previous literature. The decision-making process should have three main stages, including forecasting, scenario generation, and developing optimization problems. Thus, this paper is proposed to resolve this issue as follows:

1. It aims to introduce a roadmap and a pathway towards uncertain decision making in a smart grid environment. The roadmap includes probabilistic forecasting models of uncertain parameters, scenario generation based on probabilistic forecasts, and solving stochastic, robust, and chance-constrained optimization problems according to the results of the previous steps.
2. It tries to guide upcoming similar works by introducing the smart grid's needs in the future. In this regard, probabilistic forecasting models should be developed for a wide range of uncertain parameters and not be limited to loads, prices, and renewable generations.

### *1.2. Paper Framework and Organization*

The main goal of this paper is to introduce the roadmap and direction of making decisions in a smart grid environment, using probabilistic forecasting models. Figure 1 shows the general framework of this paper.

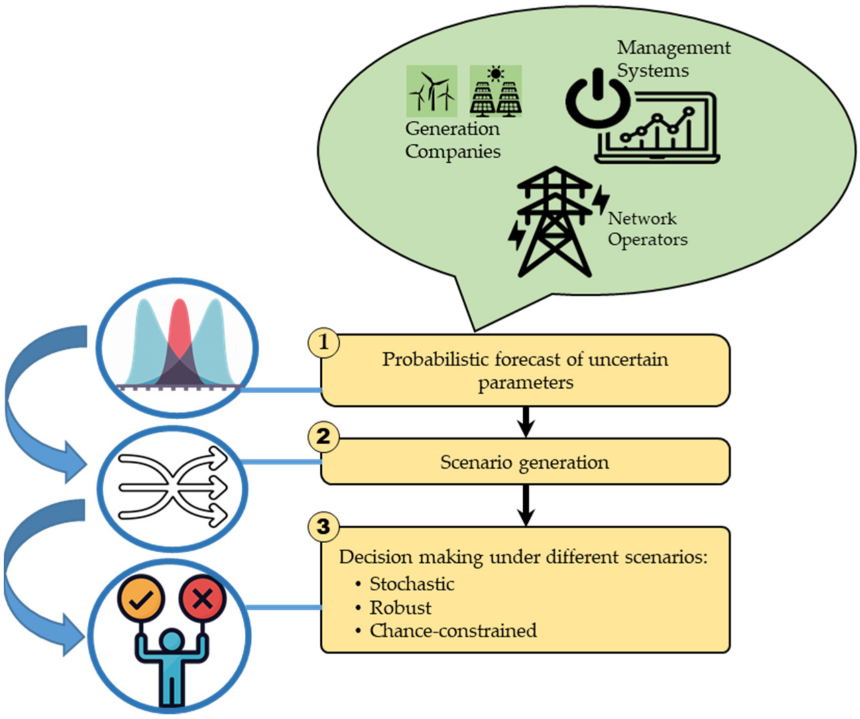


**Figure 1.** Decision-making steps in a smart grid environment.

This paper first introduces probabilistic forecasting models and reviews how the distributions of uncertain parameters are predicted based on previous works. It then presents the most common methods utilizing the predicted distributions to generate scenarios. After that, we will discuss how the scenarios generated in the previous stage can help smart grid management systems to make decisions considering different scenarios of uncertain inputs. Finally, this paper discusses two state-of-the-art applications of probabilistic forecasting that can be extended in future works. In the conclusion and discussion section, some future applications based on the future requirements of power systems are also proposed.

## 2. Probabilistic Forecasting Models

### 2.1. Examples of Parametric Probabilistic Forecasting Models

Each forecast has an error. This error was yielded by subtracting the forecasted value from the actual value in the post-processing stage. At the time of the forecast, a point forecast does not give forecasters any information about the error. Consider a linear regression model as an example. It is a forecasting model that aims to predict the response variable $Y_t$ based on some explanatory variables ($x_{t,1}, \ldots, x_{t,m}$) as follows:

$$Y_t = \hat{Y}_t + \epsilon_t \tag{1}$$

$$\hat{Y}_t = b_1 x_{t,1} + \ldots + b_m x_{t,m} \tag{2}$$

where $\hat{Y}_t$ is the point forecast in the deterministic model and $b$ denotes the weight associated with each explanatory variable. Unfortunately, as can be seen in (2), the deterministic linear regression model does not consider the forecast error. Probabilistic forecasts, on the contrary, will give forecasters different sets of forecasts that follow a known specific probability distribution function (PDF). They will then forecast the parameters of the distribution function. For instance, a probabilistic linear regression forecast assumes that the error term $\epsilon_t$ is normally distributed with a zero mean and a constant standard deviation, $\sigma^2$. Thus, the forecasted value is defined as follows [12]:

$$\hat{Y}_t \sim N\left(\mu_t, \sigma^2\right) \tag{3}$$

$$\mu_t = b_1 x_{t,1} + \ldots + b_m x_{t,m} \tag{4}$$

where (3) states that the forecasted values are normally distributed in this model. $\mu$ denotes the mean and $\sigma$ is the variance. The generalized linear models, however, consider exponential family distributions (*Exp*) of the response variables and utilize a link function $g(.)$ to model the mean value in terms of explanatory variables [12]:

$$\hat{Y}_t \sim Exp(\mu_t, \phi_t) \tag{5}$$

$$g(\mu_t) = b_1 x_{t,1} + \ldots + b_m x_{t,m} \tag{6}$$

where $\phi_t$ denotes the variance associated with the exponential family distributions.

There is a more advanced model, called the Generalized Additive Model for Location Scale and Shape (GAMLSS), that considers a huge set of distributions and is able to model all of the scale parameters related to the distributions [12]:

$$\hat{Y}_t \sim D(\mu_t, \sigma_t, v_t, \tau_t) \tag{7}$$

$$g_1(\mu_t) = b_1 x_{t,1} + \ldots + b_m x_{t,m} \tag{8}$$

$$g_2(\sigma_t) = b_1{}' x_{t,1} + \ldots + b_m{}' x_{t,m} \tag{9}$$

$$g_3(v_t) = b_1{}'' x_{t,1} + \ldots + b_m{}'' x_{t,m} \tag{10}$$

$$g_4(\tau_t) = b_1{}''' x_{t,1} + \ldots + b_m{}''' x_{t,m} \tag{11}$$

where $v$ demonstrates the skewness and $\tau$ shows the kurtosis of the distribution function. This means that the GAMLSS model is able to give us the exact shape of the distributions of our forecast.

### 2.2. Examples of Non-Parametric Probabilistic Forecasting Models

A wide range of probabilistic forecasting models fall into the non-parametric category. The non-parametric probabilistic forecasting models do not use the existing known PDFs. Instead, they build predictive distributions of the response variable based on different factors or construct quantiles/ensembles considering historical data. Since they do not limit probability distributions to specifically known distributions, the non-parametric methods are more flexible. However, compared to parametric models, they often need larger datasets to be able to estimate the response variable distributions [13].

Random forecast (RF) and quantile regression forecast (QRF) models are two examples. RF models aim to forecast the conditional mean of the response variable given the input data and without associating any known distribution functions with the variables [14]. Similarly, QRF models predict quantiles of the response variable regardless of any known parametric distributions. To obtain the quantiles, QRF minimizes the sum of errors of the mean values, considering some asymmetric weights [15,16]. Kernel density estimation (KDE) is another non-parametric method estimating the probabilistic density of the response variables using kernel functions. The kernel density function can be mathematically written as follows [17,18]:

$$F_y(h) = \frac{1}{Nh} \sum_{i-1}^{n} K\left(\frac{y - y_i}{h}\right) \quad (12)$$

where $K$ indicates the kernel function, $y_i$ are the sample points, $N$ refers to the total number of sample points and $h$ is the bandwidth referring to the smoothing parameter. In the KDE method, a proper kernel function should be selected according to the type of response variables.

Another way of obtaining ensemble forecasts is considering various initial states or different boundary conditions for the response variable, such as the lower upper bound estimate (LUBE) [19]. This method provides forecasters with prediction intervals (PI). LUBE employs artificial intelligence tools to build the PIs. In addition to LUBE, the bootstrap method can fall into this category, since it resamples the data and constructs a distribution of residuals accordingly [20]. Short range ensemble forecast (SREF), as another example of non-parametric forecasts, takes into account the uncertainties of initial states [21].

A set of different types of machine learning-based and numerical forecasts can build a non-parametric ensemble forecast. This method uses $N$ different data-driven and numerical forecasting models to predict the response variable. These forecasts are then considered as quantiles. The corresponding distribution $F(y)$ can be mathematically modeled as follows [2]:

$$F(y) = \frac{1}{N} \sum_{i=1}^{N} l(y - \hat{y_{i,t}}) \quad (13)$$

where $l(y - \hat{y_{i,t}})$ denotes a Heaviside step function that shifts $y$ to the $i$th ensemble member.

### *2.3. Artificial Neural Network-Based Probabilistic Forecasting*

Artificial neural network (ANN)-based models can be also used to develop probabilistic forecasting models. NN architectures consist of a network of neurons as processing units. The neurons connect to each other through synapses, which are weighted connections. In the training stage, the optimal weights are determined.

In general, an NN has three layers—an input layer, an output layer and one or several hidden layers. A feedforward ANN passes the data forward from input to output. On the other hand, a recurrent NN (RNN) can connect some neurons in a backward direction as well as the forward direction for further processing. In this way, RNNs have the ability to consider the autocorrelation or time dependencies of data [22]. Figure 2 compares the architecture of a feedforward NN with that of an RNN. The literature proposed various architectures and developed probabilistic forecasting models for both feedforward and recurrent ANN-based models. In the following, some important models are reviewed.

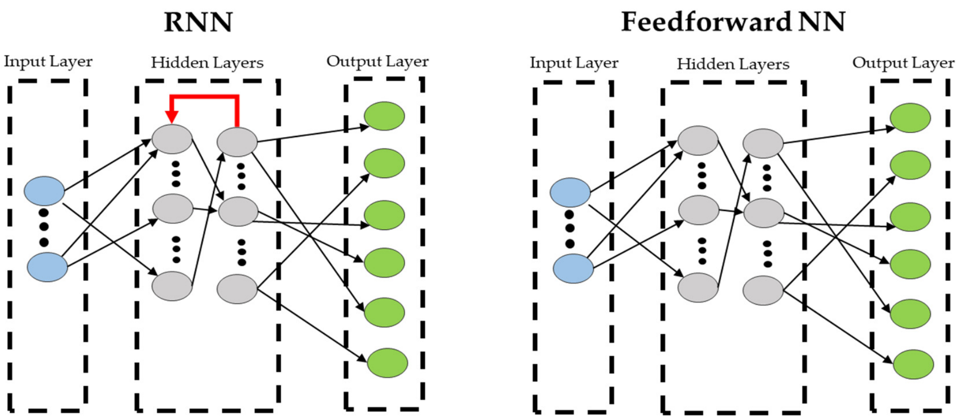


**Figure 2.** Examples of the network architectures of RNN and feedforward NN.

#### 2.3.1. Examples of Probabilistic Forecasting Models Using Feedforward ANNs

Mixture density networks (MDN) and softmax regression networks (SRN) are two of the main feedforward ANN-based models aiming to obtain the distribution of uncertain parameters [23]. Regarding MDN, as a parametric model, the associated probability density is obtained from a linear combination of kernel functions [24]:

$$F(y) = \sum_i a_i(x) K_i(y|x) \tag{14}$$

where $x$ represents the input vector of the forecasting model, $y$ is the output vector, $K_i(y|x)$ is the kernel function selected for the model, and $a_i(x)$ represents the mixing coefficients that control the inputs. In MDN models, the output neurons are the parameters of the distribution functions as well as the mixing coefficients. For example, the outputs can be the parameters of Gaussian distribution functions, including the mean values and the standard deviations as well as the mixing coefficients.

In comparison, in an SRN model, which is a non-parametric probabilistic forecasting model, each output of the neuron associates a probability fraction with a value of $y$. In this way, there should be an interval for possible values of $y$. Hence, the output of an SRN represents the probability related to each member within the interval. Figure 3 compares the architectures of MDN with SRN, two ANN-based approaches utilized for probabilistic forecasts.

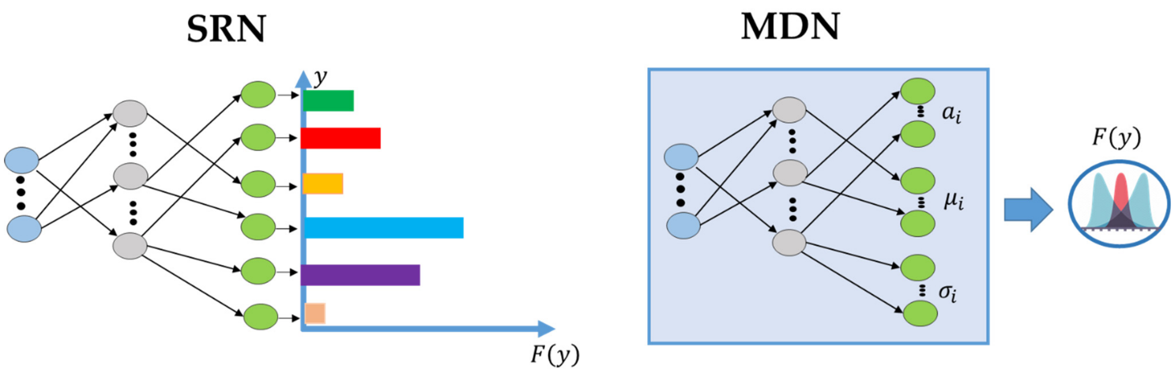


**Figure 3.** Examples of the network architectures related to two ANN-based probabilistic forecasting models.

2.3.2. Examples of Probabilistic Forecasting Models Using RNN

RNN can also be combined with long short-term memory (LSTM) units. LSTM consists of some memory blocks that are recurrently connected. Each block consists of three multiplicative units including input gate, output gate and forget gate. The input gate memorizes either the new information or the previous states of the network. The forget gate disregards the irrelevant and unnecessary information obtained from the past. The output gate extracts the important information from the memory. In this way, unnecessary information is forgotten and only necessary ones are kept within the network [25].

Reference [25] is an example of research developing two RNN-LSTM-based probabilistic forecasting models. The first model is a parametric model and quite is similar to MDN. It first tries to exact a PDF of the uncertain parameter. Then, an RNN-LSTM network is trained to find the optimal values of PDF parameters. The other model is, however, a non-parametric probabilistic forecasting model that is integrated with RNN-LSTM. It employs the QR method with the objective to predict the quantiles of the uncertain parameter. The network is trained to minimize the quantile loss by minimizing their pinball loss.

## 3. Renewable Generation and Load Probabilistic Forecasting

In general, probabilistic forecasting methods have mainly been adopted to forecast the probability distributions of renewable-based power generation and/or load in smart grids. The following sub-sections aim to review important studies that proposed parametric and non-parametric probabilistic forecasts for energy demand and/or generation in a smart grid environment. Additionally, Tables 2–4 review some selected papers that tried to develop probabilistic forecasting models for solar generation, wind generation and loads, respectively.

### 3.1. Solar Probabilistic Forecasting

Network operators, generation agents as well as premises need PV generation to be forecasted at various horizons, including very short-term, hourly and intra-hour, intra-day, as well as day-ahead forecasts [2]. In this regard, future PV generation is forecasted either based on solar irradiance or PV generations of previous times. If the forecast reference is based on solar irradiance, it builds a model according to the past meteorological data or present observations. To construct the model, it utilizes the data from weather stations, satellites, and local sensors and images as inputs [6]. It then develops a model by mapping the inputs to the solar generation.

**Table 2.** An overview of selected papers developing probabilistic forecasting models for solar generation.

| Ref. | Forecast Horizon_Forecast Resolution | Forecasting Methods | Advantages of the Work |
|---|---|---|---|
| [26] | Day-ahead_1 h | NWP-based solar irradiance forecast | The proposed probabilistic forecasting model could reflect the effects of atmospheric conditions on forecast errors |
| [27] | Two-day-ahead_30 min | NWP-based solar irradiance forecast | The paper used a post processing method that was able to improve the performance of the forecasting algorithm |
| [28] | Day-ahead_1 h | NWP-based solar irradiance forecast | It determined several confidence intervals for each region |
| [29] | Day-ahead and hour-ahead_10 min | Different parametric and non-parametric models | It assessed the effects of reconciliation on the improvement of forecasts |
| [30] | Long-term_1 h | Three parametric models | The model could describe the stochastic characteristics and features of solar irradiance |
| [31] | Intra-day (1–6 h)_1 s | Two models developed using quantile regression | It conducted graphical analysis of reliability to compare the performance of the forecasts |
| [32] | Three-day-ahead_1 h | ANN-based combined with Analog Ensemble | The combination of these two methods yielded best results compared to the individual models |
| [33] | day-ahead_1 h | LSTM-based | The proposed model performed better compared to the simpler models but got the same results as the fully connected ANN-based model |

In order to probabilistically forecast PV generation, some works proposed using numerical weather prediction (NWP) models under various scenarios. References [26–28] are some examples that employed NWP to obtain ensemble forecasts for solar irradiance and build an uncertainty model for PV generation. An NWP adopts some measured meteorological inputs, such as temperature, humidity and pressure. It then solves a set of partial differential equations to simulate the process through which solar irradiance is obtained [34]. To obtain a probabilistic forecast, an NWP method uses a training set consisting of the NWP ensemble members at timeslot $t$. After that, each member is weighted equally and utilized to make an empirical cumulative distribution function. NWP methods are usually very straightforward to implement. However, it was argued that NWP models are computationally expensive to implement, and thus it would be better to run them only a few times a day [35].

In the short-run, such as real-time and near real-time forecast horizons, probabilistic forecasters mainly utilize data-driven models including statistical and machine-learning ones [36]. For example, ref. [29] aimed to make short-horizon forecasts based on multi-step-ahead (e.g., six forecasts with 10-min time slots), considering 11 data-driven machine-learning and parametric methods, including least angle regression, least angle regression with elastic-net regularization, lasso regression, generalized linear models, generalized linear model with elastic-net regularization, Bayesian generalized linear model, gradient boosting machines, linear regression, boosted generalized linear model, multivariate adaptive regression splines, and projection pursuit regression. These models tried to probabilistically predict solar generation. The paper also discussed how the so-called "reconciliation techniques" proposed by [37] can improve the probabilistic forecasts. Additionally, ref. [30] compared three parametric probabilistic forecasting models for solar irradiance. The first model considers the use of Beta distribution with several shape factors, the second model utilizes a generalized triangular distribution and the third one combines multiple probabilistic forecasting models to construct the probability distribution of solar irradiance. Regarding non-parametric approaches, ref. [31] compared two 1-to-6-h-ahead probabilistic models for predicting global horizontal irradiance. The first model directly produces a set of quantiles for each time slot using regression methods "linear model in quantile regression (LMQR)", "quantile regression forest (QRF)", or "gradient boosting machine (GBM)". The second model, however, consists of two stages. The first stage deploys the recursive least square autoregressive and moving average (ARMArls) method to make a point forecast for the irradiance. The outputs are used in the next step to estimate quantiles for each time horizon using the same methods. As mentioned earlier, the reviewed model tried to first forecast irradiance and then predict PV generation accordingly, using a physical model and relationships. These models are often called white-box models.

By contrast, non-physical or so-called "black-box" forecasting approaches that predict PV generation are purely based on historical data and do not deal with the physical process and the meteorological data. For instance, ref. [32] developed a probabilistic forecasting model using ANN and an analog ensemble to produce 72-h forecasts of PV power. Additionally, ref. [33] utilized a more complicated approach, long short-term memory (LSTM), to probabilistically predict solar power and compared it with simpler models. Similar to NWP models, although physical models may be more accurate in day-ahead and long-term horizons, data-driven black-box models work better over short-term horizons such as intra-hour ones [38,39]. Figure 4 summarizes the probabilistic forecasting models for PV generation considering the forecasting horizon.

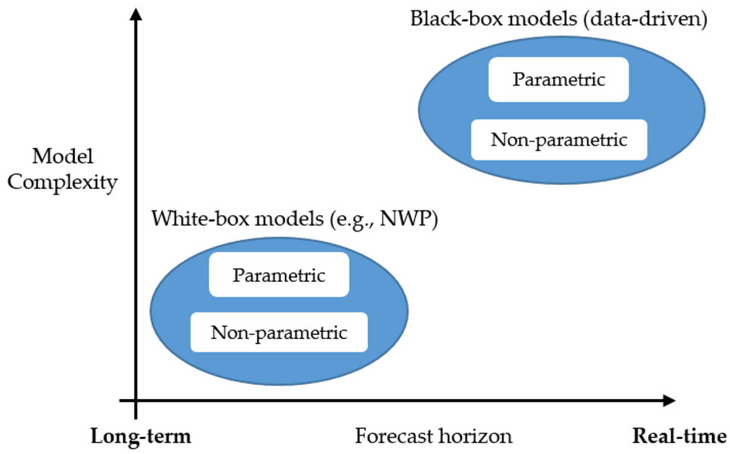


**Figure 4.** Probabilistic forecasting models for PV generation.

### 3.2. Wind Probabilistic Forecasting

There are studies trying to relate a known PDF to wind generation. They mainly adopted Gaussian and beta distributions to probabilistically forecast wind power using parametric methods [40]. Some research also tried other types of distribution functions. For example, ref. [41] proposed a modified version to generalize logit-normal distribution for wind power. Reference [42] considered the same distribution for wind generation. The authors of [43] took wind power as a double-bound variable and obtained the appropriate distribution based on this assumption. In another study, ref. [44] solved an economic dispatch problem using a versatile probability distribution for wind generation. However, it was also discussed that relating specific distributions to the distribution of wind power cannot be applied since in some cases, the predictive error of wind power distribution is changing over the prediction horizons [45].

A huge number of papers have been proposed that utilized non-parametric probabilistic forecasting models for wind generation. For instance, considering QRF-based methods, ref. [46] proposed a novel direct quantile regression (DQR) method to probabilistically predict wind power, generating quantiles without using statistical inference. The prediction was based on multi-step 10-min forecasts that combined the extreme learning machine (ELM) and QRF models to make the non-parametric probabilistic forecast and use it in a linear programming problem. Their proposed novel approach was finally compared to four different forecasting techniques, including the bootstrap-based ELM (BELM)-normal distribution, the BELM-beta distribution, the persistence model, and the radial basis function-neural network (RBF-NN) model. The final results demonstrate that the model proposed by [46] performs better in terms of the sharpness criteria. In this regard, the proposed DQR model performed 25% better compared to the persistence model and its performance was 20% better than the RBF-NN probabilistic forecasting model. In addition to the sharpness criteria, DQR model presented a more acceptable computational time equaling 63.89 s, according to the result section of [46]. As another example, ref. [47] presented a joint quantile regression (JQR) model that reproduces kernel Hilbert spaces for wind power probabilistic forecast utilizing the primal-dual coordinate descent technique. The work then employed the multi-objective salp swarm algorithm (MSSA) to optimize the final results. It then tested the forecasting model and compared it with other models on a one-step-ahead and a multi-step-ahead basis.

**Table 3.** An overview of selected papers developing probabilistic forecasting models for wind generation.

| Ref. | Forecast Horizon_Forecast Resolution | Forecasting Methods | Advantages of the Work |
|---|---|---|---|
| [41] | 10-min-ahead_1 min | Parametric (mixtures of generalized version of logit–normal distributions) | The work considered the non-linear nature and double-bounded characteristics of wind power forecast |
| [42] | 8-h-ahead_15 min | Parametric (censored normal distribution) | The work considered the effects of spatio-temporal on wind power forecast |
| [43] | Two-day-ahead_1 h | Several parametric probabilistic forecasts | It tested several distribution functions and found Beta distribution function as the most appropriate distribution for wind power |
| [44] | Day-ahead and week-ahead_1 min | Parametric (versatile distribution) | The model was integrated with the economic dispatch problems which could simplify uncertainties of wind power |
| [46] | Hour-ahead_10 min | Direct quantile regression combined with mashing learning methods | The model was proved to be high efficient, reliable, and flexible to probabilistically forecast wind power |
| [47] | One-hour-ahead and several-hour-ahead_15 min and 1 h | Joint quantile regression | The forecasting model was improved by meta-heuristics algorithm |
| [17] | Different horizons from days to hours_30 and 60 min | A tri-level adaptation function integrated with a fuzzy inference system | The model outperformed other similar approaches in terms of computational efficiency and practicality since it avoided any pre-assumptions about forecast errors and data noises, and considered cost-based optimization problems in the model |
| [48] | 1–6-h ahead and day-ahead_different time steps | Multi-distribution ensemble (MDE) forecasting model integrated with competitive and cooperative strategies | The work tried to explore the best probabilistic forecasting accuracies by considering different forecasting horizons |
| [49] | Not specified | Three neural network-based models | Reinforcement learning was also utilized to combine and improve three kinds of deep learning networks |
| [50] | Different horizons from 1–24 h_1 h | Kernel density estimation with regular vine copulas and ensemble learning | The work proved that multi-distribution mega-trend-diffusion can improve the forecast when there are insufficient data |
| [51] | Hour-ahead_1 h | Data processing techniques integrated with ensemble NWPs | The work proved that data processing techniques can improve the probabilistic forecast of wind power considerably |

Another method for obtaining the non-parametric distribution of wind power is the use of KDE. However, the model is highly impacted by using different kernel functions. In other words, the appropriate kernel function should be selected based on the type of the random variable so to avoid the boundary effects on the PDF of wind generation [52]. To resolve this issue, ref. [17] proposed applying a tri-level adaptation function integrated with a fuzzy inference system.

As examples of ensemble forecasting models, authors of [48] suggested a multi-distribution ensemble (MDE) forecasting model that is integrated with competitive and cooperative strategies. In this way, the work tried three different distributions as the ensemble members. Based on the comparison results presented by the paper, the MDE integrated with the cooperative model performed better in an hour-ahead forecast. However, the MDE integrated with the competitive model had a better performance in longer horizons including two-to-six-hours- and 24 h-ahead. Three different neural network-based probabilistic forecasting models were also presented by [49]. The work combined the ensemble deep learning method with empirical wavelet transform decomposition (EWT), which outperformed the other models considered in the paper. ref. [50] also combined improved kernel density estimation with regular vine copulas and ensemble learning to obtain an advanced probabilistic forecasting model.

Similar to solar forecast, there are some studies proposing NWP models. For instance, ref. [51] suggested wind power probabilistic forecasting using data processing techniques and ensemble NWPs. This methodology comprises data preprocessing techniques, the model of adaptive-network-based fuzzy inference system (ANFIS) integrated with fuzzy c-means (FCM) clustering model, as well as LUBE for prediction of forecast intervals. The work tried to prove that data preprocessing and post-processing processes are very important to improving the forecast models. For this purpose, it compared the model with the ANFIS model, disregarding data preprocessing. The paper concluded that the model utilizing preprocessing outperformed the other models not deploying this technique.

### 3.3. Load Probabilistic Forecasting

Similar to renewable generations, probabilistic forecasting of loads has a wide range of variety based on the type of forecasts and the forecasting horizons [8]. In terms of the variety of forecasting models, different methods have been adopted, such as hybrid Kalman filters [53], Gaussian and lognormal processes [54,55], artificial neural networks [56,57] QR [58,59], RF [60], and stochastic time-series combined with Bayesian inference (BI) [61].

**Table 4.** An overview of selected papers developing probabilistic forecasting models for electricity load.

| Ref. | Forecast Horizon_Forecast Resolution | Forecasting Methods | Advantages of the Work |
|---|---|---|---|
| [51] | Hour-ahead_5 min | Hybrid Kalman Filters | The work proved the effectiveness of hybrid Kalman filters to capture different characteristics of load components from Independent System Operator's viewpoint |
| [56] | Day-ahead_30 min | Boosting Additive Quantile Regression | The model was designed to probabilistically predict loads at the disaggregated level |
| [53] | 30-min-ahead_30 min | Gaussian Processes | The work analyzed the effects of several covariance functions on load forecasts |
| [52] | Multi-step-ahead_30 min | Gaussian and log-normal processes | The work proved that the log-normal model can generate a varying sharpness for load forecast |
| [60] | 30-min-ahead_30 min | Markov-chain mixture distribution model | The proposed model was proved not to be computationally expensive and can be insensitive to the settings of parameters |
| [61] | Day-ahead_1 h | Load probabilistic forecast based on weather ensemble prediction | The work proved that using weather ensemble predictions can improve the accuracy and uncertainty analysis of load forecasts |
| [62] | Day-ahead_1 h | Estimation of load's confidence intervals based on the quantiles of past forecast errors | The method can be adopted for security analysis of power systems since it was able to generate demand scenarios at a specified risk level |
| [63] | Day-ahead_1 h | Partially linear additive quantile regression | The work combined the forecasting model with the unit commitment problem |
| [64] | Different horizons including 30-min-, one-hour-, two-hours-, and four-hours-ahead_30 min | LSTM-based | The model was designed to probabilistically forecast the individual consumer's load |
| [65] | Day-ahead_1 h | Probabilistic methods | The novel work focused on determining the reserves based on forecasting net loads. The work demonstrated that the method can decrease the amount of reserves bought for the system |

In terms of very short-term (real-time or near-real-time) probabilistic load forecasting, reference [53] is one of the early works proposing hybrid Kalman Filters to probabilistically forecast demand considering the 5 min temporal resolution. The authors of [58] performed half-hour resolution probabilistic forecasting of electricity consumption using QR that is integrated with gradient boosting. In [55], the authors used Gaussian processes to develop a probabilistic forecasting model for residential load considering half-hour resolutions. In [54], the authors performed half-hour-resolution forecasts of residential loads utilizing a lognormal process. In one of the recent study, proposed by [62], the Markov-chain mixture distribution model (MCM) was employed for the purpose of very short-term load forecasting considering residential households in Australia. The model forecasts on a half-hour-ahead resolution basis. The authors then proved the high computational speed as well as the acceptable competitive performance of their proposed model.

Regarding interval forecasting on a day-ahead basis, the probabilistic forecasting NWP models can be adopted. For instance, the forecasting model can be constructed according to the weather ensemble prediction taking into account the consumption under different weather scenarios [63] or be built according to the quantiles of forecasting errors of the historical data [64]. In addition, a partially linear additive quantile regression model was proposed by [65] to develop a probabilistic forecast of day-ahead hourly electricity loads with a focus on the demand of peak hours in South Africa. As an example of data-driven models, the long short-term memory (LSTM) model was used to forecast the quantiles of electricity loads aiming to minimize the quantile pinball loss function [66].

Finally, ref. [67] assessed the benefits of using probabilistic methods to estimate the required day-ahead reserves. In this regard, the authors developed two probabilistic methods to forecast the system net loads. The results of probabilistic forecasts are then utilized to quantify reserves that are required to compensate for the intermittency and uncertainties of renewable generation.

## 4. Electricity Price Probabilistic Forecasting

In electricity markets, electricity prices are affected by the total system's supply and demand. However, each participant playing in these markets needs to schedule their resources according to the predicted values of the market prices, in short-term horizons. Regarding future power systems, renewable-based generation will be the main source of electricity. Their intermittent nature and real-time fluctuations increase the electricity price fluctuations [68]. Accordingly, electricity price forecasting models need to be improved to actively follow the prices' fluctuations. In addition, it can be argued that probabilistic forecasting models are attracting increasing attention since they are able to consider various uncertainties and possibilities [10].

Regarding studies that proposed parametric models, the authors of [69] proposed a first-order vector autoregressive (VAR) model considering exogenous effects and using skew t distribution in a Bayesian framework. The model was then sent to the Markov chain Monte Carlo for uncertainty analysis. Reference [70] adopted the GAMLSS method and also estimated the PIs to be time-varying quantiles of the acquired density forecasts. In [71], the authors developed generalized autoregressive conditional heteroskedasticity (GARCH)-based time-varying models to estimate the density function of the variable. As a semi-parametric model, ref. [72] introduced a semiparametric model that is combined with a time-adaptive quantile regression [34] in order to predict day-ahead market price densities. The proposed model was then compared to four well-known GARCH models considering a three-year time span. They finally proved that their proposed model is more reliable in terms of generating quantile estimates.

Recently, non-parametric data-driven probabilistic forecasting models are more often employed due to their flexibility. For instance, ref. [73] introduced a deep neural network model-based method for the probabilistic prediction of electricity prices. In this model, they first made the price distributions using its historical data. Afterward, they employed a deep convolutional neural network (DCNN) for extracting high-level features. The obtained high-level features were sent to label distribution learning forests (LDLF) in order to construct price probabilistic forecasts. In another work, ref. [74] developed a two-step model to probabilistically forecast German-Austrian day-ahead prices. It first proposed estimating the mean of correlated time series prices using ordinary least squares and the elastic net method. In the second step, they estimated the residuals using the maximum likelihood method.

## 5. Uncertainty Modeling

Uncertainty modeling itself needs comprehensive study. In general, uncertainty modeling aims to capture the dynamics of the uncertain input data and generate scenarios based on their probability distributions [75]. The results are then used as the input of stochastic programming. Figure 5 overviews some uncertainty modelling techniques utilized for stochastic programming. In addition, Table 5 states some selected works using these techniques.

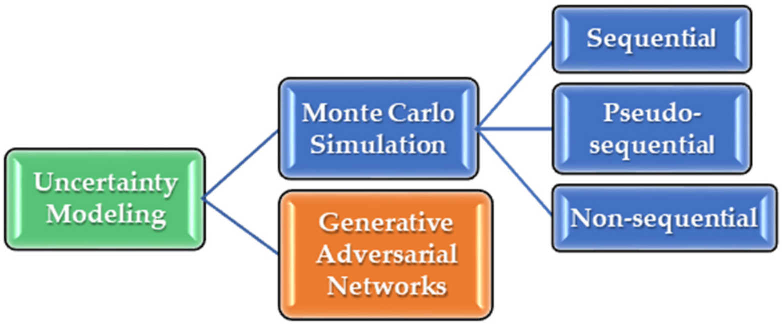


**Figure 5.** Uncertainty modelling techniques utilized in a smart grid environment.

**Table 5.** An overview of selected papers using scenario generation techniques in a smart grid environment.

| Ref. | Uncertain Parameters | Uncertainty Generation Technique | General Objective of the Work |
|---|---|---|---|
| [76] | Wind generation, generators' reliability | Sequential MCS | Minimizing the total energy generation costs |
| [77] | Wind generation, PV generation, battery storage charging/discharging output, biomass combined with heat generation, and thermal energy storage output | Sequential MCS | Minimizing the total energy costs + minimizing economic risks |
| [78] | Renewable generation, electricity demand, household hot water, and space heating and cooling parameters | Pseudo-sequential MCS | Minimizing energy generation environmental impacts + Minimizing energy costs |
| [79] | Renewable generations, electricity demand, and water inflow | Pseudo-sequential MCS | Maximizing financial profits + Minimizing economic risks |
| [80] | risks | Non sequential | Optimizing net present value and analyzing geothermal energy life-cycle for power and transportation sectors |
| [81] | Renewable generations | GAN | Generate samples for renewable generations based on historical data |

Monte Carlo simulation (MCS) is one of the most popular methods for scenario generation purposes. The PDFs of the random variables, forecasting errors of the data, and market variability, in general, are employed by the Monte Carlo simulation method in order to learn the uncertain data and generate their associated scenarios, accordingly [82]. Figure 6 illustrates the steps of achieving output from uncertain inputs, using the Monte Carlo simulation method.

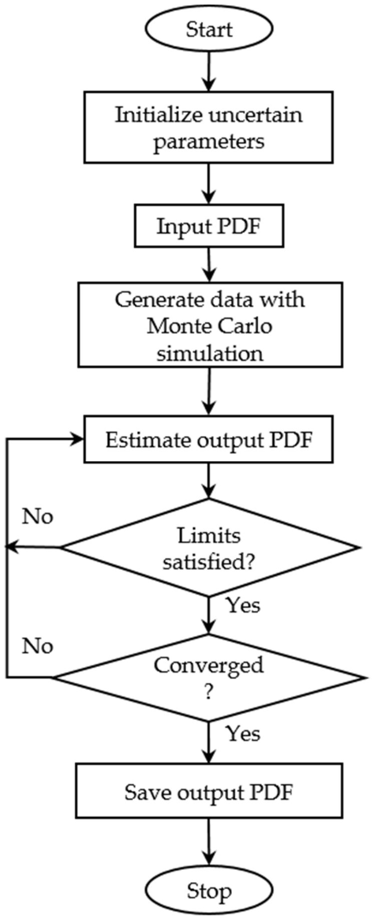


**Figure 6.** A flowchart of generating scenarios by MCS algorithm.

The advantages of the Monte Carlo simulation method can be described as follows [83]:

- The method is able to sample from random processes and supports all of the distribution functions.
- A transfer function is not required.
- It does not need a mathematical formulation since it can model a problem in the form of a black box system and can obtain output considering samples of inputs.
- The method is relatively easy to implement.
- It is able to model both non-differentiable and non-convex problems.

Recently, Monte Carlo simulation algorithms have evolved and improved. For example, sequential MCS is able to model uncertainties of inputs in chronological order. With the help of the sequential method, uncertainties of time-series inputs (such as variable generation of renewable energy resources and electricity demand) are implemented in a better way [75]. Pseudo-sequential is another extension of the MCS method which has the ability to converge faster compared to the sequential version. The pseudo-sequential method can sample states through its non-sequential capability and uses chronological simulation for the failed states [75]. Finally, the non-sequential MCS method is another family member of the Monte Carlo method which cannot model uncertainties chronologically and requires high computational costs [75].

Recently, a model-free and data-driven method, called the "Generative Adversarial Network (GAN)", has attracted more attention for scenario generation purposes. The model employs artificial neural networks (ANNs) and aims to synthesize some understanding from the training of real data. The notable advantage of GAN scenario generation is that this model does not need distribution functions of uncertain variables [81].

## 6. Decision Making under Uncertainties

The future power system is heading towards being smart and decentralized. In a new smart grid system, there will be a number of agents and stakeholders that face uncertainties in their decision-making problems. Here are some examples:

- A generation company that has renewable resources needs to submit offers to energy markets before knowing the resources' exact generation and market prices.
- Every management system in smart grids (such as microgrid energy management system and energy community management systems) needs to deal with its intermittent renewable energy resources' output as well as the uncertain resources' behavior (such as the EV charging behavior) to come up with the optimal scheduling and management of resources.
- Strategic agents try to deal with uncertain market prices and their competitors' strategies beforehand when they construct their optimal bidding strategies.
- Retailers should buy electricity based on their customers' uncertain demand.
- Balancing responsible parties require to schedule their flexible energy resources, such as their energy storage systems, based on the uncertain generation in a way to maintain the balance between their generation and their demand.
- Transmission system operators (TSO) and distribution system operators (DSO) must decide on the amount of reserves and flexibility as well as the methods to operate their network and keep the security of supply and reliability of the system within the specified limit, in spite of different uncertainties and the intermittency of renewables.

Hence, the lack of perfect information affects optimal decision making. In this regard, stochastic programming, robust programming, and chance-constrained models offer to solve optimization problems with uncertain input data.

### *6.1. Stochastic Programming*

A stochastic optimization problem models uncertainties of input data by weighting the decision-making solutions. The weights are selected based on the probabilities of occurrence, considering that each set of input data leads to a single solution. In this way, one will achieve the effects of uncertain input data on the decision-making solution [84]. A simple stochastic programming can be formulated as [6]:

$$\begin{array}{c} \min_{x} \mathbb{E}(f(x,\omega)) \\ Subject\ to: \\ g(x,\omega) = 0 \\ h(x,\omega) \leq 0 \end{array} \tag{15}$$

where $x$ is the decision variable and $\omega$ denotes the scenario. As the formulation states, uncertainties should be modeled in terms of different scenarios. The most common and simple techniques for generating scenarios need to use the inverse of the cumulative distribution function (CDF) or PDFs of the uncertain parameters. Hence, the probabilistic forecasts of the inputs are necessary to develop stochastic programming. However, it would be easier if the random input data have specifically known parametric distribution [6]. This means that parametric probabilistic forecasts are more favored in this sense. Here, if one knows the probability distributions of the inputs, they can achieve the probability distributions of the output data.

In power system concepts, an independent system operator or a generation company are proposed to conduct stochastic unit commitment by using stochastic programming [85]. In unit commitment applications, stochastic programming is divided into two-stage and multi-stage problems. Two-stage models consider both day-ahead (hear and now) and real-time (wait and see) commitment decisions. In the day-ahead stage, the conventional generators are dispatched and their commitment decisions are determined while in real-time, uncertain renewable resources and flexible energy resources are dispatched. Regarding the second (real-time) stage, to develop the two-stage problem, one needs the PDFs of renewable generation as well as those of flexible energy resources to build a large number of relevant scenarios for the PDFs of the outputs. Table 6 summarizes some of the most recent studies that considered stochastic programming to find the optimal commitment decisions for their resources.

**Table 6.** An overview of recent papers using stochastic programming for decision making in a smart grid environment.

| Ref. | Uncertain Parameters | Methods to Capture Uncertainties | Objective |
|---|---|---|---|
| [86] | Prices (day-ahead market and balancing market), renewable generations, loads, driving requirement and the availability of electric vehicles (EV) | Two-stage stochastic programming (day-ahead and real-time scheduling) | Proposing a system for microgrid support by maximizing the expected profit of a microgrid aggregator |
| [87] | EVs' arrival, and departure time, as well as EVs' daily traveled miles and types, solar irradiation and wind speed, loads | Two-stage stochastic programming | Maximizing the retailer's profit (first stage: fuel cell scheduling second stage: distributed generation scheduling) |
| [88] | Electricity demand, wind speed | Two-stage stochastic programming | Minimizing day-ahead dispatch costs of the wind-thermal-hydropower-pumped storage system along with the system's expected balancing costs |
| [89] | Renewable generations and loads | Two-stage stochastic programming | Minimizing the costs of reserving flexibility services in day-ahead forecasting and their real-time activation |
| [90] | Wind generation, demand and market prices | Two-stage stochastic programming | Maximizing microgrid's profits participating in day-ahead and real-time markets taking into account the microgrid's reconfiguration |
| [91] | Wind generation, demand and market prices | Simple scenario-based stochastic programming | Obtaining coordinated network expansion planning by minimizing the operation cost of generation + Minimizing the annual investment cost of expanding the transmission networks + Minimizing the renewable resources' annual investment costs + Minimizing the annual investment and operation costs of energy storage systems + Maximizing the flexibility index of the system |
| [92] | Renewable generations | Simple scenario-based stochastic programming | Procuring ancillary services from flexible distributed energy resources in a day-ahead operational planning by minimizing network's costs |
| [93] | Electricity demand, renewable generations, market prices | Two-stage stochastic programming | Supplying the aggregated demand through their participation in the day-ahead market and maximizing their total expected profits |
| [94] | Electricity demand and PV generation | Multi-stage stochastic programming | Operating an energy community with PV-storage system by minimizing the electricity purchased from the grid |
| [95] | Wind generation | Two-stage stochastic programming | Economic dispatch for a hybrid distribution system based on active-reactive power coordination by minimizing the cost of gas-fired operation, power purchasing from the upstream grid, penalty costs related to substations' power fluctuations, network losses, and the costs of wind curtailment and load shedding |
| [96] | Renewable generations, electric vehicles, loads, and market prices | Simple scenario-based stochastic programming | Optimal energy management of microgrids by minimizing operational costs of distributed energy resources, the costs of purchasing power from the upstream network, the costs incurred from the energy not served, and those related to EV batteries' degradation costs |

Once we make a decision for the day-ahead stage, decomposition methods are then employed to treat the real-time stage scenarios independently. This approach leads to considerably fewer scenarios, compared to the non-decomposed method [75].

Multi-stage stochastic programming models construct a scenario tree and accordingly try to capture uncertainties in a dynamical way. In multi-stage models, the uncertainties are treated chronologically, meaning that the uncertainties at time $t$ affect those at $t+1, \ldots, t+m$. However, the method comes at huge computational costs.

*6.2. Robust Programming*

The robust optimization approach aims to obtain a problem solution that is always feasible under different realizations of the uncertain inputs. In other words, the robust approach seeks optimal solutions in the worst-case realizations or worst-case scenarios [97]. Robust optimization deals with the uncertainty sets, and in the first stage aims to optimize the problem considering the scenarios under which the worst solutions are obtained. A simple robust optimization is formulated as follows:

$$\begin{gathered} \min_{x} \max_{w} f(x,\omega) \\ subject\ to: \\ g_i(x,\omega) = 0 \\ h_i(x,\omega) \leq 0 \quad \forall i \\ \omega \in W \end{gathered} \tag{16}$$

In (15), all possible sets of $\omega$ (scenarios) are included in the uncertainty set, i.e., $W$. In this way, the uncertainty sets of the uncertain parameters need to be defined adequately. The uncertainty sets are also required to cover the uncertain phenomena that can happen for the uncertain parameters. Naive and inappropriate definitions of the uncertainty sets may result in either too conservative or very risky solutions. This means that the appropriate uncertainty sets should comprise risky and conservative decisions [7]. There are other extensions of the robust optimization such as robust stochastic optimization, adaptive robust optimization and distributionally robust optimization. Although they all have the same concept, they try to keep the balance between the risky and conservative solutions in different ways and under various assumptions on uncertain parameters.

The applications of robust optimizations in smart grids and power systems can fall into one of these categories:

- Robust network and generation planning and expansion (e.g., [98,99])
- Robust capacity sizing of flexible energy resources (e.g., [100,101])
- Robust and resilient network operation under extreme and emergency conditions or climate-aware operation of resources (e.g., [102,103])
- Robust energy management and the operation of resources (e.g., [104,105])
- Robust bidding strategy for participating in energy and flexibility markets ([106,107])

A number of studies and papers utilized robust optimization or its extensions in order to solve their decision-making problems. Table 7 summarizes these papers.

**Table 7.** An overview of recent papers using robust programming for decision making in a smart grid environment.

| Ref. | Uncertain Parameters | Methods to Capture Uncertainties | Objective |
|---|---|---|---|
| [108] | Inflow and PV generation | Robust optimization | Maximizing the minimum power generated within the operation interval<br>+<br>Maximizing the operational interval<br>+<br>Maximizing the feasible solutions obtained by the operation interval |
| [109] | Electricity demand, generation capacity, as well as uncertain economic, environmental, and social parameters for customers | Robust fuzzy multi-objective optimization programming | Maximize the total profits of the whole system<br>+<br>Maximizing the social benefits of the system consumers<br>+<br>Minimizing the total negative environmental impacts |
| [110] | Energy price | Robust optimization | Minimizing the net costs of a smart home |
| [104] | Wind and PV generations | Adaptive robust optimization | Minimizing the operating costs of an isolated microgrid |

**Table 7.** *Cont.*

| Ref. | Uncertain Parameters | Methods to Capture Uncertainties | Objective |
|---|---|---|---|
| [111] | Wind speed, demand, and solar irradiance | Conditional value at risk (CVaR) combined with robust optimization | Minimizing the costs of an energy hub participating in energy and reserve markets + Minimizing the emissions of pollution |
| [105] | Wind and photovoltaic generations | Two-stage adjustable robust optimization | Minimizing the costs of multi-energy system that supplies both electricity and heat loads |
| [102] | Load and energy price | Hybrid stochastic/robust optimization | Minimizing planning, operation and resilience costs of the distribution networks considering earthquake and flood situations |
| [112] | Energy price and PV generations | Hybrid stochastic/robust optimization | Maximizing the profits of a household customer |
| [113] | Wind and PV generations, loads, and market-clearing prices | P-robust (a combination of robust and stochastic programming) | Minimizing the operating costs of diesel engine, micro turbine, procurement costs, costs of pollutant treatment, and costs of reimbursing incentive-based demand response programs |
| [114] | Availability of microgrid equipment, active and reactive loads, parameters of EVs, energy price, wind and PV generations | Hybrid stochastic/robust | Minimizing the microgrid's costs including the cost of buying energy, the operation cost of non-renewable energy sources, the reliability costs in terms of non-supplied loads |
| [115] | Renewable distributed generations | Robust model combined with prediction control | Maximizing the amount of load restoration that is controlled by the output of the power units and remote-controlled switches |
| [116] | Electricity demand and facility installation costs | Robust optimization | Minimizing the installation costs of power plants, high-voltage/low-voltage substations, and feeders, feeders' power transmission costs + Minimizing the storage power cost, power losses' costs in feeders, feeder failures' costs |
| [98] | PV and wind generations, | Robust optimization | Minimizing the annual costs of the regional distribution networks |
| [103] | Wind generation, outages, La Niña and El Niño events (a long-term warming happening for the central and eastern Pacific and vice versa) | Robust optimization | Minimizing investments' and operations' costs of the system |
| [99] | Unbalanced power percentage | Robust optimization | Minimizing the annual investment costs of transmission network lines as well as the costs related to battery superconducting magnetic hybrid energy storage system under maximum the load-shedding conditions + Reducing the insufficient supply if N-k faults happen |
| [117] | Random N-K contingency, wind and PV generation | Robust optimization | Minimizing the investment costs of building candidate lines, the generation costs of conventional generators, the costs related to scheduling downward and upward spinning-reserves, costs of renewable generation curtailment and load-shedding |
| [106] | Market participants' offers and bids as well as real-time market prices | Robust optimization | Maximizing profits of a virtual bidder (optimal bidding strategy) |
| [107] | Wind generation and electricity prices | Robust MPC-based optimization | Maximizing the profits and minimize the operating costs of a wind-storage system (optimal bidding strategy) |
| [118] | Renewable generations and electric vehicle charging behavior | Robust optimization | Optimal location and sizing of renewable distributed generation and the charging stations based on maximization the station's total payoff |
| [119] | Loads and renewable generations | Robust optimization | Designing generation resources for a microgrid to meet its demand by minimizing the total generation costs of the resources |
| [100] | Loads, wind and PV generations | Robust optimization | Positioning and sizing of the energy storage system by minimizing the operation costs of the flexible energy resources as well as those of the network |
| [101] | PV generation | Robust optimization | Planning of distributed battery energy storage from a DSO viewpoints by minimizing the batteries' degradation and operation costs |

### 6.3. Chance-Constrained Programming

Chance-constrained optimization problems aim to give an optimization constraint the possibility to be satisfied up to a specified level. It can be formulated as follows:

$$\begin{gathered} \min_{x} \mathbb{E}(f(x,\omega)) \\ \textit{Subject to}: \\ g(x,\omega) = 0 \\ \Pr\left[h(x,\omega) \leq 0\right] \geq \eta \end{gathered} \tag{17}$$

where Pr refers to probability and $\eta$ indicates the confidence level [120]. In this regard, $\eta$ should be selected between 0 and 1. According to (16), constraint $h(x,\omega) \leq 0$ needs to be satisfied up to $\eta$ level. In other words, operators or designers that use the chance-constrained method ensure that $h(x,\omega) \leq 0$ will be satisfied in $(\eta \times 100)\%$ of scenarios.

Chance-constrained programming has a wide range of applications in smart grids. Here are some examples:

1. Operations of renewable-based systems to guarantee a certain level of reliability/security/flexibility
2. Planning of distribution/transmission networks in a way to guarantee a certain level of reliability/security/flexibility
3. Determining system reserves to guarantee a certain level of reliability/security/flexibility

Table 8 summarizes some recent works that adopt chance-constrained programming methods to capture uncertainties.

**Table 8.** An overview of recent papers using chance-constrained programming for decision making in a smart grid environment.

| Ref. | Uncertain Parameters | Methods to Capture Uncertainties | Objective |
|---|---|---|---|
| [121] | Electricity prices and PV generation | Chance-constrained programming | Minimizing the costs of energy trading between the power grid and microgrids + Minimizing the fuel costs of fuel-based power generation and boiler units |
| [122] | PV generation | Chance-constrained programming | The study aims to integrate renewable energy as much as possible by minimizing the hybrid system's power curtailment + Maximizing the renewable power generation injected into the system |
| [123] | Loads, market prices, renewable generation | Chance-constrained programming | Minimizing the total operation costs of a combined, power-based, cooling, and heating microgrid: Minimizing the costs of power and gas purchased + Minimizing the operation costs of microgrid's CHP units and micro turbine + Minimizing batteries' degradation costs + Maximizing the revenues obtained from selling electricity and heat to the upstream grids |
| [124] | Loads, wind generation | Chance-constrained programming | Minimizing the costs of buying power from thermal units + Minimizing the costs of buying spinning reserves from generators as well as demand-response resources |
| [125] | Renewable generations | Chance-constrained programming | Microgrid management by minimizing the operation costs of its units + Minimizing the costs of buying power from the upstream grid + Maximizing the revenue obtained from selling electricity to the upstream grid |
| [126] | Operational modes of the microgrids | Chance-constrained stochastic conic programming | Solving multi-site microgrids' investment problem and microgrid dual-mode network operations by minimizing microgrid operation and maintenance costs, microgrid electricity transaction costs, its network loss costs, and microgrid load curtailment costs |

**Table 8.** *Cont.*

| Ref. | Uncertain Parameters | Methods to Capture Uncertainties | Objective |
|---|---|---|---|
| [127] | PV generation and ambient temperatures | Chance-constrained programming | Active distribution network management incorporating office buildings by tracking building consumption and PV generation + Minimizing network losses |
| [128] | Renewable generation and loads | Chance-constrained programming | Finding potential self-sufficient sub-networks within the existing electrical distribution grid by maximizing average load served in each sub-network |
| [129] | PV generation | Chance-constrained programming | Designing solar-based microgrid and solving related dispatch problem by minimizing the capital costs of PV panels and the capacity costs and installation costs of energy storage system, the expected costs of multi-year operation of the microgrid which include load shedding penalty costs and wind micro-turbine generation costs |
| [130] | Renewable generation | Chance-constrained programming | Minimizing the total cost of generating power and gas |
| [131] | Loads and system frequency | Chance-constrained programming | Optimal scheduling of grid-connected batteries providing frequency-related services by minimizing the cost of purchasing energy from the grid as well as the system costs |
| [132] | Renewable generation | Mixed integer second order cone chance-constrained programming | Controlled islanding strategy |

## 7. Further Probabilistic Forecasting and Applications

As can be seen in the tables (Tables 6–8) that review studies using stochastic, robust, and chance-constrained programming, smart grids need more probabilistic forecasts [124] which are made for other uncertain parameters rather than loads, renewable generation and prices. EV charging-related behaviors, battery state-of-charge (SOC), dynamic line rating (DLR), and network states are some examples. In this regard, a few papers conducted studies to develop probabilistic forecasting of other uncertain parameters that are important for decision-making in smart grids. In this section, we will review these papers that employ probabilistic forecasting models for uncertain parameters, rather than the introduced popular uncertain parameters.

### *7.1. Probabilistic Forecast of BESS SOC*

Authors of [133] developed a probabilistic forecasting model that analyzes the uncertainties of the battery energy storage system's state of the charge (BESS SOC) in providing the primary frequency control. The results were then used as inputs of the predictive optimization of BESS which schedules BESS for providing multiple flexibility services. In order to develop the probabilistic forecasts, the authors applied a multi-attention recurrent neural network (MARNN) to extract the most important contextual information in time-series forecasting. Afterward, they proposed a robust forecast, utilizing the combination of mixture density networks (MDNs) and Monte Carlo dropout (MCD). Finally, the proposed model was tested for different regulatory frameworks of primary frequency control services, using the frequency datasets of real-world power grids.

### *7.2. Probabilistic Forecast of Time and Flexibility of EV Charging*

In [134], the authors employed a quantile forecast to probabilistically predict EVs' parking duration as well as their upcoming trip distance using the forecast framework introduced by [135]. To develop the model, German datasets regarding travel logs were adopted. In this regard, the authors first determined the requirements that are used as inputs of smart charging systems. In the second stage, they extracted features from the travel logs. Then, the paper compared the charging stations' current information with those of historical parking events. If the EV users grant the permission, the travel data are extracted from the smartphone applications. As a result, the authors proposed a forecasting model based on cross-validation performance. In the final stage, the results demonstrate that the charging station operator using the proposed forecasting model can profit by selling flexibility services. The model was also proven to resolve the congestion issue within the station.

*7.3. Probabilistic Forecast of Other Uncertain Parameters*

In [136], the authors developed a probabilistic forecasting model for the current rating of transmission lines using QRF in order to solve the dynamic line rating problem with a focus on the reliability of the distribution network's lower part. In the second stage, the results were employed to conduct a cost benefit analysis using a bi-level stochastic problem. The problem considered two aspects of costs: (1) the reduced generation costs due to the higher power transfer capacity and (2) the increased reserves' adoption resulted from forecast errors.

As another application, ref. [137] investigated the probabilistic forecast of low-voltage states (voltages as well as active and reactive power) for effective operation of distribution networks. In this regard, it tested two quantile forecasting methods considering different levels of distributed renewable generation injection. The probabilistic forecasting results were then integrated with an optimization problem to avoid over voltages within the networks.

**8. Conclusions and Future Direction**

This paper discussed the roadmap towards making decisions under uncertainty in a smart grid environment. This roadmap started with introducing different types of probabilistic forecasting and continued with discussing for which uncertain variables the literature uses probabilistic forecasting. In this regard, the main focus of the literature was on obtaining the probabilistic forecasting models for renewable generation (both wind and PV generation), electricity loads, and electricity prices.

Afterward, the paper described how probabilistic forecasting models were applied in the literature. For this purpose, it reviewed some papers adopting scenario generation techniques in smart grids. Two important methods of scenario generation, i.e., Monte Carlo simulation and generative adversarial Network, were introduced, and the paper explained in what way they are related to decision making. In addition, a limited number of papers utilizing introduced scenario generation methods in smart grids have been reviewed.

In the next step, decision-making under uncertainty was discussed. It was stated that energy management systems of smart grids need to solve optimization problems in order to operate and plan their resources. In fact, uncertainties should be taken into account in the optimization problem. Accordingly, stochastic, robust, and chance-constrained programming that consider uncertainties in the optimization problem were briefly introduced. It was discussed how these problems can be used in smart grid decision makings by reviewing the most recent papers.

Furthermore, two more applications of probabilistic forecasting were reviewed. Although there exist a wide range of uncertain parameters in smart grids, the probabilistic forecasting models were only developed for a limited number of these variables. For example, there are very few papers that proposed to develop probabilistic forecasting models for uncertain parameters of BESS and EVs (such as their SOC, charging power, etc.). However, decision-makers need the distributions of these variables along with those of loads and renewable output. Thus, future studies need to be conducted to obtain and develop distributions of EV's and BESS's parameters.

Finally, it should be mentioned that future power systems are heading toward hosting a high share of renewable generation. However, at the moment, power grids are not flexible enough to tolerate this situation and need more flexibility from different flexible energy resources and flexibility solutions (e.g., related to active network management). As a result, operators need to know:

- What are the available flexible energy resources in the current system?
- What are the potential flexible energy resources that should be activated?

- How much flexibility is needed for the future power system?

  To answer these questions, the system operators need to forecast:

- The flexibility required to deal with a high share of renewables in the future such as the reserves
- The available flexibility (related to active power $P$ and reactive power $Q$) of the system at different levels of the systems (flexibility at TSO, DSO, and customer levels)
- Potential congestions (voltage and/or thermal limit violations) of lines and other passive power system key components

Point forecasts of flexibility do not give operators a comprehensive insight in order to deal with the uncertainties of the future. However, with the help of probabilistic forecasts, decision-makers can assess different operational and planning decisions considering different renewable injection scenarios.

**Author Contributions:** Conceptualization, investigation, visualization: H.K.; writing—original draft preparation: H.K. and H.L.; writing—review and editing: H.K. and H.L.; supervision: H.L. All authors have read and agreed to the published version of the manuscript.

**Funding:** This research received no external funding.

**Institutional Review Board Statement:** Not applicable.

**Informed Consent Statement:** Not applicable.

**Data Availability Statement:** Not applicable.

**Acknowledgments:** The work of Hosna Khajeh was supported by the Ella and Georg Ehrnrooth Foundation.

**Conflicts of Interest:** The authors declare no conflict of interest.

### Abbreviations

| | |
|---|---|
| ANFIS | Adaptive Network-based Fuzzy Inference System |
| ANN | Artificial Neural Network |
| ARMArls | recursive least square Autoregressive and Moving Average |
| BELM | Bootstrap-based ELM |
| BESS | Battery Energy Storage System |
| CDF | Cumulative Distribution Function |
| DCNN | Deep Convolutional Neural Network |
| DQR | Direct Quantile Regression |
| DSO | Distribution System Operator |
| ELM | Extreme Learning Machine |
| EV | Electric Vehicle |
| EWT | Empirical Wavelet Transform |
| FCM | Fuzzy C-Means |
| GAMLSS | Generalized Additive Models for Location Scale and Shape |
| GAN | Generative Adversarial Network |
| GARCH | Generalized Autoregressive Conditional Heteroskedasticity |
| GBM | Gradient Boosting Machine |
| ICT | Information and Communication Technology |
| JQR | Joint Quantile Regression |
| KDE | Kernel Density Estimation |
| LDLF | Label Distribution Learning Forest |
| LMQR | Linear Model in Quantile regression |
| LSTM | Long Short-Term Memory |
| LUBE | Lower Upper Bound Estimate |
| MARNN | Multi-attention Recurrent Neural Network |
| MCD | Monte Carlo Dropout |

| | |
|---|---|
| MCM | Markov-chain Mixture distribution model |
| MCS | Monte Carlo Simulation |
| MDE | Multi-distribution Ensemble |
| MDN | Mixture Density Network |
| MSSA | Multi-objective Salp Swarm Algorithm |
| NWP | Numerical Weather Prediction |
| PDF | Probability Distribution Function |
| PI | Prediction Interval |
| PV | Photovoltaic |
| QRF | Quantile Regression Forecast |
| RBF-NN | Radial Basis Function-Neural Network |
| RF | Random forecast |
| RNN | Recurrent Neural Network |
| SOC | State of Charge |
| SREF | Short Range Ensemble Forecast |
| SRN | Soft-max Regression Networks |
| TSO | Transmission System Operator |
| VAR | Vector Autoregressive |

## Nomenclature

| | |
|---|---|
| $t$ | time |
| $x_{t,1}, \ldots, x_{t,m}$ | explanatory variables at $t$ |
| $b_1, \ldots, b_m$ | weights associated with explanatory variables |
| $F(y)$ | PDF |
| $\epsilon_t$ | forecast error at $t$ |
| $\mu_t$ | mean value of the distribution function at $t$ |
| $\sigma_t$ | standard deviation of the distribution function at $t$ |
| $v_t$ | skewness of the distribution function at $t$ |
| $\tau_t$ | kurtosis of the distribution function at $t$ |
| $g(.)$ | link function for modeling the mean value in terms of explanatory variables |
| $K$ | Kernel function |
| $l$ | Heaviside step function |
| $N$ | total number of sample points |
| $h$ | bandwidth referring to the smoothing parameter |
| $Y_t$, $y_t$ | response variable at $t$ |
| $\hat{Y}_t$, $\hat{y}_t$ | point forecast at $t$ |
| $P$ | active power |
| $Q$ | reactive power |

## References


1. Yang, D.; Dong, Z. Operational photovoltaics power forecasting using seasonal time series ensemble. *Sol. Energy* **2018**, *166*, 529–541. [CrossRef]
2. Yagli, G.M.; Yang, D.; Srinivasan, D. Ensemble solar forecasting using data-driven models with probabilistic post-processing through GAMLSS. *Sol. Energy* **2020**, *208*, 612–622. [CrossRef]
3. Gneiting, T.; Katzfuss, M. Probabilistic forecasting. *Ann. Rev. Stat. Its Appl.* **2014**, *1*, 125–151. [CrossRef]
4. Bazionis, I.K.; Karafotis, P.A.; Georgilakis, P.S. A review of short-term wind power probabilistic forecasting and a taxonomy focused on input data. *IET Renew. Power Gener.* **2021**, *16*, 12330. [CrossRef]
5. Zhang, Y.; Wang, J.; Wang, X. Review on probabilistic forecasting of wind power generation. *Renew. Sustain. Energy Rev.* **2014**, *32*, 255–270. [CrossRef]
6. Li, B.; Zhang, J. A review on the integration of probabilistic solar forecasting in power systems. *Sol. Energy* **2020**, *210*, 68–86. [CrossRef]
7. Panamtash, H.; Mahdavi, S.; Zhou, Q. Probabilistic Solar Power Forecasting: A Review and Comparison. In Proceedings of the 2020 52nd North American Power Symposium (NAPS), Tempe, AZ, USA, 11 April 2021; IEEE: Piscataway, NJ, USA, 2021; pp. 1–6.
8. van der Meer, D.W.; Widén, J.; Munkhammar, J. Review on probabilistic forecasting of photovoltaic power production and electricity consumption. *Renew. Sustain. Energy Rev.* **2018**, *81*, 1484–1512. [CrossRef]
9. Hong, T.; Fan, S. Probabilistic electric load forecasting: A tutorial review. *Int. J. Forecast.* **2016**, *32*, 914–938. [CrossRef]

10. Nowotarski, J.; Weron, R. Recent advances in electricity price forecasting: A review of probabilistic forecasting. *Renew. Sustain. Energy Rev.* **2018**, *81*, 1548–1568. [CrossRef]
11. Zhu, W.; Yu, Y.; Yang, M.; Zhao, Y. Review on Probabilistic Short-Term Power Forecast. In Proceedings of the 2021 IEEE/IAS Industrial and Commercial Power System Asia (I & CPS Asia), Chengdu, China, 18 July 2021; IEEE: Piscataway, NJ, USA, 2021; pp. 880–884.
12. Stasinopoulos, M.D.; Rigby, R.A.; Heller, G.Z.; Voudouris, V.; De Bastiani, F. *Flexible Regression and Smoothing: Using GAMLSS in R*; CRC Press: Boca Raton, FL, USA, 2017; ISBN 1-351-98037-8.
13. Bazionis, I.K.; Karafotis, P.A.; Georgilakis, P.S. A Comprehensive Review in Wind Power Probabilistic Forecasting. In Proceedings of the 12th Mediterranean Conference on Power Generation, Transmission, Distribution and Energy Conversion (MEDPOWER 2020), Online, 9–12 November 2021; Institution of Engineering and Technology: London, UK; pp. 455–460.
14. Li, R.; Peng, L. Quantile regression for left-truncated semicompeting risks data. *Biometrics* **2011**, *67*, 701–710. [CrossRef]
15. Panamtash, H.; Zhou, Q.; Hong, T.; Qu, Z.; Davis, K.O. A copula-based bayesian method for probabilistic solar power forecasting. *Sol. Energy* **2020**, *196*, 336–345. [CrossRef]
16. David, M.; Luis, M.A.; Lauret, P. Comparison of intraday probabilistic forecasting of solar irradiance using only endogenous data. *Int. J. Forecast.* **2018**, *34*, 529–547. [CrossRef]
17. Khorramdel, B.; Chung, C.Y.; Safari, N.; Price, G.C.D. A Fuzzy adaptive probabilistic wind power prediction framework using diffusion kernel density estimators. *IEEE Trans. Power Syst.* **2018**, *33*, 7109–7121. [CrossRef]
18. Zhang, Y.; Wang, J.; Luo, X. Probabilistic wind power forecasting based on logarithmic transformation and boundary kernel. *Energy Convers. Manag.* **2015**, *96*, 440–451. [CrossRef]
19. Chen, X.-Y.; Chau, K.-W. Uncertainty analysis on hybrid double feedforward neural network model for sediment load estimation with LUBE method. *Water Resour. Manag.* **2019**, *33*, 3563–3577. [CrossRef]
20. Wan, C.; Xu, Z.; Pinson, P.; Dong, Z.Y.; Wong, K.P. Probabilistic forecasting of wind power generation using extreme learning machine. *IEEE Trans. Power Syst.* **2014**, *29*, 1033–1044. [CrossRef]
21. Belorid, M.; Kim, K.R.; Cho, C. Bias Correction of short-range ensemble forecasts of daily maximum temperature using decaying average. *Asia-Pac. J. Atmos. Sci.* **2020**, *56*, 503–514. [CrossRef]
22. Dematos, G.; Boyd, M.S.; Kermanshahi, B.; Kohzadi, N.; Kaastra, I. Feedforward versus recurrent neural networks for forecasting monthly Japanese yen exchange rates. *Financ. Eng. Jpn. Mark.* **1996**, *3*, 59–75. [CrossRef]
23. Bishop, C. *Mixture Density Networks*; Tech. Rep. No. NCRG/94/004; Neural Computation Research Group, Aston University: Birmingham, UK, 1994.
24. Vossen, J.; Feron, B.; Monti, A. Probabilistic Forecasting of Household Electrical Load Using Artificial Neural Networks. In Proceedings of the 2018 IEEE International Conference on Probabilistic Methods Applied to Power Systems (PMAPS), Boise, ID, USA, 24–28 June 2018; IEEE: Piscataway, NJ, USA, 2018; pp. 1–6.
25. Toubeau, J.-F.; Bottieau, J.; Vallee, F.; De Greve, Z. Deep learning-based multivariate probabilistic forecasting for short-term scheduling in power markets. *IEEE Trans. Power Syst.* **2019**, *34*, 1203–1215. [CrossRef]
26. Verzijlbergh, R.A.; Heijnen, P.W.; de Roode, S.R.; Los, A.; Jonker, H.J.J. Improved model output statistics of numerical weather prediction based irradiance forecasts for solar power applications. *Sol. Energy* **2015**, *118*, 634–645. [CrossRef]
27. Schulz, B.; El Ayari, M.; Lerch, S.; Baran, S. Post-processing numerical weather prediction ensembles for probabilistic solar irradiance forecasting. *Sol. Energy* **2021**, *220*, 1016–1031. [CrossRef]
28. Murata, A.; Ohtake, H.; Oozeki, T. Modeling of uncertainty of solar irradiance forecasts on numerical weather predictions with the estimation of multiple confidence intervals. *Renew. Energy* **2018**, *117*, 193–201. [CrossRef]
29. Yagli, G.M.; Yang, D.; Srinivasan, D. Reconciling solar forecasts: Probabilistic forecasting with homoscedastic gaussian errors on a geographical hierarchy. *Sol. Energy* **2020**, *210*, 59–67. [CrossRef]
30. Fatemi, S.A.; Kuh, A.; Fripp, M. Parametric methods for probabilistic forecasting of solar irradiance. *Renew. Energy* **2018**, *129*, 666–676. [CrossRef]
31. Mazorra-Aguiar, L.; Lauret, P.; David, M.; Oliver, A.; Montero, G. Comparison of two solar probabilistic forecasting methodologies for microgrids energy efficiency. *Energies* **2021**, *14*, 1679. [CrossRef]
32. Cervone, G.; Clemente-Harding, L.; Alessandrini, S.; Delle Monache, L. Short-term photovoltaic power forecasting using artificial neural networks and an analog ensemble. *Renew. Energy* **2017**, *108*, 274–286. [CrossRef]
33. Sharma, V.; Ordiano, J.A.G.; Mikut, R.; Cali, U. Probabilistic solar power forecasting: Long short-term memory network vs. simpler approaches. *arXiv* **2021**, arXiv:2101.08236.
34. Bauer, P.; Thorpe, A.; Brunet, G. The quiet revolution of numerical weather prediction. *Nature* **2015**, *525*, 47–55. [CrossRef]
35. Buizza, R. Introduction to the special issue on "25 Years of Ensemble Forecasting". *Q. J. R. Meteorol. Soc.* **2019**, *145*, 1–11. [CrossRef]
36. Sweeney, C.; Bessa, R.J.; Browell, J.; Pinson, P. The future of forecasting for renewable energy. *WIREs Energy Environ.* **2020**, *9*, e365. [CrossRef]
37. Yagli, G.M.; Yang, D.; Srinivasan, D. Automatic hourly solar forecasting using machine learning models. *Renew. Sustain. Energy Rev.* **2019**, *105*, 487–498. [CrossRef]
38. Treiber, N.A.; Späth, S.; Heinermann, J.; von Bremen, L.; Kramer, O. Comparison of Numerical Models and Statistical Learning for Wind Speed Prediction. In Proceedings of the European Symposium on Artificial Neural Networks, Computational Intelligence and Machine Learning, Bruges, Belgium, 22–24 April 2015; pp. 71–76.

39. Wang, H.; Lei, Z.; Zhang, X.; Zhou, B.; Peng, J. A review of deep learning for renewable energy forecasting. *Energy Convers. Manag.* **2019**, *198*, 111799. [CrossRef]
40. Bazionis, I.K.; Georgilakis, P.S. Review of deterministic and probabilistic wind power forecasting: Models, methods, and future research. *Electricity* **2021**, *2*, 13–47. [CrossRef]
41. Pinson, P. Very-short-term probabilistic forecasting of wind power with generalized logit-normal distributions: Probabilistic forecasting of wind power. *J. R. Stat. Soc. Ser. C Appl. Stat.* **2012**, *61*, 555–576. [CrossRef]
42. Tastu, J.; Pinson, P.; Trombe, P.-J.; Madsen, H. Probabilistic forecasts of wind power generation accounting for geographically dispersed information. *IEEE Trans. Smart Grid* **2014**, *5*, 480–489. [CrossRef]
43. Bofinger, S.; Luig, A.; Beyer, H. *Qualification of Wind Power Forecasts*; University of Applied Sciences Magdeburg-Stendal: Magdeburg, Germany, 2002; pp. 2–5.
44. Zhang, Z.-S.; Sun, Y.-Z.; Gao, D.W.; Lin, J.; Cheng, L. A versatile probability distribution model for wind power forecast errors and its application in economic dispatch. *IEEE Trans. Power Syst.* **2013**, *28*, 3114–3125. [CrossRef]
45. Hodge, B.-M.; Milligan, M. Wind Power Forecasting Error Distributions over Multiple Timescales. In Proceedings of the 2011 IEEE Power and Energy Society General Meeting, Detroit, MI, USA, 24–28 July 2011; IEEE: Piscataway, NJ, USA, 2018; pp. 1–8.
46. Wan, C.; Lin, J.; Wang, J.; Song, Y.; Dong, Z.Y. Direct quantile regression for nonparametric probabilistic forecasting of wind power generation. *IEEE Trans. Power Syst.* **2017**, *32*, 2767–2778. [CrossRef]
47. Hu, J.; Tang, J.; Lin, Y. A novel wind power probabilistic forecasting approach based on joint quantile regression and multi-objective optimization. *Renew. Energy* **2020**, *149*, 141–164. [CrossRef]
48. Sun, M.; Feng, C.; Zhang, J. Multi-distribution ensemble probabilistic wind power forecasting. *Renew. Energy* **2020**, *148*, 135–149. [CrossRef]
49. Liu, H.; Yu, C.; Wu, H.; Duan, Z.; Yan, G. A new hybrid ensemble deep reinforcement learning model for wind speed short term forecasting. *Energy* **2020**, *202*, 117794. [CrossRef]
50. Dong, W.; Sun, H.; Tan, J.; Li, Z.; Zhang, J.; Yang, H. Regional wind power probabilistic forecasting based on an improved kernel density estimation, regular vine copulas, and ensemble learning. *Energy* **2022**, *238*, 122045. [CrossRef]
51. Wu, Y.-K.; Wu, Y.-C.; Hong, J.-S.; Phan, L.H.; Phan, Q.D. Probabilistic forecast of wind power generation with data processing and numerical weather predictions. *IEEE Trans. Ind. Appl.* **2021**, *57*, 36–45. [CrossRef]
52. Juban, J.; Fugon, L.; Kariniotakis, G. Probabilistic Short-Term Wind Power Forecasting Based on Kernel Density Estimators. In Proceedings of the European Wind Energy Conference and Exhibition, Milan, Italy, 7–10 May 2007; Available online: https://hal.archives-ouvertes.fr/hal-00526011/ (accessed on 1 December 2021).
53. Guan, C.; Luh, P.B.; Michel, L.D.; Chi, Z. Hybrid Kalman filters for very short-term load forecasting and prediction interval estimation. *IEEE Trans. Power Syst.* **2013**, *28*, 3806–3817. [CrossRef]
54. Shepero, M.; van der Meer, D.; Munkhammar, J.; Widén, J. Residential probabilistic load forecasting: A method using gaussian process designed for electric load data. *Appl. Energy* **2018**, *218*, 159–172. [CrossRef]
55. van der Meer, D.W.; Shepero, M.; Svensson, A.; Widén, J.; Munkhammar, J. Probabilistic forecasting of electricity consumption, photovoltaic power generation and net demand of an individual building using gaussian processes. *Appl. Energy* **2018**, *213*, 195–207. [CrossRef]
56. Quan, H.; Srinivasan, D.; Khosravi, A. Short-term load and wind power forecasting using neural network-based prediction intervals. *IEEE Trans. Neural Netw. Learn. Syst.* **2014**, *25*, 303–315. [CrossRef]
57. Quan, H.; Srinivasan, D.; Khosravi, A. Uncertainty handling using neural network-based prediction intervals for electrical load forecasting. *Energy* **2014**, *73*, 916–925. [CrossRef]
58. Ben Taieb, S.; Huser, R.; Hyndman, R.J.; Genton, M.G. Forecasting uncertainty in electricity smart meter data by boosting additive quantile regression. *IEEE Trans. Smart Grid* **2016**, *7*, 2448–2455. [CrossRef]
59. Zhang, S.; Wang, Y.; Zhang, Y.; Wang, D.; Zhang, N. Load probability density forecasting by transforming and combining quantile forecasts. *Appl. Energy* **2020**, *277*, 115600. [CrossRef]
60. Wang, Z.; Wang, Y.; Zeng, R.; Srinivasan, R.S.; Ahrentzen, S. Random forest based hourly building energy prediction. *Energy Build.* **2018**, *171*, 11–25. [CrossRef]
61. Bracale, A.; Carpinelli, G.; De Falco, P. A Bayesian-Based Approach for the Short-Term Forecasting of Electrical Loads in Smart Grids.: Part I: Theoretical Aspects. In Proceedings of the 2016 International Symposium on Power Electronics, Electrical Drives, Automation and Motion (SPEEDAM), Capri, Italy, 22–24 June 2016; IEEE: Piscataway, NJ, USA, 2016; pp. 121–128.
62. Munkhammar, J.; van der Meer, D.; Widén, J. Very short term load forecasting of residential electricity consumption using the markov-chain mixture distribution (MCM) model. *Appl. Energy* **2021**, *282*, 116180. [CrossRef]
63. Taylor, J.W.; Buizza, R. Using weather ensemble predictions in electricity demand forecasting. *Int. J. Forecast.* **2003**, *19*, 57–70. [CrossRef]
64. Petiau, B.R. Confidence Interval Estimation for Short-Term Load Forecasting. In Proceedings of the 2009 IEEE Bucharest PowerTech, Bucharest, Romania, 28 June–3 July 2009; IEEE: Piscataway, NJ, USA, 2009; pp. 1–6.
65. Lebotsa, M.E.; Sigauke, C.; Bere, A.; Fildes, R.; Boylan, J.E. Short term electricity demand forecasting using partially linear additive quantile regression with an application to the unit commitment problem. *Appl. Energy* **2018**, *222*, 104–118. [CrossRef]
66. Wang, Y.; Gan, D.; Sun, M.; Zhang, N.; Lu, Z.; Kang, C. Probabilistic individual load forecasting using pinball loss guided LSTM. *Appl. Energy* **2019**, *235*, 10–20. [CrossRef]

67. Pierro, M.; De Felice, M.; Maggioni, E.; Moser, D.; Perotto, A.; Spada, F.; Cornaro, C. Residual load probabilistic forecast for reserve assessment: A real case study. *Renew. Energy* **2020**, *149*, 508–522. [CrossRef]
68. Yang, S.; Xu, X.; Liu, J.; Jiang, W. Data-driven analysis of the real-time electricity price considering wind power effect. *Energy Rep.* **2020**, *6*, 452–459. [CrossRef]
69. Panagiotelis, A.; Smith, M. Bayesian density forecasting of intraday electricity prices using multivariate Skewt distributions. *Int. J. Forecast.* **2008**, *24*, 710–727. [CrossRef]
70. Serinaldi, F. Distributional modeling and short-term forecasting of electricity prices by generalized additive models for location, scale and shape. *Energy Econ.* **2011**, *33*, 1216–1226. [CrossRef]
71. Huurman, C.; Ravazzolo, F.; Zhou, C. The power of weather. *Comput. Stat. Data Anal.* **2012**, *56*, 3793–3807. [CrossRef]
72. Jónsson, T.; Pinson, P.; Madsen, H.; Nielsen, H. Predictive densities for day-ahead electricity prices using time-adaptive quantile regression. *Energies* **2014**, *7*, 5523–5547. [CrossRef]
73. He, H.; Lu, N.; Jiang, Y.; Chen, B.; Jiao, R. End-to-end probabilistic forecasting of electricity price via convolutional neural network and label distribution learning. *Energy Rep.* **2020**, *6*, 1176–1183. [CrossRef]
74. Muniain, P.; Ziel, F. Probabilistic forecasting in day-ahead electricity markets: Simulating peak and off-peak prices. *Int. J. Forecast.* **2020**, *36*, 1193–1210. [CrossRef]
75. Zakaria, A.; Ismail, F.B.; Lipu, M.S.H.; Hannan, M.A. Uncertainty models for stochastic optimization in renewable energy applications. *Renew. Energy* **2020**, *145*, 1543–1571. [CrossRef]
76. Lujano-Rojas, J.M.; Zubi, G.; Dufo-López, R.; Bernal-Agustín, J.L.; Catalão, J.P.S. Novel probabilistic optimization model for lead-acid and vanadium redox flow batteries under real-time pricing programs. *Int. J. Electr. Power Energy Syst.* **2018**, *97*, 72–84. [CrossRef]
77. Zheng, Y.; Jenkins, B.M.; Kornbluth, K.; Træholt, C. Optimization under uncertainty of a biomass-integrated renewable energy microgrid with energy storage. *Renew. Energy* **2018**, *123*, 204–217. [CrossRef]
78. Di Somma, M.; Graditi, G.; Heydarian-Forushani, E.; Shafie-khah, M.; Siano, P. Stochastic optimal scheduling of distributed energy resources with renewables considering economic and environmental aspects. *Renew. Energy* **2018**, *116*, 272–287. [CrossRef]
79. Pinheiro Neto, D.; Domingues, E.G.; Coimbra, A.P.; de Almeida, A.T.; Alves, A.J.; Calixto, W.P. Portfolio optimization of renewable energy assets: Hydro, wind, and photovoltaic energy in the regulated market in Brazil. *Energy Econ.* **2017**, *64*, 238–250. [CrossRef]
80. Hanbury, O.; Vasquez, V.R. Life cycle analysis of geothermal energy for power and transportation: A stochastic approach. *Renew. Energy* **2018**, *115*, 371–381. [CrossRef]
81. Chen, Y.; Wang, Y.; Kirschen, D.; Zhang, B. Model-free renewable scenario generation using generative adversarial networks. *IEEE Trans. Power Syst.* **2018**, *33*, 3265–3275. [CrossRef]
82. Chen, D.-G.; Chen, J.D. *Monte-Carlo Simulation-Based Statistical Modeling*; Springer: Berlin/Heidelberg, Germany, 2017; ISBN 981-10-3307-2.
83. Carpinelli, G.; Caramia, P.; Varilone, P. Multi-linear Monte Carlo simulation method for probabilistic load flow of distribution systems with wind and photovoltaic generation systems. *Renew. Energy* **2015**, *76*, 283–295. [CrossRef]
84. Conejo, A.J.; Carrión, M.; Morales, J.M. *Decision Making under Uncertainty in Electricity Markets*; Springer: Berlin/Heidelberg, Germany, 2010; Volume 1.
85. Sharafi, M.; El Mekkawy, T.Y. Stochastic optimization of hybrid renewable energy systems using sampling average method. *Renew. Sustain. Energy Rev.* **2015**, *52*, 1668–1679. [CrossRef]
86. Gomes, I.L.R.; Melicio, R.; Mendes, V.M.F. A Novel microgrid support management system based on stochastic mixed-integer linear programming. *Energy* **2021**, *223*, 120030. [CrossRef]
87. Zeynali, S.; Rostami, N.; Ahmadian, A.; Elkamel, A. Stochastic energy management of an electricity retailer with a novel plug-in electric vehicle-based demand response program and energy storage system: A linearized battery degradation cost model. *Sustain. Cities Soc.* **2021**, *74*, 103154. [CrossRef]
88. Daneshvar, M.; Mohammadi-Ivatloo, B.; Zare, K.; Asadi, S. Two-stage stochastic programming model for optimal scheduling of the wind-thermal-hydropower-pumped storage system considering the flexibility assessment. *Energy* **2020**, *193*, 116657. [CrossRef]
89. Evangelopoulos, V.A.; Avramidis, I.I.; Georgilakis, P.S. Flexibility services management under uncertainties for power distribution systems: Stochastic scheduling and predictive real-time dispatch. *IEEE Access* **2020**, *8*, 38855–38871. [CrossRef]
90. Mirzaei, M.A.; Hemmati, M.; Zare, K.; Abapour, M.; Mohammadi-Ivatloo, B.; Marzband, M.; Anvari-Moghaddam, A. A novel hybrid two-stage framework for flexible bidding strategy of reconfigurable micro-grid in day-ahead and real-time markets. *Int. J. Electr. Power Energy Syst.* **2020**, *123*, 106293. [CrossRef]
91. Ansari, M.R.; Pirouzi, S.; Kazemi, M.; Naderipour, A.; Benbouzid, M. Renewable Generation and transmission expansion planning coordination with energy storage system: A flexibility point of view. *Appl. Sci.* **2021**, *11*, 3303. [CrossRef]
92. Usman, M.; Capitanescu, F. A Stochastic Multi-Period AC Optimal Power Flow for Provision of Flexibility Services in Smart Grids. In Proceedings of the 2021 IEEE Madrid PowerTech, Madrid, Spain, 28 June 2021; IEEE: Piscataway, NJ, USA, 2021; pp. 1–6.
93. Beraldi, P.; Violi, A.; Carrozzino, G.; Bruni, M.E. A Stochastic programming approach for the optimal management of aggregated distributed energy resources. *Comput. Oper. Res.* **2018**, *96*, 200–212. [CrossRef]
94. Hafiz, F.; Rodrigo de Queiroz, A.; Fajri, P.; Husain, I. Energy management and optimal storage sizing for a shared community: A multi-stage stochastic programming approach. *Appl. Energy* **2019**, *236*, 42–54. [CrossRef]

95. Kang, P.; Guo, W.; Huang, W.; Qiu, Z.; Yu, M.; Zheng, F.; Zhang, Y. Two-stage stochastic programming scheduling model for hybrid AC/DC distribution network considering converters and energy storage system. *Appl. Sci.* **2019**, *10*, 181. [CrossRef]
96. Liu, C.; Abdulkareem, S.S.; Rezvani, A.; Samad, S.; Aljojo, N.; Foong, L.K.; Nishihara, K. Stochastic scheduling of a renewable-based microgrid in the presence of electric vehicles using modified harmony search algorithm with control policies. *Sustain. Cities Soc.* **2020**, *59*, 102183. [CrossRef]
97. Khajeh, H.; Foroud, A.A.; Firoozi, H. Robust bidding strategies and scheduling of a price-maker microgrid aggregator participating in a pool-based electricity market. *IET Gener. Transm. Distrib.* **2019**, *13*, 468–477. [CrossRef]
98. Jiang, Z.; Yu, Q.; Xiong, Y.; Li, L.; Liu, Y. Regional active distribution network planning study based on robust optimization. *Energy Rep.* **2021**, *7*, 314–319. [CrossRef]
99. Wang, Y.; Hu, S.; Song, Y.; Zeng, Q.; Zheng, Z. Robust co-planning of transmission network and B-SMES. *IEEE Trans. Appl. Superconduct.* **2021**, *31*, 1–4. [CrossRef]
100. Chowdhury, N.; Pilo, F.; Pisano, G. Optimal energy storage system positioning and sizing with robust optimization. *Energies* **2020**, *13*, 512. [CrossRef]
101. Bozorgavari, S.A.; Aghaei, J.; Pirouzi, S.; Nikoobakht, A.; Farahmand, H.; Korpås, M. Robust planning of distributed battery energy storage systems in flexible smart distribution networks: A comprehensive study. *Renew. Sustain. Energy Rev.* **2020**, *123*, 109739. [CrossRef]
102. Shahbazi, A.; Aghaei, J.; Pirouzi, S.; Shafie-khah, M.; Catalão, J.P.S. Hybrid stochastic/robust optimization model for resilient architecture of distribution networks against extreme weather conditions. *Int. J. Electr. Power Energy Syst.* **2021**, *126*, 106576. [CrossRef]
103. Moreira, A.; Pozo, D.; Street, A.; Sauma, E.; Strbac, G. Climate-aware generation and transmission expansion planning: A three-stage robust optimization approach. *Eur. J. Oper. Res.* **2021**, *295*, 1099–1118. [CrossRef]
104. Sadek, S.M.; Omran, W.A.; Hassan, M.A.M.; Talaat, H.E.A. Adaptive robust energy management for isolated microgrids considering reactive power capabilities of distributed energy resources and reactive power costs. *Electr. Power Syst. Res.* **2021**, *199*, 107375. [CrossRef]
105. Lu, J.; Liu, T.; He, C.; Nan, L.; Hu, X. Robust day-ahead coordinated scheduling of multi-energy systems with integrated heat-electricity demand response and high penetration of renewable energy. *Renew. Energy* **2021**, *178*, 466–482. [CrossRef]
106. Mehdipourpicha, H.; Wang, S.; Bo, R. Developing robust bidding strategy for virtual bidders in day-ahead electricity markets. *IEEE Open J. Power Energy* **2021**, *8*, 329–340. [CrossRef]
107. Xie, Y.; Guo, W.; Wu, Q.; Wang, K. Robust MPC-based bidding strategy for wind storage systems in real-time energy and regulation markets. *Int. J. Electr. Power Energy Syst.* **2021**, *124*, 106361. [CrossRef]
108. Gong, Y.; Liu, P.; Liu, Y.; Huang, K. Robust operation interval of a large-scale hydro-photovoltaic power system to cope with emergencies. *Appl. Energy* **2021**, *290*, 116612. [CrossRef]
109. Tsao, Y.-C.; Thanh, V.-V.; Wu, Q. Sustainable microgrid design considering blockchain technology for real-time price-based demand response programs. *Int. J. Electr. Power Energy Syst.* **2021**, *125*, 106418. [CrossRef]
110. Bahramara, S. Robust optimization of the flexibility-constrained energy management problem for a smart home with rooftop photovoltaic and an energy storage. *J. Energy Storage* **2021**, *36*, 102358. [CrossRef]
111. Mokaramian, E.; Shayeghi, H.; Sedaghati, F.; Safari, A.; Alhelou, H.H. A CVaR-Robust-based multi-objective optimization model for energy hub considering uncertainty and E-fuel energy storage in energy and reserve markets. *IEEE Access* **2021**, *9*, 109447–109464. [CrossRef]
112. Akbari-Dibavar, A.; Nojavan, S.; Mohammadi-Ivatloo, B.; Zare, K. Smart home energy management using hybrid robust-stochastic optimization. *Comput. Ind. Eng.* **2020**, *143*, 106425. [CrossRef]
113. Kim, H.J.; Kim, M.K.; Lee, J.W. A Two-stage stochastic p-robust optimal energy trading management in microgrid operation considering uncertainty with hybrid demand response. *Int. J. Electr. Power Energy Syst.* **2021**, *124*, 106422. [CrossRef]
114. Dini, A.; Pirouzi, S.; Norouzi, M.; Lehtonen, M. Hybrid stochastic/robust scheduling of the grid-connected microgrid based on the linear coordinated power management strategy. *Sustain. Energy Grids Netw.* **2020**, *24*, 100400. [CrossRef]
115. Cai, S.; Xie, Y.; Wu, Q.; Xiang, Z. Robust MPC-based microgrid scheduling for resilience enhancement of distribution system. *Int. J. Electr. Power Energy Syst.* **2020**, *121*, 106068. [CrossRef]
116. Ghayoor, F.; Ghannadpour, S.F.; Imani, D.M. Bi-objective robust optimization for reliability-oriented power network planning by considering distributed generation effects: A case study in Iran. *Sustain. Energy Grids Netw.* **2021**, *26*, 100455. [CrossRef]
117. Zhang, C.; Liu, L.; Cheng, H.; Liu, D.; Zhang, J.; Li, G. Data-driven distributionally robust transmission expansion planning considering contingency-constrained generation reserve optimization. *Int. J. Electr. Power Energy Syst.* **2021**, *131*, 106973. [CrossRef]
118. Dong, H.; Wang, L.; Wei, X.; Xu, Y.; Li, W.; Zhang, X.; Zeng, M. Capacity planning and pricing design of charging station considering the uncertainty of user behavior. *Int. J. Electr. Power Energy Syst.* **2021**, *125*, 106521. [CrossRef]
119. Pandey, S.; Han, J.; Gurung, N.; Chen, H.; Paaso, E.A.; Li, Z.; Khodaei, A. Multi-criteria decision-making and robust optimization methodology for generator sizing of a microgrid. *IEEE Access* **2021**, *9*, 142264–142275. [CrossRef]
120. Nemirovski, A.; Shapiro, A. Convex approximations of chance constrained programs. *SIAM J. Optim.* **2007**, *17*, 969–996. [CrossRef]

121. Daneshvar, M.; Mohammadi-Ivatloo, B.; Asadi, S.; Anvari-Moghaddam, A.; Rasouli, M.; Abapour, M.; Gharehpetian, B.G. Chance-constrained models for transactive energy management of interconnected microgrid clusters. *J. Clean. Prod.* **2020**, *271*, 122177. [CrossRef]
122. Yuan, W.; Wang, X.; Su, C.; Cheng, C.; Liu, Z.; Wu, Z. Stochastic optimization model for the short-term joint operation of photovoltaic power and hydropower plants based on chance-constrained programming. *Energy* **2021**, *222*, 119996. [CrossRef]
123. Mianaei, P.K.; Aliahmadi, M.; Faghri, S.; Ensaf, M.; Ghasemi, A.; Abdoos, A.A. Chance-constrained programming for optimal scheduling of combined cooling, heating, and power-based microgrid coupled with flexible technologies. *Sustain. Cities Soc.* **2021**, *77*, 103502. [CrossRef]
124. Ardakani, F.F.; Mozafari, S.B.; Soleymani, S. Scheduling energy and spinning reserve based on linear chance constrained optimization for a wind integrated power system. *Ain Shams Eng. J.* **2021**, *13*, S2090447921003476. [CrossRef]
125. Marino, C.A.; Marufuzzaman, M. A microgrid energy management system based on chance-constrained stochastic optimization and big data analytics. *Comput. Ind. Eng.* **2020**, *143*, 106392. [CrossRef]
126. Cao, X.; Wang, J.; Zeng, B. Networked microgrids planning through chance constrained stochastic conic programming. *IEEE Trans. Smart Grid* **2019**, *10*, 6619–6628. [CrossRef]
127. Li, W.; Liu, Y.; Liang, H.; Man, Y.; Li, F. Distributed tracking-ADMM approach for chance-constrained energy management with stochastic wind power in smart grid. *CSEE J. Power Energy Syst.* **2021**, 1–11. [CrossRef]
128. Biswas, S.; Singh, M.K.; Centeno, V.A. Chance-constrained optimal distribution network partitioning to enhance power grid resilience. *IEEE Access* **2021**, *9*, 42169–42181. [CrossRef]
129. Dashti, H.; Cheng, J.; Krokhmal, P. Chance-constrained optimization-based solar microgrid design and dispatch for radial distribution networks. *Energy Syst.* **2021**. [CrossRef]
130. Yang, T.; Song, B.; Jiang, S.; Wang, B. Steady-State Security Region-Based Chance-Constrained Optimization for Integrated Energy Systems. In Proceedings of the 2020 IEEE 4th Conference on Energy Internet and Energy System Integration (EI2), Wuhan, China, 30 October 2020; IEEE: Piscataway, NJ, USA, 2020; pp. 1307–1312.
131. Zhong, W.; Xie, K.; Liu, Y.; Xie, S.; Xie, L. Chance constrained scheduling and pricing for multi-service battery energy storage. *IEEE Trans. Smart Grid* **2021**, *12*, 5030–5042. [CrossRef]
132. Liu, S.; Zhang, T.; Lin, Z.; Liu, Y.; Ding, Y.; Yang, L. Controlled islanding strategy considering uncertainty of renewable energy sources based on chance-constrained model. *J. Modern Power Syst. Clean Energy* **2021**, 1–11. [CrossRef]
133. Mashlakov, A.; Lensu, L.; Kaarna, A.; Tikka, V.; Honkapuro, S. Probabilistic forecasting of battery energy storage state-of-charge under primary frequency control. *IEEE J. Select. Areas Commun.* **2020**, *38*, 96–109. [CrossRef]
134. Huber, J.; Dann, D.; Weinhardt, C. Probabilistic forecasts of time and energy flexibility in battery electric vehicle charging. *Appl. Energy* **2020**, *262*, 114525. [CrossRef]
135. Hyndman, R.J.; Athanasopoulos, G. *Forecasting: Principles and Practice*; Otexts: Melbourne, Australia, 2018; ISBN 0-9875071-1-7.
136. Dupin, R.; Michiorri, A.; Kariniotakis, G. Optimal dynamic line rating forecasts selection based on ampacity probabilistic forecasting and network operators' risk aversion. *IEEE Trans. Power Syst.* **2019**, *34*, 2836–2845. [CrossRef]
137. Zufferey, T.; Renggli, S.; Hug, G. Probabilistic state forecasting and optimal voltage control in distribution grids under uncertainty. *Electr. Power Syst. Res.* **2020**, *188*, 106562. [CrossRef]

Electric Power Systems Research 205 (2022) 107767

Contents lists available at ScienceDirect

Electric Power Systems Research

journal homepage: www.elsevier.com/locate/epsr

# Flexibility Potential of a Smart Home to Provide TSO-DSO-level Services

Hosna Khajeh, Hooman Firoozi, Hannu Laaksonen *

*School of Technology and Innovations, Flexible Energy Resources, University of Vaasa, 65200 Vaasa, Finland*

ARTICLE INFO

*Keywords:*
smart homes
flexibility services
energy flexibility
demand response
controllable appliances

ABSTRACT

The high penetration of intermittent renewable-based power into modern power systems increases the need for more technical ancillary services from flexible energy resources. Smart homes could provide different flexibility services related to active power control services and therefore fulfill a part of the flexibility needs of system operators. In this regard, the estimation of the flexible capacities of each smart home's flexible device is of key importance. Correspondingly, this paper first estimates the flexible capacities of a smart home with controllable devices as flexible resources. The flexible capacity of each appliance is estimated considering its flexible and non-flexible operations. Besides, the local and system-wide flexibility services are introduced and the paper discusses whether a smart home can provide these types of services. In the simulations of this paper, the flexible capacity of each household appliance is estimated and compared to each other. Finally, the profitability of the smart home's battery energy storage multi-use is analyzed when it is providing three different types of flexibility services for the transmission system operator's needs. The results demonstrate that in some scenarios, the smart home's battery energy storage can increase its profits by providing transmission-system-level flexibility.

## 1. Introduction

### 1.1. Motivation

Modern power systems aim to host renewable-based energy as much as possible to minimize the environmental impacts of energy generation. However, the power produced by renewable resources is intermittent and uncertain. The high penetration of intermittent renewable-based power into the electricity networks increases the system operators' flexibility needs. Future power systems are required to be more flexible and be able to change their operating points constantly according to the real-time demand or/and generation fluctuations. In this regard, different types of technical ancillary services i.e. flexibility services are employed to manage the future power system with increasing flexibility needs.

In general, flexibility services are procured to fulfil local and system-wide flexibility needs. Local flexibility services help local distribution system operators (DSO) increase the flexibility of their electricity distribution networks. On the other hand, system-wide flexibility services assist transmission system operators (TSO) in controlling the frequency of the system and thus enhance the system-wide flexibility. TSOs and DSOs procure flexibility services from flexible energy resources (FER). Currently, conventional fuel-based generators are the main FERs utilized to provide system-wide flexibility services [1]. Besides, DSOs use conventional regulators and devices for the local flexibility provision. However, the employment of these devices as the only approach of operating distribution networks is not enough for the future power system with the high penetration of renewable generations [2].

To this end, both DSOs and TSOs need to employ new FERs to resolve the future flexibility requirements. Active and smart residential customers connected to distribution networks are very potential FERs that can provide flexibility for the TSOs and DSOs. Smart homes have some flexible appliances that can be controlled according to the system operators' needs. In this way, they sell their flexibility i.e. flexible capacities to the system operators and receive the monetary profits accordingly. In this way, the system operators are able to exploit the maximum flexibility potential of the active customers connected to distribution networks.

### 1.2. Literature review

In this context, there is some research proposing the participation of smart homes and residential customers in providing flexibility services. Some studies mainly focused on the provision of local flexibility services through active residential customers. For example, [3] suggested a centralized control of smart homes' appliances with the aim of providing local flexibility services. In that research, the DSO determines dynamic

* Corresponding author:
*E-mail address:* hannu.laaksonen@uwasa.fi (H. Laaksonen).

https://doi.org/10.1016/j.epsr.2021.107767
Received 18 October 2021; Received in revised form 21 December 2021; Accepted 27 December 2021
Available online 31 December 2021

**Nomenclature**

*Abbreviations*

| | |
|---|---|
| AC | Air Conditioner |
| BES | Battery Energy Storage |
| DSO | Distribution System Operator |
| EV | Electric Vehicle |
| EWH | Electric Water Heater |
| FCR | Frequency Containment Reserve |
| FER | Flexible Energy Resource |
| FFR | Fast Frequency Reserve |
| FRR | Frequency Restoration Reserve |
| HEMS | Home Energy Management System |
| SOC | State of Charge |
| TSO | Transmission System Operator |

*Sets*

| | |
|---|---|
| $t$ | Time |
| $s$ | Scenario |

*AC-related parameters*

| | |
|---|---|
| $\underline{\theta^h}$ | Lower limit of the desired temperature of the household [°C] |
| $\overline{\theta^h}$ | Upper limit of the desired temperature of the household [°C] |
| $\theta_t^{amb}$ | Ambient temperature at time $t$ [°C] |
| $\alpha$ | Constant related to the thermal characteristic of the household |
| $\beta$ | Coefficient of the AC's performance [°C /kWh][heat: $\beta > 0$, cool: $\beta < 0$] |
| $\overline{P^{AC}}$ | Nominal power consumption of the AC [kW] |

*AC-related variables*

| | |
|---|---|
| $\theta_t^h$ | Household indoor temperature at time $t$ [°C] |
| $P_t^{AC}$ | Operating power of the AC at time $t$ (in general) [kW] |
| $P_t^{AC-C1}$ | Non-flexible operating power of the AC at time $t$ [kW] |
| $P_t^{AC-C2U}$ | Operating power of the AC at time $t$ when it provides upward flexibility [kW] |
| $P_t^{AC-C2D}$ | Operating power of the AC at time $t$ when it provides downward flexibility [kW] |

*EWH-related parameters*

| | |
|---|---|
| $\underline{\theta^w}$ | Minimum temperature of the hot water [°C] |
| $\overline{\theta^w}$ | Maximum temperature of the hot water [°C] |
| $\widetilde{Q}_h^{EWH}$ | Maximum energy demand of the EWH [kWh] |
| $k$ | Constant of energy conversion [kWh/J] |
| $\rho$ | Specific heat of water [J/kg°C] |
| $v^{EWH}$ | Capacity of the EWH tank [kg] |
| $V_t^{tank}$ | Volume of the stored water in the EWH tank at time $t$ [kg] |
| $\theta^{w,ini}$ | Initial in-tank water temperature [°C] |
| $\theta^{cold}$ | Temperature of inlet cold water [°C] |
| $\overline{P^{EWH}}$ | Nominal power consumption of the EWH [kW] |

*EWH-related variables*

| | |
|---|---|
| $\theta_t^w$ | Temperature of EWH's water at time $t$ [°C] |
| $Q_t^{EWH}$ | Energy demand of the drained hot water of the EWH at time $t$ [kWh] |
| $P_t^{EWH}$ | Operating power of the EWH at time $t$ (in general) [kW] |
| $P_t^{EWH-C1}$ | Non-flexible operating power of the EWH at time $t$ [kW] |
| $P_t^{EWH-C2U}$ | Operating power of the EWH at time $t$ when it provides upward flexibility [kW] |
| $P_t^{EWH-C2D}$ | Operating power of the EWH at time $t$ when it provides downward flexibility [kW] |

*EV-related parameters*

| | |
|---|---|
| $\underline{SOC_t^{EV}}$ | Lower limit for the EV's battery SOC at time $t$ |
| $\overline{SOC^{EV}}$ | Upper limit for the EV's battery SOC |
| $Cap^{EV}$ | Maximum capacity of EV's battery [kWh] |
| $\overline{P^{AC}}$ | Maximum charging power of the EV's battery [kW] |
| $\eta^{EV}$ | Charging efficiency of the EV's battery |

*EV-related variables*

| | |
|---|---|
| $SOC_t^{EV}$ | SOC of the EV's battery at time $t$ |
| $P_t^{EV-C1}$ | Non-flexible charging power of the EV's battery at time $t$ [kW] |
| $P_t^{EV-C2U}$ | Charging power of the EV at time $t$ when it provides upward flexibility [kW] |
| $P_t^{EV-C2D}$ | Charging power of the EV at time $t$ when it provides downward flexibility [kW] |

*BES-related parameters*

| | |
|---|---|
| $\underline{SOC_t^B}$ | Lower limit for the BES SOC at time $t$ |
| $\overline{SOC^B}$ | Upper limit for the BES SOC at time $t$ |
| $\overline{P^{B,dis}}$ | Maximum discharging power of the BES [kW] |
| $\overline{P^{B,ch}}$ | Maximum charging power of the BES [kW] |
| $Cap^B$ | Maximum capacity of the BES [kWh] |
| $\eta^{B,ch}$ | Charging efficiency of the BES |
| $\eta^{B,dis}$ | Discharging efficiency of the BES |

*BES-related variables*

| | |
|---|---|
| $P_t^{B,ch-U}$ | Charging power of the BES when it provides upward flexibility [kW] |
| $P_t^{B,ch-D}$ | Charging power of the BES when it provides downward flexibility [kW] |
| $P_t^{B,dis-U}$ | Discharging power of the BES when it provides upward flexibility [kW] |
| $P_t^{B,dis-D}$ | Discharging power of the BES when it provides downward flexibility [kW] |

tariffs as well as daily network tariffs to manage the congestion in the distribution networks. However, the provision of system-wide flexibility services was not analyzed in the paper. In another work, [4] proposed a real-time re-scheduling model for shiftable appliances to respond to the DSO's flexibility requests. Then, it utilized evolutionary algorithms to solve the scheduling problem. The paper did not consider the constraints related to the operation of different appliances. For example, it did not consider the constraints imposed by the household thermal comfort and their impacts on the operation of the appliances. Reference [5] also analyzed the provision of local services through the aggregated commercial customers. However, the main focus of the paper was on the aggregation method and the interaction between the DSO and the aggregator, and not on the appliances' scheduling and the flexible capacity potential of the customers. Also, [6] suggested the use of flexible energy resources to tackle operational challenges of DSOs. The paper did not take into consideration the details about modeling these flexible energy resources. Finally, [7] presented a market environment for the participation of households in the provision of local flexibility services. Although the paper presented a comprehensive model, it did not introduce any details and mathematical models of household appliances and their flexible operations.

The contribution of residential customers to the system-wide flexibility, on the other hand, was more taken into consideration in the previous research. For instance, some authors proposed demand-side customers participating in peak-shaving programs. References [8, 9]–[12] are the examples that presented the optimal management of household appliances by shifting them to off-peak time slots and thus provide flexibility for the grid. The peak-shaving programs, however, cannot enhance the real-time flexibility of power systems and directly help the system operators deal with real-time flexibility issues resulted from intermittent renewable generation. On the other hand, [13] introduced a new local market for providing both system-wide and local flexibility services by residential prosumers. In that paper, the prosumers sell their flexible capacities to the TSO and the DSO, so that the system operators are able to follow their flexibility needs in real-time. However, the focus of the paper is more on the local capacity market clearing mechanism and the details of prosumers' scheduling were not included in the paper. Besides, [14] provided a tool that studies different aspects of demand response business models. It also presented a demand response business model canvas through which, a residential customer is able to analyze the demand response offers as well as the types of benefits that can be achieved by selling flexibility. The details and mathematical formulations about flexible capacities of these customers were not assessed in the paper. Authors of [15] developed a two-stage optimization problem aiming to maximize the revenues of small-scale prosumers that provide tertiary frequency services. Again, the constraints related to appliances' operation and the comfort level of household customers were not thoroughly modeled, similar to the works conducted by [16, 17] and [18]. These works tried to model household controllable appliances in a general way, by scheduling their working timetables, although each appliance may have its own operational and usage-based constraints. In other words, although a wide range of controllable appliances can be categorized into shiftable loads, their operations' limitations are different and thus they cannot be modeled together.

In comparison, some research analyzed the smart homes' flexibility provision capability using the details and the mathematical models of appliances. In this regard, [19] proposed two methods for controlling thermostatically controllable loads (TCL) and quantifying their available flexibility. Although the research utilized the mathematical models of TCL appliances, it does not calculate the flexibility potential of other flexible appliances. In another study, [20] presented a comprehensive work on how smart homes can provide demand response programs, solely or in an aggregated manner. This work did not mathematically model household appliances, individually. Besides, [21] proposed that the neighboring residential customers form a local energy community to provide frequency restoration reserves (FCR) as a system-wide service. The paper only considered EVs and a BES as a shared FER providing flexibility. In another research, [22] suggested a new method to forecast the flexibility of residential customers and schedule their electric water heaters (EWH) to provide frequency containment reserves (FCR) for the TSO. Household air conditioners (AC) were also proposed to be aggregated in [23], playing active roles in the operating reserve provision. Also, [24] introduced a general formulation to obtain the flexibility percentage of household appliances. The details and constraints of these appliances were not modeled in that work. In a similar study, [25] analyzed the response of TCLs, in general, that help to maintain the balance between the system's demand and generation. However, thermostatically controllable appliances and storage-based devices can be scheduled simultaneously for providing different types of flexibility services, which were not considered in the previous mentioned literature. Finally, [26] provided a review on flexibility potential of household appliances. The work, however, did not present any mathematical model to calculate the flexible capacities of these appliances and the residential customers.

### *1.3. Contribution and Structure*

In this paper, smart homes aim to provide flexibility services for system operators. Table 1 compares the reviewed literature with this paper. The first four columns analyze whether they mathematically modeled the appliance as an FER. The last column assesses if the research tried to estimate, calculate, or forecast the flexible capacities adopted by the household appliances. These flexible capacities should be obtained from comparing the normal operation and flexible operation of the appliances.

Considering Table 1, the contribution of the paper can be categorized into three main points:

1- We consider two types of appliances, thermostatically controllable appliances and storage-based devices. Thermostatically controllable appliances include an AC and an EWH whose operations affect the thermal comfort of the household. Storage-based devices include an EV and a BES. The EV charging is scheduled according to its availability and the owner's charging preference while the total capacity of the BES is utilized for flexibility purposes. To the best of the authors' knowledge, the simultaneous operation of these four appliances for providing flexibility has not been considered in the existing literature.

2- We estimate the flexible capacity of a household based on the flexible and non-flexible operations of its controllable appliances. It should be noted that estimating the flexible capacity is of vital necessity for system operators, household aggregators and the household, itself. System operators should assign monetary values according to the flexible capacities of the households and the aggregators and the household need this estimation to build bidding strategies and choose the appropriate flexibility services. However, to the best of the authors' knowledge, there exists no previous research dealing with estimating the flexible capacity of households by modeling their controllable appliances.

3- Finally, we introduce different types of flexibility services based on the European terminology of TSO-level flexibility services for frequency control. Besides, in the simulation section, multi-use scenarios of a smart home's BES is analyzed and the profitability of providing three types of system-wide (TSO-level) services is assessed considering different activation scenarios.

The rest of the paper is organized as follows. Section 3 estimates the

**TABLE 1**
A comparison between our paper and the existing literature

| Ref. | Providing mathematical models for: AC as FER | EWH as FER | EV as FER | BES as FER | Flexible capacity forecast/estimation |
|---|---|---|---|---|---|
| [3] | - | - | ✓ | - | - |
| [4] | - | - | - | - | - |
| [5] | - | - | - | ✓ | - |
| [7] | - | - | - | - | - |
| [8] | - | - | - | ✓ | - |
| [9] | - | - | - | - | - |
| [10] | ✓ | ✓ | - | ✓ | - |
| [11] | - | - | - | ✓ | - |
| [12] | - | - | ✓ | - | - |
| [13] | - | - | - | - | - |
| [14] | - | - | - | - | - |
| [15] | ✓ | - | ✓ | - | - |
| [16] | - | - | - | - | - |
| [17] | - | - | ✓ | ✓ | - |
| [18] | - | - | - | - | - |
| [19] | ✓ | | | | Quantify |
| [21] | - | - | ✓ | ✓ | - |
| [22] | - | ✓ | - | - | Forecast |
| [23] | ✓ | - | - | - | - |
| [24] | - | - | - | - | Estimation |
| [25] | ✓ | - | - | - | - |
| [26] | ✓ | - | ✓ | ✓ | - |
| Our paper | ✓ | ✓ | ✓ | ✓ | Estimation |

flexible capacities of household appliances according to their flexible and non-flexible operations. Section 4 introduces the existing TSO-level flexibility services and discusses whether a smart home can provide these services. Section 5 provides a brief discussion about the participation of a smart home in providing DSO local services. Section 6 tries to estimate and compare the flexibility of different household appliances. Finally, section 6 concludes the paper.

## 2. Estimating the flexibility of a Smart Home

The flexible capacities of a smart home need to be estimated before their activation. The reasons are twofold. First, the home energy management system (HEMS) that controls the controllable appliances should evaluate the flexibility potential of the smart home before its activation to check the availability of these appliances and to conduct cost-benefit analyses. Second, system operators need to estimate the flexible capacity of a smart home that has reacted to the operators' flexibility requests. In this way, the operators are able to assign monetary compensation based on the available flexible capacity of the smart home. However, it would be difficult to distinguish between the household's actual load and its flexibility that is resulted from its reaction to the flexibility signals. It is worth mentioning that uncontrollable appliances cannot provide flexibility. It means that only controllable appliances are able to provide flexibility. However, we can estimate their flexibility by estimating the change of controllable appliances' operation according to their reaction to flexibility signals. To this end, we propose that the flexible capacity of each controllable device is estimated by comparing the device's normal operation and its flexible operation. Fig. 1 summarizes normal and flexible operations for four types of controllable appliances. It should be noted that the focus of this work is to maximize the appliances' flexible operations in near real-time. In the following section, this paper aims to estimate the flexibility of each controllable appliance based on its specific characteristics.

### *2.1. Estimating the flexibility of thermostatically controllable loads*

Household thermostatically controllable loads (TCL) mostly come from space heating and cooling as well as the hot water consumption. In this way, this paper considers the consumption of two appliances including EWH and AC as thermostatically controllable loads. We consider two cases for the operation of these devices to estimate their flexible capacities. The first case represents the non-flexible operation of appliances whereas the second case introduces the flexible operation of the devices. It is assumed that the smart home is equipped with an intelligent HEMS that schedules the controllable appliances based on the defined objective. Fig. 2 overviews the general model of a smart home and its flexibility-related application.

#### *2.1.1. Case 1: normal operation*

For the first case, the HEMS is assumed to control thermostatically controllable devices aiming to maximize the thermal comfort level. Therefore, the objective function of the HEMS is as follows:

$$\min_{\theta_t^w, \theta_t^h, P_t^{EWH-C1}, P_t^{AC-C1}} \left|\theta_t^w - \theta^{w,des}\right| + \left|\theta_t^h - \theta^{h,des}\right| \tag{1}$$

According to (1), the HEMS aims to maximize the thermal comfort level of the household by minimizing the difference between the desired temperatures and the actual temperatures. The first term indicates the difference between the actual and desired temperature of the water whereas the second term denotes the difference between the actual and desired temperature of the household space. The introduced objective function is restricted by some operational constraints and those related to the occupants' comfort level. The HEMS should consider these constraints using the mathematical models of the appliances. For the EWH, one constraint is associated with the operation of the device which states that the temperature of the in-tank water depends on the water's temperature of the previous time step and the heat loss due to hot water demand and boiler's power rate. In fact, at each time slot, the power consumption of the boiler must be adjusted to regulate the desired temperature of outlet hot water. The related equation is indicated with (2), where the term $P_t^{EWH}\Delta t$ calculates the amount of energy needed for heating the stored water in the tank [22].

$$\theta_t^w = \theta_{t-1}^w + \frac{P_t^{EWH}\Delta t - Q_t^{EWH} - Q_t^{Loss}}{k\rho v} \tag{2}$$

There are also some settings such as maximum and minimum values for the temperature of the in-tank water that limit the operation of the EWH, as follows:

$$\underline{\theta^w} \le \theta_t^w \le \overline{\theta^w} \tag{3}$$

In addition, equation (4) refers to the required heat that increases the temperature of the specific volume of cold water to the desired level. Similarly, (5) denotes the maximum energy required to heat the full volume of the in-tank water from an initial temperature to the maximum desired temperature [27].

$$Q_t^{EWH} = k\rho v_t^{tank}\left(\theta_t^w - \theta^{cold}\right) \tag{4}$$

$$\widetilde{Q}_h^{EWH} = k\rho v^{EWH}\left(\overline{\theta^w} - \theta^{w,ini}\right) \tag{5}$$

Moreover, the EWH must fulfil the household hot water demand at each time slot, as stated in (6). Constraint (7) also guarantees that the maximum heat does not overtake the upper bound of water storage [27].

| Controllable Devices | | Objective Functions for Normal Operation: | Objective Functions for Flexible Operation: |
|---|---|---|---|
| AC |  | Minimum difference with the desired room temperatures | Maximum flexibility provision |
| EWH |  | Minimum difference with the desired in-tank water temperatures | Maximum flexibility provision |
| EV |  | Fast charging in the predefined time frame | Maximum flexibility provision |
| BES |  | - | Maximum flexibility provision |

**Fig. 1.** Objective functions of the HEMS considering normal and flexible operations of the controllable devices

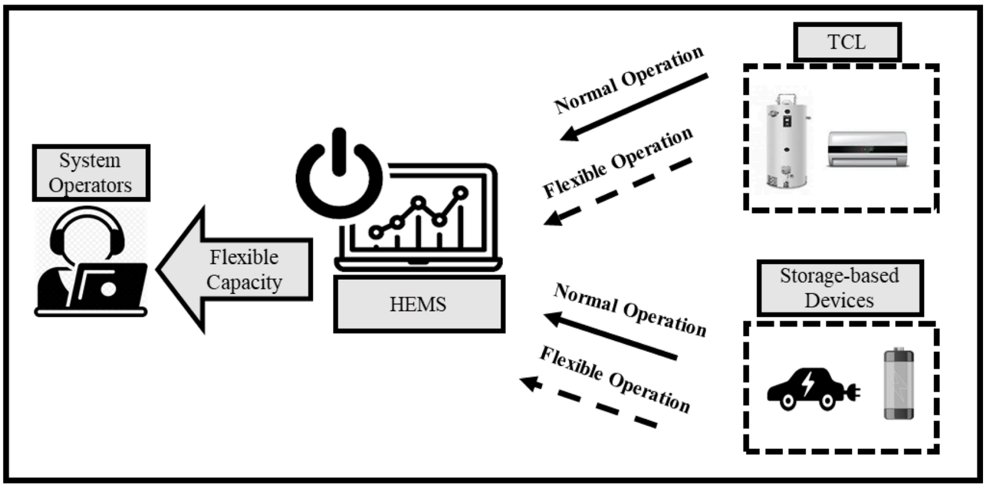


**Fig. 2.** The general model of the smart home and its application for providing flexibility

$$P_t^{EWH}\Delta t \geq Q_t^{EWH} \quad (6)$$

$$P_t^{EWH}\Delta t \leq \widetilde{Q^{EWH}} + Q_t^{EWH} \quad (7)$$

Finally, constraint (8) ensures that the power consumption of EWH's boiler does not exceed its maximum rated power.

$$0 \leq P_t^{EWH} \leq \overline{P^{EWH}} \quad (8)$$

Regarding an AC, this device has an internal thermostat which is in charge of adjusting the power consumption based on one or a range of desired temperatures. The range of desired temperatures could be predefined by the household customers or based on the factory settings. Eq. (9)-(12) are defined to model the operation of an AC. In this light, (9) shows the relationship between the indoor temperature with the outdoor temperature and the power consumption of the device. In this equation, the constant coefficient related to the thermal characteristics of the house along with the AC's thermal capacity are taken into consideration [28].

$$\theta_t^h = (1-\alpha)\theta_{t-1}^h + \alpha\theta_t^{amb} + \beta P_t^{AC}\Delta t \quad (9)$$

In addition, constraint (10) ensures that the indoor temperatures remain in a specific bandwidth defined by the household customer.

$$\underline{\theta^h} \leq \theta_t^h \leq \overline{\theta^h} \quad (10)$$

Finally, the power consumed by the AC should remain within its permissible range, as indicated by (11).

$$0 \leq P_t^{AC} \leq \overline{P^{AC}} \quad (11)$$

### 2.1.2. Case 2: flexible operation

The second case represents the flexible operation of thermostatically controllable appliances. In this case, the smart home is assumed to fully react to the flexibility requests. It provides upward flexibility if it receives the upward signal. In this regard, the smart home decreases the controllable appliances' consumption. In comparison, the smart home provides downward flexibility by increasing the controllable devices' consumption providing that it receives the downward signal. However, the AC's and EWH's operational constraints as well as the comfort level of the occupants need to be considered as well.

If the household receives an upward signal, the HEMS of the responsive smart home aims to minimize the consumption of the AC and the EWH, as follows:

$$\min_{\theta_t^w, \theta_t^h, P_t^{EWH-C2U}, P_t^{AC-C2U}} P_t^{AC-C2U} + P_t^{EWH-C2U} \quad (12)$$

The objective function (12) should be limited by the operational constraints of these two devices as well as those related to the comfort level of the occupant. Thus, the optimization problem includes (12) as an objective function and (2)-(11) as constraints of the problem.

In contrast, the HEMS needs to maximize the consumption of the AC and the EWH, if it receives the downward signal. Therefore, another optimization problem should be defined for the downward case aiming to maximize the consumption of these devices, with an objective function defined in (13):

$$\max_{\theta_t^w, \theta_t^h, P_t^{EWH-C2D}, P_t^{AC-C2D}} P_t^{AC-C2D} + P_t^{EWH-C2D} \quad (13)$$

Again, constraints (2)-(11) should be taken into account in this optimization problem.

### 2.1.3. Flexibility estimation

In the first step, the HEMS needs to estimate the introduced three optimization problems. Then, it utilizes (14) and (15) to estimate the flexile capacities of the TCL.

$$Flex_t^{TCL-up} = \left(P_t^{EWH-C1} + P_t^{AC-C1}\right) - \left(P_t^{AC-C2U} + P_t^{EWH-C2U}\right) \quad (14)$$

$$Flex_t^{TCL-dn} = \left(P_t^{AC-C2D} + P_t^{EWH-C2D}\right) - \left(P_t^{EWH-C1} + P_t^{AC-C1}\right) \quad (15)$$

Eq. (14) states that the upward flexible capacities of the thermostatically controllable loads can be estimated by calculating the amount of its decreased consumption. This amount should be the result of an external flexibility signal. In other words, if a smart home does not receive flexibility signals, its decreased consumption does not mean that it provides upward flexibility. Eq. (15) estimates the available downward flexibility of the AC and the EWH, if the household receives downward flexibility signal. In this regard, the increased consumption by these appliances is considered downward flexibility providing that it receives the downward signal. To calculate the increased and decreased consumption, the TCL operation of the responsive smart home should be compared with that of the household seeking to maximize its thermal comfort. Therefore, this deviation needs to be compensated by the system operator that sent the flexibility signals before. In this way, it motivates smart homes and encourages them to play active roles in the flexibility improvement of energy systems.

*2.1.4. Robust flexibility estimation*

Considering constraints (2), (4), (5), (6) and (7), it can be found that the EWH's consumption power is highly related to the household hot water consumption. Hence, the water consumption needs to be forecasted to solve the related optimization problem. However, the forecasted value would not be exact and there would be uncertainties due to the household uncertain behavior regarding water consumption. To capture these uncertainties, this paper utilizes the concept of robust optimization. A robust optimization problem considers the worst-case that happens regarding the water consumption of the household. In this way, HEMS should solve another optimization problem with the following objectives to find the robust values for estimating the flexible capacities of the smart home.

$$\min_{P_{t,s}^{EWH-C1},P_{t,s}^{EWH-C2U}} \left(P_{t,s}^{EWH-C1} + P_t^{AC-C1}\right) - \left(P_t^{AC-C2U} + P_{t,s}^{EWH-C2U}\right) \tag{16}$$

$$\min_{P_{t,s}^{EWH-C1},P_{t,s}^{EWH-C2U}} \left(P_t^{AC-C2D} + P_{t,s}^{EWH-C2D}\right) - \left(P_{t,s}^{EWH-C1} + P_t^{AC-C1}\right) \tag{17}$$

The robust value of the upward flexible capacities of the TCL is equal to the objective function in an optimal point (16) while the value of the downward flexible capacities equals the solution of objective function (17). The introduced objective functions are subjected to the following constraints:

$$\theta_{t,s}^{w-C1} = \theta_{t-1}^{w} + \frac{P_{t,s}^{EWH-C1}\Delta t - Q_{t,s}^{EWH} - Q_t^{Loss}}{k\rho v} \tag{18}$$

$$\theta_{t,s}^{w-C2U} = \theta_{t-1}^{w} + \frac{P_{t,s}^{EWH-C2U}\Delta t - Q_{t,s}^{EWH} - Q_t^{Loss}}{k\rho v} \tag{19}$$

$$\theta_{t,s}^{w-C2D} = \theta_{t-1}^{w} + \frac{P_{t,s}^{EWH-C2D}\Delta t - Q_{t,s}^{EWH} - Q_t^{Loss}}{k\rho v} \tag{20}$$

Where, (18) yields the consumption power of the EWH considering different scenarios for the first-case water consumption in which the HEMS is maximizing the thermal comfort level. Equation (19) calculates the EWH's consumption power considering different scenarios for the case in which the household receives upward flexibility signal. Constraint (20) calculates the same value for the case where the household receives downward flexibility signals. As a result of solving (16) and (17), the minimum flexible capacity of the household is chosen between different scenarios of water consumption. This means that if other scenarios happen in reality, the household is still able to provide the estimated flexibility.

*2.2. Estimating the flexibility of EV*

The HEMS can also change the charging power and the charging timetable of an EV in order to react to the flexibility signals. However, the charging availability of the EV and the charging preference of the EV's owner are two important factors that restrict EV's flexibility provision. This paper considers two different cases to estimate the flexible capacity of an EV. The first case considers that an EV owner tries to charge the EV with the maximum rated power within a time frame specified beforehand. In the second case, the owner sets a minimum limit for the EV's SOC at each time slot within the specified time frame and it aims to react to the flexibility signal as much as possible. In this way, the EV is able to provide flexibility while still satisfying the specified minimum charging level.

*2.2.1. Case 1: fast charging (normal operation)*

In this case, the EV is allowed to be charged only in a specific narrow timeframe which is determined by the EV owner. In addition, the owner wants to have a fully charged EV in a short period. Hence, the EV is charged with the maximum rated power to reach the higher SOC sooner. Thus, charging the EV can be mathematically modeled as follows:

$$\begin{cases} P_t^{EV-C1} = \overline{P^{ev}} \; if \; t\varepsilon \left[\underline{t^{EV-C1}}, \overline{t^{EV-C1}}\right] \; and \; SOC_t^{EV-C1} \leq \overline{SOC^{EV}} \\ P_t^{EV-C1} = 0 \quad Otherwise \end{cases} \tag{21}$$

Eq. (21) states that the EV is charged at t with its maximum rated power if t is within the time range specified by the owner and if the EV's state of charge does not exceed its upper bound.

*2.2.2. Case 2: flexible charging (flexible operation)*

In the second case, the HEMS assigns a minimum value for the SOC of EV's battery within the time frame. EV charging can modify according to the flexibility signals. However, the battery should reach the specified SOC level at each time slot. In addition, we consider the broader charging time frame for this case in which the smart home decides to be more flexible. If the HEMS receives a downward flexibility signal, the EV is charged with the maximum rated power, similar to the first case:

$$\begin{cases} P_t^{EV-C2D} = \overline{P^{EV}} if t\varepsilon \left[\underline{t^{EV-C2}}, \overline{t^{EV-C2}}\right] and \; SOC_t^{EV-C2D} \leq \overline{SOC^{EV}} \\ P_t^{EV-C2D} = 0 \; Otherwise \end{cases} \tag{22}$$

Where, the time frame $\left[\underline{t^{EV-C2}}, \overline{t^{EV-C2}}\right]$ would have a broader range compared to the charging time frame of the first case. In other words, $\left[\underline{t^{EV-C1}}, \overline{t^{EV-C1}}\right]$ can be a subset of the wider time frame $\left[\underline{t^{EV-C2}}, \overline{t^{EV-C2}}\right]$

If the HEMS receives upward flexibility signal, the EV should decrease its charging power. However, it should reach its lower bound of the SOC. Hence, the HEMS solves an optimization problem to determine the charging power of the EV. The objective function is to decrease the charging power of the EV.

$$\min_{P_t^{EV-C2U}} P_t^{EV-C2U} \tag{23}$$

The problem is subjected to the following constraints:

$$P_t^{EV-C2U} = 0 if \; t \notin \left[\underline{t^{EV-C2}}, \overline{t^{EV-C2}}\right] \tag{24}$$

$$P_t^{EV-C2U} \leq \overline{P^{EV}} \tag{25}$$

$$SOC_t^{EV} = SOC_{t-1}^{EV} + \frac{\eta^{EV} P_t^{EV-C2U}\Delta t}{Cap^{EV}} \tag{26}$$

$$\underline{SOC_t^{EV}} \leq SOC_t^{EV} \leq \overline{SOC^{EV}} \tag{27}$$

Eq. (24) states that the EV cannot be charged within the time frame that is not specified by the owner while (25) determines the upper limit of the charging power. In addition, (26) models the relationship between the SOC and the charging power of the EV's battery while (27) imposes a constraint on the upper and lower limits of the SOC [21]. According to (27), the lower limit is determined for each time slot to ensure that the EV's battery reaches the minimum limit of the SOC at each time slot. In this way, if all of the flexibility signals during these time frames are upward, the EV still reaches its acceptable SOC.

*2.2.3. Flexibility estimation*

Similar to the flexibility that comes from TCLs, the flexibility of the EV can be estimated by calculating the difference between the charging power considering the first and the second case. If the HEMS receives the upward signal, it calculates the reduced charging power in the second case, as denoted by (28):

$$Flex_t^{EV-up} = P_t^{EV-C1} - P_t^{EV-C2U} \tag{28}$$

The downward flexible capacity of the EV is estimated through calculating the increased charging power of the EV, as follows:

$$Flex_t^{EV-dn} = P_t^{EV-C2D} - P_t^{EV-C1} \tag{29}$$

### 2.3. Estimating the flexibility of BES

Unlike thermostatically controllable appliances and EVs which are must-run appliances, BESs are not must-run devices. It means that they are specifically employed for flexibility purposes. Thus, BESs are an important source of flexibility. They can inject power as well as consuming it when needed. As a result, they can create bidirectional flexibility through charging and discharging. However, unlike other introduced controllable appliances, the battery charging and discharging power can be fully used as flexibility. In this way, the HEMS discharges the battery when it receives an upward flexibility signal while the battery is charged during time slots that the HEMS receives a downward signal. In the case of the upward signal, an optimization problem with the following objective function should be solved by the HEMS:

$$\max_{P_t^{B,dis-U}} P_t^{B,dis-U} \tag{30}$$

Where, (30) states that the HEMS tries to maximize the discharging power of the BES as soon as it receives the upward signal. The objective function is subjected to (31)-(34) [21].

$$0 \le P_t^{B,dis-U} \le u_t \overline{P^{B,dis}} \tag{31}$$

$$0 \le P_t^{B,ch-U} \le (1-u_t)\overline{P^{B,ch}} \tag{32}$$

$$SOC_t^B = SOC_{t-1}^B + \frac{\eta^{B,ch} P_t^{B,ch-U}\Delta t - \eta^{B,dis} P_t^{B,dis-U}\Delta t}{Cap^B} \tag{33}$$

$$\underline{SOC^B} \le SOC_t^B \le \overline{SOC^B} \tag{34}$$

Where, (31) and (32) define the upper limit for discharging and charging power of the BES, respectively. Additionally, the binary variable $u_t$ prevents the BES from charging and discharging simultaneously. Eq. (33) models the relationship between BES charging /discharging power and the SOC of the BES. In this regard, the SOC of the BES increases when it is charging whereas discharging the BES results in an SOC decrease. Finally, (34) restricts the upper and lower limits of the battery's SOC. As a result of solving the optimization problem (30)-(34), the upward flexibility of the battery can be estimated by determining the discharging power of the battery.

$$Flex_t^{B-up} = P_t^{B,dis-U} \tag{35}$$

On the other hand, if the HEMS receives the downward signal, it tries to charge the BES as much as possible. In this way, the objective function can be defined to maximize the charging power with some constraints related to the operation of the BES as stated in (36)-(41).

$$\max_{P_t^{B,ch-D}} P_t^{B,ch-D} \tag{36}$$

$$0 \le P_t^{B,dis-D} \le u_t \overline{P^{B,dis}} \tag{37}$$

$$0 \le P_t^{B,ch-D} \le (1-u_t)\overline{P^{B,ch}} \tag{38}$$

$$SOC_t^B = SOC_{t-1}^B + \frac{\eta^{B,ch} P_t^{B,ch-D}\Delta t - \eta^{B,dis} P_t^{B,dis-D}\Delta t}{Cap^B} \tag{39}$$

$$\underline{SOC^B} \le SOC_t^B \le \overline{SOC^B} \tag{40}$$

Finally, the downward flexibility of the BES can be estimated by determining the charging power of the BES.

$$Flex_t^{B-dn} = P_t^{B,ch-D} \tag{41}$$

## 3. TSO-level Flexibility Services

A TSO requires to maintain the balance between the system's generation and demand closely to fix the system's frequency at the predefined value. The imbalance between the generation and the demand causes a frequency deviation which can risk the frequency stability of the system. Hence, the TSO procures various types of TSO-level or system-wide flexibility services to maintain the frequency within its permissible range. In this regard, there exist different flexibility services for different frequency deviation levels. Table 2 indicates the flexibility service utilized for each frequency deviation range. If smart homes are willing to contribute to the provision of system-wide flexibility services, they need to be aggregated through an aggregator to reach the minimum capacity needed for the service provision. The last column of Table 2 indicates the required minimum capacity for each service. The aggregator aggregates the flexible capacities of smart homes and activates the flexibility by measuring the frequency deviation in real-time. Without the aggregator, smart homes cannot participate in providing TSO-level flexibility services because there exists a lower limit of capacity for participation in most TSO-level markets, as illustrated in Table 2 [13]. Besides, the table summarizes the activation time required for each service. For example, according to Table 2, the FER providing FCR-N service needs to activate its full capacity (100%) in less than 180 s.

FCR services comprise FCR-N deployed for normal operations of the power system and FCR-D for disturbance situations. FCR-D service consists of two individual services for upward and downward directions whereas FCR-N is a symmetric service [29, 30, 31].It means that the FER providing FCR-N should be able to provide both upward and downward flexibility, simultaneously.

The main purpose of the FFR is to compensate for the loss of an individual producer or the loss of a high voltage direct current (HVDC) line that causes the frequency drop. The FFR service is mainly procured for the better management of the system in low-inertia situations. At the moment, this service is activated as the upward flexibility service meaning that the FERs should inject more power to the grid or reduce their consumption [32]. In Finland, the FFR service gives the FER three options including the combinations of different activation frequencies and activation time as indicated in Table 2 [32].

FRR services are categorized into automatic FRR (aFRR) and manual FRR (mFRR). In general, the main responsibility of FRR services is to restore the frequency to its nominal value and to help release the FCR that has been activated earlier. Unlike FCR and FFR services that require measuring devices to respond to the flexibility needs, the FERs providing FRR services need to continuously be in touch with the TSO and receive flexibility signals constantly.

Automatic FRR is a service associated with the Nordic power system and is an automatically activated reserve in a centralized manner [33]. It means that its activation is based on the frequency deviation of the whole Nordic synchronized area and is only utilized for certain hours in mornings and evenings [33]. Since this service is related to all Nordic areas, there should be an entity coordinating the TSOs of these areas so that they agree on the flexibility activated for restoring the frequency. In this regard, Statnett's operation control system was assigned to be in

**TABLE 2**
The technical requirements needed for each TSO-level service

| Service | Frequency deviation [Hz] | Activation time [s]- activation percentage[%] | Minimum size [MW] |
|---|---|---|---|
| FCR-N | ±0.1 | 180-100% | 0.1 |
| FCR-D | ±(0.1, 0.5) | 5-50%<br>30-100% | 1 |
| FFR | − 0.3, − 0.4, − 0.5 | 1.3, 1, 0.7-100% | 1 |
| aFRR | - | 350-100% | 5 |
| mFRR | - | 900-100% | 5 |

charge of determining the activation power of aFRR. The activation requests are sent to the TSO in each area and are then forwarded to the flexibility aggregators. For example, Fingrid, the Finnish TSO, sends the activation signal of aFRR to the balancing service providers playing the role of flexibility aggregators, every 10 seconds [33] [34] [35] [36].

Manual FRRs are procured through balancing markets. This service is used to manage the flow of the grid and used in the case of expected frequency deviations such as outages [33]. Manual FRR is localized so that the synchronous Nordic system can be balanced moment by moment. The TSO procures mFRR according to its local TSO flexibility requirements. In this way, the TSO takes into consideration the bottlenecks as well as the dimensioning faults happening in its networks and procures the mFRR accordingly [33].

### 3.1. The participation of smart homes

Firstly, it should be mentioned that the TSO does not reach every single household to provide flexibility services. The TSO and smart homes indirectly communicate through local frequency measurements. For example, as stated in table 2, if the household is going to provide FCR-N services, it should activate its upward flexibility when the frequency falls to (49.9-50) Hz and activate its downward flexibility when the frequency goes up to (50-50.1) Hz. Smart homes with flexible appliances have a considerable potential to provide the TSO with different flexibility services. However, each FER should pass the prequalification process to be qualified for the provision of that specific service. In addition, smart homes and flexible capacities of other small-scale resources need to be aggregated to be able to take part in the provision of these services. The aggregator can decide on the bidding strategy based on the estimated flexible capacities and the types of services that can be provided by its FERs including smart homes.

Regarding FCR-N services, an aggregated of smart homes with BESs (or a large-scale BES system) is able to provide this service. In this way, they are able to provide flexibility in both directions. However, for example, a BES system that is nearly full cannot provide FCR-N because it cannot simultaneously provide upward and downward flexibility. The following constraint should be taken into account for an FER contributing to the provision of FCR-N.

$$Flex_t^{up} = Flex_t^{dn} \tag{42}$$

Equation (42) states that at each time slot, the FER needs to have both upward and downward flexible capacities. Storage-based devices that have the capability of charging and discharging are potent resources. However, when the energy storage device reaches its maximum or minimum SOC level, it should interrupt the activation of the flexibility service until the direction of the frequency deviation changes or until it reaches its capability to provide the symmetric services. In this regard, designing the BES's recharging timetables is an important concern. The aggregator can be in charge of designing timetables and coordinating BESs of different households so that it leads to the maximum profits and minimum operational costs for their owners. Moreover, it is worth mentioning that the BES should have the capability to activate FCR-N reserves for 30 minutes. Hence, it requires to have a sufficient level of the SOC to be able to provide the 30-min service. Besides, the resource should be able to respond in less than 3 minutes.

Regarding FCR-D, all of the household appliances can provide these services. However, they need 30-second response time as well as the ability to activate the reserve for 30 minutes. Thus, it can be concluded that the participation of some appliances such as EWHs that their operations are restricted by the occupants' uncertain behavior should be more analyzed in future works. Other appliances such as ACs can provide FCR-D providing that they have scheduled beforehand for all of the possible activations. Besides, the HEMS should ensure that the constraints related to the thermal comfort level of the owner are satisfied during the activation period.

The household's participation in the provision of FFR is highly restricted since it requires an extremely fast response in less than a second. It means that not only the communication latency should be very low, but also the households should use the appliances whose operations are not strictly limited. In this regard, BESs are better options compared to thermostatically controllable appliances whose operations seriously affect the occupants' comfort. In comparison, the participation of smart homes in providing FRR services is more possible since they require more than 350-second activation time. However, the smart homes and the corresponding aggregator need to be constantly in touch with each other and with the TSO to receive the flexibility signals.

## 4. DSO-level Flexibility Services and Smart Home Participation

DSO-level flexibility services help DSOs to operate their networks. The main responsibilities of DSOs include congestion management and voltage control of the distribution networks [37]. In the long term, DSOs reinforce the network according to their forecasted needs in the future [38]. In this way, the DSO tries to invest in the grid's infrastructure and increases its hosting capacity for more renewable resources and be prepared for customers' increasing demand. In the short term, DSOs currently use conventional approaches to reconfigure the set points of regulators and assets of the network. DSOs may also utilize re-dispatching generation resources and request curtailment if needed. Traditionally, DSOs employ some devices such as on-load tap changer transformers, switched capacitors, and step voltage regulators to control the node voltages of their networks [39]. These mentioned devices estimate the voltage drops along the feeder and accordingly adjust the voltage. However, the high penetration of renewable-based DGs in distribution networks has restricted the operational effectiveness of these conventional methods. For example, the voltage regulator devices fail to track the variation of highly volatile voltage that results from the intermittent power of renewable-based DGs [2]. Besides, these devices incur extra costs in terms of their lifetime and maintenance if they rapidly react to the voltage variations [2]. As a result, the DSO requires new active network management schemes to operate its network. In this way, the potential of FERs connected to the distribution networks such as smart homes are less considered. Hence, the DSO needs to coordinate between traditional functionalities, distributed FERs control settings as well as possible new market structures [40–43]. Smart homes that have flexible appliances can help DSOs to operate their network more effectively. In this regard, the DSO needs to provide an appropriate incentive such as a flexibility trading marketplaces as well as a suitable clearing mechanism to coordinate the flexible capacities of smart homes according to its flexibility needs. In such a market, households play the role of sellers and the DSO is a flexibility buyer. The households benefit from the economic revenues obtained from selling flexibility while the DSO accesses several additional FERs at different locations which in turn facilitates the secure operation of the distribution network.

Regarding communication between the DSO and the smart homes, there may be a situation in which each household is located at a specific node. Hence, if the DSO needs flexibility (power injection or consumption) at that specific node, the DSO should directly communicate with the corresponding household energy management system by sending the flexibility signals.

## 5. Case Study and Simulation Results

### 5.1. Case study

In this paper, we consider a smart home with some controllable appliances, including an AC, an EWH, an EV, and a BES. The details of each appliance can be found in Table 3. It is assumed that the flexible capacity of the household is estimated for a time horizon of one hour. Thus, in a short-term time horizon, the HEMS can predict hot water consumption with acceptable accuracy. Moreover, the predicted

**TABLE 3**
The parameters related to the household controllable appliances

| AC-related Parameters | | | | | |
|---|---|---|---|---|---|
| $\overline{P^{AC}}$ [kW] | $\alpha$ | $\beta$[°C /kWh] | $\theta^{h,des}$[°C] | $\underline{\theta^{h}}$[°C] | $\overline{\theta^{h}}$[°C] |
| 2 | 0.9 | 11 | 24 | 21 | 26 |
| EWH-related Parameters | | | | | |
| $\overline{P^{EWH}}$[kW] | $\widetilde{Q^{EWH}}$[kWh] | $\theta^{w,des}$[°C] | $\underline{\theta^{w}}$[°C] | $\overline{\theta^{w}}$[°C] | $k\rho v$[kWh/°C] |
| 2.4 | 2.6 | 45 | 40 | 60 | 0.17 |
| EV-related Parameters | | | | | |
| $\overline{P^{EV}}$[kW] | $Cap^{EV}$[kWh] | Charging availability [hour] | | $\eta^{EV}$ | |
| 7.6 | 62 | 2-7, 16-24 | | 0.9 | |
| BES-related Parameters | | | | | |
| $\overline{P^{B,ch}}$[kW] | $\overline{P^{B,dis}}$[kW] | $Cap^{B}$[kWh] | | | |
| 5 | 5 | 13.5 | | | |

ambient temperature is also needed to estimate the flexibility of thermostatically controllable appliances. The hourly water consumption and ambient temperatures considered in the simulation are illustrated in Fig. 3. Manual FRR is chosen as a flexibility service that the smart home provides for the TSO. The smart home is assumed to provide the TSO's flexibility needs, based on the hourly signal. The signal is assumed to be "1" when the TSO needs upward flexible capacity, "-1" in case of downward flexibility request, and "0" when the TSO does not need flexibilities. The flexibility signals are extracted from the mFRR needs regarding the Finnish TSO, Fingrid, on 1.9.2020, and are shown in Fig. 4. We assume that the flexible capacities of the smart home are fully activated for each hour according to these flexibility signals. The proposed optimization problems were all developed as linear programming (LP) problems since they have linear and convex constraints and objective functions with continuous variables. We utilized GAMS software and the CPLEX solver to solve the proposed LP problems. It should be noted that the CPLEX solver applies dual simplex algorithm for solving LP problems [44].

### 5.2. Flexible capacities of different devices

The upward and downward capacities of each appliance are maximized based on the mFRR flexibility needs. Accordingly, we obtain the optimal operation of each device for providing the TSO with the required mFRR services. As proposed in the above sections, we estimate the operating power of each flexible appliance considering its flexible and non-flexible operation. The results associated with the flexible charging and non-flexible charging of the EV for one day are depicted in Fig. 5. The BES charging and discharging patterns for the flexibility provision are illustrated in Fig. 6. In addition, the flexible and non-flexible operations of TCLs including the AC and the EWH can be found in Fig. 7 and Fig. 8. By comparing the general patterns and behavior of these appliances in Fig. 5-8 with the pattern of flexibility signals in Fig. 4, it can be concluded that flexible appliances were able to follow the flexibility signals in most of the time slots.

To compare the flexible capacities of different appliances and to estimate the flexible capacities in more detail, we introduce an indicator that calculates the ratio of appliance's flexibility, as stated in (43).

$$Flex_t\% = \frac{Flex_t}{\overline{P_t}} \times 100 \tag{43}$$

Where $Flex_t$ is the estimated flexible capacity of each appliance and $\overline{P_t}$ denotes its maximum operating power. If $Flex_t$ of an appliance equals 100%, it means that the appliance fully decreased or increased its consumption according to the flexibility signal. If the $Flex_t$ is equal to zero, the appliance did not change its consumption due to its operational limits or those imposed by the owner.

This indicator is calculated for 24 hours considering the operation of the household's appliances, AC, EWH, EV, and the BES. The results are depicted in Fig. 9. The following results can be obtained from the Fig. 9.

- By comparing the general pattern of Fig. 9 and that of Fig. 4, it can be comprehended that the controllable appliances have followed the flexibility signals in an acceptable way.
- In this regard, storage-based devices including the EV and the BES were the most flexible devices whereas the flexibility percentage of the EWH was less than 40%. The BES was able to react to the flexibility signals with its maximum capacity at hours 1:00, 3:00, 11:00-13:00, 21:00, 22:00, and 24:00. It also responded with its 70% capacity at hour 23:00. The only constraints restricting the operation of the BES are its SOC limit as well as its working power's upper bound. Accordingly, it can be more flexible compared to other appliances since the owner does not impose any constraints on its working power and it is availability during the whole day.
- It is worth mentioning that the EV is assumed to be unavailable between 8:00-18:00. Hence, it could not provide flexibility at these hours. However, it was able to follow flexibility signals in the time span between 1:00-4:00 and at 24:00. At these hours, the EV devoted 100% percent of its capacity for the flexibility provision, except for hour 4:00, at which its flexible capacity is estimated to be 28%.
- Although the flexible capacity of the AC is not as high as that of the storage-based appliance, it was able to follow the flexibility signals at all of the hours. It means that the AC provided flexibility continuously but not much. The low flexibility percentage of the AC is due to the fact that the operation of the AC highly affects the temperature of the smart home. Hence, the temperature constraints prevent the AC from providing higher flexibility.
- In comparison, the EWH participation in providing flexibility is low because the operation of the EWH is affected by the water consumption of the household and the desired temperature of the water. These constraints are restricted the working power and thus the flexibility provision of the EWH.

### 5.3. Revenue comparison and discussion

Smart homes can be more motivated to provide flexibility, if they

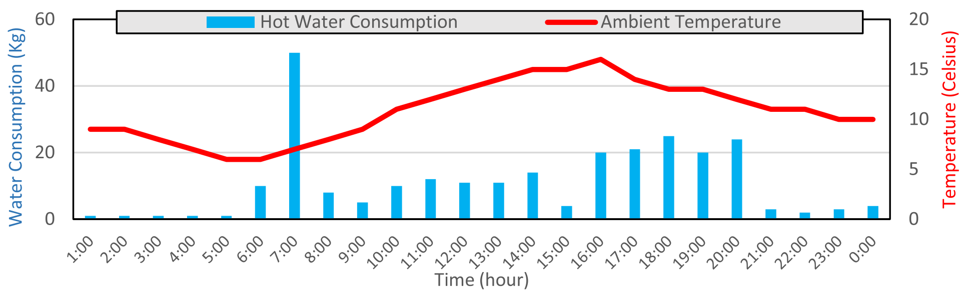


**Fig. 3.** The hourly hot water consumption and the ambient temperatures of the house

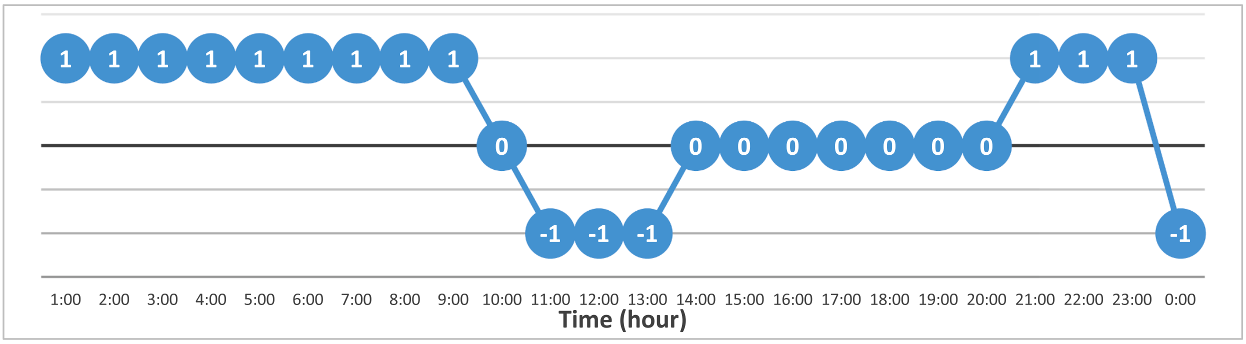


**Fig. 4.** Flexibility signals associated with mFRR services

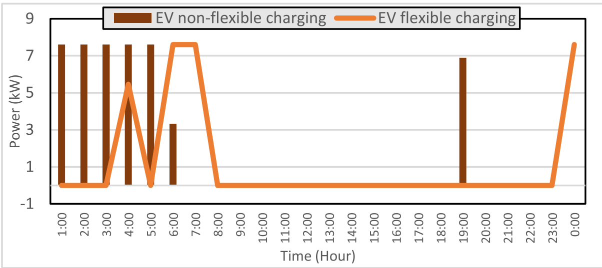


**Fig. 5.** The flexible and non-flexible charging behavior of the EV

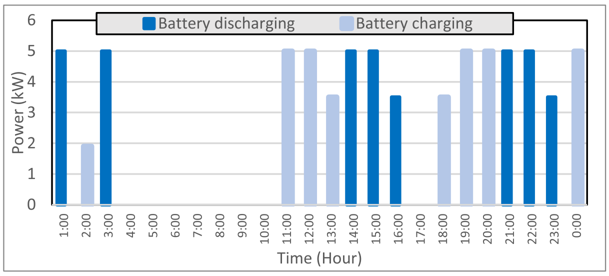


**Fig. 6.** BES's charging and discharging patterns for providing flexibility

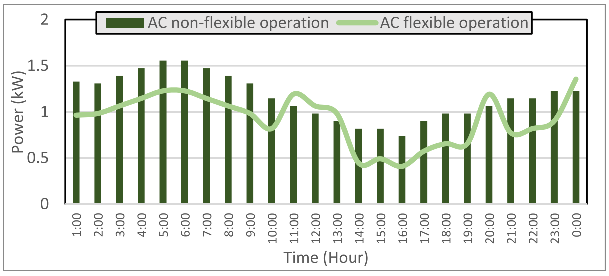


**Fig. 7.** The flexible and non-flexible operation of the AC

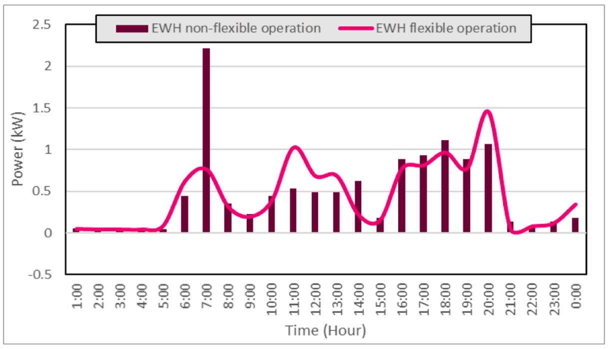


**Fig. 8.** The flexible and non-flexible operation of the EWH

achieve revenues from the flexibility provision. Regarding upward TSO-level flexibility services, the FER providing flexibility services receives a fixed amount for its flexible capacity and a variable amount based on the flexibility activation. Regarding downward TSO-level flexibility, the FER is paid a fixed amount for providing the flexible capacity and pays a variable amount based on the activation of the downward flexibility. It should be highlighted that considering balancing markets, the prices of upward flexibility are equal or higher than those of the energy markets and the prices of downward flexibility are equal or lower than those of the energy markets [35]. Accordingly, it can be concluded that the participation of must-run appliances is always beneficial since they can consume energy at lower prices and achieve extra revenues if they curtail their consumption to provide upward flexibility. However, this participation should consider the desired comfort level of the household customers as introduced in the formulation section.

Nevertheless, thorough cost-benefit analyses should be conducted for the participation of those appliances which are specially used for flexibility purposes such as BESs. These devices are not must-run and they are used to support the flexibility of the system. Thus, they need more accurate analysis to realize whether their contribution to the provision of flexibility is beneficial for the owner or not. As an example of this analysis, we calculate the income of the smart home's BES obtained from selling upward flexibility and energy at one time slot with the prices of energy and flexibility at 9:00 on 1.9.2020. In this way, the BES is considered to be discharged at this time slot. The income is calculated as the difference between the revenues and the operational costs of the BES. We use the same method applied in [21], to calculate the operational cost of the BES. The BES is considered to receive revenues for selling its flexible capacities. In addition, it receives compensation based on the flexibility activated at that time slot based on the price of the balancing energy market at that specific hour. Three types of TSO-level flexibility are considered for this case and the results are shown in Fig. 10.

As the figure explains, the black line is the income of the BES from selling its discharging power to the energy market. In comparison, the bar charts denote the revenues obtained from selling TSO-level flexibilities, considering different activation percentages. It means that in 100% case, all of the 5-kW discharging capacity of the BES is activated

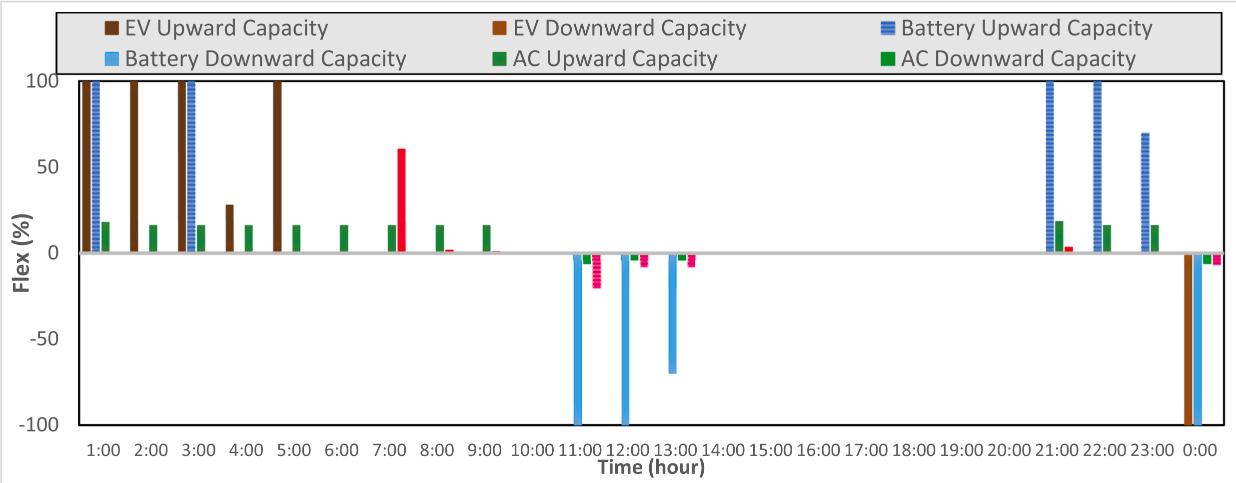


**Fig. 9.** The flexibility indicator calculated for each controllable appliance

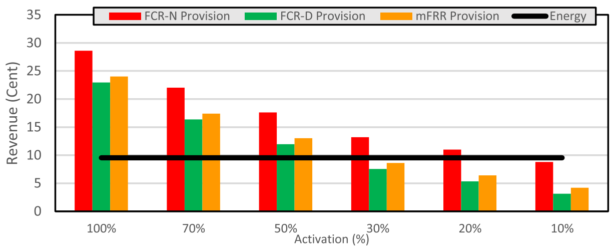


**Fig. 10.** Hourly revenues obtained from the participation of the BES in providing TSO-level services considering different activation scenarios

while in the 50% case, the BES is discharged with 2.5 kW. The results demonstrate that the provision of flexibility is highly dependent on the activation of the flexibility. However, the BES can achieve more than double income if it participates in the provision of flexibility and its whole amount of capacity is activated. In this case, if more than 50% of the capacity is activated, the provision of flexibility is still more profitable for the BES owner than selling its capacity to the energy market. However, the 10% activation was not a more profitable option in comparison with the energy case. Moreover, Fig. 10 states that providing FCR-N service is the most profitable option for the BES. Providing the mFRR service stands in the second rank and FCR-D is the least profitable service. This is due to the fact that at the moment, the capacity prices of providing FCR-N services are higher than those of the mFRR and FCR-D. The capacity price of mFRR for the considered time slot was also higher than that of the FCR-D [45].

## 6. Conclusion

This paper studied the participation of smart homes in providing flexibility services for DSO and TSO. In this way, the estimation of smart home's flexible capacities is of vital necessity because the home energy management system can schedule its controllable appliances more effectively and the system operators can assign the monetary compensation based on the available flexible capacity of the smart homes. To estimate the flexible capacity of a smart home, the flexible capacity of its controllable appliances should be estimated. Thus, this paper separately estimates the flexible capacities of four controllable appliances based on their characteristics. These appliances include an air conditioner, an electric water heater, an electric vehicle, and a battery energy storage. In addition, the constraints related to the comfort level and household customer's settings are taken into account in the flexible operations of the devices. In the next step, system-wide and local flexibility services are introduced and the paper discusses whether the smart home can provide these flexibility services.

In the simulation section, a smart home with some controllable devices was considered. The flexible capacities of the appliances were estimated assuming that the smart home provides a TSO-level service. The results indicated that storage-based devices have higher flexible capacities compared to thermostatically controllable appliances. This is due to the fact that the flexible operations of thermostatically controllable appliances are highly dependent on the thermal comfort level of the household customers. Finally, the paper analyzed whether the participation of the battery energy storage in providing system-wide flexibility services is profitable for its owner. The results demonstrated that the hourly profits of this participation are highly dependent on the activation of the flexibility. Finally, future works can be conducted in the following directions:

1- The 24-hour scheduling of a smart home or an aggregator of the smart home that participate in day-ahead flexible capacity markets, considering the flexibility prices
2- Comprehensive analysis and study on flexibility aggregators that participate in different flexibility markets, as well as their mutual interactions with households and system operators

## CRediT author statement

**H.K., H.F.**: Conceptualiazation, Methodology, Investigation, Simulation. **H.K., H.L.**: Writing- Original draft preparation. **H.K., H.L.**: Writing- Reviewing and Editing, **H.L.**: Supervision.

## Declaration of Competing Interest

The authors declare that they have no known competing financial interests or personal relationships that could have appeared to influence the work reported in this paper.

## Acknowledgement

This work was supported in part by the FLEXIMAR Project (novel marketplace for energy flexibility) through Business Finland under Grant 6988/31/2018, and in part by the Finnish companies.

## References


[1] H. Gerard, E. Rivero, J. Vanschoenwinkel, TSO-DSO Interaction and Acquisition of Ancillary Services from Distribution. TSO-DSO Interactions and Ancillary Services in Electricity Transmission and Distribution Networks, Springer, 2020, pp. 7–23.

[2] N. Mahmud, A. Zahedi, Review of control strategies for voltage regulation of the smart distribution network with high penetration of renewable distributed generation, Renew. Sustain. Energy Rev. 64 (2016) 582–595.

[3] M.A.F. Ghazvini, et al., Congestion management in active distribution networks through demand response implementation, Sustain. Energy, Grids Networks 17 (2019), 100185.

[4] F. Lezama, J. Soares, B. Canizes, Z. Vale, Flexibility management model of home appliances to support DSO requests in smart grids, Sustain. Cities Soc. 55 (2020), 102048.

[5] G. Lipari, G. Del Rosario, C. Corchero, F. Ponci, A. Monti, A real-time commercial aggregator for distributed energy resources flexibility management, Sustain. Energy, Grids Networks 15 (2018) 63–75.

[6] M.R. Monteiro, Y.R. Rodrigues, M. Abdelaziz, A.C.Z. de Souza, L. Wang, New technique for area-based voltage stability support using flexible resources, Electr. Power Syst. Res. 186 (2020), 106384.

[7] P. Olivella-Rosell, et al., Local flexibility market design for aggregators providing multiple flexibility services at distribution network level, Energies 11 (4) (2018) 822.

[8] M.H. Dadashi-Rad, A. Ghasemi-Marzbali, R.A. Ahangar, Modeling and planning of smart buildings energy in power system considering demand response, Energy 213 (2020), 118770.

[9] B.N. Silva, M. Khan, K. Han, Futuristic Sustainable Energy Management in Smart Environments: A Review of Peak Load Shaving and Demand Response Strategies, Challenges, and Opportunities, Sustainability 12 (14) (2020) 5561.

[10] H. Gong, V. Rallabandi, M.L. McIntyre, E. Hossain, D.M. Ionel, Peak Reduction and Long Term Load Forecasting for Large Residential Communities Including Smart Homes With Energy Storage, IEEE Access 9 (2021) 19345–19355.

[11] H. Golmohamadi, Operational scheduling of responsive prosumer farms for day-ahead peak shaving by agricultural demand response aggregators, Int. J. Energy Res. 45 (1) (2021) 938–960.

[12] S. Khemakhem, M. Rekik, L. Krichen, A collaborative energy management among plug-in electric vehicle, smart homes and neighbors' interaction for residential power load profile smoothing, J. Build. Eng. 27 (2020), 100976.

[13] H. Khajeh, H. Firoozi, M. R. Hesamzadeh, H. Laaksonen, and M. Shafie-Khah, "A Local Capacity Market Providing Local and System-wide Flexibility Services," IEEE Access, 2021.

[14] M. Hamwi, I. Lizarralde, J. Legardeur, Demand response business model canvas: A tool for flexibility creation in the electricity markets, J. Clean. Prod. 282 (2021), 124539.

[15] J.P. Iria, F.J. Soares, M.A. Matos, Trading small prosumers flexibility in the energy and tertiary reserve markets, IEEE Trans. Smart Grid 10 (3) (2018) 2371–2382.

[16] E. Sarker, M. Seyedmahmoudian, E. Jamei, B. Horan, A. Stojcevski, Optimal management of home loads with renewable energy integration and demand response strategy, Energy 210 (2020), 118602.

[17] S. Bahramara, Robust Optimization of the Flexibility-constrained Energy Management Problem for a Smart Home with Rooftop Photovoltaic and an Energy Storage, J. Energy Storage 36 (2021), 102358.

[18] H. Khajeh, A.A. Foroud, H. Firoozi, Robust bidding strategies and scheduling of a price-maker microgrid aggregator participating in a pool-based electricity market, IET Gener. Transm. Distrib. (2019).

[19] M.V. Gasca, F. Ibáñez, D. Pozo, Flexibility quantification of thermostatically controlled loads for demand response applications, Electr. Power Syst. Res. 202 (2022), 107592.

[20] B.S.K. Patnam, N.M. Pindoriya, Demand response in consumer-centric electricity market: Mathematical models and optimization problems, Electr. Power Syst. Res. (2020), 106923.

[21] H. Firoozi, H. Khajeh, and H. Laaksonen, "Optimized Operation of Local Energy Community Providing Frequency Restoration Reserve," IEEE Access, p. 1, 2020.

[22] K. Paridari, L. Nordström, Flexibility prediction, scheduling and control of aggregated TCLs, Electr. power Syst. Res. 178 (2020), 106004.

[23] H. Hui, Y. Ding, W. Liu, Y. Lin, Y. Song, Operating reserve evaluation of aggregated air conditioners, Appl. Energy 196 (2017) 218–228.

[24] G.G. Dranka, P. Ferreira, Load flexibility potential across residential, commercial and industrial sectors in Brazil, Energy 201 (2020), 117483.

[25] D. Xie, H. Hui, Y. Ding, Z. Lin, Operating reserve capacity evaluation of aggregated heterogeneous TCLs with price signals, Appl. Energy 216 (2018) 338–347.

[26] M. Hu, F. Xiao, S. Wang, Neighborhood-level coordination and negotiation techniques for managing demand-side flexibility in residential microgrids, Renew. Sustain. Energy Rev. 135 (2021), 110248.

[27] Y. Liu, L. Xiao, G. Yao, S. Bu, Pricing-based demand response for a smart home with various types of household appliances considering customer satisfaction, IEEE access 7 (2019) 86463–86472.

[28] X. Hou, J. Wang, T. Huang, T. Wang, P. Wang, Smart home energy management optimization method considering energy storage and electric vehicle, IEEE Access 7 (2019) 144010–144020.

[29] P.H. Divshali, C. Evens, Optimum Operation of Battery Storage System in Frequency Containment Reserves Markets, IEEE Trans. Smart Grid (2020).

[30] P.H. Divshali, C. Evens, Stochastic bidding strategy for electrical vehicle charging stations to participate in frequency containment reserves markets, IET Gener. Transm. Distrib. 14 (13) (2020) 2566–2572.

[31] Fingrid, "The technical requirements and the prequalification process of Frequency Containment Reserves (FCR)," no. January, p. 17, 2019.

[32] N. Modig et al., "Technical requirements for fast frequency reserve provision in the Nordic synchronous area," no. May, pp. 1–20, 2019.

[33] Fingrid, "TSO report on balancing in accordance with Article 60 of Commission Regulation (EU) 2017/2195 of 23 November 2017 establishing a guideline on electricity balancing," no. November 2017, 2020.

[34] Fingrid, "Terms and conditions for providers of automatic Frequency Restoration Reserves (aFRR)," no. January, 2020.

[35] P. Spodniak, K. Ollikka, and S. Honkapuro, "The relevance of wholesale electricity market places: the Nordic case," 2019.

[36] Fingrid, "Technical requirements and prequalification process for the Manual Frequency Restoration Reserve (mFRR)," no. January, pp. 1–4, 2019.

[37] H. Khajeh, H. Laaksonen, A.S. Gazafroudi, M. Shafie-khah, Towards Flexibility Trading at TSO-DSO-Customer Levels: A Review, Energies 13 (1) (2020) 165.

[38] Z. Liu, Q. Wu, S.S. Oren, S. Huang, R. Li, L. Cheng, Distribution locational marginal pricing for optimal electric vehicle charging through chance constrained mixed-integer programming, IEEE Trans. Smart Grid 9 (2) (2016) 644–654.

[39] C. Long, L.F. Ochoa, Voltage Control of PV-Rich LV Networks: OLTC-Fitted Transformer and Capacitor Banks, IEEE Trans. Power Syst. 31 (5) (2016) 4016–4025.

[40] H. Laaksonen, C. Parthasarathy, H. Hafezi, M. Shafie-khah, H. Khajeh, Control and Management of Distribution Networks with Flexible Energy Resources, Int. Rev. Electr. Eng. 15 (3) (2020) 213–223.

[41] H. Laaksonen, H. Khajeh, C. Parthasarathy, M. Shafie-khah, Hatziargyriou N, Towards Flexible Distribution Systems: Future Adaptive Management Schemes, App. Sci. (2021).

[42] H. Laaksonen, C. Parthasarathy, H. Hafezi, M. Shafie-khah, H. Khajeh, N. Hatziargyriou, Solutions to increase PV hosting capacity and provision of services from flexible energy resources, Appl. Sci. (2020).

[43] H. Laaksonen, C. Parthasarathy, H. Khajeh, M. Shafie-khah, and N. Hatziargyriou, "Flexibility Services Provision by Frequency-Dependent Control of On-Load Tap-Changer and Distributed Energy Resources, " IEEE Access, 2021.

[44] G. A. M. S. (GAMS), "CPLEX 12, GAMS Documentation Center." [Online]. Available: https://www.gams.com/33/docs/S_CPLEX.html.

[45] Fingrid Oyj, "Fingrid open data." [Online]. Available: https://data.fingrid.fi/en/.

Electric Power Systems Research 216 (2023) 109067

Contents lists available at ScienceDirect

Electric Power Systems Research

journal homepage: www.elsevier.com/locate/epsr

# A fuzzy logic control of a smart home with energy storage providing active and reactive power flexibility services

Hosna Khajeh *, Hannu Laaksonen, Marcelo G. Simões

*School of Technology and Innovations, Flexible Energy Resources, University of Vaasa, Vaasa, Finland*

ARTICLE INFO

*Keywords:*
Energy flexibility
TSO
DSO
Smart homes
Fuzzy
Inverter
Energy storage

ABSTRACT

There is a need for enhanced flexibility to allow the high penetration of intermittent renewable power into the power system. In this way, transmission system operators (TSO) need more flexible energy resources that help to control the power system frequency by using balancing services. Distribution system operators (DSO) also seek new flexible energy resources that can counteract stochasticity, control voltage level, and manage congestions in distribution networks. Smart homes located in distribution networks are potential resources. Hence, this paper considers a smart home with flexible appliances and devices, including a battery energy storage system (BESS) interfaced with an inverter, an air conditioner (AC), and an electric vehicle (EV). The smart home aims to provide the system operators with coordinated frequency and DSO-level services while respecting the thermal comfort and schedules of the household residence. The inverter-interfaced BESS not only provides active power support for TSO and DSO, but it also injects and consumes reactive power if the DSO needs local flexibility. Fuzzy logic control system is deployed to obtain this goal. In the simulation section, a smart home with flexible appliances is scheduled. Different operations and the economic outcomes are discussed for the smart home considering real-world data.

## 1. Introduction

### 1.1. Motivation

Power systems are experiencing tremendous challenges due to the high penetration of intermittent renewable generation, recent electrification in different sectors, and the decentralization of the electricity sector [1,2]. As a result, TSOs need more flexibility to keep the balance between the intermittent generation and the growing uncertain demand. In addition, most fossil fuel-based generators are phasing out in the future, and the TSOs need to deploy new sustainable sources that provide flexibility (ancillary) services [3]. Hence, flexible customers and prosumers have been recently considered as flexible resources that can provide flexibility services such as frequency control-related services for the TSOs [4].

DSOs traditionally employ mechanical devices such as on-load tap changers (OLTCs) and switched capacitors to control network voltage levels and manage congestion in the distribution networks [5,6]. However, the growing number of renewable distributed generation units make these devices unable to follow the fluctuations of voltages rapidly [5]. Thus, DSOs also need additional faster flexible energy resources for this purpose. Smart homes have some flexible appliances whose working time can be scheduled according to the operators' flexibility needs.

Nevertheless, there exists obstacles on the road to smart homes' flexibility provision. First, it needs a cooperative management system that can manage how to provide flexibility for both TSOs and DSOs in a coordinated manner. Besides, the management system needs to know how to utilize appliances in a flexible way while trying not to disturb the comfort and desires of household customers.

### 1.2. Literature review

In this context, recent research tried to model prosumers or customers providing flexibility services for the system operators. However, some works were only focused on the provision of DSO-level services and disregarded the profits that can be gained from TSO-level services. For instance, [7] modeled a smart home's energy management system that controls EVs and heat pumps to provide DSOs with congestion management services. Reference [8] worked on the flexible operation of shiftable appliances that can be shifted according to the DSO's needs. Reference [9] studied the contribution of smart homes to voltage control

* Corresponding author.
*E-mail address:* hosna.khajeh@uwasa.fi (H. Khajeh).

https://doi.org/10.1016/j.epsr.2022.109067
Received 1 August 2022; Received in revised form 24 November 2022; Accepted 5 December 2022
Available online 9 December 2022
0378-7796/

**Nomenclature**

*Sets*

$t$ Time

*Parameters*

$\pi_t^{buy}$ Price of buying electricity at time $t$ [Cent/kWh]
$\pi_t^{sell}$ Price of selling electricity at time $t$ [Cent/kWh]
$\pi_t^{BESS}$ Operating cost of using 1 kWh of the BESS capacity at time $t$ [Cent/kWh]
$\Delta t$ Scheduling time slot [h]

*Variables*

$P_t^{con}$ Active-power output of the inverter at time $t$ [kW]
$Q_t^{con}$ Reactive-power output of the inverter at time $t$ [kVAR]
$Q_t^{con-FLC}$ Inverter's active power determined by the fuzzy logic controller [kW]
$P_t^{con-FLC}$ Inverter's reactive power determined by the fuzzy logic controller [kVAR]

*AC-related parameters*

$\theta^{min}$ Lower limit of the indoor temperature of the household [°C]
$\theta^{max}$ Upper limit of the indoor temperature of the household [°C]
$\theta_t^a$ Ambient temperature of the household at time $t$ [°C]
$\alpha$ Constant parameter associated with the thermal characteristic and insulation of the household
$\beta$ Coefficient related to the AC's performance [°C /kWh] [heat: $\beta > 0$]
$P^{AC,max}$ Nominal operating power of the AC [kW]

*AC-related variables*

$\theta_t^h$ Indoor temperature of the household at time $t$ [°C]
$P_t^{AC}$ AC's operating power at time $t$ [kW]

*EV-related parameters*

$SOC^{EV,min}$ Lower limit of the EV state-of-charge (SOC)
$SOC^{EV,max}$ Upper limit of the EV SOC
$Cap^{EV}$ Maximum capacity of the EV's battery [kWh]
$P^{EV,max}$ Maximum charging power of the EV [kW]
$\eta^{EV}$ Charging efficiency of the EV battery
$\varphi_t$ A binary parameter that prevents the EV from being charged when it is unavailable at time $t$

*EV-related variables*

$SOC_t^{EV}$ EV SOC at time $t$
$P_t^{EV}$ Charging power of the EV at time $t$ [kW]

*BESS-related parameters*

$SOC^{BESS,min}$ Lower limit of the BESS SOC at time $t$
$SOC^{BESS,max}$ Upper limit of the BESS SOC at time $t$
$P^{dis,max}$ Upper limit of BESS discharging power [kW]
$P^{ch,max}$ Upper limit of BESS charging power [kW]
$Cap^{BESS}$ Maximum BESS capacity [kWh]
$\eta^{BESS,ch}$ BESS charging efficiency
$\eta^{BESS,dis}$ BES discharging efficiency

*BESS-related variables*

$P_t^{ch}$ BESS charging power at time $t$ [kW]
$P_t^{dis}$ BESS discharging power at time $t$ [kW]
$u_t$ A binary variable that prevents the BESS from being charged and discharged at the same time

in distribution networks. Authors of [10] proposed a market-based approach for smart homes that contribute to controlling voltage unbalances between the phase voltages in the distribution network. In [11], the energy management system controlled EVs and ACs to compensate for unbalances.

On the other hand, the sole focus of some papers were on the prosumers TSO-level frequency provision. For instance, [12] optimally planned energy communities to provide frequency control services. Reference [11] suggested the contribution of smart homes' heat pumps to frequency control. Authors of [13] modelled aggregated prosumers that provide the TSO with balancing services through developing a mixed-integer linear programming (MILP) problem formulation. Authors of [14] presented an NN-based model in which electric water heaters (EWHs) were scheduled to provide general flexibility services.

There are also some papers proposing the contribution of smart homes to the simultaneous provision of DSO- and TSO-level flexibility services. For example, in [15], authors developed linear programming models for the operation of smart home appliances. The smart home's appliances were scheduled to provide DSO-TSO-level flexibility services. Although the paper suggested that a smart home provides both DSO and TSO with flexibility services, the proposed method was not cooperative. In other words, it did not discuss different situations in which the smart home responds to the system operators' simultaneous needs.

Fuzzy logic rule-based control methods can be deployed in various energy management systems. These controllers can avoid intrinsic nonlinearities and integer involvement when developing devices' scheduling models and therefore, they do not require complex mathematical modeling [16]. There exists several papers proposing energy management systems integrated with fuzzy logic controllers (FLC). For example, [17] integrated the home energy management system (HEMS) with an FLC aiming to decrease the electricity costs of the household. Electricity prices, the inhabitants' presence status, and the solar irradiation were considered inputs of the FLC and the output was the shiftable load's schedule. The work did not consider reactive power flexibility and the focus was not on the flexibility provision for system operators. Reference [16] proposed the utilization of an FLC for the operation of a microgrid depending on the microgrid's components. Authors of [18] developed an FLC for a wind turbine system that can provide frequency control services for the TSO. Reference [19] designed a new FLC-equipped energy management system for a prosumer that have both a roof-mounted solar panel and a wind turbine. The proposed system seeks efficient decisions considering the electricity consumption needs and expenses. Finally, [20] introduced a inverter-interfaced BESS that provides voltage and frequency control services simultaneously. The control of voltage and frequency was done by a novel FLC. However, the work did not specify the type of services and the priority of the service provision. In reality, flexible energy resources can provide different types of frequency control services. Each service needs its own response time and technical characteristics. In addition, the flexibility provider needs to specify its priority in a case where DSO-level signals contradict the TSO-level needs. In these scenarios, if the household provides TSO-level (frequency control) services, the action will adversely affect the secure operation of the distribution network in which the household is located [21].

### 1.3. Contribution and organization

To compensate the shortcomings of the existing research, this paper develops an energy management system for a smart home equipped with an inverter-interfaced BESS. The smart home only controls its controllable appliances. It provides flexibility services for the local DSO and the TSO in a coordinated manner by utilizing controllable appliances. The

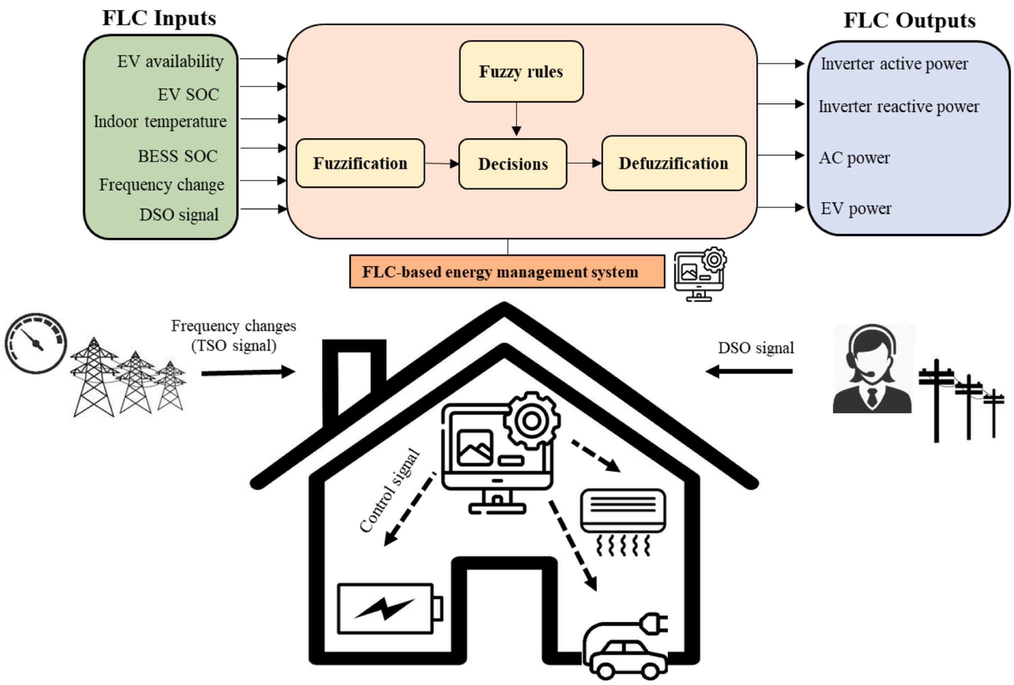


**Fig. 1.** The proposed FLC-based energy management system.

proposed energy management system utilizes a fuzzy logic control method, as follows:

- The smart home provides frequency containment reserves for normal operation (FCR-N) and offers flexibility services for the local DSO simultaneously. In cases where TSO's and DSO's needs contradict each other, the smart home gives priority to the flexibility provision of the local DSO. Otherwise, it might jeopardize the electricity supply quality of the local distribution network, where the smart home is located [21]. The frequency regulation services are provided by active power (*P*) flexibility while the DSO-level flexibility is provided by both active (*P*) and reactive power (*Q*) flexibility.
- An FLC with the minimum number of rules is designed. The objective is to provide flexibility through managing the operation of household appliances including the temperature-dependent AC, the charging timetable of the EV, as well as the active and reactive power extracted from the inverter-interfaced BESS. Although they are reacting to the flexibility signals, the appliances' operational constraints are fully respected.
- Fuzzy logic rules are defined in a way to prioritize must-run appliances in providing flexibility. They propose not to utilize the BESS much due to its operating costs unless the DSO needs high flexibility.

Also, three different cases, called price-based and self-sufficient cases, are developed to see how the household appliances react in different situations if the household is just subjected to the day-ahead market prices. Finally, it is assessed whether flexibility provision is economically efficient for the household or not, using real-world data from Finnish FCR-N and frequency open database [22].

The rest of the paper is organized as follows. Section 3 discusses the provision of DSO-TSO flexibility services. Section 4 introduces the FLC design. Section 5 develops other cases for further comparisons. Section 6 implements the control method and discusses the results. Finally, section 7 concludes the paper.

## 2. Active and reactive power flexibility provision by smart homes

### *2.1. Frequency control and DSO-level flexibility*

The smart home is assumed to provide DSO-level services which are in a form of "upward" or "downward" flexibility services. The DSO first runs an optimal power flow (OPF) calculation for the distribution network and then it might need the consumers and prosumers at some specific nodes to change their consumption or production/generation. In this way, the DSO will be able to manage congestion and voltages in the network. When the DSO needs upward flexibility it sends a signal to smart homes to increase their generation (if possible) or decrease their consumption. Otherwise, if it needs downward flexibility, it asks smart homes to increase their consumption or decrease their generation. The smart home is assumed to react to this flexibility signal by controlling the active power consumed by appliances as well as active and reactive power produced/consumed by the inverter-interfaced BESS.

On the other hand, the smart home is assumed to provide FCR-N service for the TSO. The provision of FCR-N service is based on local frequency measurement. In this way, the smart home reacts to the frequency when it varies in the range of 49.9-50.1 Hz [23–25]. When the frequency falls below 50 Hz to 49.9 Hz, the smart home decreases its consumption or increases discharging i.e. active power produced by its inverter-interfaced BESS. In cases where the frequency goes beyond 50 Hz, until 50.1 Hz, the smart home increases its consumption and charges the BESS. FCR-N was selected among frequency services since it is one of the most expensive services and the smart home can accordingly receive higher profits if it provides this frequency regulation service [26].

### *2.2. Inverter-based resource flexibility provision*

This research is based on the assumption that a smart-home will have power electronics flexibilities, based on multifunctional inverters, capable to provide both active and reactive for the DSO. The reactive power services are provided by real-time control using d-q and p-q

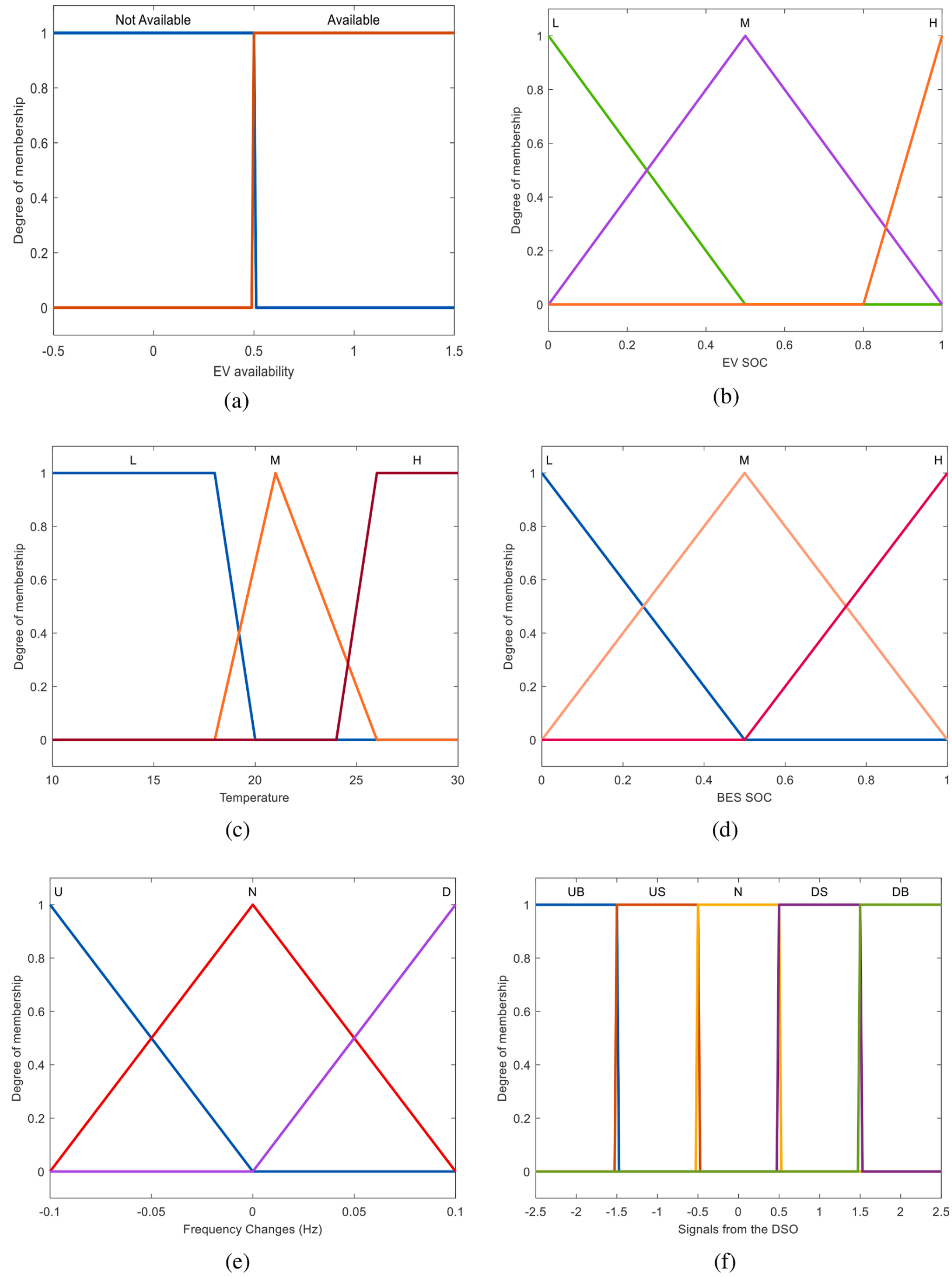


**Fig. 2.** Membership functions (MF) of the input variables: (a) MFs of EV availability, (b) MFs of EV SOC, (c) MFs of temperature, (d) MFs of BES SOC, (e) MFs of frequency changes, (f) MFs of DSO's flexibility signals.

instantaneous power theory based control for the inverter. The package is sometimes defined as a converter referring to the power electronic interfacing from the energy source (the BESS in this case) connected to the point of common coupling at the utility grid. In addition, since the BESS' output is DC, an AC/DC-inverter is used to connect it to the AC grid. We also assume that the inverter has the capability to control both consumed/produced active and reactive power in their acceptable ranges. The AC-DC inverter is considered to have oversizing option with the oversizing factor, *OSF*. Thus, the following constraint should be taken into account for the inverter:

$$P_t^2 + Q_t^2 \leq (1 + OSF\ S^{max})^2 \quad (1)$$

Where $S^{max}$ is the inverter's rated capacity, $P_t$ is its active power produced/consumed while $Q_t$ is the inverter's reactive power produced/

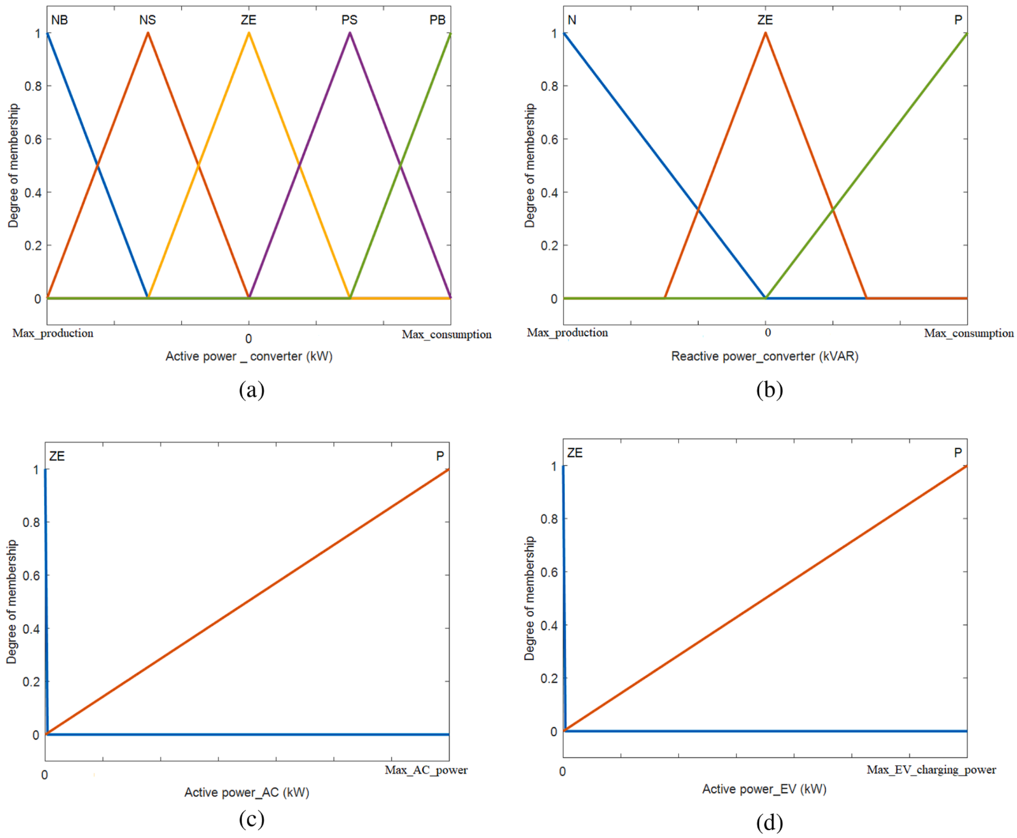


**Fig. 3.** Membership functions (MF) of the output variables: (a) MFs of inverter's active power output, (b) MFs of inverter's reactive power output, (c) MFs of AC consumption, (d) MFs of EV charging consumption.

consumed. With the help of constraint (1), the maximum reactive power i.e. $Q^{con\_max}$ can be obtained.

The output active and reactive power need to be modified after they are determined by the FLC [20]. The output is obtained as follows [20]:

$$P_t^{con} = P_t^{con-FLC} \quad (2)$$

$$Q_t^{con} = \frac{|Q_t^{con-FLC}|}{Q_t^{con-FLC}} \min\left(Q^{con\_max}, |Q_t^{con-FLC}|\right) \quad (3)$$

In (2), $P_t^{con}$ is the output active power of the inverter which is determined by the FLC's output, i.e. $P_t^{con-FLC}$. However, (3) determines the output reactive power of the inverter, $Q_t^{con}$. In (3), $Q_t^{con-FLC}$ is the reactive power obtained by the proposed FLC. The proposed FLC will be described in the next section.

## 3. Proposed fuzzy logic-based coordinated control

The paper presents a Mamdani Fuzzy Interface System (FIS) which includes three main parts. A fuzzier converts the inputs' crisp values to fuzzy values. Fuzzy rules determine how the outputs are obtained based on the inputs' fuzzy values. A defuzzifier converts back the outputs' fuzzy values to the crisp values [27]. Finally, the inverter's outputs are determined using (2) and (3). Fig. 1 explains how the proposed energy management system works and illustrates the inputs and outputs of the system.

The proposed FLC is able to coordinate active and reactive power with the operators' flexibility needs. In distribution networks, the ratio of lines' reactance to their resistance is low [28]. Thus, active power can be utilized besides reactive power to control voltages in these networks. In other words, DSOs can employ both active and reactive power services to manage the network. Active power also influences system frequency. The TSO uses active power services to control frequency in real-time. Hence, there might exist situations in which the active power provided for frequency control worsen the voltage situations at some nodes or causes congestion in the local distribution network [29, 30]. In order to avoid this situation, fuzzy rules should define different situations and determine the controller's reaction.

### 3.1. Fuzzy logic controller design

An FLC was designed with aim of coordinating active and reactive power flexibility of controllable appliances for TSO-DSO flexibility needs. This FLC accepts six inputs. The inputs consist of 1) EV pre-schedules (EV availability), 2) EV state-of-charge (SOC), 3) indoor temperature, 4) BESS SOC 4) measured frequency, and 5) flexibility signal from the DSO. The inputs' crisp values have been fuzzified via membership functions before they are sent to the FLC.

#### 3.1.1. Membership functions of inputs

Fig. 2 depicts the membership functions that are defined for each input. In this paper, the membership functions of inputs and outputs are mostly defined using Interval Estimation (IS) method. IS method aims to introduce an interval that describes the access of a value of the variable in the best way [31]. As the EV availability membership functions state, an EV is either available or unavailable to be charged. We defined some values that describe the available EV and some others that indicate the unavailable EV. The availability is determined based on the owner's

**Table 1**
Rules related to the active power output of the inverter-interfaced BESS.

| # | BESS SOC | Frequency changes | DSO signal | Inverter active power | Designed according to |
|---|---|---|---|---|---|
| 1 | M | D | N | PS | d |
| 2 | H | D | N | ZE | MR |
| 3 | L | D | N | PB | a |
| 4 | M | N | N | ZE | h |
| 5 | H | N | N | NS | b |
| 6 | L | N | N | PS | a |
| 7 | M | U | N | NS | d |
| 8 | H | U | N | NB | b |
| 9 | L | U | N | ZE | MR |
| 10 | L | N | DB | PB | a |
| 11 | M | N | DB | PS | e |
| 12 | H | N | DB | ZE | MR |
| 13 | L | N | DS | PS | a |
| 14 | M | N | DS | ZE | c |
| 15 | H | N | DS | ZE | MR |
| 16 | L | N | UB | ZE | MR |
| 17 | M | N | UB | NB | e |
| 18 | H | N | UB | NB | b, e |
| 19 | L | N | US | ZE | MR |
| 20 | M | N | US | ZE | c |
| 21 | H | N | US | NB | b |
| 22 | - | D | US | ZE | f |
| 23 | - | D | UB | ZE | f |
| 24 | - | U | DS | ZE | f |
| 25 | - | U | DB | ZE | f |
| 26 | L | U | US | ZE | MR |
| 27 | M | U | US | NB | g |
| 28 | H | U | US | NB | g |
| 29 | L | U | UB | ZE | MR |
| 30 | M | U | UB | NB | g |
| 31 | H | U | UB | NB | g |
| 32 | L | D | DS | PB | g |
| 33 | M | D | DS | PB | g |
| 34 | H | D | DS | ZE | MR |
| 35 | L | D | DB | PB | g |
| 36 | M | D | DB | PB | g |
| 37 | H | D | DB | ZE | MR |

preschedule. The membership functions of EV SOC as well as those of the BESS SOC are defined to have three ranges, low (L), medium (M), and high (H). The BESS membership functions are adopted from [20], while those of EV can be determined by the customers, using IS method. The customers determine what the high EV SOC is meant to them or to what degree each EV SOC is high, medium, or low. In this paper, the high (H) EV SOC starts from 80% and reaches its maximum in 100% as the figure states. The temperature membership functions are defined according to the standards defined by The Finnish Ministry of Social Affairs and Health's Housing Health Guide for the indoor air temperature [32]. This the temperatures lower than 18 °C and higher than 26 °C are considered to be low (L) and (H), respectively and they are not acceptable.

The energy management system receives two external signals from TSO and DSO. TSO-related signal measures frequency changes and indicates whether the TSO needs flexibility. The membership functions of frequency changes are defined to be upward (U), Downward (D), or None (N). If the frequency changes have negative values, the TSO needs upward flexibility (U). On the other hand, if the frequency changes are positive, the TSO needs more downward flexibility (D). If the frequency change shows N, it means that the household does not need to change its behavior.

The last membership functions depict the DSO's flexibility needs whose signals are sent to the household energy management system. First, the DSO runs an optimal power flow on their system. Then, it sends a flexibility signal, if it needs the flexibility of the household. The flexibility signal can be (UB, US, N, DS, DB). UB is sent when the DSO requires big upward flexibility and US shows small upward flexibility need. N means that the DSO does not need flexibility. On the other hand, DS and DB stand for downward small and big flexibility needs, respectively.

### 3.1.2. Membership functions of outputs

The FLC then gives four outputs, including active and reactive power of the AC-DC inverter, ($P_t^{con-FLC}$), ($Q_t^{con-FLC}$), the active power consumed by the AC as well as the EV charging power. The membership functions of the outputs are illustrated in Fig. 3.

Membership functions are defined based on the characteristic of the outputs. Active and reactive power of the BESS can have positive and negative values. Positive values indicate the consumption whereas negative values state that the device produces power. The inverter's output can be negative big (NB), negative small (NS), zero (ZE), positive small (PS), and positive big (PB), in terms of active power. The inverter's reactive power can be negative (N), zero (ZE), and positive (P). AC power is considered in the range of 0 to its maximum nominal power in kW. The AC can be either OFF with zero output (ZE) or ON with positive (P) active power consumption. Similarly, the EV charging power can have a zero (ZE) value or a positive (P) value. The charging power varies from 0 to its nominal power in kW. Again, IS method is adopted to determine the outputs' membership functions.

### 3.1.3. Fuzzy rules

Fuzzy Rules describe the relationship between input values and output values. A fuzzy logic-based controller is a decision-making system that defines appropriate output for a certain combination of inputs, based on a set of rules defined by heuristics and in-depth understanding of the functionalities of the overall system. A Fuzzy logic-based controller can also provide adaptively decreasing step sizes when it searches for the optimum point which leads to the fast convergence [33]. Here, the DSO is assumed to have five different flexibility needs whereas the TSO can have three of them. Rules specify how to come up with the decisions in different combinations of inputs.

The rules that are defined for each appliance are supposed to manage critical situations with counteracting services. Regarding the inverter-interfaced BESS, the active power equals zero when the DSO's and TSO's flexibility needs do not have the same direction. In these situations, the inverter reacts to the DSO signal by changing its reactive power rather than active power. On the other hand, must-run appliances that do not have reactive-power-control capability, give priority to the DSO's needs and respond to the DSO's signals in counteracting situations. The DSO mostly requires services that should be provided by specific nodes within local networks whereas TSO's frequency services can be provided by a number of resources in different regions and voltage levels. In another word, local flexible resources are more important to the local DSO than the TSO, and the smart home, as a local resource, has more impact on the flexibility of local networks. Accordingly, the rules are defined in a way that the smart home prioritizes DSO's flexibility needs in situations where TSO's and DSO's needs contradict each other.

Table 1 describes the rules associated with the active-reactive power output of the inverter-interfaced BESS. The following principles help to design the rules:

**Meta Rule (MR):** It includes the main rules of the system which should be respected in all situations. This is the rule associated with the BESS's operational constraints and prevents the BESS from high degradation costs. According to the MR, a BESS must not be charged if its SOC is high (H), and it must not be discharged if the BESS SOC is low (L). The other rules are as follows:

a) If the SOC is low (L), the active power tends to become positive values (PB, PS) in order to reach its medium (M) level. This is because the BESS with medium SOC is able to provide more flexibility in both directions. This benefits both DSO and TSO in their real-time operations.

**Table 2**
Rules related to the reactive power output of the inverter-interfaced BESS.

| # | DSO signal | Inverter reactive power |
|---|---|---|
| 38 | UB | N |
| 39 | US | N |
| 40 | N | ZE |
| 41 | DS | P |
| 42 | DB | P |

**Table 3**
Rules related to the AC output.

| # | Temperature | Frequency changes | DSO signal | AC output | Designed according to |
|---|---|---|---|---|---|
| 43 | L | - | - | P | MR |
| 44 | H | - | - | ZE | MR |
| 45 | M | N | N | ZE | d |
| 46 | M | U | N | ZE | c |
| 47 | M | D | N | P | c |
| 48 | M | - | DB | P | a, (b) |
| 49 | M | - | DS | P | a, (b) |
| 50 | M | - | UB | ZE | a, (b) |
| 51 | M | - | US | ZE | a, (b) |

**Table 4**
Rules related to the EV charging output.

| # | EV availability | EV SOC | Frequency changes | DSO signal | EV output | Designed according to |
|---|---|---|---|---|---|---|
| 52 | Not Available | - | - | - | ZE | MR |
| 53 | Available | H | - | - | ZE | MR |
| 54 | Available | - | N | N | ZE | d |
| 55 | Available | L | D | N | P | a |
| 56 | Available | M | D | N | P | a |
| 57 | Available | L | U | N | ZE | a |
| 58 | Available | M | U | N | ZE | a |
| 59 | Available | - | - | US | ZE | b, (c) |
| 60 | Available | - | - | UB | ZE | b, (c) |
| 61 | Available | L | - | DB | P | b, (c) |
| 62 | Available | M | - | DB | P | b, (c) |
| 63 | Available | L | - | DS | P | b, (c) |
| 64 | Available | M | - | DS | P | b, (c) |

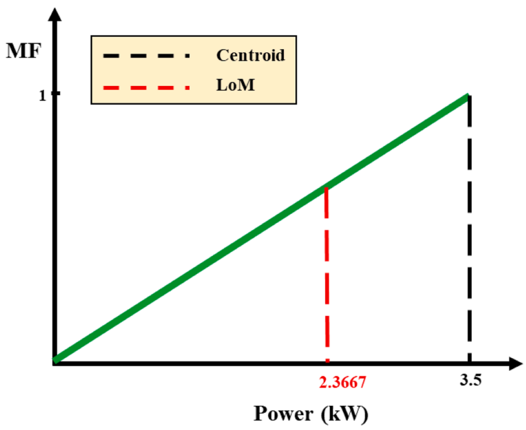


**Fig. 4.** Centroid vs. LoM defuzzification method.

b) If the SOC is high (H), the active power tends towards negative values (NB, NS) to approach the medium (M) level.
c) The BESS' active power does not react to the DSO's small flexibility needs (US and DS) and lets other must-run appliances react to these needs. Must-run appliances are those that must be operated during a specific time period. In this case, EV and AC are must-run appliances. Thus, it is more cost-efficient to use only must-run appliances' flexibility in non-emergency situations.
d) It reacts weakly (with PS and NS), in response to the positive and negative frequency changes, respectively.
e) It reacts strongly (with PB and NB), if the DSO needs higher flexibility (UB, DB).
f) It equals zero when the DSO's and TSO's flexibility needs do not have the same direction. In these situations, the inverter reacts to the DSO signal by changing its reactive power rather than active power.
g) It responds strongly (with PB and NB) if DSO's and TSO's needs have the same direction.
h) It does not react if the DSO and the TSO do not require flexibility.

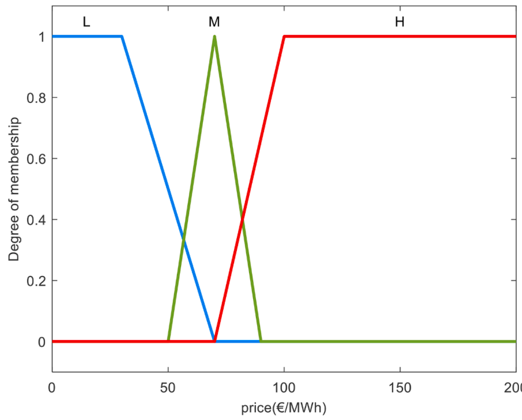


**Fig. 5.** Membership functions of the energy day-ahead price

The reactive power output of the inverter-interfaced BESS only responds to the DSO's needs. It equals a positive value when the DSO requires downward flexibility while it is negative in response to the DSO's upward needs. Table 2 illustrates the related rules.

In general, the AC's output power is set according to the real-time measured indoor temperature. However, AC's flexible operation is possible if it does not disturb the thermal comfort of the occupants. Thus, the Meta rule (MR) is that the AC must not react to the flexibility signals if the temperature is low (L) or high (H). It is because AC's first job is to maintain the temperature within the comfortable range. Other rules are applied based on the following rules and indicated in Table 3.

a) It completely reacts to the DSO's flexibility signals, by switching off the AC when it needs upward flexibility and turning on the AC in case the DSO requires downward flexibility.
b) It gives priority to the DSO's needs and responds to the DSO's signals even if DSO's and TSO's signals do not have the same direction.
c) It also responds to the frequency changes (TSO needs) if they do not contradict the DSO's requirements.
d) The AC does not respond if the DSO and the TSO do not require flexibility.

Similar to the AC, EV's priority is to fulfill DSO's flexibility needs. However, the EV should be charged in predefined time periods that were defined by the owner. This schedule is modeled by availability signals. Two Meta rules (MR) exist here. First, the EV is allowed to be charged if it is available. Second, the EV is not charged if its SOC is high (H). Table 4 describes the rules for EV charging. In general, the following rules are applied to EV charging, if the EV SOC is either low (L) or medium (M):

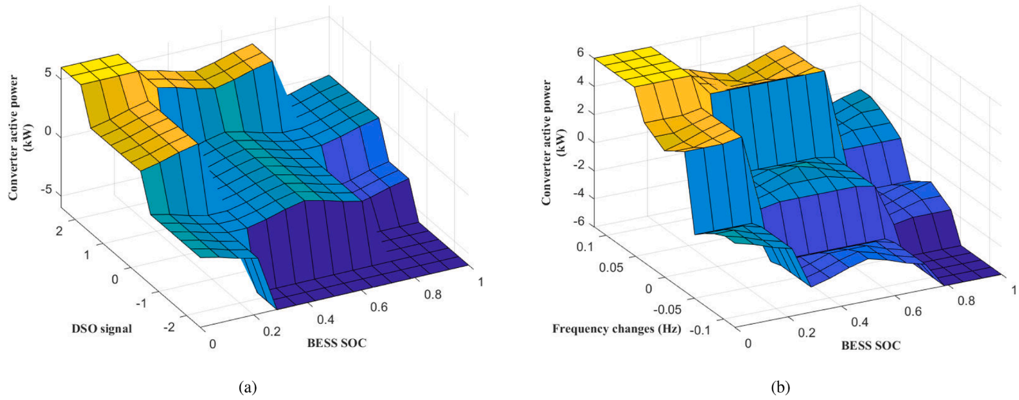


**Fig. 6.** Inverter's output in terms of flexibility signals ((a) DSO signals, (b) frequency changes) and BESS SOC.

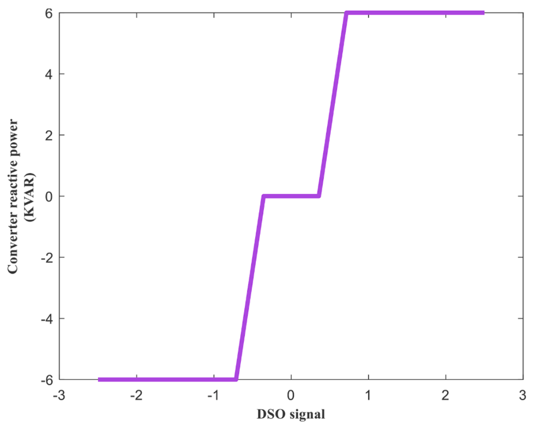


**Fig. 7.** BESS inverter's reactive power in response to the DSO's flexibility signals.

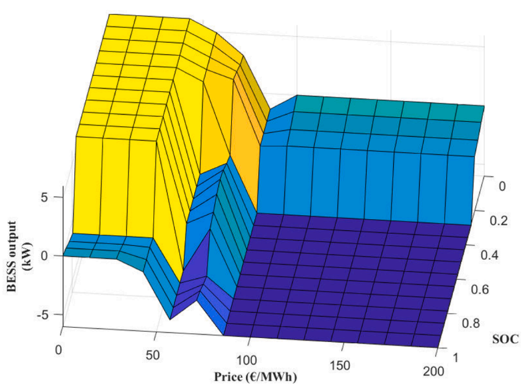


**Fig. 8.** BESS inverter's active power in response to the price signals.

a) The EV reacts to the frequency changes if its direction is not apposite of the DSO's need.
b) It completely reacts to DSO's flexibility signals.
c) It prioritizes DSO's needs if the DSO and the TSO require different flexibility signals.
d) It does not react if the DSO and the TSO do not require flexibility.

*3.1.4. Defuzzification method*

The Largest of Maximum (LoM) method is deployed to obtain the outputs' crisp values. This method gives the largest value for which the output fuzzy set is maximum. The LoM defuzzification method is proposed because we are more interested in obtaining the maximum output of each flexible appliance in response to the flexibility signals. Fig. 4 compares the crisp values yield by LoM and Centroid defuzzification methods, considering a linear membership function with 3.5 kW maximum output, such as the one associated with the AC output. Although the centroid method was adopted by most of the previous literature such as [20], it does not lead to the maximum output in Fig. 4. In our scheduling problem, it is more economical to extract the maximum output since the flexibility provided by appliances is going to be remunerated by the TSO and the DSO. Thus, LoM is more suitable especially for scheduling EVs and ACs that have similar member functions as shown by Fig. 3.

*3.2. Development of further Case studies*

Three more FLC-based models are also developed in order to be compared with our proposed model. The FCL-based cases are developed using Fuzzy Logic Toolbox in Matlab [34] while the optimization problem is solved by CVXPY in Python [35]. These cases are described in the following:

*3.2.1. Fuzzy logic price based model*

Price-based models aim to maximize the financial profits of the household and minimize its energy costs. References [36] and [37] are two examples of price-based models. The models consider that the household is subjected to hourly energy market prices as some retailers such as Finnish retailers give this option to their customers [36]. The price-based models are developed using an FLC and an optimization problem. The FLC-equipped price-based model tries to minimize energy costs in real time. When the price is low (L), the household consumes more energy which means that the BESS is charged and the other appliances are switched on as much as possible. When the price is high (H), the household consumes less and produces more. It means that the BESS is discharged, and other appliances are scheduled to consume less possible energy.

Regarding the FLC-equipped price-based model, it has five inputs including the EV availability and the EV SOC, the temperature, the BESS SOC, and the price. The membership functions of common inputs are the same as those of the proposed model. The membership functions of the price can be designed based on the definition of low (L), medium (M), and high (H) prices. This definition should consider the operational costs of household devices such as BESS operating costs. The prices of buying electricity might be different from the prices of selling electricity. In this

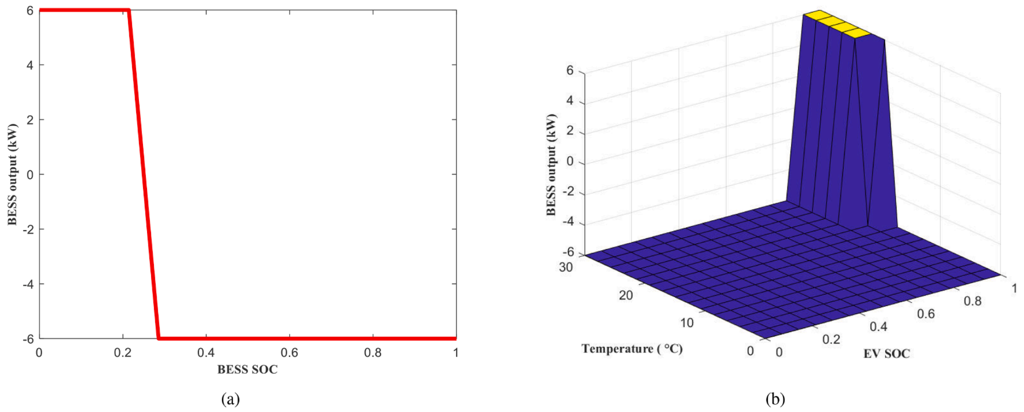


**Fig. 9.** BESS active power output (a): based on its own BESS (b) based on the EV SOC and the indoor temperature.

situation, both buying and selling prices should be added as the inputs. Fig. 5 depicts the prices' membership functions considered in this paper for both buying and selling prices. The outputs of this model are the active-power outputs of the BESS, the EV, and the AC. They have the same membership functions as shown in Fig. 3. Reactive power is disregarded in this model since the authors did not find implemented dynamic pricing for active power in a real-world system.

### 3.2.2. *Price-based model with optimization*

The price-based model can be also developed in a form of an optimization problem. This optimization problem aims to minimize household electricity costs on a day-ahead basis. Mathematically, the problem can be written as follows [18,38]:

$$\min_{P_t^{ch},\, P_t^{dis},\, P_t^{EV},\, P_t^{AC}} \sum_{t=1}^{24} \underbrace{\pi_t^{buy}\left(P_t^{ch}+P_t^{EV}+P_t^{AC}\right)}_{Cost\ I} - \underbrace{\pi_t^{sell}\left(P_t^{dis}\right)}_{Revenue} + \underbrace{\pi^{BESS}\left(P_t^{ch}+P_t^{dis}\right)}_{Cost\ II} \quad (4)$$

subject to:

$$\theta_t^h = (1-\alpha)\theta_{t-1}^h + \alpha\theta_t^a + \beta P_t^{AC}\Delta t \quad (5)$$

$$\theta^{min} \le \theta_t^h \le \theta^{max} \quad (6)$$

$$0 \le P_t^{AC} \le P^{AC,max} \quad (7)$$

$$0 \le P_t^{EV} \le \varphi_t P^{EV,max} \quad (8)$$

$$SOC_t^{EV} = SOC_{t-1}^{EV} + \frac{\eta^{EV} P_t^{EV}\Delta t}{Cap^{EV}} \quad (9)$$

$$SOC^{EV,min} \le SOC_t^{EV} \le SOC^{EV,max} \quad (10)$$

$$0 \le P_t^{dis} \le u_t P^{dis,max} \quad (11)$$

$$0 \le P_t^{ch} \le (1-u_t) P^{ch,max} \quad (12)$$

$$SOC_t^{BESS} = SOC_{t-1}^{BESS} + \frac{\eta^{BESS,ch} P_t^{ch}\Delta t - \eta^{BESS,dis} P_t^{dis}\Delta t}{Cap^{BESS}} \quad (13)$$

$$SOC^{BESS,min} \le SOC_t^{BESS} \le SOC^{BESS,max} \quad (14)$$

Where (4) denotes the objective function and (5)-(14) are the constraints that restrict the objective function. The objective function consists of *Cost I*, the total cost of electricity consumption, *Cost II*, the operating cost of the BESS, and *Revenue* representing the revenue obtained from selling electricity production. BESS operating cost can be estimated using the method proposed by [39]. Eq. (5) relates AC outputs to the indoor temperatures; (6) is the constraint associated with the indoor temperature; and (7) keeps the working power of the AC within its permissible range. In addition, (8)-(10) denote EV's operational constraints. Constraint (8) checks whether EV's charging power is within the allowable range, (9) relates the EV SOC to the charging power and (10) maintains the EV SOC within the defined range. Similarly, (11) and (12) impose constraints on the charging and discharging power of the BESS, (13) explain the mathematical relationship between the BESS SOC and its charging and discharging power. Finally, (14) denotes the upper and the lower limits of the BESS SOC.

### 3.2.3. *Self-sufficient model*

The self-sufficient model represents a scenario in which the household tries to increase their self-sufficiency by supplying the EV and the AC with its own BESS as much as possible. Reference [40] is an example trying to maximize the self-sufficiency of smart homes by managing appliances and flexible resource. In this case, the following rules are applied to the FLC-based management system:

**Meta rules (MR):** These rules aim to maintain the constraints that are embedded in appliances' characteristics or directly affect the occupants' comfort. The rules state that the AC should be ON when the temperature is low (L) and should be turned off if the temperature is high (H) or medium (M). Besides, the EV cannot be charged when it is not available and when the EV SOC is high (H).

a) The household is assumed to charge the BESS whenever the SOC is low (L).
b) In medium-BESS-SOC situations, it charges the BESS if the EV and the AC do not need to consume power.
c) The household discharges the BESS when the EV or/and the SOC consume electricity and the BESS SOC is either high (H) or medium (M).
d) The BESS is not charged or discharged, when the BESS SOC is high (H) and the EV and AC are not working.
e) EV is charged when it is available, the BESS SOC is not low (L), and the AC is not working.

## 4. Simulation results and case study

The proposed fuzzy-logic controller was designed using the Fuzzy Logic Toolbox in Matlab [34]. The rule-based Madani fuzzy logic interface system was developed for scheduling 3.5 kW AC, an EV with 8 kW charging power and also a BESS with 6 kW charging and discharging power and 14 kWh capacity.

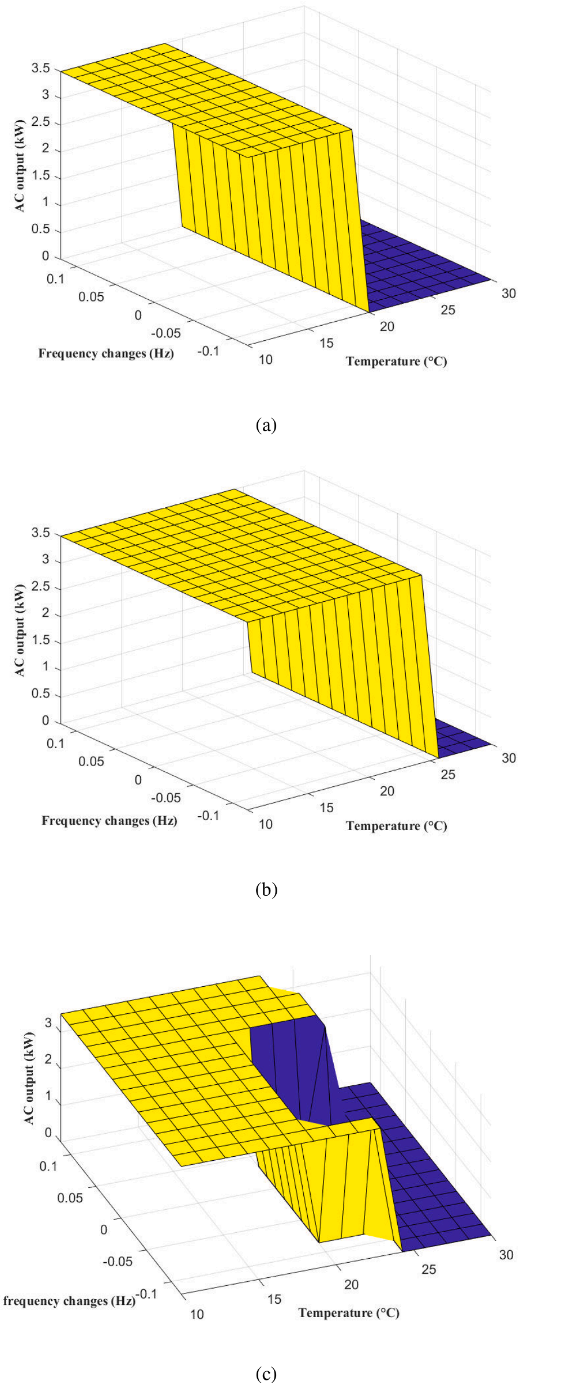


**Fig. 10.** AC output in response to frequency changes when the DSO needs (a) upward flexibility (b) downward flexibility (c) no flexibility.

## 4.1. Operations of flexible devices

### 4.1.1. Inverter-interfaced BESS operation

Fig. 6 illustrates how the BESS inverter's active power output reacts regarding the flexibility signals and the SOC. The figure shows that inverter's active power follows a descending trend when the SOC changes from 0 to 1. This means that that the BESS is mainly charged with

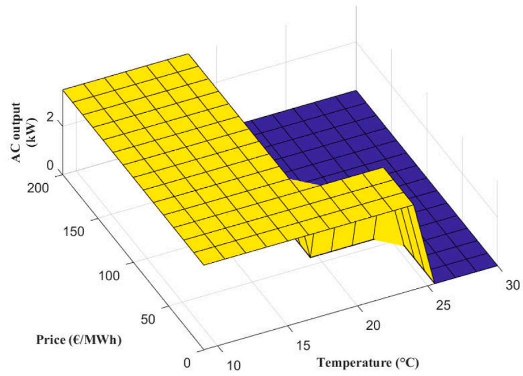


**Fig. 11.** AC output in response to the price signals.

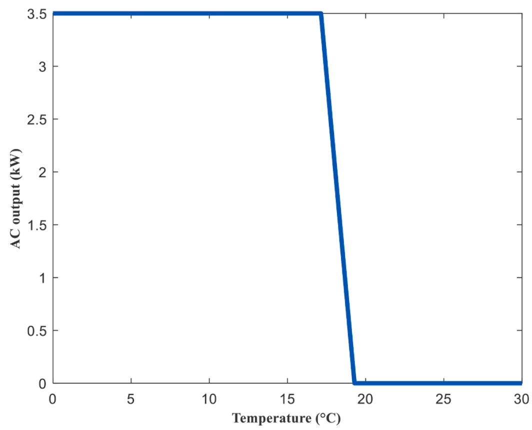


**Fig. 12.** AC output in the self-sufficient model.

positive active power when the SOC is low. Correspondingly, it is mainly discharged with a negative value of active power when the SOC is high.

Fig. 6 (a) indicates an ascending trend when the DSO flexibility changes from UB to DB. The active power has a value around zero in cases where the DSO signals are N, SD, and SU. However, it reacts strongly when the DSO requests higher flexibility. When the DSO needs UB, a range between -2.5 to -1.5, it discharges the BESS (negative active power) and when the DSO requires DB, from 1.5 to 2.5, the BESS is charged (positive active power).

As Fig. 6 (b) states, the active-power response to the frequency changes is considerable. The BESS active power equals positive values (charging mode) when the frequency changes are positive and when the TSO needs downward flexibility. Otherwise, the BESS is discharged with negative values when frequency changes are negative and the system requires upward flexibility. The figure also explains that although the BESS reacts to the operators' flexibility needs, it is neither discharged when the SOC is low nor charged when the SOC is high.

Fig. 7 plots the BESS inverter's reactive power in response to the DSO's flexibility needs. As stated before, the inverter's reactive power only reacts to the DSO flexibility needs. The figure indicates that the designed FLC can completely control reactive power based on the DSO's flexibility needs. It consumes reactive power (positive values) in cases where the DSO requests downward flexibility (positive signals). It injects reactive power when the DSO's signals are negative, meaning that the DSO asks for upward flexibility.

Fig. 8 demonstrates the BESS active power changes in the price-based models. The BESS's active power is depicted in terms of the BESS SOC

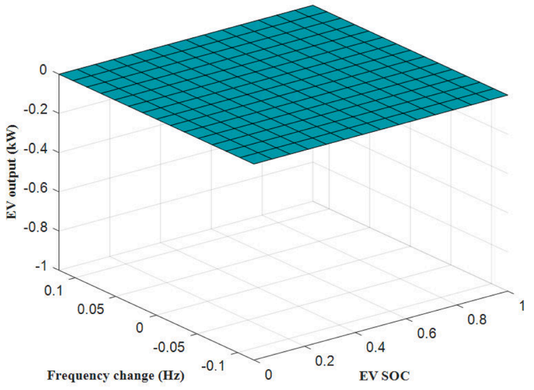


(a)

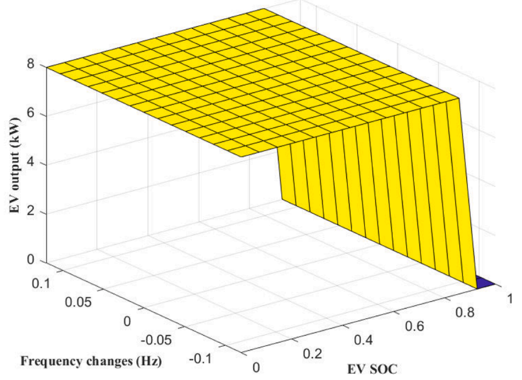


(b)

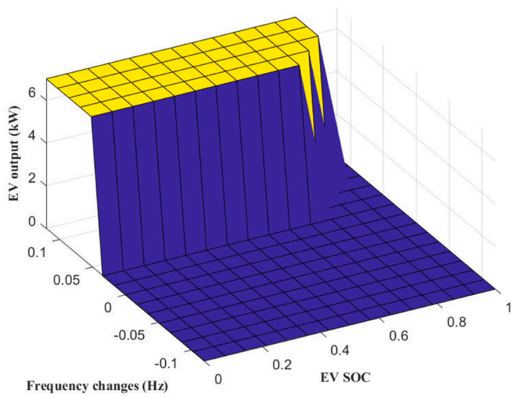


(c)

**Fig. 13.** EV charging power in response to frequency changes when the DSO needs (a) upward flexibility, (b) downward flexibility, (c) no flexibility.

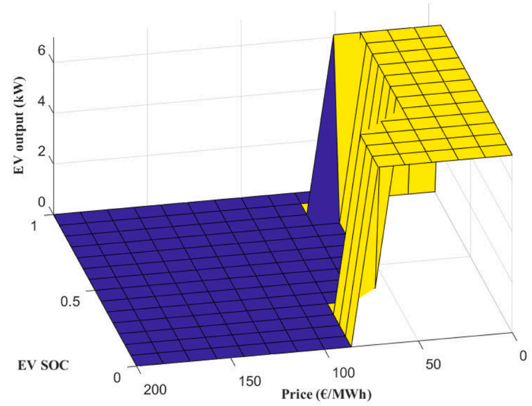


**Fig. 14.** EV charging power in response to the price signals.

and the price signal. The descending trend of the active power in terms of price states that the BESS is charged in low and medium prices and discharged in high prices. However, the SOC affects the BESS operation as well. The BESS active power only accepts negative values (discharging mode) when the SOC is high and it is positive (charging mode) when the SOC is low. This means that the FLC controls the BESS correctly according to the designed rules.

In the self-sufficient operation, however, the main idea is to use the BESS at its maximum level to increase self-sufficiency. Fig. 9 (a) shows the BESS output curve when the EV SOC is low and the temperature is medium. It demonstrates that the BESS starts being discharged as soon as it reaches the medium BESS SOC level, meaning that it is discharged when the BESS SOC is medium or high. Fig. 9 (b) indicates that the BESS is discharged in most situations. It stops being discharged when the EV SOC is high and the temperature passes the low level. It means that the BESS is only charged when the appliances do not need electricity.

#### *4.1.2. Air-conditioner operation*

Fig. 10 represents how the air-conditioner (AC) responds to frequency changes while the DSO requires different flexibility needs. The AC does not react to the frequency changes in Fig. 10 (a) and (b) as long as the DSO needs flexibility. In Fig. 10 (a), the DSO requests upward flexibility from the household and thus the AC output equals zero in medium and high indoor temperatures. In contrast, Fig. 10 (b) demonstrates a situation where the DSO needs downward flexibility. Hence, the AC provides downward flexibility until the temperature reaches its high values.

In Fig. 10 (c), the DSO does not ask for flexibility. Therefore, the AC provides upward and downward flexibility according to the frequency changes in the cases where the indoor temperature is in the medium level.

Fig. 11 presents a 3-D plot that models the AC output based on the indoor temperature and price (price-based model). Again, the AC is ON when the temperature is low and it is OFF when the temperature is high. Meanwhile, the flexible shape of the AC output can be seen when the temperature is medium. In this regard, the controller turns the AC on when the price is low and switches it off when the price is high.

Fig. 12 proves the fact that in the self-sufficient model, the AC works only according to the indoor temperature. It means that other inputs such as the EV SOC and BESS SOC cannot affect the operation of the AC in this model.

#### *4.1.3. EV operation*

Fig. 13 demonstrates that similar to the AC, EV charging output is more flexible in terms of DSO signals rather than frequency changes. In this regard, when the DSO needs either upward or downward flexibility,

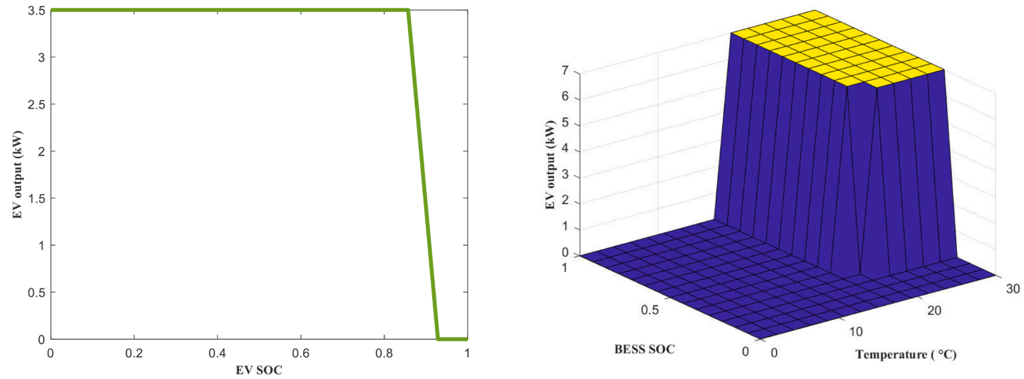


(a) (b)

**Fig. 15.** EV charging power in the self-sufficient model in terms of (a) EV SOC and (b) BESS SOC and temperature.

**Table 5**
The parameters related to the household devices that are considered in this paper.

| | | | | |
|---|---|---|---|---|
| AC-related Parameters | | | | |
| $P^{AC,max}$ [kW] | $\alpha$ | $\beta$[°C /kWh] | $\theta^{min}$ [°C] | $\theta^{max}$ [°C] |
| 2 | 0.045 | 13 | 18 | 26 |
| EV-related Parameters | | | | |
| $P^{EV,max}$ [kW] | $Cap^{EV}$ [kWh] | Charging availability [hour] | | $\eta^{EV}$ |
| 8 | 40 | (0-7) and (18-23) weekdays (0-10) weekends | | 0.9 |
| BESS-related Parameters | | | | |
| $P^{ch/dis,max}$ [kW]/ $Q^{max}$ [KVAR] | *Operating Cost* [cent/kWh] | | $Cap^{BESS}$ [kWh] | |
| 6 | 0.7 | | 14 | |

the EV does not respond to the frequency changes. However, it provides frequency control services in situations where the DSO does not ask for flexibility.

On the other hand, Fig. 14 shows the plot of EV charging output in the price-based models. According to the rules applied to the system, the EV is not charged when the price is high or it has a high SOC level.

Nevertheless, EV charging output is more complex in the self-sufficient model. If the effects of other inputs are disregarded, the EV is charged until its SOC reaches a high level, as Fig. 15 (a) depicts. The BESS SOC and the indoor temperatures, however, have effects on the EV charging schedule. Fig. 15 (b) explains that the EV is charged only when the temperature and BESS SOC are not low. In cases where the BESS SOC is low, the BESS should be charged and it decreases the self-sufficiency if the EV is simultaneously charged. In addition, if the temperature is low, the AC is ON and the BESS should supply the AC output. Thus, it would be more self-sufficient if the EV is not charged when the temperature is low and the AC is turned on.

### 4.2. *Economics analysis*

#### 4.2.1. *Case study*

The economic analyses are conducted on the household considering different operation models. We consider that the household flexible appliances are scheduled for three months from the 1$^{st}$ of January 2021 to the 31$^{st}$ of March 2021. Each flexible device is modeled linearly. The AC is linearly modelled using (5)-(7), in which the ambient temperature and the temperature of the previous time play important roles. The temperatures at the City of Vaasa, Finland, extracted from [38], are

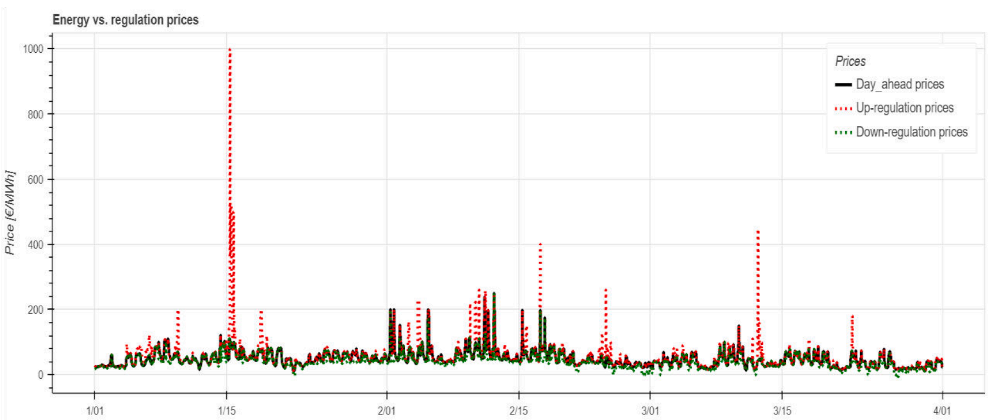


**Fig. 16.** Comparison of energy market prices with regulation prices for Jan-Apr 2021, Finland.

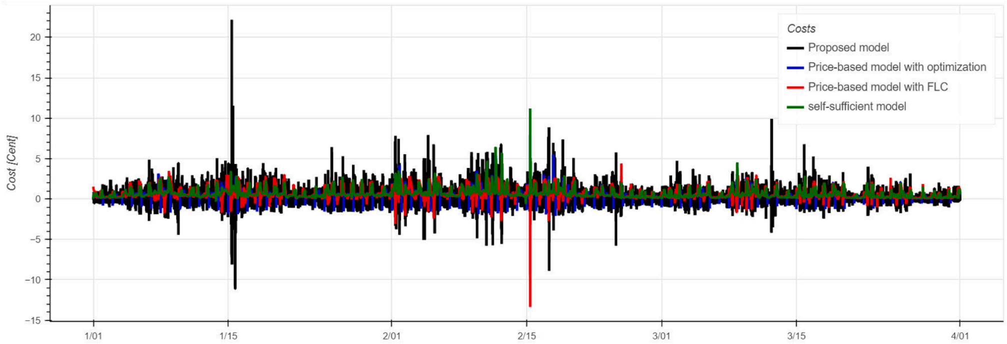


**Fig. 17.** Costs or incomes obtained from consuming and injecting power in a three-month period considering different models.

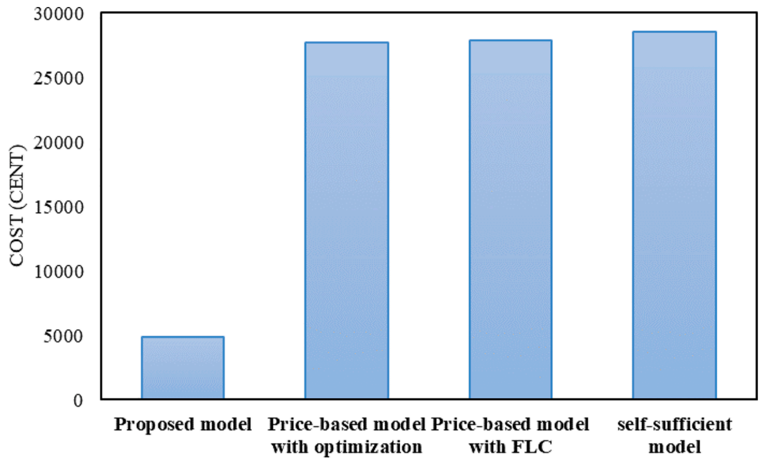


**Fig. 18.** Total three-month costs obtained from different models according to the day-ahead energy market and regulation prices.

**Table 6**
Total three-month costs and incomes of the household considering capacity incomes.

| Model / Cost [Cent] | Proposed | Price-based with FLC | Price-based with optimization | self-sufficient |
|---|---|---|---|---|
| Energy and regulation cost | 4899.19 | 27906.32 | 27735.21 | 28561.68 |
| Capacity income | ≈-21600 | - | - | - |
| Total cost | -16700.81 | 27906.32 | 27735.21 | 28561.68 |

regarded as the ambient temperatures. Besides, (8)-(10) model the EV SOC in terms of its charging power. The BESS model is developed using (11)-(14). Table 5 shows the appliances' parameters utilized in the modeling process. The household is scheduled every three minutes. Thus, $\Delta t$ is equal to 0.05.

In the proposed model, the household reacts every three minutes to the frequency changes and provides FCR-N service. The frequency real-time data is obtained from Fingrid open data for Jan-Apr 2021 [41]. Fingrid is the Finnish TSO who is responsible for frequency control in Finland. The household contributing to flexibility provision receives two sources of income: (1) First one is based on the flexible capacities that are reserved for providing flexibility and (2) Second is the payment household receives from provided upward flexibility. The household should pay for the energy consumed when it provides downward flexibility. The prices of upward flexibility are always equal to or higher than those of the day-ahead spot-/energy market whereas the prices of down-regulation are always equal to or lower than those of the day-ahead spot-/energy market. In addition, the household participating only in the day-ahead energy market (spot-market) receives one source of income which depends on how much energy it produces through its BESS discharging. Fig. 16 compares the prices of upward and downward regulations with those of the energy market for Jan-Apr 2021. In respect to Fingrid reserve resource, there are 1.25 cents if there is a reserve of 1 kW of its capacity for FCR-N provisions in 2021 [40]. In this section 5.2, we do not consider the flexibility needs of the DSO. At the moment, there does not exist price data reflecting the DSO-level flexibility. Thus, economic analyses have been conducted for households with only frequency control support related services.

In the price-based model, the household only reacts to energy market spot-prices. Day-ahead prices for the Finland region are adopted from [42] for Jan-Apr 2021.

### 4.2.2. Simulation results

Finally, a three-month economic analysis is conducted to show whether the proposed model is profitable. In this regard, the price-based and the self-sufficient models trade electricity based on day-ahead energy market prices whereas the proposed model, pays and receives payment based on downward and upward regulation prices. Fig. 17 depicts the costs and incomes that the household receives when it follows different scheduling models. The costs are denoted by positive values while incomes are indicated with negative numbers. Fig. 18 sums all costs and incomes within the three-month period and demonstrates the results by bar plots. Although the costs/incomes of the proposed model are more volatile and uncertain, they lead to a lower total cost. Fig. 18 indicates that the cost of the proposed model is approximately one-fifth of the other models. This is mainly because the proposed model consumes electricity at cheaper prices and sells electricity at more expensive prices. The price-based model with optimization solves the optimization on a daily basis. It sees a longer horizon in the optimization process. Thus, it is more economical compared to the price-based model that uses FLC on a real-time basis. Finally, the self-sufficient model that disregards prices is the less profitable model and incurs higher costs.

As stated previously, the household receives capacity incomes, in addition to regulation costs/incomes if it provides reserve services for the TSO. Regarding the three-month study, the smart home would receive 21600 cents. The capacity payment compensates for the other electricity costs and leads to the household making profits. However, the price-based and self-sufficient models do not receive the capacity payment by participating in the day-ahead energy market. Their total costs are positive values while the proposed model's total cost is equal to a negative value. Table 6 denotes the total costs/incomes of the models that are assessed in this paper.

## 5. Conclusion and future works

The future renewable-based power systems need more sources of flexibility. Households can be a flexibility provider and help DSOs and TSOs with operating their networks. In this regard, this paper proposed the integration of a fuzzy logic controller into the home energy management system. The aim is to respond to the TSO's needs by reacting to the frequency changes and to provide the DSO with the required flexibility. The paper introduced a cooperative method that prioritizes the local DSO. The proposed inverter-interfaced BESS is able to provide both active power and reactive power flexibility, although the reactive power flexibility is adopted to provide only the DSO with the flexibility.

Finally, the proposed fuzzy logic controller was implemented with enhanced performance. Three other models were also developed to be compared with the proposed model. Two of these models are price-based models in which the household reacts to the day-ahead electricity prices rather than flexibility signals. The other model is the self-sufficient model in which the household disregards the prices and flexibility signals while it tries to be self-sufficient by using its BESS as much as possible for supplying the appliances. The output of each device was analyzed and discussed for different operation models. In addition, a three-month economic analysis was conducted for the household that was scheduled based on different models. The results demonstrate that the total three-month cost of the proposed model was approximately one-fifth of that of the other three models. In addition to that, the proposed model received a considerable capacity payment (around € 216) that compensated the household costs and brought profits for the household.

Finally, this work can be expanded in the future in the following directions:

1- The proposed FLC-based management system can be developed and analyzed for a community of smart homes with smart controllable appliances and the community's shared assets. In this way, the energy community would be able to provide a considerable amount of flexibility services for system operators.
2- The FLC-based management system can be developed to control industrial devices. In this way, industrial loads would be able to provide coordinated services for both TSOs and DSOs.
3- It is very simple to retrofit the proposed fuzzy logic-based methodology on any power electronics interfaced with embedded programing and to serve utilities as services owned by prosumers with further communications on the distribution system.

## CRediT authorship contribution statement

**Hosna Khajeh:** Conceptualization, Methodology, Investigation, Formal analysis, Software, Visualization, Writing – original draft, Writing – review & editing. **Hannu Laaksonen:** Supervision, Validation, Writing – original draft, Writing – review & editing. **Marcelo G. Simões:** Validation, Writing – original draft, Writing – review & editing.

## Declaration of Competing Interest

The authors declare that they have no known competing financial interests or personal relationships that could have appeared to influence the work reported in this paper.

## Acknowledgements

The work of Hosna Khajeh was supported by The Ella and Georg Ehrnrooth Foundation in Finland.

## References

[1] J. Shair, H. Li, J. Hu, X. Xie, Power system stability issues, classifications and research prospects in the context of high-penetration of renewables and power electronics, Renew. Sustain. Energy Rev. 145 (2021), 111111, https://doi.org/10.1016/j.rser.2021.111111.
[2] D.F. Dominković, I. Bačeković, A.S. Pedersen, G. Krajačić, The future of transportation in sustainable energy systems: opportunities and barriers in a clean energy transition, Renew. Sustain. Energy Rev. 82 (2018) 1823–1838, https://doi.org/10.1016/j.rser.2017.06.117.
[3] S.I. Vagropoulos, P.N. Biskas, A.G. Bakirtzis, Market-based TSO-DSO coordination for enhanced flexibility services provision, Electr. Power Syst. Res. 208 (2022), 107883, https://doi.org/10.1016/j.epsr.2022.107883.
[4] M. Gržanić, T. Capuder, N. Zhang, W. Huang, Prosumers as active market participants: a systematic review of evolution of opportunities, models and challenges, Renew. Sustain. Energy Rev. 154 (2022), 111859, https://doi.org/10.1016/j.rser.2021.111859.
[5] M.J. Ghadi, S. Ghavidel, A. Rajabi, A. Azizivahed, L. Li, J. Zhang, A review on economic and technical operation of active distribution systems, Renew. Sustain. Energy Rev. 104 (2019) 38–53, https://doi.org/10.1016/j.rser.2019.01.010.
[6] H. Fontenot, K.S. Ayyagari, B. Dong, N. Gatsis, A. Taha, Buildings-to-distribution-network integration for coordinated voltage regulation and building energy management via distributed resource flexibility, Sustain. Cities Soc. 69 (2021), 102832, https://doi.org/10.1016/j.scs.2021.102832.
[7] M.A. Fotouhi Ghazvini, et al., Congestion management in active distribution networks through demand response implementation, Sustain. Energy, Grids Netw. 17 (2019), 100185, https://doi.org/10.1016/j.segan.2018.100185.
[8] F. Lezama, J. Soares, B. Canizes, Z. Vale, Flexibility management model of home appliances to support DSO requests in smart grids, Sustain. Cities Soc. 55 (Apr. 2020), 102048, https://doi.org/10.1016/j.scs.2020.102048.
[9] M.R. Monteiro, Y.R. Rodrigues, M. Abdelaziz, A.C.Z. de Souza, L. Wang, New technique for area-based voltage stability support using flexible resources, Electr. Power Syst. Res. 186 (2020), 106384, https://doi.org/10.1016/j.epsr.2020.106384.
[10] H. Saber, M. Ehsan, M. Moeini-Aghtaie, H. Ranjbar, M. Lehtonen, A user-friendly transactive coordination model for residential prosumers considering voltage unbalance in distribution networks, IEEE Trans. Ind. Inf. (2022), https://doi.org/10.1109/TII.2022.3141784, 1–1.
[11] F. Bünning, J. Warrington, P. Heer, R.S. Smith, J. Lygeros, Robust MPC with data-driven demand forecasting for frequency regulation with heat pumps, Control Eng. Practice 122 (2022), 105101, https://doi.org/10.1016/j.conengprac.2022.105101.
[12] C. Li, et al., Optimal planning of community integrated energy station considering frequency regulation service, J. Modern Power Syst. Clean Energy 9 (2) (2021) 264–273, https://doi.org/10.35833/MPCE.2019.000056.
[13] A. La Bella, A. Falsone, D. Ioli, M. Prandini, R. Scattolini, A mixed-integer distributed approach to prosumers aggregation for providing balancing services, Int. J. Electric. Power Energy Syst. 133 (2021), 107228, https://doi.org/10.1016/j.ijepes.2021.107228.
[14] K. Paridari, L. Nordström, Flexibility prediction, scheduling and control of aggregated TCLs, Electr. Power Syst. Res. 178 (2020), 106004, https://doi.org/10.1016/j.epsr.2019.106004.
[15] H. Khajeh, H. Firoozi, H. Laaksonen, Flexibility potential of a smart home to provide TSO-DSO-level services, Electr. Power Syst. Res. 205 (2022), 107767, https://doi.org/10.1016/j.epsr.2021.107767.
[16] M. Jafari, Z. Malekjamshidi, J. Zhu, M.-H. Khooban, A novel predictive fuzzy logic-based energy management system for grid-connected and off-grid operation of residential smart microgrids, IEEE J. Emerg. Selected Top. Power Electron. 8 (2) (2020) 1391–1404, https://doi.org/10.1109/JESTPE.2018.2882509.

[17] A.C. Duman, H.S. Erden, Ö. Gönül, Ö. Güler, A home energy management system with an integrated smart thermostat for demand response in smart grids, Sustain. Cities Soc. 65 (2021), 102639, https://doi.org/10.1016/j.scs.2020.102639.

[18] M.G. Simões, A. Bubshait, Frequency support of smart grid using fuzzy logic-based controller for wind energy systems, Energies 12 (8) (Apr. 2019) 1550, https://doi.org/10.3390/en12081550.

[19] P. Dimitroulis, M. Alamaniotis, A fuzzy logic energy management system of on-grid electrical system for residential prosumers, Electr. Power Syst. Res. 202 (2022), 107621, https://doi.org/10.1016/j.epsr.2021.107621.

[20] W. Liu, Y. Xu, X. Feng, Y. Wang, Optimal fuzzy logic control of energy storage systems for V /f support in distribution networks considering battery degradation, Int. J. Electric. Power Energy Syst. 139 (2022), 107867, https://doi.org/10.1016/j.ijepes.2021.107867.

[21] H. Khajeh, H. Firoozi, M.R. Hesamzadeh, H. Laaksonen, M. Shafie-Khah, A local capacity market providing local and system-wide flexibility services, IEEE Access 9 (2021) 52336–52351, https://doi.org/10.1109/ACCESS.2021.3069949.

[22] Fingrid, "Open data on the electricity market and the power system." [Online]. Available: https://data.fingrid.fi/en/.

[23] P.H. Divshali, C. Evens, Stochastic bidding strategy for electrical vehicle charging stations to participate in frequency containment reserves markets, IET Gen. Trans. Amp Distrib. 14 (13) (2020) 2566–2572, https://doi.org/10.1049/iet-gtd.2019.0906.

[24] P. Hasanpor Divshali, C. Evens, Optimum day-ahead bidding profiles of electrical vehicle charging stations in FCR markets, Electr. Power Syst. Res. 190 (2021), 106667, https://doi.org/10.1016/j.epsr.2020.106667.

[25] P. Hasanpor Divshali, C. Evens, Optimum operation of battery storage system in frequency containment reserves markets, IEEE Trans. Smart Grid 11 (6) (2020) 4906–4915, https://doi.org/10.1109/TSG.2020.2997924.

[26] Fingrid, "The technical requirements and the prequalification process of frequency containment reserves (FCR)," p. 17, 2019.

[27] M.G. Simões, Artificial Intelligence for Smarter Power Systems: Fuzzy Logic and Neural Networks (2021), https://doi.org/10.1049/PBPO161E.

[28] H. Laaksonen, P. Saari, R. Komulainen, Voltage and frequency control of inverter based weak LV network microgrid, in: 2005 International Conference on Future Power Systems, Amsterdam, The Netherlands, 2005, p. 6, https://doi.org/10.1109/FPS.2005.204293. –6.

[29] H. Laaksonen, C. Parthasarathy, H. Khajeh, M. Shafie-Khah, N. Hatziargyriou, Flexibility services provision by frequency-dependent control of on-load tap-changer and distributed energy resources, IEEE Access 9 (2021) 45587–45599, https://doi.org/10.1109/ACCESS.2021.3067297.

[30] H. Laaksonen, C. Parthasarathy, H. Hafezi, M. Shafie-khah, H. Khajeh, N. Hatziargyriou, Solutions to increase PV hosting capacity and provision of services from flexible energy resources, Appl. Sci. 10 (15) (Jul. 2020) 5146, https://doi.org/10.3390/app10155146.

[31] "Fuzzy sets," in *Artificial Intelligence for Smarter Power Systems: Fuzzy Logic and Neural Networks*, Institution of Engineering and Technology, 2021, pp. 65–79. doi: 10.1049/PBPO161E_ch3.

[32] "Indoor air in residential buildings." https://www.hel.fi/helsinki/en/housing/housing/functional/indoor-air/#:~:text=Indoor%20air%20temperature%20should%20not,caused%20by%20outdoor%20air%20temperature. (accessed Apr. 01, 2022).

[33] Applications of fuzzy logic and neural networks in power electronics and power systems," in *Artificial Intelligence for Smarter Power Systems: Fuzzy logic and neural networks*, Institution of Eng. Technol. (2021) 161–190, https://doi.org/10.1049/PBPO161E_ch8.

[34] MathWorks, "Fuzzy Logic Toolbox User's Guide," Mar. 2022. https://se.mathworks.com/help/pdf_doc/fuzzy/fuzzy_ug.pdf (accessed May 01, 2022).

[35] A. Agrawal, B. Amos, S. Barratt, S. Boyd, S. Diamond, J.Z. Kolter, Differentiable convex optimization layers, Adv. Neural Inf. Process. Syst. 32 (2019).

[36] H. Khajeh, H. Firoozi, H. Laaksonen, M. Shafie-khah, Comparison of optimized operation of energy community's flexibility considering different regulations and trading structures, in: CIRED 2021 - The 26th International Conference and Exhibition on Electricity Distribution, 2021, pp. 3102–3106, https://doi.org/10.1049/icp.2021.2152. Online Conference.

[37] X. Hou, J. Wang, T. Huang, T. Wang, P. Wang, Smart home energy management optimization method considering energy storage and electric vehicle, IEEE Access 7 (2019) 144010–144020, https://doi.org/10.1109/ACCESS.2019.2944878.

[38] "CLIMATE VAASA: Jan-Mar 2021." https://en.climate-data.org/europe/finland/vaasa/vaasa-6321/(accessed Feb. 01, 2022).

[39] T.A. Nguyen, M.L. Crow, Stochastic optimization of renewable-based microgrid operation incorporating battery operating cost, IEEE Trans. Power Syst. 31 (3) (2016) 2289–2296, https://doi.org/10.1109/TPWRS.2015.2455491.

[40] Fingrid, "Frequency containment reserves (FCR-N, FCR-D up and FCR-D down), transactions in the hourly and yearly markets." https://www.fingrid.fi/en/electricity-market-information/reserve-market-information/frequency-controlled-disturbance-reserve/(accessed Feb. 02, 2022).

[41] Fingrid, "Frequency - real time data." https://data.fingrid.fi/en/dataset/frequency-real-time-data (accessed Feb. 02, 2022).

[42] ENTSOE, "Day-ahead prices." https://transparency.entsoe.eu/transmission-domain/r2/dayAheadPrices/show?name=&defaultValue=false&viewType=GRAPH&areaType=BZN&atch=false&dateTime.dateTime=26.06.2022+00:00|CET|DAY&biddingZone.values=CTY|10YSE-1——K!BZN|10Y1001A1001A47J&resolution.values=PT15M&resolution.values=PT30M&resolution.values=PT60M&dateTime.timezone=CET_CEST&dateTime.timezone_input=CET+(UTC+1)+/+CEST+(UTC+2) (accessed Feb. 02, 2022).

IEEE Access
Multidisciplinary : Rapid Review : Open Access Journal

Received September 21, 2020, accepted September 26, 2020, date of publication September 29, 2020,
date of current version October 13, 2020.

*Digital Object Identifier 10.1109/ACCESS.2020.3027710*

# Optimized Operation of Local Energy Community Providing Frequency Restoration Reserve

**HOOMAN FIROOZI, HOSNA KHAJEH, (Graduate Student Member, IEEE), AND HANNU LAAKSONEN, (Member, IEEE)**
School of Technology and Innovations, Flexible Energy Resources, University of Vaasa, 65100 Vaasa, Finland

Corresponding author: Hannu Laaksonen (hannu.laaksonen@uwasa.fi)

This work was supported in part by the Business Finland undertaken as part of the FLEXIMAR Project (Novel Marketplace for Energy Flexibility) under Grant 6988/31/2018, and in part by the Finnish companies.

**ABSTRACT** In order to unlock the maximum flexibility potential of all levels in the power system, distribution-network-located flexible energy resources (FERs) should play an important role in providing system-wide ancillary services. Frequency reserves are an example of system-wide ancillary services. In this regard, this article deals with the optimal operation of a local energy community (LEC) located in the distribution network. The LEC is proposed to participate in providing manual frequency restoration reserves (mFRR) or tertiary reserves. In addition, the community is supposed to have a number of electric vehicles (EVs) and a battery energy storage system (BESS) as FERs. The scheduling of the community, which is fully compliant with the existing balancing market structure, comprises two stages. The first stage is performed in day-ahead, in which the energy community management center (ECMC) estimates the amount of available flexible capacities for mFRR provision. In this stage, control parameters are deployed by the ECMC in order to control the offered flexibility of the BESS. In the second stage, the real-time scheduling of the community is performed for each hour, taking into account the assigned and activated amount of reserve power. The target of the real-time stage is to maximize the community's profit. Finally, the model is implemented utilizing a case study considering different day-ahead control parameters of the BESS. The results demonstrate that the proposed control parameters adopted in the day-ahead stage considerably affect the real-time profitability of the LEC. Moreover, according to the simulation results, participating in the mFRR market can bring additional profits for the LEC.

**INDEX TERMS** Flexibility services, tertiary reserve, frequency restoration reserve, local energy community, flexible energy resources, mFRR, energy scheduling optimization.

## NOMENCLATURE

### ABBREVIATIONS

| | |
|---|---|
| aFRR | Automatic frequency restoration reserve |
| BCM | Balancing capacity market |
| BEM | Balancing energy market |
| BESS | Battery energy storage system |
| BSP | Balancing service provider |
| DBU | Degree of BESS utilization |
| DER | Distributed energy resource |
| DSO | Distribution system operator |
| ECMC | Energy community management center |
| EV | Electric vehicle |
| FCR | Frequency containment reserve |
| FER | Flexible energy resource |
| FFR | Fast Frequency Reserve |
| LEC | Local energy community |
| mFRR | Manual frequency restoration reserve |
| PV | Photovoltaic |
| SOC | State of charge |
| TSO | Transmission system operator |

The associate editor coordinating the review of this manuscript and approving it for publication was Shiwei Xia.

### SETS

| | |
|---|---|
| $t$ | Index of hours $\{1,\ldots,24\}$ |
| $m$ | Index of quarters (15-minute time slots) $\{1,\ldots,4\}$ |
| $s$ | Index of scenarios |
| $i$ | Index of EVs |

### FIRST-STAGE PARAMETERS

| | |
|---|---|
| $\pi_{t,s}$ | Probability of the scenario $s$ at hour $t$ |
| $P^{EV}$ | Charging power of EVs [kW] |
| $N_t^{EV}$ | The number of EVs being charged at hour $t$ |

$N_t^{plug}$ The number of EVs which are supposed to be plugged in at hour $t$
$N_t^{unplug}$ The number of EVs which are supposed to be unplugged at hour $t$
$P^{B,ch,max}$ The maximum charging power of the BESS [kW]
$P^{B,dis,max}$ The maximum discharging power of the BESS [kW]
$L_t^{net,for}$ Forecasted net load at hour $t$ [kW]
$P_t^{PV,for}$ Forecasted PV generation at hour $t$ [kW]
$\sigma_t^{PV}$ Standard deviation for the error of forecasted PV generation at hour $t$
$P^{PV,ins}$ Installed capacity of PV system [kW]
$P_t^{L,for}$ Forecasted load at hour $t$ [kW]
$\sigma_t^{L}$ Standard deviation for the error of forecasted load at hour $t$
$\Delta\mathcal{E}_{t,s}$ The error associated with the forecasted net-load at hour $t$ [kW]
$Cap^B$ Capacity of the BESS [kWh]
$SOC^{B,min}$ Minimum allowed state-of-charge of the BESS
$SOC^{B,max}$ Maximum allowed state-of-charge of the BESS
$\widetilde{SOC}_t^{min}$ Control parameters related to utilization of BESS's capacity in the day-ahead stage
$\widetilde{SOC}_t^{max}$ Control parameters related to utilization of BESS's capacity in the day-ahead stage
$\eta^{B,ch}$ Efficiency of charging of the BESS
$\eta^{B,dis}$ Efficiency of discharging of the BESS

### FIRST-STAGE VARIABLES

$F_{t,s}^{up}$ Upward offered flexibility at hour $t$ for scenario $s$ [kW]
$F_{t,s}^{dn}$ Downward offered flexibility at hour $t$ for scenario $s$ [kW]
$\mathcal{F}_t^{up}$ Expected amount of upward flexibility offer at hour $t$ [kW]
$\mathcal{F}_t^{dn}$ Expected amount of downward flexibility offer at hour $t$ [kW]
$Cap_{t,s}^{up}$ Auxiliary variable for available upward capacity at hour $t$ for scenario $s$ [kW]
$Cap_{t,s}^{dn}$ Auxiliary variable for available downward capacity at hour $t$ for scenario $s$ [kW]
$P_{t,s}^{B,ch,est}$ Estimated power of charging the BESS at hour $t$ for scenario $s$ [kW]
$P_{t,s}^{B,dis,est}$ Estimated power of discharging the BESS at hour $t$ for scenario $s$ [kW]
$SOC_{t,s}^{B,est}$ Estimated state-of-charge of the BESS at hour $t$ for scenario $s$
$u_{t,s}^{B,est}$ Binary variable preventing the BESS from being charged and discharged simultaneously at hour $t$ for scenario $s$

### SECOND-STAGE PARAMETERS

$L_{t,m}^{net}$ Forecasted net-load in quarter $m$ of hour $t$ [kW]
$\lambda_t^{sell}$ Retail prices of selling power to the grid at hour $t$ [Cent/kWh]
$\lambda_t^{buy}$ Retail prices of buying power from the grid at hour $t$ [Cent/kWh]
$\mathcal{C}^B$ Operating cost of the BESS [cent/kWh]
$\mathcal{F}_t^{up,as}$ Assigned upward flexibility at hour $t$ [kW]
$\mathcal{F}_t^{dn,as}$ Assigned downward flexibility at hour $t$ [kW]
$u_{t,m}^{up}/u_{t,m}^{dn}$ Binary parameters indicating the direction (upward/downward) of the assigned flexibility in quarter $m$ of hour $t$
$\Psi_i^{req}$ The minimum number of hours that EV $i$ needs to be charged [hour]
$t_i^{plug}$ The hour at which EV $i$ is supposed to be plugged in
$t_i^{unplug}$ The hour at which EV $i$ is supposed to be unplugged
$\Delta t_i^{plugged}$ The duration in which EV $i$ is plugged in [hour]
$Cap_i^{EV}$ Battery capacity of EV $i$ [kWh]
$SOC_{i,t-1,4}^{EV,act}$ Actual updated state-of-charge of EV $i$ in 4$^{th}$ quarter of hour $t$-1 based on activated reserve data
$SOC_{i,t-1,4}^{B,act}$ Actual updated state-of-charge of the BESS in 4$^{th}$ quarter of hour $t$-1 based on activated reserve data
$I_t^{cap}$ The income of the LEC obtained from provision of reserve capacity at hour $t$ [cent/kWh]
$I_t^{en,up}$ The income of the LEC obtained from provision of upward reserve energy at hour $t$ [cent/kWh]
$C_t^{en,dn}$ The cost of the LEC incurred for purchasing downward reserve energy at hour $t$ [cent/kWh]
$\eta^{EV}$ Efficiency of EVs' batteries

### SECOND-STAGE VARIABLES

$\hat{p}_{t,m}^{in}$ Auxiliary variable for importing power to the LEC [kW]
$\hat{p}_{t,m}^{out}$ Auxiliary variable for exporting power from the LEC [kW]
$P_{t,m}^{in}$ Imported power to the LEC [kW]
$P_{t,m}^{out}$ Exported power from the LEC [kW]
$P_{t,m}^{B,ch}$ Charging power of the BESS in quarter $m$ of hour $t$ [kW]
$P_{t,m}^{B,dis}$ Discharging power of the BESS in quarter $m$ of hour $t$ [kW]
$u_{t,m}^{B}$ Binary variable preventing the BESS from being charged and discharged simultaneously in quarter $m$ of hour $t$
$u_{i,t,m}^{EV}$ Binary variable indicating the charging status of EV $i$

$N_{t,m}^{EV,rt}$ The real-time number of EVs charging in quarter $m$ of hour $t$
$SOC_{i,t,m}^{EV}$ State-of-charge of the battery of EV $i$ in quarter $m$ of hour $t$
$SOC_{t,m}^{B}$ State-of-charge of the BESS in quarter $m$ of hour $t$

## I. INTRODUCTION

### A. MOTIVATION

Increasing the penetration of intermittent-based distributed energy resources (DERs) has led power system operators to deploy more flexibility services. In this way, system operators need to maintain the stability of the system at a specific threshold and increase the flexibility of the system using FERs. The flexibility of electrical systems could be defined as the continuous adjustability of the operating point of the network to accommodate the variations in predicted/unpredicted fluctuations of demand/generation [1]. Flexibility services can be provided by different FERs located in the transmission network and/or the distribution network. Exploiting the maximum flexibility potential of the power system requires the active utilization of FERs in all levels of the system [2]. Currently, transmission-network-connected FERs such as conventional generators are the only resources being deployed to satisfy system-wide (TSO-level) flexibility needs [3], [4]. In other words, flexibility needs of transmission networks are mostly met by transmission-network-connected FERs. However, the utilization of maximum flexible capacity of the whole system requires the contribution of FERs connected to different levels of the network. These levels include DSO- and TSO-levels [5]. Electric vehicles (EV), different types of energy storage such as batteries as well as household controllable appliances can be regarded as examples of distribution-network-located FERs [5].

System operators, including transmission system operators (TSO) as well as distribution system operators (DSO), deploy various types of flexibility services so as to fulfil their operational responsibilities. The flexibility services utilized by TSOs are commonly known as ancillary services [4]. These services are normally used to satisfy system-wide flexibility needs. This means that they are deployed mostly to maintain the system frequency at its predefined limit.

The services include reserves, both spinning and non-spinning, which assist with the efficient operation of transmission networks. The ancillary services can be different depending on the characteristics and types of disturbances occurring in the power system [5], [6]. Currently in Nordic countries, frequency reserve services are categorized into primary reserves named frequency containment reserve (FCR), secondary reserves named automatic frequency restoration reserve (aFRR) and tertiary reserves named manual frequency restoration reserve (mFRR), which are deployed based on the system flexibility requirements. The FCR is a kind of reserve required to automatically respond to the real-time frequency deviation. This type of reserve is itself divided into two categories, namely frequency containment reserve for normal condition (FCR-N), which is utilized all the time, and frequency containment reserve for disturbance conditions (FCR-D). On the other hand, the aFRR is applied to automatically restore the balance, while the mFRR is used manually in case of outages, power-constrained occurrence related to cross-border connections as well as unexpected sustained activation of the aFRR [6], [7]. Moreover, a new kind of reserve market in the Nordic countries has been introduced in 2020, entitled fast frequency reserve (FFR), which can handle rapid frequency fluctuations during extremely low inertia situations (e.g. during summertime) [8].

As mentioned earlier, the main resources providing reserve services are currently conventional generators located in the TSO-level of networks. However, in the near future, the prevailing penetration of renewable energy resources would reduce the system's inertia significantly. For this reason, the participation of distribution-network-located FERs is needed as well as in order to efficiently operate future power systems.

### B. LITERATURE REVIEW AND COMPARISON

There exist previous studies that have assessed the participation of distribution-network-located FERs in providing TSO-level flexibility by taking part in reserve markets. In terms of storage-based resources, several studies analyzed the profitability and feasibility of the participation of different types of energy storage in reserve markets. For example, the authors of [9] propose a control policy for batteries so as to achieve near-optimal performance considering an offline controller which has complete information about the expected future status of the grid. Reference [10] analyzed the contribution of energy storage for better management of the variability of demand and generation. The provision of aFRR services by a battery energy storage system (BESS) is evaluated in [11], in which the authors aim to estimate the potential revenue of the battery storage system in the balancing market. In [12], a price-maker storage system is proposed, to participate in pool-based markets including joint energy, reserve markets and balancing settlement. In this reference, the authors did not specify the exact type of balancing services as well as the reserve that the storage was proposed to provide. Finally, the participation of pumped hydro energy storage in day-ahead energy and performance-based regulation was examined in [13]. This service was designed for North American regulation markets.

An electric vehicle (EV) aggregator has also been introduced as another reserve resource in the literature. For example, [14] proposes a novel bidding strategy for an EV aggregator aiming to provide TSO-level flexibility, by participating in reserve markets. The authors did not specify the type of reserves procured from EVs. The authors of [15] developed a deterministic optimization problem in order to minimize the costs of purchasing energy and selling secondary reserves (spinning or regulation reserves in the United States [16], [17]). The study tries to schedule EVs based on the North American reserve markets formed for secondary reserve procurement. The provision of FCR services through an EV charging station is also presented by the authors of [18], where the study calculates the potential flexibility that can be procured by each charging cycle of EVs.

In addition, some studies address the roles of distribution network aggregators in providing reserves. For instance, an aggregator of prosumers is proposed to take part in a joint day-ahead and reserve markets in [19]. This reference utilized a two-stage stochastic optimization model so as to support prosumers' participation in the reserve market. In [20]–[22], various models are presented for a virtual power plant so as to maximize its profit by participating in energy and ancillary service markets. Furthermore, the aggregator introduced in [23] is capable of taking part in spinning reserve markets as well as peak-hours load reduction. The authors of [24] proposed a coordination scheme for aggregating consumers for the purpose of providing FCR services. Similarly, [25] developed a model for the utilization of grid-connected PV panels combined with a BESS, aiming to follow the regulation signals sent by the operator. Finally, a microgrid is regarded as a provider of reserve services and flexible ramping products in [26], seeking to maximize its total profits.

Considering the existing literature, previous studies assessing the potential of distribution-network-located aggregated FERs have some shortcomings which need to be addressed in the future. For instance, in most of the above-mentioned studies, scheduling of FERs was not fully conducted based on the structure of real-world two-stage reserve markets in terms of market timing and technical aspects. In this light, for example, they do not consider whether the studied small-scale reserve unit is allowed to participate solely or whether it requires an aggregator as a broker. In addition, in most of the studies the authors do not differentiate between assigned reserve and activated reserve power, which can considerably affect the scheduling of FERs and thus affect the profitability of the reserve resource.

TABLE 1 highlights the difference between the proposed method and the existing literature. It should be noted that the table includes those references which deal with the provision of TSO-level flexibility services through distribution-network-located resources. The first column of the table introduces the references. The second column states which kind of flexibility services are provided by the FERs. The third column assesses whether the research considers both day-ahead and real-time scheduling to include both capacity and energy of reserves. The fourth column analyzes whether the study takes into account the technical aspects and details of the existing reserve markets and whether the model is developed based on the existing reserve market models. Additionally, it assesses whether the relevant considerations related to the assigned and activated reserve are taken into account in the study. The fifth and sixth columns indicate whether they utilized the two important FERs in their models.

According to TABLE 1, this article offers the existing research some advantages, described below:

**TABLE 1. Comparison of the proposed model with existing research.**

| Ref. | Type of services for TSOs | Two-stage scheduling | Compliant with the existing markets | BESS as FER | EVs as FERs |
|---|---|---|---|---|---|
| [9] | Frequency regulation | - | - | ✓ | - |
| [10] | Frequency regulation | - | - | ✓ | - |
| [11] | aFRR | - | - | ✓ | - |
| [12] | Not specified | - | - | ✓ | - |
| [13] | Performance-based regulation | - | - | ✓ | - |
| [14] | Not specified | ✓ | - | - | ✓ |
| [15] | Secondary reserve | ✓ | - | - | ✓ |
| [18] | FCR | - | ✓ | - | ✓ |
| [19] | Secondary reserve | ✓ | - | - | ✓ |
| [20] | Spinning reserve | - | - | - | - |
| [21] | Spinning reserve & reactive power | - | - | - | - |
| [22] | Spinning reserve | - | - | ✓ | - |
| [23] | Spinning reserve | - | - | - | ✓ |
| [24] | FCR | - | - | - | - |
| [25] | Frequency regulation | ✓ | - | - | - |
| [26] | Ramping products (US) | | - | ✓ | - |
| This Paper | mFRR (tertiary reserve) | ✓ | ✓ | ✓ | ✓ |

1. The distribution-network-located resource is considered to provide a type of ancillary service, which has not been regarded before. It offers mFRR services to the TSO.
2. It schedules its FERs in two stages (day-ahead and real-time) so as to take into account both reserve capacity and reserve power.
3. The model is in total compliance with the existing balancing market models in Nordic countries for providing mFRR services. The technical aspects and the difference between assigned and activated reserves are fully taken into account when scheduling the FERs.
4. The paper considers scheduling of two popular FERs, including BESS and EVs, at the same time.

### C. CONTRIBUTION

In general, this article presents a two-stage model for the participation of a PV-equipped LEC with EVs and a shared BESS for providing mFRR services. The first-stage scheduling is run in day-ahead. In this stage, the LEC aims to estimate its flexible capacities and the offers which should be submitted for the provision of mFRR. In the real-time stage, the LEC is scheduled based on the assigned and activated reserve power determined in real-time. The main contribution of the paper is summarized as follows:

1) To the best of the authors' knowledge, there exists no research assessing the participation of distribution-network-located resources in providing mFRR (tertiary reserve) services. Since each type of TSO-level reserve has a specific trading structure, along with specific technical considerations and activation time, the participation of reserve resources in each reserve market needs to be specifically analyzed.
2) The participation of a local energy community in reserve markets is not regarded in the existing studies. However, an LEC can be considered as one of the potent reserve providers by exploiting different-type distribution-network-located FERs and motivating members to manage their consumption. They can also share FERs so as to increase their profits. In this manner, the expenses of resources' capital costs are shared between members while they can all benefit from the monetary income. For this purpose, this article considers an LEC as a reserve provider whose members share a PV system as well as a BESS. There exists a number of EVs in the community, which can also contribute to the LEC's flexibility provision. In this regard, the EV owners' charging satisfaction is considered as well.
3) This article considers control parameters related to the SOC of the BESS so as to manage the flexible capacity offered by the LEC in the day-ahead stage. Accordingly, different control parameters are calculated for the case study, and their impact on the community's real-time operation and profitability are discussed.

### D. PAPER ORGANIZATION

The rest of the paper is organized as follows. The model description is provided in Section II. Section III focuses on the problem formulation for both stages of this study. The case study and simulation results are discussed in Section IV. Finally, this study's conclusion and possible future works is presented in Section V.

## II. MODEL DESCRIPTION

Before describing the proposed two-stage model, the concept of an energy community should be defined and the markets' considerations need to be introduced.

### A. ENERGY COMMUNITY

A general definition of energy communities has been proposed by the literature, which refers to a group of members who voluntarily join a community. These members might appear in different forms, e.g. prosumers (proactive consumer) or/and consumers. Energy communities might also have a bulk energy storage system, wind turbine(s) and/or a PV system as shared assets between members. The aim of energy communities (i.e. its members' aim) is to minimize energy costs along with maximizing the community's revenue through trading energy with the grid as well as providing flexibility services to the networks [27].

There might be various types of energy communities in terms of members' categories (e.g. residential, industrial, rural, etc.) or based on the physical distance between the members (e.g. local energy communities or distributed energy communities). Local energy communities are communities in which the members as well as the community's assets are geographically close. In such communities, the energy produced locally is supposed to be consumed locally. In other words, there should be local proximity between prosumers and consumers [28]. Additionally, anyone from the local area can become a member of this community and can trade with other members within the community. Furthermore, the total cost and benefit of such trading must be shared between the members of the community [29]. Thus, the members will benefit from the synergy and cost-efficient outcomes of joining the community.

There are various methods for the management of energy communities. Regarding this, a non-profit manager from amongst the community members should be nominated to be in charge of community management for monetary and technical considerations [30].

This article considers a number of households as consumers who form a residential LEC. The community shares a BESS and there are also some EVs within the community, which contribute to increasing the LEC's flexibility. In addition to these resources, the community is considered to have a shared PV system as a renewable energy resource. A non-profit community manager, through an energy community management center (ECMC), is in charge of the scheduling and operation of these resources in the community. The ECMC's main goal is to increase the LEC's profit by providing TSO-level flexibility to the grid and also to schedule the community's flexible resources including EVs and the BESS.

### B. FLEXIBILITY SERVICES AND MARKET STRUCTURE

The focus of this article is on providing mFRR services. With regard to the Nordic balancing markets [31], [32], a balancing service provider (BSP) aggregates several reserve resources so as to provide suitable capacities for participation in balancing energy and capacity markets. In Finland, as an example of a Nordic country, the minimum capacity required for participation in mFRR service markets is 5 MW, which needs to consist of bids with a resolution of 1 MW [31].

The studied flexibility service, i.e. mFRR, is split into upward flexibility and downward flexibility services. In circumstances wherein systems require upward flexibility, the TSO purchases power from the BSPs, whilst during time slots requiring downward flexibility, the TSO sells power to the BSPs [7]. The type of flexibility services required in each time slot depends on the TSO's flexibility needs.

Manual FRR services are traded in the balancing capacity market (BCM) and the balancing energy market (BEM). In the BCM, participants should submit their flexibility capacities before 11:00 a.m. of the day before delivery [31]. The TSO deploys the amount of capacity required and pays a capacity fee to the corresponding BSPs. However, participants can submit and modify their balancing energy bids in the BEM 45 minutes prior to delivery [31]. The BSP submits its bids for upward/downward regulation, the prices as well as other information regarding its reserve units to the BEM. Afterwards, the TSO decides on the assigned flexibility that should be provided by the BSPs, based on their offered prices, the type of required flexibility (upward or downward) and the amount of required flexibility in each time slot.

As already mentioned, this article considers a difference between the assigned flexibility and activated flexibility. Regarding this, the TSO determines the assigned flexibility of each BSP through the settlement of the BEM, while the activated amount of flexibility is specified at the exact moment of delivery based on the TSO's real-time balancing requirements [31]. In other words, the TSO decides how much flexibility must be activated according to its instantaneous flexibility need.

### C. PROPOSED MODEL

The proposed LEC, as a reserve unit, contributes to the provision of mFRR services. In order to enable participation of a small-scale LEC, the LEC's flexibility offer should be sent to the BSP to be aggregated with those of the other reserve units and be submitted to the balancing markets. Fig. 1 depicts the main structure of the proposed LEC and its interaction with the grid and the BSP. As the figure illustrates, the LEC sells TSO-level flexibility through the BSP, and also trades energy with the upstream grid so as to fulfil its energy balance constraints.

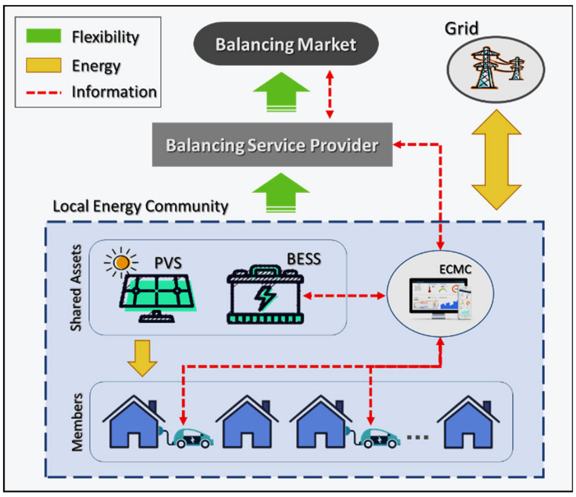


**FIGURE 1. The structure of the LEC and its interactions with the grid and BSP.**

Regarding the structure of the balancing markets introduced in the previous section, the LEC as a reserve unit is supposed to be scheduled in two stages, each with different time horizons and granularity.

In the first stage, the ECMC runs day-ahead 24-hour scheduling in order to estimate the flexible capacity of the LEC, which can be determined for each hour of the next day. The results should be submitted to the BSP before 11:00 a.m. of the day prior to delivery so that the BSP could be able to participate in the BCM and BEM with complete knowledge of its reserve units.

The second-stage scheduling, however, runs in real-time for the coming hour. Before this stage, the BSP participated in both BCM and BEM on behalf of its reserve units. Afterwards, the flexibility power that should be provided by the corresponding BSP was assigned by the TSO. Subsequently, the BSP determines the flexibility that needs to be provided by its reserve units. In this regard, the ECMC seeks to schedule the shared FERs to provide the assigned flexibility as well as maximizing the community's real-time profit.

Fig. 2 summarizes the proposed two-stage scheduling framework for the studied LEC and its interaction with the upstream entities. According to Fig. 2, the main interaction of the LEC is with the BSP in day-ahead and real-time horizons. The BSP is in charge of creating bidding strategies in order to participate in balancing markets (BCM and BEM) on behalf of its reserve units and assign the reserve power to each reserve unit. The main responsibility of the TSO regarding mFRR services is clearing the balancing markets, assigning the reserve power to each BSP according to its required frequency-based flexibility and activating the reserved power when needed. However, the main focus of this article is on the optimized operation and scheduling of the LEC. Therefore, other issues such as the bidding strategy, reserve assignment, aggregation methods applied by the corresponding BSP and reserve market clearing performed by the TSO, as well as the calculation of the related flexibility need is not within the scope of this article (see the grey blocks in Fig. 2).

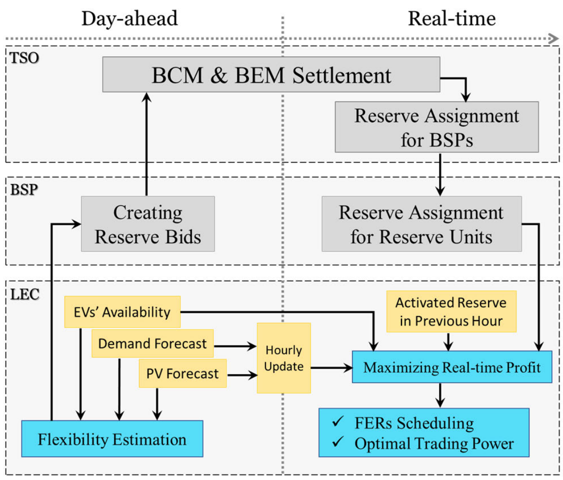


**FIGURE 2. Overview on the proposed scheduling of the LEC and the interactions with the BSP and TSO.**

The proposed two-stage operation will be fully explained in Section III.

## III. PROBLEM FORMULATION

The problem formulation of this article includes two stages, which are explained in detail as follows.

### A. STAGE I: DAY-AHEAD FLEXIBILITY OFFER

In this stage, the ECMC runs day-ahead scheduling aimed at estimating the LEC's utmost capability to provide flexibility services for the 24 hours of the next day. The following factors are taken into account in the day-ahead stage:

1. EV owners in the LEC arrange their next-day exact plugged-in and plugged-out hours and submit it to the ECMC. Thus, the ECMC has the next-day temporal charging information of EVs. Note that it is assumed that EV charging is centrally controlled by the ECMC. In addition, for the sake of simplicity, they are assumed to be charged with constant power [33].
2. The BESS can be monitored and controlled directly by the ECMC. Therefore, the ECMC has precise information regarding the BESS's capacity and estimates the BESS's next-day SOC based on its schedule.
3. The net-load of the LEC's members is predicted hourly for the 24 hours of the next day. In order to capture the stochasticity of consumption load as well as the PV generation, the error of the forecasted net-load is here taken into consideration, which can be modelled a Gaussian distribution [34]. Note that the net-load of the LEC is defined as the difference between its aggregated consumers' load and the LEC's PV generation. Regarding the probability distribution model of the net-load's forecasting error, different scenarios are considered for the first-stage schedule to consider the related uncertainties of the net-load originating from households' stochastic behavior.
4. Finally, flexibility is estimated in a time horizon of 24 hours with one-hour time granularity. Hence, each time slot refers to one hour in the first-stage scheduling.

For each time slot, the community offers its upward flexibility or/and downward flexibility power based on the community's production surplus and the capability of its FERs (i.e. BESS and EVs) to change their consumption. In time slots during which the community's surplus is positive it can submit its entire surplus as upward flexibility capacity. In contrast to this, the maximum capability of the community to increase its consumption can be considered as its downward flexible capacity. It is worth mentioning that according to the proposed strategy, the LEC may offer both downward and upward flexibility at one hour in the day-ahead stage if it simultaneously has a positive surplus and some available FERs that can increase their consumption. However, one type of offer (downward or upward) will be accepted and assigned in real-time.

#### 1) FLEXIBILITY ESTIMATION

As stated before, in the first stage the ECMC seeks to estimate the maximum upward and downward flexibility that can be offered for the 24 hours of the next day in order to submit this to the BSP for the provision of flexibility services. It is obvious that a requirement for participation in reserve markets like the mFRR is to declare capacity as reserve in previous day. Moreover, providing flexibility services is always much more profitable for the community, since the prices of balancing services is substantially higher than energy. Hence, the community should estimate the available flexibility that can be provided in the following day. The ECMC runs a stochastic optimization problem with the following objective function:

$$max. \sum_{s} \sum_{t} \pi_{t,s}(F_{t,s}^{up} + F_{t,s}^{dn}) \tag{1}$$

Equation (1) shows that the ECMC's objective is to find the maximum upward and downward available flexibility which can be offered to the BSP for all of the considered scenarios and for all 24 hours of the following day.

According to [7], regarding balancing energy markets (BEM), the price of selling upward flexibility is always greater than the price of selling power to the upstream grid or energy markets. In addition, the price of buying downward balancing flexibility is always lower than buying power from the upstream grid or energy markets. Hence, it can be concluded that participating in balancing markets is always beneficial to the LEC. Thus, in the day-ahead stage, the energy community is merely aiming to find the maximum flexible capacities which can be offered in balancing markets.

The variable that helps to calculate the maximum upward flexible capacities of the LEC is defined by (2).

$$Cap_{t,s}^{up} = P_{t,s}^{B,dis,est} - N_t^{EV,est} P^{EV} - (L_t^{net,for} + \Delta\mathcal{E}_{t,s}) \quad \forall t, \forall s \tag{2}$$

$$L_t^{net,for} = P_t^{L,for} - P_t^{PV,for} \quad \forall t \tag{3}$$

According to (2), the upward flexibility of the LEC should be obtained from the LEC's production surplus. The production surplus of the LEC is equal to the difference between the discharging power of the BESS and the aggregated values of net-load and EVs' charging power. The net-load of the LEC at hour $t$ could be obtained from (3). Equation (4) calculates the maximum downward flexible capacity which can be used for the provision of mFRR.

$$Cap_{t,s}^{dn} = P_{t,s}^{B,ch,est} + N_t^{EV,est} P^{EV} \quad \forall t, \ \forall s \tag{4}$$

The downward flexible capacity is known as the ability of the LEC's FERs to increase their consumption. Since EVs and BESS are considered as the existing FERs in this study, charging these resources can be taken into account as LEC's flexible consumption. Hence, the charging power of the mentioned resources can be considered as the LEC's available downward flexibility for scenario $s$ and time slot $t$ as stated in (4).

Equations (5) and (6) indicate that the charging and discharging power of the BESS cannot exceed their maximum rate, respectively. The binary variable $u_{t,s}^{B,est}$ in (5) and (6) is employed in order to prevent the BESS from being charged and discharged simultaneously. This variable is considered to be 1 when the BESS is in a charging state, otherwise it is equal to 0.

$$P_{t,s}^{B,ch,est} \leq P^{B,ch,max} u_{t,s}^{B,est} \quad \forall t,\ \forall s \tag{5}$$

$$P_{t,s}^{B,dis,est} \leq P^{B,dis,max} \left(1 - u_{t,s}^{B,est}\right) \quad \forall t,\ \forall s \tag{6}$$

Moreover, the net-load error is assumed to be represented by a Gaussian distribution denoted by $\Delta\mathcal{E}_t\ (\mu_t, \sigma_t)$, where $\mu_t$ is the mean value for error of forecast and $\sigma_t$ is the related standard deviation. These are obtained as follows [34]:

$$\sigma_t = \sqrt{({\sigma_t}^{PV})^2 + (\sigma_t^L)^2} \quad \forall t \tag{7}$$

$$\sigma_t^{PV} = 0.2P_t^{PV,for} + 0.02P^{PV,ins} \quad \forall t \tag{8}$$

$$\sigma_t^L = \frac{k}{100} P_t^{L,for} \quad \forall t \tag{9}$$

Equation (7) shows that the standard deviation of the net-load is obtained from consumption demand and is related to the PV located in the LEC. The standard deviation of PV production is defined in (8) while the standard deviation of the total consumption load of the community is shown in (9). In (9), $k$ is a function of the accuracy of load prediction [34].

The community can offer upward flexibility when it has a positive upward flexible capacity (i.e. the LEC's production surplus). Similarly, downward flexibility can be ascertained when the downward flexible capacity experiences a positive value, as stated by (10) and (11), respectively.

$$F_{t,s}^{up} = \begin{cases} Cap_{t,s}^{up} & Cap_{t,s}^{up} \geq 0 \\ 0 & \text{else} \end{cases} \quad \forall t, \forall s \tag{10}$$

$$F_{t,s}^{up} = \begin{cases} Cap_{t,s}^{dn} & Cap_{t,s}^{dn} \geq 0 \\ 0 & \text{else} \end{cases} \quad \forall t, \forall s \tag{11}$$

Since EVs are supposed to submit their plugged-in and plugged-out charging hours beforehand, the number of EVs being charged during each hour can be obtained simply by using (12).

$$N_t^{EV} = N_{t-1}^{EV} + N_t^{plug} - N_t^{unplug} \quad \forall t \tag{12}$$

Equation (12) states that the number of charging EVs at hour $t$ is equal to the number of EVs charged in the previous hour plus the number of those beginning to charge at hour $t$ minus the number of EVs which are supposed to be unplugged at hour $t$.

There exist constraints related to the operation of the BESS, which are indicated by (13) and (14). Equation (13) relates the estimated SOC of the BESS to its charging and discharging power. This constraint can also indicate the variation regarding the state of energy of the BESS. Equation (14) restricts the maximum and minimum permissible values of the estimated SOC, which implicitly limits the energy stored in the BESS as well.

$$SOC_{t,s}^{B,est} = SOC_{t-1,s}^{B,est} + \frac{\Delta t}{Cap^B}\left(\eta^{B,ch} P_{t,s}^{B,ch,est} - \frac{P_{t,s}^{B,dis,est}}{\eta^{B,dis}}\right) \quad \forall t,\ \forall s \tag{13}$$

$$\widetilde{SOC}_t^{min} \leq SOC_{t,s}^{B,est} \leq \widetilde{SOC}_t^{max} \quad \forall t,\ \forall s \tag{14}$$

The ECMC is proposed to adopt two control parameters, i.e. $\widetilde{SOC}_t^{min}$ and $\widetilde{SOC}_t^{max}$, to control the amount of BESS's capacity deployed for provision of flexibility services. In day-ahead scheduling, there might exist some uncertainties related to the activation of balancing services, its direction (i.e. upward or downward) and those associated with forecasting PV production and demand. Therefore, the ECMC may decide to save some part of its BESS's capacity and deploy it in real-time schedules so as to avoid the risk of penalty costs related to not providing the assigned flexibility in real-time. For this purpose, the mentioned control parameters are employed to limit the day-ahead utilization of the BESS's capacity in providing TSO-level flexibility services. These parameters should be determined within a range introduced as follows:

$$SOC^{B,min} \leq \widetilde{SOC}_t^{min} \leq SOC^{B,max} \quad \forall t \tag{15}$$

$$SOC^{B,min} \leq \widetilde{SOC}_t^{max} \leq SOC^{B,max} \quad \forall t \tag{16}$$

$$\widetilde{SOC}_t^{min} \leq \widetilde{SOC}_t^{max} \quad \forall t \tag{17}$$

In (15) and (16), the value of $SOC^{B,min}$ and $SOC^{B,max}$ indicate the lower and upper limits of state-of-charge, where their values depend on the type of BESS. Equation (17) shows that the selected value for the lower controller of state-of-charge, i.e. $\widetilde{SOC}_t^{min}$, must be smaller than the upper controller of state-of-charge, i.e. $\widetilde{SOC}_t^{max}$, at all times. Taking these constraints into account, if the gap between the adopted $\widetilde{SOC}_t^{min}$ and $\widetilde{SOC}_t^{max}$ decreases, it means that the ECMC prefers to offer a lower amount of its BESS's flexible capacity for reserve services and save a portion of its flexibility for the real-time scheduling (see Fig. 3). Fig. 3 indicates the amount of BESS's capacity deployed for flexibility offers in day-ahead.

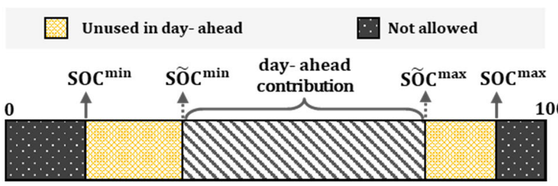


**FIGURE 3.** An illustration of the BESS utilization scheme in day-ahead according to the proposed control parameters.

Accordingly, the expected amount of upward and downward flexibility in each time slot, which is supposed to be offered to the BSP, is obtained from (18) and (19).

$$\mathcal{F}_t^{up} = \sum_s \pi_{t,s} F_{s,t}^{up} \quad \forall t \tag{18}$$

$$\mathcal{F}_t^{dn} = \sum_s \pi_{t,s} F_{s,t}^{dn} \quad \forall t \tag{19}$$

After offering the total downward and upward flexible capacity by the ECMC, the BSP will then participate in balancing markets (BCM and BEM) by aggregating the flexibility offers of its reserve units.

### B. STAGE II: REAL-TIME OPERATION AND SCHEDULING

Before the real-time stage, the TSO determines the power that should be provided by the BSP. In fact, the BSP has already participated in balancing markets and the results of the market settlement are specified in real-time. Afterwards, the BSP determines the amount of flexibility that should be provided by the LEC based on its day-ahead offer. Regarding this information, the manager of the community needs to schedule its FERs so as to achieve the following targets:

1. Fulfil the assigned power for mFRR provision
2. Maximize the total real-time monetary profits of the LEC

In this manner, this article considers that the ECMC schedules the community's FERs for the next hour regarding four temporal quarters (15-minute timeslots), based on the assigned values of flexibility. Therefore, the time horizon and time granularity of the scheduling would be one hour and 15-minutes, respectively. The following factors are also considered in this stage:

a. EV owners are assumed to adhere to their day-ahead plan. They plug in and unplug their vehicles at the exact hours they have stipulated beforehand, since they have accepted the content of the intra-community rules and must not violate their predetermined agreement signed with the community manager. In this regard, based on EV owners' desires and needs, the ECMC can schedule the vehicles for the next four quarters.
b. EV owners are supposed to submit the minimum number of hours that they want their vehicles to be charged. This constraint is applied in order to take into account the EV owners' charging satisfaction.
c. It is assumed that the ECMC monitors the real-time state of the FERs. Indeed, the ECMC updates the information regarding the SOC of the BESS and EVs at the end of each hour, based on the activated reserve. This information will be deployed for scheduling FERs for the next hour.
d. PV power generation as well as demand forecasts are updated hourly. Since predictions with very short-time horizons (i.e. one hour) are relatively more accurate than, e.g. day-ahead forecasting, the results of PV/demand predictions are considered deterministic and not to be subjected to any uncertainties.
e. After fulfilling the assigned value of TSO-level flexibility services, the ECMC trades the surplus power with the upstream grid through a DSO or a retailer.

#### 1) LEC SCHEDULING

According to the assumptions above, the ECMC runs an optimization problem with the objective of maximizing the community's real-time profit, denoted by (20). Profit is defined by (21). In addition, (22) denotes the income or cost obtained from the LEC's participation in reserve provision. By using the objective function indicated by (20), the optimization problem seeks to find a compromise between flexibility obtained from its FERs and profits of the LEC.

$$max. \sum_m Profit_{t,m}^{real-time} \Delta m \quad \forall t \tag{20}$$

$$\begin{aligned} Profit_{t,m}^{real-time} &= \underbrace{IC_{t,m}^{flex}}_{X} + \underbrace{P_{t,m}^{out}\lambda_t^{sell}}_{Income\ II} \\ &\quad - \underbrace{P_{t,m}^{in}\lambda_t^{buy}}_{Cost\ II} - \underbrace{C^B(P_{t,m}^{B,dis} + P_{t,m}^{B,ch})}_{Cost\ II} \quad \forall t, \forall m \end{aligned} \tag{21}$$

$$IC_{t,m}^{flex} = I_t^{cap} + I_t^{en,up} - C_t^{en,dn} \quad \forall t, \forall m \tag{22}$$

On the left side of (21), $Profit_{t,m}^{real-time}$ indicates the total profit of the LEC in real-time. On the right side of this equation, $X$ represents the income or cost due to the provision of capacity and energy related to mFRR services.

According to (22), the LEC receives a fixed monetary amount which is paid for offering flexibility capacities (both upward and downward), denoted by $I_t^{cap}$. In fact, this income is obtained by the participation of the BSP in the BCM. In addition, the LEC receives the income for selling upward energy ($I_t^{en,up}$) and incurs the cost for purchasing downward energy ($C_t^{en,dn}$) from the BEM. In this manner, the BSP plays the role of an intermediary by participating in the BCM and BEM.

The remaining terms of (21) are as follows. The term *Income II* denoted the revenue resulting from selling energy to the upstream grid through the DSO or the retailer. The term *CostII* denotes the cost of purchasing energy from the grid. The last term, *CostIII*, refers to the operating cost of charging and discharging the BESS. It has to be mentioned that $C^B$ is the operating costs of charging/discharging the BESS, which are considered constant over the studied time and obtained as follows [35].

$$C^B = \frac{RC^B}{Cap^B \times DOD^B \times RL^B} \tag{23}$$

where $DOD^B$ indicates depth of discharge of the BESS. The rated lifetime and the replacement cost of the BESS are denoted by $RL^B$ and $RC^B$, respectively.

The main priority of the LEC's real-time scheduling is to provide the assigned flexibility services, i.e. $\mathcal{F}_t^{up,as}$ and $\mathcal{F}_t^{dn,as}$. However, to satisfy power balance constraint within the LEC, the ECMC should trade surplus power with the upstream grid. Accordingly, (24) denotes the balance equations, when the LEC provides upward and downward flexibility services.

$$\begin{cases} L^{net}_{t,m} + P^{B,ch}_{t,m} + N^{ch}_{t,m}P^{EV} = \mathcal{F}^{dn,as}_{t} + \hat{p}^{in}_{t,m}, \\ \quad \text{if} \quad u^{up}_{t,m} = 0 \\ -L^{net}_{t,m} + P^{B,dis}_{t,m} - N^{ch}_{t,m}P^{EV} = \mathcal{F}^{up,as}_{t} + \hat{p}^{out}_{t,m}, \\ \quad \text{if } u^{dn}_{t,m} = 0 \end{cases} \tag{24}$$

In (24), $u^{up}_{t,m}$ and $u^{dn}_{t,m}$ are binary parameters which have been determined by the BSP according to the market settlement results of the BEM. In other words, these parameters provide information on whether the TSO requires downward or upward flexibility services. According to (24), in the case of providing downward flexibility, $u^{up}_{t,m}$ is equal to 0 and the consumption power of the net-load and the charging power of the BESS and EVs is supplied by the imported power from the upstream grid, as well as the downward flexibility power bought from the BEM. Similarly, in the case of providing upward flexibility, the positive power surplus of the LEC is sold to the upstream grid after fulfilling the assigned upward flexibility. It should be noted that $\mathcal{F}^{dn,as}_{t}$ and $\mathcal{F}^{up,as}_{t}$ are parameters whose values have been specified by the BSP.

If $\hat{p}^{in}_{t,m}$, which is obtained from (24), has a positive value, this means that the LEC is not self-sufficient and the required energy should be supplied by the grid. The imported power then would be equal to $P^{in}_{t,m}$. Similarly, if $\hat{p}^{out}_{t,m}$ has a positive value, this means that there exists some production surplus that should be sold to the grid. Thus, the exported power equals $P^{out}_{t,m}$, as denoted by (25) and (26).

$$P^{in}_{t,m} = \begin{cases} \hat{p}^{in}_{t,m}, & \hat{p}^{in}_{t,m} > 0 \\ 0, & \text{else} \end{cases} \quad \forall t, \forall m \tag{25}$$

$$P^{out}_{t,m} = \begin{cases} \hat{p}^{out}_{t,m}, & \hat{p}^{out}_{t,m} > 0 \\ 0, & \text{else} \end{cases} \quad \forall t, \forall m \tag{26}$$

In the proposed real-time scheduling, each EV is being scheduled to maximize the community's profit. Equation (27) – (31) are constraints related to charging the community's EVs. It should be highlighted that all EVs are supposed to be charged with a constant power rate, denoted by $P^{EV}$.

$$N^{EV}_{t,m} = \sum_{i} u^{EV}_{i,t,m} \quad \forall t, \forall m \tag{27}$$

$$\sum_{m} u^{EV}_{i,t,m} \geq \frac{4\Psi^{req}_{i}}{\Delta t^{plugged}_{i}} \quad \forall i, \forall t \in [t^{plug}_{i}, t^{unplug}_{i}] \tag{28}$$

$$SOC^{EV}_{i,t,m} = \begin{cases} SOC^{EV,act}_{i,t-1,4} + \dfrac{\eta^{EV} P^{EV} \Delta m}{Cap^{EV}_{i}} u^{EV}_{i,t,m}, \\ \quad \text{if } m = 1 \\ SOC^{EV}_{i,t,m-1} + \dfrac{\eta^{EV} P^{EV} \Delta m}{Cap^{EV}_{i}} u^{EV}_{i,t,m} \\ \quad \text{else} \end{cases}$$
$$\forall i, \ \forall t, \ \forall m \tag{29}$$

$$SOC^{EV}_{i,t,m} \leq SOC^{EV,max} \quad \forall i, \ \forall t, \ \forall m \tag{30}$$

$$u^{EV}_{i,t,m} = 0 \quad \forall i, \ \forall m, \ \forall t \notin \left[t^{plug}_{i}, t^{unplug}_{i}\right] \tag{31}$$

In (27), (29) and (30), $u^{EV}_{i,t,m}$ is a binary decision variable which determines the charging status of EV $i$ during quarter $m$ of hour $t$. This variable is equal to 1 if EV $i$ is being charged during quarter $m$ of hour $t$. Otherwise, it equals 0. Accordingly, (27) expresses that the total number of EVs that are being charged during time slot $m$ of hour $t$ is obtained through the summation of the binary variables related to the charging status of all EVs within the LEC. Equation (28) determines the number of quarters that an EV needs to be charged during a given hour. As previously stated, in the real-time stage, the scheduling time granularity is 15 minutes (one quarter) and the scheduling time horizon is one hour. Therefore, considering the one-hour time horizon, if an EV needs to be charged for $\Psi^{req}_{i}$ hour during $\Delta t^{plugged}_{i}$ hours, the EV should be charged at least $\frac{4\Psi^{req}_{i}}{\Delta t^{plugged}_{i}}$ quarters during one hour (four quarters). To elaborate this constraint, consider that EV $i$ requests to be charged for at least one hour (i.e. $\Psi^{req}_{i} = 1$). This EV, for instance, was plugged in at 8:00 and unplugged at 12:00, so it was plugged in for four hours (i.e. $\Delta t^{plugged}_{i} = 4$). Therefore, according to constraint (28), this EV should be charged at least one quarter in each hour during for which the vehicle is plugged. Through the ECMC, the community manager decides how the EVs should be charged in the plugged in periods. In order to keep all parties satisfied, it is feasible to spread the charging quarters over the plugging time, rather than charging them in a limited period. This could reduce possible peak loads during some hours.

The constraints related to EVs' battery SOC are presented by (29) and (30). It should be mentioned that the 4th quarter of hour ($t$-1) is followed by the 1st quarter of hour $t$, as explained in (29). Regarding the first equation of (29), the EVs' SOC in the 1st quarter of each hour should be determined based on its actual value in the 4th quarter of the previous hour, because the actual value of EVs' SOC may not be equal to that scheduled in the previous hour. Since the activated and assigned values of reserve power may not be equal, the scheduled values of EVs' SOC need to be replaced with the actual values. However, for the 2nd to 4th quarters of each hour, the values of EVs' SOC could be obtained based on their scheduled values in the previous quarter, as explained in the second equation of (29).

Equation (30) restricts the maximum value of the SOC of EVs' batteries. Finally, (31) ensures that the EVs will only be charged during the hours in which they are plugged in, meaning that they should be charged in a range which is part of the EV's plugged-in/plugged-out time window. Otherwise, the optimization solver should assign a zero value to the charging status of the EV.

In the following, the constraints related to the BESS are presented. Equation (32) and (33) elaborate the constraints associated with the SOC of the BESS. In (32) and (33), if we multiply both sides of the BESS's capacity, we will have the related constraints of the BESS's state-of-energy. Again, the scheduled value of the SOC for the previous hour ($t$-1) should be replaced with the actual SOC of the BESS. This value is utilized to schedule the BESS at hour $t$. The BESS will be charged/discharged only when needed. This need is the amount of energy required for balancing purposes, which is announced by the BSP/TSO. However, the BSP/TSO always asks for flexibility within the LEC's capability. The TSO would not ask for more than the LEC can offer.

Finally, (34) and (35) restrict the charging and discharging power of the BESS, respectively [36], along with the fact that the BESS is not allowed to be charged and discharged simultaneously, with the help of binary variable $u^{B}_{t,m}$.

$$SOC^{B}_{t,m} = \begin{cases} SOC^{B,act}_{t-1,4} + \left(\eta^{B,ch} P^{B,ch}_{t,m} - \dfrac{P^{B,dis}_{t,m}}{\eta^{B,dis}}\right) \dfrac{\Delta m}{Cap^{B}} \text{ if } m = 1 \\ SOC^{B}_{t,m-1} + \left(\eta^{B,ch} P^{B,ch}_{t,m} - \dfrac{P^{B,dis}_{t,m}}{\eta^{B,dis}}\right) \dfrac{\Delta m}{Cap^{B}} \quad \text{else} \end{cases} \quad \forall t, \forall m \tag{32}$$

$$SOC^{B,min} \leq SOC^{B}_{t,m} \leq SOC^{B,max} \quad \forall t, \forall m \tag{33}$$

$$P^{B,ch}_{t,m} \leq u^{B}_{t,m} P^{B,ch,max} \quad \forall t, \forall m \tag{34}$$

$$P^{B,dis}_{t,m} \leq \left(1 - u^{B}_{t,m}\right) P^{B,dis,max} \quad \forall t, \forall m \tag{35}$$

The ECMC runs this optimization problem considering (20)–(35) for each hour, to schedule its FERs including the BESS and EVs as well as its trading power with the upstream grid, aiming to maximize the community's real-time profit. Before starting the next-hour scheduling, the SOC of the BESS and EVs for the previous hour, i.e. $SOC^{B,act}_{t-1,4}$ and $SOC^{EV,act}_{i,t-1,4}$, are updated based on the real data resulted from the activated mFRR. Thereafter, the real-time scheduling is run for the next hour (next four quarters), accordingly.

It should be mentioned that decreasing the charging rate of the BESS as flexibility-up, or increasing the discharging rate of the BESS as flexibility-down, could be considered as flexibility, which actually happen in real-time operation of the BESS in the process of flexibility provision. However, counting on them as the capacity for participation in the mFRR market would not be a wise choice. For instance, in a case where we are dealing with the constant BESS's power rates, counting on the above-mentioned strategy for flexibility provision would not be generally applicable. Moreover, the change in the power rate of the BESS might not satisfy the offered flexibility.

## IV. NUMERICAL STUDIES

### A. CASE STUDY

The case study consists of a hypothetical LEC with 50 households. This community has a 100kW PV system as well as FERs, including a 50kW/200kWh (Vanadium Redox Flow) BESS and 10 EVs. The information on EVs' plugged-in/plugged-out status and the EVs' battery capacity can be found in TABLE 2.

**TABLE 2.** Information on the EVs owned by the community members.

| EV No. | $Cap^{EV}$ (kWh) | $t^{plug}$ | $t^{unplug}$ |
|---|---|---|---|
| 1 | 40 | 08:00 | 10:00 |
| 2 | 12 | 08:00 | 11:00 |
| 3 | 11.6 | 10:00 | 13:00 |
| 4 | 11.6 | 08:00 | 10:00 |
| 5 | 40 | 12:00 | 15:00 |
| 6 | 12 | 15:00 | 17:00 |
| 7 | 12 | 16:00 | 18:00 |
| 8 | 40 | 17:00 | 19:00 |
| 9 | 11.6 | 17:00 | 19:00 |
| 10 | 12 | 17:00 | 19:00 |

It is also assumed that EVs request to be charged at least for two 15-minute quarters. Moreover, the information related to the characteristics of the BESS in the simulation studies is given in TABLE 3 [37].

**TABLE 3.** Characteristics of the shared BESS in the community.

| | |
|---|---|
| Technology | Vanadium R.F. |
| Price (€/kWh) | 100 |
| Depth of Discharge (%) | 60 |
| Rated Lifetime (cycles) | 12000 |
| Capacity (kWh) | 200 |
| Max. Charging/Discharging Rate (kW) | 50 |
| Charging/Discharging Efficiency | 0.8 |

The forecasted day-ahead as well as actual values of demand and solar generation are depicted in Fig. 4. The pattern of solar irradiation is based on the historical data for July 7, 2019 in Finland [8]. The forecasting error of PV generation in the day-ahead study is represented by an independent normal distribution with a zero mean value and a 10% standard deviation. Similarly, the forecasting error of the demand load is also modelled with a zero mean value and a 2% standard deviation.

### B. SIMULATION RESULTS

The simulation in this article was executed on a laptop with an Intel Core-i5 6200U 2.3GHz CPU and 16GB of RAM. The optimization algorithms were implemented by using the well-known GAMS programming software.

#### 1) DAY-AHEAD FLEXIBILITY OFFER

In order to conduct the introduced stochastic study, 1000 scenarios were produced by utilizing Monte Carlo simulation for PV generation and load demand of each hour. Afterwards, the optimization problem defined in (1)–(19) was solved for the LEC introduced in this section. It is noticeable that a linearization technique was utilized, similar to the one deployed

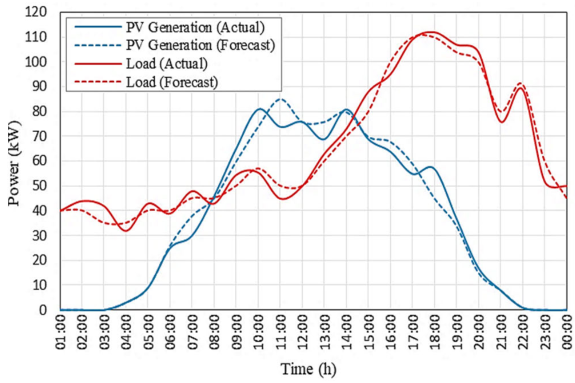


**FIGURE 4.** Actual and forecasted values of PV generation and demand.

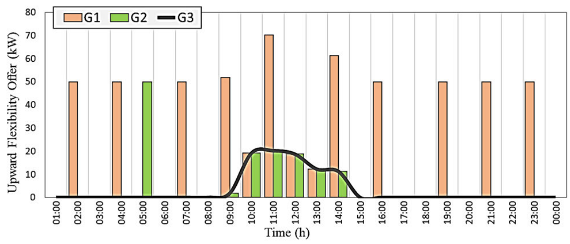


**FIGURE 5.** Upward flexibility offer by the LEC considering different cases.

in [38], so as to linearize constraints (10) and (11) (see APPENDIX). The total daily values of upward and downward flexibility offered to the BSP are calculated based on different SOC-based control parameters and the results are illustrated in TABLE 4. It should be noted that the control parameters are given as constant for 24 hours. In addition, the degree of BESS utilization (DBU) for offering flexibility is calculated for each case using the following equation (36):

$$DBU_t = \frac{\widetilde{SOC}_t^{max} - \widetilde{SOC}_t^{min}}{SOC^{max} - SOC^{min}} \times 100 \tag{36}$$

Regarding TABLE 4, all of the considered cases lead to three pairs of total upward and downward flexibility offers, i.e. $(\sum_t \mathcal{F}_t^{up} \sum_t \mathcal{F}_t^{dn})$, which are (583.9 780.5), (133.9 180.5) and (83.9 80.5). In light of this conclusion, we narrowed down all considered cases into three groups based on the values of available flexibility, namely G1, G2 and G3. These groups are illustrated by three different colors in TABLE 4.

The hourly upward and downward flexibility of these groups have been calculated and the results are depicted in Fig. 5 and Fig. 6, respectively.

According to TABLE 4, in general, the amount of upward flexibility and downward flexibility offered to the BSP decreases when $\widetilde{SOC}_t^{min}$ increases. However, this effect does not seem to be significant when the other control parameter, i.e. $\widetilde{SOC}_t^{max}$, has a lower value. Although the higher value of $\widetilde{SOC}_t^{min}$ leads to a lower amount of offered flexibility for cases 1, 2, 3 and 4, this trend does not strongly continue for

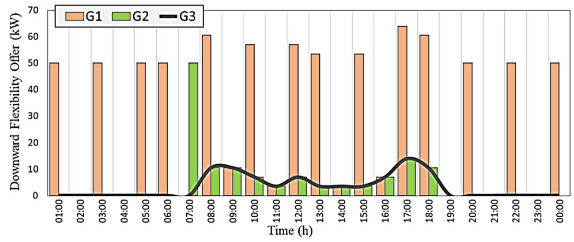


**FIGURE 6.** Downward flexibility offer by the LEC considering different cases.

**TABLE 4.** The results of total daily flexibility offers in day-ahead, based on different BESS control parameters.

| Case No. | Control Parameters $\widetilde{SOC}_t^{min}$ | Control Parameters $\widetilde{SOC}_t^{max}$ | Total Daily Upward Flexibility Offer (kW) | Total Daily Downward Flexibility Offer (kW) | DBU (%) |
|---|---|---|---|---|---|
| 1 | 0.2 | 0.8 | 583.9 | 780.5 | 100 |
| 2 | 0.3 | 0.8 | 583.9 | 780.5 | 83 |
| 3 | 0.4 | 0.8 | 133.9 | 180.5 | 67 |
| 4 | 0.5 | 0.8 | 83.9 | 80.5 | 50 |
| 5 | 0.2 | 0.7 | 583.9 | 780.5 | 83 |
| 6 | 0.3 | 0.7 | 83.9 | 80.5 | 67 |
| 7 | 0.4 | 0.7 | 83.9 | 80.5 | 50 |
| 8 | 0.5 | 0.7 | 83.9 | 80.5 | 33 |
| 9 | 0.2 | 0.6 | 133.9 | 130.5 | 67 |
| 10 | 0.3 | 0.6 | 83.9 | 80.5 | 50 |
| 11 | 0.4 | 0.6 | 83.9 | 80.5 | 33 |
| 12 | 0.5 | 0.6 | 83.9 | 80.5 | 17 |
| 13 | 0.2 | 0.5 | 133.9 | 130.5 | 50 |
| 14 | 0.3 | 0.5 | 83.9 | 80.5 | 33 |
| 15 | 0.4 | 0.5 | 83.9 | 80.5 | 17 |

G1 G2 G3

the other cases. For example, increasing $\widetilde{SOC}_t^{min}$ does not change the flexibility offer of cases 6, 7 and 8. This is due to the fact that the amount of 83.9 kW for upward flexibility and 80.5 kW for downward flexibility mainly stem from other sources of production (e.g. the surplus PV production of the LEC and EVs). Hence, decreasing the capacity of the BESS does not affect these values.

Similarly, TABLE 4 indicates that, in general, reducing control parameter $\widetilde{SOC}_t^{max}$ decreases the estimated amount of offering upward and downward flexibility. However, in some cases it does not considerably affect the amount of flexibility. As can be seen in this table, the higher amount of offered flexibility is provided by case 1, 2 and 5, with high DBU and pairs of control parameters, i.e. $(\widetilde{SOC}_t^{min} \widetilde{SOC}_t^{max})$, which are equal to (0.2 0.8), (0.3 0.8) and (0.2 0.7). In terms of offering higher flexibility, the second-ranked cases are 3, 9, and 13 with control parameters (0.4 0.8), (0.2 0.6), and (0.2 0.5). In comparison, the rest of the cases provide the minimum amount of flexibility. Based on this information, the lower values of $S\widetilde{O}C_t^{min}$ often leads to a higher amount of flexibility. For instance, the cases with $S\widetilde{O}C_t^{min} = 0.2$ ranked first and second in terms of the values of flexibility offers. Since the community's production surplus is negative in the early hours of the next day, discharging the BESS can provide upward flexibility during these time slots. As a result, the lower values of $S\widetilde{O}C_t^{min}$ enables the LEC to provide more upward flexibility through BESS discharging. In comparison, higher values of $S\widetilde{O}C_t^{max}$ do not necessarily lead to a higher amount of flexibility. Case 4 is an example with a high value of $S\widetilde{O}C_t^{max}$ while having the lowest values for the total flexibility offer.

Fig. 5 shows that the LEC is able to provide upward flexibility during 09:00–14:00, even in the cases with low DBU (i.e. G3). Considering Fig. 4, the production surplus is positive during 09:00–14:00, which enables the LEC to provide upward flexibility even without the help of the BESS. As Fig. 5 shows, for G1, the LEC can offer upward flexibility in most of time slots. In addition, the only difference between G2 and G3 is that G2 is able to offer additional flexibility during hour 05:00 by utilizing the BESS.

Fig. 6 demonstrates that the LEC of G1, G2 and G3 is able to provide downward flexibility during time slots when EVs (see TABLE 1) are being charged in all of the considered cases. As mentioned before, the only resources for the provision of downward flexibility are regarded to be EVs and the BESS. Since in G3 the LEC utilizes less than 50% of its BESS's capacity, the downward flexibility of this case is mostly provided by charging the EVs. However, G1, which deploys greater BESS capacity, is able to offer downward flexibility in most of the time slots. Although the downward flexibility offered by G2 is approximately similar to the amount offered by G3, the community of G2 utilized its BESS at 07:00 to provide more downward flexibility. Note that EVs are plugged in after 08:00, meaning that the downward flexibility offered at 07:00 was provided solely from the BESS.

### 2) REAL-TIME SCHEDULING

In real-time, the BSP specifies the amount of flexibility that should be provided by the LEC. In order to obtain the assigned amount of flexibility, we extracted information on the type of flexibility activation during the specific day (i.e. July 7, 2019) from the Finnish TSO's open data [8]. Subsequently, based on these data, the BSP accepts either the upward or the downward flexibility. In a few time slots there exist no need for mFRR deployment, which implies that no flexibility offers are accepted. Note that it is assumed that the total amount of offered flexible capacity by the LEC, which are compliant with the flexibility needs, were fully accepted and assigned by the BSP.

Fig. 7 and Fig. 8 illustrate the respective assigned and activated values of upward flexibility required to be provided by the LEC. Fig. 9 and Fig. 10 depict the respective assigned and activated values of downward flexibility required to be provided by the community. The activated amount of

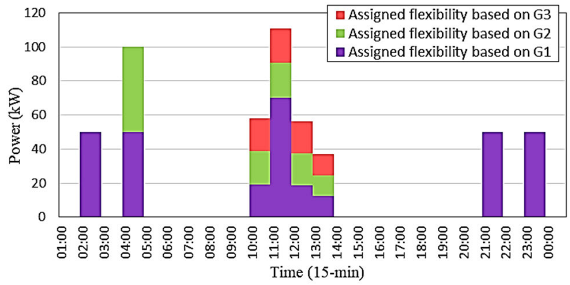


**FIGURE 7.** Assigned upward flexibility for different cases.

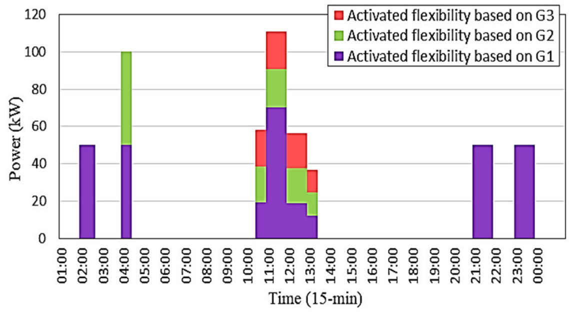


**FIGURE 8.** Activated upward flexibility for different cases.

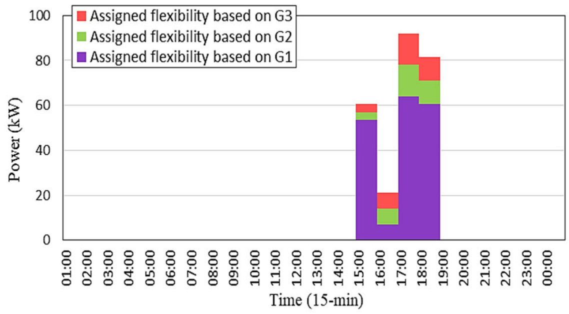


**FIGURE 9.** Assigned downward flexibility for different cases.

flexibility is also deployed based on the data of activated balancing power obtained for July 7, 2019 [8], and depicted in Fig. 7 to Fig. 10. The amount of assigned and activated flexibility is calculated for the three groups considered in the previous section, G1, G2 and G3.

The flexibility prices for provision of upward and downward balancing services are considered to be known in real-time and are presented in Fig. 11 [8]. These prices are extracted from the information on the prices of balancing energy markets on July 7, 2019, which are determined by the Finnish TSO, Fingrid. Moreover, the dynamic prices of trading energy with the grid is also shown in Fig. 11, based on one of the Finnish DSOs' open data [39]. As can be seen in the figure, the price of selling upward flexibility are always

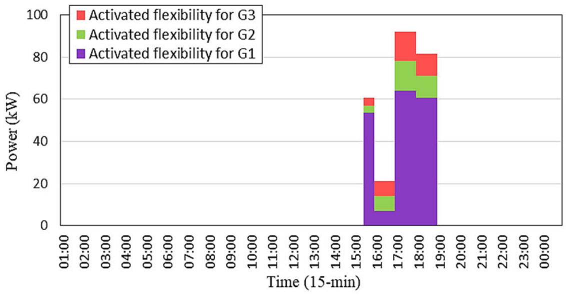


**FIGURE 10.** Activated downward flexibility for different cases.

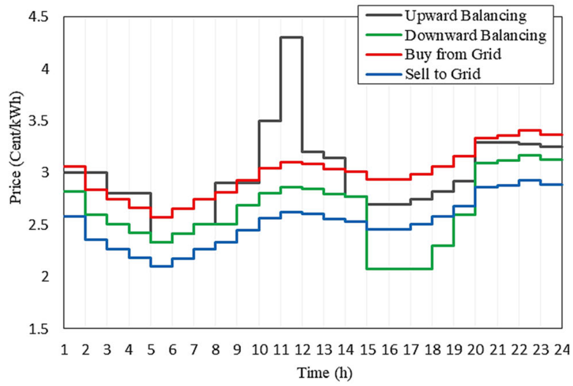


**FIGURE 11.** Prices for trading energy and flexibility, July 7, 2019 [8].

equal to or greater than the price of selling power to the grid. Additionally, the price of buying downward flexibility is always equal to or lower than the price of buying power from the grid.

The optimization problem introduced through (20)–(35) has been solved for the proposed LEC. A linearization technique (see APPENDIX) is exploited to handle the non-linearity caused by (25) and (26), with the purpose of obtaining a mixed-integer linear programming (MILP) formulation. The input data on the SOC of the EVs and the BESS were considered to be updated based on the actual activated reserve, and the results of 24 hours are obtained. Fig. 12 illustrates the hourly real-time profits of the community for one day, considering four different cases. These cases consist of three groups introduced in the previous section (i.e. G1, G2 and G3), which consider the LEC adopting different BESS control parameters in its day-ahead schedule, along with a case that suggests the LEC's operation with no contribution to reserve provision (i.e. the LEC trades only with the upstream grid and does not tend to participate in reserve provision). Fig. 13 denotes the total net-costs of the LEC on the considered day. The share of daily income and costs stemming from different resources are also illustrated in Fig. 14.

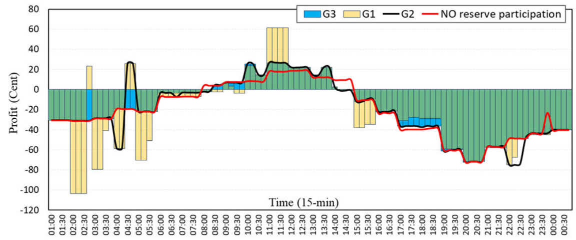


**FIGURE 12.** Hourly profits of the LEC for different cases.

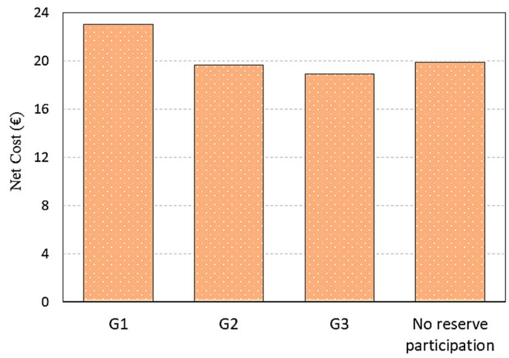


**FIGURE 13.** Total daily net-cost of the LEC considering different cases.

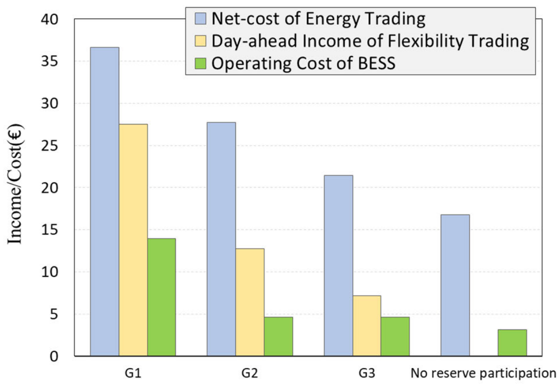


**FIGURE 14.** The LEC's monetary turnover in a single day considering different cases.

By comparing Fig. 12 with Fig. 4, it can be concluded that the profit of the LEC leads to positive values in time slots when the LEC has production surplus. However, in the rest of the time slots, the profits mostly exhibit negative values, meaning that the community is required to purchase power either from the upstream grid or by providing downward flexibility services in order to meet its demand. After solving the optimization problem for different cases, it was concluded that the LEC of G1 and G2 was not able to provide the assigned reserve during some time slots. Consequently, in these cases, the LEC is assumed to buy energy from the upstream network (through the DSO or retailer) so as to fulfil its assigned flexibility. Hence, in a few hours of the day, the profit curves related to G1 and G2 experience a considerable decrease. By comparing G1 with G3, it could be realized that G1's curve fluctuates more than G3's. Although in a limited number of hours G1's curve experiences higher profits (e.g. during time slots 02:45 and 11:15 to 11:45), it incurs more costs early in the morning (e.g. during time slots 02:00–02:15, 03:15, 05:15 and 15:00–15:45).

Fig. 13 indicates the correlation between the day-ahead selection of control parameters and the real-time net-cost of the LEC. It shows that the total net-cost of G1 is higher than that of G3 for the studied day. The same situation with a lower degree happens for G2, resulting in a higher total net-cost compared to G3 (see Fig. 13). In comparison, the case in which the LEC does not participate in reserve provision leads to the total cost which stands in the second rank, compared to the three studied cases. This means that the total net-cost of the case in which the LEC decides not to participate in reserve provision is higher than the net-costs of G3 and G2, but lower than that of G1. By comparing cases with different control parameters, i.e. G1, G2 and G3, it can be concluded that it is more profitable when the LEC deploys less BESS capacity in its day-ahead flexibility offer. In other words, according to fig. 13, the LEC made more profits when it chose a high value for $\widetilde{SOC}_t^{min}$ and a low value for $\widetilde{SOC}_t^{max}$.

Fig. 14 illustrates the sources of costs and incomes of the LEC, taking into account different cases. According to the community's day-ahead schedule, the income obtained from trading TSO-level flexibility is greater for G1, followed by G2 and G3 respectively, in terms of obtaining reserve-related income. The LEC is not able to benefit from flexibility provision if it does not claim its flexibility capacity in day-ahead, as stated in the bar chart of this case in Fig. 14.

However, the costs of real-time energy trading for G1 and G2 increase, as they need to compensate for hours during which they were not able to provide the assigned flexibility. In addition, in these cases the LEC sold a considerable amount of its production capacities through their day-ahead schedules in order to provide TSO-level flexibility. As a consequence, the community is not able to sell this part of their capacity to the upstream network, which leads to a decline in energy-trading income. Moreover, Fig. 14 implies that the higher participation of the LEC in reserve provision leads to more utilization of BESS capacity in real-time. Therefore, the operating costs of the BESS increase if the LEC provides more flexible capacity.

Fig. 15 visualizes the power sold/purchased to/from the upstream network. Positive values are related to the input power while negative values show the output power exported from the community. It expresses that the LEC of G1, G2 and G3 sells a negligible amount of its capacity to its upstream network, whereas in the case with no reserve provision, the community is able to sell all of its production surplus to the upstream grid. This is due to the fact that in G1, G2 and G3, the LEC sold most of its production capacities for reserve provision. When it comes to the amount of energy imported to the community, a short-term fluctuation for the LEC of G1 can be seen, owing to fulfilling its assigned upward flexibility offers. These fluctuations occur in few time slots during the early morning as well as from 21:00 to 23:00. Similar fluctuations could be seen for the LEC of G2 in some quarters during 22:00.

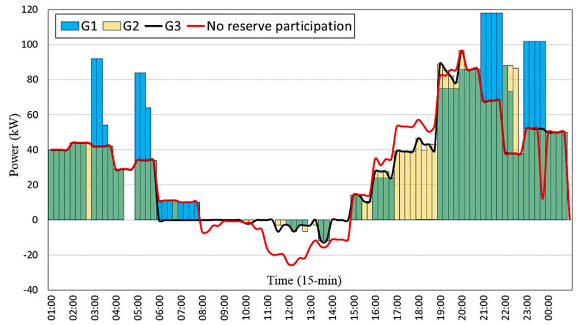


**FIGURE 15.** The power traded between the LEC and the upstream grid.

The SOC variation of the BESS for different cases is illustrated in Fig. 16. This figure explains that the participation of the BESS in reserve provision leads to greater utilization of the BESS. Comparing the SOC of the BESS for the LEC of G1 and G2 with that of G3 points out that the higher participation in reserve provision results in more variation in the SOC and thus more deployment of BESS capacity. In other words, the LEC of G1utilized a higher amount of its BESS capacities and therefore experienced more fluctuations in terms of its BESS' SOC. In comparison, these fluctuations decrease for the LEC of G2 and G3. In this manner, the case with no reserve participation deploys the BESS's capacity only from 22:00 to 24:00. In the "No reserve participation" case, the LEC does not take advantage of the charging capacity of the BESS at all. Note that the minimum allowed values of the BESS's SOC and of its initial SOC were assumed to be 0.2 and 0.5, respectively. Moreover, Fig. 16 shows that the LEC utilizes the discharging capacity more frequently than the charging capacity.

Finally, the number of EVs being charged in different time slots is illustrated in Fig. 17, considering the studied cases. The daily number of charging quarters for all of the EVs in the considered day (i.e. $\sum_i \sum_t \sum_m u_{i,t,m}^{EV}$) is shown in TABLE 5. This table explains how much the LEC utilized the charging capacity of EVs. The results discuss the fact that the number of charging EVs is greater in the case when the LEC does not tend to provide reserve, and it decreases for the other cases. The total number of charging EVs reaches its minimum value for G1, since it had to provide higher upward flexibility in most of the time slots, which leads to less utilization of charging EVs' (i.e. downward flexible capacity). In this manner, LECs of G2 and G3 place in the middle rank in terms of charging their EVs.

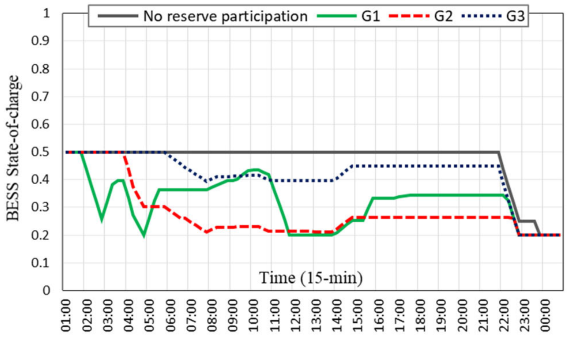


**FIGURE 16.** SOC variation of the BESS considering different cases.

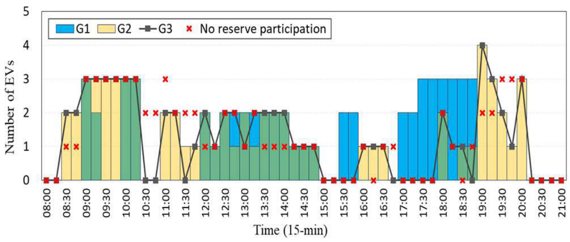


**FIGURE 17.** The hourly number of EVs being charged during the studied day considering different cases.

**TABLE 5.** The daily total number of charging quarters for all EVs considering different cases.

| Case Study | Daily number of charging quarters |
|---|---|
| G1 | 57 |
| G2 | 66 |
| G3 | 66 |
| No reserve participation | 68 |

## V. CONCLUSION AND FUTURE WORKS

This article deals with the optimal scheduling of an LEC participating in the provision of mFRR services. The LEC is considered to have shared assets, enabling it to contribute to the reserve provision. The scheduling comprises two stages. In the first stage, the ECMC seeks to determine the offered flexibility which should be submitted to the BSP in the day-ahead stage. In this stage, control parameters are deployed so as to manage the degree of the BESS utilization for offering the flexible capacity. In the second stage, the ECMC aims to maximize the community's real-time profit for each hour. The real-time stage also takes into account the assigned flexibility that should be provided in the following four quarters and the activated flexibility during the previous hour.

The proposed scheduling method was applied to a case study, comprised of a hypothetical LEC with a PV system, a BESS, EVs and several households as residential consumers. The paper utilized the structure of Finnish balancing energy and capacity markets related to mFRR procurement for the simulation. Hence, the data regarding reserve market prices, dynamic tariffs and solar power were fully extracted from the related Finnish utilities (Finnish TSO and DSO) and markets. The results demonstrate that the control parameters chosen in the day-ahead schedule can strongly affect the real-time profitability of the LEC. It was also concluded that the cases in which the LEC utilized a low capacity of the BESS in its day-ahead schedule were more profitable compared to those cases in which the BESS capacity was highly utilized. Moreover, the cases which deploy lower capacity of the BESS were more profitable in comparison with the cases where the LEC did not participate in mFRR provision. According to the simulation results, which were based on input data extracted from the real-world reserve markets, the participation in mFRR provision can be profitable for the LEC as a distribution-network-located energy resource. Hence, participating in providing mFRR ancillary services not only helps the TSO, but also increases profits for the LEC. However, the careful utilization of the BESS in estimating the LEC's day-ahead available flexibility is vitally important in real-time profitability and the LEC's optimal real-time operation. Finally, this article could be expanded in the future by analyzing the following directions:

a) LECs providing other types of flexibility services such as FCR-N or FCR-D to the TSO.
b) The provision of flexibility from LECs in the most recently introduced FFR market could also be considered as another important study.
c) Different kinds of FERs in energy communities such as thermostatically controllable loads and thermal storages could be analyzed for flexibility provision.
d) The TSO's responsibilities related to calculating flexibility needs and clearing each flexibility market (FFR, FCR, FRRs) according to the calculated requirements.

## APPENDIX

As mentioned in the simulation section, we utilized the same approach as [37] to linearize (10), (11), (25) and (26). All of these constraints are in the form of the following equation.

$$A = \begin{cases} B, & \text{if } B > 0 \\ 0, & \text{else} \end{cases} \tag{37}$$

In (37), $A$ and $B$ are two variables. In this case, an auxiliary binary variable $V$ is adopted and constraint (37) will be replaced with the following constraints:

$$A \leq VM \tag{38}$$

$$A \leq B + M(1 - V) \tag{39}$$

$$A \geq B - M(1 - V) \tag{40}$$

$$A \geq 0 \tag{41}$$

where $M$ is a large number, which was chosen to be 10000 in our problem. In this manner, if $B$ becomes negative, $V$ and $A$ equal 0. Otherwise, $V$ is equal to 1 and $A$ is equal to $B$, accordingly.

## REFERENCES


[1] B. Mohandes, M. S. E. Moursi, N. Hatziargyriou, and S. El Khatib, "A review of power system flexibility with high penetration of renewables," *IEEE Trans. Power Syst.*, vol. 34, no. 4, pp. 3140–3155, Jul. 2019.

[2] M. Džamarija, G. Leclercq, M. Marroquin, and M. Herman, "Modeling of complex systems including transmission, distribution, aggregation, ancillary services markets," in *TSO-DSO Interactions and Ancillary Services in Electricity Transmission and Distribution Networks*, G. Migliavacca, Ed. Springer, 2020, pp. 25–59. [Online]. Available: https://www.springer.com/gp/book/9783030292027

[3] M. Khoshjahan, M. Moeini-Aghtaie, and M. Fotuhi-Firuzabad, "Developing new participation model of thermal generating units in flexible ramping market," *IET Gener., Transmiss. Distrib.*, vol. 13, no. 11, pp. 2290–2298, Jun. 2019.

[4] H. Gerard, E. Rivero, and J. Vanschoenwinkel, "TSO-DSO interaction and acquisition of ancillary services from distribution," in *TSO-DSO Interactions and Ancillary Services in Electricity Transmission and Distribution Networks*, G. Migliavacca, Ed. Springer, 2020, pp. 7–23. [Online]. Available: https://www.springer.com/gp/book/9783030292027

[5] H. Khajeh, H. Laaksonen, A. S. Gazafroudi, and M. Shafie-Khah, "Towards flexibility trading at TSO-DSO-customer levels: A review," *Energies*, vol. 13, no. 1, p. 165, Dec. 2019.

[6] G. De Zotti, S. A. Pourmousavi, H. Madsen, and N. K. Poulsen, "Ancillary services 4.0: A top-to-bottom control-based approach for solving ancillary services problems in smart grids," *IEEE Access*, vol. 6, pp. 11694–11706, 2018.

[7] P. Spodniak, K. Ollikka, and S. Honkapuro, "The relevance of wholesale electricity market places: The Nordic case," ESRI, Dublin, Republic of Ireland, Tech. Rep. 631, 2019.

[8] F. Oyj, "Fingrid open data," Tech. Rep. [Online]. Available: https://data.fingrid.fi/en/

[9] B. Xu, Y. Shi, D. S. Kirschen, and B. Zhang, "Optimal battery participation in frequency regulation markets," *IEEE Trans. Power Syst.*, vol. 33, no. 6, pp. 6715–6725, Nov. 2018.

[10] R. H. Byrne, T. A. Nguyen, D. A. Copp, B. R. Chalamala, and I. Gyuk, "Energy management and optimization methods for grid energy storage systems," *IEEE Access*, vol. 6, pp. 13231–13260, 2018.

[11] M. Merten, C. Olk, I. Schoeneberger, and D. U. Sauer, "Bidding strategy for battery storage systems in the secondary control reserve market," *Appl. Energy*, vol. 268, Jun. 2020, Art. no. 114951.

[12] E. Nasrolahpour, J. Kazempour, H. Zareipour, and W. D. Rosehart, "A bilevel model for participation of a storage system in energy and reserve markets," *IEEE Trans. Sustain. Energy*, vol. 9, no. 2, pp. 582–598, Apr. 2018.

[13] H. Alharbi and K. Bhattacharya, "Participation of pumped hydro storage in energy and performance-based regulation markets," *IEEE Trans. Power Syst.*, early access, May 29, 2020, doi: 10.1109/TPWRS.2020.2998490.

[14] B. Han, S. Lu, F. Xue, and L. Jiang, "Day-ahead electric vehicle aggregator bidding strategy using stochastic programming in an uncertain reserve market," *IET Gener., Transmiss. Distrib.*, vol. 13, no. 12, pp. 2517–2525, Jun. 2019.

[15] R. J. Bessa and M. A. Matos, "Optimization models for an EV aggregator selling secondary reserve in the electricity market," *Electr. Power Syst. Res.*, vol. 106, pp. 36–50, Jan. 2014.

[16] P. González, J. Villar, C. A. Díaz, and F. A. Campos, "Joint energy and reserve markets: Current implementations and modeling trends," *Electr. Power Syst. Res.*, vol. 109, pp. 101–111, Apr. 2014.

[17] Q. Wang, C. Zhang, Y. Ding, G. Xydis, J. Wang, and J. Østergaard, "Review of real-time electricity markets for integrating distributed energy resources and demand response," *Appl. Energy*, vol. 138, pp. 695–706, Jan. 2015.

[18] P. H. Divshali and C. Evens, "Stochastic bidding strategy for electrical vehicle charging stations to participate in frequency containment reserves markets," *IET Gener., Transmiss. Distrib.*, vol. 14, no. 13, pp. 2566–2572, Jul. 2020.

[19] J. Iria, F. Soares, and M. Matos, "Optimal bidding strategy for an aggregator of prosumers in energy and secondary reserve markets," *Appl. Energy*, vol. 238, pp. 1361–1372, Mar. 2019.

[20] S. R. Dabbagh and M. K. Sheikh-El-Eslami, "Risk assessment of virtual power plants offering in energy and reserve markets," *IEEE Trans. Power Syst.*, vol. 31, no. 5, pp. 3572–3582, Sep. 2016.

[21] H. Nezamabadi and M. Setayesh Nazar, "Arbitrage strategy of virtual power plants in energy, spinning reserve and reactive power markets," *IET Gener., Transmiss. Distrib.*, vol. 10, no. 3, pp. 750–763, Feb. 2016.

[22] E. Mashhour and S. M. Moghaddas-Tafreshi, "Bidding strategy of virtual power plant for participating in energy and spinning reserve Markets—Part I: Problem formulation," *IEEE Trans. Power Syst.*, vol. 26, no. 2, pp. 949–956, May 2011.

[23] M. Mohammadnejad, A. Abdollahi, and M. Rashidinejad, "Possibilistic-probabilistic self-scheduling of PEVAggregator for participation in spinning reserve market considering uncertain DRPs," *Energy*, vol. 196, Apr. 2020, Art. no. 117108.

[24] C. Giovanelli, O. Kilkki, S. Sierla, I. Seilonen, and V. Vyatkin, "Task allocation algorithm for energy resources providing frequency containment reserves," *IEEE Trans. Ind. Informat.*, vol. 15, no. 2, pp. 677–688, Feb. 2019.

[25] T. K. Chau, S. S. Yu, T. Fernando, and H. H.-C. Iu, "Demand-side regulation provision from industrial loads integrated with solar PV panels and energy storage system for ancillary services," *IEEE Trans. Ind. Informat.*, vol. 14, no. 11, pp. 5038–5049, Nov. 2018.

[26] J. Wang, H. Zhong, W. Tang, R. Rajagopal, Q. Xia, C. Kang, and Y. Wang, "Optimal bidding strategy for microgrids in joint energy and ancillary service markets considering flexible ramping products," *Appl. Energy*, vol. 205, pp. 294–303, Nov. 2017.

[27] S. Lilla, C. Orozco, A. Borghetti, F. Napolitano, and F. Tossani, "Day-ahead scheduling of a local energy community: An alternating direction method of multipliers approach," *IEEE Trans. Power Syst.*, vol. 35, no. 2, pp. 1132–1142, Mar. 2020.

[28] P. J. M. Van Aubel, M. Colesky, J.-H. Hoepman, E. Poll, and C. M. Portela, "Privacy by design for local energy communities," in *Proc. CIRED Workshop Microgrids Local Energy Communities*, Ljubljana, Slovenia, Jun. 2018, pp. 1–4. [Online]. Available: https://www.semanticscholar.org/paper/PRIVACY-BY-DESIGN-FOR-LOCAL-ENERGY-COMMUNITIES-Aubel-Colesky/96a1dcadea80ab4d5613afa0f9314fe7054bc64e

[29] A. R. Servent, *The European Parliament*. Bamberg, Germany: Macmillan International Higher Education, 2017.

[30] N. V. Bommel, "Energy communities: An exploration into their rhetoric framings within the European Policy Context," Eindhoven Univ. Technol., Eindhoven, The Netherlands, 2019.

[31] F. Oyj, "Terms and conditions for providers of manual frequency restoration reserves (mFRR)," Tech. Rep., 2020.

[32] *Nordpool Market Data*, Nord Pool, Oslo, Norway. [Online]. Available: https://www.nordpoolgroup.com/Market-data1/#/nordic/table

[33] Z. Zhang, R. Li, and F. Li, "A novel Peer-to-Peer local electricity market for joint trading of energy and uncertainty," *IEEE Trans. Smart Grid*, vol. 11, no. 2, pp. 1205–1215, Mar. 2020.

[34] M. Hemmati, B. Mohammadi-Ivatloo, M. Abapour, and A. Anvari-Moghaddam, "Optimal chance-constrained scheduling of reconfigurable microgrids considering islanding operation constraints," *IEEE Syst. J.*, early access, Jan. 29, 2020, doi: 10.1109/JSYST.2020.2964637.

[35] T. A. Nguyen and M. L. Crow, "Stochastic optimization of renewable-based microgrid operation incorporating battery operating cost," *IEEE Trans. Power Syst.*, vol. 31, no. 3, pp. 2289–2296, May 2016.

[36] H. Khajeh, A. A. Foroud, and H. Firoozi, "Robust bidding strategies and scheduling of a price-maker microgrid aggregator participating in a pool-based electricity market," *IET Gener., Transmiss. Distrib.*, vol. 13, no. 4, pp. 468–477, Feb. 2019.

[37] *How Inexpensive Must Energy Storage Be for Utilities to Switch to 100 Percent Renewables?* IEEE Spectrum, Piscataway, NJ, USA, Sep. 2019.

[38] M. Shabanzadeh, M.-K. Sheikh-El-Eslami, and M.-R. Haghifam, "Risk-based medium-term trading strategy for a virtual power plant with first-order stochastic dominance constraints," *IET Gener., Transmiss. Distrib.*, vol. 11, no. 2, pp. 520–529, Jan. 2017.

[39] V. Sahko, "Prices for electricity products," Tech. Rep. [Online]. Available: https://www.vaasansahko.fi/en/prices-for-electricity-products-2/


**HOOMAN FIROOZI** received the M.Sc.(Tech.) degree in electrical engineering (power systems) from the Ferdowsi University of Mashhad, Mashhad, Iran, in 2016. He is currently working as a Project Researcher at the University of Vaasa, Vaasa, Finland. His research interests include the application of optimization techniques (classic and metaheuristic) in the operation and planning of smart energy systems, distributed and flexible energy resources integration, balancing services and flexibility markets, energy communities, and microgrids.

**HOSNA KHAJEH** (Graduate Student Member, IEEE) received the M.Sc.(Tech.) degree in electrical engineering (power systems) from Semnan University, Semnan, Iran, in 2016. She is currently pursuing the Ph.D. degree with the University of Vaasa, Vaasa, Finland. She is working as a Project Researcher at the University of Vaasa. Her research interests include future electricity market concepts (such as flexibility markets and local peer-to-peer markets), smart grid and microgrid scheduling, and renewable energy integration.

**HANNU LAAKSONEN** (Member, IEEE) received the M.Sc.(Tech.) degree in electrical power engineering from the Tampere University of Technology, Tampere, Finland, in 2004, and the Ph.D.(Tech.) degree in electrical engineering from the University of Vaasa, Vaasa, Finland, in 2011. His employment experience includes working as a Research Scientist at VTT Technical Research Centre of Finland and the University of Vaasa. He has previously worked as a Principal Engineer at ABB Ltd., Vaasa. He is currently a Professor of Electrical Engineering with the University of Vaasa. He is also the Manager of the Smart Energy Master's Program. His research interests include the protection of low-inertia power systems (including microgrids), active management of distributed and flexible energy resources in future smart energy systems and future-proof technology, and market concepts for smart grids.

# Flexibility of Microgrids with Energy Management Systems

Hooman Firoozi[1,*], Hosna Khajeh[2] and Hannu Laaksonen[3]

Flexible Energy Resource, School of Technology and Innovations, University of Vaasa, 65200 Vaasa, Finland

[1]hooman.firoozi@uwasa.fi , [2]hosna.khajeh@uwasa.fi , [3]hannu.laaksonen@uwasa.fi ,

[*]Corresponding author: Hooman Firoozi (hooman.firoozi@uwasa.fi)

**Keywords:** *flexibility, flexible energy resources, microgrid energy management systems, microgrids, scheduling, renewable energy resources*

## 1 INTRODUCTION

In recent years, approaches towards energy transition and sustainable development have been ever-increasing due to the need for mitigating climate change issues and the efficient utilization of existed energy resources. With this regard, state-of-the-art technologies and infrastructures along with active operation and control of different energy resources would become crucial. Amongst all energy resources, microgrids (MGs) are believed to be one of the highly potent resources to deal with the issues of electrical systems. In other words, active operation and control of MGs in which there exist different kinds of demands and energy resources (e.g. energy storages, micro-generation units, etc.) would be beneficial not only for MG stakeholders in terms of cost-benefit efficiency but also for power system operators in terms of MGs' contribution to grid's flexibility.

In order to unlock the active utilization of MGs, cutting-edge technologies along with efficient infrastructure are a necessity. These technologies together in communication with the MGs' energy resources are known as energy management system (EMS). EMSs are intelligent automated systems that contribute to, for instance, lowering/shifting energy consumption in critical moments along with a reduction in the MGs' costs. Although the utilization of EMS might consider other objectives such as $CO_2$ emission reduction or self-sufficiency, they mostly employ optimization techniques either as single-objective or multi-objective approaches. EMSs can also enable either the bidirectional energy exchange with the network in grid-connected mode, or stand-alone operation of MGs in islanded-mode.

In this chapter, the focus of the study is on the MGs equipped with EMS. There have been introduced several approaches to the energy management of MGs. However, in most of them, economic aspects, i.e. cost reduction, are the top priority desire of the problem from the MG stakeholders' point of view. This could be done in different ways. On the one hand, reducing the total costs of the MGs by maximum utilization of self-production facilities (PV panels, wind turbines, etc.) as well as changing the energy consumption over time from peak hours to off-peak hours during the day. On the other hand, exploiting MGs' flexibility so as to help the upstream grid in critical moments for monetary profits in return. Accordingly, the authors first present an introduction to flexible energy resources (FERs) in MG along with their characteristics in Section 2. Afterward, the MGEM modeling approaches are widely presented in Section 3. In this section, first, the different kind of management method deployed in the MGs are illustrated. Then, various objectives for energy management in MGs will be introduced. Regarding this section, we introduce a number of approaches based on well-known optimization algorithms considering different MG-related as well as grid-related constraints. Microgrids' constraints are related to the physics and limitations of the MG's resources whilst the constraints of the grid are related to the limitation of energy exchange with the upstream grid (e.g. congestion management, emission reduction and/or energy loss reduction). Moreover, the application of the MGEM system in MGs with FERs such as energy storages, electric vehicles (EVs), and thermostatically controllable loads (TCLs) which exchange energy and flexibility with the grid will be discussed as well which is followed by the flexibility services that MGs could provide to the different levels of power system. Finally, the chapter will be summarized and concluded in Section 4.

## 2 FLEXIBLE ENERGY RESOURCES IN MICROGRID

There could be various types of energy sources in MGs. They might be supplied by either fossil fuels or renewable sources such as wind, solar, etc. [1]. Fig. 1 depicts the most common energy resources in MGs. In general, any energy resource that is located in the MG's demand-/generation-side, and enables the MG's reacting to the needs, could be defined as flexible energy resources. However, based on the amount of flexibility, these energy resources could be divided into two main categories namely high-flexible energy resources and low-flexible energy resources.

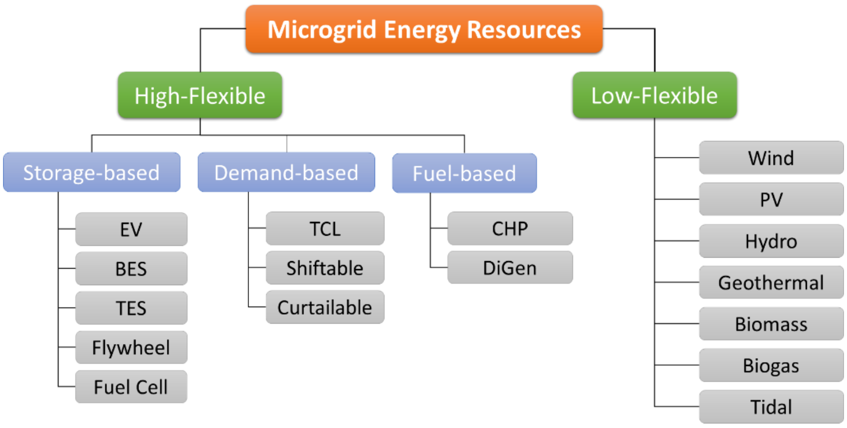


Fig. 1. An overview of microgrids' energy resources

The low-flexible energy resources in the MG consist of renewable generation units which their output power is not fully controllable. This originates from the fact that renewable energy sources such as wind, solar radiation, etc. depending on meteorological conditions. In certain situations, the only way to take action for low-flexible energy resources is to curtail their generation from MG's generation side. Therefore, in MGEM systems, they could be entitled to low-flexible energy resources.

On the contrary, there might be some flexible energy resources in MGs which could help to increase the flexibility of the MG. These types of energy sources could be entitled to high-flexible energy resources. The high-flexible resources could be utilized either in demand-side or generation-side of the MG. In other words, they might be among the consumers' assets, consumers' load, or as a part of a bulk PV system. Having employed the high-flexible energy resources in MGs, the MGEM system could take advantage of them to enhance the flexibility of MG by the active utilization of these resources. Therefore, the focus of this section is on the high-flexible energy resources in MGs. In the following subsections, the explanation about the characteristics of the high-flexible energy resources in MGs is presented.

## 2.1 Storage-based Flexible Resources

The storage-based FERs refers to the devices that could store the energy in different shapes (i.e. electrical, thermal, mechanical, etc.) in order to utilize it when there is a shortage or in critical moments. Energy storages could help the MGs to enhance their flexibility by injecting the power back to the MG, especially in islanding situations. Storage-based energy resources could be mostly categorized as electric vehicles, battery energy storages, thermal energy storages, flywheels, fuel cells, etc. In the following subsections, the most common storage-based flexible resources are illustrated.

### 2.1.1 Electric Vehicle (EV)

Electric vehicles as one of the ever-increasing types of flexible energy resources in future smart grids are believed to be among the potential solutions to systems' flexibility. These FERs are adjustable, shiftable, and fast-response which could considerably enhance the MG's flexibility in flexibility services provision. Moreover, EVs could be charged when the prices are at the lowest level meaning that they could be contributing to the cost-reduction target at all system levels. Although the EVs act as the load consumption when they are in charging mode, the recent version of EVs with new charging facilities makes the EVs capable of injecting power back to the grid (i.e. vehicle-to-grid mode) when it is needed. The equations related to the EV's operation are defined as follows. Eq. (1) presents the energy stored in the EV's battery at time *t*:

$$E_t = E_{t-1} + \begin{cases} \eta^{ch} P_t^{ch} \Delta t & \text{charging} \\ \dfrac{P_t^{dis}}{\eta^{dis}} \Delta t & \text{discharging} \\ 0 & \text{unplugged} \end{cases} \qquad (1)$$

Where $\eta^{ch}/\eta^{dis}$ are the charging/discharging efficiency and $P_t^{ch}/P_t^{dis}$ are the power of charging/discharging, respectively. $\Delta t$ is the duration time at which the EV is being charge or discharge. According to this equation, the energy of EV's battery depends on its current level of energy as well as its current mode of charging. The EVs' battery are mostly chosen from Li-Ion technology batteries since they are highly efficient compared to the other types of batteries. However, the capital cost of these batteries is nowadays high. Therefore, it is recommended to restrict the lower and upper levels of the battery's stored energy in MGEM systems. This restriction could be considered as a constraint in MGEM problems as in (2) which helps to reduce the number of charging or discharging cycles over a time span.

$$E^{min} \le E_t \le E^{max} \qquad (2)$$

$$0 \le P_t^{ch}, P_t^{dis} \le P^{max} \qquad (3)$$

Another constraint related to the EVs' battery could be found in (3). This one similarly helps to limit the charging/discharging power of the battery to avoid the battery from early depreciation. Note that, in order to take advantage of flexibility provision by EVs, the EVs, as well as the charging facilities, must have the capability of working in the vehicle-to-grid mode.

### 2.1.2 Battery Energy Storage (BES)

Battery energy storages are one of the best solutions for future smart grids. They could be centrally controlled, they have very rapid response, and also they could be useful in remote local energy systems, islanded MGs, or in power shortage situations. Moreover, they could effectively help the grid in terms of stability, resiliency, and flexibility. BESs could be found in different sizes, from domestic level to MG level or even grid levels. There have been introduced several materials used in manufacturing BESs such as Li-Ion, Vanadium Redox Flow, etc. The equations related to BES are similar to those mentioned in the previous subsection. However, all the BESs support the bidirectional power flow since they are meant to be discharged when it is needed.

#### 2.1.3 Thermal Energy Storage (TES)

Thermal energy storages are used to store the thermal energy and utilized it when it is required. These storages could be beneficial in MGEM systems in order to store the heat in off-peak low-price times over night for using in high-price moments. The heat might be coming from combined heat and power (CHP) units, the waste heat from biomass/biogas units, or the exhausting heat from industrial units. They can be also beneficial not only for storing heat in summers but also for preserving the cold in the winters and reverting it to the MG's facilities in summers (i.e. seasonal TES). Thermal storages could be various in size and also in response time. Table I presents the typical types of thermal storages with their characteristics [2].

Table I. The typical types of thermal storages with their characteristics

| Technology | Capacity (kWh) | Power (kW) | Efficiency (%) | Cost (€/kWh) | Storage Time |
|---|---|---|---|---|---|
| Sensible | 10-50 | 1-10000 | 50-90 | 0.1-10 | days-month |
| Phase-change | 50-150 | 1-1000 | 75-90 | 10-50 | hours-month |
| Chemical | 120-250 | 10-1000 | 75-100 | 8-100 | hours-days |

#### 2.1.4 Flywheel

Flywheel is a mechanical energy storage which consists of a rotational part and other facilities for connecting to the system. In charging mode, flywheel is speeding up to its nominal rotational speed and store energy as kinetic type. Afterward, the stored kinetic energy is preserved in standby mode. When energy is required, the flywheel starts to discharge the stored energy back to the grid [3].

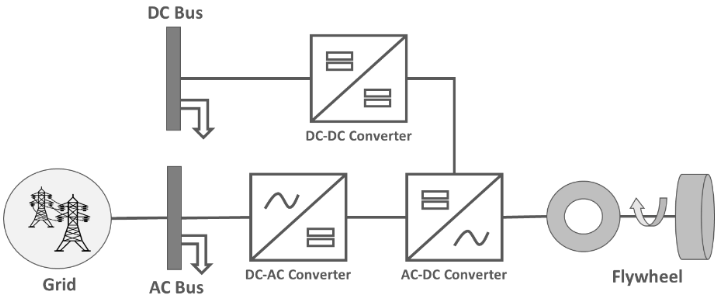


Fig. 2. Flywheel storage utilization in a hybrid grid-connected MG

Fig. 2, depicts a flywheel storage utilization in a hybrid grid-connected MG. In order to calculate the energy of a flywheel storage the following well-known formula is [3]:

$$E = \frac{1}{2} m r^2 \omega^2 \qquad (4)$$

In (4), $E$ is the kinetic energy stored in the flywheel and $m$, $r$ and $\omega$ are the mass of cylinder, radius and rotational speed, respectively.

#### 2.1.5 Fuel Cell (FC)

Fuel cell (FC) as another high-flexible energy resources could also be utilized in MG applications. FCs can produce electricity by converting the chemical energy originating from hydrogen-oxygen reactions into electrical energy. The capacity of FC could be different based on their applications from 100 kW to 100 MW [4]. In solid-oxide FC, for example, anode supplies hydrogen and catalytically split it into a number of protons and electrons. The electrons are then flowing towards the positive side (i.e. the cathode) by flowing through the external circuit. The oxygen then reacts with the protons and also the electrons flowing in the circuit, forming water formula [5]. Solid-oxide FC can operate in parallel with MG’s PV panels, meaning that it can be integrated with solar power as a hybrid PV system since they can store the produced energy for hours [4]. Therefore, in the night time, when PV panels cannot produce electricity, the FC could be employed to supply the demand. This could help the MG to have the flexibility to reduce the power exchange with the connected grid aiming at a generation cost reduction or provision of flexibility to the grid for monetary profits in return.

### 2.2 Demand-based Flexible Resources

The demand-based FERs refers to the devices that only consume energy. In residential MGs, for example, they might be found in the residential home appliances [6]. In other types of MGs, they might be in the shape of an industrial unit's demand or a commercial building's load. In general, all the devices in demand-side that their consumption power could be controlled, are considered as demand-based FER. Since a great number of demand-based FERs are widely being utilized in residential/commercial units, it would be beneficial for MGs to unlock the flexibility that could be emerged from these resources. Thereby, the demand-based FERs in the consumers' premises that are capable of controlling, changing, or shifting are at the center of attention for MGs' manager/operator. Note that, the demand response programs [7] could be a key factor for incentivizing small-scale consumers in MGs for flexibility provision. In the following subsections, some of these demand-based FERs that could enhance the flexibility of MG are presented.

### 2.2.1 Thermostatically Controllable Load (TCL)

Thermostatically controllable loads refer to the loads that their power consumption could be adjusted by sending command signals to their thermostat. These loads have a great portion of the total demand. In summers, the power consumption is used for cooling whilst in winters, the power consumption is utilized to heat the internal spaces of houses, offices, etc. For instance, electric water heaters (EWH), heating, cooling, air conditioning systems (HVAC), and refrigerators could be categorized in TCLs. These appliances are closely intertwined with the thermal comfortness and other consumers' preferences. Therefore, in MGEM systems, in addition to the operational constraints of appliances, the constraints regarding TCLs must also be considered. One of these constraints is thermal comfort of the users for HVACs and EWHs which could be found in (5)-(6):

$$\theta_i^{min} \leq \theta_{i,t} \leq \theta_i^{max} \quad (5)$$

$$\theta_i^{w,min} \leq \theta_{i,t}^{w} \leq \theta_i^{w,max} \quad (6)$$

Where $\theta_i^{min}$ and $\theta_i^{max}$ are the minimum and maximum desired temperature requested by user *i,* respectively. $\theta_i^{w,min}$ and $\theta_i^{w,max}$ are the minimum and maximum desired temperature of hot water requested by user *i,* respectively. Finally, $\theta_{i,t}$ and $\theta_{i,t}^{w}$ is the interior and hot water temperature of user *i*, respectively.

In order to unlock the flexibility from TCLs in an MG, they must be aggregated. Aggregating several TCLs in an MG could help to reduce or increase the power consumption in certain moments for the provision of upward or downward flexibility services to the connected upstream network. However, it is worth mentioning that the response time of some TCLs is a bit low. Therefore, they might not be suitable for all kinds of flexibility services but still beneficial for those services that have a slow activation time.

### 2.2.2 Shiftable Load

Shiftable loads are those that their consumption power cannot be controlled, however, the operating time could be shifted from high-price to low-price hours. These loads also need to work for a constant cycle and they could not be disconnected once they started which means shiftable loads must run a cycle completely. Therefore, the MGEM system can only schedule the related start time. Dishwasher, washing machine, and clothes dryer, as the devices which might be found mostly in residential households in the MG, could be grouped in shiftable loads' category [8]. A MG operator could take advantage of shiftable loads for energy scheduling during a day considering the consumers' comfortness constraints.

### 2.2.3 Curtailable Load

The power consumption of curtailable loads could be adjusted, usually without any significant effect on consumers' comfortness. These adjustments limit the energy consumption of devices by changing the settings thorough a command signal, without any consequences. As an example, lighting devices could be curtailed by a command during the day or as an automated function of natural daylight [8].

## 2.3 Fuel-based Flexible Resources

The fuel-based FERs are those that could be categorized in the generation side. Naturally, these FERs produce power by using fossil fuels as input energy sources. However, their output generating power could be regulated according to the system's needs. The output power generation of fuel-based FERs could be adjusted by changing the amount of intake fuel. Therefore, these FERs could contribute to increasing the MG's flexibility. Although these resources could not be categorized as a totally sustainable energy resource, their power production could be controlled in critical moments for flexibility provision targets. In the following subsections, a brief overview of the most important fuel-based FERs are provided.

### 2.3.1 Combined Heat and Power (CHP)

The most famous fuel-based flexible resource in MGs is combined heat and power (CHP) unit. A CHP unit is generally a power generation unit which combines the heat production with electricity generation. CHPs could be regarded as a decentralized distributed generator located at the MG level. This DG has the ability to produce heat and electricity simultaneously which could be beneficial in increasing the efficiency and flexibility of the MG. The exhausted heat from the power generation cycle in the CHP could be utilized to provide the required energy for the heating load as well as hot water within the MG internal network. In the MG level, the size of the CHPs depends on the size of the MG which could be found up to 20 MW. CHPs, however, could also be installed in customer-level applications with a maximum capacity of 15 kW [9]. Although the energy efficiency of the CHP unit can be assumed to be constant, the CHP unit's efficiency practically differs with dynamic operation due to the variation of output power. This could help the MGs to enhance their flexibility or providing flexibility services to the upstream grid. Note that, ramping constraints need to be considered in MGEM problems since the CHP unit requires some time to reach the steady-state condition after changing its set point [10].

### 2.3.2 Diesel Generator (DiGen)

Diesel generator as one of the fuel-based FERs could be beneficial in MGEM. This FER may be utilized when there is a power shortage in the MG. They could also be considered as flexibility sources when upward flexibility is needed from the upstream network. However, the sizing of the diesel generators in the MG is quite crucial since the ramping rate of the generator should be adequate for fulfilling the MG's/network's need. In fact, diesel generators play a quite important role when, for example in an islanded MG, the power generation is not enough and the energy storages are almost discharged. Therefore, these FERs are also called backup units in local energy systems. They could be different in size from 5 kW to 5 MW or more. The equation regarding fuel consumption of the diesel generator can be calculated from (7) that should be considered in MGEM optimization problems [11].

$$Cost = c_1 \times P^{DG} + c_2 \times P^n \tag{7}$$

In (7), $P^{DG}$ and $P^n$ is the produced power and the nominal power of the generator, respectively. $c_1$ and $c_2$ are the coefficients related to fuel consumption's curve which typically considered $c_1 = 0.246$ l/kW and $c_2 = 0.08145$ l/kW, respectively [12].

## 3 MODELLING THE MICROGRID ENERGY MANAGEMENT

Microgrid, as one of the potential solutions to the future smart grids, usually confronts the lack of power generation. This is due to the variability and intermittency both from generation and demand sides [13]. Energy management methods have been believed as one of the solutions to this issue. The most important target of energy management is to find the optimal operation point of different kinds of energy resources in order to supply the requested demand constantly and efficiently [14]. It should be mentioned that the main objective of these studies is reducing consumption costs whilst taking advantage of the MGs' flexible capacity for the provision of energy and flexibility services. However, there might be various approaches and tools towards this target. Before discussing the MGEM tools and techniques, the MG management methods are briefly illustrated in the next subsection.

### 3.1 Microgrid Energy Management Methods

The approaches toward the control and operation of MG resources as well as dispatchable loads are known as MG management methods. These management method could be deployed by having an agreement between the MG operator and the MG's members/stakeholders. The microgrid energy management (MGEM) could be defined in two perspectives [15]:

1) Decentralized energy management
2) Centralized energy management
3) Distributed energy management

In decentralized MGEM, the control and operation of FERs located at the MG have more degree of freedom. This means the FERs' adjustability in this management method helps more to meet the preferences of the stakeholders/consumers. In centralized MGEM, however, a central controller decides how the FERs and generation units should be operated. It has to be mentioned that in both centralized and decentralized management methods, the technical constraints of the MG must be taken into account. The most important constraint would be the balance between load and production within the MG [16].

Distributed MGEM as another management method in MGs is presented in the literature as well. This type of management method is mostly based on game-theoretic approaches. In distributed MGEM, game players, as the agents in the MG, seek the best management method for their own objectives taking into account the overall goal of the MG regarding energy management considerations [17].

Having mentioned the above approaches, the MGEM problems generally aim at scheduling the operation of generation units, storage systems, and even controllable loads in the MG [18]. These problems have been presented with various objectives. In the following section, some of these objectives with the related considerations are elaborated.

### 3.2 Microgrid Energy Management Objectives

#### 3.2.1 Cost Reduction / Profit Maximization

One of the most important objectives of energy management is reducing the total operation cost of MGs' components. This operational cost includes, for instance, the fuel cost, cost of purchasing energy from the grid, degradation cost of battery energy storages, etc. [19]. The cost reduction in an MGEM could be over different time spans from real-time to daily, monthly, or even yearly periods. However, energy management sometimes might be defined for real-time operation. In this case, the real-time operational cost of MG is the objective of the problem. Accordingly, the generation and demand as well as the scheduling of the FERs should be in a way that the overall cost of the MG tends to be minimized in real-time [20]. Accordingly, the MGEM system is in charge of scheduling the generation and flexible loads so that the total cost of energy purchasing from the grid as well as the operational costs of the DGs become minimized as in (8).

$$\min \quad \mathrm{Cost}^{\mathrm{MG}} = \sum_t \left( Cost_t^{EN} + \sum_i Cost_t^{DG_i} + \sum_j Cost_t^{BES_j} + \sum_j Cost_k^{EV_k} \right) \tag{8}$$

$$\text{Subject to:} \quad \text{Constraint}\,\{\text{DGs, FERs}\}$$

In (8), $Cost_t^{EN}$ is the cost of purchasing energy from the grid at time *t*. Accordingly, the total temporal operational cost of DGs, BESs and degradation cost of EVs that must be paid to the EV owners for vehicle-to-grid contribution, are $\sum_i Cost_t^{DG_i}$, $\sum_j Cost_t^{BES_j}$ and $\sum_j Cost_k^{EV_k}$ , respectively.

This objective could also be considered in a different shape which says the MGEM objective is to maximize the total profit of the MG instead of operational cost. The monetary profit for a MG mostly comes from selling energy to the grid or providing flexibility services to balancing responsible parties. Accordingly, the objective function of the MG could be defined considering the following formulation:

$$\max \quad \mathrm{Profit}^{\mathrm{MG}} = \sum_t \left( P_t^{sell} \lambda_t^{sell} - P_t^{buy} \lambda_t^{buy} - Cost_t^{MG} \right) \tag{9a}$$

$$\max \quad \mathrm{Profit}^{\mathrm{MG}} = \sum_t \left( F_t^{up} \lambda_t^{up} + F_t^{dn} \lambda_t^{dn} - P_t^{EN} \lambda_t^{EN} - Cost_t^{MG} \right) \tag{9b}$$

$$\text{Subject to:} \quad \text{Constraint}\,\{\text{DGs, FERs, Grid Limits}\}$$

Eq. (9a) indicates the objective function of MGEM problem for a grid-connected MG which only exchange energy with the grid while the (9b) presents the objective for a flexibility provider MG. In (9a)-(9b), $P_t^{sell}$ and $\lambda_t^{sell}$ are the exported power to the grid and the price of selling to the grid, respectively. $P_t^{buy}$ and $\lambda_t^{buy}$ are the imported power from the grid and the price of energy to the grid, respectively. $F_t^{up}$ and $F_t^{dn}$ are the upward and downward flexibility provided to the network, respectively. $\lambda_t^{up}$and $\lambda_t^{dn}$ are the price of upward and downward flexibility, respectively. $P_t^{EN}$and $\lambda_t^{EN}$ are the quantity and price of purchased energy from the grid, respectively. Finally, $Cost_t^{MG}$ refers to the total operational cost of the MG which includes degradation cost of energy storages, EVs as well the operational cost of generation-side resources. Note that, in both definitions, the constraints related to the operational consideration of the assets as well as members' comfortness must be taken into account in MGEM problem.

### 3.2.2 Self-sufficiency

One of the important targets of MGEM in MG is self-sufficiency. A MG is self-sufficient when there is a balance between the generation and consumption within the MG. In other words, the power produced by the MG's resources could fulfill its demand over a period of time. This objective becomes pivotal mostly when an islanding situation is predictable since, in that case, the MG becomes disconnected from the grid and the stability of the MG becomes critical. The MGEM with an objective of self-sufficiency could be tackled by reducing the peak demand, load shedding as well as discharging the storage-based flexible resources. In this way, based on the level of emergency, the MGEM should define a priority for the utilization of fast-response FERs located in the MG. However, this objective could have other targets inside itself. For example, the self-sufficiency of MG in moments at which the renewable energy resources have production and the energy storages have a sufficient level of charge could be deployed to reduce energy purchasing from the grid. Therefore, fewer greenhouse gases emission as well as cost reduction could also be considered as the results of self-sufficiency objective. The objective function regarding the self-sufficiency in MGEM systems must satisfy the following constraint:

$$G_t^{MG} \geq D_t^{MG} \tag{10}$$

$$G_t^{MG} = \sum_i P_t^{DG_i} + \sum_j P_t^{dis_j} \tag{11}$$

$$D_t^{MG} = P_t^{BL} + \sum_i P_t^{FL_i} + \sum_j P_t^{ch_j} \tag{12}$$

In the above equation, $G_t^{MG}$ is the MG total generation and $D_t^{MG}$ is the MG total demand at time *t*. In (10)-(12), the $P_t^{DG_i}$ is the production of DG *i* at time *t*. $P_t^{BL}$ and $P_t^{FL_i}$ are the baseline load and power consumption of flexible load *i* in the MG at time *t*, respectively. $P_t^{dis_j}$ and $P_t^{ch_j}$ are the discharging and charging power of storage-based resources $j$ at time *t*, respectively. It has to be mentioned that the other constraint regarding the simultaneous charging/discharging limitation and the operational constraints of DGs also must be taken into account.

### 3.2.3 Flexibility Provision

As the traditional power systems have been experiencing a fast and vast transition to the smart, local, and decentralized ones, the flexibility services concept has been introduced in order to cover the whole system-related issues. In this light, MGs as the local energy systems is believed to be a suitable choice in providing local and system-wide flexibility. Flexibility services could be provided by MGs through the effective utilization of FERs and also distributed energy resources in MG by using MGEM systems. However, before mentioning the flexibility services provision by the MGs, the definition of flexibility in an electrical system should be clarified. A comprehensive definition of the flexibility of electrical systems could be the ability of the system to adjust its operating point continuously and also to resist the predicted and unpredicted differentiations happening in operating conditions. Accordingly, a flexible electrical system must adapt to the possible changes both in generation and consumption in a temporal manner [21]. Therefore, another possible objective of MGEM might be providing flexibility services by MGs to the connected upstream networks. These services could appear in different shapes. An overview of the flexibility services (e.g. in Nordic countries [22]) that MG can provide to other entities are presented in Fig. 3.

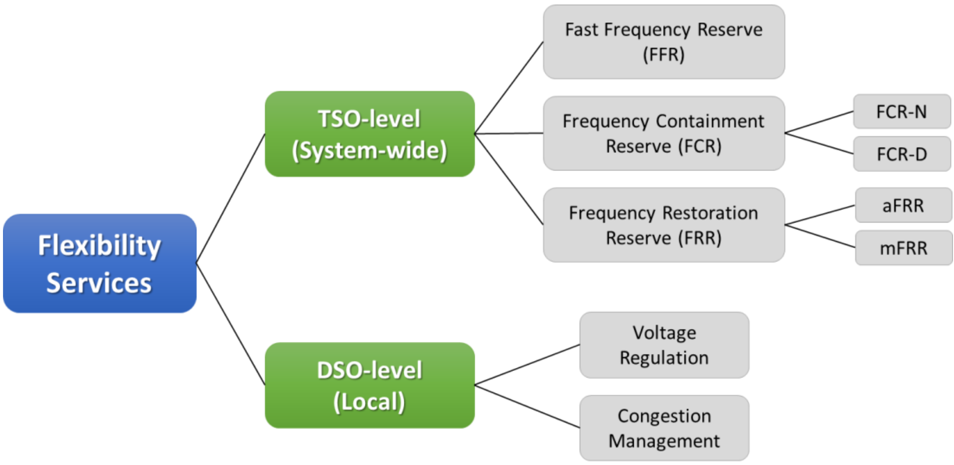


Fig. 3. An overview of the flexibility services (in Nordic)

### 3.2.3.1 TSO-level Flexibility Services

The transmission system operator is the responsible party for TSO-level balancing issues which could be addressed by the contribution of all system-level flexible resources, e.g. MGs. There are three types of services that local energy systems can contribute to flexibility provision to transmission-level needs, which are fast frequency reserve (FFR), frequency containment reserve (FRR), and frequency restoration reserve (FCR). TSO-level flexibility services have been the conventional generation units' responsibility. However, recently and more increasingly in future power systems, MGs as the potent sources of flexibility, would be among the flexibility service responsible parties. Depending on the size of grid-connected MGs and the flexibility needs of the upstream entities, MGs could contribute to one or more specific flexibility services in singular or aggregated manners. The TSO-level flexibility services (e.g. in Finland [23]) with their characteristics are summarized as in the Table II. The flexibility services in this table are categorized as reserve product services [23].

Table II. The characteristics of the Nordic flexibility services

| Service | FFR (new) | FCR-D | FCR-N | aFRR | mFRR |
|---|---|---|---|---|---|
| Application | In very low-inertia situations | In big frequency deviations | Always in use | In certain hours | Incidents/imbalances of balancing parties |

| Activation | 1 sec. | Less than 1 min. | 1-5 min. | 5 min. | 15 min. |
|---|---|---|---|---|---|
| Min. Bid Size | Not defined yet | 1 MW | 0.1 MW | 5 MW | 5 MW |

- **FFR:** The FFR service as the recently introduced flexibility service in Nordic will be utilized in extremely low-inertia situations when there are ±0.5 Hz frequency fluctuations. The maximum amount of FFR services need in Nordic is estimated 300 MW.
- **FCR-D:** The FCR-D service is needed in huge frequency deviations which at least 50% of it needs to be activated in 5 seconds and the rest is required to be activated in 30 seconds. The system's need in this service is only for under-frequency situations (i.e. increase in generation or decrease in demand)
- **FCR-N:** The FCR-N service is for normal operation of the system and is being activated all the time. The system's need in this service is only for both under-frequency and over-frequency situations (i.e. increase/decrease in generation or demand). Note that, this service is symmetrical which means the flexibility providers like MGs must be able to provide the flexibility needs equally for upward and downward flexibility.
- **aFRR:** The aFRR service is activated when . In this service, unlike FCR, the asymmetrical bids are also accepted which means the upward and downward flexibility bids could be submitted separately. Note that, the activation price to the service providers will be paid according to the price of balancing energy market.
- **mFRR:** The mFRR service is activated manually in 15 minutes. Bids are needed to be delivered 45 minutes prior to activation hour. In this service, like aFRR, the upward/downward flexibility bids are being submitted separately. Note that, in this service, the prices are constantly greater than day-ahead energy prices so that it is quite beneficial for flexibility providers like MGs.

#### 3.2.3.2 DSO-level Flexibility Services

There are two types of flexibility services that are introduced in the electrical systems namely voltage regulation and congestion management in which MGs can contribute as DSO-level flexibility providers. Voltage regulation services could be provided by MG's power electronic devices like FERs' converters and also by injected active power control through the point of common coupling (PCC) with the distribution grid. The power electronic devices are able to control the reactive power which is effective in voltage regulation applications. Similarly, congestion management services could be provided by the mentioned FERs. In DSO-level flexibility provision by MGs, along with the MG-related constraints, the distribution network's limitations such as active and reactive power and injected current should also be taken into account.

### 3.3 Microgrid Energy Management Tools and Techniques

There have been introduced various types of MGEM modeling techniques in the previous literature. These techniques include the optimization approaches along with intelligence control tools such as model predictive control, game theory methods, etc. In the following subsections, some of the most popular tools and methods will be introduced.

#### 3.3.1 Optimization Methods

The basic approach to energy management problems would be based on optimization algorithms. This originates from the nature of the energy management since it is supposed to minimize or maximize an objective depending on the targets of MG's stakeholders as well as the method of asset management [24]. There have been introduced many optimization techniques which could be employed correctly depending on the type of the problem. In general, the optimization techniques could be split into two main categories, convex and non-convex. Fig. 4, presents a general overview of the proposed types of optimization problems [25].

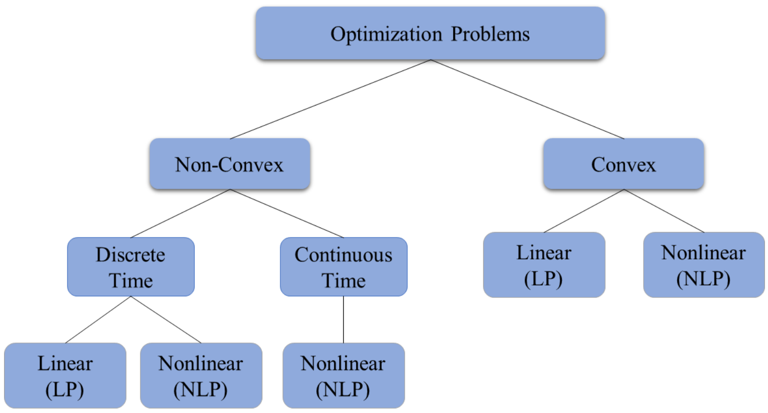


Fig. 4. General categorization of optimization problems

The type of optimization technique could be chosen correctly depending on the problem's characteristics. In MGEM, the type of problems mostly are convex or the problems are defined in a way that they could be solved with convex techniques (i.e. convex relaxation). This is due to the fact that the convex problems give better convergence compared to the non-convex ones [25]. Furthermore, there could be many uncertainties in MG operation due to the nature of MG components. For instance, the intermittent renewable components such as wind turbines, photovoltaic units, and on the top of them, the unpredictable demand could create the mentioned uncertainties [26]. These uncertainties, however, could be addressed by means of some well-known mathematical and statistical techniques during the definition of optimization problems for MGEM. In order to analyze the impact of uncertainty of data, the following three types of optimization methods have been proposed:

- Deterministic Optimization
- Stochastic Optimization
- Robust Optimization

Although the deterministic approach for defining an optimization problem could be beneficial for comparing the results of the problem with other approaches, robust and stochastic optimization solutions are believed as the most effective techniques in energy management problems which are illustrated in details in the following subsections [27].

#### 3.3.1.1 Deterministic Optimization

Deterministic problems are those that have a unique output for any kind of input [25]. As an example, wind speed or solar radiation which are variable over a time span could directly affect the output power of wind turbines or PV systems. Therefore, for different values of wind speed and solar radiation, the power generation of these renewable units would change. However, the power generation function of these renewable units could be defined deterministic meaning that, for any wind speed and solar radiation, the output power of wind and PV units are considered as certain values. This type of problem formulation would not take place in reality, however, there are some applications for deterministic approaches. Furthermore, this method could be beneficial when the aim is to have an idea about the overall operating points of the system in a certain condition. In MGEM problems, there is some component in the system that has strong stochasticity (e.g. renewables, demand, etc.) and could not be modeled as deterministic functions. Consequently, the other types of optimization techniques (i.e. stochastic and robust) are usually recommended that will be introduced in the following subsections.

#### 3.3.1.2 Stochastic Optimization

In stochastic optimization, the problem of energy management could be presented by a statistical objective function. In this light, the uncertain parameters of the problem such as the output power of renewable energy units could be modeled as the well-known probability distribution functions. These distribution functions might be different due to the difference in the nature of renewable sources such as solar irradiation or wind power. They also might be different due to the uncertainties stemming from the stochastic behavior of consumers such as the behavior of EV owners and the pattern of charging their vehicles. However, all these uncertainties are can be considered as the most popular distribution functions since their sources mostly follow a predictable pattern. The general formulation of a stochastic optimization problem could be found in (13):

$$\min_{x \epsilon \chi} \sum_{\omega \epsilon \Omega} \pi(\omega)\, F(x, \omega) \quad (13)$$

In (13), $\pi(\omega)$ is the probability of scenario $\omega$, $\Omega$ is the set of scenarios, $\chi$ is the set of decision variables. The function $F(x, \omega)$ could be different based on the objective of the MGEM problem. According to the stochastic optimization method, the main objective function of the problem could be written as the sum of the objective function of each scenario multiplied by the scenario probability. In this method, the value of uncertain variables in the system is considered by defining several possible scenarios. Note that, for each scenario, a probability of occurrence should be considered in a way that the summation of the probability of all scenarios must be equal to one as follow:

$$\sum_{\omega} \pi(\omega) = 1 \quad (14)$$

There have been presented a number of computational methods for generating the above scenarios. Amongst these methods, one of the most popular scenario generation techniques is the Monte-Carlo method which is widely employed in the literature [28]. The number of the considered scenarios for the problem has a direct impact on the accuracy of the problem. In other words, by increasing the number of these scenarios the result would be more accurate. However, a large number of considered scenarios for the stochastic optimization problems could result in a huge computational cost. In order to reduce the computational cost of solving, the number of scenarios should be reduced. Therefore, one could use a mathematical method to limit the possible scenarios. For instance, the K-means clustering technique is proposed in order to tackle a large number of scenarios [29]. In the following sub-sections, uncertainty modeling methods for different sources of stochasticity are illustrated.

#### 3.3.1.3 Robust Optimization

The robust optimization method was first introduced in 1973 [30]. This method has been introduced and employed in many research as one of the most powerful approaches towards energy management in order to act as an alternative for modeling the problems with uncertain parameters. The robust optimization is employed when the energy management problems confront a limited amount of data but at the same time several uncertainties. In this optimization method, unlike the stochastic optimization with many possible scenarios, we consider only one scenario which means this optimization does not need any kind of probability distribution function [31]. This scenario is assumed to be the worst-case regarding the uncertain situations in the optimization procedure. In energy management problems, the worst-case scenario is the one that is believed to have the most severe outcome that happens in the real situation. In other words, in this method, it is assumed that the uncertain parameters are in their worst condition [30]. This could help to have a realistic paradigm towards the occurring scenario and if possible, it could improve the results of the optimization in comparison with stochastic methods [32].

In this method, the optimal result of the optimization has two features. First, less data is needed for uncertain parameters here which means only minimum, maximum, and mean of the uncertain parameter is required. Second, the optimal solution of the problem is feasible for all conditions which could be quite beneficial in decision making.

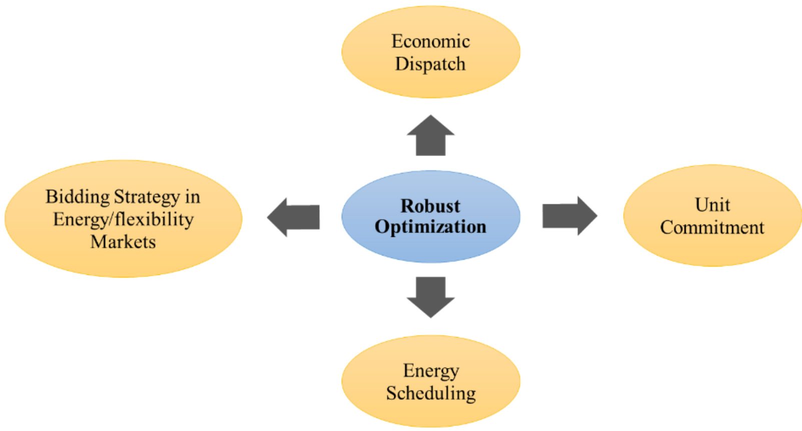


Fig. 5. Applications of the robust optimization

The robust optimization approach has many applications in MGEM such as bidding strategy [33]. These applications could be dealing with the uncertainty of renewable energy units' generation, consumers' load, and energy/flexibility market prices. Fig. 8, provides a summarized overview of the most important applications of the robust optimization techniques in MGs.

In general, the basic formulation of a robust optimization problem would be as follow:

$$\min_{x \epsilon \chi} \max_{\omega \epsilon \Omega} \mathbb{C}(x, \omega) \qquad (27)$$

Where $\chi$ is the set of uncertainties and $\Omega$ is the decision variables' space [34]. In MGEM problems, for instance, the robust optimization technique could be employed in order to minimize the cost function of MG (i.e. $\mathbb{C}$) while the baseline demand of the MG is at the highest possible value. In the following subsection, the uncertainty characterization methods are presented.

### 3.3.2 Uncertainty Characterization

#### 3.3.2.1 Uncertainty of Wind Units

The uncertainty of the wind power units is due to the variable nature of wind speed in different weather conditions. The uncertainty related to the generation output of wind power units has been specifically studied in the previous works like [35], [36] and [37]. In order to model the uncertainty of wind power production the well-known Weibull distribution function is proposed [36]. The introduced formula of Weibull probability distribution function is as follows:

$$f_s(s) = \left(\frac{k}{c}\right)\left(\frac{s}{c}\right)^{k-1} e^{-\left(\frac{v}{c}\right)^k} \qquad k, c > 0 \tag{15}$$

In (15), $c$ and $k$ refers to the scale factor and shape factor, respectively. This distribution function could be divided into $N_{sc}$ scenarios in which the probability of occurrence of each scenario could be defined and written as follows:

$$\pi_\omega = \int_{S_\omega}^{S_{\omega+1}} f_s(s)\, ds \qquad \omega = 1,2,\dots,N_{sc} \tag{16}$$

In (16), the $S_w$ denoted the wind speed of the scenario $w$. Accordingly, the output power of the wind, $P^{WT}$, unit could be obtained by using the following equation:

$$P^{WT} = \begin{cases} 0 & 0 \le S_\omega < S_i \\ P_r(A + S_\omega B + S_\omega^2 C) & S_i \le S_\omega < S_r \\ P_r & S_r \le S_\omega < S_o \\ 0 & S_\omega \ge S_o \end{cases} \tag{17}$$

The power generation curve of wind units could be found in Fig. 5.

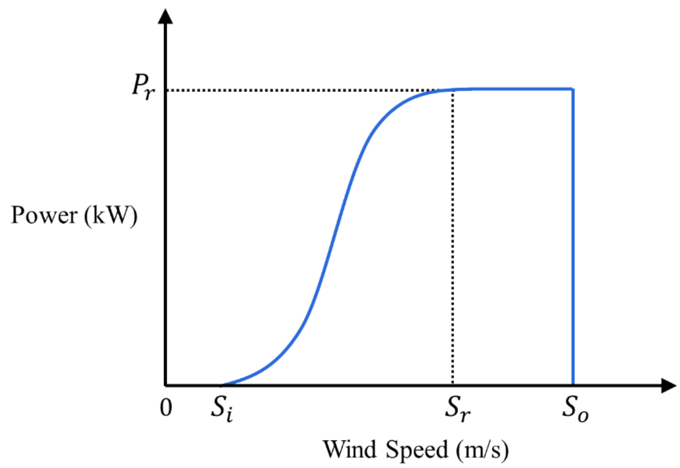


Fig. 6. Output power of wind units based as a function of wind speed

The generation of the wind unit directly depends on the wind speed in a specific time-step. In (17), the constant values A, B and C could be achieved, for example from [38], and are related to the characteristics of the wind turbine. Note that, $S_i, S_o, S_r$ and $P_r$ indicate the cut-in speed, cut-out speed, rated speeds and rated power, respectively.

### 3.3.2.2 Uncertainty of PV Units

The uncertainty related to the photovoltaic units stems from the variable amount of solar irradiation. Solar irradiation could be different from one location to another which results in the intermittent generation of PV units. The amount of solar radiation is dependent on the weather temperature, weather conditions, and the angle of photovoltaic panels. However, by studying the long-term patterns of solar radiation, for instance, in a specific location, it can be realized that they mostly follow a pattern. These patterns could be modeled as one of the most popular probability distribution functions. The most utilized distribution that is being used to model the generation of PV units would be Beta distribution [39]. This function is introduced as following equation:

$$f_{\mathcal{R}} = \begin{cases} \mathcal{R}^{\alpha+1}(1-\mathcal{R})^{\beta-1}\left(\frac{\Gamma(\alpha+\beta)}{\Gamma(\alpha)\Gamma(\beta)}\right) & 0 \le \mathcal{R} \le 1\,;\alpha,\beta \ge 0 \\ 0 & \text{otherwise} \end{cases} \tag{18}$$

$$\alpha = \left(\frac{\mu}{1-\mu}\right)\beta \tag{19}$$

$$\beta = \frac{\mu(1-\mu^2)}{\sigma^2} - (1-\mu) \tag{20}$$

In (18)-(20), the parameters $\alpha$ and $\beta$ denote the features of function which can be obtained by means of (19) and (20), respectively [40]. The Beta distribution curve for different values of $\alpha$ and $\beta$ is depicted in Fig. 6. The variable $\mathcal{R}$ refers to the solar radiation in kW/m$^2$. Note that, the $\Gamma$ refers to well-known Gamma function.

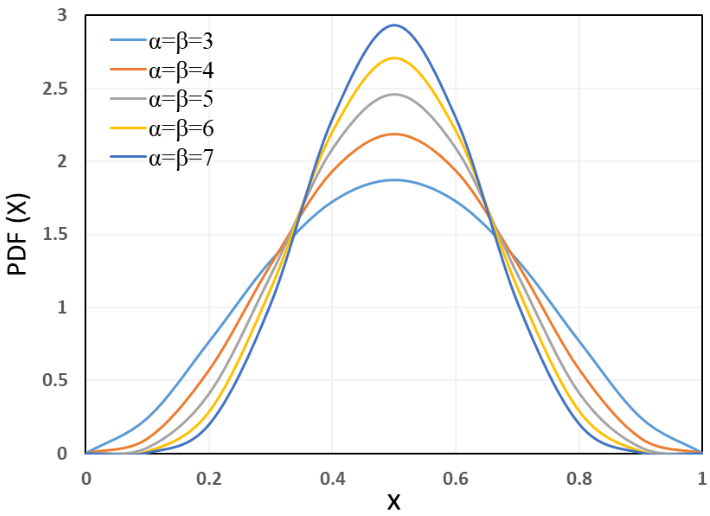


Fig. 7. The Beta distribution curve for different values of $\alpha$ and $\beta$

In (19)-(20), the mean and standard deviation of solar radiation could be denoted by $\mu$ and $\sigma$. Accordingly, the output power of the photovoltaic unit can be calculated using the following equation [39]:

$$P^{PV} = N_p\, \mathcal{R}\, (V_{oc} - k_v\theta_c)(I_{sc} + k_c\theta_c - 25k_c)\left(\frac{V_{mpp}I_{mpp}}{V_{oc}I_{sc}}\right) \quad (21)$$

Where $P^{PV}$ is the power generation of PV system and the parameter $N_p$ refers to the number of panels in the PV unit. $\mathcal{R}$ is the solar radiation at the location of PV unit. The constants $k_v$ and $k_c$ are related to coefficient temperatures of voltage and current, respectively. $V_{mpp}$ and $I_{mpp}$ denotes the respective voltage and current in the maximum power point condition. $V_{oc}$ and $I_{sc}$ refers to the voltage in open-circuit and current in short-circuit conditions, respectively. $\theta_c$ is the temperature of solar cells that can be approximated using the following equation:

$$\theta_c = \theta_{amb} + \frac{\mathcal{R}(\theta_n - 20)}{0.8} \quad (22)$$

In (22), the term $\theta_{amb}$ is the ambient temperature of PV panels and $\theta_n$ is the temperature in nominal operation condition.

### 3.3.2.3 Uncertainty of EV Owners' Behavior

In order to model the uncertain behavior of EV owners, for example in an MG, a distribution function is needed that could correctly represent the usage pattern of EVs. The most usual probability distribution that is used to model the uncertainty of EVs is truncated Gaussian distribution function [41], [42] and [43]. In the case of an MG, the EVs owned by the MG stakeholder, residential/commercial units, and/or a charging station could be considered in the uncertainty modeling with single or multiple probability distributions. In this light, for every single EV, the initial state-of-charge (SoC) and the availability of the EV in the understudy time horizon could be taken into account.

$$SoC_i^{ini} = f_{TG}(x, \mu^{soc}, \sigma^{soc}, SoC_i^{min}, SoC_i^{max}) \tag{23}$$

In (23), the $SoC_i^{ini}$ is the initial SoC of EV $i$. $\mu^{soc}$ and $\sigma^{soc}$ are the mean and standard deviation of EVs' SoC, respectively. $SoC_i^{min}$ and $SoC_i^{max}$ are the minimum and maximum possible SoC of EVs in the MG. This equation could be utilized to generate the possible scenarios for initial SoC of the EVs.

According to the above equation, the truncated Gaussian distribution that could be used for modeling the initial SoC of an EV is depicted in Fig. 7 [44]. In this exemplary figure, the minimum and maximum SoC for EVs considered 0.3 and 0.9, respectively. In Fig. 7, the value of mean and the standard deviation are considered 0.5 and 0.25, respectively. The exact value of the parameters could be estimated by studying the historical and regular patterns of EVs' behavior.

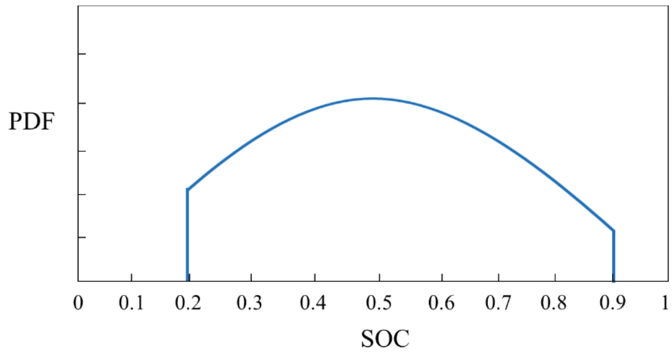


Fig. 8. Truncated distribution of EV's SOC

Moreover, the most probable availability times of each EV have to be in hand for modeling the behavior of EVs. This could happen by considering the historical plug-in and plug-out times of EVs to the grid. Accordingly, the plug-in and plug-out times of EVs in the MG could be modeled with a distribution function as follows:

$$\begin{cases} t_i^{in} = f_{TG}(x, \mu^{in}, \sigma^{in}, t_i^{in,min}, t_i^{in,max}) & \forall i \\ t_i^{out} = f_{TG}(x, \mu^{out}, \sigma^{out}, t_i^{out,min}, t_i^{out,max}) & \forall i \end{cases} \tag{24}$$

In (24), $t_i^{in}$ and $t_i^{out}$ are the times of plug-in and plug-out by EV $i$, respectively. This equation could be employed to generate several possible scenarios for plug-in and plug-out times of EVs in the MG.

#### 3.3.2.4 Uncertainty of Flexibility Needs

In order to schedule and operate the MG in an efficient manner, the flexibility needs of the system should be predicted in advance. The concept of flexibility needs refers to the amount of regulation up/down needed for maintaining the system's balance in a predefined bandwidth. In fact, the flexibility need for a specific time is determined by the system's operator by the time of activation. However, the MG manager/aggregator should have the idea about the approximate values of flexibility that are supposed to be assigned from the system's operator. The flexibility need is always uncertain due to its dependency on several factors that need to be modeled by stochastic methods.

In order to model the uncertainty related to the flexibility needs, one can deploy a probability distribution function. It is obvious that the amount of flexibility need from the upstream grid that needs to be activated has a value between zero and the assigned value by the MG. In other words, the minimum activated amount of flexibility is zero when the MG is not supposed to provide any flexibility for a time step, and in contrast, the maximum value of the activated flexibility by the MG when the MG is supposed to provide the entire amount of assigned flexibility to the upstream network. However, the MG aggregator must schedule the demand and generation in a way that provides all the offered flexibility to the upstream network. With this regard, the activated amount of upward and downward flexibility from the system's operator could be modeled as uniformly distributed between zero and its maximum value [44].

$$UF_{w,t} = f(x) = \frac{1}{F_t^{up}} \qquad 0 \le x \le F_t^{up} \tag{25}$$

$$DF_{w,t} = f(x) = \frac{1}{F_t^{dn}} \qquad 0 \le x \le F_t^{dn} \tag{26}$$

In (25) and (26), the $UF_{w,t}$ and $DF_{w,t}$ are the upward and downward activated flexibility. $F_t^{up}$ and $F_t^{dn}$ refers to the upward and downward assigned flexibility.

### 3.3.3 Model Predictive Control

Model predictive control (MPC) as a subfield of optimal control has several applications in electrical energy systems operation and control, especially in the energy management systems. Generally, MPC is a technique that makes a decision at a time through solving an approximate model over future horizons. There might be many engineering problems where the model is not in hand. In the MPC method, at least, an approximate model of the system is required. MPC is mostly employed to solve a problem with stochastic parameters which is modeled by means of a deterministic approximation. MPC might also utilize a stochastic model of the system in the future, however, the solution may be hard to converge [34]. In this method, the actions about the future configurations are realized by making the decisions now. Alternatively, it might utilize sampled approximations for the future, introduced as MPC in some literature, which are standard strategies in stochastic programming [45]. The overview of the MPC strategy for more clarification is depicted in Fig. 9. This figure states that how the decision made by MPC at the current moment, could predict the optimal trajectory of the system towards the future changes in the next time steps. This procedure will iterates every time step until the controller find the best solution.

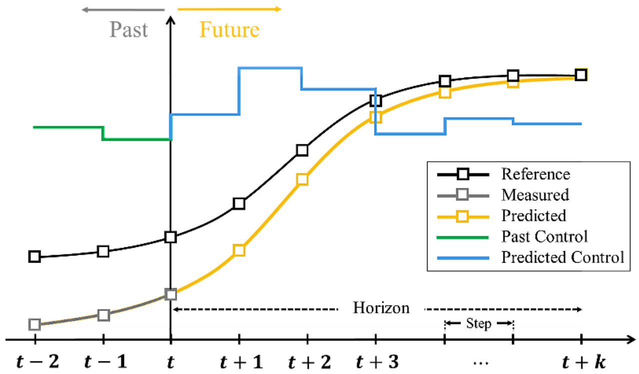


Fig. 9. Model predictive control analogy

The MPC method is believed to be applicable in MGEM systems, especially when there are many stochasticities within the MG. Some of the most important applications of MPC method in MGs could be classified as follows [46]:

- ✓ Providing an optimal solution to control the operation of MG's FERs for different objectives in MGEM systems.
- ✓ Providing a control-based decision making to deal with the intermittency of consumers (demand, EVs, etc.) as well as renewable energy resources (wind, PV, etc.) in the MGEM optimization problems in order to tackle the stochasticity and randomness of these components.
- ✓ MPC is useful in handling some binary variables that need to be considered in MGEM problem. This could be beneficial when the situation of some components (e.g. charging mode of BESs, availability of EVs, ON-OFF mode of flexible loads) might possibly change and the new decisions should be made based on the situation.
- ✓ MPC could be beneficial in dealing with sudden changes in the MG where the new decisions should be made based on the new situation to maintain the MG in its normal operating point. This could help the MG to improve its degree of freedom in unusual conditions.

- ✓ MPC is also helpful when a distributed management method is taken within the MG. In this case, there might be several agents in the MG who make the MGEM problem complicated. Hence, MPC is believed to be a suitable choice in dealing with such problems.

Despite the above advantages and usefulness of the MPC method, it might have a high computational cost due to several optimization problems that need to be run in each time step over a horizon. More information regarding different types of MPC formulation can be found in [46]. In the following subsection, a brief overview of the game-theory application in MGs are presented.

### 3.3.4 Game-theory

Another potential approach to MGEM problems is game theory. Game theory is believed to be among potential techniques in the operation of MGs due to the capability of enabling distributed management for MGs' resources [47] [48]. In order to implement a MGEM problem as a game theory problem, the resources located at the MG could be considered as game participants. Despite the game theory's shortcomings in problem convergence, it is still a good choice for multi-agent-based decision making studies.

Game theory has many applications from the energy industry to economic studies in complex systems. In general, its concept refers to mathematical techniques that model the interaction between multiple decision-makers [49]. The choice of one decision-making entity could affect the choices of the other entities. One of the applications of game theory could be in distributed management of MGs. In order to implement a MGEM problem as a game theory problem, the resources located at the MG could be considered as game participants. The following four steps should be taken for a game-theoretic problem:

a) Defining players of the proposed game
b) Defining the individual and overall goal
c) Dealing with the coupled constraints
d) Finding the Nash equilibrium

Game theory methods could be split into two categories: cooperative game and non-cooperative game [50]. A cooperative game is the one with a number of entities in which the main goal of these players are in-line with each other. In contrast, the non-cooperative game refers to a game in which the entities are in conflict with each other and they try to act independently regarding their goals [51]. However, the choice of the suitable game-theory approach for MGEM problems directly depends on the method of MG management and the agreements between MG operator and members.

## 4 SUMMARY AND CONCLUSION

The MG is an autonomous or semi-autonomous system that consists of DGs, RESs, FERs as well as dispatchable loads working together which are able to operate in both grid-connected and islanded mode. MGs as the potential sources of sustainability are designed to expand the decentralization goals along with cooperation with the whole system toward flexible electrical energy systems. However, the increasing penetration of renewable sources and the decentralization in either MG or system-level networks have resulted in several stability and resiliency issues. Consequently, the EMSs are proposed to efficiently control and manage the operation of all energy resources locate in generation-side and demand-side so as to deal with the stochastic outcomes of a deregulated system. Moreover, the smart power systems in the future will confront several uncertainties due to the very low-inertia situations which must be addressed by the EMS as well as the novel control techniques in advance.

In MG concepts, the EMS also could play a pivotal role in dealing with the aforesaid issues since they could be employed to satisfy several objectives in operation and control of the MG. The EMSs could also be beneficial in providing different kinds of services to the national or regional grids. Accordingly, MGEM systems could be designed and planned carefully so that they can take into account all the individual or environmental constraints and limitations of consumers' electrification. Hence, in order to have an efficient and synergetic contribution by MGs, the MGEM problems should be defined by problem formulations in which all the uncertainty, stochasticity, restrictions, and also monetary payback for its stakeholders are considered precisely.

Different types of optimization formulations were used for the MGEM problems. Most of them focused on minimizing MG's operating costs such as fuel costs, maintenance costs, and the cost of imported energy from the grid. These optimization techniques could be categorized based on their optimization types, objective functions, constraints, and also tools that are utilized to solve MGEM problems. The most popular ones include stochastic and robust optimization techniques. Furthermore, there have introduced some tools such as model predictive control, intelligent techniques, and game-theory in order the make the MGEM more efficient and predictable.

To sum up, the utilization of MGs equipped with the MGEM system could be a potential solution to future power systems issues. The control and optimization techniques in MGEM system enable the active and sustainable utilization of energy resources. These energy management systems could help to enhance the flexible utilization of energy resources as well as the flexibility of the whole power system by providing different types of balancing and ancillary services. However, in order to make the most out of these MGEM plans, the smart selection of control and optimization trajectories are of the necessity.

## 5 References


[1] H. Shayeghi, E. Shahryari, M. Moradzadeh, and P. Siano, “A survey on microgrid energy management considering flexible energy sources,” *Energies*, vol. 12, no. 11, p. 2156, 2019.

[2] A. Hauer, “Storage Technology Issues and Opportunities, International Low-Carbon Energy Technology Platform,” in *Proceedings of the Strategic and Cross-Cutting Workshop “Energy Storage—Issues and Opportunities”, Paris, France*, 2011, vol. 15.

[3] F. Faraji, A. Majazi, and K. Al-Haddad, “A comprehensive review of flywheel energy storage system technology,” *Renew. Sustain. Energy Rev.*, vol. 67, pp. 477–490, 2017.

[4] “Energy Storage enabling Flexibility in Electrical Grid Systems,” Strasbourg, 2017.

[5] W. Bai, M. R. Abedi, and K. Y. Lee, “Distributed generation system control strategies with PV and fuel cell in microgrid operation,” *Control Eng. Pract.*, vol. 53, pp. 184–193, 2016.

[6] Y. Liu, L. Xiao, G. Yao, and S. Bu, “Pricing-based demand response for a smart home with various types of household appliances considering customer satisfaction,” *IEEE access*, vol. 7, pp. 86463–86472, 2019.

[7] H. Khajeh, M. Shafie-khah, and H. Laaksonen, “Blockchain-based demand response using prosumer scheduling,” in *Blockchain-based Smart Grids*, Elsevier, 2020, pp. 131–144.

[8] J. Leitão, P. Gil, B. Ribeiro, and A. Cardoso, “A survey on home energy management,” *IEEE Access*, vol. 8, pp. 5699–5722, 2020.

[9] J. Wang, S. You, Y. Zong, C. Træholt, Z. Y. Dong, and Y. Zhou, “Flexibility of combined heat and power plants: A review of technologies and operation strategies,” *Appl. Energy*, vol. 252, p. 113445, 2019.

[10] D. Li, X. Xu, D. Yu, M. Dong, and H. Liu, “Rule Based Coordinated Control of Domestic Combined Micro-CHP and Energy Storage System for Optimal Daily Cost,” *Appl. Sci.*, vol. 8, no. 1, p. 8, 2018.

[11] J. M. Lujano-Rojas, C. Monteiro, R. Dufo-López, and J. L. Bernal-Agustín, “Optimum load management strategy for wind/diesel/battery hybrid power systems,” *Renew. Energy*, vol. 44, pp. 288–295, 2012.

[12] T. Khatib and W. Elmenreich, “Novel simplified hourly energy flow models for photovoltaic power systems,” *Energy Convers. Manag.*, vol. 79, pp. 441–448, 2014.

[13] Y. Zheng, B. M. Jenkins, K. Kornbluth, A. Kendall, and C. Træholt, “Optimization of a biomass-integrated renewable energy microgrid with demand side management under uncertainty,” *Appl. Energy*, vol. 230, pp. 836–844, 2018.

[14] B. Li, R. Roche, D. Paire, and A. Miraoui, “A price decision approach for multiple multi-energy-supply microgrids considering demand response,” *Energy*, vol. 167, pp. 117–135, 2019.

[15] C. Dou, M. Lv, T. Zhao, Y. Ji, and H. Li, “Decentralised coordinated control of microgrid based on multi-agent system,” *IET Gener. Transm. Distrib.*, vol. 9, no. 16, pp. 2474–2484, 2015.

[16] W. L. Theo, J. S. Lim, W. S. Ho, H. Hashim, and C. T. Lee, “Review of distributed generation (DG) system planning and optimisation techniques: Comparison of numerical and mathematical modelling methods,” *Renew. Sustain. Energy Rev.*, vol. 67, pp. 531–573, 2017.

[17] J. Bai, Z. Zhou, S. Zhou, and M. Tariq, “Distributed energy management in smart grid with dominated electricity provider and multiple microgrids,” in *2014 International Conference on*

*Power System Technology*, 2014, pp. 3249–3256.

[18] Q. Fu, A. Nasiri, V. Bhavaraju, A. Solanki, T. Abdallah, and C. Y. David, "Transition management of microgrids with high penetration of renewable energy," *IEEE Trans. Smart Grid*, vol. 5, no. 2, pp. 539–549, 2013.

[19] Y. Liu, S. Yu, Y. Zhu, D. Wang, and J. Liu, "Modeling, planning, application and management of energy systems for isolated areas: A review," *Renew. Sustain. Energy Rev.*, vol. 82, pp. 460–470, 2018.

[20] Z. Iqbal *et al.*, "A domestic microgrid with optimized home energy management system," *Energies*, vol. 11, no. 4, p. 1002, 2018.

[21] H. Khajeh, H. Laaksonen, A. S. Gazafroudi, and M. Shafie-khah, "Towards Flexibility Trading at TSO-DSO-Customer Levels: A Review," *Energies*, vol. 13, no. 1, p. 165, 2020.

[22] "Fingrid Open Data Source." [Online]. Available: https://www.fingrid.fi/en/.

[23] "Reserve Products and Marketplaces."

[24] H. Firoozi and H. Khajeh, "Optimal day-ahead scheduling of distributed generations and controllable appliances in microgrid," in *2016 Smart Grids Conference (SGC)*, 2016, pp. 1–6.

[25] M.-H. Lin, J.-F. Tsai, and C.-S. Yu, "A review of deterministic optimization methods in engineering and management," *Math. Probl. Eng.*, vol. 2012, 2012.

[26] Z. A. Farhath, B. Arputhamary, and L. Arockiam, "A Survey on ARIMA Forecasting Using Time Series Model," *Int. J. Comput. Sci. Mob. Comput*, vol. 5, pp. 104–109, 2016.

[27] W. Wei, F. Liu, S. Mei, and Y. Hou, "Robust energy and reserve dispatch under variable renewable generation," *IEEE Trans. Smart Grid*, vol. 6, no. 1, pp. 369–380, 2014.

[28] T. Baležentis and D. Streimikiene, "Multi-criteria ranking of energy generation scenarios with Monte Carlo simulation," *Appl. Energy*, vol. 185, pp. 862–871, 2017.

[29] Y. Dvorkin, Y. Wang, H. Pandzic, and D. Kirschen, "Comparison of scenario reduction techniques for the stochastic unit commitment," in *2014 IEEE PES General Meeting| Conference & Exposition*, 2014, pp. 1–5.

[30] M. Nazari-Heris and B. Mohammadi-Ivatloo, "Application of robust optimization method to power system problems," in *Classical and recent aspects of power system optimization*, Elsevier, 2018, pp. 19–32.

[31] W. Hu, P. Wang, and H. B. Gooi, "Toward optimal energy management of microgrids via robust two-stage optimization," *IEEE Trans. Smart Grid*, vol. 9, no. 2, pp. 1161–1174, 2016.

[32] S. Cui, Y.-W. Wang, J.-W. Xiao, and N. Liu, "A two-stage robust energy sharing management for prosumer microgrid," *IEEE Trans. Ind. Informatics*, vol. 15, no. 5, pp. 2741–2752, 2018.

[33] H. Khajeh, A. A. Foroud, and H. Firoozi, "Robust bidding strategies and scheduling of a price-maker microgrid aggregator participating in a pool-based electricity market," *IET Gener. Transm. Distrib.*, vol. 13, no. 4, pp. 468–477, 2018.

[34] W. B. Powell, "A unified framework for stochastic optimization," *Eur. J. Oper. Res.*, vol. 275, no. 3, pp. 795–821, 2019.

[35] A. Nasri, S. J. Kazempour, A. J. Conejo, and M. Ghandhari, "Network-constrained AC unit commitment under uncertainty: A Benders' decomposition approach," *IEEE Trans. power Syst.*, vol. 31, no. 1, pp. 412–422, 2015.

[36] R. Karki, P. Hu, and R. Billinton, "A simplified wind power generation model for reliability evaluation," *IEEE Trans. Energy Convers.*, vol. 21, no. 2, pp. 533–540, 2006.

[37] S. J. Kazempour and A. J. Conejo, “Strategic generation investment under uncertainty via Benders decomposition,” *IEEE Trans. Power Syst.*, vol. 27, no. 1, pp. 424–432, 2011.

[38] P. Giorsetto and K. F. Utsurogi, “Development of a new procedure for reliability modeling of wind turbine generators,” *IEEE Trans. power Appar. Syst.*, no. 1, pp. 134–143, 1983.

[39] Y. Li and E. Zio, “Uncertainty analysis of the adequacy assessment model of a distributed generation system,” *Renew. Energy*, vol. 41, pp. 235–244, 2012.

[40] Y. M. Atwa, E. F. El-Saadany, M. M. A. Salama, and R. Seethapathy, “Optimal renewable resources mix for distribution system energy loss minimization,” *IEEE Trans. Power Syst.*, vol. 25, no. 1, pp. 360–370, 2009.

[41] M. Amini and A. I. Sarwat, “Optimal reliability-based placement of plug-in electric vehicles in smart distribution network,” 2014.

[42] S. I. Vagropoulos and A. G. Bakirtzis, “Optimal bidding strategy for electric vehicle aggregators in electricity markets,” *IEEE Trans. power Syst.*, vol. 28, no. 4, pp. 4031–4041, 2013.

[43] M. H. Amini *et al.*, “Plug-in electric vehicle owner behavior study using fuzzy systems,” *Int. J. Power Energy Syst.*, vol. 35, no. 2, p. 40, 2015.

[44] M. Shafie-Khah, P. Siano, D. Z. Fitiwi, N. Mahmoudi, and J. P. S. Catalao, “An innovative two-level model for electric vehicle parking lots in distribution systems with renewable energy,” *IEEE Trans. Smart Grid*, vol. 9, no. 2, pp. 1506–1520, 2017.

[45] G. Schildbach and M. Morari, “Scenario-based model predictive control for multi-echelon supply chain management,” *Eur. J. Oper. Res.*, vol. 252, no. 2, pp. 540–549, 2016.

[46] C. Bordons, F. Garcia-Torres, and M. A. Ridao, *Model Predictive Control of Microgrids*. Springer, 2020.

[47] P. Li, J. Ma, and B. Zhao, “Game theory method for multi-objective optimal operation of microgrid,” in *2015 IEEE Power & Energy Society General Meeting*, 2015, pp. 1–5.

[48] E. Mojica-Nava, C. A. Macana, and N. Quijano, “Dynamic population games for optimal dispatch on hierarchical microgrid control,” *IEEE Trans. Syst. Man, Cybern. Syst.*, vol. 44, no. 3, pp. 306–317, 2013.

[49] P. Aristidou, A. Dimeas, and N. Hatziargyriou, “Microgrid modelling and analysis using game theory methods,” in *International Conference on Energy-Efficient Computing and Networking*, 2010, pp. 12–19.

[50] M. J. Osborne and A. Rubinstein, “A course in game theory Cambridge,” *MA MIT Press [Google Sch.*, 1994.

[51] W. Saad, Z. Han, H. V. Poor, and T. Basar, “Game-theoretic methods for the smart grid: An overview of microgrid systems, demand-side management, and smart grid communications,” *IEEE Signal Process. Mag.*, vol. 29, no. 5, pp. 86–105, 2012.

Energy 285 (2023) 129490

Contents lists available at ScienceDirect

Energy

journal homepage: www.elsevier.com/locate/energy

# Optimized siting and sizing of distribution-network-connected battery energy storage system providing flexibility services for system operators

Hosna Khajeh *, Chethan Parthasarathy, Elahe Doroudchi, Hannu Laaksonen

*School of Technology and Innovations, Flexible Energy Resources, University of Vaasa, 65100, Vaasa, Finland*

ARTICLE INFO

Handling Editor: Neven Duic

ABSTRACT

This paper develops a two-stage model to site and size a battery energy storage system in a distribution network. The purpose of the battery energy storage system is to provide local flexibility services for the distribution system operator and frequency containment reserve for normal operation (FCR-N) for the transmission system operator. In the first stage, the priority is to fulfil the flexibility needs of the distribution system operator by managing congestions or interruptions of supply in the local network. Thus, the first stage allocates the battery to ensure reliable electricity supply in the local distribution network. The minimum required size of the battery is also determined in the first stage. The second stage optimally sizes the battery energy storage system to boost the profit by providing frequency containment reserve for normal operation. The first and second stages both solve stochastic optimization problems to design the battery energy storage system. However, the first stage considers worst-case scenarios while the second stage utilizes the most probable scenarios derived from the historical data. To validate the proposed model, real-world data from the years 2021 and 2022 in Finland are employed. The battery placement is conducted for both the IEEE 33-bus system and a Finnish case study. The profitability of the model is compared across different cases for the Finnish case study. Finally, the paper assesses the impacts of cycle aging on the battery's total profit.

## 1. Introduction

Future power systems will face challenges because of the increasing amount of intermittent renewable-based power. In addition, more uncertain demand is added to the system due to the huge electrification in different sectors such as transportation sectors. On one hand, power system operators require more flexibility to deal with the growing uncertainties arising from renewable distributed energy resources (DER) within the system. On the other hand, they can benefit from the flexibility of DERs and take advantage from their potent flexibility to operate distribution and transmission networks.

### 1.1. Motivation

One highly flexible DER is rapidly controllable battery energy storage system (BESS). The European Association for the Cooperation of Transmission System Operators for Electricity (ENTSO-E) has introduced batteries as fast and versatile resources that are capable of providing ancillary services to both DSOs and TSOs [1]. A BESS, functioning as a flexible energy resource, can provide support for the power system frequency, offer local voltage and congestion management as well as back-up power during supply interruptions at different voltage levels. With the help of a BESS, DSOs can actively control the active and reactive power flows in their network to manage congestions and avoid violation of voltage and thermal limits. Beyond its services for local networks, a BESS can assist TSOs with frequency regulation services. It exhibits the ability to rapidly respond to frequency deviations, enabling participation in frequency service markets for profit. Consequently, both TSOs and DSOs can employ BESSs as flexible energy resources to enhance the efficiency of their network operations.

Nevertheless, thorough ex-ante analyses are required before buying a BESS. The BESS should be sized in a way that the revenue obtained from the BESS must outweigh its capital and operational costs. Besides, the BESS needs to be sited optimally if it aims to help with the operation of the distribution network.

### 1.2. Literature review

The existing literature tried to address BESS citing and sizing with

* Corresponding author.
*E-mail address:* hosna.khajeh@uwasa.fi (H. Khajeh).

https://doi.org/10.1016/j.energy.2023.129490
Received 16 April 2023; Received in revised form 23 October 2023; Accepted 26 October 2023
Available online 31 October 2023

**Nomenclature**

*Abbreviations*

| | |
|---|---|
| BESS | Battery Energy Storage System |
| DSO | Distribution System Operator |
| FCR-N | Frequency Containment Reserve for normal operation |
| PoC | Point of Coupling |
| SOC | State of Charge |
| TSO | Transmission System Operator |

*Sets*

| | |
|---|---|
| $t$ | Timeslot [hour = h] |
| $n$, $n'$ | $cn$ Nodes Candidate node |
| $s$ | Scenario |
| $q$ | 3-min time slot |
| $j$ | Partition used in piece-wise linearization |

***Constants***

| | |
|---|---|
| $N^{BESS}$ | The maximum number of BESSs |
| $E^{cell}$ | Energy capacity of the battery cell [kWh] |
| $I^{max}_{n,n'}$ | Maximum permissible current that can flow between $n$ and $n'$ [A$^2$] |
| $N^{par}$ | The number of partitions |
| $N^{NL,S1/S2}$ | The number of net loads' clusters in the first/second stage |
| $N^{f+,S2}$ | The number of clusters for positive frequency deviations in the second stage |
| $N^{f-,S2}$ | The number of clusters for negative frequency deviations in the second stage |
| $P^{cell}$ | Rated charging/discharging power of the battery cell [kW] |
| $P^{NL}_{n,t,s}$ | Net load at node $n$ and timeslot $t$ of scenario $s$ [kW] |
| $prob^{S2}_s$ | Probability of scenario $s$ of the second stage |
| $Q^{NL}_{n,t,s}$ | Reactive power consumed by the load at node $n$ and timeslot $t$ of scenario $s$ [kVar] |
| $R_{n,n'}$ | The resistance of the line between $n$ and $n'$ [Ω] |
| $SOC^{min}$ | BESS minimum SOC |
| $SOC^{max}$ | BESS maximum SOC |
| $v^{min}_n$ | Minimum voltage of node $n$ (0.95 Per-unit) |
| $v^{max}_n$ | Maximum voltage of node $n$ (1.05 Per-unit) |
| $v^{rated}$ | Rated voltage (1 Per-unit) |
| $X_{n,n'}$ | The reactance of the line between $n$ and $n'$ [Ω] |
| $Z_{n,n'}$ | The impedance of the line between $n$ and $n'$ [Ω] |
| $\Delta f_{q,t}$ | Frequency deviation in the $q$ timeslot at hour $t$ [Hz] |
| $\Delta f^{up}_{t,s}$ | Mean value of upward frequency deviation at $t$ [Hz] |
| $\Delta f^{up}_{t,s}$ | Mean value of downward frequency deviation at hour $t$ [Hz] |
| $\Delta q$ | 3 min = 1/20 hour |
| $\Delta S_{n,n'}$ | Maximum power in the piecewise-linearized power flow [kW] |
| $\Delta t$ | 1 h |
| $\pi^{DCC}$ | Price of daily-based BESS capital cost [€/$kWh$] |
| $\pi^{M\&O}$ | Price of BESS maintenance and operation cost [€/ $kWh$] |
| $\pi^{FCR}_t$ | FCR-N price for reserving capacity on the FCR-N day-ahead market [€/$kWh$] |
| $\pi^{reg,up}_t$ | Up regulation price [€/$kWh$] |
| $\pi^{reg,down}_t$ | Down regulation price [€/$kWh$] |
| $\pi^{da}_t$ | Day-ahead spot market price [€/$kWh$] |
| $\pi^{cycle}$ | Price of BESS cycling aging for one cycle [€/$kWh$] |
| $\eta^{ch}$ | BESS charging efficiency |
| $\eta^{dis}$ | BESS discharging efficiency |

*Variables*

| | |
|---|---|
| $Cap^{FCR}_{t,s}$ | Power capacity reserved for FCR-N at timeslot $t$ of scenario $s$ [kW] |
| $E^{BESS}$ | BESS energy capacity [kWh] |
| $P^{up,S1}_{cn,t,s}$ | Activated upward power at node $cn$ and timeslot $t$ of scenario $s$ [kW] |
| $P^{down,S1}_{cn,t,s}$ | Activated downward power at node $cn$ and timeslot $t$ of scenario $s$ [kW] |
| $P^{+}_{n,n',t,s}$ | Active power flowing in a downstream direction from $n$ to $n'$, at timeslot $t$ of scenario $s$ [kW] |
| $P^{-}_{n,n',t,s}$ | Active power flowing in an upstream direction from $n$ to $n'$, at timeslot $t$ of scenario $s$ [kW] |
| $P^{BESS}$ | BESS rated power [kW] |
| $P^{ch,da}_{n=OBP,t,s}$ | BESS charging power with day-ahead spot market prices at timeslot $t$ of scenario $s$ [kW] |
| $P^{dis,da}_{n=OBP,t,s}$ | BESS discharging power with day-ahead spot market prices at timeslot $t$ of scenario $s$ [kW] |
| $P^{FCR-up}_{n=OBP,t,s}$ | BESS activation power in the upward direction at timeslot $t$ of scenario $s$ [kW] |
| $P^{FCR-down}_{n=OBP,t,s}$ | BESS activation power in the downward direction at timeslot $t$ of scenario $s$ [kW] |
| $P^{PoC}_{n=PoC,t,s}$ | Active power coming to the local network through PoC at timeslot $t$ of scenario $s$ [kW] |
| $Q^{PoC}_{n=PoC,t,s}$ | Reactive power coming to the local network through PoC at timeslot $t$ of scenario $s$ [kVar] |
| $Q^{+}_{n,n',t,s}$ | Reactive power flowing in a downstream direction from $n$ to $n'$, at timeslot $t$ of scenario $s$ [kVar] |
| $Q^{-,S1}_{n,n',t,s}$ | Reactive power flowing in an upstream direction from $n$ to $n'$, at timeslot $t$ of scenario $s$ [kVar] |
| $SOE^{BESS}_{t,s}$ | BESS state of energy at timeslot $t$ of scenario $s$ [kWh] |
| $SI_{n,n',t,s}$ | Auxiliary variable for squared current flowing between $n$ and $n'$ at timeslot $t$ of scenario $s$ [A$^2$] |
| $SV_{n,t,s}$ | Auxiliary variable for squared voltage at timeslot $t$ of scenario $s$ [v$^2$] |
| $u^{BESS}_{cn}$ | Binary variable representing if the BESS can be located in candidate node $cn$ |
| $\Delta P_{n,n',j,t,s}$ | Active power flowing between $n$ and $n'$ of partition $j$ at timeslot $t$ of scenario $s$ [kW] |
| $\Delta Q_{n,n',j,t,s}$ | Reactive power flowing between $n$ and $n'$ of partition $j$ at timeslot $t$ of scenario $s$ [kVar] |

different objectives. Some aimed to address the challenges related to the distribution networks while others focused on the peak shaving and TSO-related services.

Most of the literature proposed to size a BESS to enhance the operation of the distribution network or the local microgrid. They, however, did not consider other profitable services that can be provided by the BESS such as frequency control services. For example, Ref. [2] sized a BESS for PV system owners to invest in buying BESSs. It concluded that not only the BESS assists the DSO and improves the power supply quality in distribution networks, but it also brings profits for the owners. Authors of [3] deployed a two-stage stochastic bi-level programming method to allocate and size a BESS in a deregulated distribution network. In the upper level, the BESS revenue is maximized whereas the lower level clears the distribution market. In Ref. [4], authors proposed

**Table 1**
Comparing the paper with the existing literature that developed planning problems for a BESS.

| Ref. | Site the BESS | Size the BESS | Provide DSO flexibility services | Provide TSO flexibility services |
|---|---|---|---|---|
| [2] | × | ✓ | ✓ | × |
| [3] | ✓ | ✓ | ✓ | × |
| [4] | ✓ | ✓ | ✓ | × |
| [5] | × | ✓ | × | × |
| [6] | ✓ | ✓ | ✓ | × |
| [7] | ✓ | ✓ | ✓ | × |
| [8] | ✓ | ✓ | ✓ | × |
| [9] | ✓ | ✓ | ✓ | × |
| [10] | ✓ | ✓ | ✓ | × |
| [11] | ✓ | ✓ | ✓ | × |
| [12] | × | ✓ | × | × |
| [13] | × | ✓ | × | Frequency response |
| [14] | × | ✓ | × | × |
| [15] | × | ✓ | × | Balance services for a fully standalone system |
| [16] | ✓ | ✓ | × | Transient frequency regulation services and transmission-level services for the network |
| [17] | × | ✓ | × | Frequency regulation service and energy arbitrage |
| [18] | ✓ | ✓ | Peak-shaving for distribution network | Frequency regulation in abnormal conditions |
| [20] | ✓ | ✓ | Supports for operation unbalanced network | Frequency regulation |
| This paper | ✓ | ✓ | ✓ (Voltage and congestion management services) | FCR-N service in normal operations |

to help distribution system planners to allocate a BESS and isolation devices as well as to size the BESS. It aimed to improve the system reliability and boost its revenue by using energy arbitrage. Ref. [5] designed a BESS by solving a security-constrained optimal power flow within a microgrid. The paper proposed to recover the costs of PV forecasting errors by a joint operation of PV-BESS. It stated that the BESS can recoup the PV uncertainty costs under a specific degree of the BESS operation. Authors of [6] identified the optimal BESS placement in a radial distribution network to enhance the reliability of the network. The paper sized the BESS considering the system load and the outage data. In Ref. [7], the authors aimed to mitigate the fluctuations resulting from renewable energy resources and thus increase power reliability and quality. It allocated and sized the BESS to enhance the performance of the distribution network. The objective of the problem was defined to minimize the costs of voltage fluctuations, losses, and peak demand. In Ref. [8], authors proposed a multi-stage model to size a utility-scale BESS. The level of the penetration of dispersed PV panels was assumed to be increasing and the BESS had to accommodate the renewable solar generation in the short-time operation. Similarly [9], tried to allocate a BESS in distribution systems to provide voltage support for the distribution network. A network was assumed to bear a high penetration of PV power. In Ref. [10], the focus was on determining the optimal location and size of a BESS within a distribution network featuring a high number of renewable distributed generations. The objective of the BESS was to mitigate the costs associated with voltage deviations and power losses in the distribution network. Similarly [11], aimed to size the BESS to offer a wide array of flexibility services to the DSO. These services included addressing distribution network outages, non-wires-alternative solutions, and voltage support.

Some other papers focused on other types of services and ignored the effect of BESS on the operation of distribution networks. For instance Ref. [12], developed an interesting work on sizing a BESS in order to reduce the total cost of an extremely fast EV charging station. The sizing objective was to satisfy the station's demand during peak hours, to take advantage of the energy arbitrage and to reduce the total demand charges. Ref. [13] proposed an intelligent approach to size a BESS in a stand-alone microgrid. It also suggested utilizing hybridization sources to improve the frequency responses of the microgrid. In Ref. [14], authors assessed the sizing of a BESS situated in a photovoltaic-equipped energy community. The battery size was determined based on the community's energy consumption and peak demand profiles of households.

Nevertheless, there are a few studies that designed a BESS to provide frequency regulation or other TSO-related services. As examples, In Ref. [15], a BESS was planned to provide energy balance services. The methodology obtains the BESS minimum size to make a fully standalone system. In Ref. [16], authors designed a BESS for post-disturbance situations. The proposed multi-objective problem sites and sizes the BESS to firstly recover post-disturbance line overloads at transmission levels and secondly to arrest frequency excursion. The paper did not consider the BESS revenue obtained from providing these services. Ref. [17] sized a BESS to take advantage of energy arbitrage and provide frequency regulation services. Interestingly, the paper concludes that the BESS should be sized to its highest capacity power when it comes to providing frequency regulation services. Ref. [18] used a heuristic method to determine the optimal BESS placement and capacity in transmission and distribution networks. It performed a sensitivity analysis to allocate the BESS in a transmission network. It then solved power flow and economic dispatch problems to optimally size the BESS. The BESS was considered to minimize peak loads in a distribution network and provide frequency regulation support. In the mentioned literature, the BESS was not tailored to a specific frequency service type [19]. In addition [20], sized and allocated a BESS in a distribution network to provide support for the network as well as frequency regulation services designed for North America. However, frequency regulation services have different capacity market structures and technical requirements, such as activation characteristics and payment methods, which vary from country to country. For the practical application of the sizing problem using real-world data, it is crucial to select the country where the BESS is located. Subsequently, the planning problem can be developed based on the specific regulation service type. In this paper, we assume that the BESS is providing FCR-N service in Finland.

In terms of BESS operation for FCR-N provision, for example [21,22], developed a methodology for the operation of a BESS and electric vehicles to participate in FCR markets, respectively. The main focus was on the BESS and electric vehicle's battery scheduling to meet FCR markets' requirements and how the battery recovers its state of charge (SOC). Ref. [23] proposed bidding strategies for a BESS to participate in FCR capacity markets. Authors of [24] analyzed the operation of a BESS when it participates in FCR provision. According to the paper's results, when the FCR is remunerable, scheduling BESS leads to profits in central European countries. Moreover, the main focus of [25] was on the BESS real-time operation when it provides FCR-N. The aging impacts were also analyzed in that paper. However, these reviewed papers have

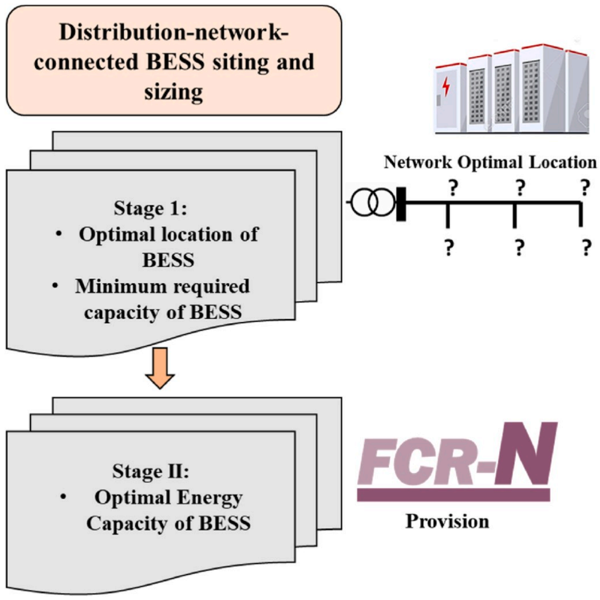


**Fig. 1.** The main architecture of the proposed model.

focused on the operation of the BESS and disregarded its capacity planning and location in the distribution network.

Table 1 provides a comparison between this paper and existing literature that presents models for designing a BESS. The second column indicates whether the paper addressed the issue of BESS allocation. The third column highlights whether the research included an analysis of BESS optimal capacity. In the fourth column, it is indicated whether the studied BESS offered flexibility provision services to the DSO, while the fifth column denotes whether the research explored any forms of TSO-related flexibility.

### *1.3. Contribution and organization*

Although the existing literature mainly focused on either DSO- or TSO-related services, this paper sites and sizes a distribution-network-connected BESS for providing both types of flexibility services at the same time. The BESS provides active power support so that the voltages of nodes/buses stay in their permissible range and the power flow constraints are respected. In addition, the proposed method boosts the BESS profit by providing FCR-N services. Currently, FCR-N is one of the profitable services and a suitable option for the BESS since the battery can react in both upward and downward directions, according to the frequency changes [26]. Also, Finnish TSO lists BESS as suitable a technology for providing FCR-N service. To the best of authors' knowledge, there does not exist any study that size the BESS for FCR-N provision. Hence, the main contribution of this paper can be summarized as follows.

1) It develops a two-stage model with two stochastic optimization problems. The first optimization problem allocates the BESS to help the DSO operate the local network in a secure way. The first stage also determines the minimum required size of the BESS. The second stage considers that the BESS is providing FCR-N and aims to determine the BESS size by maximizing its profits.
2) It proposes two different scenario extraction methodologies to develop the first- and second-stage stochastic optimization problems. For the first-stage, worst-case scenarios are extracted to ensure the secure operation of the local network. The second-stage scenarios are selected from the highest-probability scenarios within the historical horizon considered.
3) In the simulation section, the paper compares the BESS optimal size in four cases. It assesses the outcomes if the BESS provides FCR-N and if the BESS works with only day-ahead spot market prices. We use the real-world data of 2021 and 2022 to compare the models together. Finally, the paper analyzes the effects of cycle aging and BESS capacity fade on the profits.

The rest of the paper is organized as follows:

Section 3 provides the detail and the problem formulation of the proposed model. Section 4 introduces the case studies. Section 5 presents the results considering four different cases. Finally, section 6 concludes the paper.

## 2. Problem formulation

This paper considers that a private company owns and designs a specific type of Lithium-ion (Li-ion) BESS. The BESS consists of battery cells as well as other required equipment such as a converter, transformer, and the control system. The BESS is going to be utilized as a service to ensure the secure operation of the local distribution network and provides the DSO with its required flexibility. In addition, it aims to boost the profits by participating in FCR-N markets. In this regard, the BESS planning model has two main goals. First, it should be sited and sized to avoid violation of voltages and thermal limits of the network and secondly, to increase the profits by providing FCR-N services for the TSO. To achieve these two goals, the proposed planning model consists of two stages. The first stage finds the optimal placement of the BESS in the local network. It also determines the minimum charging and discharging power of the BESS to ensure the secure operation of the local network. The second stage, on the other hand, aims to minimize the costs of the BESS while simultaneously providing DSO-related and FCR-N services. Fig. 1 summarizes the main architecture of the paper.

The two-stage methodology offers distinct advantages including distinguishing between the BESS design for DSO- and TSO- related services, the possibility of considering worst-case scenarios to place and size the BESS for the worst-case situations of the distribution network and having the most probable scenarios for the profit maximization purpose of the second stage, and ultimately resulting in the formulation of two optimization problems with fewer dimensions.

### *2.1. Proposed model of lithium-ion battery energy storage system*

To develop the BESS model, experimental data from accelerated aging tests on a Li-ion battery cell in laboratory conditions were utilized. More details about the aging tests can be found in Ref. [27]. In the first stage, cell capacity characterization tests were measured in Ah at regular intervals of cycling, in this case at 0, 500, 800, 1200 and 1600 cycles. Then, *Cell Capacity* in Ah was converted to its energy capability in Wh at different cycle intervals, using the following equation:

$$E^{cell}(Cycles) = Cell\ Capacity\ (Cycles) * V_{cell} \quad (1)$$

Where, $V_{cell}$ is the cell voltage in volts. Simultaneously, the rated power of the cell was calculated at 0, 500, 800, 1200, and 1600 cycles. Fig. 2 presents the variations of cell energy and rated power in terms of cycles. Fig. 2 shows how the BESS capacity fade has a non-linear trend. The decreasing slope of the curve becomes steeper when the BESS is more aged. This will also have an impact on the BESS participation in FCR-N market and its profits. The effect will be calculated in section 5.3 of this paper.

To design a BESS, we need to build a battery pack. A battery pack is formulated by multiplying the cell energy capacity by the number of cells in series $N^{series}$ and in parallel $N^{parallel}$. The same equation can be applied for the battery pack's rated power:

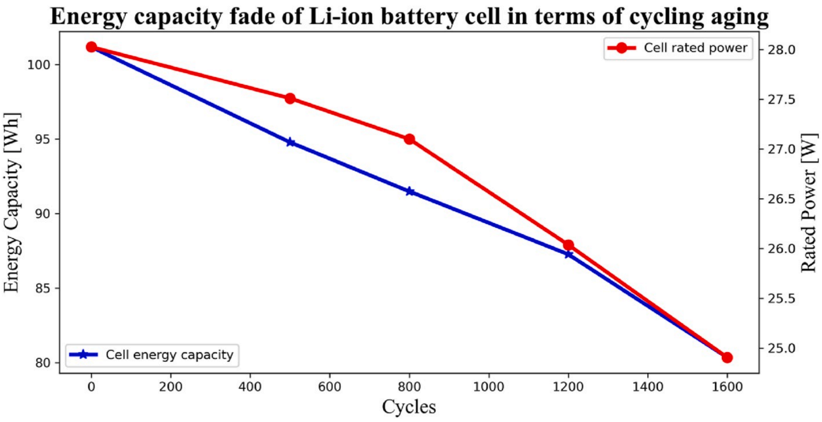


**Fig. 2.** BESS energy capacity face in terms of cycles for our Li-ion BESS.

$$E^{BESS} = N^{series} \times N^{parallel} \times E^{cell} \tag{2}$$

$$P^{BESS} = N^{series} \times N^{parallel} \times P^{cell} \tag{3}$$

Equations (2) and (3) can give us (4), which will be used in the second-stage optimization problem:

$$E^{BESS} = \frac{E^{cell}}{P^{cell}} P^{BESS} \tag{4}$$

### *2.2. Stage I: placement and minimum sizing in distribution network*

The first stage optimally places and designs the Li-ion BESS to avoid voltage violations and congestions within its distribution network. This stage is designed to simultaneously handle BESS placement and minimum sizing. We utilize a piecewise-linearized power flow model to obtain the optimal place and minimum flexible power and to check the voltage and current limits of the network. This model has been previously presented in Ref. [28]. If the local network needs upward flexibility at timeslot $t$, the BESS is discharged with power $P^{up,S1}_{n,t,s}$ and if the network asks for downward flexibility at $t$, the BESS is charged with power $P^{down,S1}_{n,t,s}$.

The objective is to find the minimum flexible power that helps operate the network in a secure way [29]:

$$\min_{P^{up,S1}_{cn,t,s}, P^{down,S1}_{cn,t,s}} \sum_t \sum_n P^{up,S1}_{cn,t,s} + P^{down,S1}_{cn,t,s} \tag{5}$$

The constraints associated with the active and reactive power balance are indicated with (6) and (7), respectively:

$$P^{PoC,S1}_{n=PoC,t,s} - P^{NL}_{n,t,s} + P^{up,S1}_{cn,t,s} - P^{down,S1}_{cn,t,s} - \sum_{n'} \begin{pmatrix} P^{+,S1}_{n,n',t,s} - P^{-,S1}_{n,n',t,s} \\ +R_{n,n'} SI^{S1}_{n,n',t,s} \end{pmatrix} + \sum_{n'} \Big( P^{+,S1}_{n',n,t,s} - P^{-,S1}_{n',n,t,s} \Big) = 0 \forall n, t, s \tag{6}$$

$$Q^{PoC,S1}_{n=poC,t,s} - Q^{NL}_{n,t,s} - \sum_{n'} \begin{pmatrix} Q^{+,S1}_{n,n',t,s} - Q^{-,S1}_{n,n',t,s} \\ +X_{n,n'} SI_{n,n',t,s} \end{pmatrix} + \sum_{n'} \Big( Q^{+,s1}_{n',n,t,s} - Q^{-,s1}_{n',n,t,s} \Big) = 0 \forall n, t, s \tag{7}$$

The flexible injected/consumed active power of BESS affects balance constraint (6). The balance constraint keeps the balance between the power coming into/leaving the local network at the Point of Coupling (PoC), the net load consumed at each node, the BESS's flexible power at node $n$, and the power flowing through the lines. Correspondingly, (7) ensures the reactive power balance in the local network. The effect of the power flowing through the lines on the voltage of each node is modeled using (8):

$$SV^{S1}_{n,t,s} - SV^{S1}_{n',t,s} - Z^2_{n,n'} SI^{S1}_{n,n',t,s} - 2R_{n,n'} \Big( P^{+,S1}_{n,n',t,s} - P^{-,S1}_{n,n',t,s} \Big) - 2X_{n,n'} \Big( Q^{+,S1}_{n,n',t,s} - Q^{-,S1}_{n,n',t,s} \Big) = 0 \forall n, n', t, s \tag{8}$$

Where, the squared voltage and squared current are replaced with two auxiliary variables *SV* and *SI* to linearize the model. These two variables should not go beyond the range between their maximum and minimum values, as (9) and (10) state:

$$\left(v^{min}_n\right)^2 \le SV^{S1}_{n,t,s} \le \left(v^{max}_n\right)^2 \forall n, t, s \tag{9}$$

$$\left(I^{min}_{n,n'}\right)^2 \le SI^{S1}_{n,n',t,s} \le \left(I^{max}_{n,n'}\right)^2 \forall n, n', t, s \tag{10}$$

The above constraints limit the active and reactive power flowing through the lines to avoid congestion within the network:

$$P^{+,S1}_{n,n',t,s} + P^{-,S1}_{n,n',t,s} \le v^{rated} I^{max}_{n,n'} \forall n, n', t, s \tag{11}$$

$$Q^{+,S1}_{n,n',t,s} + Q^{-,S1}_{n,n',t,s} \le v^{rated} I^{max}_{n,n'} \forall n, n', t, s \tag{12}$$

Piecewise linearization is applied to the power flow constraints. These constraints are stated below [30]:

$$\left(v^{rated}\right)^2 SI^{S1}_{n,n',t,s} = \sum_j (2j-1) \Delta S_{\boldsymbol{n},\boldsymbol{n'}} \Delta P^{S1}_{\boldsymbol{n},\boldsymbol{n'},j,t,s} + \sum_j (2j-1) \Delta S_{\boldsymbol{n},\boldsymbol{n'}} \Delta Q^{S1}_{\boldsymbol{n},\boldsymbol{n'},j,t,s} \forall n, n', t, s \tag{13}$$

$$P^{+,S1}_{\boldsymbol{n},\boldsymbol{n'},t,s} + P^{-,S1}_{\boldsymbol{n},\boldsymbol{n'},t,s} = \sum_j \Delta P^{S1}_{\boldsymbol{n},\boldsymbol{n'},j,t,s} \forall n, n', t, s \tag{14}$$

$$Q^{+,S1}_{\boldsymbol{n},\boldsymbol{n'},t,s} + Q^{-,S1}_{\boldsymbol{n},\boldsymbol{n'},t,s} = \sum_j \Delta Q^{S1}_{\boldsymbol{n},\boldsymbol{n'},j,t,s} \forall n, n', t, s \tag{15}$$

$$0 \le \Delta P^{S1}_{\boldsymbol{n},\boldsymbol{n'},j,t,s} \le \Delta S_{\boldsymbol{n},\boldsymbol{n'}} \forall n, j, n', t, s \tag{16}$$

$$0 \le \Delta Q^{S1}_{\boldsymbol{n},\boldsymbol{n'},j,t,s} \le \Delta S_{\boldsymbol{n},\boldsymbol{n'}} \forall n, j, n', t, s \tag{17}$$

$$\Delta S_{\boldsymbol{n},\boldsymbol{n'}} = \frac{v^{rated} I^{max}_{\boldsymbol{n},\boldsymbol{n'}}}{N^{par}} \forall n, n', t, s \tag{18}$$

The following constraints determine the optimal BESS's place (OBP)

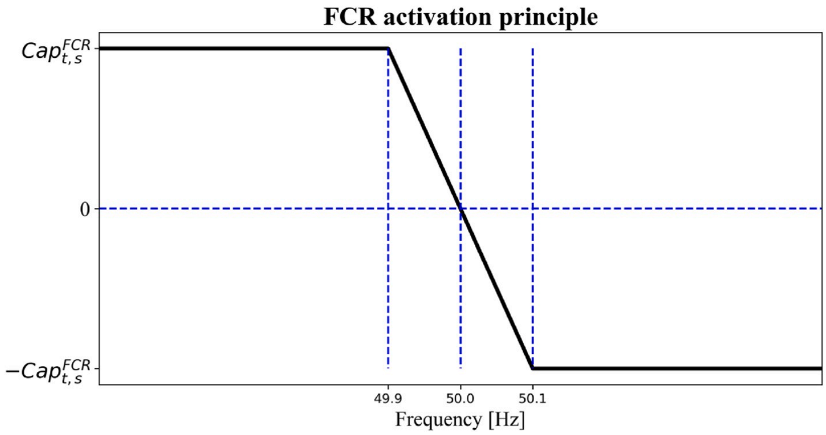


**Fig. 3.** Activation of FCR-N active power capacity according to the system frequency.

which is chosen among candidate nodes (cn):

$$P_{cn,t,s}^{up,S1} \leq Mu_{cn}^{BESS} \forall cn, t, s \tag{19}$$

$$P_{cn,t,s}^{down,S1} \leq Mu_{cn}^{BESS} \forall cn, t, s \tag{20}$$

$$\sum_{cn} u_{cn}^{BESS} \leq N^{BESS} \tag{21}$$

Where, $M$ is a large number. Constraints (19), (20) and (21) indicate that the flexible power should be injected/consumed only at BESS-located nodes. The binary variable $u_{cn}^{BESS}$ equals one for the optimal nodes at which the BESSs are going to be located. The other nodes, on the other hand, have a zero $u_{cn}^{BESS}$. The maximum number of BESSs, i.e., $N^{BESS}$, is assumed to be a parameter that was predefined by the BESS designers.

In addition, the below constraints specify positive variables:

$$P_{cn,t,s}^{up,S1}, P_{cn,t,s}^{down,S1}, P_{n,n',t,s}^{+,S1}, P_{n,n',t,s}^{-,S1}, Q_{n,n',t,s}^{+,S1}, Q_{n,n',t,s}^{-,S1}, \Delta P_{\boldsymbol{n},\boldsymbol{n}',j,t,s}^{S1}, \Delta Q_{\boldsymbol{n},\boldsymbol{n}',j,t,s}^{S1} \geq 0 \tag{22}$$

After solving the minimization problem (5)-(22), the optimal flexible power of the worst-case scenario determines the minimum BESS rated power. The worst-case scenario obtained from the timeslot and scenario in which $P_{cn,t,s}^{up,S1}$ *or* $P_{cn,t,s}^{down,S1}$ are maximum. These optimal values and their maximums are denoted by $P_{n=OBP,t,s}^{up,S1}$, $P_{n=OBP,t,s}^{down,S1}$, $\max(P_{n=OBP,t,s}^{up,S1})$, *and* $\max(P_{n=OBP,t,s}^{down,S1})$, respectively. OBP is the optimal BESS' place that is obtained by solving (5)–(22). Moreover, the BESS' rated power should support both charging and discharging of the BESS. Therefore, minimum rated power of the BESS, $P^{BESS,min,S1}$, yields as follows:

$$P^{BESS,min,S1} = \max\left(\max\left(P_{n=OBP,t,s}^{up,S1}\right), \max\left(P_{n=OBP,t,s}^{down,S1}\right)\right) \tag{23}$$

Finally, the OBP and $P^{BESS,min,S1}$ are sent to the second stage.

*2.3. Stage II: sizing and cost minimization through FCR-N participation*

After receiving the optimal location and minimum rated power of the BESS, the second stage boosts the revenues by providing FCR-N services. This stage aims to find the optimal energy capacity and rated active power $P$ of the BESS that leads to the maximum revenue. Thus, the objective of the second stage minimizes the daily net costs associated with the battery considering different scenarios:

min $OF$

$$OF = \underbrace{\pi^{DCC} E^{BESS}}_{Daily-based\ Capital\ Cost} + \sum_s prob_s^{S2} \sum_t \Bigg\{ \underbrace{\pi^{M\&O}\left(P_{n=OBP,t,s}^{ch,da} + P_{n=OBP,t,s}^{dis,da} + P_{n=OBP,t,s}^{FCR-up} + P_{n=OBP,t,s}^{FCR-down}\right)}_{M\&O\ Cost} + Cost_{t,s}^{cycle} - \underbrace{\pi_t^{FCR} Cap_{t,s}^{FCR}}_{FCR\ Capacity\ Revenue}$$
$$- \underbrace{\pi_t^{reg,up} P_{n=OBP,t,s}^{FCR-up}}_{Activation\ Revenue} + \underbrace{\pi_t^{reg,down} P_{n=OBP,t,s}^{FCR-down}}_{Activation\ Cost} - \underbrace{\pi_t^{da} P_{n=OBP,t,s}^{dis,da}}_{DA\ Revenue} + \underbrace{\pi_t^{da} P_{n=OBP,t,s}^{ch,da}}_{DA\ Cost} \Bigg\} \Delta t \tag{24}$$

Where the *"Daily – based Capital Cost"* of the BESS is assumed to be a linear function of the BESS's capacity. The *"M&O Cost"* represents the maintenance and operational cost of the BESS which is considered a linear function of the BESS's charging and discharging power. The cycle cost of BESS is denoted by *"*$Cost_{t,s}^{cycle}$*"*. The BESS which is participating in FCR-N markets receives capacity revenue for reserving its capacity, indicated by *"FCR Capacity Revenue"* e. The BESS reserved capacity for FCR is then activated according to the frequency. If the capacity is activated in the upward direction, the BESS is charged and receives revenue, called "*Activation Revenue*". Otherwise, if the activation is downward, the BESS is discharged and incurs costs, called "*Activation Cos t*". This paper considers that in the cases where the BESS is not providing FCR-N, for example when the BESS is being recovered, it can be charged and discharged with day-ahead spot market prices. Hence, The BESS receives revenue, *"DA Revenue"*, based on the day-ahead spot market prices if it is discharged. If the BESS is charged with the day-ahead spot market prices, it should pay *"DA Cost"*.

The cost minimization objective function is constrained by the balance equation:

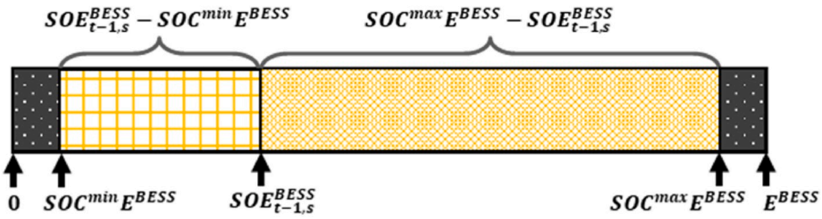


**Fig. 4.** The available BESS state of energy at the beginning of timeslot t.

$$P^{PoC,S2}_{n=PoC,t,s} + P^{FCR-up}_{n=OBP,t,s} - P^{FCR-down}_{n=OBP,t,s} - P^{NL}_{n,t,s} + P^{dis,da}_{n=OBP,t,s} - P^{ch,da}_{n=OBP,t,s} - \sum_{n'} \left( \begin{array}{c} P^{+,S2}_{n,n',t,s} - P^{-,S2}_{n,n',t,s} \\ + R_{n,n'} SI^{S2}_{n,n',t,s} \end{array} \right) + \sum_{n'} \left( P^{+,S2}_{n',n,t,s} - P^{-,S2}_{n',n,t,s} \right) = 0 \forall n,t,s \quad (25)$$

Where (25) states that the FCR-N downward-activated and the charging power traded with day-ahead prices consume power at the BESS node/bus. Correspondingly, the FCR-N upward-activated and discharging power traded with day-ahead prices inject power into the BESS node. The net load at each node, $P^{NL}_{n,t,s}$, consumes power whereas the power leaves/enters the local network through the PoC node can have both positive and negative values. If $P^{PoC,S2}_{n=PoC,t,s}$ is positive, the power is consumed in the local network while negative $P^{PoC,S2}_{n=PoC,t,s}$ indicates that the power is fed from the local network. It should be highlighted that PoC and OBP are two different nodes unless the first stage determines that the BESS can be put at the PoC. The following constraints restrict the power capacity offered to the FCR-N capacity market:

$$Cap^{FCR}_{t,s} + P^{ch,da}_{n=OBP,t,s} \leq P^{BESS} \forall t,s \quad (26)$$

$$Cap^{FCR}_{t,s} + P^{dis,da}_{n=OBP,t,s} \leq P^{BESS} \forall t,s \quad (27)$$

The power capacity offered to the FCR-N market plus the power traded with day-ahead prices should not exceed the rated power of the BESS. The FCR-N power capacity should be symmetrical. It means that the BESS needs to submit a power capacity that is able to be activated in both directions, upward and downward directions. Taking into account the downward direction, the FCR-N power capacity and the day-ahead charging power should be lower than the BESS rated power, as denoted by (26). Regarding the upward direction, (27) states that the FCR-N power capacity plus the day-ahead discharging power is upper limited by the rated active power of the BESS.

Equations (28) and (29) relate the upward and downward activated power to the power capacity:

$$P^{FCR-up}_{n=OBP,t,s} = \frac{\Delta f^{up}_{t,s}}{0.1} Cap^{FCR}_{t,s} \forall t,s \quad (28)$$

$$P^{FCR-down}_{n=OBP,t,s} = \frac{\Delta f^{down}_{t,s}}{0.1} Cap^{FCR}_{t,s} \forall t,s \quad (29)$$

The active power capacity of the BESS is submitted to the FCR-N

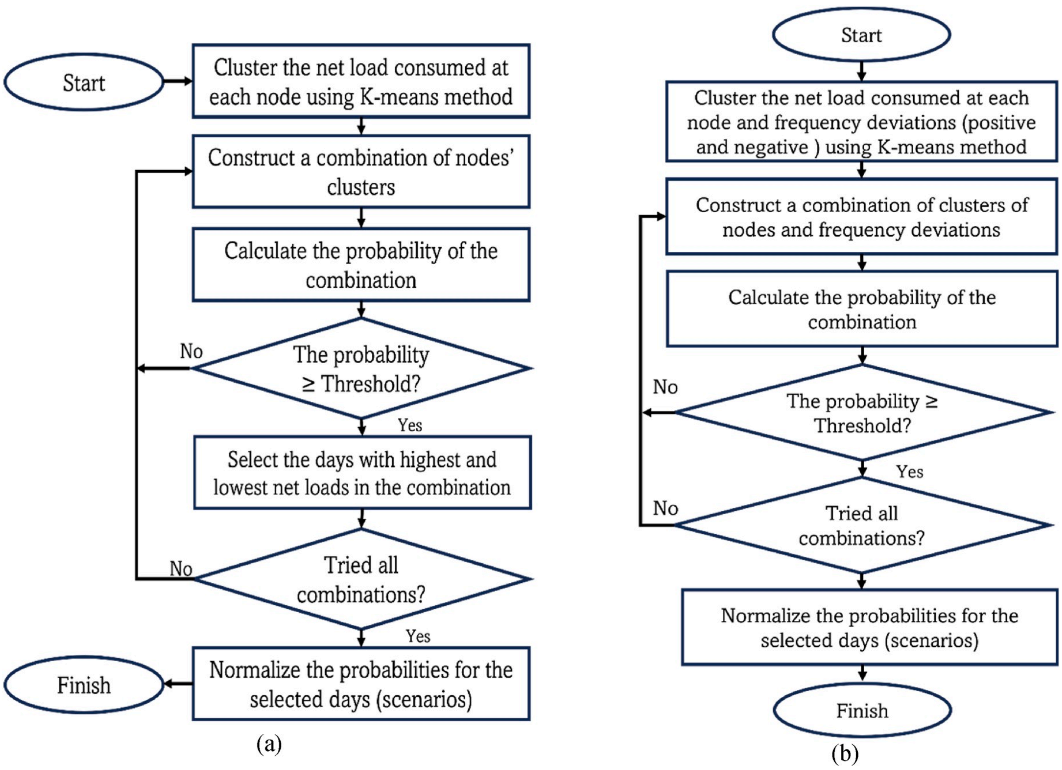


**Fig. 5.** Flowcharts of (a) Algorithm I, first-stage scenario generation & reduction and (b) Algorithm II, second-stage scenario generation & reduction.

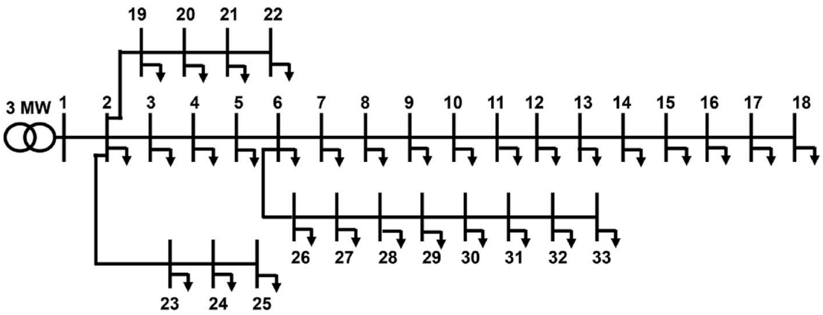


**Fig. 6.** Single diagram schematic of IEEE 33-bus radial distribution system.

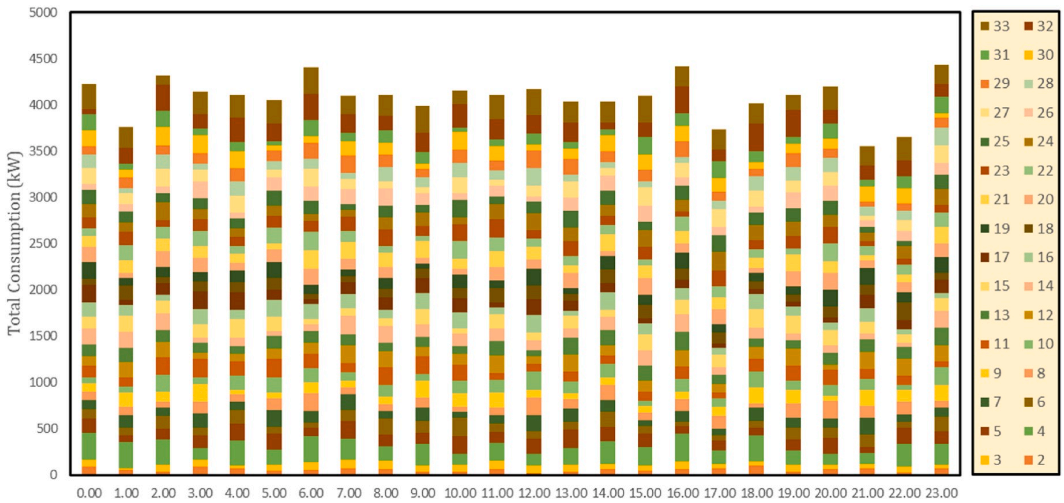


**Fig. 7.** Hourly net load considered for IEEE 33-bus radial distribution system.

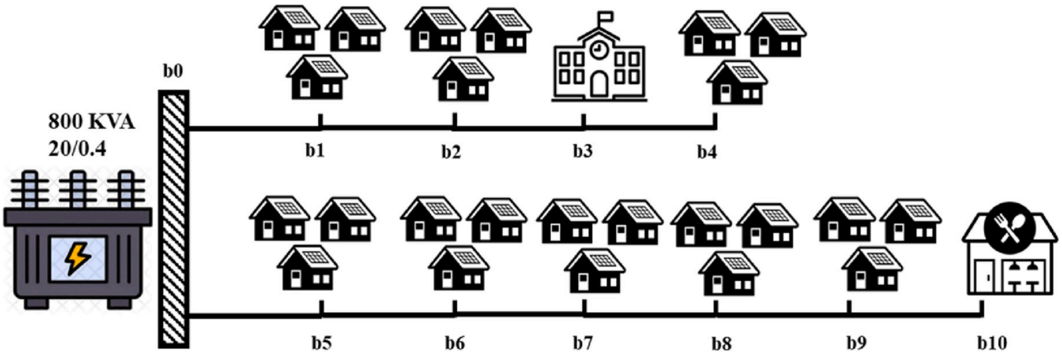


**Fig. 8.** The Finnish local network considered in the paper.

capacity market one day before the actual activation. If the power capacity is accepted, the BESS needs to activate the power capacity according to the frequency. Fig. 3 illustrates the FCR-N activation principle. If the frequency is greater than 50 Hz, the BESS activates in a downward direction. Otherwise, if the frequency is lower than 50 Hz, the BESS activates in an upward direction.

As Fig. 3 shows, the amount of activation should be proportional to the frequency deviation if frequency deviations are lower than 0.1 Hz. Since the paper considers 1-h timeslot, hourly frequency deviations are calculated as follows:

$$\Delta f_t^{up} = \sum_{q=1}^{q=N_q} \left|\Delta f_{q,t}\right| \Delta q \quad if \quad \Delta f_{q,t} \geq 0 \forall t \tag{30}$$

$$\Delta f_t^{down} = \sum_{q=1}^{q=N_q} \left|\Delta f_{q,t}\right| \Delta q \quad if \quad \Delta f_{q,t} < 0 \forall t \tag{31}$$

$$\Delta f_{q,t} = 50 - f_{q,t} \forall t, q \tag{32}$$

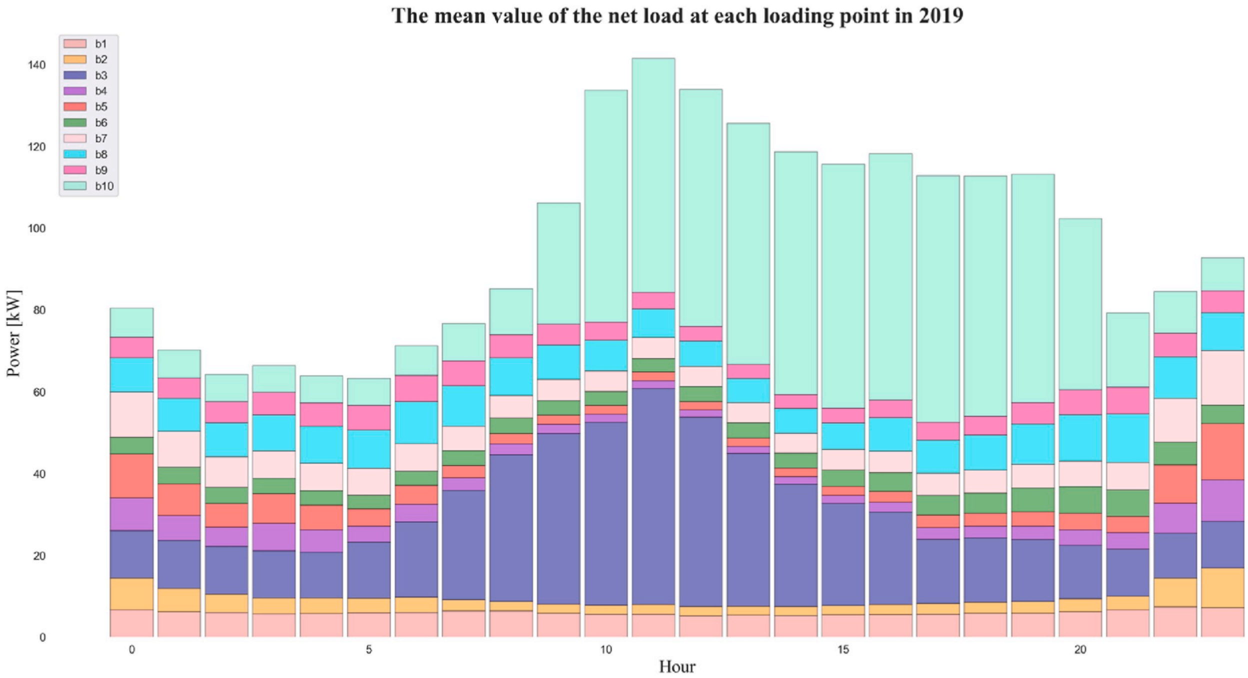


**Fig. 9.** Hourly net loads' mean values considering one year.

**Table 2**
Used BESS parameters.

| $SOC^{min}$ | $SOC^{max}$ | $\eta^{ch}/\eta^{dis}$ | $E^{cell}$ [kW] | $P^{cell}$ [kW] | Cycle life | $\pi^{cycle}$ [€/kWh] | $\pi^{DCC}$ [€/kWh] | $\pi^{M\&O}$ [€/kWh] |
|---|---|---|---|---|---|---|---|---|
| 0.05 | 0.95 | 90 % | 0.1 | 0.028 | 6000 | 0.1 | 0.095 | 0.001 |

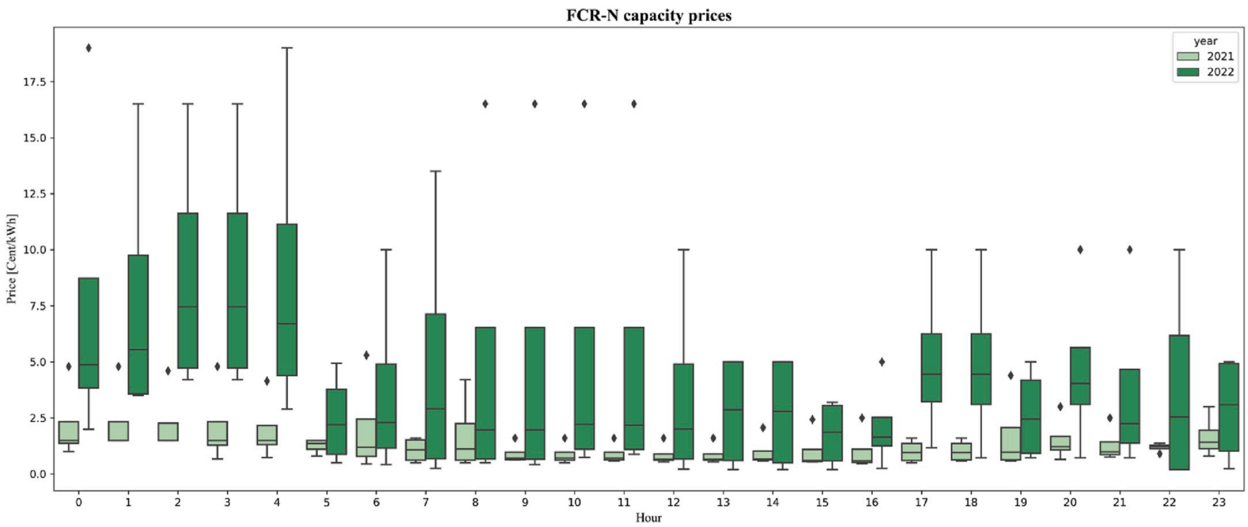


**Fig. 10.** Box plot of FCR-N capacity prices for scenarios of 2021 and 2022.

$$\Delta f_{q,t} = 0.1 \quad if\ f_{q,t} \geq 50.1\ or\ f_{q,t} \leq 49.9 \tag{33}$$

It is assumed that the frequency is measured in every $\Delta q$, where $\Delta q < \Delta t$. We consider $\Delta t$ to be 1 h and the frequency is measured every 3 min, i.e., $\Delta q = 1/20$ and $N_q = 20$. According to the technical requirements of the FCR-N, the full capacity should be activated in less than 3 min. Thus, 3-min frequency measurement can be acceptable. The mean value of all positive frequency deviations at time slot $t$ is equal to $\Delta f_t^{up}$. This value is multiplied by the power capacity and shows the upward activation, $P_{n=OBP,t,s}^{FCR-up}$, as (28) states. Correspondingly, the power capacity times the

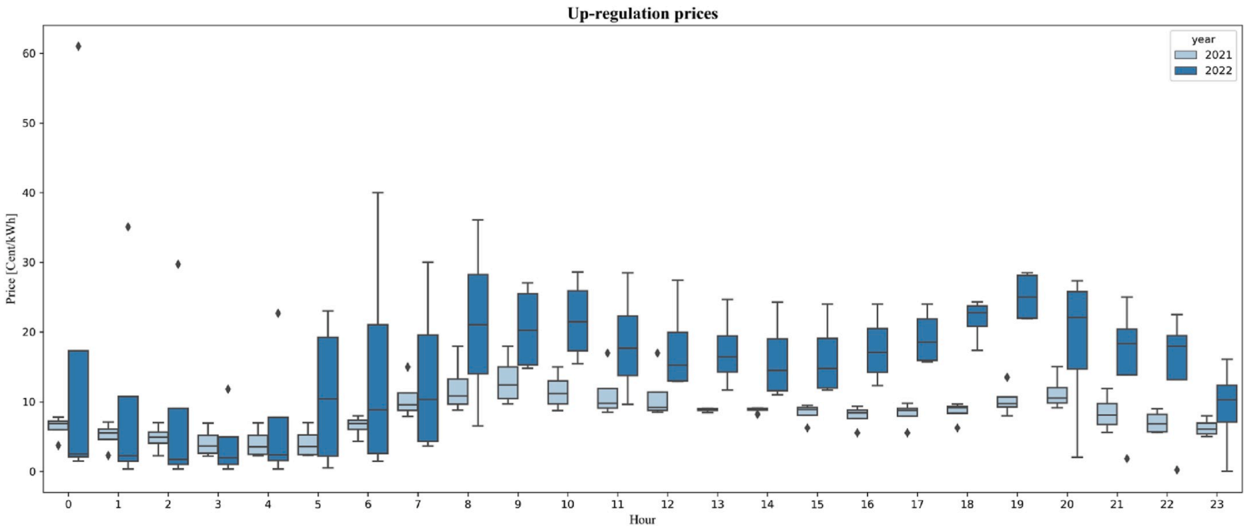


**Fig. 11.** Box plot of up-regulation prices for scenarios of 2021 and 2022.

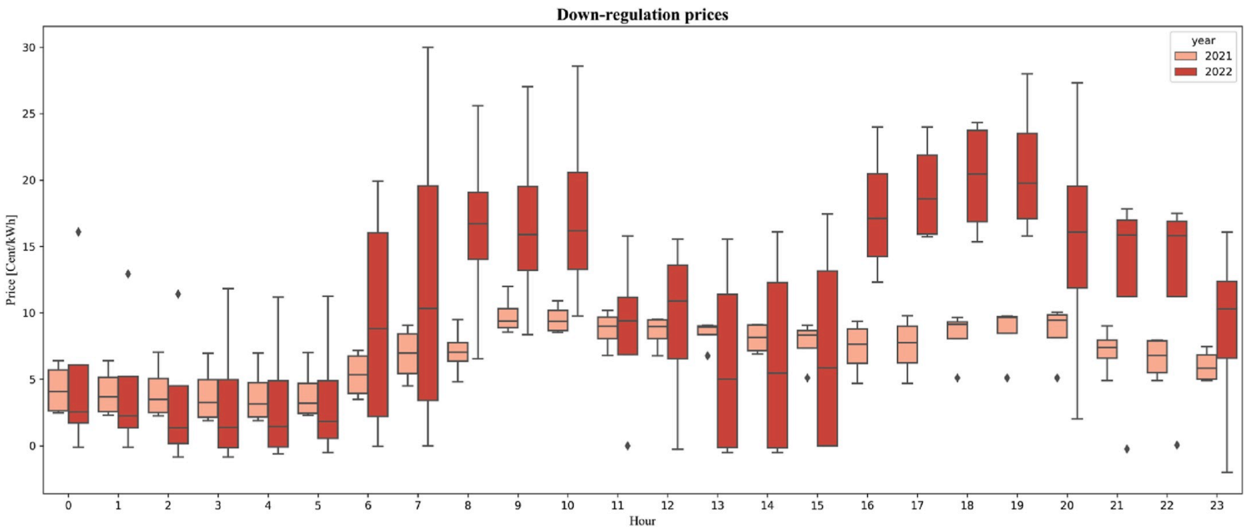


**Fig. 12.** Box plot of down-regulation prices for scenarios of 2021 and 2022.

**Table 3**
The aggregated capacities and the location of the BESS(s) required for the secure operation of IEEE 33 bus system if the number of BESSs varies.

| Number of BESSs | Optimum location (nodes) | Aggregated power capacities of all BESSs [kW] | Aggregated energy capacities of all BESSs [kWh] |
|---|---|---|---|
| 1 | 12 | 2799.25899 | 10 106.8281 |
| 2 | 16, 33 | 1829.17907 | 6604.3186 |
| 3 | 15, 18, 33 | 2147.44668 | 7753.4356 |
| 4 | 14, 16, 18, 33 | 2387.43912 | 8619.9372 |
| 5 | 14, 16, 17, 18, 33 | 2470.10113 | 8918.3915 |
| 6 | 13, 14, 16, 17, 18, 33 | 2602.51608 | 9396.4805 |
| 7 | 13, 14, 15, 16, 17, 18, 33 | 2694.09477 | 9727.12882 |
| 8 | 13, 14, 15, 16, 17, 18, 32, 33 | 2826.10600 | 10203.7602 |

mean value of all negative frequency deviations equals the downward FCR-N activated power, $P^{FCR-down}_{n=OBP,t,s}$, represented by (29).

Equations (34) and (35) show the state of energy at the end of each time slot, which is affected by BESS charging and discharging power. BESS charging power includes upward activated power and the power charged with day-ahead prices. BESS discharging power consists of downward activated power and power discharged with day-ahead prices.

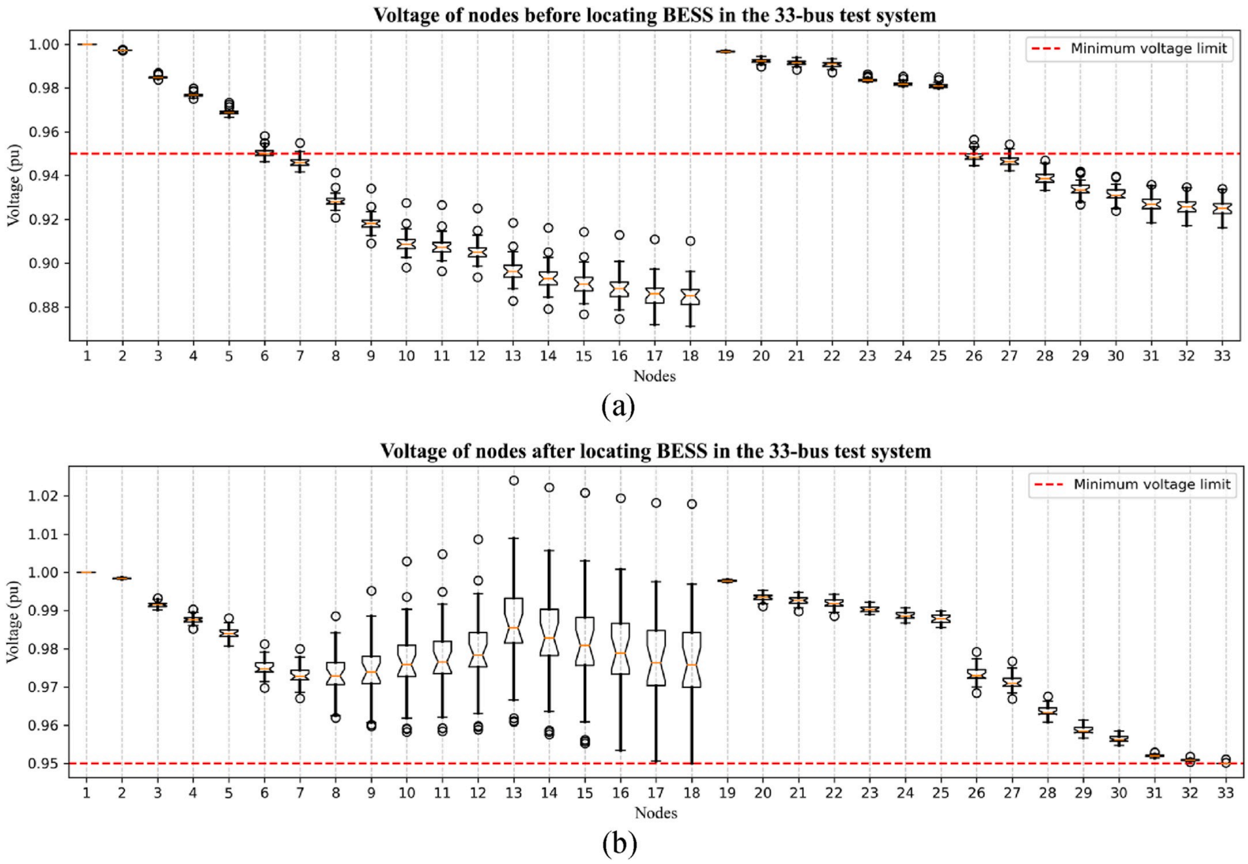


**Fig. 13.** The node voltages before and after placing a BESS at node 12 within IEEE 33 bus system.

$$SOE^{BESS}_{t,s} = SOE^{BESS}_{t-1,s} + \left\{ \eta^{ch}\left(P^{ch,da}_{n=OBP,t,s} + P^{FCR-down}_{n=OBP,t,s}\right) - \frac{1}{\eta^{dis}}\left(P^{dis,da}_{n=OBP,t,s} + P^{FCR-up}_{n=OBP,t,s}\right)\right\}\Delta t \forall t \geq 2, \forall s \tag{34}$$

$$SOE^{BESS}_{t,s} = SOE^{BESS,ini}_{s} + \left\{ \eta^{ch}\left(P^{ch,da}_{n=OBP,t,s} + P^{FCR-down}_{n=OBP,t,s}\right) - \frac{1}{\eta^{dis}}\left(P^{dis,da}_{n=OBP,t,s} + P^{FCR-up}_{n=OBP,t,s}\right)\right\}\Delta t \forall t = 1, \forall s \tag{35}$$

According to the technical requirements for FCR-N provision, a BESS must be able to get fully activated for at least 30 min in each direction [31]. Equations (36) and (37) ensure that the available state of energy of the BESS at the beginning of timeslot $t$ (or at the end of timeslot $t-1$) should be higher than 30-min (½ hour) activation of FCR-N power capacity in either direction. Fig. 4 illustrates the available BESS state of energy at the beginning of timeslot t, which also refers to the terms on the right side of (36) and (37).

$$SOE^{BESS}_{t-1,s} - E^{BESS}SOC^{min} \leq \frac{1}{2}Cap^{FCR}_{t,s} \forall t, s \tag{36}$$

$$\frac{1}{2}Cap^{FCR}_{t,s} \leq SOC^{max}E^{BESS} - SOE^{BESS}_{t-1,s} \forall t, s \tag{37}$$

Constraint (38) indicates minimum and maximum permissible values for the BESS state of energy at time slot $t$.

$$E^{BESS}SOC^{min} \leq SOE^{BESS}_{t,s} \leq E^{BESS}SOC^{max} \forall t, s \tag{38}$$

The minimum power that yields from the first stage restricts the BESS rated power as follows:

$$P^{BESS} \leq P^{BESS,min,S1} \tag{39}$$

The relationship between the BESS rated power and the BESS energy capacity is stated by (40). This relationship applies the same constraint, (41), on the minimum BESS energy capacity:

$$E^{BESS} = \frac{E^{cell}}{P^{cell}}P^{BESS} \tag{40}$$

$$E^{BESS} \leq \frac{E^{cell}}{P^{cell}}P^{BESS,min,S1} \tag{41}$$

In order to estimate the cost of BESS from cycling aging, it is assumed that we have $\pi^{cycle}$ which is a price of cycling aging for one kWh of consumed/injected energy in each cycle. Since the half cycle includes one full charging or discharging [32], the BESS "kWh cycle" is equal to $\frac{1}{2}\eta^{ch}(P^{ch,da}_{n=OBP,t,s} + P^{FCR-down}_{n=OBP,t,s})\Delta t$ when the BESS is being charged and $\frac{1}{2}\frac{1}{\eta^{dis}}(P^{dis,da}_{n=OBP,t,s} + P^{FCR-up}_{n=OBP,t,s})\Delta t$ when it is being discharged at $t$. Thus, the cycling cost is estimated as follows:

$$Cost^{cycle}_{t,s} = \pi^{cycle}\left\{\frac{1}{2}\left(P^{ch,da}_{n=OBP,t,s} + P^{FCR-down}_{n=OBP,t,s}\right) + \frac{1}{2}\left(P^{dis,da}_{n=OBP,t,s} + P^{FCR-up}_{n=OBP,t,s}\right)\right\}\Delta t \forall t, s \tag{42}$$

The distribution network's constraints can also bind the BESS operation and its maximum energy capacity. They need to be considered in the problem as well:

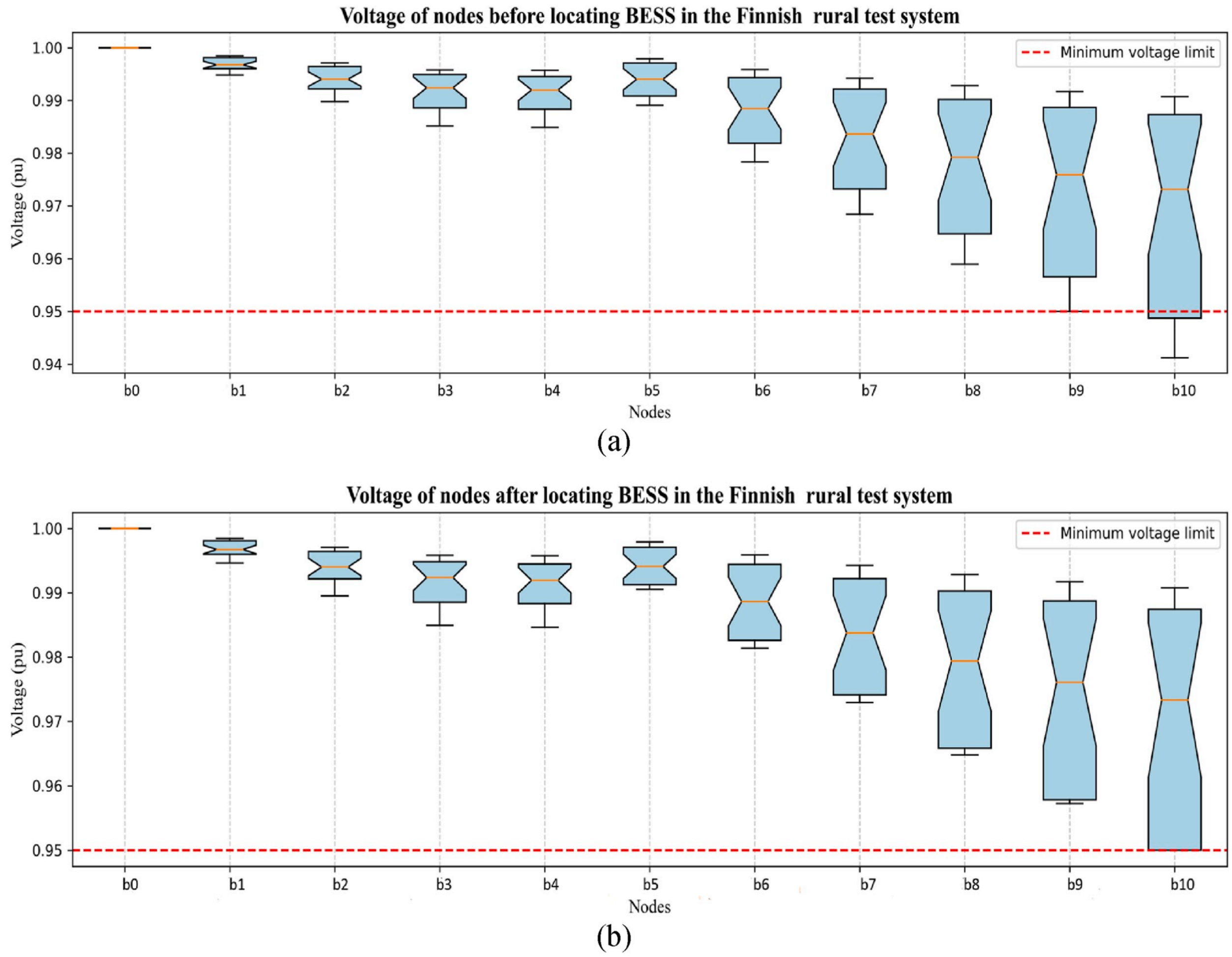


**Fig. 14.** The voltage of nodes before and after placing a BESS at node 12 of the Finnish test system.

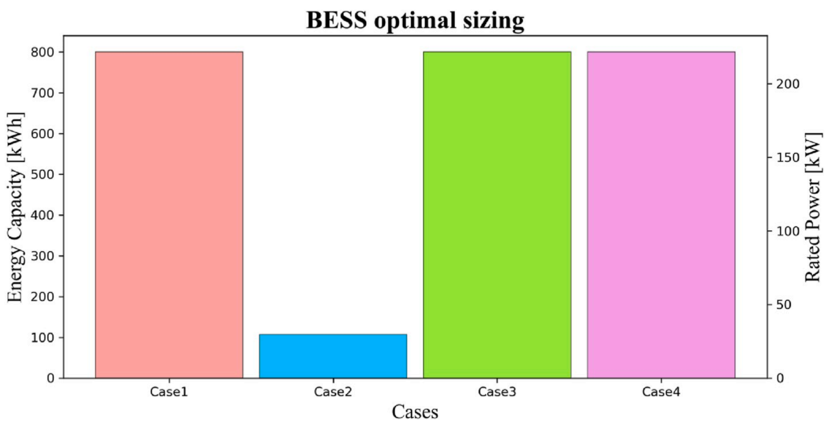


**Fig. 15.** The optimal rated power and energy capacity of the BESS considering four cases.

(8) – – (43)

Finally, positive variables are indicated in the following:

$$P^{ch,da}_{n=OBP,t,s}, P^{FCR-down}_{n=OBP,t,s}, P^{dis,da}_{n=OBP,t,s}, P^{FCR-up}_{n=OBP,t,s}, Cap^{FCR}_{t,s}, P^{BESS}, E^{BESS}, P^{+,S2}_{n,n',t,s}, P^{-,S2}_{n,n',t,s}, Q^{+,S2}_{n,n',t,s}, Q^{-,S2}_{n,n',t,s} \geq 0 \forall n, n', t, s \quad (44)$$

By solving minimization problem (24)-(44), the BESS optimal energy capacity and rated power is obtained.

### 2.4. Scenario extraction

This paper deploys two different methods to extract representative scenarios for the first and for the second stage. The first stage aims to find the minimum required flexible power for the worst-case scenarios. In this way, we are looking for scenarios that may cause the worst situations for the network's operation. Algorithm I is proposed to extract these scenarios. Fig. 5 illustrates the algorithms and clarifies the stages of scenarios' generation and reduction for the first and second stages.

**Algorithm I:** First-stage Scenario Generation & Reduction

**Input:** Historical data on daily net load of each node for each hour
**Output:** Scenarios for a daily net loads of each node for each hour
Time series **clustering using K-means:**

1 For each node:
- Determine optimal number of clusters for the daily net load using Elbow Method
- Categorize daily net loads (365 samples) into $N^{NL,S1}$ clusters

2 Calculate the probability for each combination of nodes' clusters
**Scenario** generation **& reduction:**

3 Select the combination with probabilities higher than the threshold
4 Among the selected combinations:
- The days in which the highest total hourly loads and the highest hourly production (or lowest hourly loads) happened, are selected

5 Normalize the probability of the final selected scenarios

Since the second-stage problem deals with the net cost minimization, the scenarios with highest probabilities are more important. Algorithm II is utilized to extract the second-stage scenarios.

**Algorithm II:** Second-stage Scenario Generation & Reduction

**Input:** Historical daily data for

1) Net loads of each node for each hour
2) Positive frequency deviations for each hour, calculated using (26)
3) Negative frequency deviations for each hour, calculated using (27)

**Output:** Scenarios for

1) A daily net loads of each node for each hour
2) The hourly positive and negative frequency deviations

**Time series clustering using K-means:**

1 For each node:
- Determine optimal number of clusters for the daily net load using Elbow Method
- Categorize daily net loads (365 samples) into $N^{NL,S2}$ clusters

2 Determine optimal number of clusters for positive and negative frequency deviations using Elbow Method
3 Categorize daily positive and negative frequency deviations into $N^{f+,S2}$ and $N^{f-,S2}$, respectively
4 Calculate the probability for each combination of nodes' clusters and frequency deviations' clusters
**Scenario generation & reduction:**

5 Select the days among a combination with the probability higher than the threshold
6 Normalize the probability of the final selected scenarios

## 3. Case studies

### 3.1. IEEE 33-bus radial distribution system

The first case study analyzes the optimal location for the BESS to ensure the secure operation of the network. Fig. 6 illustrates the distribution network, with further details and line parameters provided in Ref. [33]. Using nominal loads, we generated a worst-case scenario for the network's net loads. Fig. 7 displays bar plots depicting the net consumption at various nodes within the system.

### 3.2. Finnish rural network

Fig. 8 illustrates the modified typical Finnish rural network that was presented by Ref. [34]. In the case study, a 800-kVA MV/LV- transformer feeds two LV feeders. The distance between each loading point is 100 m. The network's details including the line impedance's, resistance's, reactance's, and line maximum currents can be found in Ref. [34]. Each loading point feeds three detached houses that has a PV panel, except for loading points b3 and b10 that feed a school and a big restaurant, respectively. We used the hourly net load of detached houses, a school and a restaurant in Vaasa, Finland during 2019. Fig. 9 depicts the net loads' mean values for each hour considering one year. The restaurant and school's net loads are considerably higher than those of detached houses at other nodes. Contrary to the PV-panel-equipped detached houses whose net load decreases during daytime, the school net load experiences a peak at 11 a.m. The net load of the restaurant increases during 10–20.

Table 2 denotes the detailed data on the BESS that was used in our paper. The parameters $E^{cell}$, $P^{cell}$, and cycle life were obtained from the field experiment [27] whereas the data of daily-based BESS cost was estimated based on the value of BESS energy rating cost and the BESS lifespan proposed by Ref. [12]."Algorithm I" (presented in section 3.4) was used in the first stage and it selected 10 extreme scenarios from the historical data to determine the location of the BESS and to find the minimum required rated power of the BESS. In the second stage, "algorithm II", proposed by section 3.4, selected 4 scenarios that have the highest probabilities. The historical horizon is assumed to span one year, specifically the most recent years, 2021 and 2022. It should be noted that our implementation is constrained by the availability of consumption data for a single year.

Regarding frequency data, we used the frequency of the Finnish power system that was measured in Fingrid's operation control system, every 3 min. Fingrid is the Finnish TSO. The data is available in Ref. [35]. The FCR-N hourly market prices as well as up-regulation and down-regulation prices were also extracted from Fingrid's open data website [36–38] whereas the day-ahead spot market prices are obtained

**Table 4**
Energy capacity of the BESS in case of relaxing the maximum energy capacity limit.

| Cases | Case 1 | Case 2 | Case 3 | Case 4 |
|---|---|---|---|---|
| Energy capacity [MWh] | 5.3 | 0.1 | 50 | 4.07 |

**Table 5**
Daily profit obtained by BESS for different cases.

| Cases | Case 1 | Case 2 | Case 3 | Case 4 |
|---|---|---|---|---|
| Profit [€] | 55.80 | −2.18 | 280.30 | 77.47 |

from Entsoe Transparency Platform [39].

In this paper, the BESS is sized according to four cases.

**Case 1).** Price and frequency data of year 2021 and the BESS net cost minimization based on FCR-N and spot market prices (proposed method)

**Case 2).** Price and frequency data of year 2021 and the BESS net cost minimization based on only spot market prices

**Case 3).** Price and frequency data of year 2022 and the BESS net cost minimization based on FCR-N and spot market prices (proposed method)

**Case 4).** Price and frequency data of year 2022 and the BESS net cost minimization based on only spot market prices

This means that in the second and fourth cases, the BESS is not participating in FCR-N provision. Thus, it is only charged and discharged with the day-ahead spot market prices. Regarding the extracted scenarios, Figs. 10–12 compare 2021 prices with those of 2022. As the figure shows, prices of 2022 have increased at most of timeslots.

We consider that the BESS energy capacity cannot exceed that of the transformer. Thus, the BESS capacity cannot be higher than 800 kWh. It should be noted that we used the same data as the net loads of 2021 and 2022 due to our limited data on the households' net loads in Finland.

## 4. Simulation results

We utilized the CVXPY package in Python to model both optimization problems [40]. For problem-solving, we employed the Gurobi solver on a desktop PC equipped with a 2.4 GHz CPU and 6 Gigabytes of RAM. For the first-stage problem, the solution process took 31.7 s for the Finnish case study and 144.4 s for the IEEE 33 bus system. The completion time for solving the second-stage problem was 310 s.

### 4.1. First-stage results

Firstly, the first-stage optimization problem was executed for the IEEE 33-bus system. We systematically increased the maximum number of BESSs that can be connected to the system by modifying the right side of equation (21). Through this approach, we compared the aggregated capacities of all BESSs needed to ensure a secure distribution network. The results are presented in Table 3. As shown in the table, increasing the number of BESSs up to 7 leads to a reduction in the required BESS capacity. However, introducing 8 batteries results in a higher aggregated capacity for the battery system. Nonetheless, a comprehensive techno-economic analysis is imperative to determine the optimal number of batteries required for a distribution network.

Fig. 13 depicts the node voltages before and after the installation of a BESS at node 12. As evident from the figure, a significant portion of the

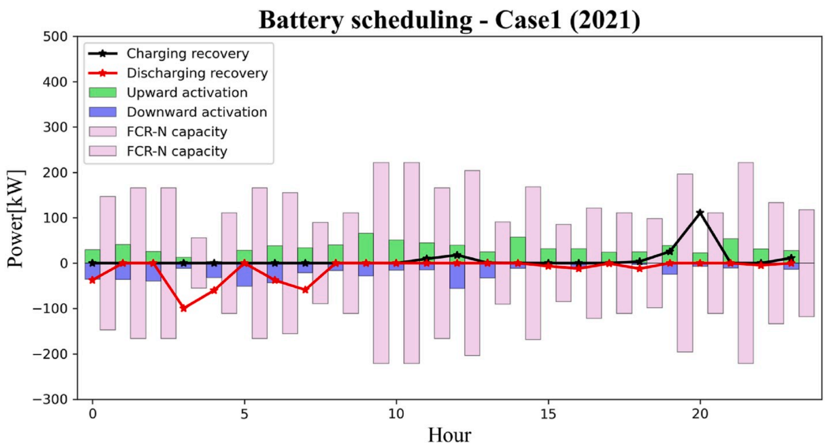


**Fig. 16.** BESS scheduling for Case 1.

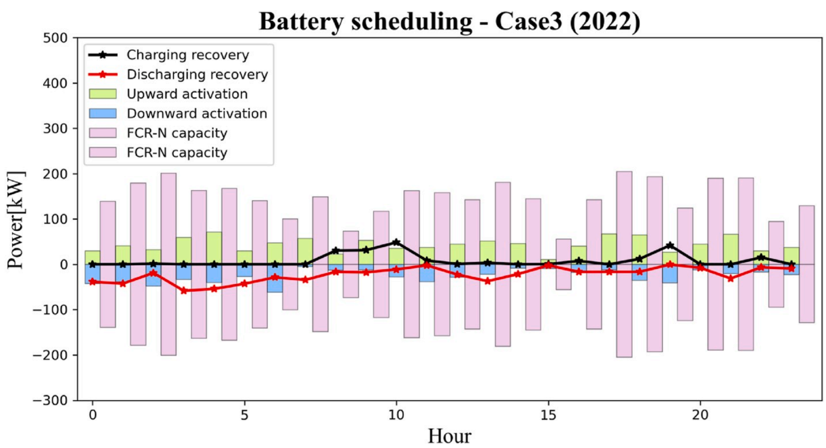


**Fig. 17.** BESS scheduling for Case3.

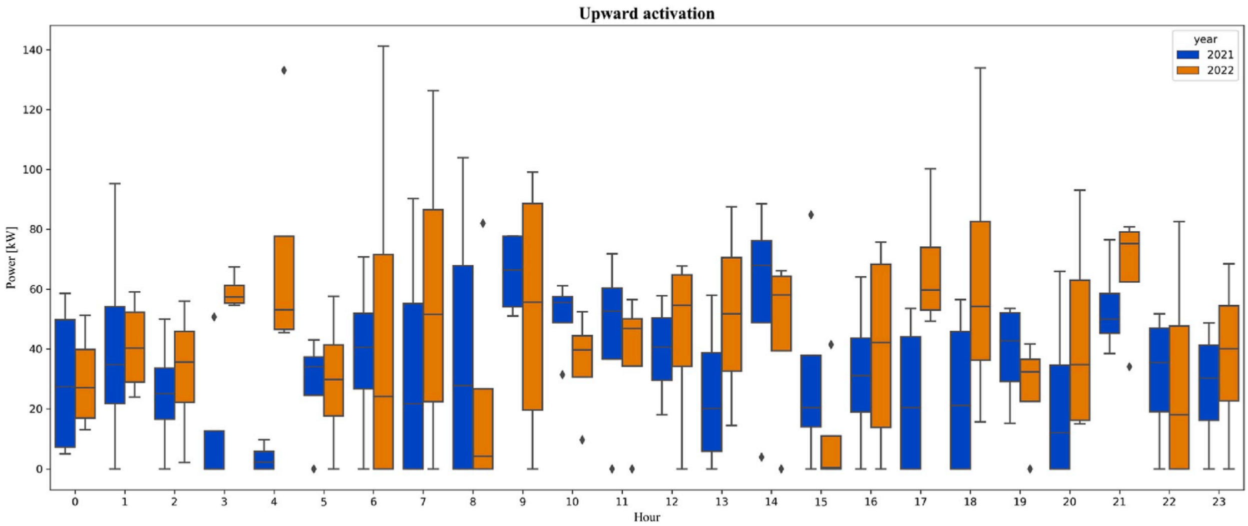


**Fig. 18.** Box plot comparing upward activation for scenarios of 2021 and 2022.

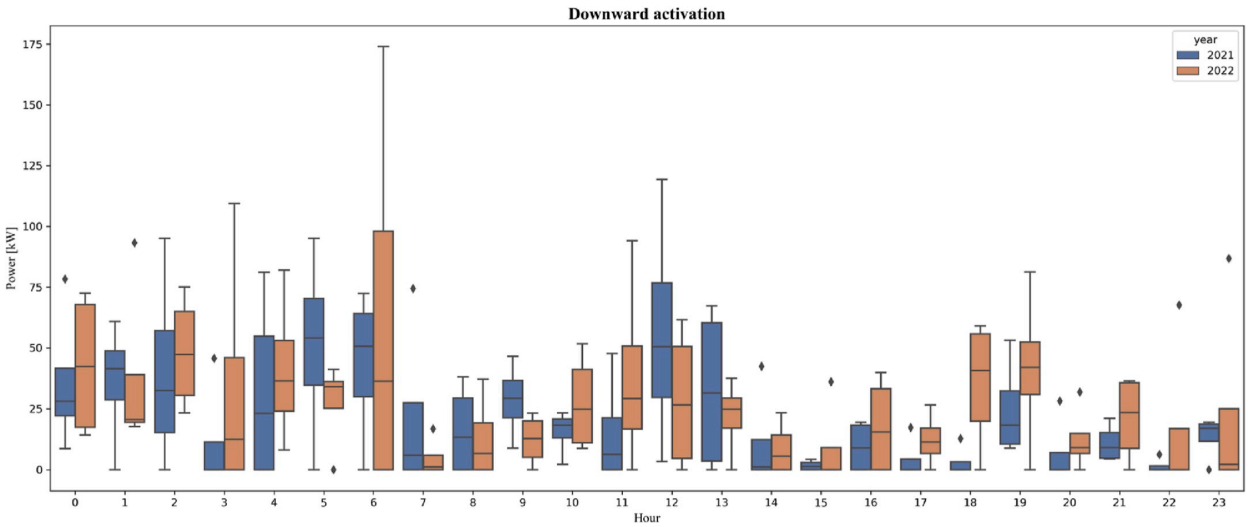


**Fig. 19.** Box plot comparing downward activation for scenarios of 2021 and 2022.

voltages falls below the minimum permissible limit of 0.95 pu. The introduction of the BESS at node 12 effectively mitigates the under-voltage instances, ensuring that the node voltages remain within the acceptable range.

The first-stage problem was resolved using the Finnish test case. The outcomes reveal a necessity for a BESS with a minimum rated power of 23.5627 kW within the local network. Based on the battery cell data, this rated power necessitates a minimum energy capacity of 85.074 kWh. Additionally, the optimal placement for the BESS (OBP) is identified at node b10, coinciding with the location of the restaurant. Furthermore, we experimented with increasing the number of BESSs in equation (21); however, the results remained consistent. This implies that the system requires flexibility solely at node b10. Fig. 14 offers a comparison of node voltages before and after the implementation of the BESS. The results indicate that the placement of the BESS effectively mitigates the under-voltage scenarios that may arise at node b10.

### 4.2. Second-stage results

In the next step, second-stage optimization problem (24)-(44) was solved for 4 different cases. The BESS optimal rated power (kW) and energy capacity (kWh) are calculated for these four cases and the results are illustrated in Fig. 15.

The right-side vertical axis in Fig. 15 shows the optimal rated power whereas the left-side one indicates the optimal BESS energy capacity. According to our results, the best BESS size is equal to the maximum energy capacity, i.e. 800 kWh, if the BESS has the opportunity to provide FCR-N (Case 1 & Case 3). In our case the maximum energy capacity is imposed by the maximum capacity of the distribution network's transformer. If the BESS cannot participate in FCR-N provision, the optimal BESS energy capacity equals 107.399 kWh in 2021 which is slightly higher than the minimum energy capacity needed by the local network (Case 2 in Fig. 15). However, the BESS can still increase its revenue by participating only in spot markets with 800 kWh capacity in 2022 (Case 4 in Fig. 15). This is because of the fact that market prices have

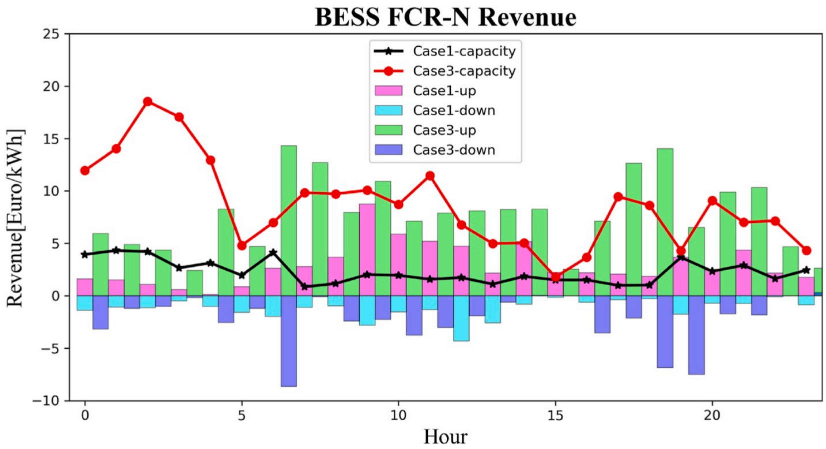


**Fig. 20.** BESS revenue from FCR-N provision.

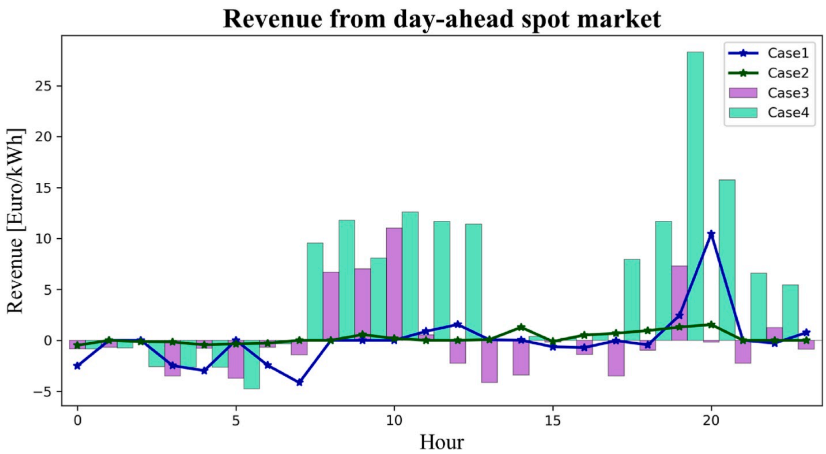


**Fig. 21.** BESS revenue from spot market prices.

considerably increased in 2022.

For the sake of better comparison, we calculated the BESS capacities with the relaxation of the constraint related to maximum energy capacity. The outcomes of this analysis are depicted in Table 4. Notably, as indicated in the table, if the LV/MV transformer's impact on BESS maximum capacity is disregarded, Case 3's capacity can be expanded to 50 MWh. Similarly, in this scenario, the energy capacity for Case 1 amounts to 5.3 MW in 2021. This variation is attributed to substantially higher prices in 2022. However, it is crucial to acknowledge the transformer's capacity. Consequently, it's important to clarify that all presented results, except for those in Table 4, consider the limitation pertaining to the maximum transformer capacity.

Table 5 compares the daily profit of each cases with the designed BESS. Table 5 proves how the profit can be boosted by providing FCR-N. In 2021 (Case 1), the BESS brings 55.8 € of revenue when it provides FCR-N. In 2022 (Case 3), the BESS makes 280.3 € of profit by providing FCR-N. This profit is 3.6 times higher than the case where the BESS is not participating in FCR-N provision.

The second-stage problem also determines the FCR-N capacity that should be offered on a day-ahead basis. Moreover, it calculates upward and downward activations according to the frequency deviations. The BESS may need to be charged and discharged based on the spot market prices to recover its SOC. By recovering the SOC, the BESS is able to provide more FCR-N capacity and therefore make more profits [21]. The hourly mean value of the BESS FCR-N capacity, FCR-N activations, and recovery charging and discharging power for Case 1 and Case 3 are shown in Figs. 16 and 17. The FCR-N capacity should be symmetrical, meaning that the BESS must provide both upward and downward directions, when needed. We bar-plotted the FCR-N capacity in both directions to compare the offered capacity with the activations. The figures show that in most cases, less than 50 % of the capacity is activated. Figs. 18 and 19 demonstrate the box plot of upward and downward activations, respectively, for the extracted scenarios. The plots show that in total, 2022 requires more amount of FCR-N activation.

The BESS makes profits for reserving its capacity and for activating the capacity in the upward direction. The FCR-N capacity payment was assumed to be based on FCR-N day-ahead capacity market prices. The BESS is paid for the upward activation based on up regulation prices. If the activation direction is downward the BESS incurs costs and should pay according to the down regulation prices. Fig. 20 compares the revenue obtained from FCR-N provision for Case 1 and Case 3. In the early morning, the BESS of Case 3 makes considerable profit by reserving its capacity for FCR-N. However, the activations' amount is quite smaller. During the day and evening, the upward activation may increase the BESS revenue and the downward cost does not highly affect the BESS total profit. The profits of the BESS boosts considerably in 2022 since the prices of 2022 are higher than those in 2021.

In order for the BESS to provide symmetrical FCR-N capacity, its SOC

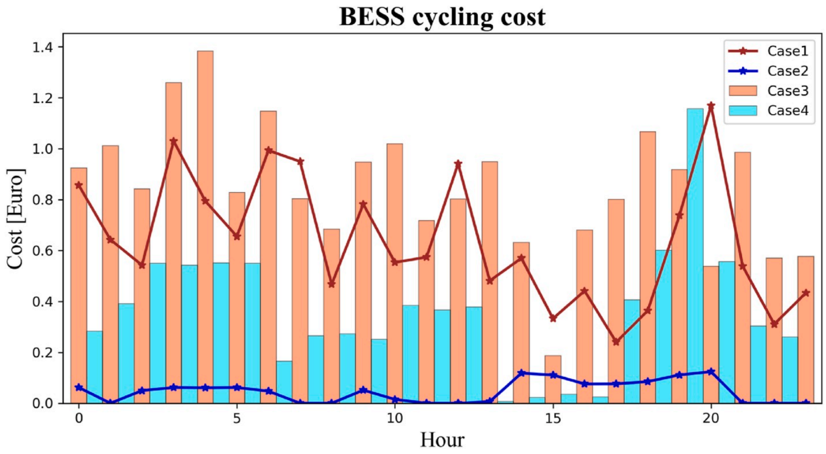


**Fig. 22.** BESS cycling costs for four cases.

should be recovered when required. In Case 1 and Case 3, the BESS SOC can be recovered by charging or discharging with day-ahead spot market prices. Fig. 21 compares the revenue and costs of discharging and charging with market prices. The figure shows that the optimization leads the BESS adopting more revenues by scheduling the recovery-based charging and discharging. It should be noted that recovery is done based on the activated flexibility for the Case 1 and Case 3 while Case 2 and Case 4 are mostly following spot prices.

Finally, Fig. 22 depicts the cycling costs for the considered cases. The participation in the FCR-N market increases the cycling costs for Case1 and Case3. This cost is even higher for Case 3 which has more amount of activations. However, as Table 5 states, the total value of the costs are lower than the profits that are brought from FCR-N provision.

**Table 6**
Effect of BESS cycles on the BESS energy capacity, rated power, and profits if it provides FCR-N in 2022.

| Cycles | 0 | 500 | 800 | 1200 | 1600 |
|---|---|---|---|---|---|
| Rated power [kW] | 221.57 | 217.49 | 214.25 | 205.85 | 196.90 |
| Energy capacity [kWh] | 800 | 749.35 | 723.30 | 689.91 | 635.20 |
| Daily profit [€] | 280.3 | 270.76 | 264.46 | 252.46 | 237.92 |

### 4.3. *Effect of cycle aging on the profits*

It is assumed that the BESS siting and sizing are completed using the proposed methodology. This section analyzes the effects of capacity fade and cycle aging on the BESS profits. We used the data in 2022, thus all analyses are conducted for Case3.

We solved the second-stage optimization for the aged BESS and the results are illustrated in Table 6 and Fig. 23. The results show that the cycle aging can considerably decrease the profits. The aged BESS has less energy capacity and also less rated power. In addition, the aged BESS incurs higher cycle costs which eventually decreases the profits. After passing 1600 cycles, the BESS profit decreases by 15.1 %. Since cycle aging impacts the BESS scheduling and profits, it should be taken into account in ex-ante analyses. The cycle aging depends on the type of the BESS and it needs experimental analyses to determine the exact cycle aging trend.

## 5. Conclusion

A two-stage model was developed to site and size distribution-network-connected BESS that is owned by a private company. The first stage solved a robust stochastic optimization problem with worst-case scenarios to determine the optimal location of the BESS. This stage also guaranteed the secure operation of the distribution network

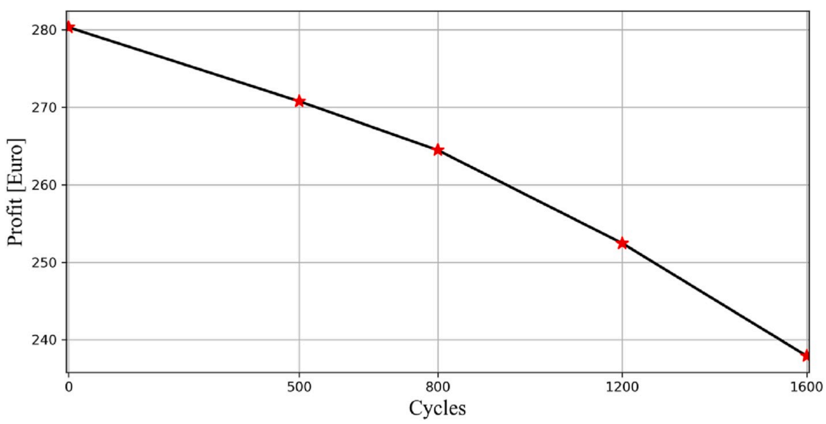


**Fig. 23.** Illustration of BESS profit in terms of cycles.

by establishing the minimum required BESS power capacity. In the second stage, the stochastic optimization problem aimed at maximizing the profit by participating in the FCR-N market. This stage determined the most profitable BESS energy capacity by considering scenarios with the highest probabilities.

The proposed planning methodology was implemented through two case studies. The first case study was IEEE 33-bus radial distribution network whereas the second case study was a rural distribution network in Finland. In the second case study, all data including frequency deviations, net load, FCR-N market prices as well as regulations and spot market prices were extracted from the real-world data of 2021, and 2022 in Finland.

The first-stage problem was solved for both case studies and the results proved considerable improvements in the voltage profile of all nodes. Regarding the second stage, we compared the results of the year 2021 with those of 2022. In addition, the profits and BESS size were assessed in the cases where it does not participate in FCR-N provision. According to our results, the best BESS size is equal to the maximum size if the BESS provides frequency support through FCR-N market participation. Otherwise, the optimal energy capacity decreases for the case where spot market prices were low. In addition, by participating in FCR-N market, the BESS daily profit increased from € −2.18 to € 55.80 in 2021 and from € 77.47 to € 280.3 in 2022. Finally, the paper analyzed the effects of cycle aging and the capacity fade on the profitability of the proposed model. The study concluded that BESS profits could decline by 15.1 % after undergoing 1600 cycles.

This research could be extended in the future by conducting a techno-economic analysis of the number of BESS units placed within the distribution network. Furthermore, a separate study could explore the establishment of a pricing mechanism when a BESS offers diverse types of flexibility services for DSOs.

### CRediT authorship contribution statement

**Hosna Khajeh:** Conceptualization, Methodology, Investigation, Formal analysis, Software, Visualization, Writing – original draft, Writing – review & editing. **Chethan Parthasarathy:** Conceptualization, Writing – original draft, Writing – review & editing. **Elahe Doroudchi:** Writing – original draft, Writing – review & editing. **Hannu Laaksonen:** Conceptualization, Supervision, Validation, Writing – original draft, Writing – review & editing.

### Declaration of competing interest

The authors declare that they have no known competing financial interests or personal relationships that could have appeared to influence the work reported in this paper.

### Data availability

Data will be made available on request.

### Acknowledgements

This work has been done as a part of "Smart Grid 2.0" project funded by Business Finland with grant No. 1386/31/2022. The work of Hosna Khajeh has been partly supported by "Finnish Foundation for Technology Promotion". The work of Elahe Doroudchi is supported by the Academy of Finland under Project No. 338540.

### References

[1] entsoe. "Battery technology.". Accessed: Aug. 09, 2023. [Online]. Available: https://www.entsoe.eu/Technopedia/techsheets/battery-technology.
[2] Liao J-T, Chuang Y-S, Yang H-T, Tsai M-S. BESS-sizing optimization for solar PV system integration in distribution Grid. IFAC-PapersOnLine 2018;51(28):85–90. https://doi.org/10.1016/j.ifacol.2018.11.682.
[3] Wang X, Li F, Zhang Q, Shi Q, Wang J. Profit-oriented BESS siting and sizing in deregulated distribution systems. IEEE Trans Smart Grid 2022. https://doi.org/10.1109/TSG.2022.3150768. 1–1.
[4] Lai K, Wu X, Conejo AJ. Co-optimizing the siting and sizing of batteries and the siting of isolation devices in distribution systems. IEEE Trans Power Deliv Aug. 2022;37(4):2482–91. https://doi.org/10.1109/TPWRD.2021.3111643.
[5] Lee Y-R, Kang H-J, Kim M-K. Optimal operation approach with combined BESS sizing and PV generation in microgrid. IEEE Access 2022;10:27453–66. https://doi.org/10.1109/ACCESS.2022.3157294.
[6] Wu X, Conejo AJ, Mathew S. Optimal siting of batteries in distribution systems to enhance reliability. IEEE Trans Power Deliv Oct. 2021;36(5):3118–27. https://doi.org/10.1109/TPWRD.2020.3034095.
[7] Boonluk P, Siritaratiwat A, Fuangfoo P, Khunkitti S. Optimal siting and sizing of battery energy storage systems for distribution network of distribution system operators. Batteries Nov. 2020;6(4):56. https://doi.org/10.3390/batteries6040056.
[8] Tang Z, Liu Y, Liu J, Li R, Wen L, Zhang G. Multi-stage sizing approach for development of utility-scale BESS considering dynamic growth of distributed photovoltaic connection. J Modern Power Syst Clean Energy Oct. 2016;4(4):554–65. https://doi.org/10.1007/s40565-016-0242-3.
[9] Babacan O, Torre W, Kleissl J. Siting and sizing of distributed energy storage to mitigate voltage impact by solar PV in distribution systems. Sol Energy Apr. 2017;146:199–208. https://doi.org/10.1016/j.solener.2017.02.047.
[10] Barla MC, Sarkar D. Optimal placement and sizing of BESS in RES integrated distribution systems. Int J Syst Ass Eng Manag Jul. 2023. https://doi.org/10.1007/s13198-023-02016-w.
[11] Wang Y, et al. Value stacking of a customer-sited BESS for distribution Grid support: a utility case. IEEE Trans Power Syst 2023:1–12. https://doi.org/10.1109/TPWRS.2023.3242295.
[12] ur Rehman W, Bo R, Mehdipourpicha H, Kimball JW. Sizing battery energy storage and PV system in an extreme fast charging station considering uncertainties and battery degradation. Appl Energy May 2022;313:118745. https://doi.org/10.1016/j.apenergy.2022.118745.
[13] El-Bidairi KS, Nguyen HD, Mahmoud TS, Jayasinghe SDG, Guerrero JM. Optimal sizing of Battery Energy Storage Systems for dynamic frequency control in an islanded microgrid: a case study of Flinders Island, Australia. Energy Mar. 2020;195:117059. https://doi.org/10.1016/j.energy.2020.117059.
[14] Morcilla RV, Enano NH. Sizing of community centralized battery energy storage system and aggregated residential solar PV system as virtual power plant to support electrical distribution network reliability improvement. Renew Energy Focus Sep. 2023;46:27–38. https://doi.org/10.1016/j.ref.2023.05.007.
[15] Kichou S, Markvart T, Wolf P, Silvestre S, Chouder A. A simple and effective methodology for sizing electrical energy storage (EES) systems based on energy balance. J Energy Storage May 2022;49:104085. https://doi.org/10.1016/j.est.2022.104085.
[16] Cao Y, Wu Q, Zhang H, Li C. Multi-objective optimal siting and sizing of BESS considering transient frequency deviation and post-disturbance line overload. Int J Electr Power Energy Syst Jan. 2023;144:108575. https://doi.org/10.1016/j.ijepes.2022.108575.
[17] Wu X, Zhao J, Conejo A. Optimal battery sizing for frequency regulation and energy arbitrage. IEEE Trans Power Deliv Jun. 2022;37(3):2016–23. https://doi.org/10.1109/TPWRD.2021.3102420.
[18] Motalleb M, Reihani E, Ghorbani R. Optimal placement and sizing of the storage supporting transmission and distribution networks. Renew Energy Aug. 2016;94:651–9. https://doi.org/10.1016/j.renene.2016.03.101.
[19] Khajeh H, Laaksonen H. Potential ancillary service markets for future power systems. In: 2022 18th international conference on the European energy market (EEM). Ljubljana, Slovenia: IEEE; Sep. 2022. p. 1–6. https://doi.org/10.1109/EEM54602.2022.9921133.
[20] Muqbel A, Al-Awami AT, Parvania M. Optimal planning of distributed battery energy storage systems in unbalanced distribution networks. IEEE Syst J Mar. 2022;16(1):1194–205. https://doi.org/10.1109/JSYST.2021.3099439.
[21] Hasanpor Divshali P, Evens C. Optimum operation of battery storage system in frequency containment reserves markets. IEEE Trans Smart Grid Nov. 2020;11(6):4906–15. https://doi.org/10.1109/TSG.2020.2997924.
[22] Divshali PH, Evens C. Stochastic bidding strategy for electrical vehicle charging stations to participate in frequency containment reserves markets. IET Gener, Transm Distrib Jul. 2020;14(13):2566–72. https://doi.org/10.1049/iet-gtd.2019.0906.
[23] Casla IM, Khodadadi A, Soder L. Optimal day ahead planning and bidding strategy of battery storage unit participating in nordic frequency markets. IEEE Access 2022;10:76870–83. https://doi.org/10.1109/ACCESS.2022.3192131.
[24] Hu Y, Armada M, Jesús Sánchez M. Potential utilization of battery energy storage systems (BESS) in the major European electricity markets. Appl Energy Sep. 2022;322:119512. https://doi.org/10.1016/j.apenergy.2022.119512.
[25] Khajeh H, Parthasarathy C, Laaksonen H. Effects of battery aging on BESS participation in frequency service markets – Finnish case study. In: 2022 18th international conference on the European energy market (EEM). Ljubljana, Slovenia: IEEE; Sep. 2022. p. 1–6. https://doi.org/10.1109/EEM54602.2022.9921139.
[26] Khajeh H, Firoozi H, Laaksonen H. Flexibility potential of a smart home to provide TSO-DSO-level services. Elec Power Syst Res Apr. 2022;205:107767. https://doi.org/10.1016/j.epsr.2021.107767.
[27] Arunachala R, Parthasarathy C, Jossen A, Garche J. Inhomogeneities in large format Lithium ion cells: a study by battery modelling approach. ECS Trans Aug. 2016;73(1):201–12. https://doi.org/10.1149/07301.0201ecst.

[28] Shafie-Khah M, Siano P, Fitiwi DZ, Mahmoudi N, Catalao JPS. An innovative two-level model for electric vehicle parking lots in distribution systems with renewable energy. IEEE Trans Smart Grid Mar. 2018;9(2):1506–20. https://doi.org/10.1109/TSG.2017.2715259.

[29] Khajeh H, Firoozi H, Hesamzadeh MR, Laaksonen H, Shafie-Khah M. A local capacity market providing local and system-wide flexibility services. IEEE Access 2021;9:52336–51. https://doi.org/10.1109/ACCESS.2021.3069949.

[30] Fitiwi DZ, Olmos L, Rivier M, de Cuadra F, Pérez-Arriaga IJ. Finding a representative network losses model for large-scale transmission expansion planning with renewable energy sources. Energy Apr. 2016;101:343–58. https://doi.org/10.1016/j.energy.2016.02.015.

[31] ENTSOE. Technical requirements for frequency containment reserve provision in the nordic synchronous area. Accessed: Jan. 12, 2022. [Online]. Available: https://www.fingrid.fi/globalassets/dokumentit/fi/sahkomarkkinat/reservit/fcr-technical-requirements-2022-06-27.pdf.

[32] Koller M, Borsche T, Ulbig A, Andersson G. Defining a degradation cost function for optimal control of a battery energy storage system. In: 2013 IEEE grenoble conference. Grenoble, France: IEEE; Jun. 2013. p. 1–6. https://doi.org/10.1109/PTC.2013.6652329.

[33] Toronto Metropolitan University. 33-BUS test system. Accessed: Aug. 01, 2023. [Online]. Available: https://www.torontomu.ca/content/dam/cue/research/reports/33bus%20test%20system.pdf.

[34] Laaksonen H, Saari P, Komulainen R. Control of voltage and frequency in inverter and synchronous generator based urban LV microgrid. 2006. p. 26–8.

[35] Fingrid. Frequency - real time data. Accessed: Feb. 02, 2022. [Online]. Available: https://data.fingrid.fi/en/dataset/frequency-real-time-data.

[36] Fingrid. Up-regulating price in the Balancing energy market. Accessed: Jan. 12, 2022. [Online]. Available: https://data.fingrid.fi/en/dataset/up-regulating-price-in-the-balancing-energy-market.

[37] Fingrid. Down-regulation price in the Balancing energy market. Accessed: Jan. 12, 2022. [Online]. Available: https://data.fingrid.fi/en/dataset/down-regulation-price-in-the-balancing-energy-market.

[38] Fingrid. Frequency Containment Reserve for Normal operation, hourly market prices. Accessed: Jan. 12, 2022. [Online]. Available: https://data.fingrid.fi/en/dataset/frequency-containment-reserve-for-normal-operation-prices.

[39] ENTSOE, "Day-ahead prices." Accessed: Feb. 02, 2022. [Online]. Available: https://transparency.entsoe.eu/transmission-domain/r2/dayAheadPrices/show?name=&defaultValue=false&viewType=GRAPH&areaType=BZN&atch=false&dateTime.dateTime=26.06.2022+00:00|CET|DAY&biddingZone.values=CTY|10YSE-1——————K!BZN|10Y1001A1001A47J&resolution.values=PT15M&resolution.values=PT30M&resolution.values=PT60M&dateTime.timezone=CET_CEST&dateTime.timezone_input=CET+(UTC+1)+/+CEST+(UTC+2).

[40] Diamond S, Boyd S. CVXPY: a Python-embedded modeling language for convex optimization. J Mach Learn Res 2016;17(1):2909–13.

# Optimized Operation of Hybrid Wind-Hydrogen System to Provide Flexibility for Transmission System Needs

Hosna Khajeh, Sahar Seyyedeh-Barhagh, *Student Member, IEEE*, Hannu Laaksonen, *Member, IEEE*

***Abstract*—The focus of this paper is to study the optimized and coordinated operation of a hybrid system with wind turbines, a hydrogen electrolyzer, and hydrogen storage. In this paper, the main aim of the hybrid wind-hydrogen system is to provide flexibility for the transmission system operator's needs by offering frequency control support through frequency containment reserves (FCR) and also to manage congestion on transmission lines close to the wind-hydrogen system. The proposed optimized operation strategy enables effective participation in three reserve markets (FCR-N, upward, and downward FCR-D) as well as simultaneous robust management of wind power forecasting uncertainties by utilizing the flexibility of the hydrogen electrolyzer and hydrogen storage. This strategy utilizes historical data of FCR activation during normal grid operation and disturbances and robustly handle the uncertainties of frequency-driven activation. The effectiveness of the proposed method is presented through a case study using real-world data on frequency deviations and market prices in Finland. Also, the proposed operation strategy is compared with two alternative strategies: optimization based on spot market prices and another strategy prioritizing Self-sufficiency over financial gains.**

***Index Terms*—TSO, Hydrogen Electrolyzer, FCR, Hydrogen Storage, Reserve Markets.**

## I. NOMENCLATURE

- *Abbreviations*

  FCR-D: Frequency Containment Reserve for Disturbances
  FCR-N: Frequency Containment Reserve for Normal operations
  HSEW: A hybrid system that includes Hydrogen Storage, Electrolyzer, Wind
  NN: Non Negative variable
  TSO: Transmission System Operator

- *Sets*

  $c$: Scenario pertaining to either upward or downward activation $\in \{1, 2\}$
  $d$: Time (day) $\in \mathcal{D}$
  $m$: Time (minute) $\in \mathcal{M}$
  $n, n'$: Nodes $\in \mathcal{N}$
  $r$: Segment in piece-wise linearization $\in \mathcal{R}$
  $s$: Scenario associated with wind power forecasts $\in \mathcal{S}$
  $t$: Market timeslot $\in \tau$

- *Variables*

  $\theta_{n,t,c}$: Voltage angle at node $n$ and time $t$ for scenario $c$
  $A^{-N,up/down,max}_{n=HSEW,t,c}$: Maximum activation of FCR-N in upward/downward direction at $t$ and HSEW node for scenario $c$ (NN)
  $A^{-D,up/down,max}_{n=HSEW,t,c}$: Maximum activation of upward/downward FCR-D at $t$ and HSEW node for scenario $c$ (NN)
  $H^{pro}_t$: Hydrogen produced at $t$ (NN)
  $H^{dir}_t$: Hydrogen going directly to demand at $t$, without storing in the storage (NN)
  $H^{in,sto}_t$: Hydrogen injected into the storage at $t$ (NN)
  $H^{out,sto}_t$: Hydrogen extracted from the storage at $t$ (NN)
  $H^{demand}_t$: Hydrogen delivered to the demand at $t$ (NN)
  $SOC^{sto}_t$: State of charge of the storage at $t$ (NN)
  $P^e_t$: Power consumed by electrolyzer at $t$ (NN)
  $P^e_{r,t}$: Power consumed by electrolyzer in segment $r$ at $t$ (NN)
  $P^{-N}_t$: FCR-N capacity offered by the HSEW at $t$ (NN)
  $P^{-D,up/down}_t$: Upward/downward FCR-D capacity offered by the HSEW at $t$ (NN)
  $P^{2grid}_{n=n_0,t,c}$: Power coming to the grid from slack node ($n_0$) at $t$ for scenario $c$
  $P^{com}_t$: Power consumed by the compressor at $t$ (NN)
  $u^{ON/OFF}_t$: Binary variable indicating whether the electrolyzer is ON/OFF at $t$
  $u^{sb}_t$:Binary variable indicating whether the electrolyzer is in the standby state at $t$
  $u^{su}_t$: Binary variable indicating whether the electrolyzer starts up at $t$
  $u_{r,t}$:Binary variable indicating whether segment $r$ is active at $t$

- *Parameters*

  $\alpha_r, \beta_r$: Parameters associated with hydrogen's piece-wise linearization
  $\pi^{-N}_t$: Price of reserving FCR-N capacity at $t$
  $\pi^{-D,up/down}_t$: Price of reserving upward/downward FCR-D capacity at $t$
  $\pi^H$: Hydrogen price
  $\pi^{reg,up/down}_t$: Up/down regulation price at $t$
  $\pi^{su}$: startup cost of electrolyzer
  $\theta^{min/max}$: Minimum/maximum voltage angle allowed
  $\overline{\Delta f^{-N,up/down}_t}$: Average frequency deviation associated with upward/downward activation of FCR-N at $t$
  $\overline{\Delta f^{-D,up/down}_t}$: Average frequency deviation associated

The authors are affiliated with the Flexible Energy Resources Team at the School of Technology and Innovations, University of Vaasa.

with upward/downward activation of FCR-D at $t$
$\Delta \widehat{f_t^{-N,up/down}}$: Maximum of frequency deviation average associated with upward/downward activation of FCR-N at $t$
$\Delta \widehat{f_t^{-D,up/down}}$: Maximum of frequency deviation average associated with upward/downward activation of FCR-D at $t$
$\overline{\Delta P_t^w}$: Average error regarding wind power forecast scenarios
$B_{n,n'}$: Susceptance of the line between nodes $n$ and $n'$
$\widehat{SOC^{sto}}$: Maximum state of charge of hydrogen storage
$\widehat{D^H}$: Maximum hydrogen demand that should be delivered throughout a day
$f_{t,m}$: Frequency measured at minute $m$ and market timeslot $t$
$\widehat{H^{out,sto}}$: Maximum hydrogen that can be extracted from the storage
$K^c$: Compression coefficient
$P_{n,t}^p$: Power produced at $t$ and node $n$
$P_{n,t}^d$: Power consumed at $t$ and node $n$
$P_t^{wind,min/max}$: Minimum/maximum forecasted wind power at $t$
$P^{e,min/max}$: Minimum/maximum power that can be consumed by the electrolyzer
$P_{n,n'}^{e,min/max}$: Minimum/maximum power that can flow between nodes $n$ and $n'$
$P^{sb}$: Power consumed by the electrolyzer in its standby mode

## II. Introduction

EUROPE aims to lead in hydrogen production and infrastructure development, aligning with the EU Green Deal's goal of accelerating renewable energy construction, with a particular emphasis on green hydrogen [1]. This involves doubling hydrogen valleys across Europe [1]. However, integrating large-scale electrolyzers poses challenges for both local transmission grids and broader energy systems [1]. These challenges include disrupting system balance and causing network congestion. Therefore, effective coordination between hydrogen production and energy systems is crucial to enable the electrical grid to accommodate the widespread integration of hydrogen.

Some studies conclude that the flexible and optimized operation of hydrogen systems could, in turn, decrease electricity prices and reduce renewable curtailments. For example, Reference [2] argued that the flexible operation of hydrogen can stabilize the price of renewable energy in future renewable-based power systems. The study conducted by [3] indicated that an increase in hydrogen demand by deploying more hydrogen fuel cell electric vehicles could not only support effective grid operation but also lower electricity costs. The authors of [4] discussed that the utilization of hydrogen as a fuel for heating residential houses can affect energy prices and lower renewable generation curtailment. Reference [5] analyzed the positive impacts of the hydrogen system on market clearing results and the hydrogen system's role in electricity prices. Finally, Reference [6] concluded that the hybrid system of hydrogen and renewable energy systems led to up to 30 % cost savings.

Besides optimization based on electricity prices, another economically efficient coordination solution is to use hydrogen systems to offer ancillary services to power system operators. In this regard, some research analyzed the technical feasibility of providing ancillary services by hydrogen systems. For example, Reference [7] focused on the technical aspects of Proton Exchange Membrane (PEM) electrolyzer technologies, analyzing their eligibility to comply with the requirements of European ancillary services markets. Reference [8] analyzed the technical potential of the Alkaline electrolyzer plant when it provides dynamic frequency regulation service to the TSO. In another work, Reference [9] reviewed the papers proposing the flexible operation of electrolyzers and discussed that hydrogen electrolyzers' capabilities to provide ancillary services. The research conducted by [10] assessed the dynamic characteristics and potential of the electrolyzer's stack for frequency regulation for a power system dominated by solar photovoltaic units. Reference [11] investigated the provision of fast frequency reserve by electrolyzers in low inertia situations. The paper gave special emphasis to the nonlinearity of modeling the electrolyzer and the impacts on its service provision. In Reference [12], authors conducted extended research on a dynamic model of the electrolyzer interfaced with power electronics equipment that provides fast frequency services for the TSO. Reference [13] proposed a method to aggregate electrolyzers with VPP that provides voltage control services to the local distribution system operator.

In addition to technical aspects, limited research has been done to focus on estimating the flexible capacity of hydrogen systems to participate in ancillary service markets complying with the requirements of the specific ancillary service. For example, Reference [14] conducted a long-term profitability analysis by developing a mathematical model of a PV producer integrated with battery storage and a hydrogen system participating in the multi-energy markets as well as balancing markets. The work utilized the general "balancing service" term and did not specify the type of balancing service. However, each frequency regulation service defined in a specific area has its own technical requirements and market characteristics. Authors of [15] developed an optimization-based approach for a system consisting of PV and hydrogen systems based on the concept of power-to-power trading. It also provides secondary frequency control service for TSO. Results showed that participation in the day-ahead and ancillary service markets can be financially viable and beneficial, particularly when markets exhibit significant price volatility. In another work, Reference [16] modeled hydrogen electrolyzers that provide frequency control services, including virtual inertia as well as primary and secondary frequency response with a focus on Australian ancillary service markets. Reference [17] examined how electrolyzers can support the operation of an energy island when combined with offshore wind energy. In [18], authors presented a method for a wind-electrolysis joint system to provide secondary frequency regulation aiming to reduce the production cost of green hydrogen. This flexibility provision

TABLE I
COMPARISON OF THE MAIN FACTORS CONSIDERED IN THE LITERATURE WITH THOSE IN THIS PAPER

| Reference | Hydrogen system | Service provided | Uncertainty of renewables | Uncertainty of activation |
|---|---|---|---|---|
| [14] | Electrolyzer, compressor, storage, fuel cell | Balancing service | No | Not exactly |
| [15] | Electrolyzer, compressor, storage, fuel cell | Secondary frequency reserve | No | No |
| [16] | Electrolyzer | Virtual inertia, frequency reserves | No | No |
| [17] | Electrolyzer | Balancing service | Yes | No |
| [18] | Electrolyzer, compressor, storage | Secondary frequency reserve | Yes | No |
| [19] | Electrolyzer | FCR-N, FCR-D | No | No |
| This paper | Electrolyzer, compressor, storage | FCR-N, FCR-D, network-related service | Yes | Yes |

does not consider the network and also did not model the real-time activation impacts on the system's operation.To the best of authors' knowledge, [19] is the only research that suggests using an electrolyzer for FCR provision. However, the authors did not consider the impact of frequency-driven reserve activation on the electrolyzer's operation and the electrolyzer's effects on the transmission grid.

Table I compares the literature in terms of the hydrogen system analyzed, the type of ancillary service proposed, and whether a model was proposed to handle uncertainties of renewables integrated with the hydrogen system, as well as uncertainties associated with frequency-driven service activation. The final row highlights this paper, showcasing its unique features that distinguish it from the others.

In most ancillary service markets, participants estimate their flexible capacity one day in advance. To accurately estimate their flexible capacity, hydrogen systems need to consider different service activation scenarios, which can significantly affect their revenue. This challenge is heightened when hydrogen systems are integrated with renewable energy sources like wind, due to the inherent unpredictability of renewable energy forecasts. Despite this, current literature does not offer a comprehensive method for addressing all key uncertainties involved in estimating the flexible operation of hydrogen systems. To address the gap, this paper proposes an optimization approach to coordinate the operations of a hydrogen storage, electrolyzer, and wind (HSEW) system (see Fig. 2). The goal is to provide flexibility services to the transmission system operator (TSO). The flexibility services studied include frequency control support through FCR markets and participation in congestion management for transmission lines near the HSEW system. Additionally, the study adopts the piecewise three-state model of an alkaline electrolyzer to account for the non-linear behavior of the hydrogen system. The primary contributions of this paper are as follows:

- This paper examines the HSEW system's participation in three reserve markets (FCR-N, upward and downward FCR-D) while simultaneously managing congestion in the nearby transmission network. The technical and market requirements of these services are all modeled and considered in this paper.
- It proposes novel robust approaches to handle uncertainties from frequency-driven activation of FCRs and uncertainties in wind power forecasts for day-ahead flexible capacity estimation.

Furthermore, the paper develops two other strategies, named Spot and Self-sufficiency strategies, which operate under different frameworks. The paper compares hydrogen production, operation, and profitability of the HSEW in the proposed model with these two strategies using real-world market data from Finland.

The rest of the paper is organized as follows: Section III describes the characteristics of the FCR services including the payment and market participation. Section IV develops the optimization problem regarding the coordinated operation of the HSEW. The case study is introduced in Section V and the results are visualized and discussed in Section VI. Finally, Section VII concludes the paper.

## III. FCR PROVISION

FCR providers competitively submit bids on a daily or annual basis to provide FCR, allowing the TSO to secure its required flexible capacity strategically. In real-time, these frequency control support providers must adjust their power generation or consumption to match grid frequency deviations, aligning with their accepted capacity reservations. Fig. 1 demonstrates how providers modify their active power generation or consumption, precisely matched to their allocated capacity, in response to observed frequency changes [20].

FCR markets consist of three primary products: FCR-N, upward FCR-D, and downward FCR-D. These products are designed to respond to specific frequency deviations and ensure grid stability. FCR-N is a symmetric product that can adjust power output in both upward and downward directions. It is typically activated when the frequency deviates 0.1 Hz from the nominal value of 50 Hz. Upward FCR-D providers act as disturbance responders when the frequency deviation is between 49.1 and 49.5 Hz. They inject more power into the grid (decrease consumption or increase production) to bring the frequency back up. Downward FCR-D providers step in to restrain frequency increases that surpass from 50.1 up to 50.5 Hz. Downward flexibility products consume more power by increasing consumption or decreasing production to reduce frequency.

If the HSEW provides FCR-N, it earns revenue based on the price of the FCR-N capacity market. Additionally, it receives revenue in line with the up-regulation price when the FCR-N activates in the upward direction [21]. However, the HSEW incurs a payment if the FCR-N capacity activates in the downward direction, in accordance with the down-regulation price [21, 22]. On the other hand, FCR-D services do not entail energy remuneration. The HSEW only receives revenue by

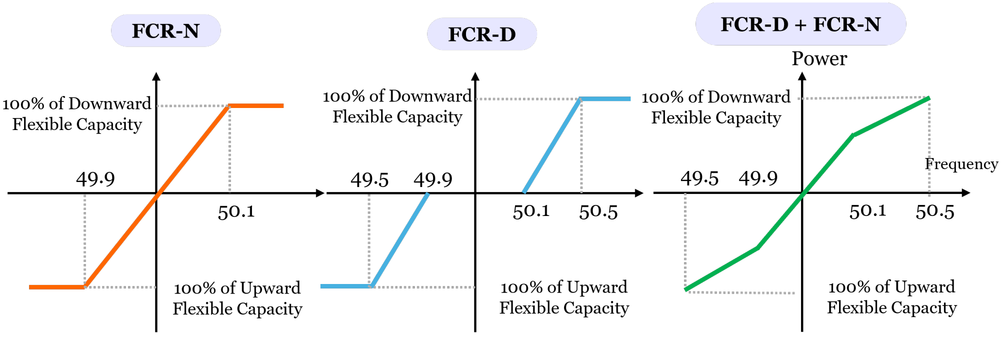


Fig. 1. Illustration of $Pf$ droop profiles for providing FCR services

reserving its capacity for FCR-D, and no payment is transacted in either activation direction [22].

In this paper, HSEW is daily scheduled to provide FCR services, including FCR-N, upward FCR-D, and downward FCR-D. When the grid frequency drops below 50 Hz, the HSEW injects wind power into the grid. To counteract frequency increases above 50 Hz, the HSEW increases the power consumption of electrolyzer. Moreover, we assume a fixed-term contract between the TSO and the HSEW so that the HSEW prevents congestion in the local transmission grid.

## IV. Problem Formulation

The objective function maximizes the HSEW's revenue from providing FCR services and selling hydrogen:

$$\max_{P_t^{-N}, P_t^{-D,up}, P_t^{-D,down}} \sum_{t\in\tau} \overbrace{H_t^{demand}\pi^H}^{\text{Hydrogen Selling Revenue}} + \underbrace{P_t^{-N}\pi_t^{-N} + P_t^{-D,up}\pi_t^{-D,up} + P_t^{-D,down}\pi_t^{-D,down}}_{\text{Capacity Revenue}} + \underbrace{\overline{\Delta f_t^{-N,up}} P_t^{-N}\pi_t^{reg,up}}_{\text{Activation Revenue}} - \underbrace{\overline{\Delta f_t^{-N,down}} P_t^{-N}\pi_t^{reg,down}}_{\text{Activation Cost}} - \underbrace{\pi^{su}u_t^{su}}_{\text{Startup Cost}} \quad (1)$$

Where, Hydrogen Selling Revenue indicates the revenue from selling hydrogen at the fixed price $\pi^H$. Capacity Revenue comprises the revenues earned by reserving capacity for FCR-N, upward FCR-D and downward FCR-D. If FCR-N capacity is activated upward, the HSEW receives Activation Revenue according to up-regulation prices. Conversely, if FCR-N activates downward, the HSEW incurs the Activation Cost based on down-regulation prices. The last term in (1) refers to the cold startup cost of the electrolyzer, which is incurred during each startup.

The introduced objective function is subjected to the constraints that explain the HSEW's operational limits as well as FCR services' requirements. Besides offering FCR services, the HSEW also provides the TSO with network congestion management services, ensuring that network constraints are upheld even in the worst-case FCR activations. In this context, the equation of power balance for each node is considered a constraint and expressed as follows:

$$\begin{aligned} & A_{n=HSEW,t,c}^{-N,up,max} - A_{n=HSEW,t,c}^{-N,down,max} + A_{n=HSEW,t,c}^{-D,up,max} \\ & -A_{n=HSEW,t,c}^{-D,down,max} + P_{n=n_0,t,c}^{2grid} - P_{n,t}^{d} + P_{n,t}^{p} = \\ & \textstyle\sum_{n'\in\mathcal{N}-n} B_{n,n'}(\theta_{n,t,c} - \theta_{n',t,c}) \\ & \forall n' \in \mathcal{N}, \forall t \in \tau, \forall c \in \{1,2\} \end{aligned} \quad (2)$$

In the power balance equation, the worst-case activation of upward FCRs is represented with a positive sign, while the activation of downward FCRs is denoted with a negative sign. This convention reflects that upward flexibility contributes to increased production, while downward flexibility corresponds to increased consumption.

In the first worst-case activation scenario ($c = 1$), the TSO activates only downward for both FCR-N and FCR-D capacities throughout the entire timeslot, meaning that threre is no upward activations:

$$A_{n=HSEW,t,c=1}^{-N,up,max} = 0 \quad \forall t \in \tau \quad (3)$$

$$A_{n=HSEW,t,c=1}^{-D,up,max} = 0 \quad \forall t \in \tau \quad (4)$$

$$A_{n=HSEW,t,c=1}^{-N,down,max} = \frac{\widehat{\Delta f_t^{-N,down}}}{0.1} P_t^{-N} \quad \forall t \in \tau \quad (5)$$

$$A_{n=HSEW,t,c=1}^{-D,down,max} = \frac{\widehat{\Delta f_t^{-D,down}}}{0.4} P_t^{-D,down} \quad \forall t \in \tau \quad (6)$$

In equations (5) and (6), the values 0.1 and 0.4 represent the slope of the $Pf$ droop, as illustrated in Fig. 1, and are specific to the determination of FCR-N and FCR-D services. In this paper, we calculate the maximum average frequency deviations as follows:

$$\widehat{\Delta f_t^{-D,down}} = \max_{d\in\mathcal{D}} \mathcal{R}^{-D\downarrow} = \max_{d\in\mathcal{D}} \begin{cases} \frac{1}{N_m}\sum_m (f_{d,t,m} - 50.1), \\ \text{if } 50.1 \le f_{d,t,m} \le 50.5 \\ 0.4, \text{ if } f_{d,t,m} \ge 50.5. \\ 0 \text{ otherwise.} \end{cases} \quad (7)$$

$$\widehat{\Delta f_t^{-N,down}} = \max_{d\in\mathcal{D}} \mathcal{R}^{-N\downarrow} = \max_{d\in\mathcal{D}} \begin{cases} \frac{1}{N_m}\sum_m (f_{d,t,m}-50), \\ \text{if } 50 \le f_{d,t,m} \le 50.1 \\ 0.1, \text{ if } f_{d,t,m} \ge 50.1. \\ 0 \text{ otherwise.} \end{cases} \quad (8)$$

Where $\mathcal{R}^{-N\downarrow}$ and $\mathcal{R}^{-D\downarrow}$ indicate the frequency deviation functions for downward FCR-N and FCR-D, obtained from Fig. 1. Equation (7) examines historical events $\mathcal{D}$, find situations where frequencies have surpassed 50.1, and computes the average deviations for downward FCR-D at each timeslot $t$. It then identifies its maximum frequency deviations as the value of $\widehat{\Delta f_t^{-D,down}}$. In our paper, we adopt a frequency resolution of 1 minute and have analyzed the frequency data over the past year. Correspondingly, Equation (8) calculates maximum of average frequency deviations for downward FCR-N at each timeslot $t$ ($\widehat{\Delta f_t^{-N,down}}$) when frequencies have exceeded 50.

In the second worst-case activation scenario ($c = 2$), only upward activation is requested for both FCRs, with the downward activations set to zero:

$$A^{-N,down,max}_{n=HSEW,t,c=2} = 0 \quad \forall t \in \tau \quad (9)$$

$$A^{-D,down,max}_{n=HSEW,t,c=2} = 0 \quad \forall t \in \tau \quad (10)$$

$$A^{-N,up,max}_{n=HSEW,t,c=1} = \frac{\widehat{\Delta f_t^{-N,up}}}{0.1} P_t^{-N} \quad \forall t \in \tau \quad (11)$$

$$A^{-D,up,max}_{n=HSEW,t,c=1} = \frac{\widehat{\Delta f_t^{-D,up}}}{0.4} P_t^{-D,up} \quad \forall t \in \tau \quad (12)$$

Where, the calculation of maximum frequency deviations for upward activation of FCRs is computed as follows:

$$\widehat{\Delta f_t^{-D,up}} = \max_{d\in\mathcal{D}} \mathcal{R}^{-D\uparrow} = \max_{d\in\mathcal{D}} \begin{cases} \frac{1}{N_m}\sum_m (49.9-f_{d,t,m}), \\ \text{if } 49.5 \le f_{d,t,m} \le 49.9. \\ 0.4, \text{ if } f_{d,t,m} \le 49.5. \\ 0 \text{ otherwise.} \end{cases} \quad (13)$$

$$\widehat{\Delta f_t^{-N,up}} = \max_{d\in\mathcal{D}} \mathcal{R}^{-N\uparrow} = \max_{d\in\mathcal{D}} \begin{cases} \frac{1}{N_m}\sum_m (50-f_{d,t,m}), \\ \text{if } 49.9 \le f_{d,t,m} \le 50. \\ 0.1, \text{ if } f_{d,t,m} \le 49.9 \\ 0 \text{ otherwise.} \end{cases} \quad (14)$$

$\mathcal{R}^{-N\uparrow}$ and $\mathcal{R}^{-D\uparrow}$ indicate the frequency deviation functions for upward FCR-N and FCR-D, obtained from Fig. 1. As (13) and (14) indicate, the maximum frequency deviation for each timeslot is determined by calculating the average frequency deviations over the past year and selecting the maximum deviation value for each timeslot.

This paper assumes that when upward FCRs are activated, the HSEW injects its wind power into the grid. Conversely, in situations where downward activation is necessary, the electrolyzer increases the consumption of electricity. In the downward situation, although wind power may still be generated, the electrolyzer is configured to absorb wind power to prevent any injection into the grid.

Given that the HSEW scheduling is conducted on a day-ahead basis, wind power is susceptible to forecast errors. Consequently, we have devised various scenarios for wind power and selected the scenario with the minimum wind power as the upper limit for upward capacity to consider the robust scheduling:

$$P_t^{-N} + P_t^{-D,up} \le P_t^{wind,min} \quad \forall t \in \tau \quad (15)$$

$$P_t^{wind,min} = \min_{s\in\mathcal{S}} P_{t,s}^{wind} \quad \forall t \in \tau \quad (16)$$

As expressed in constraint (15), the upward capacity of the HSEW can subsequently be allocated between FCR-N and upward FCR-D. For the downward capacity, to guarantee the provision of downward FCRs, the worst-case scenario is contemplated by anticipating that the electrolyzer should absorb the maximum forecasted wind production:

$$P_t^{-N} + P_t^{-D,down} \le P^{e,max} - P_t^{wind,max} \quad \forall t \in \tau \quad (17)$$

$$P_t^{wind,max} = \max_{s\in\mathcal{S}} P_{t,s}^{wind} \quad \forall t \in \tau \quad (18)$$

As indicated in Equation (17), the maximum downward capacity of the HSEW is determined by subtracting the maximum forecasted wind power at time $t$ from the maximum consumption capacity of the electrolyzer. Since FCR-N capacity is symmetric it needs to be considered to both upward and downward capacity constraints i.e. (15) and (17).

The following constraints ensure that the voltage angles of nodes and the limits on line power flow are maintained within their permissible ranges:

$$P_{n,n'}^{min} \le B_{n,n'}(\theta_{n,t,c} - \theta_{n',t,c}) \le P_{n,n'}^{max} \quad \forall t \in \tau, \forall n \in \mathcal{N}, \forall c \in \{1,2\} \quad (19)$$

$$\theta^{min} \le \theta_{n,t,c} \le \theta^{max} \quad \forall t \in \tau, \forall n \in \mathcal{N}, \forall c \in \{1,2\} \quad (20)$$

This paper adopts the three-state model for alkaline electrolyzers, originally proposed in [23]. At each timeslot, the electrolyzer can operate in only one of three modes: $ON$ (active hydrogen generation), $OFF$ (complete shutdown), or standby (partial power, enabling quick startup):

$$u_t^{ON} + u_t^{OFF} + u_t^{sb} = 1 \quad \forall t \in \tau \quad (21)$$

The power consumption in the ON state must stay within the specified minimum load limit and maximum capacity of the electrolyzer while the standby state has a constant consumption ($P^{sb}$):

$$P_t^e \le u_t^{ON} P^{e,max} + u_t^{sb} P^{sb} \quad \forall t \in \tau \quad (22)$$

$$P_t^e \ge u_t^{ON} P^{e,min} + u_t^{sb} P^{sb} \quad \forall t \in \tau \quad (23)$$

During each cold startup, the electrolyzer transitions from the $OFF$ (not $ON$ or stand-by) state at $t-1$ to the $ON$ state at $t$, as modeled by (24):

$$u_t^{su} \ge u_t^{ON} - u_{t-1}^{ON} - u_{t-1}^{sb} \quad \forall t \in \tau \quad (24)$$

However, the electrolyzer cannot come from the $OFF$ to the standby state:

$$u_{t-1}^{OFF} + u_t^{sb} \le 1 \quad \forall t \in \tau \quad (25)$$

No startup costs are considered during the initial timeslot:

$$u_{t=1}^{su} = 0 \tag{26}$$

This paper suggests introducing a constraint, which was not considered in [23] to ensure that the binary variable representing startup does not equal one when the electrolyzer is not ON:

$$u_t^{ON} \geq u_t^{su} \tag{27}$$

The following constraint estimates the minimum real-time power consumption of the electrolyzer, influenced by both the activation of FCR services and various wind power injection scenarios:

$$P_t^e \geq \overbrace{\frac{\overline{\Delta f_t^{-N,down}}}{0.1} P_t^n + \frac{\overline{\Delta f_t^{-D,down}}}{0.4} P_t^{-D,down}}^{\text{Consumption regarding downward FCRs activation}} + \underbrace{P_t^{-N} + P^{-D,up} - (\frac{\overline{\Delta f_t^{-N,up}}}{0.1} P_t^{-N} + \frac{\overline{\Delta f_t^{-D,up}}}{0.4} P_t^{-D,up})}_{\text{Non-activated upward FCRs}} + \overline{\Delta P_t^w} \quad \forall t \in \tau \tag{28}$$

In (28), the terms $\frac{\overline{\Delta f_t^{-N,up/down}}}{0.1}$ and $\frac{\overline{\Delta f_t^{-D,up/down}}}{0.4}$ denote the mean values of activation ratio, which are estimated from the historical activations, as illustrated by equations (29), (30), (31), and (32):

$$\overline{\Delta f_t^{-D,up}} = \frac{1}{N_D} \mathcal{R}^{-D\uparrow} \tag{29}$$

$$\overline{\Delta f_t^{-D,down}} = \frac{1}{N_D} \mathcal{R}^{-D\downarrow} \tag{30}$$

$$\overline{\Delta f_t^{-N,up}} = \frac{1}{N_D} \mathcal{R}^{-N\uparrow} \tag{31}$$

$$\overline{\Delta f_t^{-N,down}} = \frac{1}{N_D} \mathcal{R}^{-N\downarrow} \tag{32}$$

As per (28), the electrolyzer is designed to consume energy in response to the activation of downward FCRs. Additionally, it is required to absorb the non-activated segment of upward FCRs originating from wind power. Given our consideration of the minimum wind power scenario, the electrolyzer must also account for absorbing the average error in forecasted wind. The error is estimated based on the minimum wind power scenario considered when determining the maximum reserve capacity limit. Estimating this average error involves analyzing different wind scenarios and their respective probabilities:

$$\overline{\Delta P_t^w} = \sum_{s \in \mathcal{S}} \rho_s (P_{t,s}^{wind} - P_t^{wind,min}) \quad \forall t \in \tau \tag{33}$$

Where $\rho_s$ refers to the probability of scenario $s$.
As suggested in [23], the function representing the electrolyzer's hydrogen production in relation to its electricity consumption has been linearized in a piecewise manner to model the non-linear efficiency of the electrolyzer. The resulting function is as follows:

$$H_t^{pro} = \sum_{r \in \mathcal{R}} \alpha_r P_{r,t}^e + \beta_r u_{r,t} \quad \forall t \in \tau \tag{34}$$

Also, each linearized segment needs to remain within its lower and upper bounds:

$$P_{r,t}^{e,min} u_{r,t} \leq P_{r,t}^e \leq P_{r,t}^{e,max} u_{r,t} \quad \forall t \in \tau, \forall r \in \mathcal{R} \tag{35}$$

The electrolyzer in its on-state operates exclusively within the efficiency that is obtained from (36):

$$u_t^{ON} = \sum_{r \in \mathcal{R}} u_{r,t} \quad \forall t \in \tau \tag{36}$$

The following formulation specifies that the electricity consumption of the electrolyzer is determined by the sum of linearized segments when it is ON, and by a constant power when it is in standby mode:

$$P_t^e = \sum_{r \in \mathcal{R}} P_{r,t}^e + u_t^{sb} P^{sb} \quad \forall t \in \tau \tag{37}$$

A portion of the total hydrogen produced by the electrolyzer is immediately routed to meet current demand, while the remainder is stored in the hydrogen storage system, as depicted in Fig. 2. Equation (37) precisely articulates the balance among hydrogen production, its immediate demand, and the amount reserved in the storage:

$$H_t^{pro} = H_t^{dir} + H_t^{in,sto} \quad \forall t \in \tau \tag{38}$$

Additionally, there is another equation that explains how the hydrogen delivered to meet demand can come from storage (as the output of storage) or directly from the electrolyzer. This concept is shown in Fig. 2 and written in math like this:

$$H_t^{demand} = H_t^{dir} + H_t^{out,sto} \quad \forall t \in \tau \tag{39}$$

This paper operates under the assumption of a daily minimum threshold for required hydrogen, as shown in (40):

$$\sum_{t \in \tau} H_t^{demand} = \widehat{D^H} \tag{40}$$

As depicted in Fig. 2, the hydrogen must first pass through the compressor before being sent to storage. The compressor consumes electricity, which varies according to the storage inputs:

$$P_t^{com} = K^c H_t^{in,sto} \quad \forall t \in \tau \tag{41}$$

The time-varying state of charge of the storage and its maximum allowable capacity are mathematically modeled in equations (42) and (43), respectively.

$$SOC_t^{sto} = SOC_{t-1}^{sto} + H_t^{in,sto} - H_t^{out,sto} \quad \forall t \in \tau \tag{42}$$

$$SOC_t^{sto} \leq \widehat{SOC^{sto}} \quad \forall t \in \tau \tag{43}$$

## V. Case Study

The case study presents a simplified model of the standard European High Voltage (HV) transmission network, using line parameters obtained from [24]. In Fig. 3, the network under consideration is illustrated, alongside the net production values for each node during the simulation. As the figure illustrates, the HSEW is located at bus $b3$ while other nodes include various types of generation units and demand. The timeslot is contemplated one hour. The hourly net production of other nodes is calculated by subtracting their hourly demand

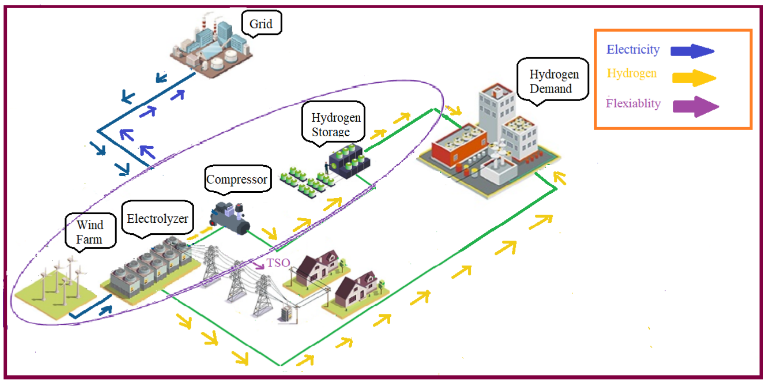


Fig. 2. Illustration of the HSEW providing flexibility services to the TSO while selling hydrogen to the demand

from their hourly production. Positive net production indicates that the production exceeds the demand, while negative net production signifies higher demand than production. All specific details about the hydrogen electrolyzer, compressor and storage are sourced from [23]. The capacities are as follows: 52.25 MWh for the electrolyzer, 22 kg for hydrogen storage, and 42 MWh for the wind park. The daily demand for hydrogen is assumed to be 1222.44 kg.

This paper analyzes real-world price data from Finland on

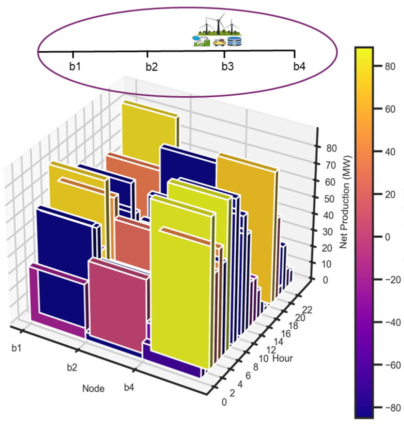

Fig. 3. Illustration of the case study along with the hourly net production of the nodes

April 1, 2023. We focus on the annual capacity prices for three FCR markets: FCR-N, upward FCR-D, and downward FCR-D capacity markets. Figure 4 illustrates a comparison of these prices.

This paper examines the activation ratios for FCRs by analyzing one-year historical frequency data from Finland, spanning from April 1, 2022, to March 31, 2023. The maximum frequency deviation values are determined using equations (7), (8), (13), and (14), while the mean frequency deviation values are estimated using equations (29)–(32). The activation ratios are computed by dividing the frequency deviations for FCR-N by 0.1 and those for FCR-D by 0.4, in order to account for their activation droop characteristics. Fig. 5 represents the estimated

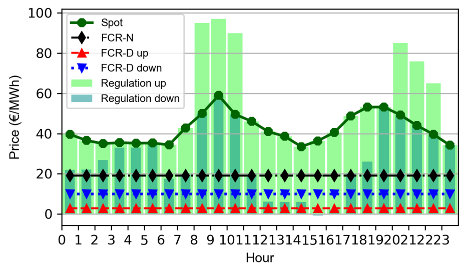


Fig. 4. Comparison of spot, FCRs, and regultaion prices on 1.4.2023 in Finland

activation ratios for FCRs. For improved clarity in presentation, the mean values of FCR-D activation are depicted based on the left y-axis, while the remaining activation values are illustrated based on the right y-axis.

Furthermore, we consider six onshore wind turbines with full

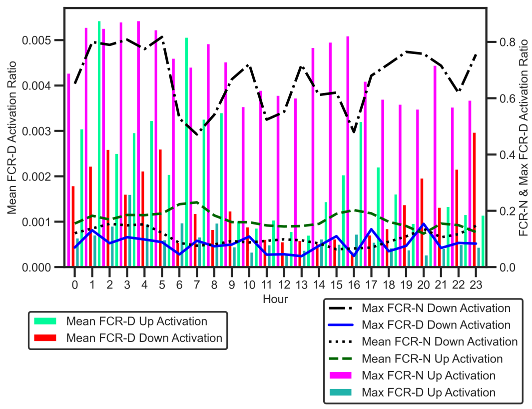


Fig. 5. The mean and maximum values of activation ratio estimated for the case study

power converters, each with a capacity of 7 MWh, aligning with the 2020 ATB NREL turbine outlined in [25]. Essential turbine parameters and power curves can be referenced in the provided source. We utilized quantile regression to forecast wind power from forecasted wind speed, generated different scenarios from the quantiles and assign probability to each scenario using the CDF of the quantile [26]. Accordingly, 10 scenarios (s1-s10) are considered. Figure 6 visually represents the scenario values alongside the respective probabilities considered for each scenario.

For comparison purposes, this paper examines three different

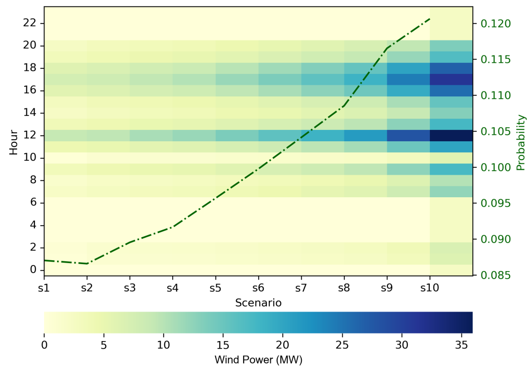


Fig. 6. The heatmap and line plots representing the probability and the wind power values for each scenario

operation strategies. In all strategies, the HSEW plays a role in managing network congestion. However, their operation strategies differ as follows:

- Proposed operation strategy: the model suggested by this paper in which HSEW contributes to both FCR-N and FCR-D provision.
- Spot strategy: Introduced by [23] which optimizes HSEW operation based on spot market prices.
- Self-sufficient strategy: Designed to enhance Self-sufficiency. This model aims to minimize the power flowing into the local transmission network. The costs are also calculated based on spot market prices.

## VI. Simulation Results

The optimization problem described by equations 1 through 43 has been formulated and solved using the JuMP package in Julia. Figure 7 illustrates the optimized decision values, representing the FCR capacities to be offered in reserve markets. Given the paper's focus on addressing wind power uncertainties robustly, the proposed operation strategy with optimal scheduling prioritizes allocating more capacity to downward flexible capacities. Fig. 7 showcases that the majority of HSEW capacity is allocated to downward FCR-D provision, with lesser capacity dedicated to symmetrical FCR-N provision, and none allocated to upward FCR-D capacity.

Furthermore, the Spot and Self-sufficient strategies were developed and solved using the JuMP package. Figure 8 compares daily hydrogen production between these three strategies. "H2D" represents hydrogen delivered to meet demand, while "Total Hydrogen" signifies overall hydrogen production from the electrolyzer. The proposed operation

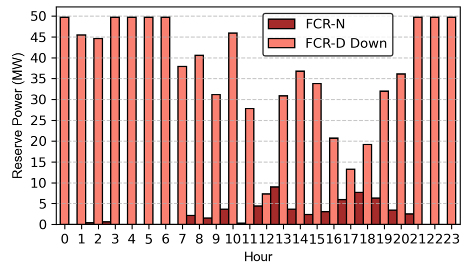


Fig. 7. Optimal capacities devoted to each reserve product in the proposed operation strategy

strategy prioritizes hydrogen production alongside FCR market operations. Notably, it utilizes hydrogen storage and compression, leading to higher total hydrogen production compared to H2D at certain hours. In contrast, the Spot strategy follows spot market price patterns, with lower prices resulting in increased hydrogen production. The Spot strategy does not view hydrogen storage as a profitable option. Conversely, the Self-sufficient strategy minimizes hydrogen production to prevent excessive power entering the local grid. Hydrogen production occurs during hours of positive net production in the local transmission network. Similar to the Spot strategy, the Self-sufficient strategy does not utlize the storage. Figure 9 further demonstrates that the proposed operation strategy maximizes the consumption of the electrolyzer, while the Spot strategy adjusts electrolyzer consumption according to spot prices. In contrast, the Self-sufficient strategy minimizes electrolyzer's electricity usage altogether. In this figure, the white square denotes the mean value of electrolyzer's consumption for each strategy.

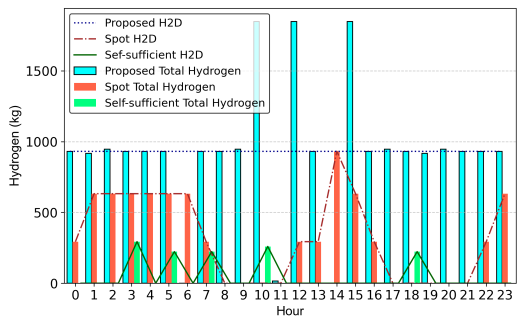


Fig. 8. Optimal hydrogen delivered to demand (H2D) and the total hydrogen produced by the electrolyzer (Total Hydrogen) for three studied strategies

Figure 10 depicts the revenues and costs in the proposed operation strategy. Hydrogen selling revenue is shown on the right y-axis, while other costs and revenues are displayed on the left y-axis. The figure highlights that after hydrogen selling, a significant portion of HSEW revenue comes from FCR capacity revenue. Activation costs for downward FCR-N are relatively minor compared to its capacity revenue. Additionally, the optimized scheduling maintains the electrolyzer in ON-

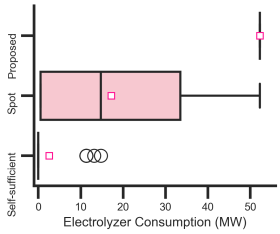


Fig. 9. The box plot representing the distribution of electrolyzer's consumption in three studied strategies

mode operation due to its high startup cost.

In contrast to the proposed operation strategy, the Self-

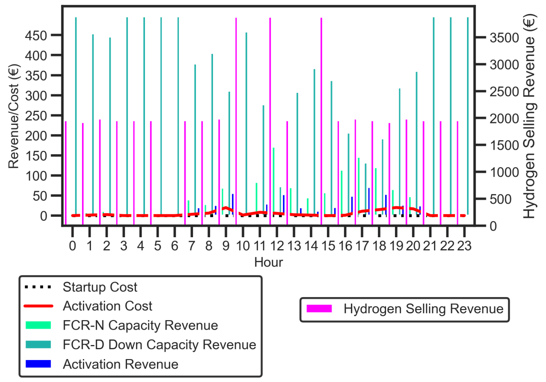


Fig. 10. The hourly illustration of costs and revenues brought from the proposed operation strategy.

sufficient and Spot strategies have limited revenue sources. HSEW profits solely from selling hydrogen and, if net production is positive, from selling wind power production at spot market prices. Conversely, when net production is negative, HSEW incurs costs for electricity consumption. Figure 11 illustrates the costs and revenues when HSEW is optimized according to spot market prices. The figure reveals that buying electricity results in negative revenue when HSEW produces hydrogen. However, when hydrogen production ceases, HSEW can generate revenue by selling its wind production at spot market prices. Figure 12 presents the revenues and costs associated with the Self-sufficient strategy. In this scenario, the electrolyzer is turned off for 5 hours, as the Self-sufficient strategy prioritizes Self-sufficiency over economics. However, the high startup cost imposes significant expenses on HSEW in the Self-sufficient strategy.

Finally, Table II compares the daily profits obtained from these three strategies. The results show that participating in FCR markets can increase HSEW's profit by more than 2.6 times compared to when HSEW operates solely based on spot market prices. Additionally, the significant impact of startup costs is evident in the Self-sufficient strategy, where profits are 8 times lower than in the proposed operation strategy.

TABLE II
COMPARISON OF TOTAL DAILY PROFIT FOR THREE STUDIED STRATEGIES

| Strategies | Proposed | Spot | Self-sufficient |
|---|---|---|---|
| Profit (€) | 57428.31 | 21440.37 | 7029.08 |

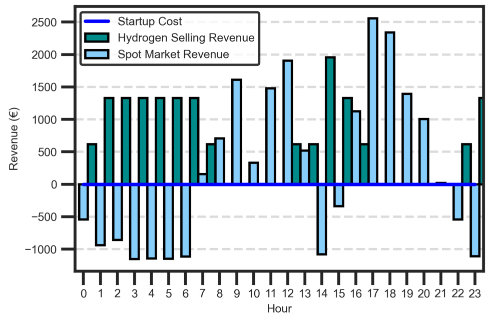


Fig. 11. The hourly illustration of costs and revenues brought from the spot-market-participation-based operation strategy.

## VII. CONCLUSION

This paper introduced a novel method to optimize the coordination of HSEW operation to align with the requirements of the TSO. HSEW can serve multiple purposes, including providing FCR for normal operation and disturbance scenarios, as well as assisting with congestion management. The method addressed wind power uncertainty robustly while considering detailed electrolyzer states and FCR market characteristics, including activation features.

In the simulation section, we compared the performance and profitability of our proposed operation strategy with two others: Spot, which operates based on spot prices, and Self-sufficient, which emphasizes the grid's Self-sufficiency. The results showed that our proposed FCR-market-participation-based strategy produces significantly more hydrogen compared to the other strategies whereas the Self-sufficient operation strategy minimizes hydrogen production. Also, utilizing the hydrogen storage was only found to be profitable in the proposed operation strategy. In profitability, our FCR participation strategy earns 2.6 times more than the Spot-market-participation-based operation strategy and 8 times more than the Self-sufficient one.

## REFERENCES

[1] Antonio Iliceto et al. "Hydrogen's impact on grids: Impact of hydrogen integration on power grids and energy systems". In: (2023).

[2] Oliver Ruhnau. "How flexible electricity demand stabilizes wind and solar market values: The case of hydrogen electrolyzers". In: *Applied Energy* 307 (2022), p. 118194. ISSN: 0306-2619. DOI: https://doi.org/10.1016/j.apenergy.2021.118194. URL: https://www.sciencedirect.com/science/article/pii/S0306261921014641.

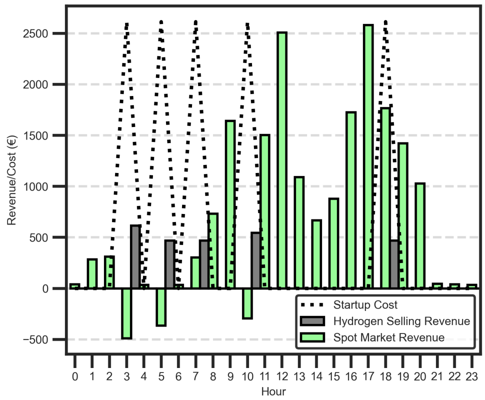


Fig. 12. The hourly illustration of costs and revenues brought for the Self-sufficient strategy.


[3] Cong Zhang et al. "Flexible grid-based electrolysis hydrogen production for fuel cell vehicles reduces costs and greenhouse gas emissions". In: *Applied Energy* 278 (2020), p. 115651. ISSN: 0306-2619. DOI: https://doi.org/10.1016/j.apenergy.2020.115651. URL: https://www.sciencedirect.com/science/article/pii/S0306261920311491.

[4] Genaro Longoria, Muireann Lynch, and John Curtis. "Green hydrogen for heating and its impact on the power system". In: *international journal of hydrogen energy* 46.53 (2021), pp. 26725–26740.

[5] Chenjia Feng et al. "Day-ahead strategic operation of hydrogen energy service providers". In: *IEEE Transactions on Smart Grid* 13.5 (2022), pp. 3493–3507.

[6] Weiping Zhang, Akbar Maleki, and Mohammad Alhuyi Nazari. "Optimal operation of a hydrogen station using multi-source renewable energy (solar/wind) by a new approach". In: *Journal of Energy Storage* 53 (2022), p. 104983. ISSN: 2352-152X. DOI: https://doi.org/10.1016/j.est.2022.104983. URL: https://www.sciencedirect.com/science/article/pii/S2352152X22009884.

[7] Feras Alshehri et al. "Modelling and evaluation of PEM hydrogen technologies for frequency ancillary services in future multi-energy sustainable power systems". In: *Heliyon* 5.4 (2019), e01396. ISSN: 2405-8440. DOI: https://doi.org/10.1016/j.heliyon.2019.e01396. URL: https://www.sciencedirect.com/science/article/pii/S2405844018367471.

[8] Chunjun Huang et al. "Analytical Modeling and Control of Grid-Scale Alkaline Electrolyzer Plant for Frequency Support in Wind-Dominated Electricity-Hydrogen Systems". In: *IEEE Transactions on Sustainable Energy* 14.1 (2023), pp. 217–232. DOI: 10.1109/TSTE.2022.3208361.

[9] Simone Mucci, Alexander Mitsos, and Dominik Bongartz. "Power-to-X processes based on PEM water electrolyzers: A review of process integration and flexible operation". In: *Computers and Chemical Engineering* 175 (2023), p. 108260. ISSN: 0098-1354. DOI: https://doi.org/10.1016/j.compchemeng.2023.108260. URL: https://www.sciencedirect.com/science/article/pii/S0098135423001308.

[10] Md Biplob Hossain et al. "Power system dynamic performance analysis based on frequency control by proton exchange membrane electrolyzers". In: *IEEE Transactions on Industry Applications* (2023).

[11] Mehdi Ghazavi Dozein, Antonella Maria De Corato, and Pierluigi Mancarella. "Fast Frequency Response Provision from Large-Scale Hydrogen Electrolyzers Considering Stack Voltage-Current Nonlinearity". In: *2021 IEEE Madrid PowerTech*. 2021, pp. 1–6. DOI: 10.1109/PowerTech46648.2021.9494906.

[12] Mehdi Ghazavi Dozein, Ahvand Jalali, and Pierluigi Mancarella. "Fast Frequency Response From Utility-Scale Hydrogen Electrolyzers". In: *IEEE Transactions on Sustainable Energy* 12.3 (2021), pp. 1707–1717. DOI: 10.1109/TSTE.2021.3063245.

[13] Antonella Maria De Corato, Shariq Riaz, and Pierluigi Mancarella. "Impact of hydrogen electrolyzers on flexibility and network voltage profiles of a virtual power plant". In: *2020 Australasian Universities Power Engineering Conference (AUPEC)*. 2020, pp. 1–6.

[14] Ivan Pavić, Nikolina Čović, and Hrvoje Pandžić. "PV–battery-hydrogen plant: Cutting green hydrogen costs through multi-market positioning". In: *Applied Energy* 328 (2022), p. 120103. ISSN: 0306-2619. DOI: https://doi.org/10.1016/j.apenergy.2022.120103. URL: https://www.sciencedirect.com/science/article/pii/S0306261922013605.

[15] E. Crespi et al. "Energy storage with Power-to-Power systems relying on photovoltaic and hydrogen: modelling the operation with secondary reserve provision". In: *Journal of Energy Storage* 55 (2022), p. 105613. ISSN: 2352-152X. DOI: https://doi.org/10.1016/j.est.2022.105613. URL: https://www.sciencedirect.com/science/article/pii/S2352152X22016012.

[16] Mehdi Ghazavi Dozein, Antonella Maria De Corato, and Pierluigi Mancarella. "Virtual Inertia Response and Frequency Control Ancillary Services From Hydrogen Electrolyzers". In: *IEEE Transactions on Power Systems* 38.3 (2023), pp. 2447–2459. DOI: 10.1109/TPWRS.2022.3181853.

[17] Alexandra Lüth et al. "Electrolysis as a flexibility resource on energy islands: The case of the North Sea". In: *Energy Policy* 185 (2024), p. 113921.

[18] Xiang Cheng et al. "A Coordinated Frequency Regulation and Bidding Method for Wind-Electrolysis Joint Systems Participating Within Ancillary Services Markets". In: *IEEE Transactions on Sustainable Energy* 14.3 (2023), pp. 1370–1384. DOI: 10.1109/TSTE.2022.3233062.

[19] Marco Saretta, Enrica Raheli, and Jalal Kazempour. "Electrolyzer scheduling for Nordic FCR services". In: *2023 IEEE International Conference on Communications, Control, and Computing Technologies for Smart Grids (SmartGridComm)*. IEEE. 2023, pp. 1–6.

[20] *FCR-Design Project Summary report by ENTSO-E*. URL: https://www.statnett.no/globalassets/for-aktorer-i-kraftsystemet/utvikling-av-kraftsystemet/nordisk-frekvensstabilitet/fcr-design-project-summary-report.pdf.

[21] Hosna Khajeh et al. "Optimized siting and sizing of distribution-network-connected battery energy storage system providing flexibility services for system operators". In: *Energy* 285 (2023), p. 129490.

[22] *Terms and conditions for providers of Frequency Containment Reserves (FCR) by Fingrid*. URL: https://www.fingrid.fi/globalassets/dokumentit/fi/sahkomarkkinat/reservit/terms-and-conditions-for-providers-of-frequency-containment-reserves-fcr-as-of-22-may-2023.pdf.

[23] Manuel Tobias Baumhof et al. "Optimization of hybrid power plants: When is a detailed electrolyzer model necessary?" In: *2023 IEEE Belgrade PowerTech*. IEEE. 2023, pp. 1–10.

[24] Stefano Barsali et al. *Benchmark systems for network integration of renewable and distributed energy resources*. 2014.

[25] NREL. *2020ATB NREL Reference 7MW 200*. URL: https://nrel.github.io/turbine-models/2020ATB_NREL_Reference_7MW_200.html.

[26] Davide Burba. *Probabilistic ML with Quantile Matching: an Example with Python*. URL: https://towardsdatascience.com/probabilistic-ml-with-quantile-matching-an-example-with-python-c367eee85f18.